ABSTRACT

The research described in this feasibility study concludes that The Ocean Cleanup Array is likely a feasible and viable method to remove large amounts of plastic pollution from the North Pacific Gyre. Computer simulations have shown that floating barriers are suitable to capture and concentrate most of this plastic. Combined with ocean currents models to determine how much plastic would encounter the structure, a cleanup efficiency of 42% of all plastic within the North Pacific gyre can be achieved in ten years using a 100 km array. In collaboration with offshore experts, it has been determined that this array can be made and installed using current materials and technologies. The estimated costs are €317 million in total, or €31.7 million per year, which translates to €4.53 per kilogram of collected ocean debris.

AUTHORS

THE REPORT HAS BEEN AUTHORED BY:

Boyan Slat, Emile Arens, Evelien Bolle, Hyke Brugman, Holly Campbell, Pierre-Louis Christiane, Marijn Dekker, Stella Diamant, Bernd van Dijk, Mark van Dijk, Sjoerd Drenkelford, Norbert Fraunholcz, John Clinton Geil, Christian Goebel, Joost de Haan, Jort Hammer, Richard Hildreth, Tadzio Holtrop, Edd Hornsby, Sam van der Horst, Nick Howard, Wouter Jansen, Jochem A. Jonkman, Nicholas P. Katsepontes, David Kauzlaric, Raphael Klein, Stephan Koch, Tim Landgraf, Ezra Hildering van Lith, Jaime López, Richard Martini, Maximilian Michels, Bonni Monteleone, Elena Pallares, Leonid Pavlov, Kauê Pelegrini, Gabrielle S. Prendergast, Maira Proietti, Jill Randolph, Alexander Rau, Julia Reisser, Marleen Roelofs, Sebastiaan van Rossum, Rebecca Rushton, Stefan van Ruyven, Bruno Sainte-Rose, Sebastiaan van Schie, Moritz Schmid, Katherine Schmidt, Nandini Sivasubramanian, Paula Walker, Adam Walters, Nathan Walworth, Niklas Wehkamp, Robbert Zuijderwijk, Jan de Sonneville.

THE REPORT HAS BEEN EDITED AND PROOFREAD BY:

Boyan Slat, Agnes Ardiyanti, Johanna Buurman, Norbert Fraunholcz, Goli Habibi-Kenari, Edd Hornsby, Hester Jansen, Nicholas P. Katsepontes, Mukul Kumar, Elizabeth Ooi, Kelly Marie Osborn, Leonid Pavlov, Julia Reisser, Michiel van der Spek, Robbert Zuijderwijk, Jan de Sonneville

LIST OF AUTHORS AND AFFILIATIONS

	Boyan Slat	Personal title
dr.	**Agnes Ardiyanti**	Personal title
	Emile Arens	Huisman Equipment BV, Schiedam, the Netherlands
	Evelien Bolle	Personal title
	Hyke Brugman	internship Engineering, Design & Innovation, Hogeschool van Amsterdam, the Netherlands
J.D., LLM., Ph.D.	**Holly Campbell**	Instructor at the Oregon State University
Msc. (Magna Cum Laude)	**Pierre-Louis Christiane**	Personal title
	Bill Cooper	Personal title
Bsc.	**Marijn Dekker**	MSc student TU Delft, Delft, the Netherlands
	Stella Diamant	Personal title
Msc.	**Bernd van Dijk**	Personal title
Msc.	**Mark van Dijk**	Personal title
Bsc.	**Sjoerd Drenkelford**	MSc student TU Delft, Delft, the Netherlands
ir.	**Jabe Faber**	USG engineering
dr.	**Norbert Fraunholcz**	Recycling Avenue BV, Delft, the Netherlands
	John Clinton Geil	Co-founder, International Ocean Law and Science Institute. J.D. Lewis and Clark Law School. A.B. Occidental College, Assistant Attorney General for the State of Oregon
Msc.	**Christian Göbel**	Instituto Federal Rio Grande do Sul
	Dario Grassini	Personal title
Bsc	**Joost de Haan**	MSc student TU Delft, Delft, the Netherlands
Msc.	**Jort Hammer**	Personal title
	Richard G. Hildreth	Board of Directors, International Ocean Law and Science Institute. J.D. University of Michigan; Frank Nash Professor of Law and Director of the University of Oregon Ocean & Coastal Law Center
	Tadzio Holtrop	Personal title
	Edward Hornsby	Personal title
	Sam van der Horst	Personal title
	Nick Howard	Personal title
	Hester Jansen	Personal title
Bsc.	**Wouter Jansen**	MSc student TU Delft, Delft, the Netherlands
	Jochem A. Jonkman	Recycling Avenue BV, Delft, the Netherlands
	Nicholas P. Katsepontes	Retired, personal title
		Freiburg Institute for Advanced Studies, University of Freiburg, Germany; Laboratory for Simulation, Department of Microsystems Engineering (IMTEK), University of Freiburg, Germany
	David Kauzlaric	Freiburg Institute for Advanced Studies; Laboratory for Simulation, Department of Microsystems Engineering (IMTEK), University of Freiburg, Germany
Bsc.	**Raphael Klein**	MSc student TU Delft, Delft, the Netherlands

	Stephan Koch	ETH Zürich, Institute of Geophysics
dr.	**Tim Landgraf**	Freie Universität Berlin, Berlin, Germany
	Remko Leinenga	El-tec Elektrotechniek BV
	Christophe Limouzin	MRE Business Development Manager, Vryhof Anchors, Paris, France
Bsc.	**Ezra Hildering van Lith**	student TU Delft, Delft, the Netherlands
dr.	**Jaime López**	Personal title
	Wart Luscuere	Personal title
	Richard Martini	Personal title
	Maximilian Michels	MSc student, Computer Science, Freie Universität Berlin, Berlin, Germany
	Bonnie Monteleone	Personal title
	Frank Nash	Personal title
dr.	**Senol Ozmutlu**	Projects Director, Vryhof Anchors, Capelle aan de Yssel, the Netherlands
	Elena Pallares	Labaratori d'Enginyeria Marítima (LIM-UPC)
	Leonid Pavlov	Engineer, ATG Europe, Noordwijk, The Netherlands
	Herbert Peek	El-tec Elektrotechniek BV
dr.	**Kauê Pelegrini**	Polymers Laboratory, University of Caxias do Sul, Brazil
dr.	**Gabrielle S. Prendergast**	Personal title
	Maira Proietti	Universidade Federal do Rio Grande
	Jill Randolph	Personal title
	Alexander Rau	MSc student, Computer Science, Freie Universität Berlin, Berlin, Germany
Msc.	**Julia Reisser**	The University of Western Australia
	Marleen Roelofs	Personal title
Bsc.	**Sebastiaan van Rossum**	MSc student TU Delft, Delft, the Netherlands; intern, Vuyk Engineering Rotterdam BV
	Rebecca Rushton	Third-year law student at the University of Oregon
	Stefan van Ruyven	Huisman Equipment BV, Schiedam, the Netherlands
	Bruno Sainte-Rose	LEMMA, Paris, Head of Office
	Sebastiaan van Schie	BSc student TU Delft, Delft, the Netherlands
	Moritz Schmid	Takuvik Joint International Labatory, Laval University, Canada; CNRS, France; Département de biologie et Québac-Océan, Université Laval, Québec, Canada
	Katherine Schmidt	Personal title
	Nandini Sivasubramanian	Intern, Freiburg Institute for Advanced Studies, Freiburg, Germany
Bsc.	**Kathleen Laura Stack**	Personal title
	Paula Walker	Co-founder, International Ocean Law and Science Institute. J.D. Lewis and Clark Law School
	Adam Walters	Oceans, Coasts, and Watersheds Fellow at the University of Oregon School of Law
	Nathan Walworth	University of Southern California
MSc.	**Niklas Wehkamp**	MSc. in Microsystems Engineering
Bsc.	**Robbert Zuijderwijk**	Student Leiden University, Leiden, the Netherlands
dr.ir.	**Jan de Sonneville**	Personal title

COPYRIGHT INFORMATION

The Ocean Cleanup wishes to respect all third party rights. The Ocean Cleanup has no intention to violate any of those rights. Although The Ocean Cleanup takes the utmost care in the use of third party materials, infringements of third party rights may accidentally occur. In that case, The Ocean Cleanup will endeavour to cease these infringements as soon as possible or come to an agreement with those third parties about the use of their materials.

Version 1.1

REVIEWERS

Before release this document has been evaluated for scientific falsities by a selected group of scientific peers, as a response to the authors' request. The independent scientists outlined in this chapter have agreed to the conclusions, exclusively based on their own field of knowledge.

The Ocean Cleanup Foundation and the authors of this report highly appreciate critical feedback, as well as suggestions for future work. Please send your input to:

feasibility@theoceancleanup.com

If you are interested in contributing to the success of our future work, please visit:

www.theoceancleanup.com

"It is commendable that The Ocean Cleanup feasibility report brings together a vast array of concepts and disciplines that are brought across in an ordered and understandable way. The summarized description of the oceanography associated with the subtropical ocean gyres, where plastics are believed to be concentrated, is accurate, albeit it being generalized. The summary provides a good starting point of knowing where to focus the core of the project. Before full project implementation, I would suggest that more regionally specific analysis is completed on the gyres that The Ocean Cleanup intends to target, as this would provide efficiency to the cleanup process."

Dr. Sebastiaan Swart
Senior Researcher – Southern Ocean Carbon and Climate Observatory
Council for Scientific and Industrial Research (CSIR)

"In the Ocean Cleanup report several options have been proposed for the boom, the skirts, the station keeping system, and the installation procedures. Through a series of preliminary feasibility assessments, mainly through simplified time domain dynamic models, the fundamental challenges of this novel concept have been individuated. A series of conceptual/preliminary technical solutions for these challenges are proposed, and most importantly the areas to be further investigated have been individuated. As a result, a first methodology for the design and analysis has been established.

Based on the conclusions on the report, the concept seems to be challenging but technically within the capabilities of state of the art offshore engineering technology."

Maurizio Collu, PhD, CEng
Cranfield University, Offshore Renewable Energy Engineering Centre

"The Ocean Cleanup's exploratory CFD simulations use measured and modeled plastic distribution and oceanic conditions to determine the appropriate shape for their passive barrier concept. They also determine reasonable estimates for the efficiency of their design in collecting plastic debris of different sizes and densities. Although the design is unable to remove the smallest microplastics from the ocean, the high efficiency of the barriers in dealing with larger plastics would significantly reduce the overall mass of plastic debris in the North Pacific Subtropical Gyre."

Nicole Sharp, Ph.D.
Aerospace engineer and author, FYFD

"The strategy of the study is conventional and efficient, with a first two dimension analysis of the ocean flow around the boom and the skirt, and a particle model to have a first idea of the plastic parts potentially captured, depending on their size, density and depth. Despite some mesh size discontinuities, and the lack of boundary layer on the skirt degrading the flow precision near the wall, the results give a good idea of the efficiency of the system and the influence of the parameters.

Then two 3D studies are completed to analyze the effect of the boom angle on the flow and the catch probability. A large scale simulation is performed with COMSOL and gives the 3D flow with several boom angle. Some hypothesis are not clear (condition used on the boundary at the end of the barrier and on the barrier, pressure gradient due to gravity not present at the outlet), but the results give more information on the effect of the boom angle. The finer study with CFX models the barrier more precisely, but with a too coarse mesh near the skirt and a domain too small to impose a pressure at the outlet. Nevertheless, the 3 studies give the same parameters range which allow the particles to be caught, and a good idea of the efficiency of the global system."

Stéphane Dyen
Design team manager and CFD expert of Hydros / Hydroptère Suisse SA

EXECUTIVE SUMMARY

BOYAN SLAT • HESTER JANSEN • JAN DE SONNEVILLE

EXECUTIVE SUMMARY

Every year we produce about 300 million tons of plastic, a portion of which enters and accumulates in the oceans. Due to large offshore currents, plastic concentrates in vast areas called gyres, of which the Great Pacific Garbage Patch between Hawaii and California is the best-known example.

The damage to sea life is staggering: at least one million seabirds, and hundreds of thousands of marine mammals die each year due to the pollution. Even worse, the survival of many species, like the Hawaiian Monk Seal and Loggerhead Turtle, is directly jeopardized by plastic debris.

Marine species often become entangled in larger debris, leading to "injury, illness, suffocation, starvation, and even death" (NOAA, 2014). Smaller fragments can be mistaken for food and eaten, causing malnutrition, intestinal blockage and death. When marine animals eat plastic, harmful chemicals move up the food chain. Ingestion of and entanglement in marine debris by marine animals has increased by 40 percent in the last decade. Furthermore, plastics can transport invasive species and toxic substances over great distances.

The problem does not end there. Marine debris causes an estimated $1.27 billion in fishing and vessel damage annually in the region of the Asia-Pacific Economic Cooperation (APEC) alone. Moreover, the removal of garbage from coastlines costs up to $25,000 per ton of plastic.

Figure 1 Albatross with plastic in its stomach. Photo by Chris Jordan

Figure 2 Schematic overview of the five rotating currents, called gyres, where floating plastic accumulates

Figure 3 A preliminary design of a collection platform (Erwin Zwart – Fabrique Computer Graphics)

IN SEARCH OF A SOLUTION

Even if we manage to prevent any more plastic from entering the oceans, the natural loss of plastic from the gyres is likely low; therefore, a cleanup is still necessary. Since the problem gained widespread attention at the beginning of this century, several cleanup concepts have been proposed, each based on vessels with nets – essentially, fishing for plastic. Unfortunately, even though the concentration of plastic in these five subtropical gyres is extremely high compared to the rest of the oceans, plastic is still spread over millions of square kilometers. Hence, it would likely take many billions of dollars and thousands of years to clean up such an area using those methods (Moore, 2011). By-catch and emissions would likely be problematic using this approach. Furthermore the ocean is not a particularly friendly place to work. Why move through the oceans, if the oceans can move through you?

ABSTRACT

The world's oceans are characterized by a system of large-scale rotating currents, called 'gyres'. The ocean systems are constantly moving as a result of the turning of the earth and wind patterns. The five major gyres are the Indian Ocean Gyre, the North Atlantic Gyre, the North Pacific Gyre, the South Atlantic Gyre and the South Pacific Gyre. If the ocean's water is constantly moving according to predictable patterns, so is the plastic pollution. This led to the idea of a 'passive cleanup': using an array of floating barriers fixed to the sea bed to catch the debris as it flows past on the natural ocean currents.

THE CONCEPT

The Ocean Cleanup Array utilizes long floating barriers which - being at an an angle - capture and concentrate the plastic, making mechanical extraction possible. One of the main advantages of this passive cleanup concept is that it is scalable. Using the natural circulation period of the North Pacific Subtropical Gyre, cleanup duration could be reduced to a minimum of just 5 years.

Using a passive collection approach, operational expenses can potentially be very low, making the cleanup more viable. Furthermore, converting the extracted plastic into either energy, oil or new materials could partly cover execution costs.

Because no nets would be used, a passive cleanup may well be harmless to the marine ecosystem and could potentially catch particles that are much smaller than what nets could capture.
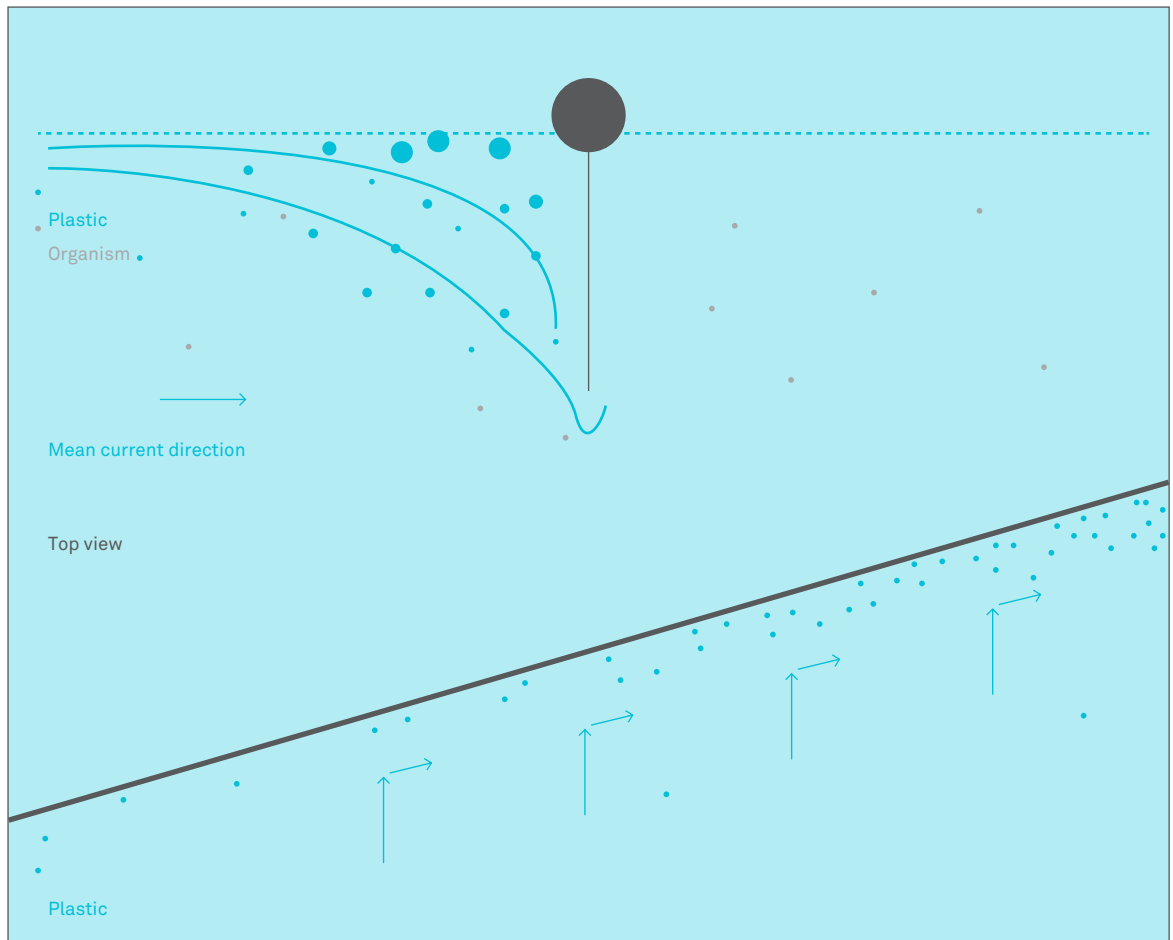
Figure 4 Simplified and schematic cross-section view of a floating barrier. The red dots represent plastic particles, while the green particles are organisms. Simplified and schematic top view of a floating barrier. The red dots represent plastic particles.

THE FEASIBILITY STUDY

Between April 2013 and May 2014, The Ocean Cleanup has been investigating the technical feasibility and financial viability of The Ocean Cleanup Array concept. With costs covered by a crowd funding campaign, a global team of over 100 people, companies and institutes have collaborated to produce an in-depth study.

This feasibility study examines the physical properties of plastic pollution; technical feasibility in terms of fluid dynamics, structural engineering and operations; and describes the large-scale test that has been performed. It assesses any possible negative environmental effects and legal consequences. Moreover, the study evaluates the quality of ocean plastics, as well as possible methods to process it - including a cost-benefit analysis. Finally, the feasibility study outlines recommendations for future work.
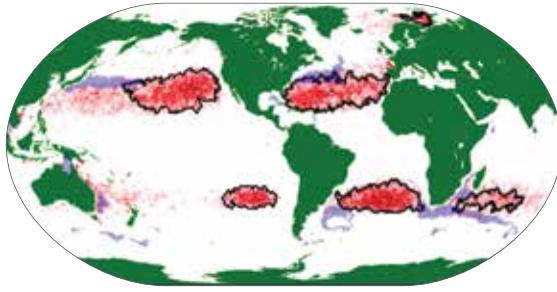
Figure 5 Initial simulation plastic distribution. The locations where plastic release begins are visualised in red and purple.
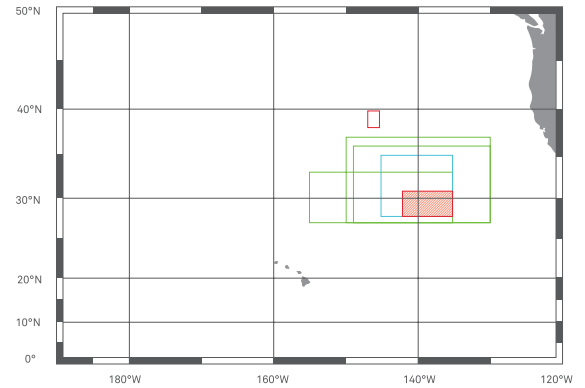
Figure 6 Map showing the areas in which the highest concentration of plastic debris has been predicted by Maximenko et al. ,2012, Van Sebille et al.,2012 and Lebreton et al., 2012, in green. The highest measured plastic concentration is displayed in blue, while the areas containing favorable seabed conditions are depicted in red."

PLASTIC POLLUTION HOTSPOTS IN OCEAN GYRES

Based on ocean surface current models indicating plastic pollution hotspots, the scope of the research was narrowed down to the subtropical gyres. Subsequently, the focus was further narrowed to only include the North Pacific Subtropical Gyre through the use of measurement data. The Ocean Cleanup conservatively estimates the mean mass of floating plastic in the North Pacific accumulation zone at 140 thousand metric tons: 21 thousand tons of plastic smaller than 2 cm and 119 thousand metric tons of plastic larger than 2 cm. However, more research is needed to increase the accuracy and reliability of these figures. Sampling of ocean plastic is still limited - both spatially and temporally - particularly for large (centimeter/meter-sized) plastic items.

DETERMINATION OF LOCATION

On the basis of ocean current models, ocean depth and measured plastic concentrations, The Ocean Cleanup has chosen 30°N, 138°W as the preliminary coordinates for placement of the Array.

ENVIRONMENTAL CONDITIONS IN THE NORTH PACIFIC GYRE

Using data from weather buoys and satellite recordings, current, wave and wind conditions were estimated for the area of interest, see Figures 6-8.

The following values have been used as input parameters for structural engineering and fluid dynamic chapters of the report: waves predominantly derive from the northwest (NW), and to a lesser extent also from the northeast (NE) sector. Waves from the northwest (NW) sector are swells generated in the North Pacific Ocean, and waves from the northeast (NE) sector are sea waves. Over 95% of waves are lower than 4.5 – 5.5 m. The maximum significant wave height (H_s) is 12.2 m with a 100-year return period. The wind predominantly comes from the northeast to east (NE-E) sectors. A mean current velocity of 14 cm/s has been calculated for the area.

H$_S$ (m)

>=20,0	8,0 – 12,0	Calms: 0,00%
16,0 – 20,0	4,0 – 8,0	
12,0 – 16,0	0,0 – 4,0	
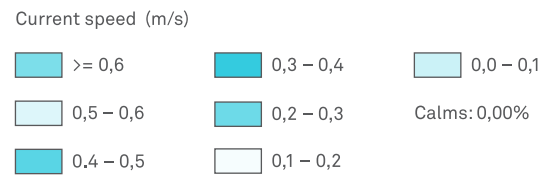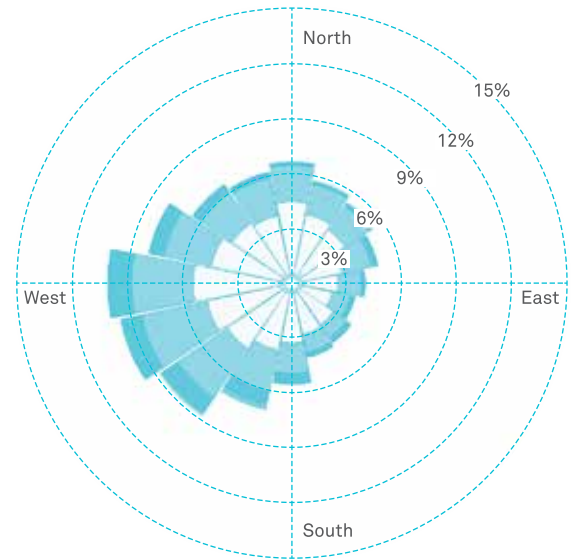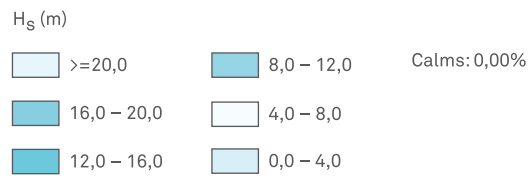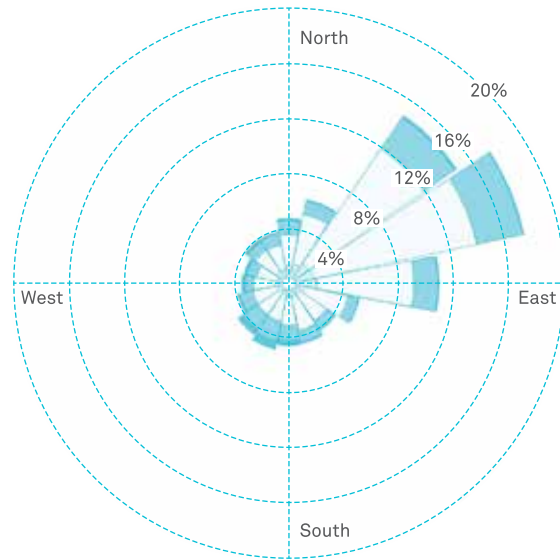
Figure 7 Wind from direction rose for NOGAPS reanalysis data

Current speed (m/s)

>= 0,6	0,3 – 0,4	0,0 – 0,1
0,5 – 0,6	0,2 – 0,3	Calms: 0,00%
0,4 – 0,5	0,1 – 0,2	

Figure 8 Surface layer current rose

H$_S$ (m)

>=7,5	3,0 – 4,5	Calms: 0,00%
6,0 – 7,5	1,5 – 3,0	
4,5 – 6,0	0,0 – 1,5	
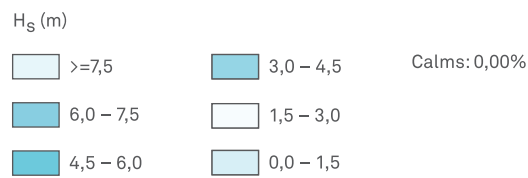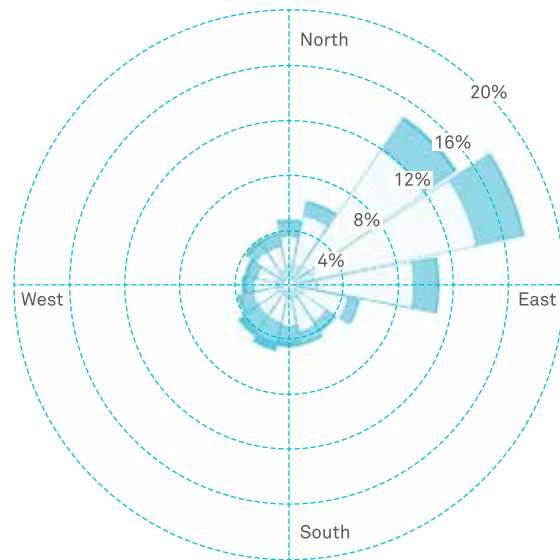
Figure 9 Significant wave height – wave from direction rose

Figure 10 The multi-level trawl, used for sampling plastic concentrations

VERTICAL DISTRIBUTION OF PLASTICS

To measure the vertical distribution of the plastic debris, a net system was created capable of sampling the oceans from the surface to a depth of 5 meter. The plastic concentration (grams and pieces per m³) was measured in the North Atlantic Gyre during two separate expeditions. The observations indicate that plastic maintains a depth profile of higher mass close to the water surface with mass decreasing exponentially with depth. Therefore, a floating barrier depth of 2-3 m was chosen because it would be able to capture most of the total plastic pollution mass. The data also suggests there is a relationship between wind speed and vertical distribution, but more measurements are necessary to confirm this.
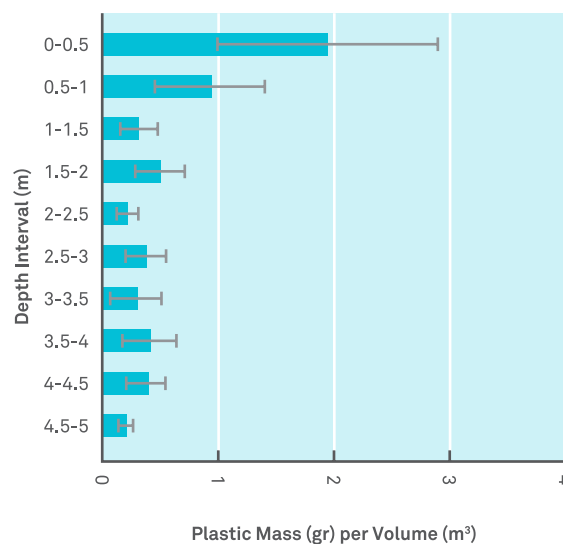
Figure 11 Depth profile of plastic pollution (N = 12 trawls) plastic concentrations in mass per volume at different depth intervals; plastic concentrations in pieces per volume at different depth intervals.
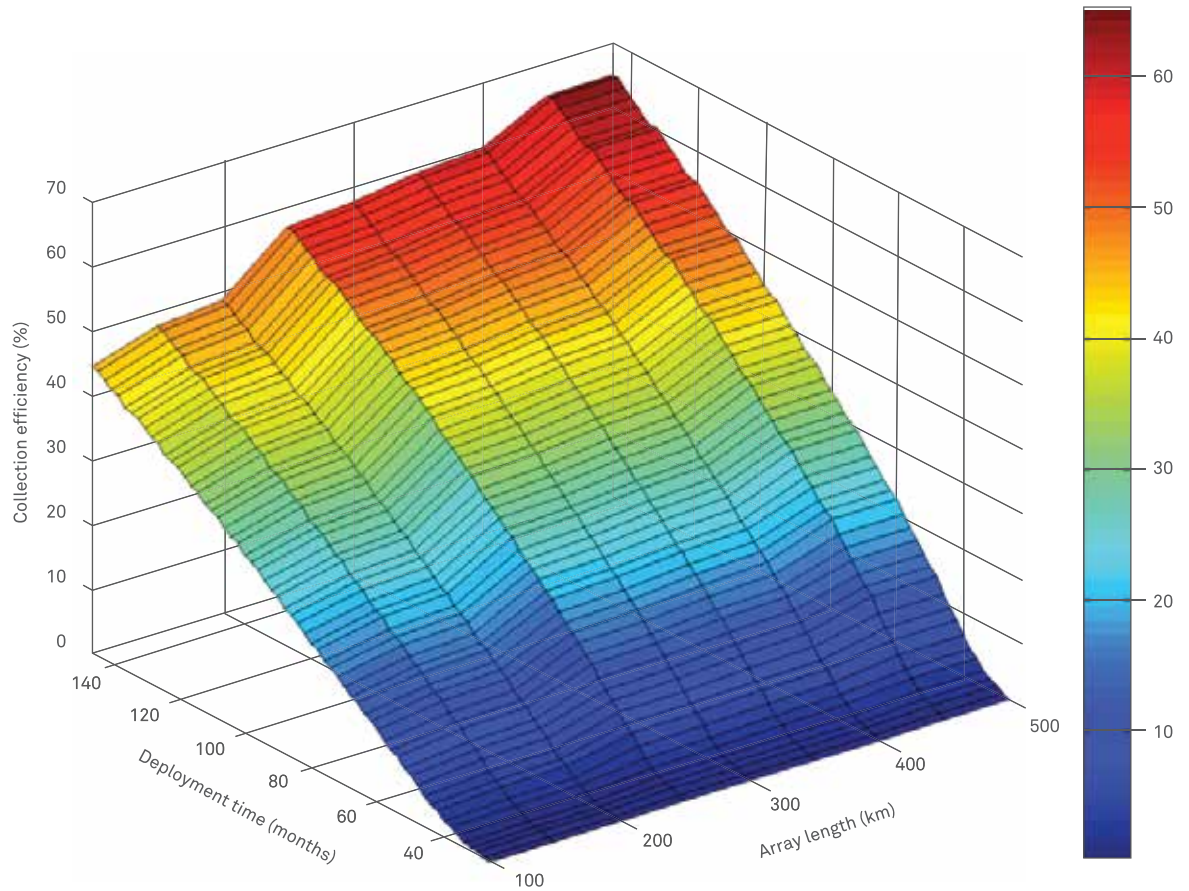
Figure 12 A graphic representation of the dependency between the field efficiency, total array length and deployment time. To increase field efficiency, either the total array length or deployment time has to increase

CLEANUP TIME AND REQUIRED ARRAY LENGTH

The Ocean Cleanup investigated the relation between array length, deployment time and field efficiency. It follows that to increase field efficiency, either the total array length or deployment time has to increase. A deployment time of 10 years and an array length of 100 km was chosen, resulting in a field efficiency of 40-45%

INVESTIGATING BASIC PRINCIPLES

Computational Fluid Dynamics (CFD) has been used to study the catch efficiency, the transport of plastic along the boom, and the forces acting on the boom.

Variables such as particle size, density and release depth were taken into account in determining which particles would be caught by or escape underneath the boom. Combining this data with modeled mass distribution and vertical distribution, a capture efficiency of 79% of mass was calculated. No micro plastics (particles smaller than 2 cm) were captured under the modeled conditions. However, all medium and large size plastics (irrespective of the depth within the top 3 m) are caught. Furthermore, the capturing of large debris prevents the creation of small debris by photo-degradation.

CFD simulations also showed that particles travel along the boom when encountering a boom that is under an angle relative to the direction of the surface current, meaning booms can concentrate plastic pollution. The velocity of the plastic along the barrier depends on the boom angle, but is about 40% of the initial velocity when placed at an angle of 30°.
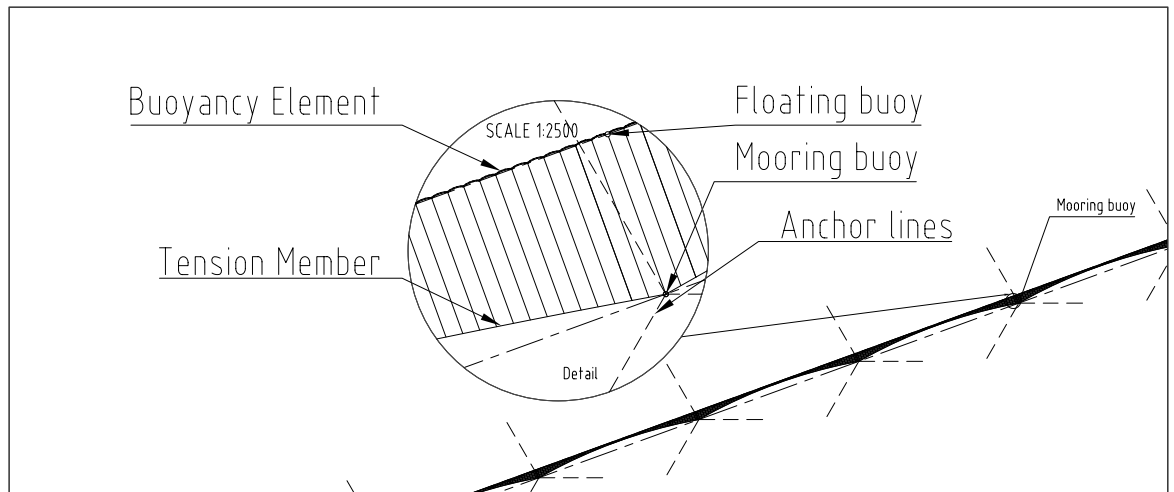
Figure 13 Tension cable impression

LOADS ON THE BOOM

A boom-and-mooring model was set up in Orcaflex to determine the mid-effective tension (the load on the boom) as function of boom length. Forces were determined for a generic boom with a draft of 3 m, at a significant wave height of 5.5 m, which was set as the maximum operational significant wave height.

For boom lengths used in the simulation, the relationship between force and boom length was found to be essentially linear. The fact that for the Dyneema-tensioned boom the tension is higher than both neoprene and steel boom is due to its high stiffness compared to the other options. The steel boom has neoprene links that lower the stiffness significantly. Although the boom likely would not be entirely manufactured out of Dyneema, its readings were used during the dimensioning of the materials as a conservative estimate.

OVERTOPPING

Orcaflex also found that if the boom were too long, high tension would prevent the boom from following the waves, resulting in overtopping. This is an undesired effect, because plastic would likely be lost in the process, impacting capture efficiency.

In the above image, the boom can follow the shape of the wave, but in the second image the tension force spans the boom in such a way that it remains straight and waves overtop it. If overtopping is to be avoided, it was found that the maximum length of an individual boom should be 1.4 km.

TENSION CABLE CONCEPT DESIGN

The Ocean Cleanup developed a boom design in which the boom and tension cable are separated. This design allows the boom to move with the waves, rather than being restricted by the load carrying part of the boom - regardless of the stiffness of the tension cable. The boom is connected to the tension cable every 60 m, transferring its load to the cable. Furthermore this design allows the boom to move along with the rotational motion of the waves, reducing the forces on the tension cable. The use of a tension cable is also included in a patent application from The Ocean Cleanup.
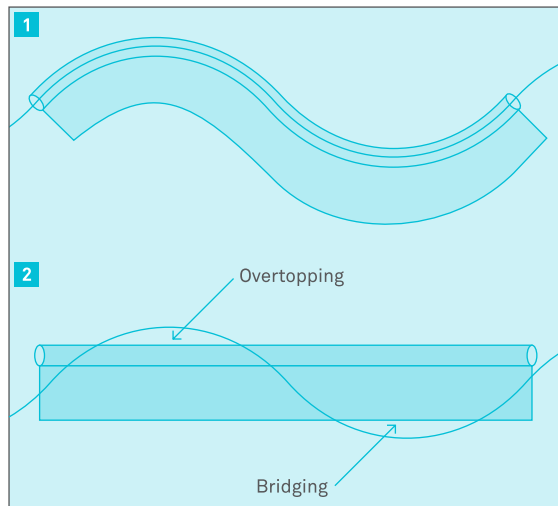
Figure 14 Effect of a too high tension force along the boom: in the top image, the boom can follow the shape of the wave, but in the bottom image, the tension force spans the boom in such a way that it remains straight

Figure 15 Preliminary design of a classic spar as a processing platform.

MOORING

The mooring systems required for station-keeping the structure are novel due to the unprecedented depths at which they would be placed. Given an average depth of about 4 km, a fiber rope mooring system is the only option available. To ensure durability of the system, chain and wire rope is used at the bottom and top ends. A Stevmanta Vertical Load Anchor (surface area 14 m²) is sufficient to withstand the design loads including the safety factor. A three-line system was chosen for all mooring points.

Vryhof Anchors confirmed that with current knowledge, mooring at the given water depths is feasible and installation of all system components can be done from the water surface. The mooring configuration is similar to proven solutions at 2,500 m of water depth.

THE PROCESSING PLATFORM

The platform design is based on a spar, being a stable, cost-effective and proven hull-type. This design consists of a buffer for the collected plastic in the hull of the spar, with a processing-equipment deck as a topside. The hull has a cylindrical shape with a diameter of 11m and a height of 58m. For the storage of plastic, a volume of 3,000 m³ is reserved in the hull. Although for transport a volume of 6,000 m³ has been reserved, this includes the added water necessary to pump it from platform to ship.

The plastic collection rate will total 65 m³/day, which means the plastic collected has to be picked up by a ship every 45 days.

The main deck features processing equipment, including the top of the mesh conveyor, a shredder for large debris and electrical systems. Additionally, the deck incorporates a workshop and a 50-ton crane to lift spare machinery. Photovoltaic panels mounted on the roof over the main deck will provide the primary power supply. The platform is equipped with a slurry pump to extract small particles, coupled to a centrifugal separator for dewatering purposes.

Taking into account a cost of €5 per kg of steel (including construction), and a total weight 2,800 tons of steel, the costs of the platform are an estimated €14 million (excluding equipment and mooring). For transshipment and transport of the collected debris a second slurry pump will be used. The costs to transport the garbage to land have been calculated to be €1 million euro per year, or €0.14 per kg plastic.

r=35cm

3m skirt

2kg lead
weight per 2m

Boom cross-section
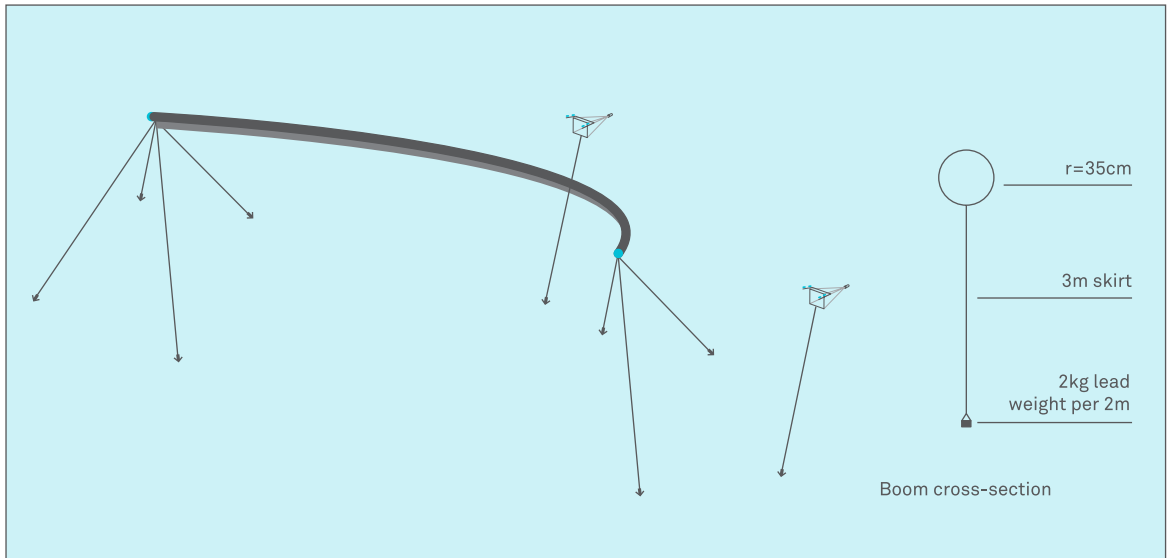
Figure 16 Mooring configuration. Schematic drawing of the planned mooring configuration of the booms and trawls

ENVIRONMENTAL IMPACT

Because they are effectively neutrally buoyant, both phytoplankton and zooplankton are likely to pass underneath the barriers along with the current. But even assuming the worst - The Ocean Cleanup Array would harvest all the plankton it encounters - this would constitute a maximum loss of 10 million kg of planktonic biomass annually. Given the immense primary production of the world oceans, it would take less than 7 seconds to reproduce this amount of biomass.

With regard to vertebrates, harm caused by the barriers seems unlikely because non-permeable barriers are used, although some bycatch may occur in the near vicinity of the platform's extraction equipment. To prevent the possible impact on vertebrates, active deterrent techniques could be implemented near the extraction equipment.

The carbon footprint analysis showed the greenhouse gas emissions of the entire Ocean Cleanup project are 1.4-5 million kg of CO^2, depending on the chosen scenario. To put this into perspective, it is equal to the production of only 370-1,400 cars based on an average consumption of driving 20,000 km per year. The calculation of the carbon footprint revealed that the life-cycle stage 'Marine Transport' has the largest environmental impact. This impact can be reduced by limiting the on-site time of the vessel, as well as by using a highly energy-efficient vessel. The transportation of more plastic per vessel and per cycle could lead to a longer cycle time and a smaller carbon footprint. The use of solar energy reduces the platform's carbon footprint.

Figure 17 Cod ends. Cod ends with its zooplankton contents, bottom one as control, and the top one from behind the boom

Figure 18 Volunteers collecting beached debris. Photo by Megan Lamson / HWF

PROOF OF CONCEPT

A first proof-of-concept test performed at the Azores Islands validated the capture and concentration potential of a floating barrier with a skirt depth of 3 m, in moderate environmental conditions. In addition, qualitative data suggested that the barrier does not catch zooplankton as the net behind the boom appeared to have caught an equal amount of zooplankton as the net next to the boom.

PLASTIC MATERIAL ANALYSIS AND PROCESSING OPTIONS

Although the possibility of processing plastic into a useable and valuable material does not determine the feasibility of the Array, a valid question would be: what The Ocean Cleanup would do with the plastic once this process has been completed.

In order to investigate a representative sample of North Pacific Gyre debris, half a ton of plastic was collected on a remote beach on Hawaii Island. See figure 18.

From the degradation tests, it can be concluded that the polyolefin samples were less degraded than expected. The degree of degradation of high-density polyethylene (HDPE) appears particularly mild both when compared to studies of accelerated aging under controlled conditions and when compared to the degradation found for polypropylene (PP) from the same sample origin.

Pyrolysis tests have showed that there is at least one method in which ocean plastic can be reused. According to the companies involved in the testing, the quality of the pyrolysis oil obtained from the polyolefin fraction of marine debris is comparable to that obtained as regular input in their pyrolysis plants. It appears that the production of marine fuel is more attractive due to its substantially higher yield of 77% for the target fraction when compared to the gasoline producing process with a final yield of 53% for the gasoline fraction.

LEGAL ISSUES

This study also provides a high-level overview of key legal issues that may impact The Ocean Cleanup.

First, concerning the question of who owns the plastic in the oceans, there are three different legal constructs in play. As most plastic is unlabeled and degraded before being caught, the owner of the plastic cannot be traced, and therefore salvage is not possible. Laws of abandonment cannot be used, as virtually all the traces, including owner information, are lost in the high seas. This leaves the law of the finds, that is based on the following principles: i) intent of the finding party to establish possession over the property in question; ii) actual possession as in exerting physical control over the property; and iii) a determination that the property has been abandoned by the owner. Based on this law, it is assumed that The Ocean Cleanup can take ownership of the plastic collected in the high seas.

Second, because The Array presents a unique situation that poses questions regarding shipping right-of-ways and hazards to shipping traffic, it may have to abide by additional safety regulations from either the flag-state or the International Maritime Organization (IMO). For this feasibility study The Ocean Cleanup assumes that platforms will not be flagged by a state and will thus not be subject to state law. The question remains if the UN would have some jurisdiction over the platforms, either by flagging or otherwise.

Third, as the Ocean Cleanup Project has the objective of passive collection of floating plastic waste, it would not qualify as a fishing activity. Therefore it does not fall under the current by-catch laws or the laws addressing "taking" of endangered migratory species. While assessing that The Ocean Cleanup bycatch will likely be minimal, the mere prospect of bycatch might bring The Ocean Cleanup into the realm of regulatory oversight.

Last, a proposal for a legal framework is postulated for international ocean rehabilitation projects.

FINANCIALS

The Ocean Cleanup Array is estimated to be 33 times cheaper than conventional cleanup proposals per extracted mass of plastics. In order to extract 70 million kg (or 42 percent) of garbage from the North Pacific Gyre over 10 years, we calculated a total cost of 317 million euro.

In the calculations, a limited lifetime of 10 years is applied instead of a general economic lifetime (for most equipment 20 years). This is because projections indicate the mean amount of plastic mass will decrease with time. Thus, the average mass of plastic that will be collected per year will likely be lower than what has been calculated using the 10-year deployment time. As expected with the passive cleanup concept, capital expenditures outweigh the operating expenditures. The total annual estimated operating expenditures is estimated at five million euro.

A break-even cost of €4.53 per kg of plastic collected must be realized in order for The Ocean Cleanup Array to be profitable. This amount falls in the range of beach cleanup costs, estimated to be €0.07 – €18.0 per kg. This is also less expensive than the plastic-caused damage to the maritime industry in the APEC region.

Based on the current estimates of costs and the amount of plastic in the oceans, the costs outweigh the profits generated by high-volume solutions, like incineration or pyrolysis, but it is unknown what the financial prospective would be for mechanical recycling. This should be investigated in a later phase.
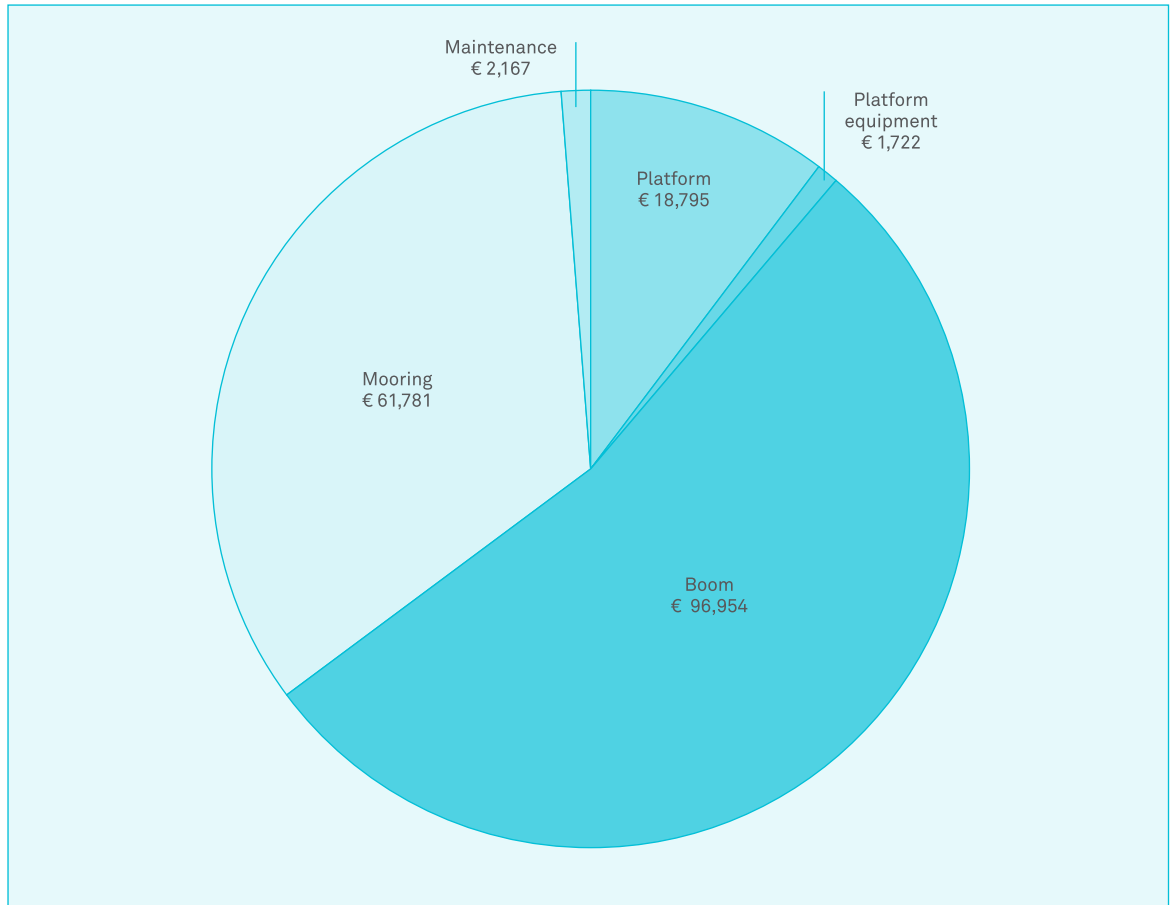
Figure 19 Estimated initial Base Capital Expenditure in euro '000s
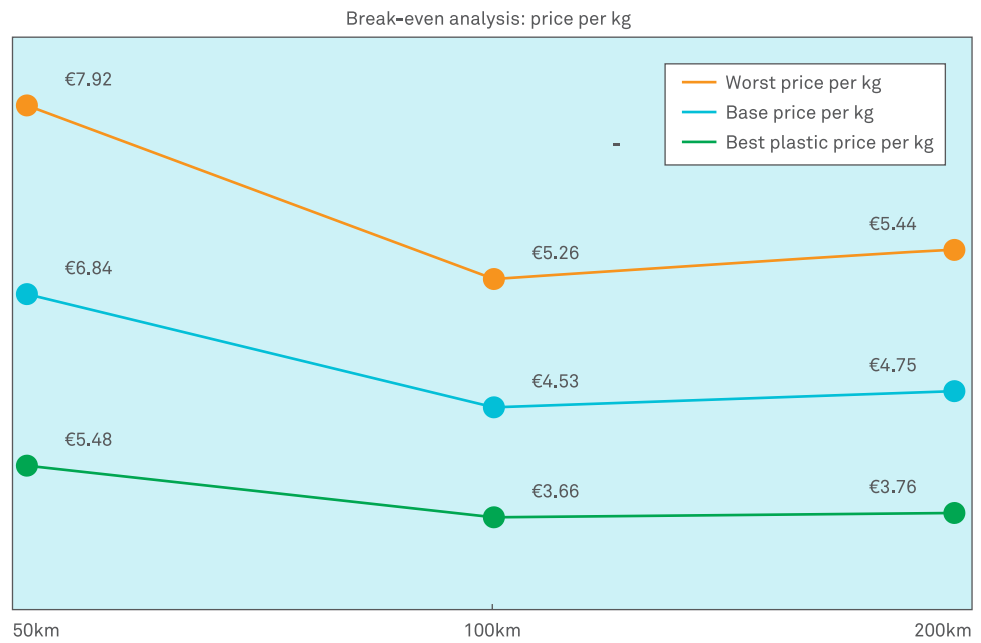
Figure 20 Break-even analysis in price per kg for each Array length in km.

	Best	Base	Worst
Initial Capital Expenditure	€ 147,984,453	€180,193,050	€202,684,608
CapEx Replacement Costs after 5 yrs	€ 61,035,640	€70,198,000	€ 78,191,390
Operating Expenditures over 10 yrs	€ 34,276,271	€ 49,997,283	€ 68,860,495
Decommissioning cost after 10 yrs	€ 12,607,500	€ 16,810,000	€ 18,491,000
Total Cost over 10 yrs **Including Replacement & Decommissioning Costs**	€ 255,903,864	€ 317,198,333	€ 368,227,492

Figure 21 OpEx in relation to CapEx, euro (best-, base-, and worst-case) over ten years.
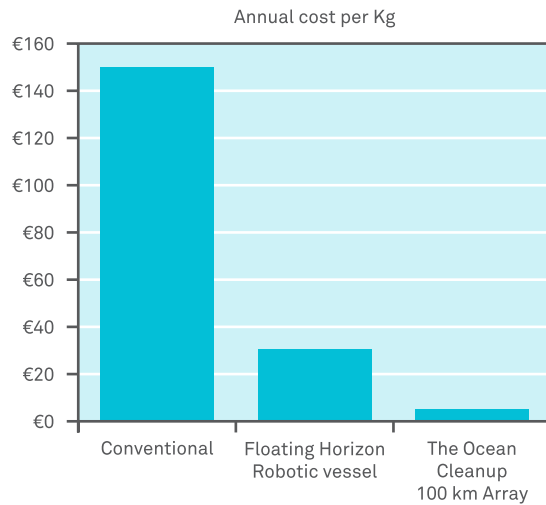
Figure 22 A comparison of cleanup costs per concept per kg

Phase 0	Phase 1	Phase 2	Phase 3
Project initiation	Preliminary engineering	Iterating and validating	Construction, operation and decomissioning

```
                              ┌─────────────────────────┐
                              │   Detailed Engineering   │
                              └─────────────────────────┘
                                    ↑            ↑
┌──────────────┐  ┌──────────────┐  ┌──────────────┐  ┌──────────────────┐  ┌──────────────┐
│  Conceptual  │→ │ Feasibility  │→ │  Up-scaling  │  │  Large-scale     │  │Implementation│
│   Design     │  │    Study     │  │   testing    │  │ operational pilot│  │              │
└──────────────┘  └──────────────┘  └──────────────┘  └──────────────────┘  └──────────────┘
                                    ↓            ↓
                              ┌─────────────────────────┐
                              │Oceanographic Field Research│
                              └─────────────────────────┘
```
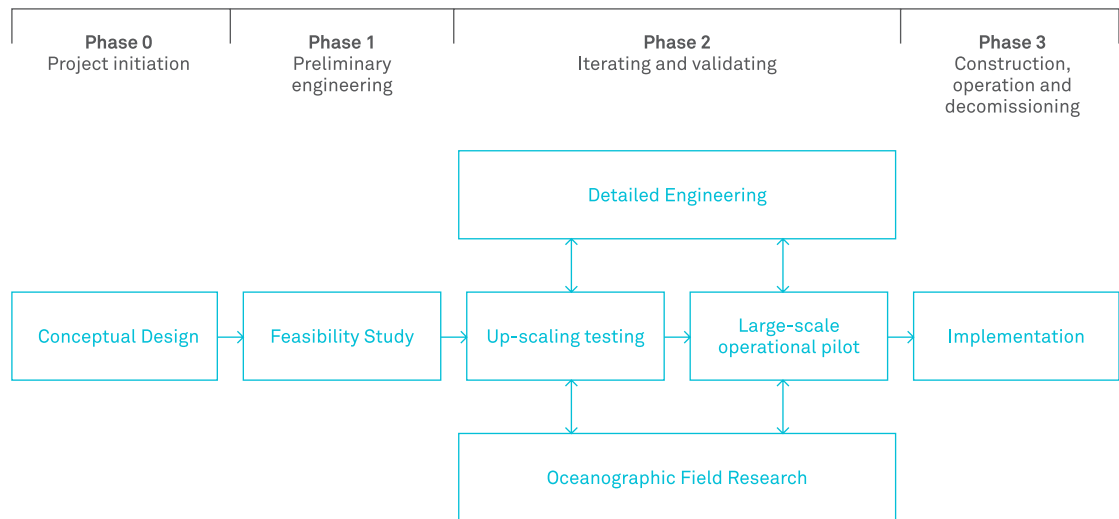
Figure 23 Phasing of The Ocean Cleanup project

LOOKING AHEAD

To address the remaining uncertainties identified in the feasibility study, a second phase of the project is proposed to prepare for implementation. In this phase, The Ocean Cleanup would develop a series of up-scaling tests, working towards a large-scale operational pilot in 3 to 4 years.

The scale of these tests will likely range from ~10m at the scale model test (1:1000) to ~10km at the large-scale operational test (1:10). Besides assessing new engineering results in a real-world environment, these tests also serve to uncover any unforeseen interactions between the structure and the environment, while allowing for the practicing of operational procedures.

In terms of research, the two essential elements in the second phase of the project are:

1 The in-depth engineering and optimization of the structure;
2 Improving the plastic mass estimate, by taking spatial and temporal variability, as well as measured vertical distribution into account.

To be more cost-efficient, The Ocean Cleanup will act as a facilitator of the research, outsourcing most of the fundamental research to institutes, and collaborating with offshore and engineering companies to cover most of the tests' costs.

CONCLUSIONS

Based on this collected evidence, it is concluded that The Ocean Cleanup Array is likely a feasible and viable method for large-scale, passive and efficient removal of floating plastic from the North Pacific Garbage Patch.

However, for this project to be successful in reducing the amount of plastics in the Great Pacific Garbage Patch, it is essential for the influx of new plastic pollution into the oceans to be radically reduced.

CHAPTER 1

INTRODUCTION

What are the causes and effects of plastic pollution? What are the potential benefits of a cleanup operation? What work has already been done in the field, and why haven't they succeeded? How does The Ocean Cleanup plan to change this? These questions are covered in the first chapter of this feasibility study.

THE PLASTIC LIFECYCLE IS BROKEN

BONNIE MONTELEONE • BILL COOPER

Plastics are highly valued for their light and durable qualities, and are widely used not just in packaging but also in consumer goods, building and construction, electronics, medical supplies, and transportation. Most plastics are made from non-renewable petroleum and natural gas resources, and contain chemical additives that have a significant impact on the environment and human health. Unfortunately, despite efforts to reduce their use and recycle, humanity uses increasingly more plastic, and much of it ends up in our oceans. This is not just an eyesore, it is a threat to the world's biodiversity. Plastics do not biodegrade, rather they break down into minute pieces, releasing their chemical additives and masquerading as food to marine life. In fact, in 2011 the United Nations Environment Program listed plastic pollution in oceans as a top priority issue, citing its potential impact on ecosystems and human health.

Figure 1.1 Plastic debris on Kanapou, Hawaii, USA, 2006 (Courtesy NOAA, Marine Debris Programme)

1.1.1 A BRIEF HISTORY OF PLASTIC

The end of World War II marked the start of the modern plastic era, or "Our plastic age" (Thompson, Swan, Moore, & vom Saal, 2009). Derived from oil or gas, plastics possess properties that are ideal for the manufacture of many everyday items: they are light, cheap, flexible, strong, and durable (Thompson et al., 2009).

Not surprisingly, global plastic production has grown exponentially. From 1950-2007 plastic production rose from 1.5 million tons to 270 million tons per year, an expansion which kept pace with the simultaneous global population growth from 2.7 to over 7 billion (Rochman, Browne, et al., 2013). In 2012 alone, 288 million tons of plastic were produced (PlasticsEurope 2013), which is approximately the same weight of the entire human biomass (Walpole et al., 2012).

Two specific issues are associated with this sharp rise in plastic production: impacts on human health, such as increased risk of cancer and neurological problems (Breast Cancer Foundation 2013); and the growing amounts of plastic debris entering the marine environment (United Nations Environment Programme 2013).

1.1.2 PLASTIC IN THE OCEANS

Plastics are made of essential polymers, synthetically produced from petroleum, natural gas, or coal, and mixed with a complex blend of chemicals known as additives. These additives have the ability to alter or improve the polymers' properties. For example, polyethylene terephthalate, or PET, is the nearly indestructible plastic used to make most containers and bottles. Other common additives include: UV stabilizers, antioxidants, brominated flame-retardants, and bisphenol-A. Some of these chemicals are known endocrine disrupters or carcinogens and can seriously affect the health of organisms.

Plastic is unlikely to biodegrade, yet does photo-degrade. However, this requires prolonged exposure to ultra-violet light. Physical abrasion also contributes to its decomposition (A. L. Andrady, Hamid, Hu, & Torikai, 1998; D.K.A. Barnes, Galgani, & Thompson, 2009; Colton Jr., Knapp, & Burns, 1974; Gregory, 1977; Thompson et al., 2004). Still, it can take 400 to 1000 years, and even longer in a marine environment for plastics and their chemical additives to break down into carbon dioxide, water, and small inorganic molecules, a process called mineralization.

[2] Marine debris is defined as "any persistent solid material that is manufactured or processed and directly or indirectly, intentionally or unintentionally, disposed of or abandoned into the marine environment."
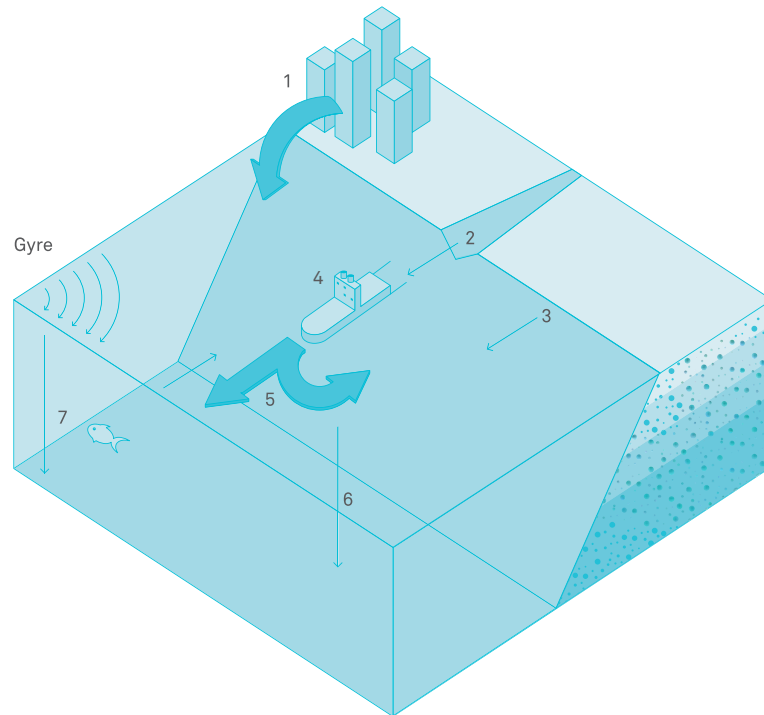
Figure 1.2 Pathways of plastic pollution. Plastic enters the ocean from coastal urbanization (1), through rivers (2), from beaches (3), and from ships (4). Through currents and wind, plastic gets transported through the ocean or sea (5), finally ending up on coastlines or in a gyre. Heavier-than-water plastics are likely to sink not far from the coast (6), unless the plastic encapsulates air. Possible sinks for the plastic in the gyre include sinking due to loss in buoyancy, ingestion, biodegradation, and natural loss onto coastlines due to currents (7).

1.1.3 BREAKING THE CYCLE

The discovery of fragmented plastic during plankton tows of the Sargasso Sea in 1971 led to one of the earliest studies of plastic in the marine environment. Using a 333 micron surface net trawl, Carpenter and Smith collected small fragments of plastics in 1971, resulting in estimates of the presence of plastic particulates at an average of 3,500 pieces and 290 g/km^2 in the western Sargasso Sea (Carpenter and Smith, 1972). Shortly after, Colton et al., (1974) surveyed the coastal waters from New England to the Bahamas and confirmed distribution of plastic all along the North Atlantic. These studies have been recently updated in two comprehensive studies of the North Atlantic gyre (K. L. Law et al., 2010; Moret-Ferguson et al., 2010). Indeed, plastic is found in most marine and terrestrial habitats, including bays, estuaries, coral reefs, lakes and the open oceans. (Rochman et al., 2014, Wright et al., 2013)

Even though the monitoring of plastic debris in the ocean began over 40 years ago, volumes are difficult to estimate as conditions vary across different bodies of water and over time. However, it is known that while marine debris[2] may be made up of a variety of materials, including glass, rubber and Styrofoam, the majority of it (60% to 80%) is plastic. (EPA, 2011)

Plastic pollution has two major sources, 80% is estimated to come from land and 20% from shipping, and is most commonly the result of the improper disposal of single use plastics and manufacturing materials (Allsopp, Walters, Santillo, & Johnston, 2000; D.K.A. Barnes et al., 2009). Plastic enters the marine environment via runoff, rivers, beach litter, lost cargo, direct dumping, and episodic events. The ocean is downhill from everywhere; therefore, plastic waste can be washed down streams and rivers from mountains, hills, and valleys. It can enter waterways via storm drains and runoff. Riverine transport contributes substantially to the proportion of land originating plastic pollution (Ryan, 2008).

Once plastic is in the ocean, wind, currents, and wave action disperse it both laterally and vertically through the water column. At the same time, currents and wind tend to concentrate debris into accumulation zones, often referred to as "garbage patches". This is a misleading term, because it evokes images of a large floating plastic island, when in reality much of the plastic is in small fragments mixed into the top layer of water (NOAA, 2014). Perhaps the most telling research and modeling of how plastics travel in the ocean is the Ocean Surface Current Simulator (OSCURS). To develop this model, tracking devices were released into the North Pacific and their movements observed over a 12-year period. OSCURS revealed that marine debris would eventually accumulate in the mid-latitudes after traveling for nearly six years around the North Pacific gyre (Arthur, 2009).

1.1.4 WHAT IS THE PROBLEM

Being lightweight, durable, strong, and inexpensive, the very properties that make plastic so useful are also responsible for its large negative impact on marine environments. Today, plastic marine debris is found in oceans and sediment worldwide and affects marine life along most of the food chain (Wright, Thompson, & Galloway, 2013).

Marine species can become entangled in larger debris, leading to "injury, illness, suffocation, starvation, and even death" (NOAA, 2014). Smaller fragments can be mistaken for food and eaten, which can cause malnutrition, blockage and death, as well as provide a pathway for transport of harmful chemicals up the food chain (Teuten, Rowland, Galloway, & Thompson, 2007). Ingestion of and entanglement in marine debris by marine animals has increased by 40% in the last decade (GEF, 2012). Furthermore, plastics can transport invasive species and toxic substances great distances. (D. K. A. Barnes & Fraser, 2003)

These adverse effects are concentrated in the convergence zones, where marine species tend to congregate and plastic debris tends to collect. (A more detailed review of the scope of the problem is presented in the following section.)

So far progress towards halting the rise of marine plastic pollution has been limited. Important short-term mitigation strategies include beach cleanup activities, which are performed on the shorelines of many countries, and ocean cleanups on coastal and oceanic regions where high levels of plastic pollution are affecting many species.

The long-term solution for this environmental issue involves decreasing plastic waste and creating better disposal practices on land and at sea, at an international level. MARPOL 73/78 is the international convention for the prevention of marine pollution, and prohibits the disposal of plastic from ships anywhere in the world's oceans. However, its enforcement varies globally, and clearly this regulation effects, at most, only 20% of all plastics entering the seas. Other measures to reduce the detritus of plastics in the environment are ordinances banning plastic single use items such as plastic bags and polystyrene[3].

Despite these efforts, the use of plastic worldwide continues to grow.

---

[3] Currently, 29 countries have plastic bag legislation, 14 U.S. States with at least one county ordinance and 26 States with proposed legislation. Hawaii is the first State to ban plastic bags countywide. (Duboise, 2014).

OBSERVATIONS OF OCEANIC PLASTIC POLLUTION

JULIA REISSER

Plastics are transported from populated areas to the oceans by rivers, the wind, tides, rainwater, storm drains, sewage disposal, and flood events. They can also reach the marine environment from boats and offshore installations. Surface net tows and visual observations from vessels show that although marine plastics are widespread across all oceans, their concentration levels vary. Hotspots occur close to populated coastal areas, in the Mediterranean Sea, and in offshore, subtropical areas associated with large-scale oceanic gyres.

Figure 1.3 Examples of surface nets used to sample plastics at the ocean surface. Left: Neuston Net; Right: Manta Net.

1.2.1 PLASTIC POLLUTION AS QUANTIFIED BY NET TOWS

Plastics that float in seawater will either be cast ashore by inshore currents and winds, or accumulate in convergence zones such as the five large-scale subtropical gyres (South and North Pacific, South and North Atlantic, and Indian). To gain a better understanding of the environmental hazards associated with marine plastic pollution, several studies have attempted to quantify marine plastic debris ranging from 0.001 millimeter to several meters in size (Hidalgo-Ruz, Gutow, Thompson, & Thiel, 2012; W. G. Pichel et al., 2012). Floating marine plastics have been quantified through visual counts from vessels and airplanes sampling (I. A. Hinojosa, M. M. Rivadeneira, & M. Thiel, 2011; Ivan A Hinojosa, Marcelo M Rivadeneira, & Martin Thiel, 2011; William G Pichel et al., 2007; W. G. Pichel et al., 2007; William G Pichel et al., 2012; W. G. Pichel et al., 2012), and by sampling devices that collect plastics from the oceans. Such instruments include Plankton Recorder Bottles (Ng and Obbard 2006), and zooplankton nets (Carpenter & Smith, 1972).

1.2.1.1 MARINE PLASTIC POLLUTION AS QUANTIFIED BY NET TOWS

Zooplankton nets, such as Neuston and Manta nets are by far the most common devices used to sample small plastics in the open sea (Hidalgo-Ruz et al., 2012). Towed from vessels, the surface nets systematically sample buoyant plastics at the air-seawater interface where floating plastics tend to gather (Kukulka et al., 2012). The main advantage of such nets is their capacity to concentrate buoyant material from a relatively large volume of water (Hidalgo-Ruz et al., 2012). After each net tow, the content captured by the net is carefully examined to separate plastics from biological material. Detected plastics are then counted and/or weighed and usually reported in pieces per area (Hidalgo-Ruz et al., 2012), although pieces per volume, mass per area, and mass per volume are also used.

Table 1.1 shows the findings of 17 empirical studies that conducted surface net tows, all reported in pieces per km². Fragmented pieces of larger plastics were by far the most common plastic type described in the "net tow" reports. Plastic pellets, the raw material used to make larger plastic items, were very common in reports from the 1970s and 1980s.

Marine plastics, mostly smaller than 5 mm, were widespread in the sampled marine regions and mean concentrations higher than 10,000 pieces per km² were found in the Mediterranean Sea and oceanic subtropical areas of the North Pacific, South Pacific, and North Atlantic (Figure 1.4) at the sea surface as estimated by net tows. Circle positions show approximate location of each measurement and letters next to circles indicate the study that reported each mean value: a)Carpenter and Smith 1972, b)Shaw 1977, c)Ryan 1988, d)Morris 1980b, e)Wilber 1987, f)Gregory 1990, g)Day et al., 1990, h)Moore et al., 2001, i) Law et al., 2010, j)Yamashita and Tanimura 2007, k)Collignon et al., 2012, l)Van Cauwenberghe et al., 2013a, m) Eriksen et al., 2013, n)Reisser et al., 2013b, o)Reisser et al., 2013a, p)Zhou et al., 2011, q)Dufault and Whitehead 1994.).

At the present, several gaps exist in the global dataset, particularly in the Indian Ocean. However, this is likely to decrease in the near future, as some studies on global observations of marine plastic debris collected by net tows are currently being conducted. Taking into account the findings of such observations and the global models of plastic dispersal (Lebreton, Greer, & Borrero, 2012; Maximenko, Hafner, & Niiler, 2012; van Sebille, England, & Froyland, 2012), it can be concluded that small marine plastics are concentrated over large subtropical areas of the oceans, i.e., oceanic gyres, as well as in the Mediterranean Sea.

REFERENCE	YEARS OF SAMPLING
Carpenter and Smith 1972	1971
Shaw 1977	1974-75
Shaw 1977	1974-75
Ryan 1988	1977-78
Morris 1980	1979
Wilber 1987	1984
Wilber 1987	1984
Wilber 1987	1984
Wilber 1987	1984
Gregory 1990	1984
Gregory 1990	1984
Gregory 1990	1985-88
Day et al., 1990	1985-88
Day et al., 1990	1985-88
Day et al., 1990	1985-88
Day et al., 1990	1985-88
Dufault and Whitehead 1994	1990
Moore et al., 2001	1999
Law et al., 2010	1986-2008
Law et al., 2010	1986-2008
Law et al., 2010	1986-2008
Yamashita et al., 2007	2000-01
Zhou et al., 2011	2009-10
Collignon et al., 2012	2010
Van Cauwenberghe et al. 2013	2011
Eriksen et al., 2013	2011
Reisser et al., 2013a,b	2011-12
Reisser et al., 2013a,b	2011-12
Reisser et al., 2013a,b	2011-12
Reisser et al., 2013a,b,c	2011-13

MARINE REGION	CS PIECES PER KM²	SAMPLING DETAILS PROVIDED
Sargasso Sea	3537	11 0.5–5.7h tows using a 1m diameter mouth, 0.33mm mesh net
Bering Sea	68	20 15min tows using a 0.4m wide mouth, 0.33mm mesh net
Gulf of Alaska	132	51 15min tows using a 0.4m wide mouth, 0.33mm mesh net
Eastern South Atlantic	3639	1224 2min net tows using a 1.57x.42m mouth, 0.36mm mesh Neuston Net
Eastern South Atlantic	1874	10 20–45min tows using a Neuston sledge (0.32mm mesh)
Sargasso Sea	11000	78 1 Nautical Mile tows using a 1x.5m mouth, 0.33 or 0.50mm mesh Neuston net
Sargasso Sea	2500	127 1 Nautical Mile tows using a 1x.5m mouth, 0.33 or 0.50mm mesh Neuston net
Caribbean Sea	1400	154 1 Nautical Mile tows using a 1x.5m mouth, 0.33 or 0.50mm mesh Neuston net
Gulf of Maine	700	72 1 Nautical Mile tows using a 1x.5m mouth, 0.33 or 0.50mm mesh Neuston net
North New Zealand	1000	"Neuston net tows"
South New Zealand	20	"Neuston net tows"
Bering Sea	100	66 10min tows using 1.3 m ring net or a Sameoto Neuston sampler (both 0.55 mm mesh)
Western North Pacific	12800	64 10min tows using 1.3 m ring net or a Sameoto Neuston sampler (both 0.55 mm mesh)
Western North Pacific	57000	60 10min tows using 1.3 m ring net or a Sameoto Neuston sampler (both 0.55 mm mesh)
Eastern North Pacific	61000	2 10 min tows using 1.3 m ring net or a Sameoto Neuston sampler (both 0.55 mm mesh)
Japanese waters	74700	11 10min tows using 1.3 m ring net or a Sameoto Neuston sampler (both 0.55 mm mesh)
Nova Scotia	67150	25 20 min tows using a 0.4x0.4 m mouth, 0.30 mm mesh net
Eastern North Pacific	334271	11 5-19 km tows using a 0.9x0.15 m Neuston net
Caribbean Sea	1414	30 min tows using a 1x.5 m mouth, 0.33 mm mesh Neuston net
Gulf of Maine	1534	30 min tows using a 1x.5 m mouth, 0.33 mm mesh Neuston net
Western North Atlantic	20328	30 min tows using a 1x.5 m mouth, 0.33 mm mesh Neuston net
Japanese waters	174000	76 10 min tows using a 0.5x.5 m mouth, 0.33 mm mesh net
South China Sea	3165	"Trawl net method"
Mediterranean Sea	116000	40 20 min tows using a .6x.2 m mouth, 0.33 mm mesh net
Belgian waters	3875	24 1km tows using a 2x1 m mouth, 1 mm mesh Neuston net
Eastern South Pacific	26898	48 60 min tows using a 0.61x0.16 mouth,0.33 mm mesh Nesuton net
Western South Pacific	4305	33 15 min. tows using a 1x.17 m mouth, 0.33 mm mesh Manta net
Southern Australia	5353	27 15 min. tows using a 1.2x.6 m mouth, 0.33 mm mesh Neuston net
Eastern Australia	6267	54 15 min. tows using a 1x.17 m mouth, 0.33 mm mesh Manta net
North-western Australia	7344	57 15 min. tows using a 1x.17 m mouth, 0.33 mm mesh Manta net

Table 1.1 Details of "net tow" studies reporting plastic concentrations (pieces per km²) at different marine regions of the world's ocean. This compiled data is presented in chronological order (sampling years; from older to newer) shows the findings of 17 empirical studies that conducted surface net tows4, all reported in pieces per km². Fragmented pieces of larger plastics were by far the most common plastic type described in the "net tow" reports. Plastic pellets, the raw material used to make larger plastic items, were very common in reports from the 1970s and 1980s.

REFERENCE	YEARS OF SAMPLING	MARINE REGION	CS PIECES PER KM'	SAMPLING DETAILS PROVIDED
Venrick et al. 1973	1972	Eastern North Pacific	2.24	Strip transect
Morris 1980	1979	Mediterranean Sea	1300	Strip Transect of 10m
Dixon and Dixon 1983	1982	North Sea	0.85	Strip Transect of 100m
Dahlberg and Day 1985	1984	Eastern North Pacific	3.15	Strip transect
Dahlberg and Day 1985	1984	Eastern North Pacific	0.1	Strip transect
Dahlberg and Day 1985	1984	Western North Pacific	3.15	Strip transect
Day and Shaw 1987	1985	Bering Sea	0.23	Strip transect of 50m
Day and Shaw 1987	1985	Eastern North Pacific	0.94	Strip transect of 50m
Day and Shaw 1987	1985	Eastern North Pacific	1.83	Strip transect of 50m
Ryan 1990	1987-88	Eastern South Atlantic	0.06	-
Dufault and Whitehead 1994	1990	New Scotia	21.3	Strip transect of 50m
Alani et al 2003	1997, 2000	Mediterranean Sea	8.8	Strip transect of 100m
Shiomoto and Kameda 2005	2000	Japanese waters	0.37	Strip transect of 100m
Barnes and Milner 2005	2002	Western South Atlantic	0	Strip transect
Barnes and Milner 2005	2002	Western South Atlantic	0.1	Strip transect
Barnes and Milner 2005	2002	Western South Atlantic	0.16	Strip transect
Barnes and Milner 2005	2002	Central South Atlantic	1.15	Strip transect
Barnes and Milner 2005	2002	Central South Atlantic	1.5	Strip transect
Barnes and Milner 2005	2002	Western South Atlantic	3	Strip transect
Barnes and Milner 2005	2002	Eastern North Atlantic	4.2	Strip transect
Barnes and Milner 2005	2002	Western South Atlantic	4.28	Strip transect
Barnes and Milner 2005	2002	Eastern North Atlantic	5.5	Strip transect
Barnes and Milner 2005	2002	Eastern North Atlantic	5.6	Strip transect
Thiel et al 2003	2002	Chilean waters	11.15	Strip Transect of 10m
Hinojosa and Thiel 2009	2002-05	Chilean waters	20	Strip transect of 20m
Thiel et al 2013	2002-05	Chilean waters	21.89	Strip Transect of 10m
Williams et al. 2011	2004-06	Inside Passage, Canada	1.48	Line Transect
Titmus and Hyrenbach 2011	2009	Eastern North Pacific	2.89	Line Transect
Titmus and Hyrenbach 2011	2009	Eastern North Pacific	4.97	Line Transect
Titmus and Hyrenbach 2011	2009	Eastern North Pacific	110.9	Line Transect
Titmus and Hyrenbach 2011	2009	Eastern North Pacific	111.66	Line Transect
Titmus and Hyrenbach 2011	2009	Eastern North Pacific	2330.2	Line Transect
Zhou et al 2011	2009-10	South China Sea	0.02	Strip transect
Reisser 2014	2011	Tasman Sea	0	Strip transect of 20m
Reisser 2014	2011	Southern Australia	2.3	Strip transect of 20m
Reisser 2014	2012	Fijian waters	17.16	Strip transect of 20m
Ryan 2013a	2012	Bay of Bengal	8.7	Strip transect of 50m
Ryan 2013a	2012	Strauts of Malacca	578	Strip transect of 50m
s.Ryan 2013b	2013	Eastern South Atlantic	2.9	Strip transect of 50m
Ryan 2013b	2013	South African waters	67	Strip transect of 50m

Table 1.2 Details of "visual surveys" studies reporting plastic concentrations (pieces per km²) at different marine regions of the world's ocean. This compiled data is presented in chronological order (sampling years; from older to newer).
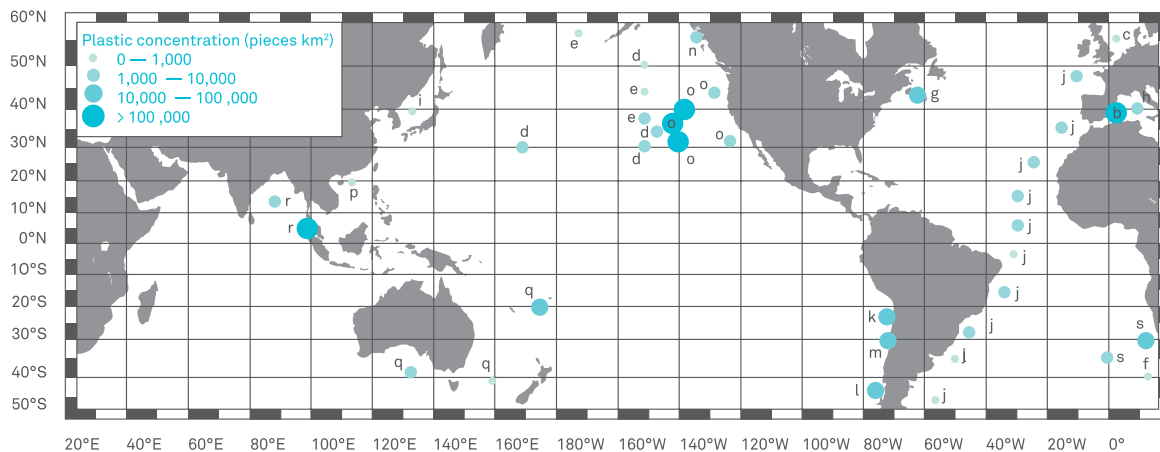
Figure 1.4 Mean plastic concentration (pieces per km²) at the sea surface as estimated by net tows. Circle positions show approximate location of each measurement and letters next to circles indicate the study that reported each mean value: a)Carpenter and Smith 1972, b)Shaw 1977, c)Ryan 1988, d)Morris 1980b, e)Wilber 1987, f)Gregory 1990, g)Day et al., 1990, h)Moore et al., 2001, i)Law et al., 2010, j) Yamashita and Tanimura 2007, k)Collignon et al., 2012, l)Van Cauwenberghe et al., 2013a, m)Eriksen et al., 2013, n)Reisser et al. 2013b, o) Reisser et al., 2013a, p)Zhou et al., 2011, q)Dufault and Whitehead 1994.

Figure 1.5 Mean plastic concentration (pieces per km²) at the sea surface as estimated by visual surveys. Circle positions show approx-imate location of each measurement and letters next to circles indicate the study that reported each mean value: a)Venrick et al., 1973, b)Morris 1980a, c)Dixon and Dixon 1983, d)Dahlberg and Day 1985, e)Day and Shaw 1987, f)Ryan 1990, g)Dufault and Whitehead 1994, h) Alani et al., 2003, i)Shiomoto and Kameda 2005, j)Barnes and Milner 2005, k)Thiel et al., 2003, l)Hinojosa and Thiel 2009, m)Thiel et al., 2013, n)Williams et al., 2011, o)Titmus and Hyrenbach 2011, p)Zhou et al., 2011, q)Reisser 2013b, r)Ryan 2013b, s)Ryan 2013a

1.2.2 PLASTIC POLLUTION AS QUANTIFIED BY VISUAL OBSERVATIONS

Counting floating objects while aboard vessels is the most common method for estimating the number of large plastics in surface waters. Generally, an observer stands on the flying bridge looking for floating objects as the ship moves through the area. Binoculars are sometimes used to confirm the characteristics of the sighted objects (e.g. material, size, color)..

Table 1.2 summarizes the findings of 19 empirical studies[5] that conducted visual surveys in the course of four decades. In these studies, plastic pollution levels have been reported in pieces per km². Many factors influence the reported means, such as the state of the sea, distance from which objects were observed, minimum plastic size and so forth. As such, comparison between studies should be done cautiously. Nevertheless, such pooled data may still adequately capture plastic pollution trends over large spatial scales.

Generally, centimeter-sized fragments resulting from the disintegration of larger plastic objects were the most common type of debris observed, particularly during offshore surveys (Dahlberg & R.H., 1985; Titmus & Hyrenbach, 2011; Venrick et al., 1973). Plastic items, such as bags, Styrofoam blocks, bottles, packaging, and fishing gear were also common, especially in coastal waters (Reisser, Shaw, et al., 2013; Thiel et al., 2003; Williams et al., 2011)

[5] Venrick et al., 1973; Morris 1980a; Dixon and Dixon 1983; Dahlberg and Day 1985; Day and Shaw 1987; Ryan 1990; Dufault and Whitehead 1994; Aliani et al., 2003; Thiel et al., 2003; Barnes and Milner 2005; Shiomoto and Kameda 2005; Hinojosa and Thiel 2009; Titmus and Hyrenbach 2011; Williams et al., 2011; Zhou et al., 2011; Reisser et al., 2013b; Ryan 2013a; Ryan 2013b; Thiel et al., 2013)

Large marine plastics were widespread in the sampled marine regions and mean concentrations higher than 10 plastics per km² occurred close to populated coastal areas (e.g. Indonesian, Fijian, Chilean, Canadian, and South African waters), oceanic subtropical waters of the North Pacific (North Pacific "Garbage Patch"), and the Mediterranean Sea (Figure 1.5 Mean plastic concentration (pieces per km²) at the sea surface as estimated by visual surveys.

Circle positions show approximate location of each measurement and letters next to circles indicate the study that reported each mean value: a)Venrick et al. 1973, b)Morris 1980a, c)Dixon and Dixon 1983, d)Dahlberg and Day 1985, e)Day and Shaw 1987, f)Ryan 1990, g)Dufault and Whitehead 1994, h)Alani et al. 2003, i)Shiomoto and Kameda 2005, j)Barnes and Milner 2005, k)Thiel et al., 2003, l) Hinojosa and Thiel 2009, m)Thiel et al., 2013, n)Williams et al., 2011, o)Titmus and Hyrenbach 2011, p)Zhou et al., 2011, q)Reisser 2013b, r)Ryan 2013b, s)Ryan 2013a).

Vast areas of the oceans are yet to be sampled and more data is required to better our understanding of specific regions where large-scale concentrations of plastic debris accumulate. Many of the plastic objects observed during visual surveys have a relatively large surface exposed to air. Therefore their movements and distribution are likely to be influenced not only by surface ocean currents, but also by wind (Richardson 1997). The development of global models accounting for such wind forces is pivotal to better foresee the distribution of large floating items at the oceans' surface (Kako, Isobe, Seino, & Kojima, 2010).

Studies performed at different marine regions reported distinct trends when examining temporal patterns of plastic pollution levels. For instance, in the North Pacific Gyre, plastic debris concentrations were estimated to have increased by two orders of magnitude between 1972-1987 and 1999-2012 (Goldstein, Rosenberg, & Cheng, 2012), while no trend was observed between 1986 and 2008 (Law et al., 2010).

PLASTIC IN THE MARINE ENVIRONMENT

There are three main types of impacts of marine plastic pollution: ecological, economic and eco-toxicological. First, plastics are light and durable, and discarded objects can thus easily be transported long distances from their source. It is therefore not uncommon for marine wildlife to come into contact with these materials, even in the most remote locations. The most visible ecological impact is entanglement, but ingestion and the transport of invasive species are also observed in studies.

Determining the full economic cost of marine litter is challenging. While the expense of fixing or replacing damaged equipment can be directly measured, it is more difficult to calculate all of the costs resulting from impaired ecosystem services.

Finally, plastic is made of essential polymers mixed with a complex blend of chemicals known as additives that can have serious impacts on the health of an organism. Moreover, plastics may also "adsorb" contaminants in the marine environment, such as insecticides and pesticides. For microplastics in particular, absorption of contaminants and the leaching of additives receive great attention since these particles are easily ingested and form a pathway for chemicals to enter an organism.

SPECIES GROUP	TOTAL NUMBER OF SPECIES WORLDWIDE	NUMBER & PERCENTAGE OF SPECIES WITH ENTANGLEMENT RECORDS	NUMBER & PERCENTAGE OF SPECIES WITH INGESTION RECORDS
SEA TURTLES	7	6 (86%)	6 (86%)
SEABIRDS	312	51 (16%)	111 (36%)
PENGUINS (SPHENISCIFORMSES)	16	6 (38%)	1 (6%)
GREBES (PODICIPEDIFORMES)	19	2 (10%)	0
ALBATROSSES, PETRELS, SHEARWATERS (PROCCLLARIIFORMES)	99	10 (10%)	62 (63%)
PELICANS, BOOBIES, GANNETS, CORMORANTS, FRIGATEBIRDS, TROPICBIRDS (PELICANIFORMS)	51	11 (22%)	8 (16%)
SHOREBIRDS, SKUAS, GULLS, TERNS, AUKS CHARADRIIFORMES)	122	22 (18%)	40 (33%)
OTHER BIRDS	-	5	0
MARINE MAMMALS	115	32 (28%)	26 (23%)
BALEEN WHALES (MYSTICETI)	10	6 (60%)	2 (20%)
TOOTHED WHALE (ODONTOCETI)	65	5 (8%)	21 (32%)
FUR SEALS & SEA LIONS (OTARIIDAE)	14	11 (79%)	1 (7%)
TRUE SEALS (PHOCIDAE)	19	8 (42%)	1 (5%)
MANATEES & DUGONGS (SIRENIA)	4	1 (25%)	1 (25%)
SEA OTTER (MUSTELLIDAE)	1	1 (100%)	0
FISH	-	34	33
CRUSTACEANS	-	8	0
SQUID	-	0	1
SPECIES TOTAL		**136**	**177**

Table 1.3 List of marine species with entanglement and ingestion records (Reprinted with permission from Laist 1997)

1.3.1 ECOLOGICAL IMPACTS
JORT HAMMER • STELLA DIAMANT

The properties that make plastics so desirable in the modern world can make them lethal for marine wildlife (Hammer, Kraak, & Parsons, 2012). Marine species can either get entangled in plastic nets, fishing wire or other objects, or ingest plastics when the material is mistaken for food. Laist et al., (1997) argues at least 267 marine species worldwide suffer from entanglement and ingestion of plastics. Moreover, the proliferation of floating plastic debris in the marine environment has caused an increase in marine rafting of many species, which has been identified as a threat (Barnes 2002).

1.3.1.1 ENTANGLEMENT

Entanglement can cause suffocation, strangulation or starvation of marine organisms (Allsopp et al., 2007). Entanglement itself is the most visible effect of plastics on organisms in the marine environment and thus ought to be easily observed and studied. However, entanglement of marine organisms often occurs in remote areas and is therefore hard to monitor. Laist et al., (1997) estimates that a total of 136 marine species are affected by entan-

glement in plastic debris (Table 1.3).

The "accidental" entanglement of fish species in plastic debris such as discarded fishing nets is hard to quantify since most organisms that die in the these nets do quickly degrade and leave no trace of their entanglement. Lost or discarded nets, i.e. ghost nets, continue to 'fish' for many years while never being emptied. Fish entangled in these nets die and attract bigger predators that in turn get stuck. The dead fish degenerate but the nets cannot biodegrade and thus will keep catching fish (UNEP, 2009). Another way to quantify accidental entanglement of fish in plastic debris is by-catch. While by-catch is mostly not caused by plastic debris, it can still emphasize the impact of discarded fishing nets on different fish species. For instance, between 1978 and 2000, 28,687 sharks were caught in nets that were used to protect people at popular swimming spots in South Africa. A small percentage of these sharks were also found with plastic strapping bands around their bodies (Cliff et al., 2002).

Entanglement in plastic debris also impacts bird species that forage in waters at great distances from the coast. These birds tend to dive for food and when diving six-pack rings and discarded fishing lines can easily be mistaken for a small fish or jellyfish (Allsopp et al., 2007). Just as marine mammals, birds need to surface every couple of minutes, making them susceptible to drowning. The gannet is a common victim. Studying their death in relation to plastic debris, researchers attributed 29 percent of total deaths on Helgoland, Germany (Schrey & Vauk, 1987), and 5.9 percent of deaths along the Dutch coast to entanglement (Camphuysen, 2001). These gannets most likely died from exhaustion caused by the effect of the entanglement while transmigrating along the Dutch

coast (Camphuysen 2001). According to Laist (1997) entanglement is most common for gannets and albatrosses. A more tropical species often affected by plastic debris is the sea turtle. Juvenile sea turtles are easily caught in discarded fishing nets. Larger marine animals are often capable of swimming with plastic debris attached to their fins. However, this affects their ability to feed and can result in starvation. Sea turtles are known to feed on jellyfish and easily mistake plastic bags for food. Orós et al., (2005) attributed 25 percent of observed sea turtle deaths in the Canary Islands to discarded fishing nets.

For marine mammals, drowning is the most common death caused by entanglement in plastic debris. While marine mammals such as seals, whales and dolphins can generally dive longer and deeper than most marine birds, they still need to surface once every 20 minutes and entanglement in plastic debris such as discarded fishing lines or nets can be fatal.

The pinniped is a marine mammal that often falls victim to entanglement. Due to their curious and playful nature, especially with young seals, they are quickly attracted to floating plastic debris. By swimming through or poking their heads trough loops, they get stuck, and removal is very difficult due to the backward direction of the seal's hair (Hammer et al., 2012). When the seal grows, the plastic tightens and can inhibit eating or even breathing. Unlike bigger organisms such as whales, seals are not strong enough to escape from submerged fishing nets when entangled. A seal in such a situation is not able to reach the surface and will drown. In the Dutch coastal waters, where visibility is limited due to sediments from nearby rivers, entanglement in fykes causes the death of

Figure 1.6 A stranded humpback whale on the Dutch coast (a). The whale was entangled in a nylon rope which had cut into its body (b-c-d) causing its death (Photos from Bruin (2004))

15 gray- and harbor-seals yearly (Ecomare, 2010).

Unlike cetaceans, most seals tend to stay relatively close to their haul-out site when foraging (McConnell et al., 1999). The material responsible for entanglement of seals therefore mostly originates from local fisheries. A study at Farallon Island, California, observed a total of 914 pinnipeds with indications of entanglement or implications from past entanglement. The majority of victims were California sea lions and these were mostly observed with neck constrictions. The plastic debris in this area primarily consisted of packaging material, and many pinnipeds were also seen with fishing hooks hanging from their jaws (Hanni and Pyle, 2000). The Farallon Islands are well-known fishing grounds and this is an example of the impact of debris originating from local activities. Page et al., (2004) studied the deaths of pinnipeds on the shores of Australia and New Zealand, and estimated that 1,478 fur seals and sea lions annually die from entanglement. In the Australian region entanglement was mostly caused by monofilament gillnet originating from shark fishery, while in New Zealand entanglement was often caused by packaging material and trawl net fragments from re-gional trawl fisheries (Page et al., 2004).

Besides pinnipeds, cetacean species have also been observed as affected by plastic debris. The larger size whale species often drag fishing gear along with them, which can cause strangulation and can affect the feeding ability of the animal, causing it to starve (Figure 1.6). Johnson et al (2005) observed in a study in the North Atlantic ocean that whales mostly get entangled around the mouth and tail area. The authors also found that the highest percentage of entangled gear (89 percent) originated from pots and gill nets. Such fishing gears are located on the seafloor and have surface buoys attached to them. Often large whale species become stuck between the buoy and pot structure, and drag the fishing gear away while getting entangled in the connection lines (Johnson et al. ,2005). Between 1983 and 2009, 83 cases of entangled whales were reported along the Atlantic coast of the USA and Canada (PCCS, 2010). Another case of entanglement was reported in 2004 when a humpback whale stranded on the Dutch coast. The whale was entangled in a nylon rope that was wrapped around the head, probably causing the death of the animal (Hammer et al., 2012).

Figure 1.7 The unaltered stomach contents of a dead albatross chick photographed on Midway Atoll National Wildlife Refuge in the Pacific in September 2009 (Photo taken by Chris Jordan, Source: Wikimedia Commons).

1.3.1.2 INGESTION

While plastic debris in the marine environment is easily detected in the case of entanglement, ingestion of plastics by marine organisms, although common, is difficult to observe. Ingestion primarily occurs when plastics are mistaken for food. The smaller fragments mostly pass through the gut without hurting the organism. However, when a larger fragment becomes trapped inside the stomach or digestive tract, it can cause damage or induce starvation.

Little is known about the impact of plastic ingestion among smaller fish species because it is hard to determine if ingestion is an important cause of mortality. Various larger fish species, however, have been known to ingest many items of plastic debris including plastic bottles, bags and caps (Randall, 1992). Studying flounders in the Bristol Channel, the authors observed plastic fragments in 21 percent of the examined organisms (Derraik ,2002). Along the coast of New England, USA, plastic fragments were found in 8 of 13 (62 percent) fish species that were examined (Derraik, 2002). Some larvae and small fish species in the North Pacific Subtropical Gyre were found to have plastic pellets or small fragments thereof in their guts. The ingestion rate of plastic particles by mesopelagic fish species in this area is estimated between 12,000 and 24,000 ton/year (Davison and Asch, 2011).

While it is difficult to monitor ingestion by fish species, this is generally easier in the case of marine birds. As chicks are fed with fish or other food from the open sea, monitoring their food intake may give an indication of plastic ingestion by certain species. Moreover, marine birds not only ingest plastic particles directly, but also receive a proportion through the guts of their pray (Hammer et al., 2012). A study from Robarts et al., (1995) in the Subarctic North Pacific Ocean, observed 4,417 plastic particles in the gut contents of 1,799 birds, 76% of which consisted of plastic pellets.

A marine bird species well known for being a good biomonitor for plastic ingestion is the northern fulmar. This planktivorous bird species feeds on plankton and small fish. Studying the rate of plastic ingestion by the northern fulmar in the Davis Strait, Canada, revealed 36 percent of the examined birds had at least one piece of plastic in their guts (Mallory, Roberston, & Moenting, 2006). Other studies on the North Pacific and the North Atlantic Ocean showed ingested plastic particles in 79% to 99% of the examined northern fulmars (Moser & David, 1992). The OSPAR commission, aiming to protect and conserve the North-East Atlantic Ocean, defined an acceptable ecological quality when no more than 10% of fulmars exceed

the weight of 0.1 g plastic in their stomach; (Hammer et al., 2012; OSPAR 2008). In their study of 1,295 dead fulmars that were washed ashore in het North Sea, Franeker et al. (2011) found that 58% of the birds exceeded the minimum of 0.1 g of plastic particles in their stomach. Another study on northern fulmars in the eastern North Pacific found plastic particles in 92.5% of the examined fulmars, with an average of 0.385 g per specimen (Avery-Gomm et al., 2012).

Another species infamous for their ingestion of plastic debris is the Laysan Albatross. These birds pass plastic debris to their chicks through regurgitation. A study including 251 Laysan Albatross chicks from Midway Atoll, USA, revealed that only six specimens did not contain plastic fragments in their guts. Most fragments, e.g., buttons, cigarette lighters, PVC fragments, light sticks and markers, were stuck in their digestive paths, causing starvation of the chicks (Auman, Ludwig, Giesy, & Colborn, 1997). Many bird species, including fulmars and albatrosses, are known to feed selectively on plastic fragments with a specific color or shape. Therefore, ingestion can often be directly related to their feeding habits and foraging techniques.

For sea turtles, plastic debris is a great concern as transparent plastic bags or sheets are easily mistaken for food (Bugoni, Krause, & Petry, 2001; Derraik, 2002; Oros et al., 2005).. Studying the green turtles in southern Brazil, researchers observed that 60% of the examined turtles had ingested plastic particles, and this had caused the death of 13 percent of the turtles (Bugoni et al., 2001). In a different study in the Mediterranean Sea, Tomás et al., (2002) found plastic debris in 60% of examined juvenile loggerhead turtles.

Plastic ingestion is less reported than plastic entanglement by pinnipeds since the former is harder to observe. Most ingestion studies involving pinnipeds show a relative small sample size (Baulch & Perry, 2014; Derraik, 2002). Furthermore, since pinnipeds are higher in the trophic food chain it is more difficult to distinguish direct ingestion from ingestion through the seal's pray. Eriksson and Burton (2003) examined the feces of fur seals at the Macquarie Island, Australia, and found a total of 164 plastic fragments in the excrement of 145 seals, i.e.more than one fragment per seal.

As is the case for pinnipeds, reports of plastic ingestion by cetaceans are very limited. Whale species that ingest plastic debris live in remote areas and may sink after they die. Moreover, many cetaceans are protected, which makes it difficult to study their plastic intake. The sample size of studies that focus on ingestion is mostly very small and limited to specimens washed ashore. A report from Texas, USA, concluded a sperm whale washed ashore had died from ingesting a corn chip bag, plastic sheets, a garbage can liner and a bread wrapper (Derraik ,2002). Similarly, Walker and Coe (1989) reported 30 p% of stranded toothed whale species died due to the ingestion of plastic debris, mostly plastic sheeting and bags. According to the authors the ingestion was primarily incidental and probably occurred while consuming benthic prey. Denuncio et al., (2011) studied the stomachs of 106 Franciscana dolphins in Argentina and found plastic debris in 28.1% of the specimens, mostly plastic packaging and fishing gear. An interesting conclusion of this study was the increase in ingested plastic debris by younger dolphins in their weaning phase, during which the mammals are yet to learn what is edible. A more recent study shows anthropogenic debris, mainly plastic, was found in at least 48 cetacean species (Baulch and Perry, 2014).

1.3.1.3 INVASIVE SPECIES

Natural debris, such as tree trunks or volcanic rocks, has always provided a way for organisms to be transported far from their original habitat. The introduction of floating plastic debris into the marine environment has caused an increase in marine rafting of many species and is considered a serious threat (Barnes 2002). Mussels and algae are often found as exotic species when attached to plastic fragments and washed ashore (Aliani and Molcard 2003; AMRF 2010; Goldstein et al., 2012).

Most natural debris is heavy and carried by currents. Wood also tends to sink after being exposed to seawater for a long time. In contrast, plastic debris is light and often not totally submerged. It can therefore easily be transported in any direction by the wind, which creates new paths for organisms to colonize other areas. Due to its non-biodegradable nature, plastic can be used as a raft for a very long time (Hammer et al., 2012), although biotic rafts like wood and kelp provide a food source for organisms, and increase their chance of survival (Bravo et al., 2011). Interestingly, a piece of floating debris was recently discovered at the Dutch coast which contained tropical biota, including self-fertilizing corals (Hoeksema et al., 2012).

Many different plastic substrates with various forms and surface topography are used as rafting materials by various organisms. It has been observed that the type of plastic and the form of the fragments strongly influence the kind of species that are harbored by the rafting material and also host different communities than natural substrates (Pister 2009; Bravo et al., 2011). Large amounts of plastic debris found ashore the Pacific Islands are a great concern in terms of invasive species due to the vulnerability of these relatively small ecosystems (McDermid and McMullen 2004; Goldstein et al., 2012).

1.3.2 ECONOMIC IMPACTS
PIERRE-LOUIS CHRISTIANE

Determining the full cost of marine litter is challenging. While the expense of fixing or replacing damaged equipment can be directly measured, it is more difficult to calculate all of the costs resulting from impaired ecosystem services (Mouat, et. al., 2010). And, according to UNEP Scientific and Technical Advisory Panels the true costs are likely underestimated due to a lack of available data. (STAP, 2011). Like many other types of pollution, the impact of plastic in the marine environment is a negative externality – the costs are not borne directly by plastic producers or consumers, but instead are transferred to unrelated third-parties.

1.3.2.1 DIRECT AND INDIRECT COSTS

The costs of marine litter can be categorized as direct or indirect. Direct effects are those that impact marine-related markets; in other words, where the market activity has an immediate connection to the marine environment. One example of a direct cost would be the fishing opportunities lost when gear must be cleared of, or is damaged by, plastic debris. Another is fish that cannot be sold because they were contaminated or killed by plastic waste. Fisheries can also experience a reduction in stock due to by-catch in lost nets, which can in turn lead to further costs caused by interference with reproduction (US EPA). The Scottish fishing fleet loses 5% of its total annual revenue, or $15 to $17 million as a consequence of marine litter (Mouat, et. al., 2010). In addition, rescue vessels are disabled due to fouled propellers, damaged drive shafts, or blocked engine intakes. In the waters of the United Kingdom alone, recovering these vessels cost $2.8 million in the year 2008, excluding related repairs (Kershaw, 2011). Additionally, there is the cost of accidents from SCUBA diving and snorkeling accidents caused by submerged debris; lost tourism revenue due to littered beaches, bays and diving areas; and the expense of cleaning up polluted areas.

Vessel damage and incidents	Cost of coastguard rescues	Statutory duty
Awards such as ISO 14001 and Golden Anchors	Shipping	Negative publicity
Removal of litter from harbours and marinas	Additionional dredging in harbours and marinas	

	Restricted catch due to litter in nets	
Contamination incidents	Sea fisheries	Lost and damaged fishing gear
Reduced earnings and lost fishing time	Vessel damage and staff downtime	

Figure 1.8 A visualization of impacts of plastic pollution to fisheries and shipping industries

The North Pacific gyre, which is the focus of this feasibility study, lies within the Asia-Pacific Economic Cooperation Region. Here, McIlgorm found: "From data on the marine economy, the damage from marine debris on the fishing, shipping and marine tourism sectors has a damage value of $1,265 billion (U.S.) per annum in the APEC region. The marine debris damage is estimated at US$364 million to the fishing industry, US$279 million to shipping and US$622 million to marine tourism." (McIlgorm, F., & J, 2009, p. 19).

The indirect effects of plastic pollution in the oceans include lost ecosystem functions and reduced biodiversity. For example, plastic marine debris that enters the food chain can indirectly result in increased human medical expenses. There are also costs tied to invasive species transported by plastic waste "rafts" (U.S. EPA). Persistent Organic Pollutants attach to floating plastic pellets and become part of the food chain when marine animals ingest them. Unfortunately, these costs are difficult to quantify. In strict economic terms, an incentive exists to implement an ocean cleanup strategy if the cost to do so is less than the direct and indirect costs combined. Using the precautionary principle, we believe it is preferable to develop such a solution rather than wait to measure and quantify the full economic impact later, when it could already be too late for the effort to succeed.

1.3.3 ECOTOXICOLOGICAL IMPACTS
JORT HAMMER • STELLA DIAMANT

Plastics are made of essential polymers mixed with a complex blend of chemicals known as additives. Additives have the ability to alter or improve the polymer´s properties. The essential polymers in plastics have a relatively large molecular structure and thus are often considered to be biochemically inert. Given their small molecular size, added chemicals are often not bound to the polymer and are therefore able to leach from the material. Since most of these additives are lipophilic, when ingested they adsorb to cell membranes and remain inside an organism rather than being excreted. These chemicals may cause biochemical interactions and affect the health of an organism.

Besides additives, plastics in the marine environment may also contain adsorbed chemicals from the surrounding water. Since plastics are hydrophobic, other hydrophobic (or lipophilic) chemicals have an affinity for the polymer. Most contaminants in the marine environment, such as insecticides and pesticides are hydrophobic and therefore tend to accumulate at plastic surfaces (Andrady 2011). For microplastics in particular, adsorption of contaminants and the leaching of additives receive great attention since these particles are easily ingested and form a pathway for chemicals to enter an organism.

1.3.3.1 TOXIC ADDITIVES IN PLASTIC

The use of common plastics in today's user products is not possible without the use of additives. Some polymers, such as polyvinyl chloride (PVC), are known to be very sensitive to thermal- and photo-degradation and cannot be used without the addition of stabilizer additives (Andrady 2003). UV stabilizers and antioxidants are additives that prevent polymers degrading due to sunlight. Stabilizers prevent UV rays degrading the polymer, as the rays may cause a free radical chain reaction, and antioxidants prevent oxidations caused by any free radical chain reactions that do occur. However, when ingested some of these additives are toxic to organisms (Lithner et al., 2012).

Flame-retardants are added to plastics to inhibit the production of flames in the material. The first generation of flame retardants, polychlorinated biphenyls (PCBs), were banned in 1977 after the compounds proved to be hazardous to organisms. Due to their hydrophobic characteristics they accumulate in fat when ingested. PCB's are found to damage the liver and stomach, and may induce acne-like skin conditions. Today, most flame-retardants are brominated flame retardant (BFRs). BFRs are not only very effective in preventing fires but they also have a minimal impact on a material's other properties. Their wide-ranging popularity poses a serious threat to the world's environment. BFRs are found in rivers and waters up to the arctic regions, and are reported in organisms such as the Canadian Arctic belugas (Tomy et al., 2008) and blue mussels (Gustafsson et al., 1999). Some chemicals related to BFRs are known reproductive and carcinogenic disruptors and can cause neurotoxicological effects on organisms (Darnerud 2003; Legler 2008).

A well-known constructive monomer that is used in plastics as a plasticizer, stabilizer and antioxidant is bisphenol A (BPA) (Yamamoto & Yasuhara 1999). Several studies have observed this compound to be leaching from PVC or other plastics into the aquatic environment (FDA 2010). BPA is a known endocrine disruptor – it closely mimics the structure of the hormone estradiol and is able to activate the same receptors.

Studies have linked prenatal exposure to physical and neurological effects (Okada et al., 2008; Rubin 2011). The leaching rate of BPA, and probably of other additives, is dependent on the temperature and may be higher in tropical regions (Sajiki & Yonekubo 2003).

Phthalates are a group of plasticizer chemicals that are added as an additive to polymers. Leaching of phthalates from the plastics causes the material to become more brittle, making it more susceptible to fragmentation. These chemicals are ubiquitous in the environment and in humans (Diamanti-Kandarakis 2009; Sax 2009). Phthalates can induce genetic aberrations (Teuten et al., 2009). Moreover, their adverse impacts in the developmental and reproduction phase of several fish, crustacean and amphibian species has been documented (Oehlmann et al., 2009).

1.3.3.2 ABSORPTION OF CONTAMINANTS BY PLASTIC

Most insecticides, pesticides and herbicides are hydrophobic compounds, which means they are repelled from water and often cluster together when in water. Plastics are more hydrophobic than most natural sediments and therefore hydrophobic contaminants (such as polyethylene, polypropylene, and PVC) tend to adsorb onto plastics (Teuten et al., 2009). Adsorption to plastics is primarily studied in relation to small fragments of plastics such as microplastics and plastic pellets. For these fragments the adsorption of several environmental contaminants has been observed.

Although banned more than 30 years ago, polychlorinated biphenyls (PCBs) – once used as coolants, insulating fluids and flame-retardants – are present in waters all over the world due to leakage, dumping, and leaching. PCB concentrations found adsorbed to plastic pellets along the coast of the USA, Japan and Europe, were shown to be much higher than anywhere else in the world. In these areas, PCB concentrations can be directly correlated to past use (Teuten et al., 2009).

Besides PCBs, plastic pellets are also able to adsorb other contaminants including hexachlorocyclohexane (HCH), dichloride diphenyl trichlorethane (DDT), and aromatic hydrocarbons (PAHs) (Teuten et al., 2009). Rios et al., (2007), found the presence of PCBs in 50 percent of the floating marine plastic debris studied in the North Pacific Gyre, pesticides (DDT and its metabolites) in 40 percent, and PAHs in nearly 80 percent of the fragments. The plastic was mostly made of polyethylene and remained on or near the ocean surface. In another study by Van et al., (2012), PCBs, DDTs, PAHs and Chlordane were found on plastic debris collected from Californian beaches. The observed PAH concentrations on polystyrene foam in this study were much greater than for other persistent organic pollutants (POPs). The authors suggest that PAHs may be a byproduct, produced during the production of PS foam, since pre-production pellets of PS did not show such high concentrations of PAHs. This means that it is possible that some plastics may also be a source of PAHs in the environment.

Adsorption of contaminants seems to be different for different plastic materials. For example, Mato et al., (2001) found polyethylene pellets adsorb four times more PCBs than polypropylene pellets. A recent study into the adsorption of different contaminants onto different plastic materials showed that high- and low- density polyethylene (HDPE and LDPE), and polypropylene (PP) contained much greater concentrations of PAHs and PCBs than plastics like polyethylene terephthalate (PET) and PVC (Rochman et al., 2013).

Thus, since the concentration in the water is usually too low to be measured directly, plastic pellets can function as a solid-phase extraction substrate for contaminants, and can be used as a cheap and fast sampling approach to determine contamination in coastal areas (IPW 2010).

1.3.3.3 TRANSFER OF CONTAMINANTS TO ORGANISMS

As previously explained, contaminants such as PCBs, DDTs, and PAHs have an affinity for hydrophobic plastic material and adsorb onto their surface rather than remain in the water. However, when plastic fragments are ingested by organisms and end up in the digestive tract, this change in environmental conditions may cause the contaminants to desorb from the plastic material and accumulate in tissue or blood.

The concentration of these contaminants may increase with progression through a food web, also referred to as bioaccumulation. Organisms from a higher trophic level are exposed to enriched concentrations of contaminants via their prey (Hammer et al., 2012). Although not all contaminants accumulate through the food web at the same rate (biomagnification), many compounds are found in marine organisms at high trophic levels (De Laender et al., 2011). A few studies have shown a positive correlation between the concentrations of PCBs found in streaked shearwaters and the ingestion of plastic fragments (Tanaka et al., 2013). Browne et al., (2013) found that microplastics, when ingested by worms living in marine sediments, can cause an increase in concentration of additives and adsorbed contaminants in the organisms. However, some additives may be more problematic than adsorbed contaminants and at times leach at a higher rate than adsorbed chemicals desorb from plastic (Browne et al., 2013; Teuten et al., 2009). Another study concluded that fish, exposed to a mixture of polyethylene with contaminants adsorbed from the marine environment, bioaccumulate these chemicals and suffer liver toxicity and pathology (Rochman et al., 2013).

While the previous studies contain evidence that contaminants and additives have the ability to indeed desorb and leach from plastics into organisms, the overall magnitude of the effects is reported to be fairly low and may not be relevant from a risk assessment perspective (Koelmans et al., 2013). However, more research on this topic is needed as there is little known about the impact on organisms higher in the food chain and the susceptibility to biomagnification. Contaminants are transferred within food webs over the world and the oceans are often a sinkhole for dumped and leached pollutants, which makes the marine food web especially vulnerable.

Many mammals, such as polar bears, dolphins, seals and humans, are at the top of the marine food chain and therefore susceptible to pollutants that have accumulated through organisms in the marine food web. Several studies observed the transfer of contaminants form seafood to humans. Mezzetta et al., (2011) investigated concentrations of dioxin-like PCBs in fish found on an Italian fish market and observed the overall concentrations to be relatively low (meaning, under acceptable concentrations) for most species. However, concentrations found in eel and few other species exceeded the limit. This may be related to the fact that eels tend to live in sediments on the seafloor, where hydrophobic pollutants are more present than in the water phase. In a study of the relation between seafood and infant size at birth, it was observed that higher maternal intake of canned tuna and crustaceans could be associated with increased risk of a small size for gestational age births (Andrady et al., 1998; Mendez et al., 2010). Some population groups regularly consume high quantities of certain fish species and this could significantly impact their health due to intake of contaminants (Bocio et al. 2007). However, total human exposure is difficult to measure since data concerning levels of contaminants in marine organisms is very specific to region or country and varies by the way food is prepared.

ARGUMENTS FOR A CLEANUP

SEBASTIAAN VAN SCHIE • WOUTER JANSEN • KATHLEEN LAURA STACK • JAN DE SONNEVILLE • BOYAN SLAT

The global general public is increasingly aware of the problem of marine plastic pollution. Since the turn of the century, many initiatives aimed at helping address it, were set up or proposed by individuals, academics, NGO's, corporations, and governments. An overview of initiatives is shown in Table 1.4. Given that an estimated 8 million pieces of plastic enter the oceans each day (McIlgorm et al.,, 2008), preventing plastic from entering the oceans should be a top priority. This report shows what the costs of cleaning are when such prevention has failed and plastic waste has reached the North Pacific gyre, as it does today.

Plastic takes thousands of years to degrade (see Chapter 9), therefore plastic waste in the Ocean has a long time to cause harm if not cleaned up. Cleaning and prevention reinforce each other, as one without the other will not lead to a clean ocean in the foreseeable future.

To strengthen this argument, we examine next the increase of plastic consumption and marine plastic pollution, and natural plastic loss from the ocean gyres.

Measure	Examples
The introduction of alternatives to plastic	Bio-plastics
Prevention of pollution by producer	Nurdle spillage prevention (nurdles are pre-production micro-plastic pellets)
The reduction of the use of plastics through sustainable product design	Reusable or sustainable products, reduction in the amount of packaging
Prevention of pollution by consumer through legislation	Banning or increasing tax on high-risk products such as plastic bags or micro beads
Prevention of pollution by consumer through social change	Education, awareness
Prevention of pollution by improvement of collection infrastructure	Garbage cans, garbage collection, closed landfills
Adding value to plastic waste	Development of profitable recycling methods, deposits, post-consumer responsibility
Prevention of pollution entering the oceans	River interception techniques, filters in water treatment plants, beach cleanups
Collection of pollution from the oceans	The Ocean Cleanup

Table 1.4 An overview of proposed and implemented measures to help reduce the amount of plastic in the oceans through both prevention and extraction.

1.4.1 TRENDS IN PLASTIC USAGE

As discussed previously in this chapter, ever since the invention of the first plastics, a variety of new plastics have been formulated, each with its own unique properties. In the early days, plastic use was limited to luxury products. Nowadays, plastics are an indispensable part of society and are used in almost every industry imaginable. For a long time, plastics were thought to be an ideal material: able to be tailored to the specific needs of a specific application, relatively cheap to produce, and lightweight. As a result, plastic consumption has grown steadily, as illustrated in Figure 1.9. Currently, the greatest increase in yearly plastic consumption comes from developing economies where people are rapidly gaining more wealth and, in turn, increasing their consumption of plastic. In these areas, the waste collection infrastructure is less efficient than in for example European countries. (OECD, 2010)

One can also note that the total plastic consumption of Europe has been relatively stable the last couple of years. This is in contrast to the global (non-biodegradable) plastic production, which is still increasing steadily, despite the economic crisis of 2008.

Sampling plastic debris suggests that plastic debris concentrations have increased by two orders of magnitude between 1972-1987 and 1999-2012 in the North Pacific Gyre (Goldstein et al., 2012). During the same period the annual plastic production has increased six-fold, from roughly 50 to 300 million tonnes. This discrepancy can partly be explained by the time needed for the plastic debris to reach the gyre, as will be explained in more detail with plastic flow simulations in Chapter 2.7. This delay also means that a continuous rapid increase is expected in the years to come. In this respect, the trends in plastic production can serve as an indirect indicator of the release of plastic into the environment.

1950	1976	1989	2002	2009	2010	2011	2012
1,7	47	99	204	250	270	280	288
0,35	19,8	27,4	56,1	55	57	58	57

Mtonne

[Chart showing World plastics productions and European plastics productions from 1950 to 2020, with Mtonne on the y-axis ranging from 50 to 300 and Year on the x-axis]
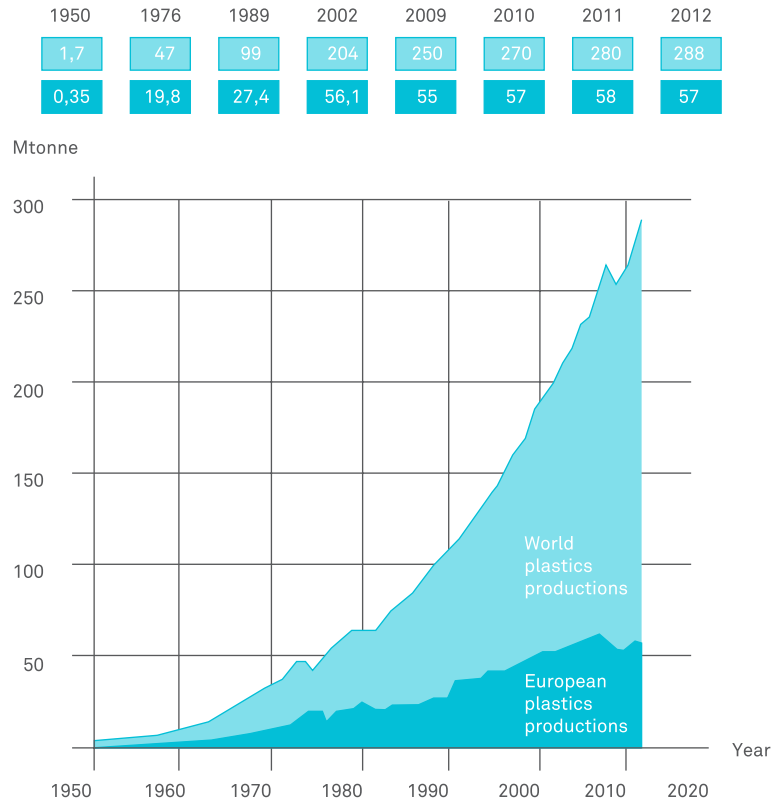
Figure 1.9 The amount of plastic production for each year, both for Europe and worldwide (PlasticsEurope, 2013)

1.4.2 NATURAL PLASTIC LOSS FROM THE GYRES

There are several ways for plastic to escape from the subtropical gyres, including A) sinking (due to a loss of buoyancy, either because of biofouling, or caused by a reduction in particle size), B) biodegradation, C) ingestion by organisms and D) the natural loss of plastics onto coastlines.

There is some evidence for biodegradation by micro-organisms living on the surface of plastic debris, but this is yet to be confirmed and quantified (Zettler et al., 2013). When organisms like fish and birds ingest plastic, die and sink, the organism sinks (Pierce 2004) and thereby removes plastic from the surface. The ingestion rate of plastic by lantern fish in the North Pacific gyre has, for example, been estimated to be between 12 and 24 kilotons annually (Davidson and Asch 2011). However, no studies have yet attempted to quantify the natural loss of plastics through beaching. Our simulations confirm this effect, however the software is currently not able to reliably quantify the amounts.

It is likely, however, that the natural plastic loss from the North Pacific Gyre due to beaching is low. One explanation could be the lack of landmass in the area of highest concentration, the Hawaiian Islands being the closest. In waters just south of the island of Hawaii island, of the 33 net tows taken between 18-19° N, 150-160° W by K.L. Law et al., only one (3%) indicated a concentration of greater than 100,000 parts per km², while in the center of the high concentration area (between 30-35° N, 135-145° W) 25 out of 42 tows (60%) contained concentrations of greater than 100,000 parts per km² (Law et al., 2014).

1.4.3 MORAL ARGUMENTS

Besides the technical challenges (outlined in Chapter 1.5), some have argued that cleanup propositions are incompatible with other (primarily prevention) efforts, and thereby only serve as a distraction, and perhaps even as a reason to continue polluting.

There are several arguments against such criticisms of moral hazard:

Firstly, cleanup concepts have demonstrated the potential to attract attention, including the concept that is the subject of this feasibility study as introduced in Chapter 1.7 (Slat, 2012). If used wisely, this attention could not only emphasize the scale and urgency of the plastic pollution problem, but can also be used to help preventive measures, by stressing the importance of closing the tap first. And since the cost of preventing and cleaning plastic pollution on land is likely to be lower than offshore, this could also quantify the financial incentive for improved pollution control on land.

Secondly, a cleanup would be able to make the problem more visible. Although the numbers (by both mass and particle count) are large, it is hard to visualize, because the debris is dispersed over a vast area, with concentrations ranging from 0.01 to 10 parts per m³ (Goldstein et al., 2013). However, by concentrating and/or extracting a significant percentage of plastic from the oceans, coverage of this collection process could help in raising awareness about the problem as well.

Finally, a cleanup project contributes to the scientific understanding of the oceanic plastic pollution problem. Both the research in the R&D phases before a cleanup as well as a large-scale cleanup itself would provide much better insights into the amount and composition of plastics in the oceans. Most recently for example, it has been recommended reducing the uncertainties of debris mass estimates "by developing large-scale, cost-effective techniques to monitor subtropical gyre accumulation zones that are millions of square kilometers in size" (Law et al., 2014).

1.4.4 CONCLUSIONS

Many initiatives have been set up with the aim of trying to combat plastic pollution (especially in the past 10-15 years), ranging from prevention to extraction. Although not completely understood, the currently known sinks of the North Pacific gyre are likely to be small, and a large and continuous increase in plastic pollution has been measured over time (see Chapter 2). Given the implications for ecology, economics and human health as explained in Chapter 1.3, a cleanup would reduce these negative impacts. Based on the counterarguments outlined in 1.4.3 above, the statement that the solution to the plastic pollution problem should be either prevention or cleanup is not valid. A cleanup could also benefit preventive efforts as well. Hence, the effect of a combination of both prevention and cleanup will be greater than either of them alone, and this combination is the only solution that could reduce the amount of plastic pollution in the oceans within our lifetimes.

CHAPTER 1.5

CLEANUP CHALLENGES

SEBASTIAAN VAN SCHIE • KATHLEEN LAURA STACK

BOYAN SLAT

1.5.1 SCALE AND DEPTH

An ocean clean-up attempt may seem daunting simply due to scale. The amount of plastic in the oceans is enormous, estimated in the order of millions of tons (Clark, 1997). Yet, with the oceans as vast as they are, this can be difficult to accurately measure. Most plastic marine debris has accumulated in the five oceanic gyres (Moore et al., 2001), with one the size of an entire continent. A successful clean-up concept must be effective at this immense scale.

Another complication is the local depth of the sea. For example, the depth at the North Pacific Gyre is approximately 5,000 meters, as shown in Figure 1.10. This presents a challenge to any clean-up concept that relies on moorings. Moorings have been placed at greater depths (National Data Buoy Center), but no large structures have been placed at depths greater than 2.5 km (Reuters, 2010).

1.5.2 PLASTIC SIZE AND DEPTH DISTRIBUTION

Plastic particles in the ocean can be quite small. Plastics released into the marine environment degrade over time, become brittle and break down into smaller and smaller pieces. Even particles too small to be seen by the naked eye continue to fragment (Andrady, 2011). There are also medium sized pieces and large debris such as ghost nets (Pichel, 2007). Thus, a successful clean-up scheme must be able to deal with a wide range of debris sizes.

There is little quantitative data available on the vertical distribution of plastic particles in the gyres, but these particles are generally considered to be 'neustonic' (i.e. present in the top layer of the sea). The distribution may vary though, due to factors such as local wind speeds (Kukulka et al., 2012), suggesting that turbulent water movement can mix the plastics below the surface. Any potential clean-up system must account for uncertain plastic distributions in varying weather conditions.

1.5.3 DESTRUCTIVE MARINE ENVIRONMENT

The environment in any of the oceanic gyres presents many challenges for any potential clean-up concept. The structure must continue to function despite strong currents, waves, and winds, while avoiding wear and tear from various abiotic and biotic factors.

Currents will place heavy loads on any system designed to resist it. Winds can be high in the open ocean and have a tendency to blow in a direction not parallel to the currents. Perpetual wave motion will keep all components moving, especially stressing joints., see Figure 1.11.

These mechanical complications can drastically increase during storms, during which 13 to 14 meter waves can be reasonably expected (Met Office, 2010), putting heavy strain on any ocean structure. If the structure remains at sea during a 100-year storm, it will experience waves, winds, and currents five to ten times greater than their average values (See Chapter 2.6 – Wave, wind, and current data). An effective clean-up concept must be able to withstand or avoid such storms.

In addition to the stresses and strains from these mechanical factors, the structure must also be designed to resist degradation of its exterior from solar radiation and saline water corrosion, among other things. The build-up of underwater organisms on the structure, also known as bio fouling, can exacerbate). Bio-fouling is problematic not only because it degrades the structure but also because it alters the flow dynamics around it.

Elevation, m
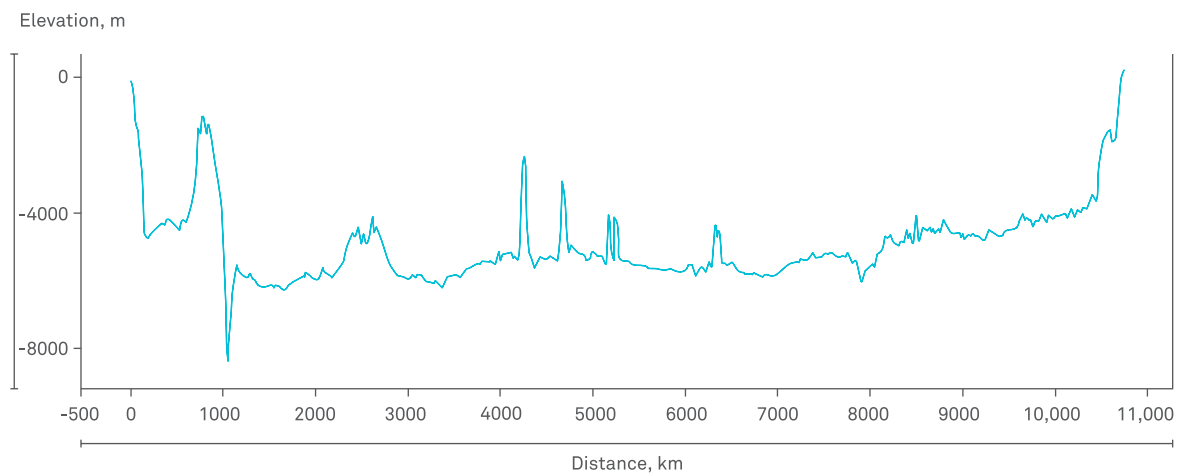
Figure 1.10 Ocean depths across the North Pacific along the latitude of 31 degrees North, ranging from 0 m to 9000 m (source: GeoMa-pApp)
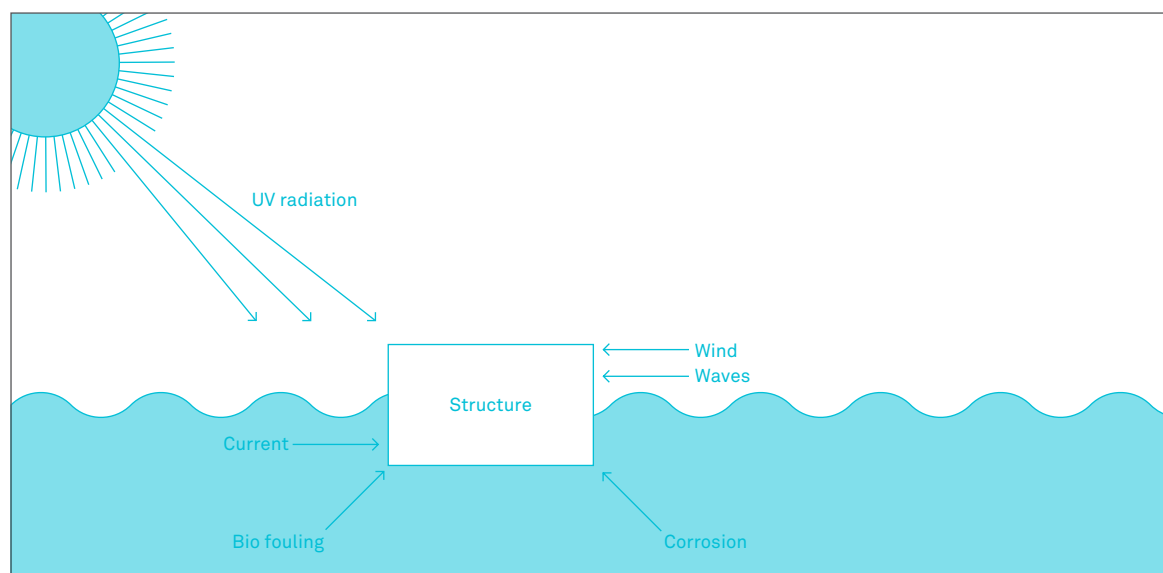
Figure 1.11 Diagram showing the different environmental influences on a structure floating on the sea surface.

1.5.4 ENVIRONMENTAL IMPACT

Any ocean clean-up project should be designed to avoid harming the environment while in the process of cleaning it. Care must be taken to avoid by-catch of marine life, as well as minimize the carbon footprint of the construction, use, and eventual deconstruction of the structure.

By-catch is an enormous problem for filtration-based ocean clean-up strategies. A device which filters water to extract plastics in the commonly reported size range of 0.3 to 4.7 mm (Moore et al., 2001) would also filter out similarly-sized plankton species. Other species remain at risk of becoming by-catch with a larger net-based solution. The sea creatures can be attracted to the organisms growing on an ocean structure, as well as to the plastics themselves, raising the incidence of by-catch.

An ocean clean-up project is created primarily for its environmental benefit, and for that reason, negative environmental consequences of its production and operations should be minimized. Sustainable fabrication of the components and environmentally friendly deconstruction at the end of the functional lifespan should be planned. Consideration should also be given to environmental impact during operation, including minimizing the production of greenhouse gases in powering the system and transporting collected plastic. Once the plastic has been removed from the ocean something must be done with it; if it is not burned on the platform, it will be brought to land, where it still must be processed or stored.

1.5.5 LEGAL CHALLENGES

Aside from mechanical and environmental challenges, there are many legal questions to be considered. A more detailed discussion of the legal issues identified thus far can be found in Chapter 8. The following is a brief review. Resolution of these legal ambiguities could be key to a successful clean-up effort.

To start, there is possibility that sea traffic could be obstructed by such an operation. It would be vital to know whether international laws exist concerning the blockage of sea lanes that could complicate or block an ocean clean-up effort. There is also the matter of the legal designation of a platform located in the ocean, with uncertainty as to whether it should be registered as a ship under a nation-state flag, or if some other designation is more appropriate.

Another question is one of ownership. Who owns the plastic that would be collected? Do the customary rules of salvage apply? Once collected, the plastic material must be transported to shore. It should be understood which – if any - international and bilateral treaties apply as the material passes from international into territorial waters. And once imported to land, would it be considered a hazardous material? Would it be taxable as an imported good? What other national laws would apply?

Out at sea, there is a possibility of by-catch – or the unintentional capture of marine species – by the system. National and international laws and treaties exist to protect threatened and endangered species, such as sea turtles. It is important to know which of these apply in the case by-catch does occur.

ALTERNATIVE CLEANUP CONCEPTS

SEBASTIAAN VAN SCHIE • KATHLEEN LAURA STACK
BOYAN SLAT

Since the marine plastic pollution problem has become known, many possible solutions have been proposed and this section will discuss some of these. The concepts can be broadly divided into three technical based sections: autonomous drone-based systems, ship or vessel based systems and 'floating islands'. Each type's conceptual strengths and weaknesses will be assessed separately in the following sections, although the reader should be reminded that each of these theoretical concepts are still in their preliminary design phases.

1.6.1 DRONE-BASED CONCEPTS

Several ocean cleanup concepts employ the use of automated drones to remove ocean plastics, including Drone 1-001-1 proposed by Elie Ahovi, the Oceanic Cleaning System by Erik Borg, Cesar Harada's Project Protei, the Pod Project by the Abundant Seas Foundation and Project Floating Horizon, by Ralph Schneider. Renderings of some of these concepts mentioned are shown in Figure 1.12.

The general premise behind a drone-based concept is to deploy a large number of small floating or neutrally buoyant vehicles to collect plastic, which would eventually return to a central mother-ship. The drones would be equipped with batteries or photovoltaic (PV) systems as a power supply and would be able to operate autonomously. Using a propulsion system, the drones would move through the water and collect plastic that they encounter. When full they would either return to the mother-ship or be picked up by a maintenance vessel, where repairs could take place and batteries could be recharged or replaced.

An advantage to this method over vessel-based concepts is the drones' deployment flexibility. If there is a location where the concentration of plastic is very high, it is easy to move drones accordingly. Furthermore, in the case of a breakdown impact to the system as a whole may be minimal and small units may be relatively inexpensive to replace. As a whole, operational expenditures could be lower than vessel-based concepts, with the potential for lower fuel and employment costs. While the drones could be fitted with small-meshed nets, enabling them to catch small particles. These may present an advantage over conventional nets that pose a risk to sea life through entanglement.

However, there are also potential problems. First of all if the drones were required to travel at a high speed in response to currents etc., the combination of a high drag caused by fine-meshed nets and the limited energy capacity of batteries would likely require many pit-stops or other charging moments. Furthermore, both the drones and the mother-ship would have a limited capacity, requiring the ship to frequently travel great distances between the cleanup location and land to empty its buffer. Due to the small span of each drone, it is likely a certain area will be covered more than once, reducing field efficiency. It is also unknown how the small drones would be able to deal with large debris, like parts of vessels or ghost nets. Most importantly however, the areas in which plastic tends to concentrate are large, and, in conjunction with the above impediments, covering these areas would likely require a combination of many units and hundreds to thousands of years (Charles Moore, 2012)
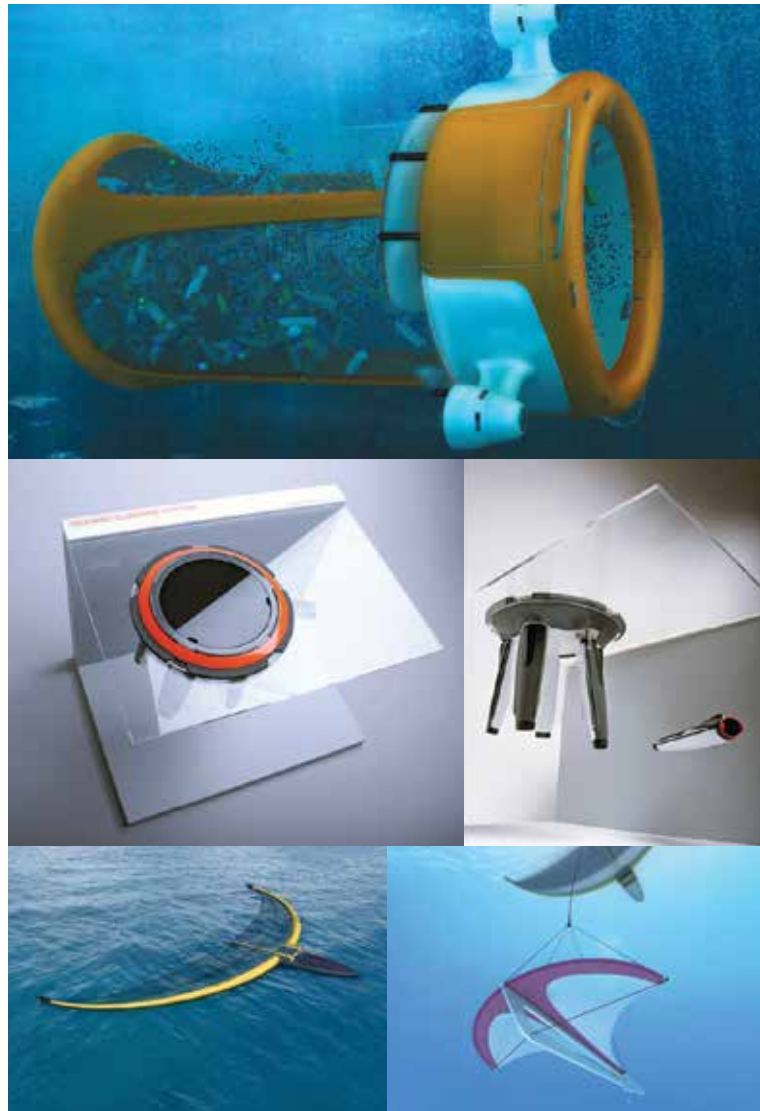
Figure 1.12 Drone concept renderings, from top to bottom: Drone 1-001-1 of Elie Ahovi (Elie Ahovi, 2013), Oceanic Cleaning System of Erik Borg (Erik Borg, 2010) and Project Floating Horizon of Ralph Schneider (Ralph Schneider, 2012)

1.6.2 VESSEL-BASED CONCEPTS

Ship-based solutions, whether sailing or industrial vessels, have been frequently proposed. This is generally a more conservative approach to the issue at hand as it mostly uses existing technology. Variations commonly include using modified ships fitted with nets or other extraction equipment. Examples of this are Project Kaisei, Bo Atkinson's Plastic Baler, the Clean Oceans Project and Saraswater. Generally, the cleaning method consists of sailing through the oceanic gyres and using nets attached to the ships to skim the surface for plastics, just like a fishing vessel, but often with a finer mesh.
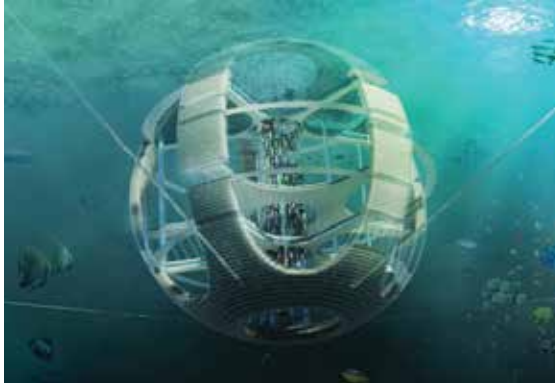
Figure 1.13 The Plastic Fish Tower as seen from under the sea surface (eVolo, 2012)

Figure 1.14 "Seawer: The Garbage-Seascraper" is the name of another floating skyscraper design filtering plastics (eVolo, 2014)

A major benefit to using ship-based concepts is that almost all the technology involved already exists. This removes the need for extensive research in the field of engineering, which can cut pre-costs. Furthermore, the use of mass produced or second-hand vessels could also cut capital expenditures.

However, vessel-based cleaning concepts generally face the same challenges and risks as drone-based concepts. Again, problems of scale mean that either thousands of vessels or thousands of years (or a balance between the two) would be required. These concepts would have the added disadvantage that these vessels would need to be manned (for both practical and legal reasons) and would burn more fuel, increasing expenditure. Furthermore, these vessels would probably release atmospheric emissions, and hence the end net balance of environmental impacts must be considered. It is furthermore unlikely that small particles could be caught, due to the large drag force created by large area, fine-meshed nets.

1.6.3 FLOATING ISLANDS

The last, and most exotic, group of concepts consists of 'floating islands'. A further distinction between two types of proposals can be made here: 1) ideas of constructing floating skyscrapers with the added function of filtering the water for plastic, and 2) floating habitats created from ocean plastics itself. Examples of the floating skyscrapers are the Plastic Fish Tower (designed by Hongseop, Cho Hyunbeom, Yoon Sunhee and Yoon Hyungsoo), the Seawer: The Garbage-Seascraper (by Korean designer Sung Jin Cho), and Rudolph Eilander's Plastic Island. An example of the latter type is Ramon Knoester's Garbage Island.

Both the Plastic Fish Tower and the Seawer concepts plan to use an underwater superstructure, anchored to the seafloor. While not primarily designed to clean marine-borne plastics, the designers claim that this is also one of the possibilities of the concept. The 'seascrapers' would be like a small city at sea, providing living and leisure space.

Using plastics fished out of the ocean to build an artificial island has been proposed on multiple occasions. The potential advantage would be that there is no need to transport the captured plastics back to land. However, due to various environmental impacts, for example UV degradation, the plastics loose some of their material properties, potentially making it unsuitable for mechanical recycling. Moreover, an added challenge would be that the same degradation processes that once broke down the plastics would again be working on the 'island', potentially creating a source for more marine debris. Further still, compressing the plastic into a floating habitat is a way to deal with the plastics once it's out of the ocean, but it does not address the step of extracting the plastic from the ocean. No technical details of these concepts have been released, and their technical feasibility cannot be judged. Moreover, these structures face the same problem as drone-based and vessel-based concepts, as the area that would be covered is (almost) negligible compared to the area of the gyres.

1.6.4 COMPARISON OF CONCEPTS

As can be seen in the table below, there are a number of reasons that make the implementation of these concepts impractical. Most of these arguments stem from the fact that the gyres have a large surface area, and the plastic, even though it has been concentrated in these areas, is still dispersed. In terms of engineering, these devices would also have to overcome challenging offshore environments – structural details of these concepts have not been published. However, it is quite possible that active methods to remove plastic through drones and vessels may be more suitable (and commercially viable) for rivers and coastal areas, where several of these limiting factors are reduced.

	PROS	CONS
DRONES	+ units are inexpensive to replace + can potentially catch small particles + unmanned + deployment flexibility	- will take very long time - potential for by-catch - high operating expenditure - logistically impractical - low field efficiency - frequent pit-stop necessity likely - unable to catch very large debris

VESSELS	+ existing technology,
	   so low capital expenditures
		- will take very long time
		- potential for by-catch
		- atmospheric emissions
		- high operating expenditure
		- logistically impractical
		- low field efficiency
		- catching small particles unlikely
		   due to drag

FLOATING ISLANDS	+ cleaning plastic is often its secondary
	   goal, i.e. there is a different 'business plan'
	   involved
		- costs
		- similar challenges as vessel-based and
		   drone-based concepts, but technical
		   details to confirm this are unknown

Table 1.5 Comparison of plasting capturing methods

OUR CONCEPT

BOYAN SLAT • JAN DE SONNEVILLE

The Ocean Cleanup concept consists of an array of floating barriers (or booms) and platforms, moored to the seabed, where buoyant plastic particles can be caught, while neutrally buoyant marine organisms remain underneath the boom in the flow of water. Through this concept, plastic can efficiently be extracted from seawater in three phases. In the initial phase, the particles are caught in front of the boom, by rising from the main ocean flow into the almost stationary water in front of the booms. During the second phase, the particles accumulate while slowly progressing along the boom towards the platform, and new particles are continuously added to this stream. In the final phase, streams of particles from both sides of the array meet in front of the platform and the increased concentration allows for efficient collection. These three stages are explained in more detail below.
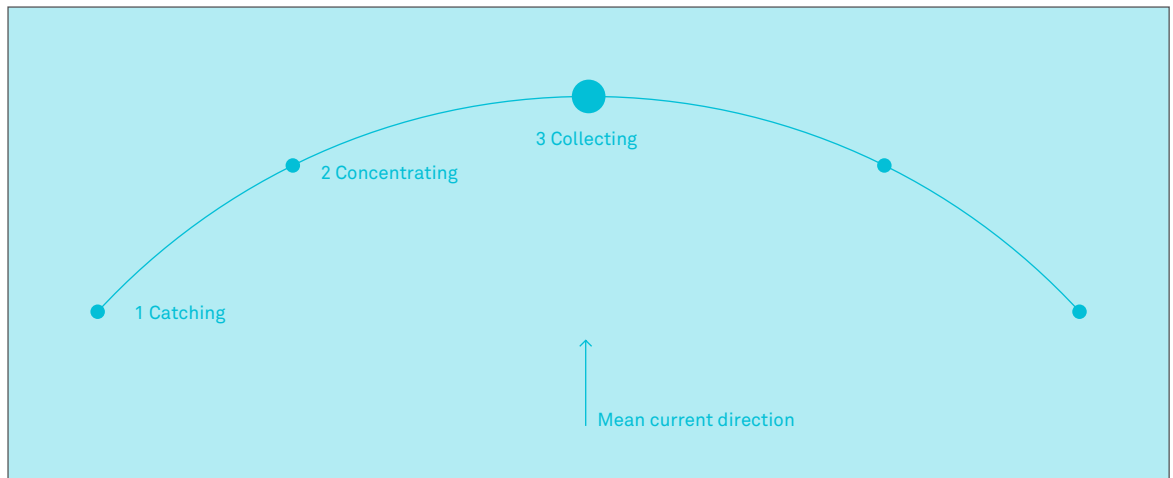
Figure 1.15 Simplified and schematic top view of an Ocean Cleanup Array. The line represents floating barriers, the small dots are buoys (where moorings attach), and the large dot represents the collection platform.
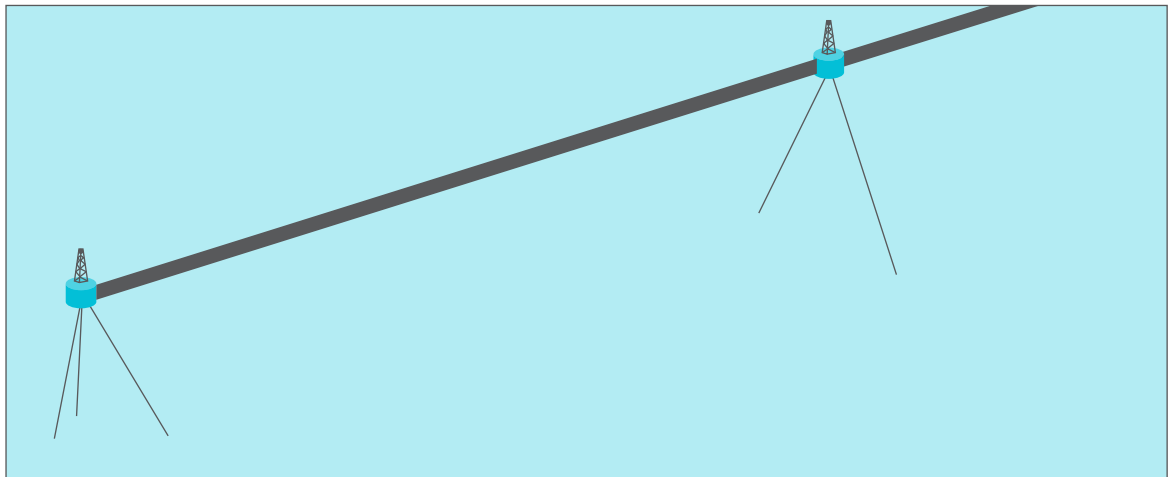
Figure 1.16 Schematic representation of two moorings, attached to buoys, between which booms are spanned.

1.7.1 THE ARRAY

The floating barrier spans across a hundred kilometers so that a vast area can be covered (see Figure 1.15). To ensure that marine plastic debris can be collected passively by using the natural rotational current of the gyre, a difference in velocity between the floating barriers and the water needs to be created. This will be achieved by fixing the array to the seabed, which also ensures that the loads on the floating barriers are transferred through these moorings.

Buoys will be used to compensate for the downward pull of the mooring lines, as shown in Figure 1.16. Because the mid-ocean depths can exceed 4,000 meters, large amount of lightweight fiber cables are required.

1.7.2 THE CATCHING PHASE

During the accumulation of plastics no nets are used in order to avoid entanglement of marine organisms. It is imperative to note that this concept is based on the notion that surface currents propel the plastic pollution towards the floating barrier. The upper part of the boom is designed in a way to keep the entire structure afloat and prevent over-topping of water and accompanying plastic debris. The lower part consists of a skirt that stretches several meters, catching near-surface plastic debris. Neutrally buoyant organisms are carried underneath the booms by the current, thus preventing by-catch, while positively buoyant plastic particles are separated from this flow by rising to the surface in front of the boom. Since the skirt is made of non-permeable material, the size of the plastic debris that can be captured is only limited by the particle's buoyancy force. Following this logic, it is likely that microplastics, i.e., particles smaller than 5 mm, may get caught.

1.7.3 THE CONCENTRATION PHASE

Arranging the booms in a V or U-shape with the opening against the water flow, allows a small force of the current to transport the debris towards a central collection point. While directly removing debris from the ocean could be considered inefficient due to the relatively low concentration of plastics and the vastness of the gyres, the accumulation of the particles along the booms results in an area of high concentration, from which debris can be removed more effectively.

1.7.4 THE COLLECTION PHASE

Plastic debris, accumulated at the center of the array in very high concentrations, can be extracted using conventional techniques including scoops, conveyor belts, pumps or similar techniques. It is important to highlight here that the Array is designed such that plankton will not be accumulated by it; this is also discussed and assessed within the report.

After removal from the ocean surface, the plastic debris arrives inside the platform where it is filtered out of the water. This will be done by allowing the polluted water to pass through a series of self-cleaning filter screens. Hereafter, the discharge fluid containing the smaller particles will run through a centrifugal separator, reducing the amount of water. The volume of the collected debris can be reduced by compressing and/or shredding, after which it can be stored internally (e.g. within a silo) or externally (e.g. a barge or vessel), before being transported to land. The platforms could be autonomous, operating without any personnel on board, and for extended periods through the employment of renewable energy sources. By separating the two actions of plastic collection and transportation to land, the removal of debris can continue unhindered, thereby increasing efficiency.
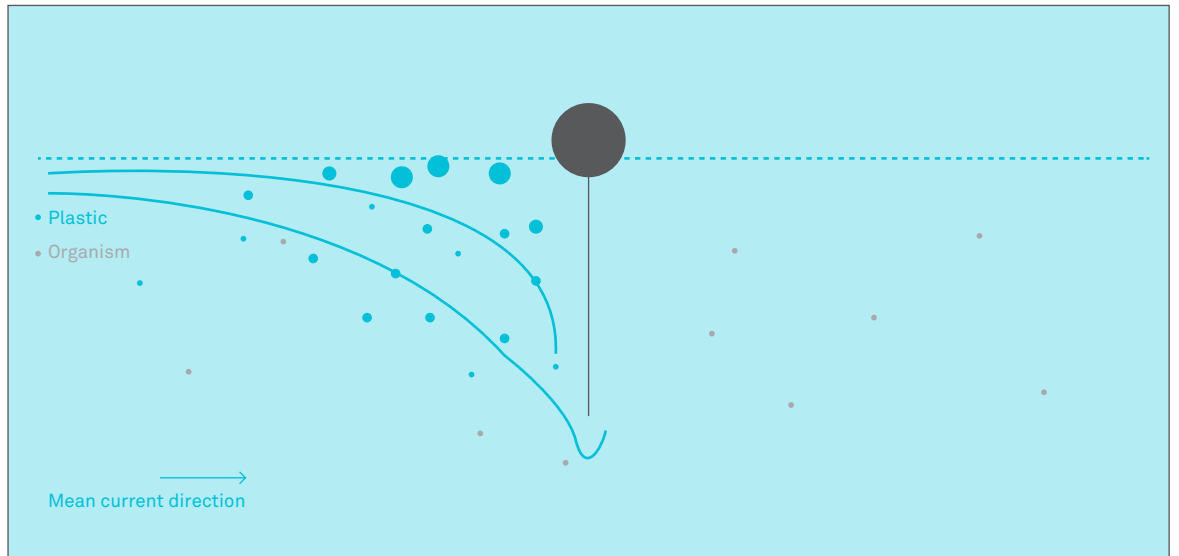
Figure 1.17 Simplified and schematic cross-section view of a floating barrier. The blue dots represent plastic particles, while the grey particles are organisms
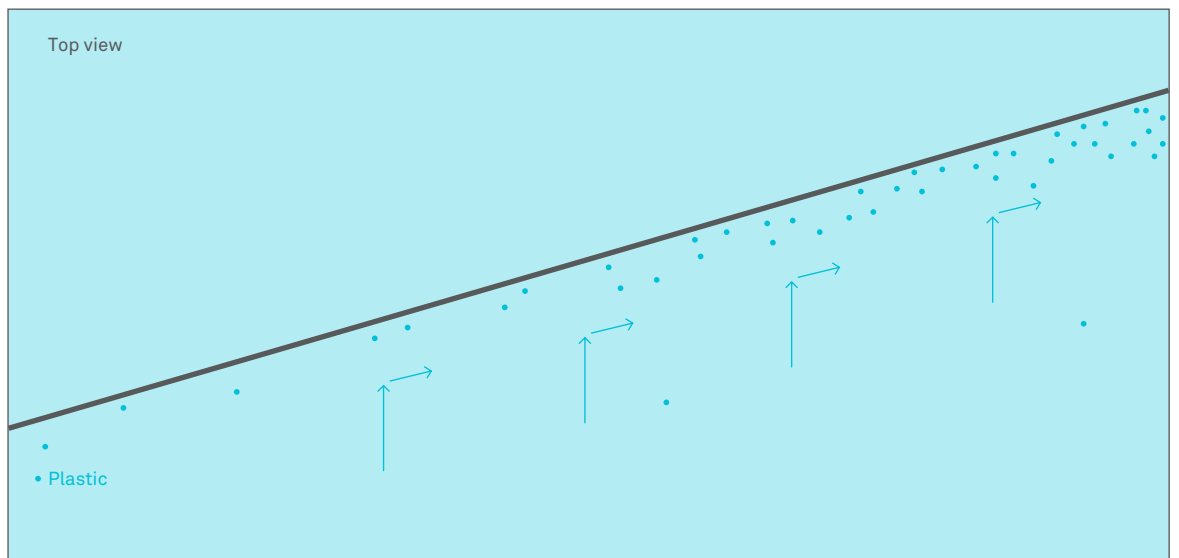
Figure 1.18 Simplified and schematic top view of a floating barrier. The blue dots represent plastic particles.

Figure 1.19 A preliminary design of a collection platform (Erwin Zwart – Fabrique Computer Graphics)
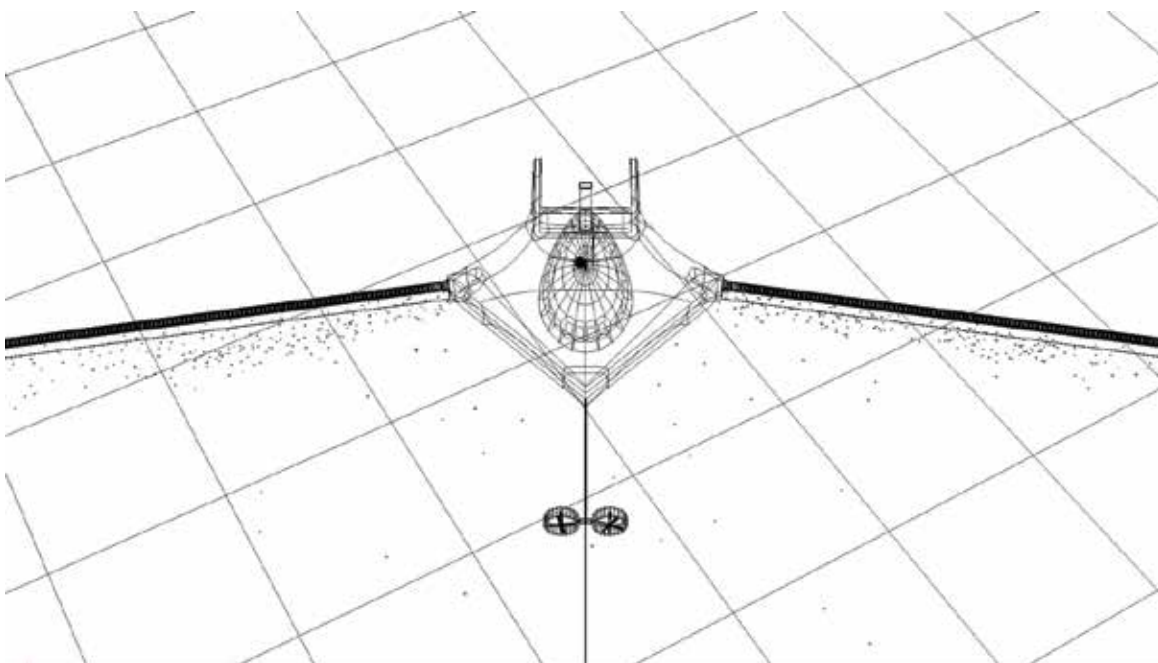
Figure 1.20 Early conceptual designs of The Ocean Cleanup Array, wireframe, August 2012. (Erwin Zwart – Fabrique Computer Graphics)

1.7.5 MAIN ADVANTAGES

The main advantage of passive cleanup is that it is scalable. Using conventional ship-and-net methods, it has been estimated that it would take about 79,000 years to remediate the Great Pacific Garbage Patch (Moore and Philips 2011). And that estimate assumes that vessels cover the entire oceanic area, and that the plastic pollution is spatially static. While the former assumption is perhaps naive or unrealistic, the latter is false. Ship-and-net methods are less efficient as the high variability in current directions caused by eddies makes them either repeat their run on the same patch of the sea or to miss some of the plastics.

In contrast, our concept uses the natural movement of the water to its advantage. In combination with the circulation period of the North Pacific Subtropical Gyre, the cleanup duration could be drastically reduced (a minimum of 5 years).

Due to the passive collection approach, operational expenses can potentially be very low, making the cleanup more cost-effective. Furthermore, converting the extracted plastic into energy, oil or new materials could cover (a large part of) the costs of the execution.

Furthermore, passive cleanup poses less harm to the marine ecosystem, and can potentially catch plastic particles that are much smaller than what nets could capture.

FEASIBILITY STUDY OBJECTIVES

BOYAN SLAT

The Ocean Cleanup Feasibility Study investigated the technical feasibility, financial viability, and scalability of large-scale passive plastic removal from the North Pacific Gyre using the Ocean Cleanup Array concept. The concept has been analyzed from several perspectives including oceanographic, engineering, fluid dynamics, ecology, legal, processing, and financial.

1.8.1 DEFINITION OF FEASIBILITY

'Feasible' is a quality of a proposed concept that is hard to define. The Oxford English Dictionary defines feasible as "Of a design, project, etc.: Capable of being done, accomplished or carried out; possible, practicable."

Since a similar concept has never before been proposed, 100 percent certainty on the ability of the concept to execute the plan can only be given after the project has been realized. Hence, the aim of a feasibility study is to prove with a high degree of certainty that a project can realistically be executed. This investigation is based on existing knowledge and supplemented with empirical evidence.
The questions that are covered in the Feasibility Study can be divided into two sets. The first set of questions focus on whether the concept works, e.g., "Can plastic debris get caught by a floating barrier, and is collection possible?" The second set of questions is directed at the execution of the concept and questions its viability, e.g., "Can the structure survive the extreme conditions faced during the chosen deployment time?"

While the first set contains questions that can be answered with a yes or no, this is (nearly) impossible with the questions of the second set. Continuing with the above-mentioned examples, fluid dynamics determines if the plastic is transported along the boom. However, whether the structure survives extreme weather conditions not only depends on fixed values (environmental conditions and material limits), but also on the available budget.

In other words, two kinds of answers can be expected as a conclusion to the study: a simple yes or no as to the projects theoretical feasibility and then a more qualified conclusion considering real-world requirements and limitations.

Solving engineering challenges is heavily dependent on the available budget. Hence, it is essential to combine the technical, ecological and legal investigations with an indication of the financial viability of the project. To do this, the total costs per ton will be determined based on the input of the technical development groups. The cost per ton can then be compared to other values, like revenue, current plastic pollution remediation efforts, direct and indirect costs, and other concepts. Based on this comparison, an assessment of the financial viability will be made.

It should however be noted that the cost per ton is heavily dependent upon the scale of the project execution. Due to economies of scale, the cost per ton will initially decrease as the scale of execution increases. However, after a certain peak size, the cost per ton will increase, since the array will be expanding away from the area of ocean with the highest concentration of plastic.
Hence, along the way, assumptions will have to be made on variables where no optimum exists, e.g., deployment time and array length, which will ultimately depend on the available budget, but do not influence the core principles of the concept. Nevertheless, a minimum scale will be established for the requirements of capture efficiency so as to help determine the required scale.

FINANCIAL
VIABILITY

COST PER
WEIGHT UNIT

LOW

HIGH

PROFITABLE

BREAK-EVEN

CHEAPER THAN
CURRENT MEASURES

MEDIUM

CHEAPER THAN
DIRECT COSTS

CHEAPER THAN
INDIRECT COSTS

LOW

CHEAPER THAN
OTHER CONCEPTS

MORE EXPENSIVE
THAN THE ABOVE

HIGH
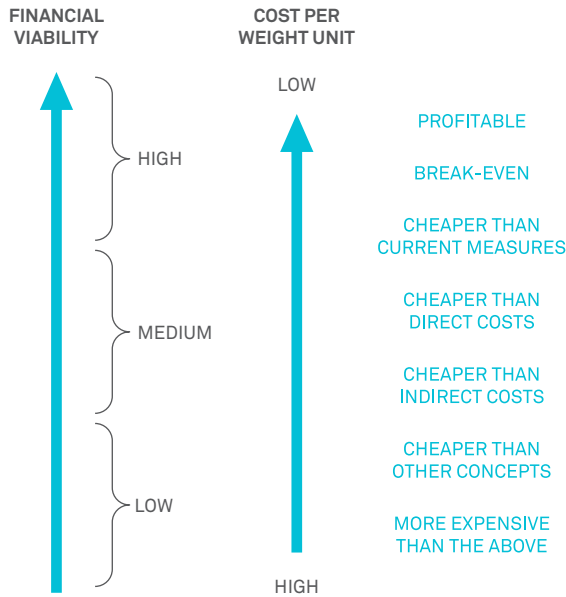
Figure 1.22 Scheme of cost considerations

TOTAL COST

ECONOMIES OF SCALE

REDUCTION IN
CONCENTRATION

TOTAL MASS COLLECTED
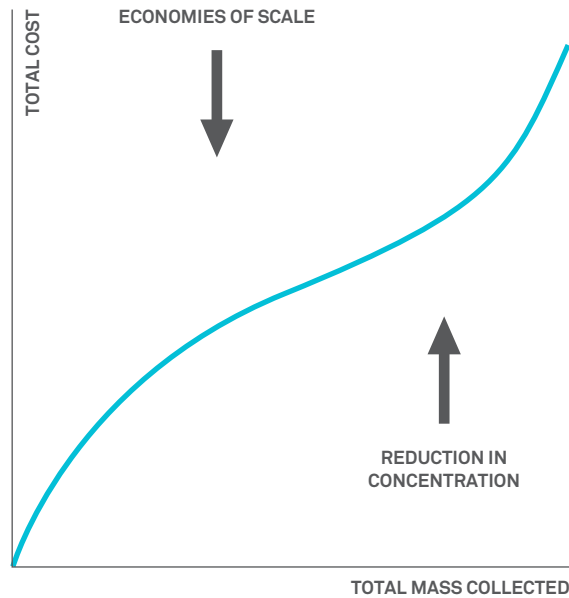
Figure 1.23 Relation between mass of plastic collected and total cost

1.8.2 MAIN QUESTIONS

Although many other questions will be answered throughout the feasibility, the results of the following questions directly lead to conclusions influencing the feasibility and financial viability of the proposed concept.

For a system capturing at least 25 percent plastic available in the North Pacific Gyre in 10 years,
Is the concept feasible to be executed?

TECHNICAL
- Can the boom skirt stretch deep enough to cover the highest concentration of plastics?
- Do the surface currents transport the plastic into the array?
- Does a floating barrier capture plastic?
- Does plastic get transported along a floating barrier?
- Can the structure survive the extreme conditions faced during the chosen deployment time?
- Can the structure be placed and operated?
- Can the large floating structure be moored at mid-ocean depths?

ECOLOGICAL
- Is the overall balance of impacts of our passive cleanup on the environment positive or negative?

LEGAL
- Will it be legally permissible to place and operate The Ocean Cleanup Array in international waters?

FINANCIAL
- Is the concept financially viable, and is the concept a time-efficient way of significantly reducing the amount of plastic in the oceans?
- Cost per ton compared to revenue
- Cost per ton compared to current plastic pollution measures
- Cost per ton compared to direct costs of plastic pollution
- Cost per ton compared to indirect costs of plastic pollution
- Cost per ton compared to other cleanup concepts

INTRODUCTION   STUDY   CONCLUSION

| Problem assessment | System development | Cost of execution |

| System requirements | Proving underlying principles | Does it work? Yes/no |
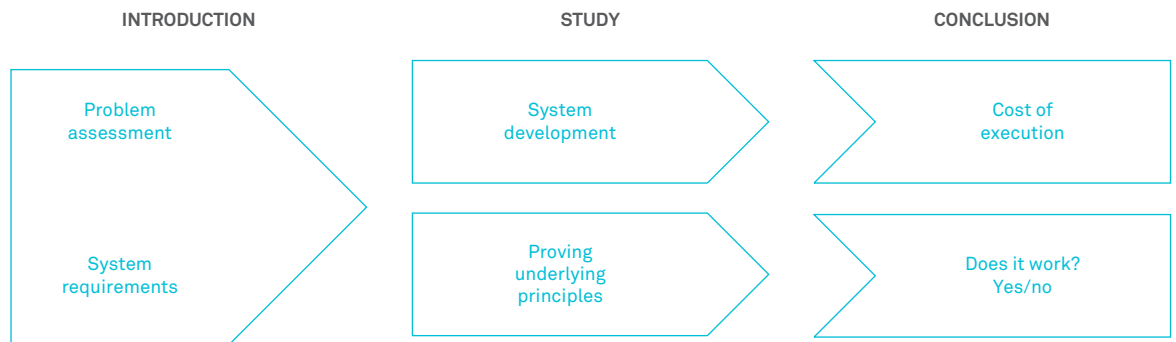
Figure 1.21 Scheme of the steps taken during feasibility study

1.8.3 OVERVIEW OF THE STUDY

In Chapter 2, an overview of the current oceanographic knowledge (supplemented with new fundamental knowledge) will be provided, investigating the technical feasibility from an oceanographic perspective.

Chapters 3, 4 and 5 will built upon the environmental conditions mapped in Chapter 2, and cover the technical feasibility in terms of fluid dynamics, structural engineering and operations.

Chapter 6 investigates whether or not the negative environmental effects of the operation are negligible.

Chapter 7 describes the performed large-scale test, serving as a validation for fluid dynamics simulations.

Chapter 8 investigates the feasibility of implementing and operating the system from the perspective of maritime and environmental law.

Chapter 9 outlines our investigation into the quality of ocean plastics, as well as possible methods to process it.

Chapter 10 will feature a calculation of the projected cost of the cleanup, as well as a cost-benefit analysis.

Finally, all results of the research will be concluded in chapter 11, where also recommendations for future work will be outlined.

THE GYRES

In order to be able to formulate the system requirements for an engineering solution to concentrate and capture floating plastic debris from the oceans, both the physical properties of the plastic pollution problem, as well as the present environmental conditions, must be determined. This chapter covers the vertical and geographical distribution of plastic pollution, the determination of a preliminary location, and two computer simulations that show the cleaning effect of an ocean cleanup array.

A FEASIBILITY STUDY

INTRODUCTION TO THE SUBTROPICAL GYRES

JULIA REISSER • CHRISTIAN GÖBEL • MAIRA PROIETTI

The subtropical gyres are the five largest systems of rotating ocean currents (Talley, Pickard, Emery, & Swift, 2011) that combined cover about 40% of the Earth's surface (Figure 2.1) Their horizontal extension occupies an area approximately 10° north to 10° south of the equator to 45° east and west in each hemisphere, while in terms of depth they can extend to nearly 2 km beneath the sea surface (Pedlosky, 1990). The gyres in the Northern Hemisphere (North Pacific and North Atlantic Gyres) rotate clockwise, while those in the Southern Hemisphere (South Pacific, South Atlantic, and Indian Gyres) spin counter-clockwise.

Wind driven surface circulations form a strong and narrow western boundary current, and a weak and broad eastern boundary current, shaping these ocean systems. The ocean surface interiors of these gyres have low concentrations of nutrients and biomass throughout the year (Figure 2.2). However, their immense size makes their total biological productivity significant in the context of the world's ocean ecosystem (McClain, Signorini, & Christian, 2004).
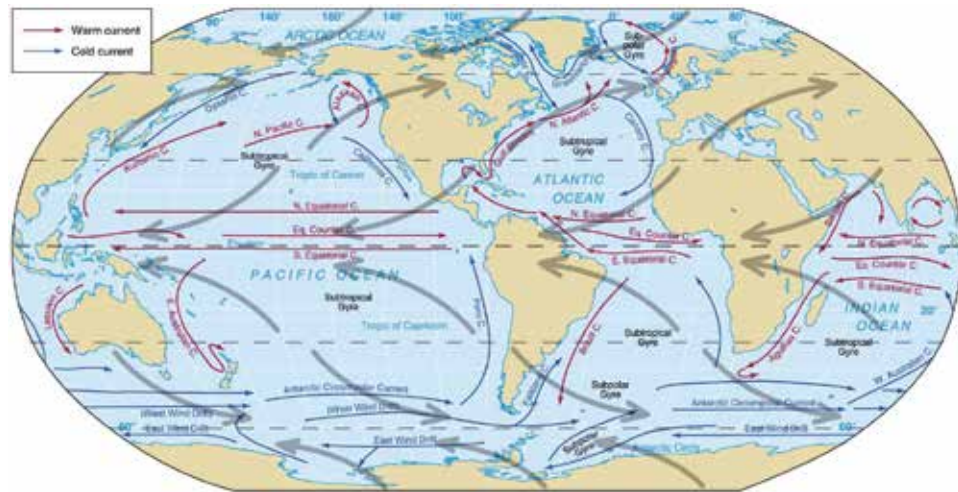
Figure 2.1 World ocean surface circulation. Source: (Talley et al., 2011).

The detection of very high concentrations of plastic in the subtropical waters of the North Pacific – with a mass of plastic six times that of plankton (Moore, Moore, Leecaster, & Weisberg, 2001) – caught the attention of researchers and the general public. Subsequent modelling work and at-sea surveys confirmed that such oceanic mid-latitude plastic hotspots occur within all five subtropical gyres (Eriksen et al., 2013; K. L. Law et al., 2010; Lebreton, Greer, & Borrero, 2012; Maximenko, Hafner, & Niiler, 2012; van Sebille, England, & Froyland, 2012).

This chapter reviews how subtropical gyres are formed, explains the surface currents that shape each of them, and describes identified hotspots of plastic pollution.

2.1.1. THE NORTH PACIFIC SUBTROPICAL GYRE
The North Pacific Gyre is one of the largest oceanic gyres, covering a vast surface area of the ocean. This gyre extends from slightly above the equator (around 10°N) to the Subarctic Frontal Zone (around 42°N), has a circular clockwise-spinning flow, and is formed by four main oceanic currents, including the Kuroshio Current, North Pacific Current, California Current, and North Equatorial Current (see Figure 2.1).

The Kuroshio Current is a strong, narrow, northwards-bound current that is formed at approximately 14°N latitude. It changes direction at around 35°N, where it begins to flow eastward into offshore waters of the North Pacific. This portion of the current is referred to as the Kuroshio Extension, and it connects the Kuroshio Current to the broader, weaker, eastwards-flowing North Pacific Current. When the North Pacific Current reaches waters off California, the flow turns southwards into the California Current. At around 10°N this current separates from the eastern boundary and starts to move westward, flowing into the North Equatorial Current. When this current reaches waters off the Philippines, at about 14°N, it bifurcates into two separate flows, one being the Kuroshio Current, and the North Pacific Subtropical Gyre loop is closed. The area to the east of the Kuroshio Extension is characterized by two meanders and a recirculation gyre to the south. While a semi-permanent feature, the overall strength of the recirculation gyre is related to fluctuations in the wind stress field.

2.1.2. THE SOUTH PACIFIC SUBTROPICAL GYRE
The South Pacific Gyre extends from the equator to approximately 45°S. Since it is located in the Southern Hemisphere, it rotates counter-clockwise. Four main ocean currents form this gyre. These include the Eastern Australian Current, South Pacific Current, Peru-Chile Current, and South Equatorial Current (see Figure 2.1).
The Eastern Australian Current, which is the western limit of this subtropical gyre, flows southwards along Australia's east coast. When this current reaches approxi-
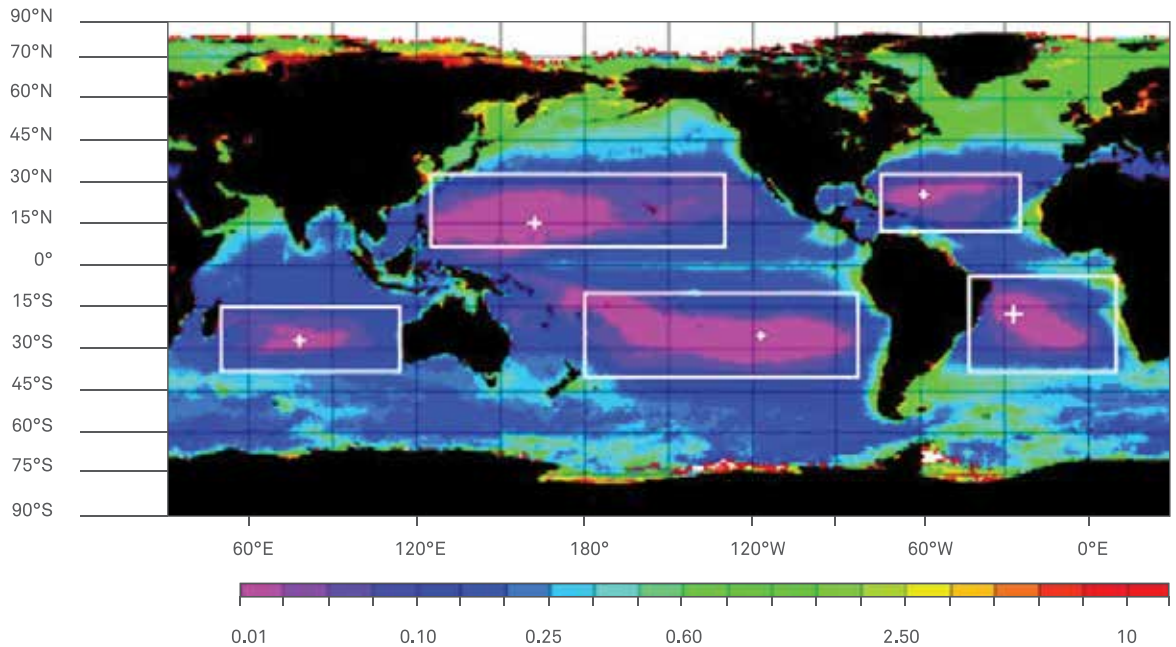
Figure 2.2 Global distribution of chlorophyll concentration. Map derived from a January 1998 – December 2000 SeaWiFs (http://oceancolor.gsfc.nasa.gov/SeaWiFS/) composite. Crosses show estimated location of the minimum chlorophyll concentration and boxes represent the main region of each subtropical gyre. Source: (McClain et al., 2004). Permission requested.

mately 30-35°S it flows eastwards towards New Zealand, where it then flows to the south of New Zealand's east coast (East Auckland Current). This current system is very dynamic and produces a series of smaller gyres known as eddies, which can rotate clockwise, i.e., cyclonic, or counter-clockwise, i.e., anti- cyclonic (Mata, Wijffels, Church, & Tomczak, 2006). At about 40°S this western boundary current departs the waters off eastern New Zealand and begins flowing eastwards; it is then called the South Pacific Current. This broad eastern flow delimits the southern border of the South Pacific Gyre, and crosses the South Pacific Ocean associated with the Antarctic Circumpolar Current. When the South Pacific Current arrives at waters off Chile, it turns northwards, becoming the Peru-Chile Current. This current system forms the eastern boundary of the South Pacific Gyre, flowing along the coast off South America until reaching the Equatorial region, when its direction turns westwards. Such westward flow is the South Equatorial Current, which is located between 20°S to approximately 5°N. This current reaches waters off eastern Australia, where it bifurcates and feeds the East Australian current; and the loop is closed.

2.1.3. THE NORTH ATLANTIC SUBTROPICAL GYRE

The North Atlantic gyre extends from the equator to approximately 45°N, and rotates clockwise. This gyre consists of mainly four oceanic currents, including the Gulf Stream, North Atlantic Current, Canary Current, and North Equatorial Current (see Figure 2.1).

This gyre presents the largest western boundary current, the Gulf Stream System, which transports large amounts of heat to medium and high latitudes. This current is fast and narrow, with a north-eastern flow off the North American coast until it reaches around 45°N. Here, the Gulf Stream is divided into two branches, one of which forms the eastwards-flowing North Atlantic Current. This is a wider and more diffuse eastward flow that turns to the south upon reaching waters off the European continent, forming the Canary Current. The eastern boundary Canary Current flows towards the equator until reaching around 15°N, where it turns westwards joining the trans-Atlantic North Equatorial Current. This current flows to the west until reaching the Caribbean region where it turns northwards into the Florida current, which in turn becomes the Gulf Stream and closes the subtropical gyre.

2.1.4. THE SOUTH ATLANTIC SUBTROPICAL GYRE

The South Atlantic gyre extends from the equator to approximately 40°S, and rotates counter-clockwise. It comprises four surface currents, including the Brazil Current, South Atlantic Current, Benguela Current and South Equatorial Current (see Figure 2.1).

The Brazil Current is a relatively weak western boundary current that runs southwards along the coast of Brazil to about 38°S, where it meets the north- flowing Falklands Current. This is known as the Brazil-Falklands Confluence Zone, one of the most energetic regions in the oceans. The Brazil Current is then deflected to the east, feeding the South Atlantic Current, which is the southern branch of the subtropical gyre. It is difficult to distinguish between this southern boundary of the gyre and the northern boundary of Antarctic Circumpolar Current. When reaching waters off the southern tip of the African continent, the South Atlantic Current partially deflects northwards into the eastern boundary Benguela Current, which flows along the African coast until reaching approximately 20°S, where it turns westward and feeds the South Equatorial Current. The South Equatorial Current is a broad, westward flowing current that extends from around 15 - 20°S to 4°N. The westward flowing trans-Atlantic South Equatorial Current bifurcates as it approaches the continental shelf around 10°S, with waters flowing north becoming the North Brazil Current, which joins the North Equatorial Current linking the two Atlantic gyres. Meanwhile, the branch flowing south turns into the Brazil Current, which closes the South Atlantic Gyre.

2.1.5. THE INDIAN SUBTROPICAL GYRE

The Indian Ocean is quite unique, as it has no northern latitudes higher than 25°N. As a consequence, it only has one subtropical gyre, located in the Southern Hemisphere. The major currents that form the Indian Subtropical Gyre include the Agulhas Current, South Indian Current, West Australian Current, and South Equatorial Current.

The Agulhas Current is a strong, narrow current flowing southwards, delimiting the western portion of the Indian Gyre. It is a unique western-boundary current in the sense that it surpasses the end of the African coast, creating a retroflection south of Africa, and turning eastwards at approximately 40°S. This eastward flow is the South Indian Current, which is connected to a broad northward flow in the eastern part of the gyre, usually called the West Australian Current. The northern limit of this subtropical gyre is the South Equatorial Current, which transports fresher water from the Indonesian archipelago to the west, resulting in a front with high variation in salinity. The Indonesian archipelago is an important connection to the Pacific Ocean. In the tropics and the northern Indian Ocean, surface ocean circulations are strongly seasonal, forced by the reversing Southwest and Northeast Monsoons (see Figure 2.3 to visualise seasonal winds of this region).

Figure 2.3 Satellite-tracked buoy being released in Australian waters aboard the Solander research vessel. Photo by Julia Reisser.
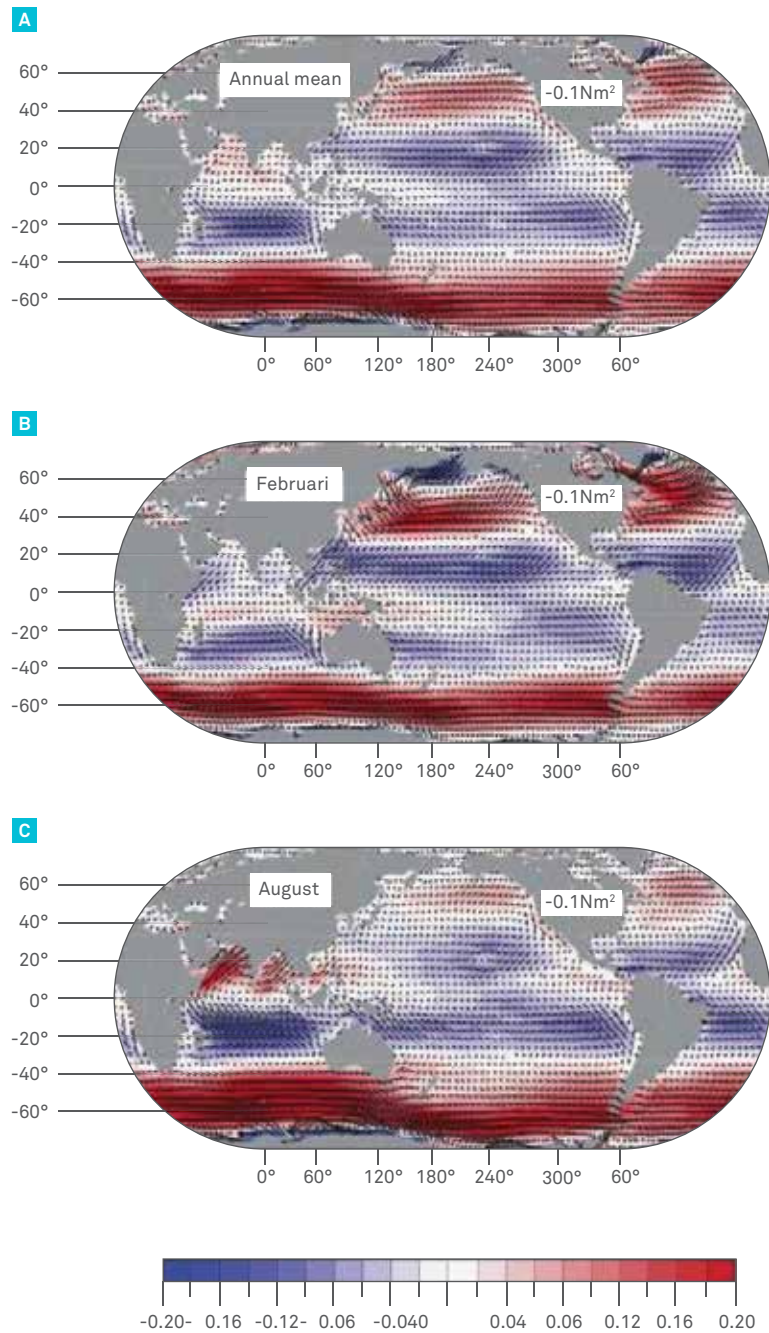
Figure 2.4 Mean wind stress (arrows) and zonal wind stress (color shading) in N m⁻² from NCEP reanalysis (esrl.noaa.gov/psd/data/gridded/data.ncep.reanalysis.html). a. Annual mean (1968 - 1996); b. February mean (1968 - 1996); c. August mean (1968 - 1996). Source: (Talley et al., 2011).
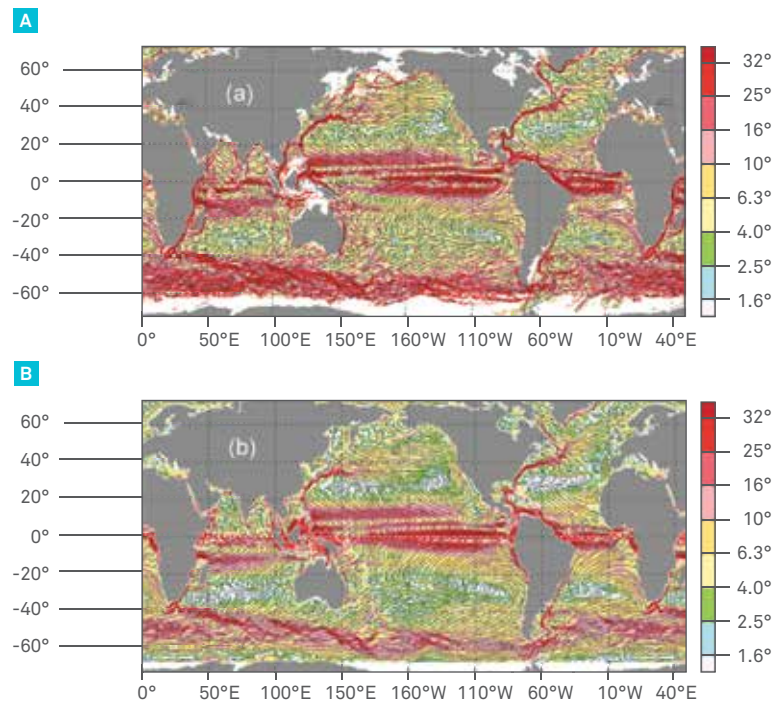
Figure 2.5 Mean streamlines calculated from (a) 0.25° ensemble-mean velocities of satellite-tracked drifting buoys drogued at 15 m depth (1979 – 2007) smoothed to 1°, and (b) a combination of the mean geostrophic and Ekman velocities using method described in (Maximenko et al., 2009). Colors are magnitude of (a) mean drifter velocity and (b) mean geostrophic plus Ekman velocity to compute the streamlines; units are cm / s. Source: (Maximenko et al., 2009). Permission requested

D   Tracer accumulation after 50 years
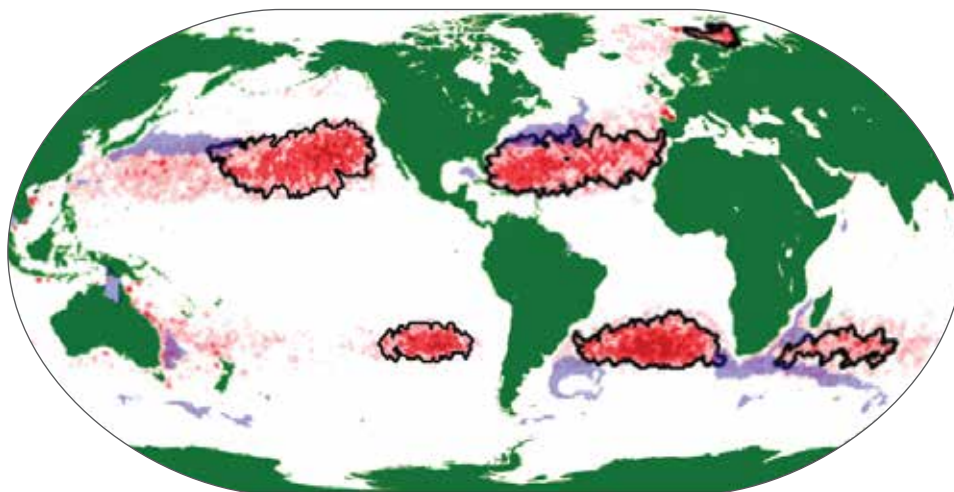
Figure 2.6 The locations of six plastic pollution hotspots as predicted by (Erik van Sebille et al., 2012) after 50 years of tracer ("debris") movement from coastal sources.
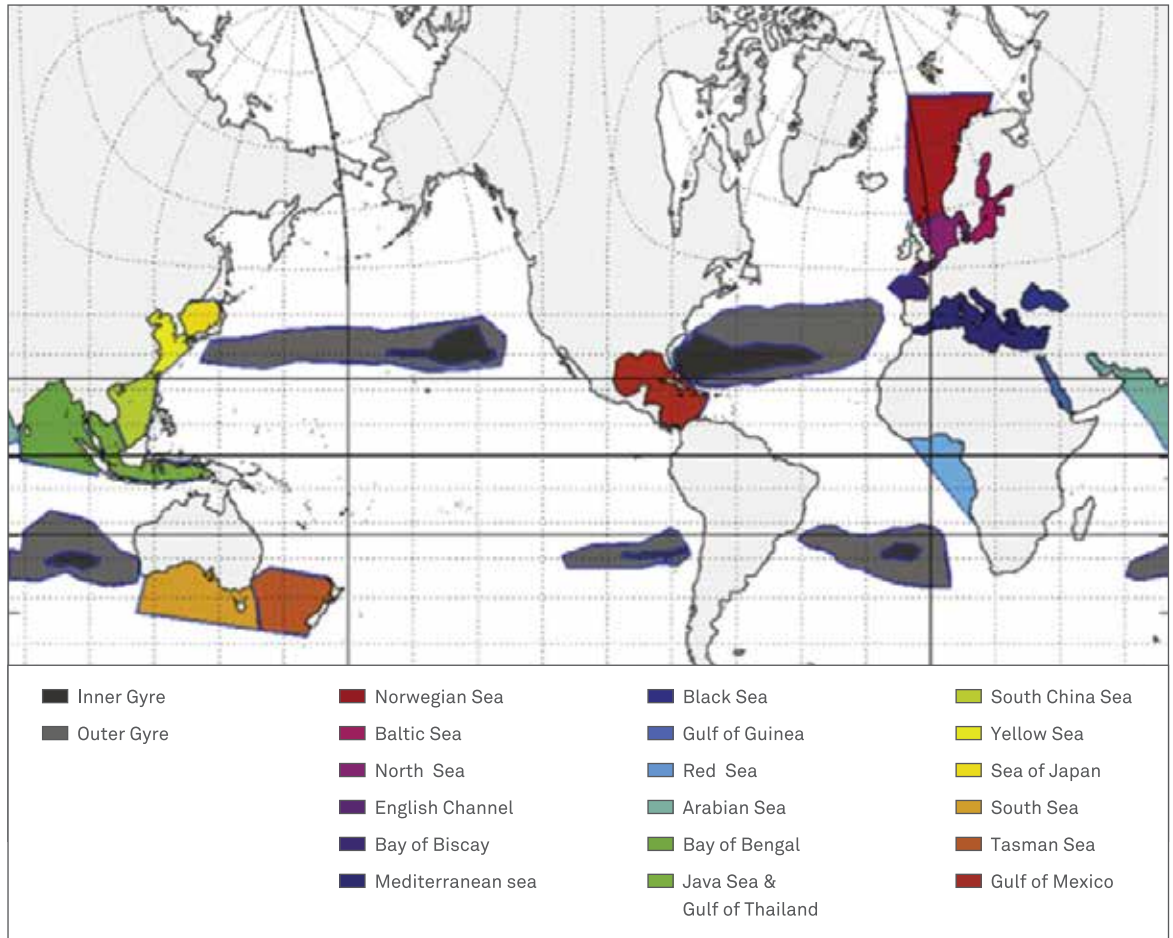
Figure 2.7 Plastic accumulation zones as predicted after 30 years of simulated plastic input and circulation. Source: (L. C. M. Lebreton et al., 2012). Permission requested.

2.1.6. PLASTIC POLLUTION HOTSPOTS

As demonstrated in the previous chapter, a great amount of plastic debris ends up in the oceans. There is an increasing need to remove the debris from the marine environment, particularly at areas with high concentrations. In order to figure out where plastic accumulates, it is necessary to understand where currents at the upper layer of the oceans converge, as floating plastic debris is concentrated at these areas. The dynamics of the upper ocean, where most plastics float, is very complex. Significant improvements on databases from satellite-tracked buoys (NOAA, 2014) as shown in Figure 2.4 and satellite altimetry (GRACE) have led to a far better understanding of the near-surface ocean currents. Through maps derived from such datasets, visualization of important convergent zones in the subtropical oceans has been improved (Maximenko et al., 2009), see Figure 2.5.

Studies modelling the pathways of plastic debris at the world's sea surface have predicted the existence of plastic pollution hotspots at these convergence zones (Maximenko et al., 2012). Data on quantities of plastic debris collected by net tows have consistently confirmed the occurrence of plastic pollution hotspots at some of these five convergence zones (Eriksen et al., 2013; K. L. Law et al., 2010; Moore et al., 2001). Other recent modelling studies that take into account sources and quantities of plastic debris at different coastal and oceanic zones have predicted that other large-scale plastic hotspots may occur (Lebreton et al., 2012; van Sebille et al., 2012). There is still a need to perform further at-sea surveys with better spatiotemporal coverage to validate and calibrate such plastic concentration predictions (Figure 2.6 and Figure 2.7).

MASS OF OCEAN PLASTIC

BOYAN SLAT • JULIA REISSER

Modeling predictions and sampling data suggest that the five subtropical gyres form large-scale accumulation zones with distinct plastic pollution levels, spatial and temporal dynamics, and extensions (K.L. Law et al., 2014; K. L. Law et al., 2010; Lebreton et al., 2012; Maximenko et al., 2012; van Sebille et al., 2012). For instance, some models predict that the three accumulation zones formed by the southern hemisphere subtropical gyres are smaller, with lower concentrations of plastic, and with a higher degree of connectivity due to the eastward transport of plastic by the Antarctic Circumpolar Current, which runs completely around the globe and is associated with high eddy activity and mixing (Lebreton et al., 2012; van Sebille et al., 2012).

The accumulation zone formed within the North Pacific subtropical gyre is relatively well studied, both through model predictions (Kubota, Takayama, & Namimoto, 2005; Lebreton et al., 2012; Maximenko et al., 2012; van Sebille et al., 2012) and sampling (Dahlberg & R.H., 1985; Day & Shaw, 1987; Day, Shaw, & Ignell, 1990; Goldstein, Rosenberg, & Cheng, 2012; Goldstein, Titmus, & Ford, 2013; K.L. Law et al., 2014; Moore et al., 2001; Titmus & Hyrenbach, 2011; Venrick et al., 1973). Due to hydrodynamic processes and spatial distribution of major plastic pollution sources, the North Pacific "garbage patch" seems to possess relatively high plastic concentrations when compared to the other four large-scale accumulation zones formed by subtropical gyres (K.L. Law et al., 2014; Lebreton et al., 2012; van Sebille et al., 2012). For that reason, it has been decided to narrow the scope of this feasibility study to the deployment of a The Ocean Cleanup platform within the large-scale accumulation zone of the North Pacific.

In this section we make an estimate of the total mass of plastic currently floating in the North Pacific accumulation zone. This is only an approximation, hopefully within the same order of magnitude of the actual amounts. However, that may not be the case given that many approximations and assumption were taken. There is limited information on the mass of ocean plastic, both spatially and temporally, particularly for large (centimeter/meter-sized) plastic items. Furthermore, there are no comprehensive datasets on microscopic plastic concentrations (smaller than 0.5 mm), mostly due to the difficulty of sampling microscopic particles using zooplankton nets (333-335 micron mesh) and identifying the material type of microscopic particles (i.e. differentiating polymer micro-particles from organic matter, inorganic marine dust, and contamination from air dust).

2.2.1 MASS OF MILLIMETER-SIZED PLASTICS

An extensive survey of floating plastic debris in the eastern North Pacific from more than 2,500 surface net tows has just been published (K.L. Law et al., 2014). In this study, the authors defined the North Pacific accumulation zone to occur from 25° to 41°N latitude and from 130° to 180°W longitude. It was within this accumulation zone, the so-called North Pacific garbage patch, that 93% of all plastic pieces of this survey were collected (2001 – 2012). The median plastic concentration of all tows within this accumulation zone was $3,309*10^4$ pieces per km², while outside this zone the median value was 0 pieces per km². Global models predict similar centers of plastic accumulation within the North Pacific gyre and they strongly correspond to the area of accumulation described in Law et al. 2014 (Figure 2.8).
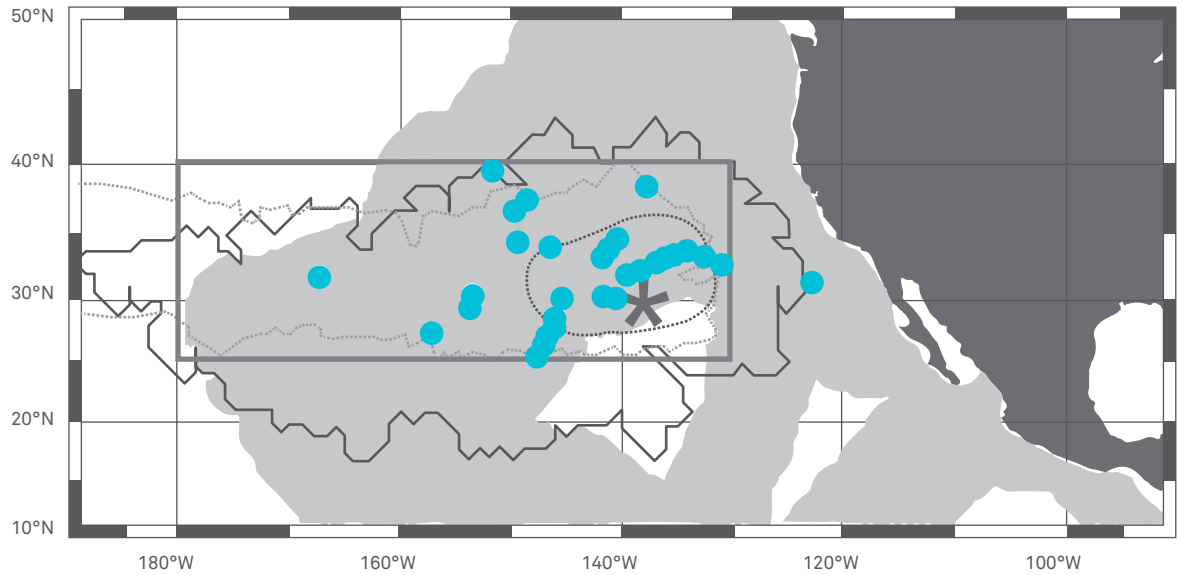
Figure 2.8 North Pacific accumulation zone, the so-called North Pacific garbage patch. Dark grey asterisk displays proposed location for installation of the Ocean Cleanup Platform, and gray square shows plastic accumulation zone as defined by Law et al. 2014 and used here to calculate mean mass of plastic within the North Pacific accumulation zone. Centers of plastic accumulation as previewed by different models are indicated by a dashed black line (N. Maximenko et al., 2012), dashed gray line (E. van Sebille et al., 2012), and continuous black line (L. C. M. Lebreton et al., 2012). Gray background indicate area sampled by Law et al. (2014) and blue dots show locations of net tows that sampled waters with plastic concentration higher than 200,000 plastics per km².

Law et al. 2014 utilized all available net tow data collected in the eastern Pacific Ocean since 1999. They used this data to estimate the average mass of floating plastic by integrating the plastic concentration over the areas where it exceeds 25,000 pieces km-2. They then multiplied this by the average particle mass (1.36*10-5 kg), as estimated by (Moret-Ferguson et al., 2010) (Figure 2.9). This resulted in a total mass estimation of at least 18,280 metric tons. When data was adjusted for wind-driven vertical mixing (Kukulka, Proskurowski, Morét Ferguson, Meyer, & Law, 2012), the estimate increased by 17 percent to 21,290 metric tons.

2.2.2. MASS OF CENTIMETER TO METER-SIZED PLASTICS

Currently, there are no published estimates of centimeter/meter-sized plastic mass within the North Pacific accumulation zone. As such, an estimate was made based on reported numerical mean values of centimeter/meter-sized plastic concentrations (in pieces per km²), as estimated by visual searches (Titmus & Hyrenbach, 2011). Titmus and Hyrenbach (2011) conducted visual searches from around 30° to 46°N and from 115° to 145°W, sighting 3,868 pieces of marine debris. More than 95.5% of this debris was identified as plastic. While some intact objects were seen, fragments were the most dominant type of plastic debris (90% of total, N=3,464). Their work used correction factors to calculate plastic concentration (pieces per km²) at three debris length classes: 2 – 10 cm, 10 – 30 cm, and larger than 30 cm.
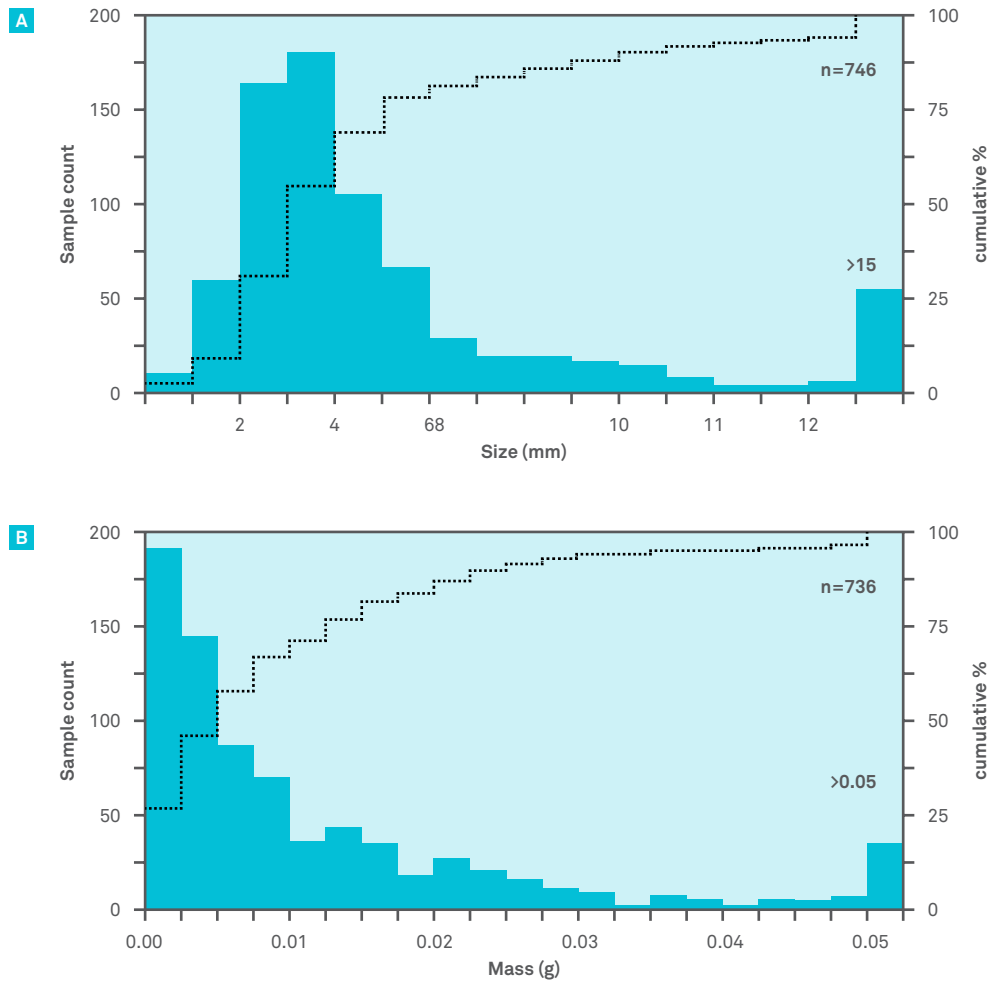
Figure 2.9 Size and mass of marine plastic collected by net tows in the North Atlantic. Bars indicate number of plastic pieces within each size (a) and mass (b) category and dotted lines represent cumulative percentage. (Morét-Ferguson et al., 2010). Permission requested.

Using these concentration values and the mean weight of beached plastic fragments with similar dimensions (Table 2.1), we estimated mean plastic concentration in grams per km² for these three debris size classes: 5,650 g per km² of plastic with length between 2 and 10 cm, 3,806 g per km² of plastic with length between 10 and 30 cm, and 4,986 g per km² of plastic longer than 30 cm. Assuming these are the mean mass concentration of centimeter/meter-sized plastic within the North Pacific accumulation zone (25°- 41°N, 130° - 180°W), we then multiplied the area of this zone (8.3 million km²) by these estimated mass concentrations (Table 2.2). Using this method, we estimate that the mean mass of small (2-10 cm), medium (10-30 cm) and large (larger than30 cm) plastics to be equal to 46,656 tons, 31,431 tons, and 41,168 tons, re-

spectively. The higher mass of larger items (larger than 30 cm) when compared to medium-sized items (10-30 cm) may be a consequence of the fact that some items, such as Styrofoam objects and closed PET plastic bottles, sink to the seafloor after there is no air within its heavier-than-seawater polymer.

SIZE CLASS	LARGE	MEDIUM	SMALL
Surface Area (cm²)	**2500.0**	**500.0**	**52.0**
Approximate Length (cm)	**50.0**	**22.0**	**7.0**
Weight Fragment 1	142.0	74.0	16.0
Weight Fragment 2	220.0	70.0	14.0
Weight Fragment 3	116.0	83.0	7.0
Weight Fragment 4	194.0	70.0	15.0
Weight Fragment 5	140.0	67.0	6.0
Weight Fragment 6	100.0	40.0	19.0
Weight Fragment 7	152.0	45.0	11.0
Weight Fragment 8	26.0	38.0	16.0
Weight Fragment 9	694.0	117.0	27.0
Weight Fragment 10	1300.0	40.0	7.0
Weight Fragment 11	1317	83.9	10.3
Weight Fragment 12	946	50.4	28.3
Weight Fragment 13	34	127.7	18.5
Weight Fragment 14	161	119.3	26.8
Weight Fragment 15	174	301.7	10.8
Weight Fragment 16	47	49.8	2.4
Weight Fragment 17	53	52.3	12.2
Weight Fragment 18	105	68.5	6.2
Weight Fragment 19	83	372.3	9.0
Weight Fragment 20	81	46.5	13.0
Average Weight (g)	**304.3**	**95.8**	**13.8**

Table 2.1 Mass in grams of randomly selected plastic fragments recovered from a remote beach in Big Island, Hawaii. To come up with an average sized fragment, we took the lower and higher boundary of the size range used in Titmus and Hyrenbach (2011) , converted that to an area (assuming a square fragment), and averaged. The square root of that average surface area was used as a target length of the fragments weighed. Please note that for the size class smaller than 30 cm there is no upper boundary, and hence simply measured particles that were longer than 30 cm (for the 30+ diameter, on average it was 35 cm).

SIZE CLASS	PIECES/KM²	MEAN WEIGHT	G/KM²	TOTAL MASS (TONS)
>30 CM	16.40	304	4,986	41,168
10-30 CM	39.65	96	3,806	31,431
2-10 CM	403.59	14	5,650	46,656

Table 2.2 Numerical concentration (pieces per km²), mean weight (grams), mass concentration (grams per km²), and total mass of floating plastic within the North Pacific accumulation zone. Values are given for floating plastic (1) longer than 30 cm, (2) with length between 10-30 cm, and (3) 2-10 cm.

2.2.3. TOTAL MASS OF FLOATING PLASTIC IN THE NORTH PACIFIC GARBAGE PATCH

Our estimate of the mean mass of floating plastic in the North Pacific accumulation zone is of 140,546 metric tons: 21,290 metric tons of plastic smaller than 2 cm and 119,256 metric tons of plastic larger than 2 cm. However, we acknowledge that more research is needed to increase the accuracy and reliability of these results. There is limited sampling of ocean plastic, both spatially and temporally, particularly for large (cm/m-sized) plastic items.

Nevertheless, we believe that ours is more likely an underestimate of the actual amounts rather than an overestimate. One of the reasons for this is that mass of plastics longer than 30 cm may be higher than estimated here: we assumed that all the plastic within this category are fragments of about 50 cm in length and items far much heavier than this, such as ghost nets and floats, occur in this area (Pichel et al., 2007). Additionally, Law et al. (2014) did not quantify amounts of microscopic plastic, which are likely to occur in the area (Desforges, Galbraith, Dangerfield, & Ross, 2014).

Marcus Eriksen and collaborators estimated that the current global mass of floating plastic is 500,000 tons (Parker, 2014). As such, our mass estimate for the North Pacific garbage patch corresponds to 28% of this global mass of floating plastics. By way of comparison, recent modeling studies predict that 12 to 20 percent of ocean plastics older than 30 years is within this North Pacific accumulation zone (Lebreton et al., 2012; van Sebille et al., 2012).

In the following chapters, the mass estimates reported here are used for various efficiency and dimensioning problems. For example, the mass of plastic of different sizes will dictate the percentage of plastic that will be caught by the structure (Chapter 3.3). The estimated amount of plastic to be captured by the platform will then be used to dimension various processing and transport processes (Chapter 4), and estimate how much it would, on average, cost to remove a certain mass of plastics from the oceans using the proposed system (Chapter 10).

DEPTH PROFILE OF PLASTIC POLLUTION: A PILOT STUDY

JULIA REISSER • HYKE BRUGMAN • BOYAN SLAT

Plastics with a diameter of less than 5 mm, coined microplastics, formed from the fragmentation of plastic objects, are abundant at the ocean surface. As previously explained in section 1.2, concentrations of this type of pollutant are commonly estimated using data collected by surface nets that only sample the top few centimeters of seawater. Only recently did a study based on data from a series of 12 surface and subsurface trawls comprehensively demonstrate that small plastics are vertically distributed within the ocean's water column due to wind-driven mixing (Kukulka et al., 2012). The findings showed that the amount of microplastics at the air-seawater interface is inversely proportional to wind stress. In other words, as a portion of the plastics is transported by turbulence to greater depths, the higher the wind speed, the less plastic is located in the area sampled by surface nets. Therefore studies must take into account the effects of wind-driven vertical movement and previous estimates of plastic concentration may be biased (Kukulka et al., 2012; Reisser et al., 2013).
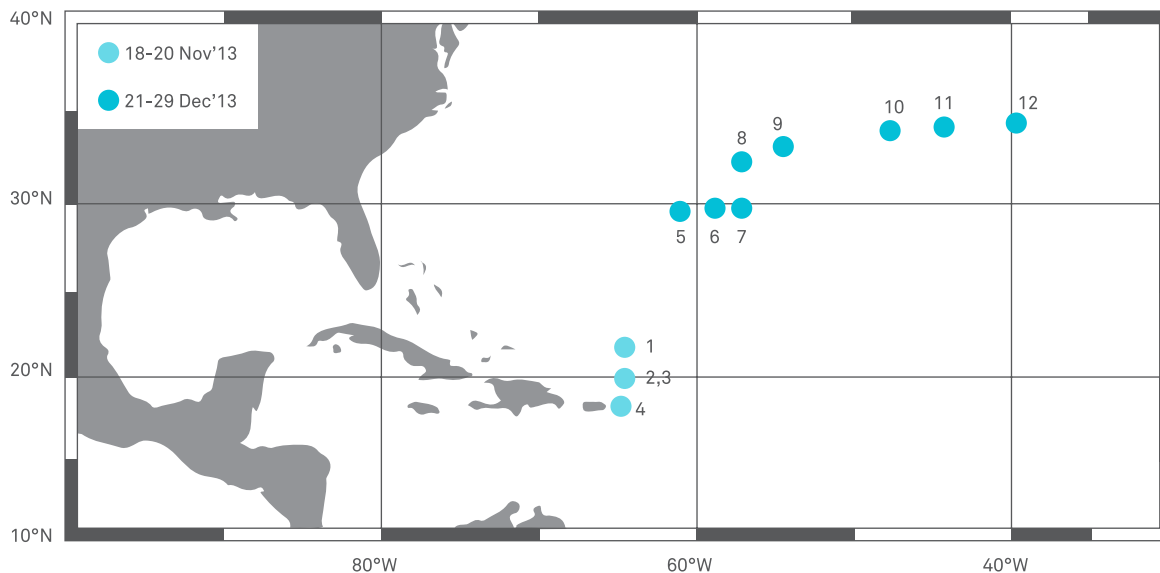
Figure 2.10 Location of the net tows undertaken during this study (N = 12). Dot colors indicate the voyage in which the location was sampled and numbers follow the chronological order of sampling. The Multi-level Trawl developed and used during this study is shown in subsequent pictures.

It is also essential to know the vertical distribution of plastic as, besides making it possible to accurately calculate total plastic pollution levels, this will directly affect the efficiency of The Ocean Cleanup Array. This information will greatly influence design choices, as it is needed to understand the relationship between the depth of the boom used and the volume of plastics captured. However, as currently plastic depth profile observations are scarce and the phenomenon is still poorly understood, the Ocean Cleanup team decided to design a net system capable of sampling the oceans from the air-seawater interface to a depth of 5 meters. This Multi-level Trawl is capable of obtaining high-resolution data (with net dimensions of 0.5 m H x 0.3 m W) on plastic pollution depth profiles, from 0 to 5 m, under different environmental conditions. This section outlines the depth profiles of plastic concentration (g and pieces per m³) observed under wind speeds varying from 2.6 to 12 m/s (5 – 23 knots). These observations indicate that while plastic particles can be well mixed throughout the water column, plastic maintains a depth profile of higher mass close to the air-water interface and exponentially decreases with depth. As such, it was inferred that a 3 meter-deep boom would be able to capture a large proportion of the total plastic pollution mass floating in the oceans.

2.3.1. MATERIALS AND METHODS

During two voyages to the North East Atlantic, 12 net tows sampled from the surface to a depth of 5 meters using a Multi-level Trawl designed by the Ocean Cleanup team (Figure 2.9 – 2.11). Tow durations ranged between 59-124 minutes and were all undertaken while the vessel was travelling at a speed of 0.6 – 1.8 knots. During each net tow, a shipboard anemometer located at approximately 25 meters above mean waterline measured wind velocity and direction. The net system is composed of 11 nets with rectangular openings (0.5 m H x 0.3 m W) towed by several ropes that ensure its stability in the water column. During the tows, the top 1 - 1.5 net remained above mean waterline, while the other nets were submerged. As such, the sampled depth intervals considered were at (i) 0 - 0.5 m, (ii) 0.5 - 1 m, (iii) 1 - 1.5 m, (iv) 1.5 - 2 m, (v) 2 - 2.5 m, (vi) 2.5 - 3 m, (vii) 3 - 3.5 m, (viii) 3.5 - 4 m, (ix) 4 - 4.5 m, and (x) 4.5 - 5 m. Table 2.2 contains more data about the sampling.

VOYAGE VESSEL NAME	DATE (UTC)	START TIME (UTC)	DURATION (MIN)	WIND SPEED (M/S)	START LATITUDE	START LONGITUDE
1 SEA DRAGON	18.11.13	15:52	60	10	21.765ºN	64.482ºW
1 SEA DRAGON	19.11.13	11:17	123	3	19.937ºN	64.599ºW
1 SEA DRAGON	19.11.13	13:37	124	2.6	19.964ºN	64.586ºW
1 SEA DRAGON	20.11.13	9:04	63	5	18.276ºN	64.849ºW
2 RV PELAGIA	21.11.13	20:22	72	9	29.589ºN	61.109ºW
2 RV PELAGIA	22.11.13	16:33	84	10	29.753ºN	58.843ºW
2 RV PELAGIA	23.11.13	11:36	67	10	29.782ºN	57.109ºW
2 RV PELAGIA	24.11.13	13:14	65	4	32.341ºN	57.169ºW
2 RV PELAGIA	25.11.13	12:15	59	12	33.157ºN	54.493ºW
2 RV PELAGIA	27.11.13	16:26	76	9	34.004ºN	47.718ºW
2 RV PELAGIA	28.11.13	12:23	69	10	34.154ºN	44.325ºW
2 RV PELAGIA	29.11.13	15:21	69	11	34.400ºN	39.726ºW

Table 2.3 Information of the Multi-level Trawl (0 to 5 m) conducted during this study (N = 12): Voyage number and Vessel Name; date in Coordinated Universal Time (UTC); start time in UTC; duration in minutes; wind speed in meters per second; start latitude and longitude, both in degrees.

Figure 2.11 Multi-level Trawl attached to the spinnaker pole of vessel Sea Dragon, for the first expedition through the North Atlantic Gyre. Picture by Allard Faas [Figure 1b.] Courtesy of of Allard Faas. Please note that the boxes in front of the top two nets were removed after testing, and hence were not used during trawling.

Figure 2.12 Multi-level Trawl in action during expedition 1 (left) and 2 (right). As can be seen, the trawl was higher in the water due to the angle from which it was pulled. Picture by Allard Faas

All net frames were fitted with 2.1 meter-long polyester nets, initially with a 70-µm mesh. This mesh was shown to be too fragile, leading to the loss of some samples due to net damages. To solve this, 150-µm meshes were used in the second expedition. After each tow, the collected contents were transferred to a 63-µm sieve and kept in sealed bags or tubes for transportation. Once in the laboratory, samples were washed in petri dishes using a spray bottle and plastics were separated from organic material with the aid of a microscope (10x eyepieces), tweezers, and dissecting needles. The plastic pieces found in each sample were counted, air-dried in a flow cabinet for 24-72 hours, weighted on a 1/1000 gram sensitive scale, photographed using a microscope-mounted camera, and then stored in sealed bags. To compare plastic pollution levels observed in this study with those from other areas of the globe (see section 1.2), the sea surface plastic concentration was estimated in pieces per km². To do so, the number of plastic pieces found in the top 2 nets (0 - 0.5 m) was divided by the sampled area, which was estimated by multiplying net opening width by tow lengths (determined by GPS position data; (K. L. Law et al., 2010).

We arrived at an estimate of plastic concentrations at each of the sampled depths, by dividing the number of plastic pieces and the total plastic mass of by the volume sampled (reported in pieces per m³ and grams per m³). Towed volume was estimated using net opening dimensions and readings from the mechanical flow meter (Goldstein et al., 2013) attached to the Multi-level Trawl at a depth of approximately 3.75 meters.

Finally, the mean and standard error of plastic concentrations (grams per m³ and pieces per m³) were calculated for each of the depth intervals. To investigate how the depth profile of plastic concentrations changes with wind speed, these mean and standard error values were calculated considering all trawls (N = 12), as well as only data from trawls conducted under "low" and "high" wind speeds (< 10 m/s and → 10 m/s, respectively).
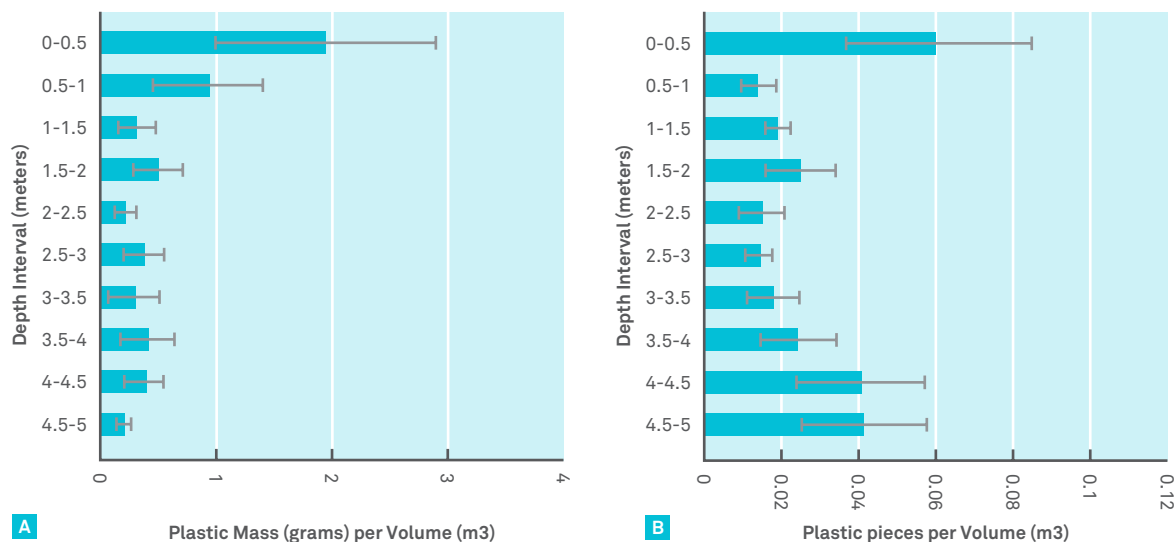
Figure 2.13 Depth profile of plastic pollution (N = 12 trawls) (a) plastic concentrations in grams per volume at different depth intervals; (b) plastic concentrations in pieces per volume at different depth intervals. Bars represent mean values and lines standard errors

2.3.2. RESULTS AND DISCUSSION

All 12 trawls collected plastic and this study registered 587 plastic pieces with a total mass of 1.2 grams. The collected plastic pieces where less circular in shape when compared to manufactured plastic particles (e.g. industrial pellets), thus strongly suggesting they are a result of the fragmentation of larger items. Mean sea surface (0 to 0.5 m) plastic concentrations ranged from 0 to 41,774 pieces per km² (median = 9,205.4 pieces per km², mean ± standard error = 12,472.8 ± 3,717.95 pieces per km²). Such values are similar to those reported by previous studies sampling oceanic waters at intermediate latitudes (see Figure 1.2 of section 1.2).

Mean plastic mass concentration (grams per m³) was higher in the top 0.5 m of the sampled locations and seemed to decrease exponentially with depth (Figure 2.13 a). Interestingly, the pattern of higher mass concentrations at the sea surface was present not only at "low" wind conditions (< 10 m/s, N = 6 trawls, Figure 2.14a, but also at "high" winds (→ 10 m/s, N = 6 trawls, Figure 2.14c). In contrast, mean plastic count concentration (plastic pieces per m³) did not present a consistent depth profile shape (Figure 2b). Plastic particles were concentrated at the sea surface at "low" wind conditions (< 10 m/s, N = 6 trawls, Figure 2.14b), but at "high" winds these plastics were equally distributed throughout the 5 meters of water sampled (→ 10 m/s, N = 6 trawls, Figure 2.14c). As such, these preliminary findings are in accordance with previous studies indicating a strong association between surface plastic concentration and wind speed (Kukulka et al., 2012; Reisser et al., 2013).

To the best of our knowledge, this is the first study assessing the depth profile of plastic concentration in terms of mass. Even at "high" winds, the plastic mass peak remained at the sea surface, exponentially decreasing with depth. This, it was deduced, is a consequence of larger plastics being more resistant to turbulent transport due to their higher mass, and therefore higher buoyancy values. The preliminary results presented here, together with the fact that large buoyant plastic objects (e.g. buoys, large fragments) are relatively resistant to wind-mixing processes, indicate that a platform fitted with a 2-3 meter-deep boom would capture the majority of the plastic mass present at its deployment location; at least when within the wind speed range experienced during this experiment. Further sampling using this new Multi-level Trawl, together with the development of models able to predict plastic mass depth profiles under different environmental conditions and plastic characteristics, will enhance our ability to quantify the capture efficiency of the proposed Ocean Cleanup Array.

WIND SPEED < 10M/S

A   Plastic Mass (grams) per Volume (m3)

B   Plastic pieces per Volume (m3)

WIND SPEED > 10M/S

C   Plastic Mass (grams) per Volume (m3)

D   Plastic pieces per Volume (m3)
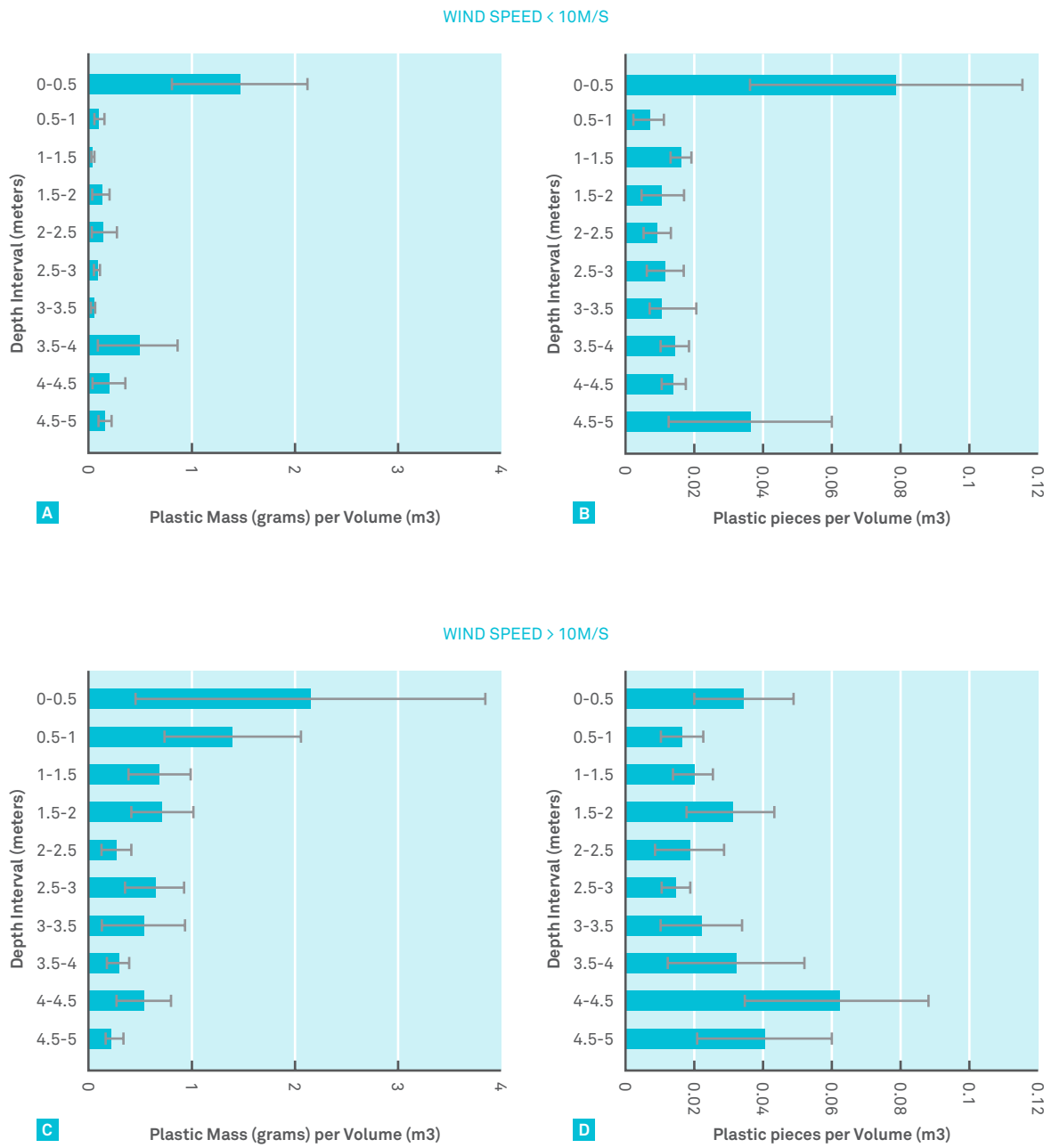
Figure 2.14 Depth profile of plastic pollution observed during "low" and "high" wind speed conditions. (a,b) plastic concentrations when wind speed was lower than 10 m/s (N = 6 trawls); (c,d) plastic concentrations when wind speed was higher or equal to 10 m/s (N = 6 trawls). Bars represent mean values and lines standard errors.

DETERMINATION OF LOCATION

BOYAN SLAT • EZRA HILDERING VAN LITH JAN DE SONNEVILLE

The choice of a preliminary location for our feasibility study will enable us to determine environmental conditions, seabed conditions, ocean depth and plastic finding efficiency; parameters essential as input data for later chapters concerning structural requirements, mooring configurations and logistics.

So far, we have been able to identify the North Pacific Subtropical Gyre as the focus area for this study, but since the region of highest plastic concentration has an estimated area of 1.5 million square kilometers, a more specific location is needed to be able to determine the above parameters.

We identified the following factors that influence decision-making, in approximate order of importance: Plastic pollution flux, ocean depth, shipping traffic density, environmental conditions and jurisdiction. However, changes in shipping traffic density and environmental conditions within the area of focus (which are within a significant wave height of 1 meter (Cox & Swail, 2001) will not be taken into consideration for determining a suitable location. Since the plastic accumulation zone within the North Pacific is, as a whole, located outside of national jurisdictions, this is also not a variable for the determination of the position.

Hence, in this chapter our understanding of plastic flux simulations, ocean depths and plastic sampling data will be combined to determine a suitable preliminary location.

2.4.1. POSSIBLE LOCATIONS BASED ON DISTRIBUTION MODELS

In the past few years, 3 models have been produced predicting the concentration of plastic debris in the world's oceans (Lebreton et al., 2012; Maximenko et al., 2012; van Sebille et al., 2012). All of them show a high concentration of plastic debris in the North Pacific subtropical gyre, but all show slightly different areas of highest concentration. Based on the images in their papers, Maximenko et al.'s model defines the area between 27-37° N and 130-150° W, Van Sebille et al.'s model shows that the highest concentration is between 27-36° N and 130-149° W, while Lebreton et al.'s model shows that it is between 27-33° N and 135-155° W.

2.4.2. POSSIBLE LOCATIONS BASED ON OCEAN DEPTH

The average ocean depth is around 5,000 meter for the area between 20 and 40 degrees North and 125 and 160 degrees West. As depth has enormous consequences for mooring costs, it is of great value to review shallower locations. With this in mind, looking at the map shown in Figure 2.15, it can be seen that two areas in this wide range are of potential interest; one featuring two closely located high mountains around 39° N, 147° W, and a larger area featuring many smaller mountains between 132-142° W and 27-33° N, especially between 28-31° N and 135-142° W. In both detailed maps the Ocean Cleanup Array is plotted to visualize the scale. At the bottom of this figure two height profile graphs are visible, taken from the dashed line, demonstrating the underwater topography.

2.4.3. POSSIBLE LOCATIONS BASED ON PLASTIC MEASUREMENTS

During their 1999 expedition Charles J. Moore et al. measured an average plastic concentration of 334,271 plastic particles per square kilometer in the top 15 cm of the water column (Moore et al., 2001). Based on 2,529 net tows during 2001- 2012, Law et al. mapped the concentration of plastic across the Northeast pacific, measuring a high concentration of plastics between approximately 28-35° N and 135-145° W. The highest concentration was found to be around 31°N, 139°W. All measurements with 106 or more particles km^{-2} were found within 1,100 km from this point, as seen in Figure 2.16 (K.L. Law et al., 2014).

2.4.4. CHOICE OF LOCATION

Plotting the search areas from the three plastic distribution models, the two relatively shallow areas, and the area in which the highest concentration of plastic was measured, the map in Figure 2.17 was produced.

It can be seen from Figure 2.17 that all three parameters, the computer models of high concentration areas (green), the measured high concentration area (blue), and an area with favorable seabed topography (red), intersect in an area stretching from 28° N to 31° N and from 135° W to 142° W. Based on the underwater topography in this area, the coordinates 30° N, 138° W have been chosen as the preliminary coordinates for this project.
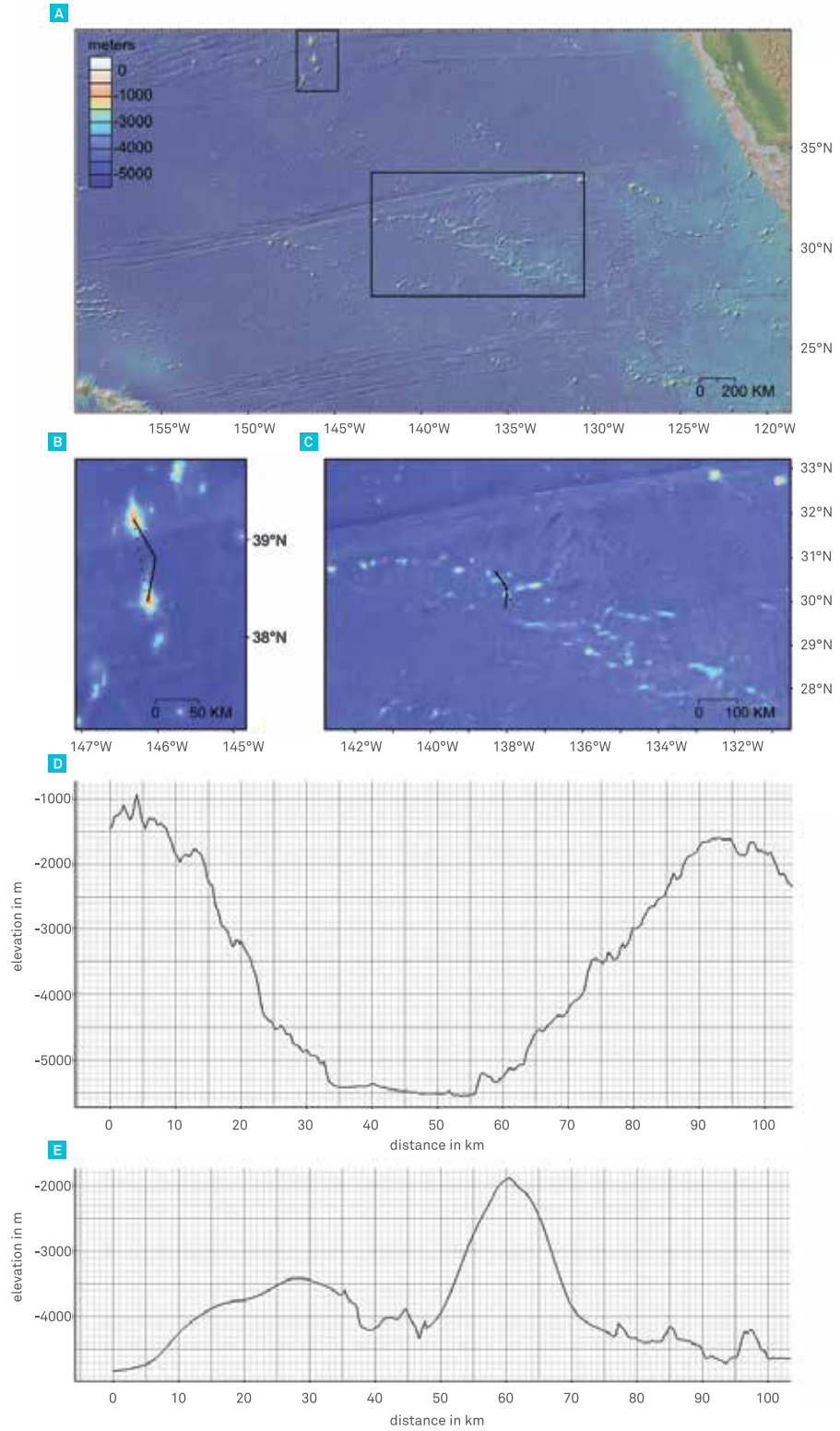
Figure 2.15 Combined satellite and bathymetric maps of A) the North Pacific Gyre, B) the Kermit Roosevelt Seamount and C) area between 132-142° W, 27-33° N, followed by depth profiles of D) the Kermit Roosevelt Seamount and E) area around 30° N, 138° W.

Longitudes histogram
of high concentration
latitudes (25°–41°)

Latitude histogram
of sampled
longitudes
(80°–180°W)
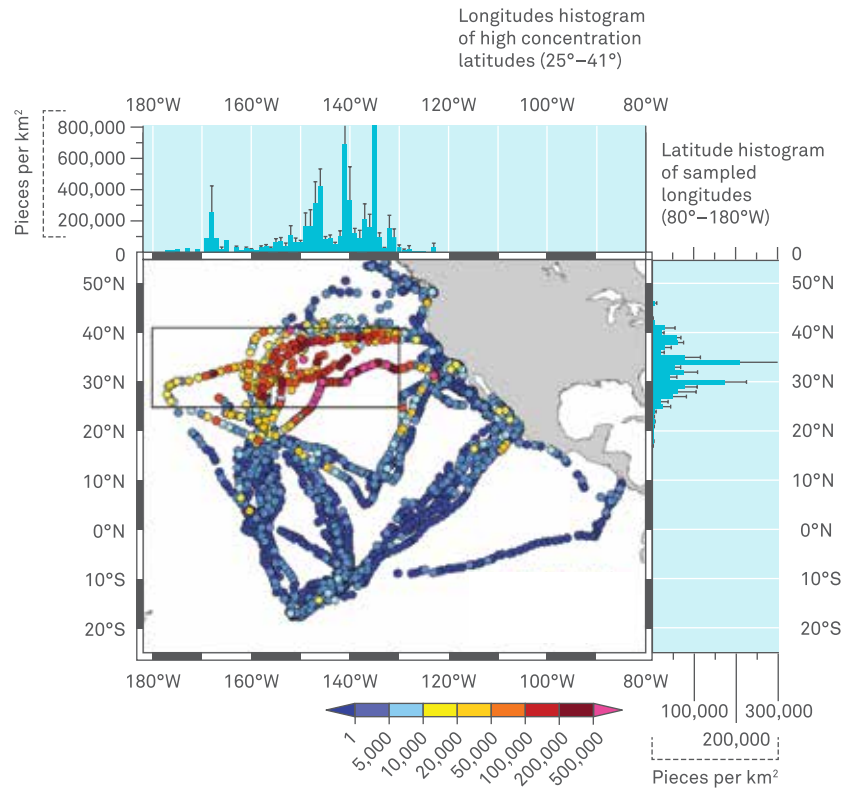
Figure 2.16 Map of microplastic concentration measurements by count, taken between 2001 and 2012. (Source: Law et al., 2014)
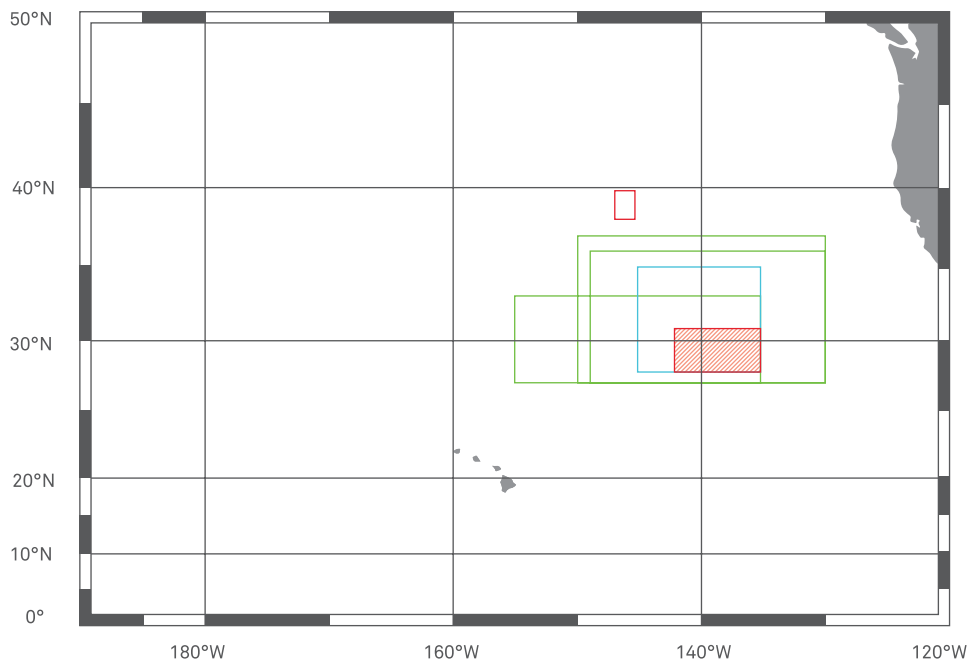
Figure 2.17 Map showing the areas in which the highest concentration of plastic debris has been predicted by Maximenko et al., Van Sebille et al. and Lebreton et al. (green), the highest measured plastic concentration (blue) and the areas containing favorable seabed conditions (red).

ENVIRONMENTAL CONDITIONS

JAIME LÓPEZ • ELENA PALLARES • EDWARD HORNSBY

It is important to understand the meteo-oceanographic conditions the Array will be exposed to on site. The local environment will have a high potential to impact the efficiency of the system. This will occur in two ways; either due to extreme weather causing physical damage or, as the Array is static, currents, winds and waves determining the rate at which plastic is collected. Data for the waves, wind and currents at 31°N, 142°W was analyzed. However, due to the lack of specific measurements at this location (excluding remote sensing data), reliable data from numerical modeling reanalysis was used. The results of this chapter will be used for engineering decisions like the calculation of the forces and dimensions relevant for the boom and platform designs. The results will be also used to calculate the predicted movement of plastic along the booms.

Please note that the location examined here (31°N, 142°W) was a preliminary location early in the study and is not the same preliminary location used in other sections (30°N, 138°W). However, although the site examined here lies 400 km to the west of the current preferred location, conditions are presumed to be fairly similar and the conclusions drawn are still viewed as appropriate.

The scope of this chapter will be the waves, winds and currents. However, we are aware other environmental influences are relevant, such as UV radiation (110-150 J/cm²) and salinity (36.8 g/kg). These factors will not be further explored in this chapter.

2.5.1. WAVES

Wind waves can be described as a vertical motion of the free surface at one horizontal position. These waves are present in the surface of oceans, seas, lakes or any water mass, and are generated by the wind. The duration, intensity and fetch (longitude) of the blowing wind will determine wave characteristics.

When the wind starts blowing the waves appear on the free surface and continue interacting with the wind and growing until they reach a maximum possible size for those conditions or until the wind stops. These waves are called wind sea or just sea. Once the winds stop no more waves are generated, but only propagated along the ocean. These waves, generated elsewhere and not affected by the local wind at that time, are called swell.

The characteristics of both types of waves are different. Wind sea is more energetic and irregular, with a greater wave height and shorter wave period. As waves propagate away from the generation area (become swell), they split into groups of common direction and wavelength, resulting in more regular waves, with longer periods.
Wind waves can be described as a stochastic process, however, they have been widely studied and this knowledge makes it possible to predict the sea state with numerical models.
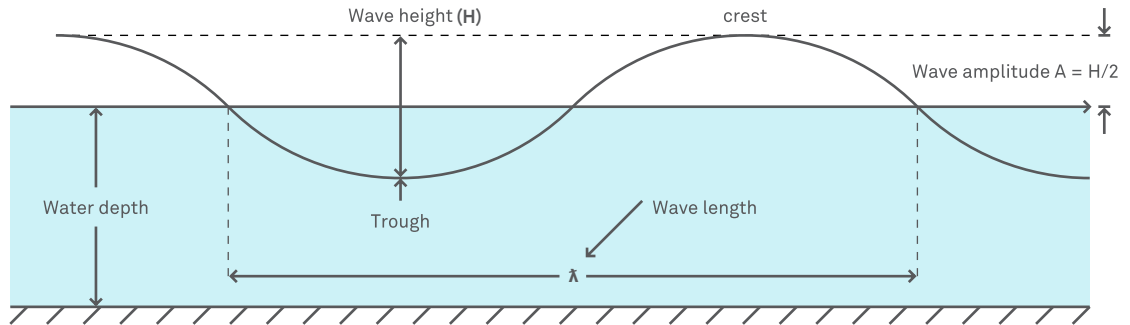
Figure 2.18 Wave parts

WAVE CHARACTERISTICS

There are several factors that can influence the generation of waves (see Figure 2.18). The most important are wind speed, fetch (defined as the distance of open water over which the wind blows constantly) and duration. Some other factors that can be considered are the width of the area affected by the fetch and the water depth.

The characteristics of the waves are determined by these factors:

- Wave height: the vertical distance between the highest (crest) and the lowest (trough) surface elevation in a wave
- Wave length: the horizontal distance between two consecutive crests
- Wave period: the time interval between the start and the end of the wave - wave direction: the propagation direction of the waves in degrees

Since wind waves are a stochastic process, the wave characteristics vary from one wave to another. However, in a given area a typical range of heights and periods are present. It is commonly accepted to use a mean value that represents all the waves for a period of time. Those variables are known as the significant wave height and significant wave period, and are obtained as the mean of the highest third of the values.

Figure 2.19 represents an average height of the highest one-third of the waves in a given time period.

WAVE GENERATION

The generation of surface wind waves (Figure 2.20) can be explained by the following mechanism:

1 Wind flows over the ocean surface
2 Wind turbulence results in pressure fluctuations over the surface
3 The surface rises and falls to account for these pressure changes
4 As the wind continues to blow a positive feedback between surface roughness and pressure fluctuations occurs. This shear instability means the surface waves grow exponentially.

Waves are therefore generated by wind-induced surface pressure, not by wind- induced surface friction.

ORBITAL MOTION

Wave velocity can be calculated as a function of the force of gravity, the wave length and the depth (Figure 2.21). The relationship between wave length and depth (whether the wave is in shallow, intermediate or deep water) is important for the calculation of speed.
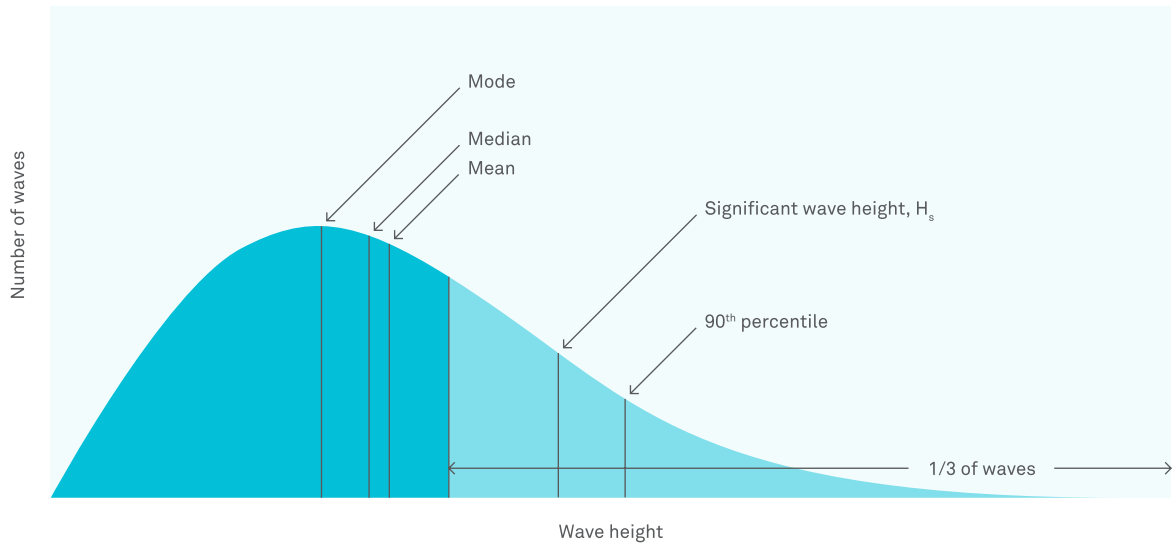
Figure 2.19 Statistical wave distribution

The velocities of particles of water are called orbital velocities because they correspond to the motion of the particles in closed, circular or elliptical orbits. It is important to note that the velocities in the crest of the wave are always oriented in the down-wave direction of the wave propagation, while the velocities in the trough of the wave are always oriented in the up-wave direction. Wavelength determines the size of the orbits, but depth determines the orbits' shape.

In deep water, the orbital radius decreases and particles move in circular paths. The particle velocities decrease exponentially with the distance to the surface. On the other hand, the orbits of water molecules in waves moving through shallow water are flattened by the proximity of the sea surface bottom, generating ellipses and, if shallow enough, the waves to 'break'.

STOKES DRIFT
In general, the particles move in closed orbits. However, as the wave height increases the orbits are no longer perfectly closed, and particles are displaced slightly from their previous position. This phenomenon is known as Stokes drift.

In Figure 2.22 and Figure 2.23, representations of this phenomenon are presented for both deep and shallow waters.

CONVENTIONS
Directional values are given in 16 equal sectors of 22.5° centered on 000°, 022.5°, and 337.5°.
Directional conventions are those commonly used in offshore engineering: wind and wave directions are taken from the approach; current directions are those towards which they flow.

Extreme values are given for a selection of return periods (2, 5, 10, 25, 50, 100, 200 and 500 years). These periods have been calculated through the adjustment of a Gumbel distribution function. It is important to note that the extreme values are usually calculated with long time series of instant measures. In this report, due to the lack of these measures in the area, the records contained in the different model data sets, which correspond to 1-hour average values every 3 hours, have been used. Therefore, some maximum values may have been missed due to working with partial samples. Consequently, this effect would lead to an underestimation in the extreme analysis. This underestimation is even more noticeable in the case of waves and currents where time series are shorter than desirable for this analysis.
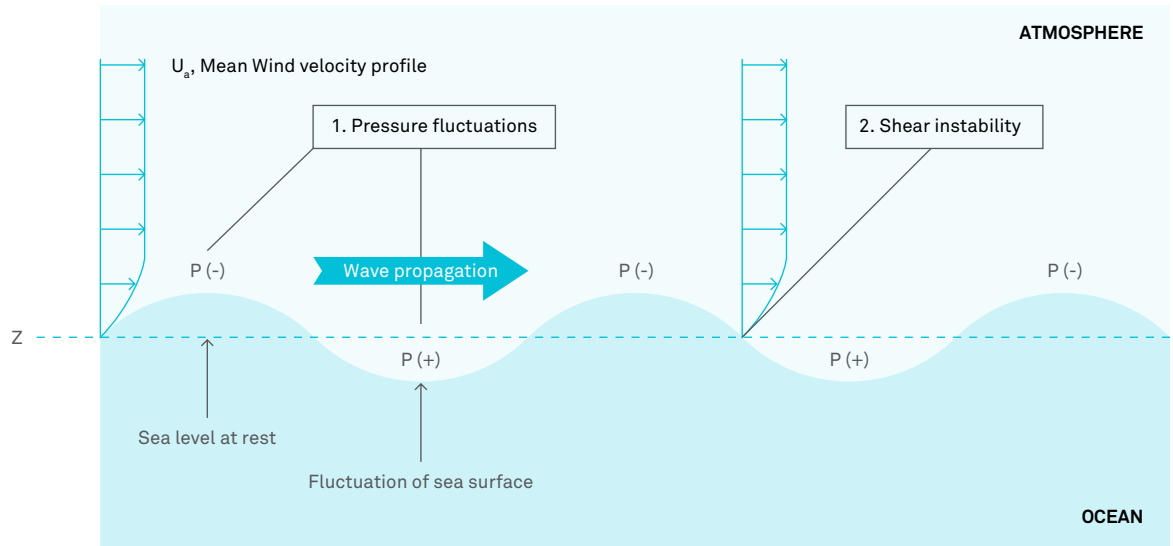
Figure 2.20 Wave generation

Wind values at 10 m height have been used in the analysis, due to the difficulty of taking surface winds, and also as the 10 m height level is frequently used in offshore engineering.

UNITS OF VARIABLES

The units of the variables used throughout the document are:

Direction	Degrees ($^{\circ}$)
Wind velocity	Meters per second (m/s)
Current velocity	Meters per second (m/s)
Significant wave height (H_s)	Meters (m)
Mean wave period (T_z)	Seconds (s)

The following analyses have been performed with numerical model data results at the location: 31°N-142°W.

WAVE SOURCE

Data from the USGODAE project (http://www.usgodae.org) was used for the wave analyses. GODAE stands for Global Ocean Data Assimilation Experiment and is a practical demonstration of near-real-time, global ocean data assimilation that provides, regular, complete descriptions of the temperature, salinity and velocity structures of the ocean in support of operational oceanography, seasonal-to-decadal climate forecasts and analyses, and oceanographic research.

Wave fields calculated with the Wave Watch III - NOAA/NCEP 3rd Generation Wave Model are available in the project server (Sharfstein, Dimitriou, & Hankin, 2005). Time series of significant wave height, primary wave direction and primary wave period every 3 hours, from 16th September 2003 to 25th January 2014 are also available there. However, after a first inspection of data, only data since 22nd January 2009 was analyzed.

Deep water

Wave direction

Intermediate depth

Wave direction

Very shallow water

Wave direction

Bottom

Bottom

Bottom
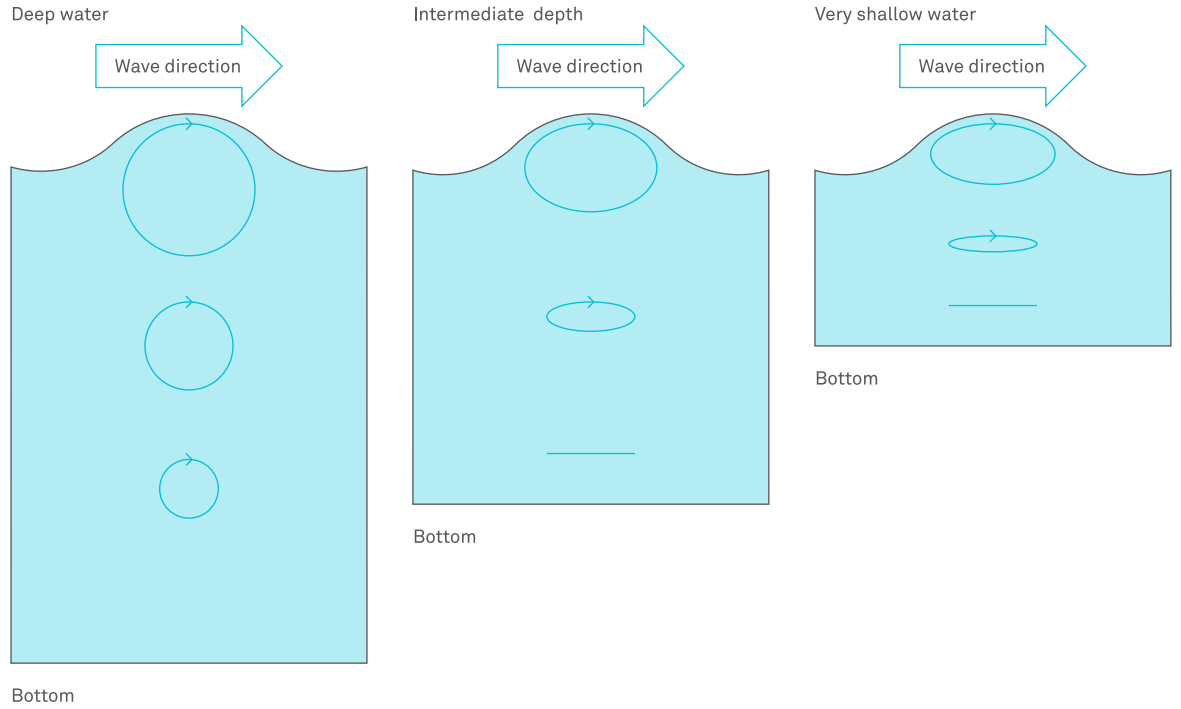
Figure 2.21 Orbital motion in deep water, intermediate-depth water, and very shallow water
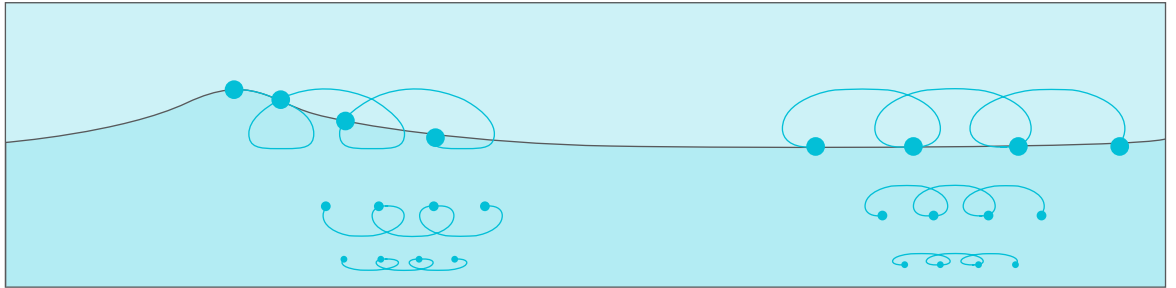
Figure 2.22 Stokes drift in shallow water waves
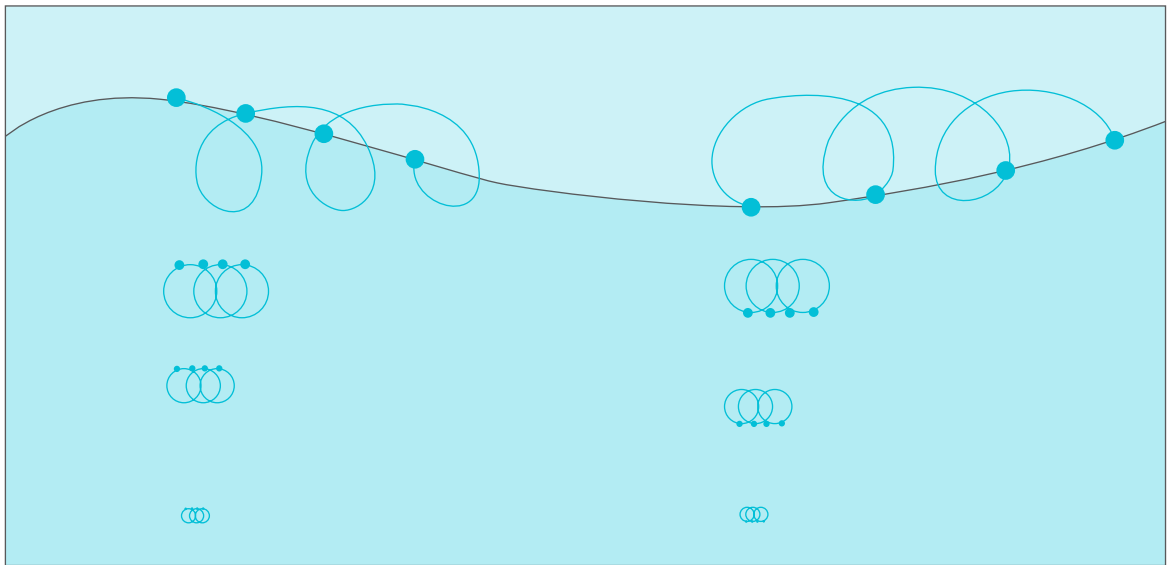
Figure 2.23 Stokes drift in a deeper water wave

TIME SERIES STATISTICAL DESCRIPTION

A significant wave height (H_s) and mean period (T_z) statistical description obtained for the Wave Watch III reanalysis, is shown in Table 2.4.

WAVE ROSE

Figure 2.24 calculated with the Wave Watch III reanalysis, shows predominant waves from the NW sector, and also some importance of the NE sector. Taking into account the wind analysis (Section 2.4.2), it can be said that waves from the NW sector are swells generated in the North Pacific Ocean, and that waves from the NE sector are sea waves.

RETURN PERIOD	H_s (M)	T_z (S)
MEAN	2.31	8.36
STANDARD ERROR	0.76	1.21
MEDIAN	2.09	8.09
STANDARD DEVIATION	1	1.76
VARIANCE	1.01	3.11
KURTOSIS	3.09	6.75
SKEWNESS	1.49	-0.91
RANGE	8.61	15.67
MAXIMUM	8.61	15.67
MINIMUM	0	0

Table 2.4 Significant wave Height (H_s) and mean period (T_z) statistical description

H_S (m)

>=7,5		3,0 − 4,5	Calms: 0,00%
6,0 − 7,5		1,5 − 3,0	
4,5 − 6,0		0,0 − 1,5	
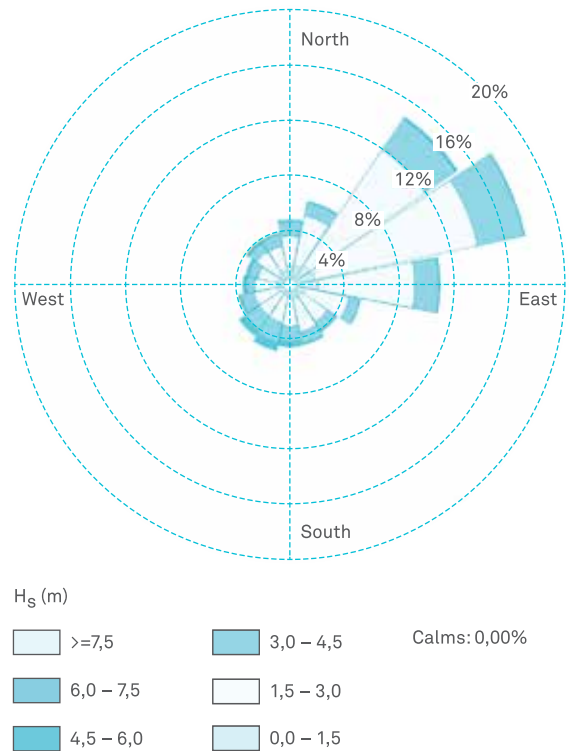
Figure 2.24 Significant wave height − wave from direction rose

Dir./Wind speed (m/s)	0.0 - 1.5	1.5 - 3.0	3.0 - 4.5	4.5 - 6.0	4.5 - 6.0	> 7.5	Total
N	0.49%	4.17%	1.02%	0.11%			5.79%
NNE	0.47%	3.42%	0.35%	0.01%			4.24%
NE	0.81%	5.02%	0.22%				6.04%
ENE	1.52%	6.55%	0.21%				8.27%
E	1.58%	3.91%	0.09%				5.58%
ESE	1.71%	1.82%	0.08%				3.61%
SE	1.84%	1.72%	0.12%				3.67%
SSE	1.99%	1.08%	0.14%	0.01%			3.22%
S	1.68%	1.07%	0.16%	0.01%			2.92%
SSW	1.07%	0.94%	0.20%	0.03%	0.03%		2.27%
SW	0.79%	1.23%	0.23%	0.06%	0.02%		2.32%
WSW	0.76%	1.62%	0.55%	0.23%	0.01%		3.18%
W	0.77%	2.79%	1.23%	0.45%	0.11%		5.35%
WNW	0.78%	8.00%	3.80%	1.07%	0.27%	0.03%	13.96%
NW	0.84%	11.98%	4.67%	1.05%	0.17%	0.04%	18.74%
NNW	0.73%	6.67%	2.91%	0.46%	0.06%		10.82%
Sub-total	17.83%	61.99%	15.95%	3.48%	0.68%	0.07%	99.99%
Calms							0.00%
Missing/Incomplete							0.01%
Total							100.00%

Table 2.5 Significant wave height/wave from direction joint frequency distribution

Dir./Wind speed (m/s)	5.0 - 7.0	7.0 - 9.0	9.0 - 11.0	11.0 - 13.0	>= 13.0	Total
N	0.21%	3.16%	2.11%	0.29%	0.03%	5.79%
NNE	0.40%	2.68%	1.01%	0.15%		4.24%
NE	0.82%	4.16%	0.98%	0.08%		6.04%
ENE	1.06%	5.73%	1.38%	0.11%		8.27%
E	0.92%	3.81%	0.77%	0.08%	0.01%	5.58%
ESE	0.22%	2.16%	1.18%	0.03%	0.02%	3.61%
SE	0.16%	1.63%	1.76%	0.12%		3.67%
SSE	0.16%	0.94%	1.74%	0.38%		3.22%
S	0.07%	0.73%	1.45%	0.66%	0.01%	2.92%
SSW	0.10%	0.83%	0.90%	0.38%	0.06%	2.27%
SW	0.08%	0.92%	0.90%	0.37%	0.05%	2.32%
WSW	0.10%	1.29%	1.44%	0.28%	0.08%	3.18%
W	0.10%	1.72%	2.52%	0.88%	0.13%	5.35%
WNW	0.08%	2.46%	7.10%	3.55%	0.76%	13.96%
NW	0.14%	3.50%	10.74%	3.93%	0.45%	18.74%
NNW	0.27%	3.82%	5.34%	1.24%	0.14%	10.82%
Sub-total	4.91%	39.53%	41.31%	12.53%	1.72%	99.99%
Calms						0.00%
Missing/Incomplete						0.01%
Total						100.00%

Table 2.6 Mean period/wave from direction joint frequency distribution table

JOINT FREQUENCY DISTRIBUTION TABLES

The joint distribution table significant wave height vs direction is shown in Table 2.5.

The joint distribution table mean period vs direction is shown in Table 2.6.

Both Table 2.5 and Table 2.6, summarizing the Wave Watch III reanalysis data, confirm the predominance of waves from the NW and the adjacent sectors, with more than 43% of the total waves. More than 60% of the significant wave height records are included in the range between 1.5 and 3m, and more than 95% of the waves are smaller than 4.5 m. More than 80% of the analyzed mean wave periods, are in the 7 to 11 seconds range.

EXTREME WAVES

Different return periods for significant wave height and mean period are shown in Table 2.7.

As explained before, these values have been calculated with the available data (Wave Watch III reanalysis). Real values for the different return periods, calculated with wave buoys measurements, should be higher than those presented here.

RETURN PERIOD	HS (M)	T_z (S)
2	6.71	14.77
5	8.19	15.58
10	9.16	16.12
25	10.39	16.79
50	11.31	17.29
100	12.21	17.79
200	13.12	18.29
500	14.31	18.94

Table 2.7 Return periods for significant wave heights (H_s) and mean periods (T_z)

	WIND SPEED (m/s)
MEAN	6.23
STANDARD ERROR	2.12
MEDIAN	6.05
STANDARD DEVIATION	2.74
VARIANCE	7.52
KURTOSIS	1.14
SKEWNESS	0.65
RANGE	21.88
MAXIMUM	21.95
MINIMUM	0.07

Table 2.8 Wind speed statistical description for the NOGAPS reanalysis data

EVENTS

For design purposes it is important to know the number of times that certain values of significant wave height are exceed, and the duration of those episodes. For the present study, values of 5, 5.5, 6, 6.5, 7 and 7.5 m of H_s have been chosen.

Criteria to set the events duration:

1 Eight records per day are available, so 1 record corresponds to a 3 hour time interval. This way, each time the threshold value is exceeded, the duration will be increased in 3 hours.

2 Single peak events duration will be counted from the first value over the threshold to the last value over the threshold.

3 During the event, if H_s falls under the threshold value minus 10% of the threshold value, the event is closed, however, if the value decreases under the threshold value but not under the threshold value minus 10% of the threshold value, and after that the threshold is exceeded, only one double peak event would be counted with the total duration. The duration will be counted until the last value over the threshold (not the value over the threshold minus 10% of the threshold value).

NUMBER OF EVENTS WHERE H_s > 5 m AND DURATION.

2009. 12 events. Duration (h): 15, 6, 12, 45, 24, 15, 9, 6, 39, 9, 12, 45
2010. 18 events. Duration (h): 12, 21, 63, 3, 126, 12, 18, 27, 30, 12, 24, 30, 12, 12, 21, 45, 6, 36
2011. 5 events. Duration (h): 9, 15, 9, 45
2012. 9 events. Duration (h): 18, 33, 3, 93, 21, 18, 39, 42
2013. 4 events. Duration (h): 9, 6, 3, 18

NUMBER OF EVENTS WHERE H_s > 5.5M AND DURATION.

2009 . 8 events. Duration (h): 3 , 12 , 15 , 6 , 3 , 18 , 3, 24
2010 . 11 events. Duration (h): 12, 39, 120, 15, 6, 15, 24, 27, 3, 15, 21 2011 . 2 events. Duration (h): 12, 36
2012. 7 events. Duration (h): 12, 9, 54, 21, 15, 27, 30
2013 . 1 events. Duration (h): 9
Number of events where H_s > 6m and duration.
2009. 4 events. Duration (h): 6, 3, 12, 12
2010. 8 events. Duration (h): 21, 114 , 6 , 12 , 12 , 18 , 12 , 6
2011. 1 event. Duration (h): 3
2012. 5 events. Duration (h): 12, 12, 3, 15, 21
2013. 1 event. Duration (h): 6

NUMBER OF EVENTS WHERE H_s > 6.5 M AND DURATION.

2010. 5 events. Duration (h): 21, 24, 39, 6, 9 2012. 2 events. Duration (h): 9, 9
Number of events where H_s > 7m and duration.
2010. 4 events. Duration (h): 9, 9, 36, 9
Number of events where H_s > 7.5m and duration.
2010. 1 event. Duration (h): 30

2.5.2. WIND

WIND SOURCE
WIND source link can be found in USGODAE website (US-GODAE, 2014) http://www.usgodae.org/pub/outgoing/fn-moc/models/nogaps

As in the case of waves, data from the USGODAE project have been used for this analysis.

Wind fields from the Navy Operational Global Atmospheric Prediction System (NOGAPS) model of the Navy's Fleet Numerical Meteorology and Oceanography Center (FNMOC) are available on the project server.

Time series of wind at 10 m height (u and v components) from 1st January 2004 to 12th March 2013, with a record every 3 hours, have been analyzed. However, since the boom only stretches up to 1 m to 1.5 m above the water surface, a power law can be calculated with $v = v10\ m*(z/10)alpha$, where alpha is the shear coefficient.

In the literature, the wind shear coefficient is generally approximated between 0.14 and 0.2 (Sen, 2012). This way a wind of 10 m/s at 10 m over the sea level, should represent a wind between 6.3 and 7.24 m/s at 1m height. This way the results obtained and shown in this section, can be transformed for necessary purposes.

TIME SERIES STATISTICAL DESCRIPTION
Wind speed statistical description for the NOGAPS reanalysis data is shown in Table 2.8.

WIND ROSE
Figure 2.25 calculated for the NOGAPS reanalysis data shows that predominant wind blows from the NE-E sectors.

Hs (m)

>=20,0	8,0 – 12,0	Calms: 0,00%
16,0 – 20,0	4,0 – 8,0	
12,0 – 16,0	0,0 – 4,0	
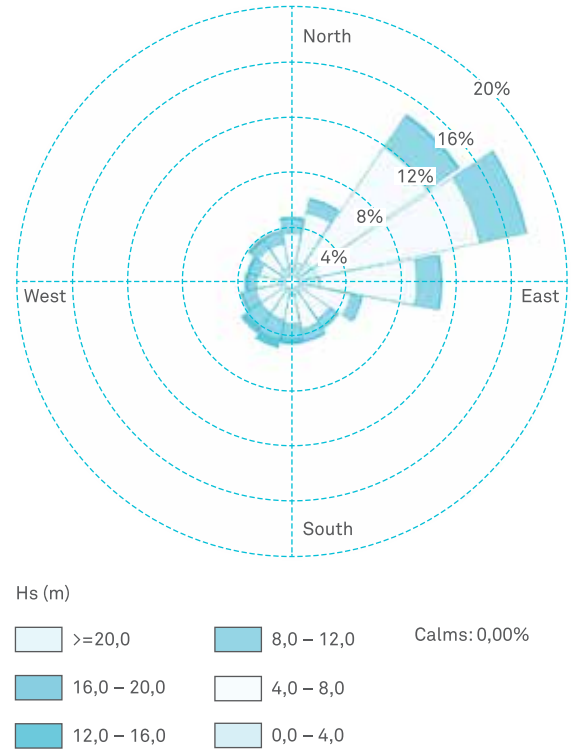
Figure 2.25 Wind from direction rose for NOGAPS reanalysis data

Dir./Wind speed (m/s)	0.0 – 4.0	4.0 – 8.0	8.0 – 12.0	12.0 – 16.0	16.0 – 20.0	>= 20.0	Total
N	1.40%	2.19%	0.98%	0.15%	0.02%	0.02%	4.73%
NNE	1.49%	3.65%	0.96%	0.12%			6.22%
NE	1.78%	10.07%	2.72%	0.17%			14.74%
ENE	1.88%	12.01%	3.45%	0.09%			17.42%
E	2.01%	7.02%	1.76%	0.09%			10.89%
ESE	1.22%	3.18%	0.82%	0.03%			5.25%
SE	1.06%	2.20%	0.74%	0.09%	0.02%		4.10%
SSE	1.04%	2.46%	0.86%	0.09%	0.02%		4.46%
S	0.98%	2.02%	1.12%	0.34%	0.03%		4.49%
SSW	0.87%	1.92%	1.48%	0.51%	0.08%	0.01%	4.87%
SW	0.81%	1.90%	1.28%	0.39%	0.10%	0.02%	4.50%
WSW	0.93%	1.76%	0.94%	0.20%	0.03%		3.85%
W	1.12%	1.46%	0.60%	0.19%	0.02%	0.01%	3.40%
WNW	0.91%	1.49%	0.69%	0.22%	0.03%		3.35%
NW	1.12%	1.82%	0.72%	0.19%	0.04%		3.88%
NNW	1.11%	1.77%	0.86%	0.12%	0.00%		3.87%
Sub-total	19.70%	56.91%	20.00%	2.95%	0.40%	0.04%	100.00%
Calms							0.00%
Missing/Incomplete							0.00%
Total							100.00%

Table 2.9 The wind speed vs wind direction joint frequency distribution

JOINT FREQUENCY DISTRIBUTION TABLES
The wind speed vs wind direction joint distribution is shown in Table 2.9

Table 2.9, summarizing the NOGAPS reanalysis data, shows that more than 55% of the analyzed winds blow with a speed between 4 and 8 m/s, and more than 95% of the wind speed records are lower than 12 m/s. 43% of wind records blow from the ENE and adjacent sectors.

EXTREME WINDS
Different return periods for wind speed are shown in Table 2.10.

As explained earlier, these values have been calculated with the available data. Real values for the different return periods, calculated with wind measurements, should be higher than the ones presented.

RETURN PERIOD	WIND SPEED (M/S)
2	19.1
5	22.63
10	24.97
25	27.93
50	30.12
100	32.3
200	34.47
500	37.33

Table 2.10 Return periods for wind speed

	SURFACE LAYER	2M DEPTH LAYER
MEAN	0.14	0.14
STANDARD ERROR	0.06	0.06
MEDIAN	0.13	0.13
STANDARD DEVIATION	0.08	0.08
VARIANCE	0.006	0.006
KURTOSIS	0.24	0.26
SKEWNESS	0.61	0.61
RANGE	0.52	0.51
MAXIMUM	0.52	0.51
MINIMUM	0	0

Table 2.11 Statistic values for the current speed at the surface and the 2 m depth layers.

2.5.3. CURRENTS

CURRENTS SOURCE

Currents source link can be found in (Ecowatch, 2014) http://ecowatch.ncddc.noaa.gov/thredds/catalog.html The U.S. Navy Operational Global Ocean Model (NCOM) was developed by the Naval Research Laboratory Journal and is maintained by the Naval Oceanographic Office. It includes OSU Tides (http://volkov.oce.orst.edu/tides/) forcing (C. N. Barron, Kara, Hurlburt, Rowley, & Smedstad, 2004; C.N. Barron, Kara, Martin, Rhodes, & Smedstad, 2006).

Surface currents and currents at 2 m depth have been analyzed for the period: 2009/05/04-2013/03/18 with a record every 3 hours.

TIME SERIES STATISTICAL DESCRIPTION

Current speed (m/s) statistical description for the NCOM reanalysis data at surface layer and 2m depth layer are shown in Table 2.11.

Statistical results are similar for both layers. That implies that, as expected, the first few meters layer of the ocean show barotropic behavior at the analyzed point, and it is possible to venture that these currents are generated due to wind effects.
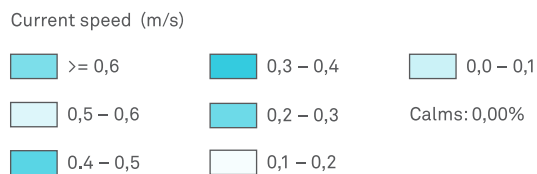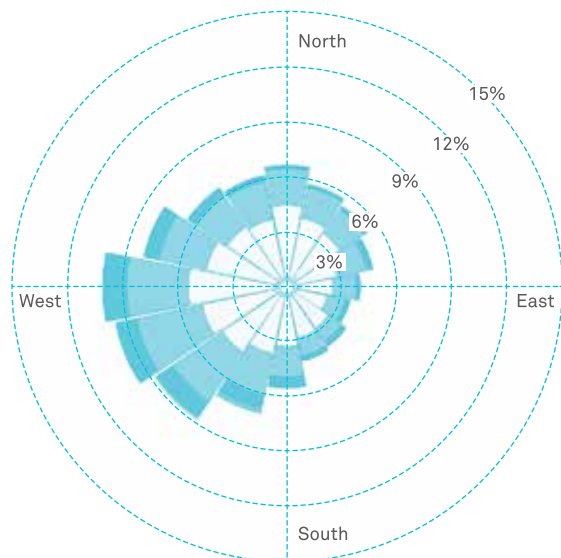
Figure 2.26 Surface layer current rose
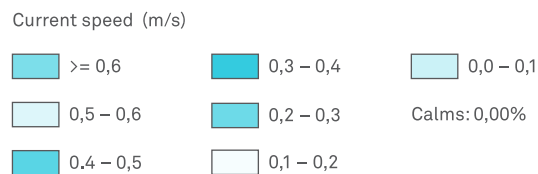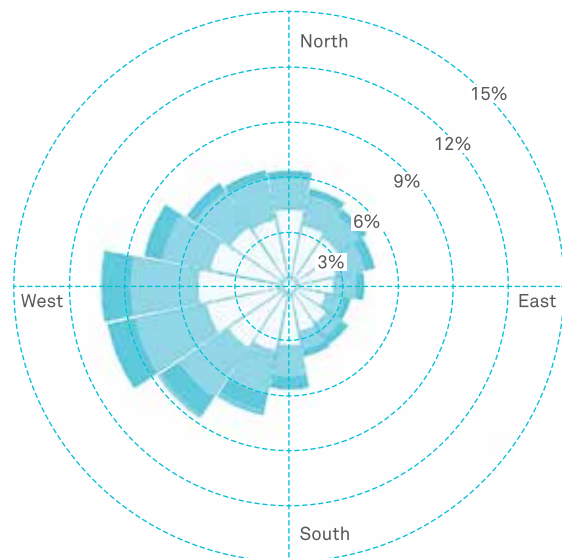
Figure 2.27 2 m depth layer current rose

CURRENT ROSES

Current roses for the NCOM reanalysis data, at the surface and at 2 m depth are shown in Figure 2.26 and Figure 2.27.

These current roses agree with the wind rose, where NE-E winds cause currents in the ocean (at least at the surface) to the W-SW sectors. Main winds main are from ENE, which corresponds to a main current to the WSW, however, and due to the Ekman (NASA, 2014) spiral, the main current direction shows an angle to the right (W) with regard to the wind direction.

JOINT FREQUENCY DISTRIBUTION TABLES

The surface current speed vs surface current direction joint frequency distribution is shown in Table 2.12.

The 2 m depth layer current speed vs 2 m depth layer current direction joint frequency distribution is shown in Table 2.13.

For both tables, obtained with the NCOM reanalysis data, the current speeds at the surface and at the 2 m depth are between 10 and 20 cm/s in almost 50% of the data sets, and 90% of current speeds are less than 30 cm/s.

Dir./Wind speed (m/s)	0.0 - 0.1	0.1 - 0.2	0.2 - 0.3	0.3 - 0.4	0.4 - 0.5	>=0.5	Total
N	0.55%	3.66%	1.73%	0.30%	0.04%	0.02%	6.21%
NNE	0.54%	2.90%	1.67%	0.27%	0.04%		5.36%
NE	0.61%	2.63%	1.49%	0.31%	0.03%		5.01%
ENE	0.53%	2.11%	1.63%	0.42%	0.06%		4.69%
E	0.59%	1.86%	1.25%	0.31%	0.03%		3.99%
ESE	0.42%	1.64%	1.03%	0.25%	0.04%		3.34%
SE	0.42%	2.05%	0.97%	0.38%	0.02%		3.79%
SSE	0.55%	2.01%	1.06%	0.25%	0.07%		3.89%
S	0.61%	2.66%	1.72%	0.53%	0.09%	0.01%	5.55%
SSW	0.62%	3.04%	2.42%	0.79%	0.28%	0.03%	7.10%
SW	0.54%	3.55%	3.29%	1.10%	0.22%	0.02%	8.60%
WSW	0.70%	3.99%	4.02%	1.39%	0.06%		10.02%
W	0.69%	4.33%	3.71%	1.45%	0.10%		10.15%
WNW	0.60%	3.86%	2.70%	0.87%	0.06%		7.99%
NW	0.57%	3.37%	2.37%	0.47%	0.02%		6.71%
NNW	0.58%	3.18%	2.31%	0.36%	0.02%		6.37%
Sub-total	8.97%	46.24%	32.96%	9.33%	1.18%	0.06%	98.74%
Calms							0.00%
Missing/Incomplete							1.26%
Total							100.00%

Table 2.12 Frequency distribution of surface current speed vs surface current direction

Dir./Wind speed (m/s)	0.0 - 0.1	0.1 - 0.2	0.2 - 0.3	0.3 - 0.4	0.4 - 0.5	>=0.5	Total
N	0.56%	3.92%	1.96%	0.21%	0.02%	0.02%	6.59%
NNE	0.56%	3.30%	1.70%	0.16%	0.01%		5.66%
NE	0.71%	2.83%	1.55%	0.26%			5.29%
ENE	0.51%	2.28%	1.69%	0.32%	0.02%		4.77%
E	0.62%	1.92%	1.28%	0.19%	0.02%		3.98%
ESE	0.58%	1.67%	1.03%	0.22%	0.04%		3.50%
SE	0.50%	2.22%	0.91%	0.29%	0.02%		3.90%
SSE	0.59%	2.26%	0.99%	0.25%	0.04%		4.09%
S	0.48%	2.78%	1.67%	0.53%	0.07%	0.01%	5.47%
SSW	0.58%	3.15%	2.29%	0.72%	0.28%	0.02%	6.96%
SW	0.65%	3.64%	3.32%	0.96%	0.15%	0.01%	8.62%
WSW	0.72%	4.02%	3.68%	1.13%	0.05%	0.01%	9.48%
W	0.81%	4.59%	3.38%	1.23%	0.06%		9.94%
WNW	0.58%	3.92%	2.68%	0.79%	0.04%		7.91%
NW	0.71%	3.29%	2.07%	0.49%	0.02%		6.49%
NNW	0.57%	3.24%	2.11%	0.27%	0.01%		6.12%
Sub-total	9.58%	48.41%	31.91%	7.94%	0.85%	0.05%	98.74%
Calms							0.00%
Missing/Incomplete							1.26%
Total							100.00%

Table 2.13 Frequency distribution of 2 m depth layer current speed vs 2 m depth layer current direction

RETURN PERIOD	SURFACE CURRENT SPEED (M/S)	2M DEPTH LAYER CURRENT SPEED (M/S)
2	0.48	0.45
5	0.53	0.51
10	0.56	0.55
25	0.60	0.60
50	0.63	0.64
100	0.66	0.68
200	0.68	0.71
500	0.72	0.76

Table 2.14 Return periods for current speed at the surface and at 2 m depth

EXTREME CURRENTS

Different return periods for current speed at the surface and at 2m depth are shown in Table 2.14.

As explained earlier, these values have been calculated with available data. Real values for the different return periods, calculated with current meter measurements, should be higher than the ones presented.

COUNTERCURRENT EVENTS

Due to the presence of eddies or other phenomena, during some time periods currents in the operation area can flow in a direction that does not match with the expected. These countercurrent events, mainly in case of long events, are an important problem because during these events the plastics do not reach the booms.

In order to know the importance and, mainly, the duration of these events, the mean current direction has been calculated with the full time series. The resultant mean current velocity and direction obtained for the full analyzed period is 0.038 m/s to 265°.

For this analysis, the episodes of currents with directions under 175° or over 355°, from the NCOM reanalysis data, have been used, and their duration has been calculated and the results are depicted in Figure 2.28.

More than 90% of the countercurrent events have durations of 18 hours or less and for almost 60% of the events the duration is shorter than or equal to 9 hours.
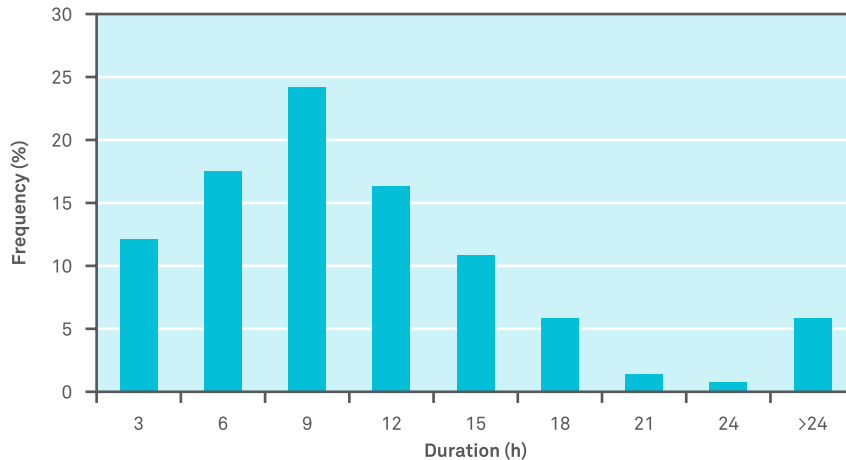
Figure 2.28 Countercurrent frequencies at various durations

2.5.4. PLASTIC DRIFTING CAUSES

Plastics in the ocean are exposed to winds, waves and currents. These forces are strongly related and the interaction between them is not negligible.

Wave conditions, by means of the Stokes drift, the radiation stress and wave breaking, can modify the currents. For nonlinear and periodic water waves, accurate results on the Stokes drift have been computed and tabulated (J. M. Williams, 1981; J.M. Williams, 1986). Currents also have a contribution on waves, basically due to wave refraction. The interaction between surface winds and waves was studied by Charnock (1955) who proposed an estimation of the surface drag created by the waves as a function of the wind speed (Charnock, 1955). More recent studies have revisited the topic proposing new parameterizations (e.g. (Johnson, Højstrup, Vested, & Larsen, 1998)). Wind-stress is also altered due to sea surface roughness, Taylor and Yelland (2001) proposed a dependence of the surface roughness on the wave height and the wave length (Taylor & Yelland, 2001).

As explained, the interaction between winds, waves and currents is significant, and so, all these forces act on the plastics and contribute to the plastic drift. However, the main forces involved in plastic drift are winds and currents, where winds would be the dominant drifting force for larger plastics with an emerged part, and currents would be dominant for submerged microplastics. In order to confirm this hypothesis and also to quantify the contribution of each force, laboratory experiments are required.

DETERMINATION OF ARRAY LENGTH AND CLEANUP TIME

Although the amount of plastic that will be captured depends on many efficiency factors (including boom capture efficiency and collection efficiency), field efficiency is probably the most dominant factor. Field efficiency is defined as the percentage of plastics that will be caught by the cleanup array during its deployment time within the gyre, assuming that boom capture efficiency and collection efficiency are both 1. This factor is determined by two parameters; the total length of the structure perpendicular to the dominant direction of the current (referred to as total array length or total collection width), and the deployment time. When either one or both of these variables increase, it should result in an increase in field efficiency.

To study the relation between the field efficiency, total array length and deployment time, two different computational models predicting the geographical distribution and trajectories of plastic pollution in the oceans have been used.

2.6.1. VAN SEBILLE MODEL

ALEXANDER RAU • MAXIMILIAN MICHELS
TIM LANDGRAF • JAN DE SONNEVILLE • LEONID PAVLOV

Near-surface debris flows in the oceans are used as the basis of this model. The used model was provided by Eric van Sebille, and is based on previous published work (Eric van Sebille et al., 2012).

Van Sebille and coworkers used observational drifter (a type of buoy) data from the Global Drifter Program to create the model. In their paper (van Sebille et al., 2012) the results from global flow simulations over a period of 1,100 years are presented. After the first 10 years of simulation, the model confirms high plastic concentrations in five subtropical gyres. The simulation also predicts a sixth garbage patch forming in the Barents Sea. For the following years the simulation suggests a dynamic process of patch shrinking and growing. The simulation shows that within 500 years, patches reach their maximum size and begin to shrink afterwards, with the exception of the North Pacific patch, which is said to be the largest attractor of global debris.

2.6.1.1. MODEL EXPLANATION

The Van Sebille model uses the drifter data, and calculates predictions based on the chance that a drifter buoy will arrive in another place two months later. As the starting place is not a single point, but an area of 1° longitude x 1° latitude, two buoys in this starting area can end up in two different locations after two months. These possible end- location areas all receive a certain probability of occurrence, the sum of all probabilities always being equal to unity up to 1, see Figure 2.29.
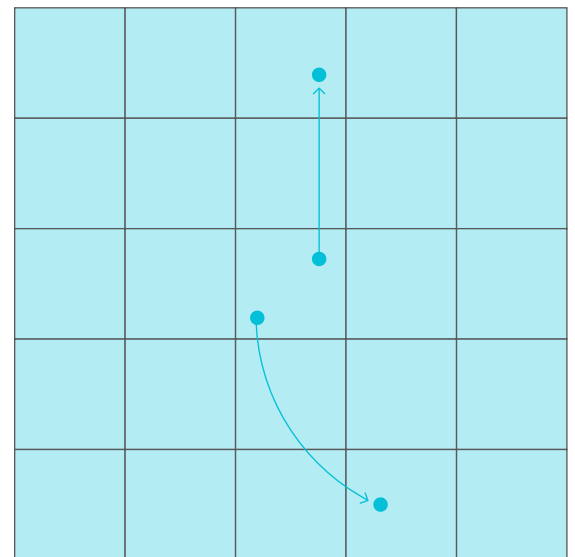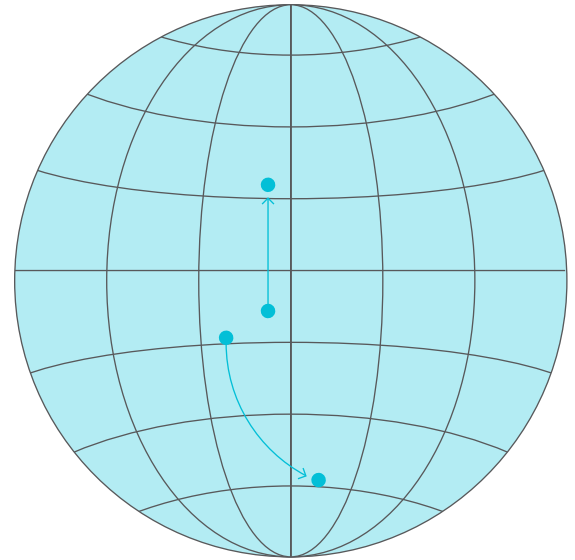
Figure 2.29 From within one area of 1° longitude x 1° latitude, two example drifter buoys' trajectories are recorded for a period of two months. These end locations then obtain an occurrence probability of 0.5 each.

Using repeated prediction, one can look at the probability of a drifter buoy ending up at a certain location after two iterations (four months) or longer. As ocean flows are different throughout the year, the probability scores, based on the drifter buoy data, are estimated six times, each time representing a two month period - thus amounting to a whole year. One degree of latitude corresponds to approximately 111 km everywhere on the planet, but 1° in longitude has a metric distance of something between 111 km at the equator and 0 km at the poles. Since the five large gyres are located relatively close to the equator, the estimated average grid cell area used in the computations was set to ~10,000 km².

INTRODUCING THE OCEAN CLEANUP ARRAY

The Ocean Cleanup array is modeled as a line with a specific position, orientation and length. More precisely, the position and length were translated into two points representing the ends of the line segment. With respect to the initial position, orientation, length and especially longitude the calculated two points tackled the mentioned problem of non-linear longitude distances. The line extremities are placed in the centers of the cells. See also Figure 2.30.

PLASTIC CAPTURE

Each non-zero probability for an end position corresponds to plastic flows that are assumed to be linear. Plastic debris that crosses the cleaning array line is assumed to be captured by the array. For this process it is irrelevant:

A from which side of the cleaning array line the flow of debris passes;

B what is the incidence angle at which the debris approach the array;and

C what the absolute mass or volume of the plastic flowing through the array is.
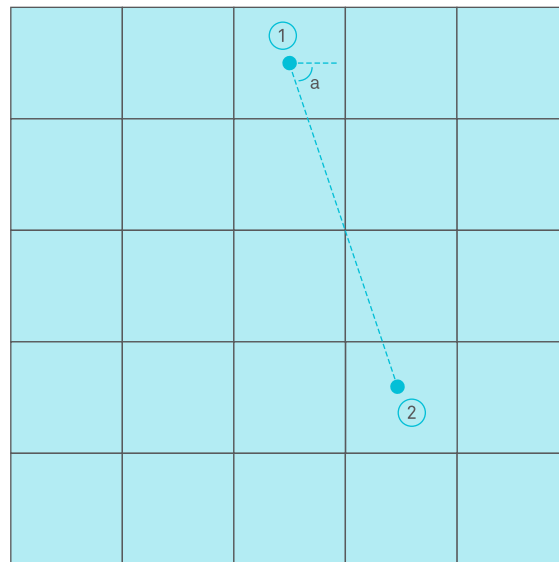
a = 0 . 15 . 30 .45 .60 .75 .90...360°

Figure 2.30 Schematic representation of The Ocean Cleanup array

2.6.1.2. METHODS

The plastic is released into the model at different starting locations corresponding to the coastal areas (see Figure 2.31). In the current implementation of the model the global mass of plastic is not expressed in quantities such as mass or volume, but instead an equivalent value of unity is used to represent the total amount of plastic particles in the model. The results of all efficiency calculations in turn are given as fractions of the total amount of particles. Based on the drifter buoy data, the location of certain plastic particles in the ocean is predicted based on the recorded paths of the drifters. Each path can be visualized as a line, and caries a certain fraction of total debris.

An example of debris capture is shown in Figure 2.32. As the particle flow is predicted the intersection/collision with the array can be detected. The equivalent plastic content corresponding to each equivalent particle allows monitoring the plastic capture over time. All lines with a color other than blue intersect the array.
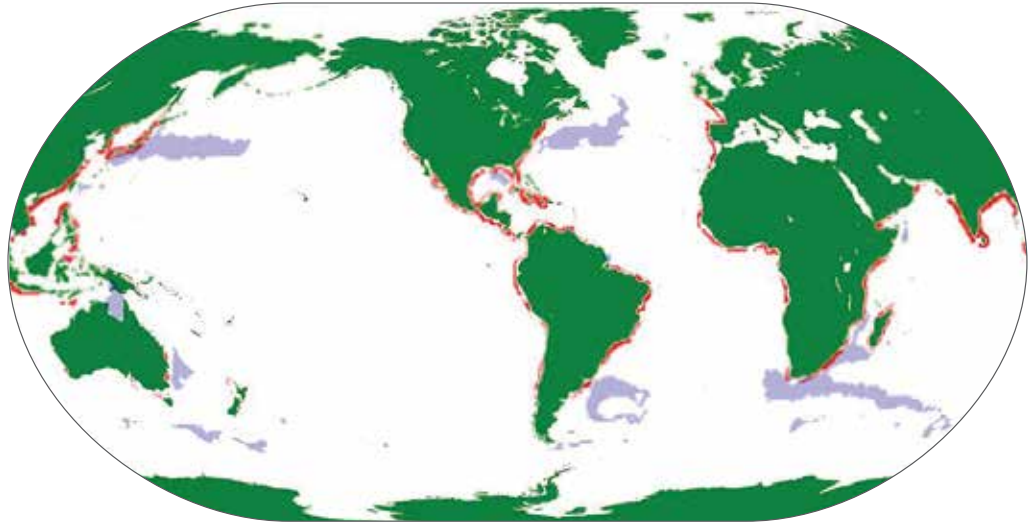
Figure 2.31 Initial simulation of plastic distribution. In red and light-blue the start locations of plastic release are visualized.
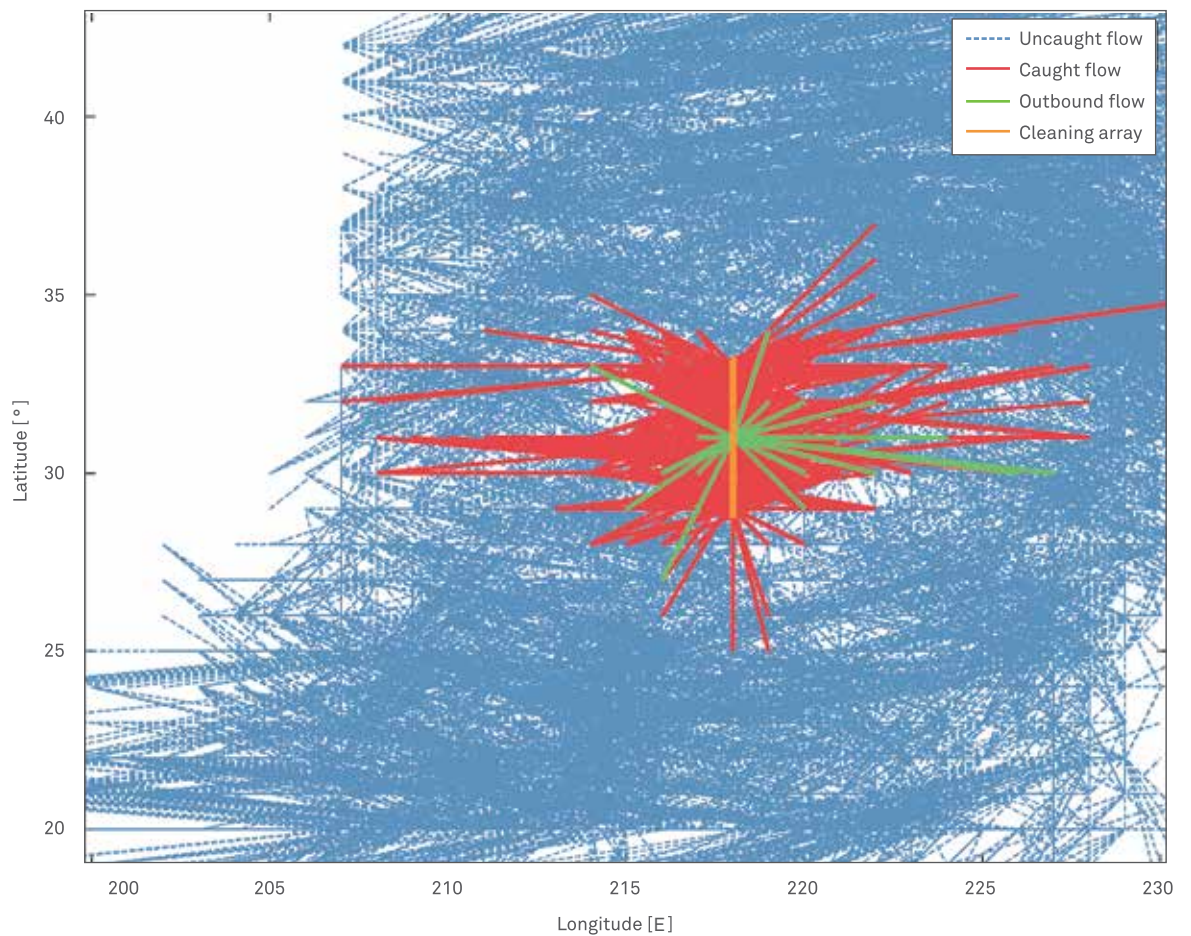
Figure 2.32 The debris flow within a certain area around the ocean cleanup array is depicted as dashed blue lines. Caught debris is bold red. Debris originating from the area where the array is placed is colored green (those are modeled to be captured as well). The line segment that defines the ocean cleanup array is shown in orange.

GYRES	MIN LATITUDE (º)	MAX LATITUDE (º)	MIN LONGITUDE (º)	MAX LONGITUDE (º)
NORTH PACIFIC	18	45	180	240
SOUTH PACIFIC	-40	-20	230	280
NORTH ATLANTIC	14	40	275	340
SOUTH ATLANTIC	-40	-20	320	359
SOUTH INDIAN	-40	-20	30	90

Table 2.15 Overview of gyre boundaries used for the automated search of optimal cleaning array configurations.

Since the locations of the five gyres are roughly known the search for optimum array positioning was reduced to these known areas in order to save computational time. (see Table 2.15). The given boundaries were chosen manually on the basis of van Sebille's simulation. Within these borders, a grid of 1º x 1º, was used; array lengths were varied in steps of 50 km and various array orientations were investigated in steps of 15°. A typical optimization run would test all configurations within the defined gyre area bounds and pre-defined steps and increments.

For the sake of simplicity, each gyre was handled separately with only one array at a time.

IMPLEMENTATION IN MATLAB

The flow model was implemented in Matlab. A single simulation run used an Ocean Cleanup Array position, orientation and length as a fixed four parameter array configuration. The initial plastic distribution was mostly released from the coast. For each array configuration the debris flow for every two months of the 20 years of total simulation time was calculated. Debris that crossed the array line is removed, reducing the total amount of debris. The overall efficiency of a given cleaning array configuration was computed as the difference between the final (relative) amount of plastic after 20 years of simulation time and the initial concentration.

With an estimate of 1 minute per simulation run approximately 330 days for the entire search process would be needed. A parallelized computation was therefore implemented with the support of the Computer Science Faculty of the Freie Universitat Berlin. About 50 Linux machines were utilized during night times in order to execute distinct parts of the total global computation. In the end, a final script has verified that all data has been analyzed and extracted the best configurations.
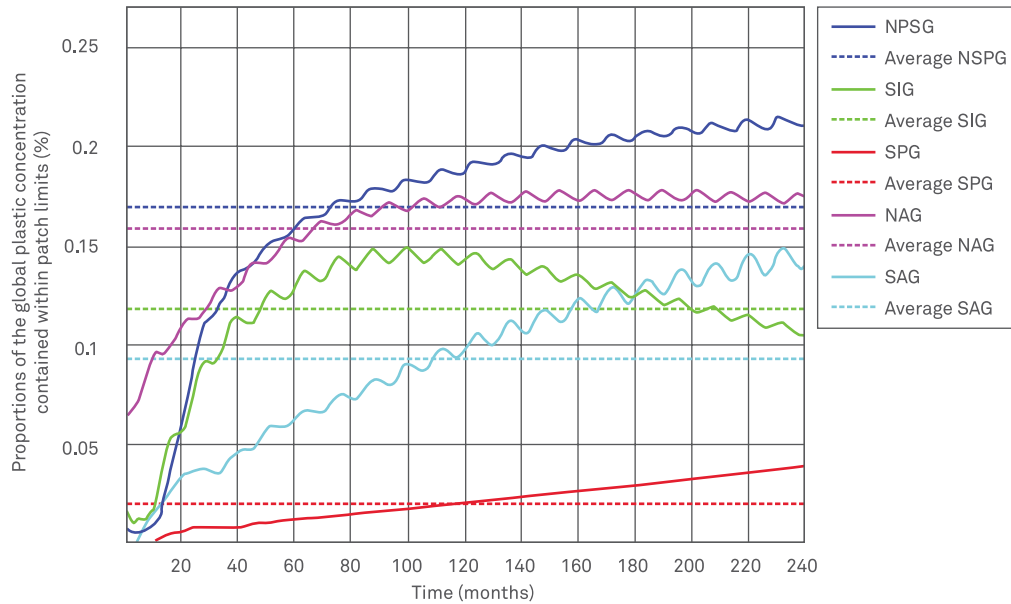
Figure 2.33 Accumulation of the plastic contained within the gyre limits as % from the total amount of particles in the model. The NPSG shows the largest accumulation of plastic over time, The South Indian gyre shows an increase, followed by a natural decrease of plastic over time.

2.6.1.3. RESULTS

The plastic accumulation per gyre can be used to normalize the efficiency results per gyre. It is important to note, that gyres might exchange particles over the course of time. This effect has been taken into account by this model, hence that is why the NPSG continues accumulating plastic, while the South Indian gyre plastic concentration decreases after some time, as is apparent in the Figure 2.33.

To find the optimal location for the cleanup array in the North Pacific gyre debris reduction for each possible location the global was measured. Figure 2.34 vizualizes an example of the results obtained by using the model. The example is based on an array of 350 km length and 0° orientation. White area in the top right represents the coast. The obtained efficiencies reach their maximum at a position relatively close to the coast; in this case over 20% of the global plastic debris can be collected over the 20 years simulation time.
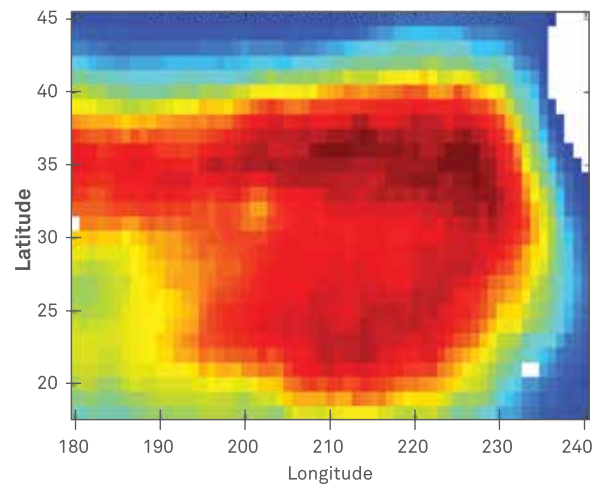
Figure 2.34 Efficiency map of a cleaning array of length 350 km, oriented vertically (0°), within the boundaries of the north pacific garbage patch. All locations (except the white areas) were tested by running a full simulation over a 20-years period. The resulting total efficiency is color-coded. Dark red are very efficient (maximum value is 21.6 % global plastic reduction, with respect to the total plastic content in the world ocean) and dark blue are close to zero.
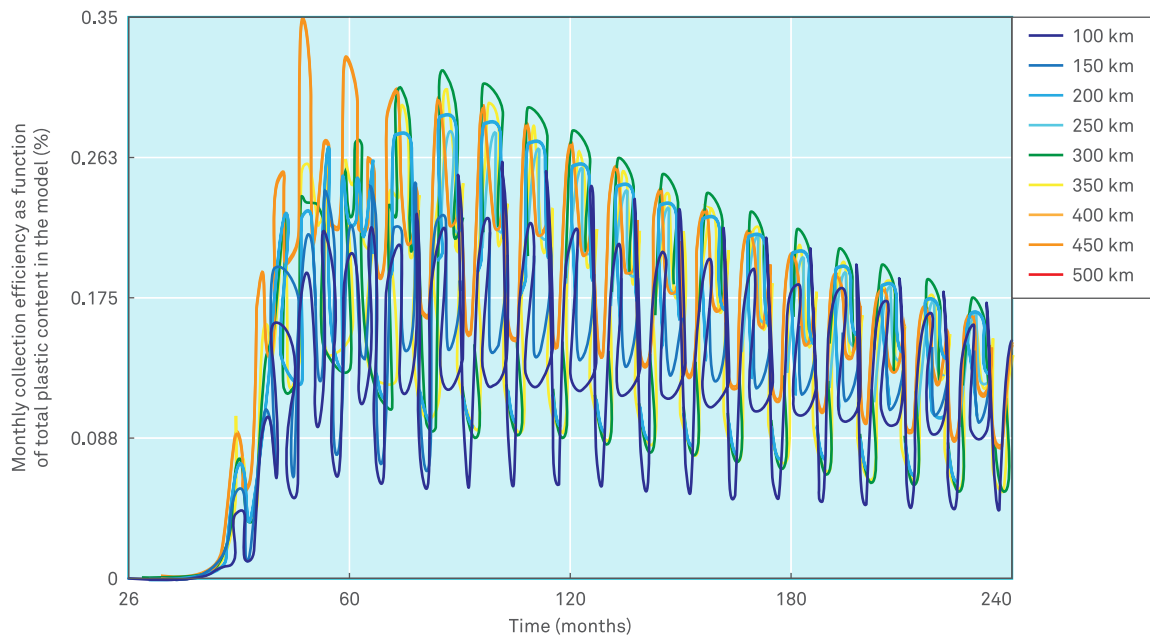
Figure 2.35 Monthly efficiency of a cleaning array centered on (31°N, 218°W) over a total simulation duration of 120 months.

If one were to plot the monthly field efficiency over time for a given location and a given orientation, an oscillation of the array efficiency would be visible for every two months (see Figure 2.35). Since the simulation starts with most plastic distributed near the coasts, only very low amounts of plastic can be caught in the first 26 simulation months. After this "start-up" period the field efficiencies for all array lengths increase and periodically oscillate with a further decay of average monthly field efficiency. Note that the field efficiencies of the arrays do not differ proportionally to their lengths partly due to the cell nature of the model used.

The cumulative efficiency of different array lengths at one location in the NPSG is plotted in Figure 2.36. As expected, longer arrays have higher total efficiencies. However, there is practically no difference between the two longest arrays, which suggests that there is a limited volume of plastic contained within a gyre, irrespective of continuous new debris flowing in from other gyres. When the efficiency of the 100 km array in the North Pacific Gyre is evaluated over time, compared to the total amount of plastic within this gyre itself (not the global plastic content), it can be seen that after a model setup time of 26 months, the efficiency after ten years is about 45 percent (see also Figure 2.37).
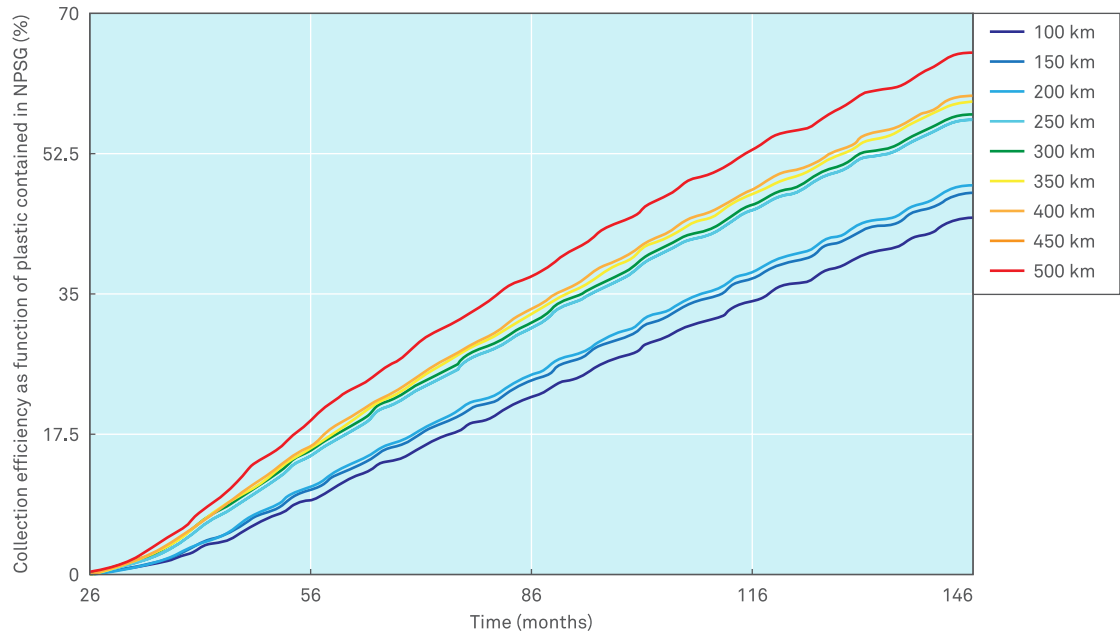
Figure 2.36 Total efficiency of cleaning arrays centered at (31°N, 218°W) as a fraction of the particles contained within the bounds of the gyre (not the global plastic content)

As can be seen in Figure 2.33, the total amount of plastic contained in NPSG compared to the total amount of plastic contained in the model asymptotically reaches the value of ~21.4 percent, which is why the total efficiency shown in Figure 2.36 seems to have an upper limit. This can be seen in the fact that the arrays of 450 and 500 km length catch the same amount of particles over time. This implies that these arrays can already extract close to 100 percent of gyres plastic and thus their efficiency is limited by the amount of plastic contained in the gyre.
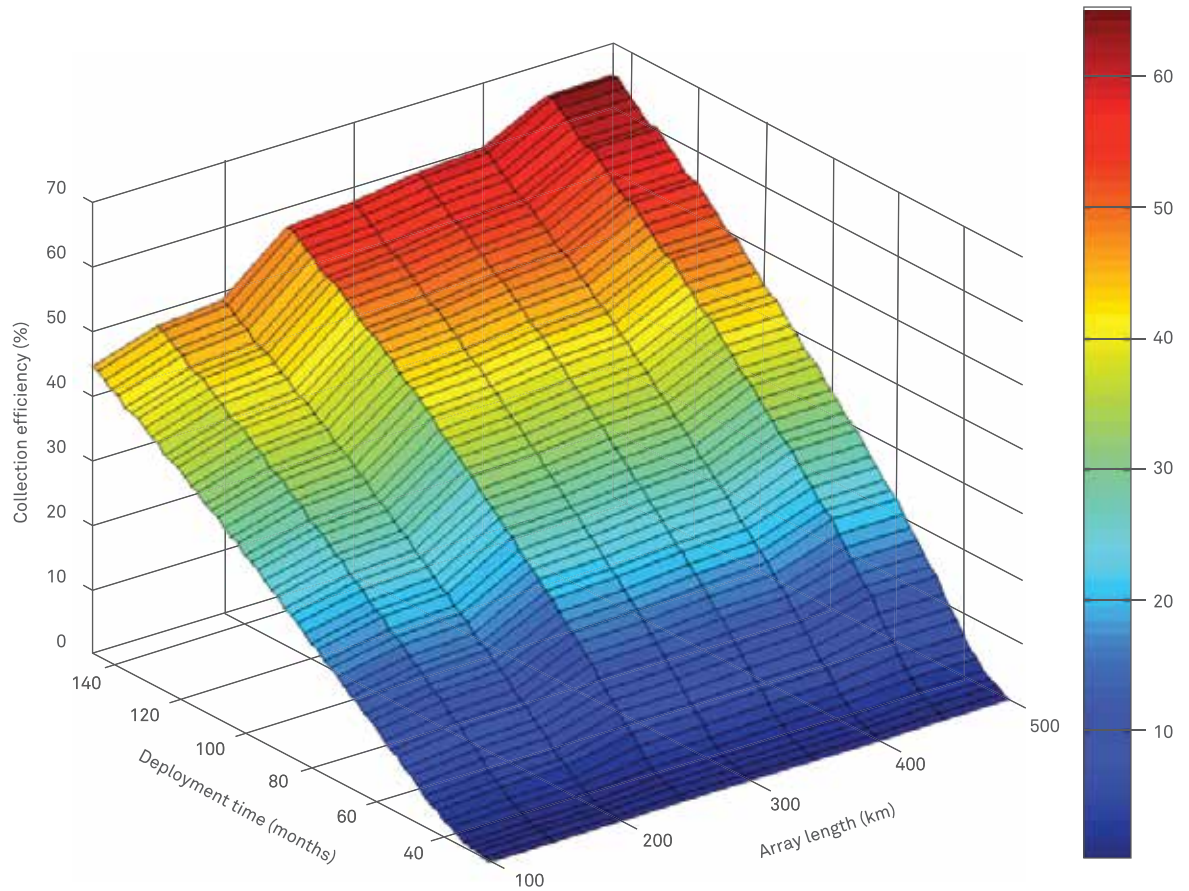
Figure 2.37 A graphic representation of the dependency between the field efficiency, total array length and deployment time. To increase field efficiency, either the total array length or deployment time has to increase

By combining the data of the total collection efficiency (Figure 2.36) with the proportion of global plastic contained in the NPSG (Figure 2.33) a plot of relative collection efficiency can be obtained. This is visualized in Figure 2.37. Here the efficiency is visualized starting from month 26 up to month 146 (10 years) since before month 26 virtually no plastic is caught due to the "start-up" cycle of the model.

DISCUSSION

The model is a fit to a rather coarse data set. The Global Drifter Program logs the positions of many thousands of drifters in all oceans. Drifters are buoys that float in the upper layer of the water and are moved by a sum of influencing forces, such as wind and ocean currents. By design, the transition matrix can only reflect the general motion which was interpolated from the observational data. The model relies on the following assumptions:

- The measured drifter motion can be generalized to affect smaller (plastic) particles similarly.
- The plastic debris motion repeats periodically (gyres have periods of rotation)
- The actual mass or volume of the debris has no effect on the movement.
- Particle movement is assumed linear from cell to cell.

The model can be evaluated very quickly and is based on real-world observations. The gyre predictions match observations. However, the assumptions made and the low spatial resolution have implications for the obtained results.

The model described in this section simplifies a rather complex process. To begin with, the transition model of van Sebille and colleagues is a two-dimensional model and so is the model of the cleaning array. Flow direction, orientation and debris mass are ignored in this model, but all are likely to have an influence on the amount of plastic being caught. The current implementation thus yields an upper limit of cleaning efficiency, i.e. it is very unlikely to achieve better results than those computed by the current model. It is very likely that the arrays are indeed less efficient. Plastic might not be caught for various reasons. A likely one is that particles pass either above or below the array. Plastic particles that hit the array at its tips take longer to be caught at the center and therefore are more probable to pass. Also the shape of the array, in the original idea V-shaped, is modeled as a line segment. In a realistic model the direction from where the plastic hits the array would determine whether the respective particle is caught or not. Other efficiency losses will be addressed in chapter 3.

However, on a coarse scale this model should capture the order of magnitude of array efficiency. The results of our simulations point to locations within the gyres to be optimal with respect to efficiency, as shown in the next section.

It has been shown how the model of van Sebille et al. (2012) was augmented in order to simulate the process of filtering marine plastic debris. We have run an exhaustive search over all feasible combinations in the space parameter and have reported a list of locations and configurations of cleaning arrays that yield high efficiencies. Our analyses yield realistic optimal locations within the gyres. However, there are large assumptions and simplifications used in modeling the plastic flow and the Array. As discussed above the actual efficiency values should be understood as upper limits. It is unlikely that this model captures the seemingly complex spatial and temporal dynamics of the process of catching plastic. The numeric values that we have produced rather give a hint

indicating where plastic is likely to cross a certain linear space. Since our simulations result in rather minor differences in efficiency over a range of different orientations, lengths and locations it might make sense to implement an array model that is sensitive to flow direction. This might help in pinpointing locations that have a strong unidirectional flow.

2.6.2. LEBRETON MODEL
WOUTER JANSEN • LEONID PAVLOV
JAN DE SONNEVILLE • STEPHAN KOCH
The Lebreton model (Lebreton et al., 2012) is based on a slightly different set of assumptions than the Van Sebille model and is of a higher resolution, both spatially and temporally.

A global ocean circulation model was coupled to a particle tracking model to simulate 30 years of input, transport and accumulation of floating debris in the world oceans. The working principle of this model is schematically represented in Figure 2.38. The input of new plastic debris comes from either marine or land based sources. Faris and Hart (1994) estimate that 80 percent of the total plastic mass enters the ocean by land and it is assumed that the remaining 20 percent is derived from maritime activities such as commercial and recreational fishing, cruises and shipping. The release of plastic debris increases over time to represent the growth in worldwide plastic consumption and waste. The rate of increase in particle release was built on the assumption that the release of marine debris worldwide doubles every decade (Halpern et al., 2008).

2.6.2.1. WORKING PRINCIPLE

The model consists of a two-stage process; first a hydrodynamic model solves the equations of motion to describe water movement throughout the model domain. In the second stage, virtual particles are introduced into the flow field and move through hydrodynamic forcing.

In the first stage sea surface currents are extracted from the oceanic circulation modeling system HYCOM/NCODA (Cummings, 2005). The HYCOM model includes wind stress, wind speed, heat flux and precipitation. The model provides daily ocean circulation on a global scale. In the second stage the velocity data extracted from HYCOM was coupled to a particle tracking model 'Pol3DD' (Black & Gay, 1990) and used to drive the dispersion of floating material across the ocean surface. The HYCOM model contained 32 vertical layers, but only the velocities in the surface layer were used as the principal driver of floating particles.

Particles were tracked on a Meridian grid between 78 °S and 47 °N (North Pacific Gyre). The grid consists of 1500 x 1100 grid cells at ~21 km resolution and was later converted to a 2D grid as it is illustrated in Figure 2.39. The simulations were run at hourly time steps for a period of 30 years. The model output updated particles position and the history of particle visits per cell on a weekly basis.

The model deals with 'particles', which do not relate to real individual plastic particles, but have a more abstract representation. Since it is not known exactly how much plastic mass is added to the oceans, these particles represent a relative amount of plastic mass instead of an absolute value.

Every week new equivalent particles are added to the model. The exact source and quantity of input material varies depending on the coastal population density at the given location.

There is a fixed number of particle release points defined, which can be divided in two main categories: land-based and ocean-based release points. Land-based release points are mainly locations at the coastline but also contain locations inland which contribute to ocean pollution through rivers and urban runoff. Ocean-based release points represent marine input i.e. plastic debris dumped overboard on the high seas. Each release point is denoted by a specific number, which is assigned to each particle that is released from this point (see Figure 2.40). Hence every particle can be tracked to where it originally came from. Apart from this 'release point' ID number, each particle is weekly assigned x and y coordinates. Unlike the release point number, the x and y coordinates change every week as the particle moves through the ocean. Finally it is also possible that particles are removed from the model because they are washed ashore.

2.6.2.2. THE GOAL

The 30-year simulation of the Lebreton model resulted in a large dataset containing weekly x and y coordinates for an increasing amount of particles. Now the goal is to use this data to provide the information that relates the amount of caught particles over time to the array length, array orientation and array deployment time.

2.6.2.3. OPTIMAL LOCATION

The determination of the optimal boom location would be a very expensive optimization process, because a 10-year simulation for only a single boom length already takes 8 computer cores around one week to solve. However for the 'best' location, besides the optimal location in terms of boom efficiency, there are other factors that should be considered. These factors are, for example, the sea depth, the local climate and the average flow velocity. As sea depth is one of the factors with the greatest economic impact, this was considered to be one of the most important requirements for the selection of the boom location. First, a region of the gyre with an acceptable current speed and plastics flow was selected and then the final location (31°N-142°W) was selected based on a low seabed depth, but still good catch efficiency. This location was then simulated in order to determine the array orientation, length and deployment time.
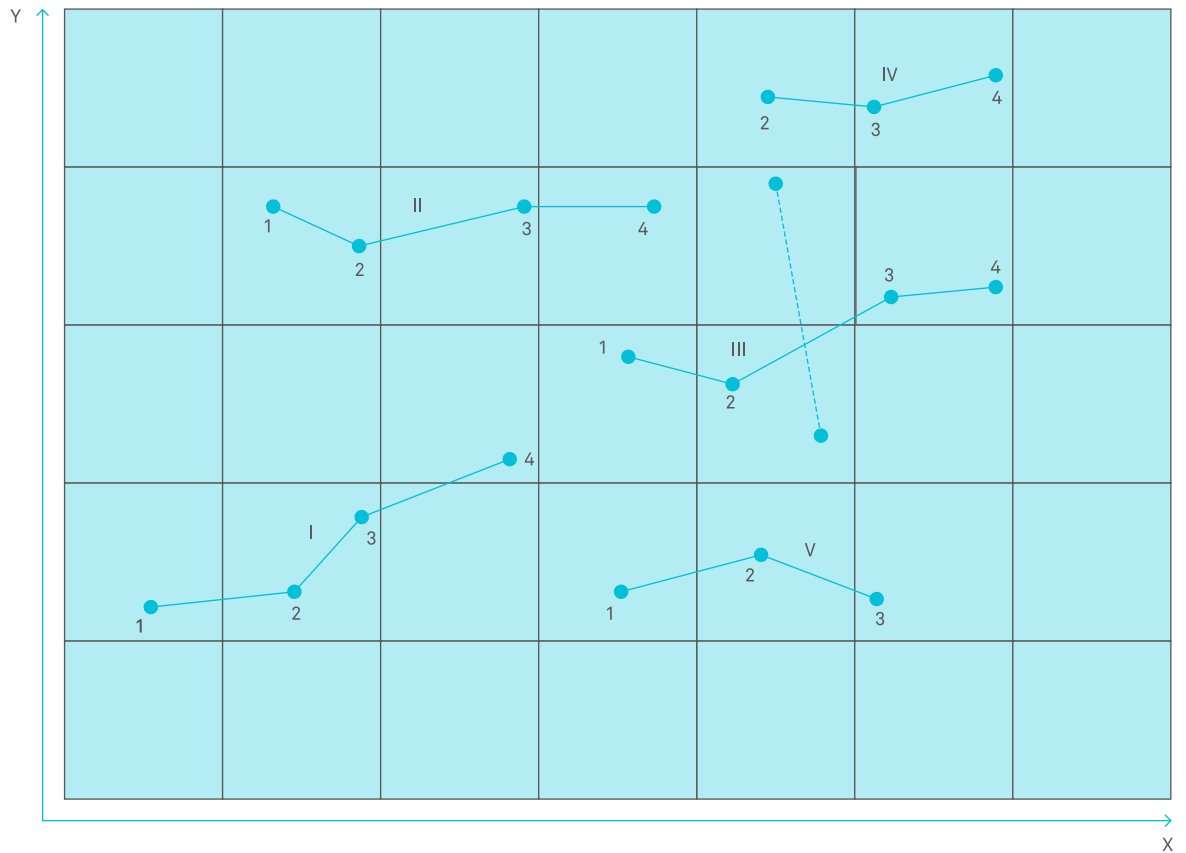
Figure 2.38 As an example, 5 particles (I,II,III, IV, andV) are represented on a x- y grid for 4 weeks. Particle V is washed ashore after week 3 and particle IV is released in week 2. The dashed line represents the boom and it can be seen that particle III would have been caught between week 2 and 3
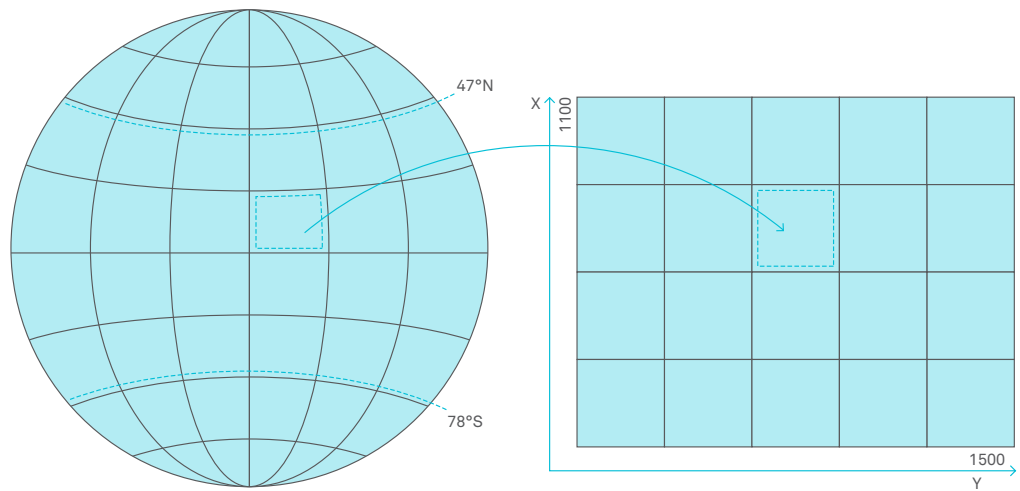
Figure 2.39 Conversion from a Meridian grid to a 2D grid

Figure 2.40 Schematic representation of particle release points. Each point is denoted with a specific number.

In order to find the best boom location in terms of efficiency, the plastics flow is the most interesting aspect to consider. The plastics flow is defined as the amount of particles that cross a grid cell over a certain time interval, and is therefore directly related to the quantity of plastics that can be caught. In order to analyze the flow, the model was used to quantify, how many particles cross each grid cell over a certain time interval. The direction of a particle crossing a grid cell was not taken into account here. In Figure 4 the results are represented for a time interval of 5 years.

In Figure 2.41, the North Pacific Subtropical Gyre (NPSG) is marked by a yellow dashed line. A boom of 200 km is represented by the black line at the location (31°N 142°W). It can be seen that the location of the boom is in a region with a large particle flow, but it definitely is not the optimal location in terms of efficiency.

2.6.2.4. OPTIMAL ORIENTATION

The first step in the simulation is to determine the optimal orientation of the boom. It is assumed that the optimal orientation is constant for different boom lengths and perpendicular to the flow direction in the selected point. A simple method to approximate the direction of the flow in a point is illustrated in Figure 2.42.

A circle of radius 'r' is defined around a location 'P'. Every week all the particles that are located within this circle are tracked to determine their individual direction. By averaging the flow direction of all the individual particles over a certain time interval, the flow direction is approximated. The direction of the flow is expressed in the angle , which is defined as the angle with respect to the equator. An angle of 90o is for example in the direction of the meridians (North).

In order to check the variation of the flow direction, was approximated on a weekly basis for 5 years. The result of this analysis is visualized in Figure 2.43. It can be seen that the flow direction actually varies a lot. Even between two consecutive weeks the direction can change drastically, with a total range variation of between +90 and -90 degrees. This variation corresponds to the observations in chapter 2.6 about the varying surface currents.
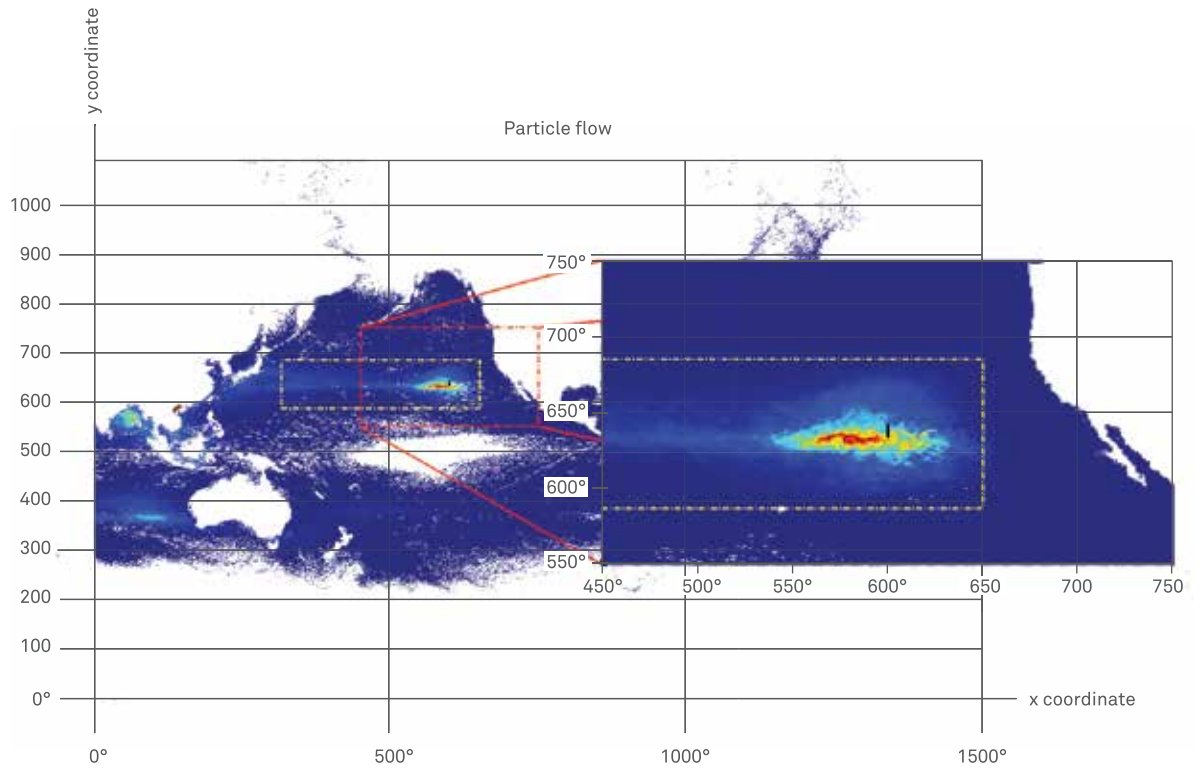
Figure 2.41 Plastics flow based on a five-year time interval. The NPSG is marked by the yellow dashed line and a boom of 200 km is represented by a black line at 31°N 142°W. The figure does not contain a legend, because the particles in the model do not represent an absolute value of plastic mass.
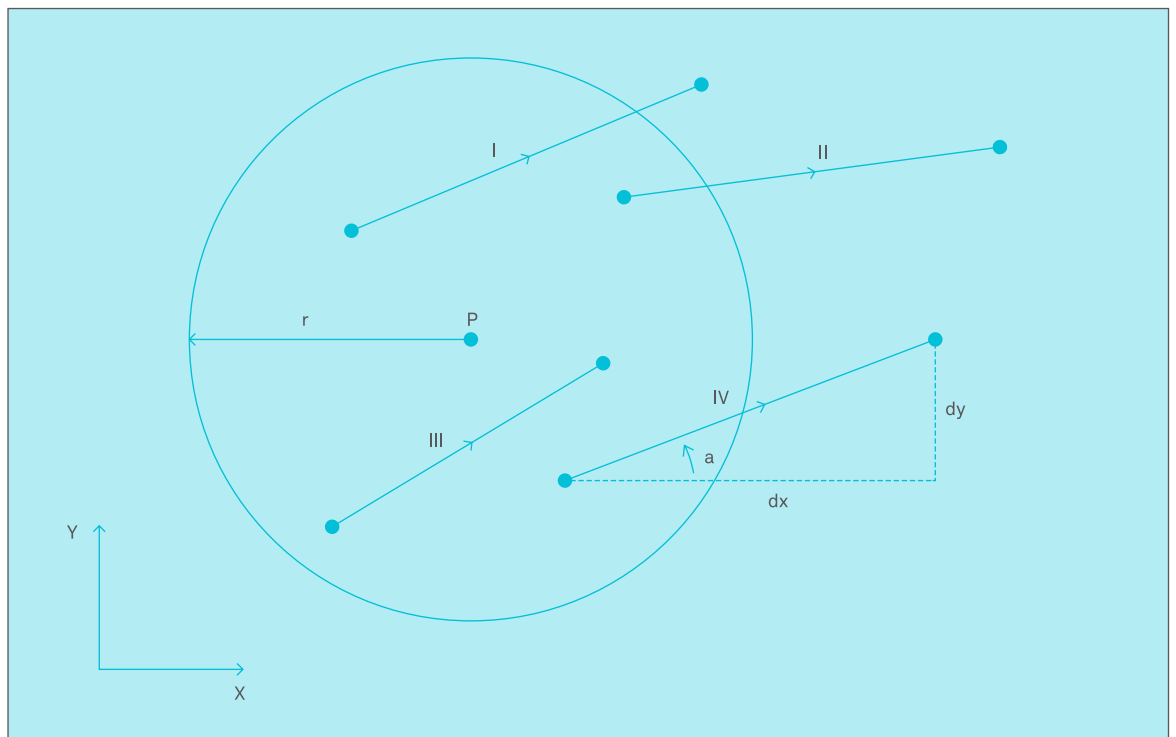
Figure 2.42 Schematic representation of the determination of the average plastic flow direction in a point P

Plastic flow direction at 31°N-142°W
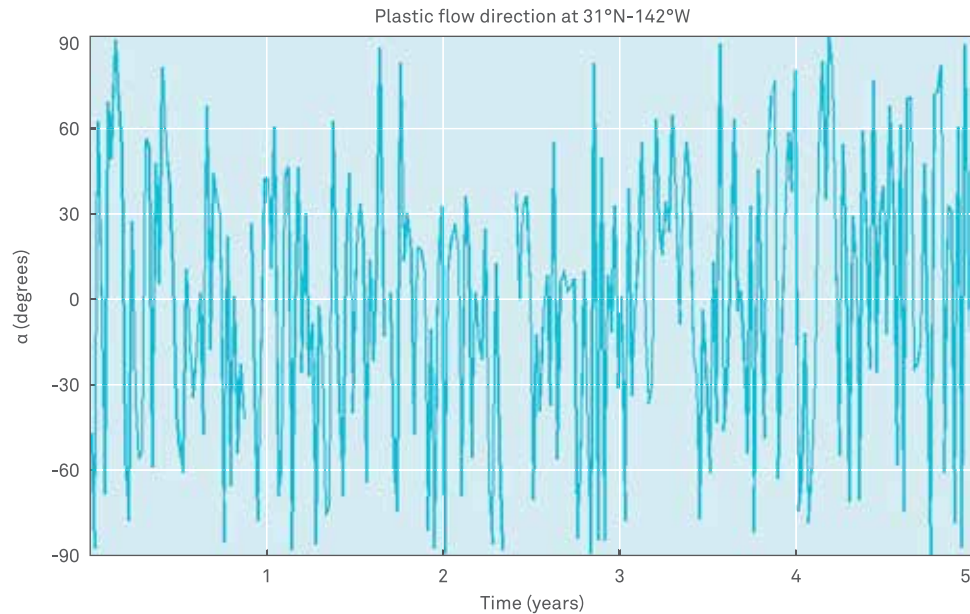
Figure 2.43 Weekly plastic flow direction ᵃ where ᵃ is defined as the angle with respect to the equator

Still, an average flow direction can be determined for the simulation; however, the result will depend strongly on the start and end point of the chosen time interval. For the simulation the flow direction was approximated by averaging the flow direction over a 5 year time interval using a circle of radius r of 1 km around the location P (31°N 142°W). This resulted in an average flow direction of 0.6 degrees. The boom is therefore placed perpendicular to the direction of the flow at an angle of 90.6 degrees, which is almost parallel to the meridians.

Once the boom location and orientation were determined, simulations were done to determine the 'efficiency' over time for different boom lengths. The efficiency was defined as the amount of particles caught by the boom over the total amount of particles that would be present in the NPSG if no boom were present. The area defining the NPSG is marked by the yellow dashed line in Figure 2.41. It is stressed again that these particles represent a relative amount of plastic mass instead of an absolute value. So this model can only be used to quantify a percentage of plastic that is caught and not the actual amount of plastic mass.

Initially only one location was investigated: 31°N 142°W. For this location, first the optimal boom orientation was determined and then simulations were performed for the following boom lengths: 50, 100 and 200 kilometers. Although 30 years of data was available, a simulation was only done for 10 years due to computation time. As initially in the model there is no plastic in the oceans, the simulation was started after the first 15 years of the available data to give the model time to settle from its initial conditions.

In the simulations the boom is described as a simple line as it is illustrated in Figure 2.38 by the dashed line. Each particle travels in a straight line between two consecutive weeks and if this line intersects the line of the boom it is assumed that the particle is caught, independent from the angle at which the particle approaches the boom.

All the particles that intersect the boom line are counted and removed from the data in subsequent weeks. The result of the 10-year simulation is represented in Figure 2.44. In Figure 2.44 the efficiency is obtained by normalizing the amount of caught particles by the amount of particles that would have been in the NPSG if no boom were placed.
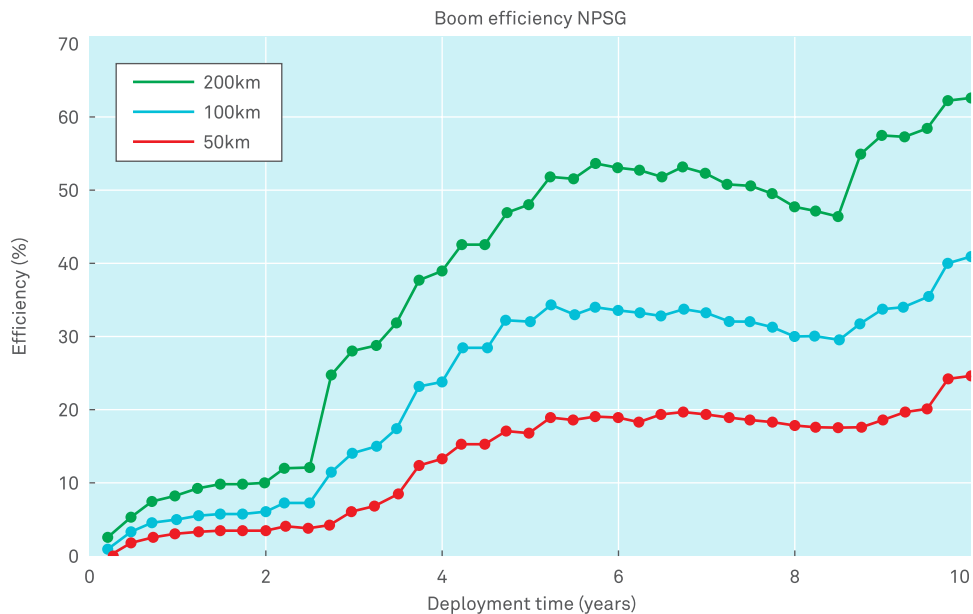
Figure 2.44 Boom efficiency (normalized with respect to the increasing amount of particles in the NPSG)]

2.6.2.6 CONCLUSIONS

First of all, as expected, it can be seen that the efficiency of the boom increases positively with boom length. The efficiency also increases over time. One would expect that after some time the efficiency of the boom would reach a steady state value. Initially this seems to happen after 2.5 years, but then suddenly the efficiency increases sharply. Six years later more or less the same feature occurs. The cause for is assumed to be, that the available 6 years of ocean circulation data was looped 5 times to represent 30 years of ocean circulation, assuming that global circulation patterns have not changed significantly in recent decades. It is not clear if the efficiency has reached an equilibrium state after 10 years or that it will increase even further after 10 years.

The efficiency plot alone presents a very good result, however, if the total amount of particles in the NPSG is considered, the result looks less positive. In Figure 2.45 it can be seen that the total amount of particles is still increasing over time, even if a boom of 100 km is placed. This is because, apparently, more plastic is added to the oceans than is caught by the boom. The red line in Figure 8 represents the case where no boom is deployed, and an even steeper increase in particles in the NPSG can be seen as a consequence.

Hence, just placing a boom of 100 kilometers in the ocean cannot solve the problem; it is essential to also prevent new plastic particles to enter the oceans. The blue dashed line in Figure 2.45 represents this case. Here it can be seen that the total amount of plastic is reduced by almost 50 percent in 10 years.

In the rest of the report it is assumed that no more new plastic particles will enter the oceans by the time the boom is deployed. As this probably is not a very realistic situation, the transport and processing costs in Chapter 4 and 9 will become higher in reality, but the cost per kilogram of extracted plastic in Chapter 10 will be very conservative as a consequence.
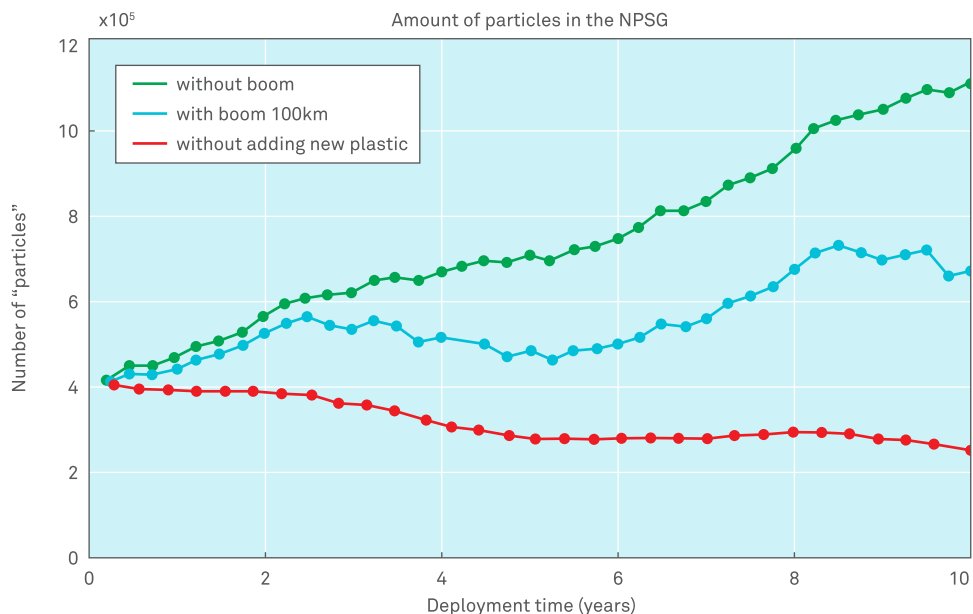
Figure 2.45 Comparison of the amount of particles in the NPSG in case of a 100 km boom and no boom. The blue dashed line represents the case when no new particles are added to the ocean and a boom of 100 km is placed.

2.6.3. CONSIDERATION BETWEEN ARRAY VARIABLES
BOYAN SLAT • LEONID PAVLOV

The variability in the directions of incidence of the flow with respect to the selected orientation of the array (shown in Figure 2.43) is contradicting one of the assumptions used in the study. This variability is likely to be applicable to both models. The periodicity of the gyre is therefore questionable and so is the assumption about having a predominant direction of the flow at the selected location. The periodicity of the gyre does not seem to be a problem per se since its periods might still exist, but just span a longer time interval than the one investigated. However, the inexistence of predominant flow direction could become an additional complication where special attention needs to be paid in the selection of the array layouts and orientations. At the moment, this issue is the main recommendation for future work since an in depth investigation into it might change some of the fundamental assumptions and increase our understanding of the Ocean Cleanup Array concept.

Since no optimum can be found in the relation between deployment time, array length and the amount of plastic collected (see Figure 2.36 and Figure 2.44, the actual deployment time and array length will only depend on the available budget. Hence, for this feasibility study assumptions for these parameters will have to be made, since a budget has not been defined in advance. These assumptions are:

Total array length **100 KILOMETERS**
Deployment time **10 YEARS**

Based on the work in 2.6.1, if the first twenty 2-month periods are not taken into account (since no plastic is collected in that period according to the model), after 10 years (at '80' on the vertical axis in Figure [Gyre accumulation]), 20 percent of all plastic in the model would be within the area defined as the North Pacific gyre. After 10 years, Figure 2.36 indicates a field efficiency of 9 percent of all particles in the model. To calculate the field efficiency relative to the amount of plastics in the area defined as the North Pacific gyre: 0.09/0.20 = 0.45, resulting in a theoretical removal of 45 percent of the plastics in that accumulation zone. According to the results of 2.6.2, a 100 kilometer array would collect 40% of the debris in the North Pacific gyre in 10 years.

It's difficult, however, to compare the results of the two models. First, although the boundary coordinates of both models include the area of high concentration they did not define the same area as the North Pacific gyre. Furthermore, the location of the area of highest concentration in the Lebreton model does not exactly correspond to the measured area of highest concentration (see Chapter 2.5) and the chosen coordinate (30°N 138°W), and hence the 40 percent could be an underestimation. For the use of material flow calculations in this feasibility study, we will therefore work with a field efficiency of 0.45.

BOOMS AND MOORINGS

The most critical elements of the passive concept described in chapter 1 are the floating barriers and moorings. Currents and waves subject structures near the sea surface to great forces. Furthermore, the structure will have to be placed in an area where depths average about 4 km. This chapter describes the engineering process of these novel elements, chosen concepts and cost estimates.
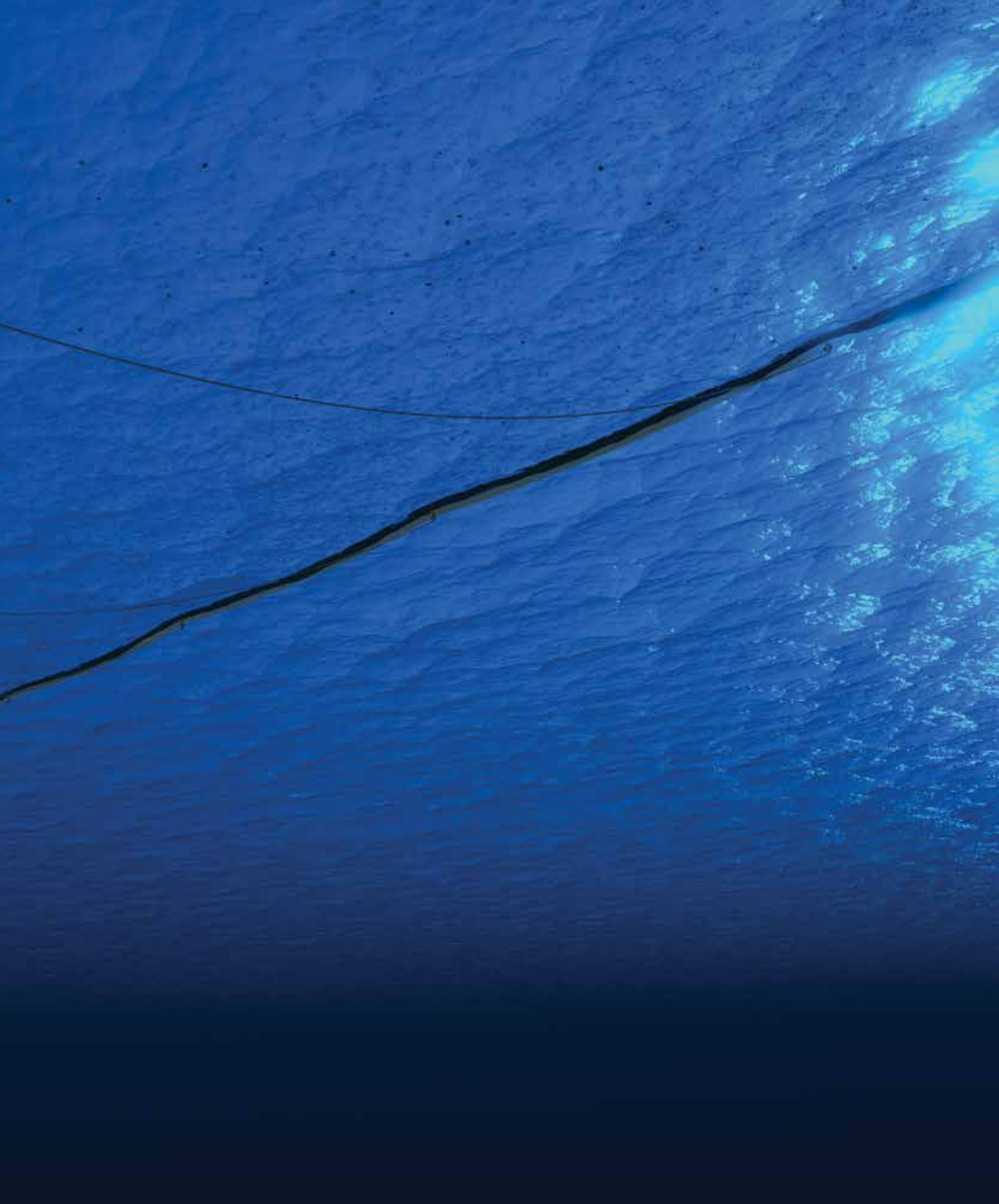
BASIC OVERVIEW

JOOST DE HAAN • JAN DE SONNEVILLE • BOYAN SLAT
KATHLEEN LAURA STACK

Before the plastics can be extracted and transported to land, they must be caught in front of the booms and migrate along the booms to concentrate near the center platform. For this to occur, the boom design must overcome certain environmental and structural challenges. Other design challenges relate to the moorings, as the structure will be bound to the seafloor at record depths. Analysis must be conducted to ensure that the booms will capture the majority of plastic down to the defined depth and transport it to the collection platform while withstanding the forces upon them.
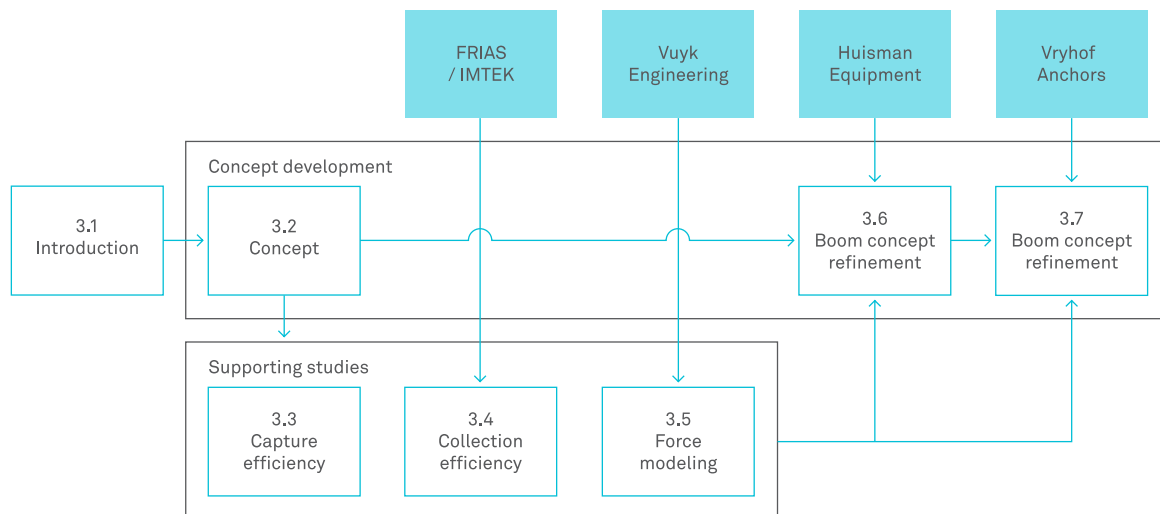
Figure 3.1 Chapter structure

3.1.1. CHAPTER CONTENTS

Chapter 3 presents the concept as developed in the feasibility study. The focus here is on the boom and mooring design. The chapter first presents the initial iteration of concept options. It is followed by multiple calculations regarding particle flow and forces. Using the (qualitative) results from these studies, the most promising concept is outlined. The chapter closes with a presentation of the mooring system and system cost optimization using parameters from the calculations. Figure 3.1 shows the chapter structure, containing concept development and the supporting studies, and also shows the three companies who supported the development of Chapter 3.

CONTENT PER SUBCHAPTER

Subchapter 3.2 discusses multiple boom concepts. First, important design requirements are outlined. The presented concepts include rigid steel floating barriers and flexible polymer based barriers.

Subchapter 3.3 shows a 2-dimensional CFD (Computational Fluid Dynamics) approach for simulating the velocity profile of water near the boom. Simulations are performed using different current speeds, plastic particle density and size. The study gives an estimate of the boom's capture efficiency at these different conditions. The skirt length can be designed according to the desired efficiency.

Subchapter 3.4 continues with 3-dimensional CFD to investigate the particle velocity parallel to the boom with varying angles of incidence. This velocity is required for transportation of plastic particles towards the collection platform.

Subchapter 3.5 outlines force calculations executed in a 3-dimensional multi-body dynamics computer program. This program simulates a structural boom model exposed under environmental forces. Besides obtaining resulting forces, simulations are run to optimize the boom design.

Using the outcomes of the studies, subchapter 3.6 presents the building blocks of the most promising boom concept in more detail.

Subchapter 3.7 closes with a presentation of the mooring and anchoring concept. This concept is briefly described and cost optimization is discussed. The subchapter ends with an outline of the design steps required for the final design.

3.1.2. CONCEPT INTRODUCTION

The Ocean Cleanup concept is composed of three main parts: the booms, the mooring system and the collection platform. It was briefly introduced in Chapter 1.7. The booms and mooring system are discussed in this chapter, while the collection platform will be discussed in Chapter 4.
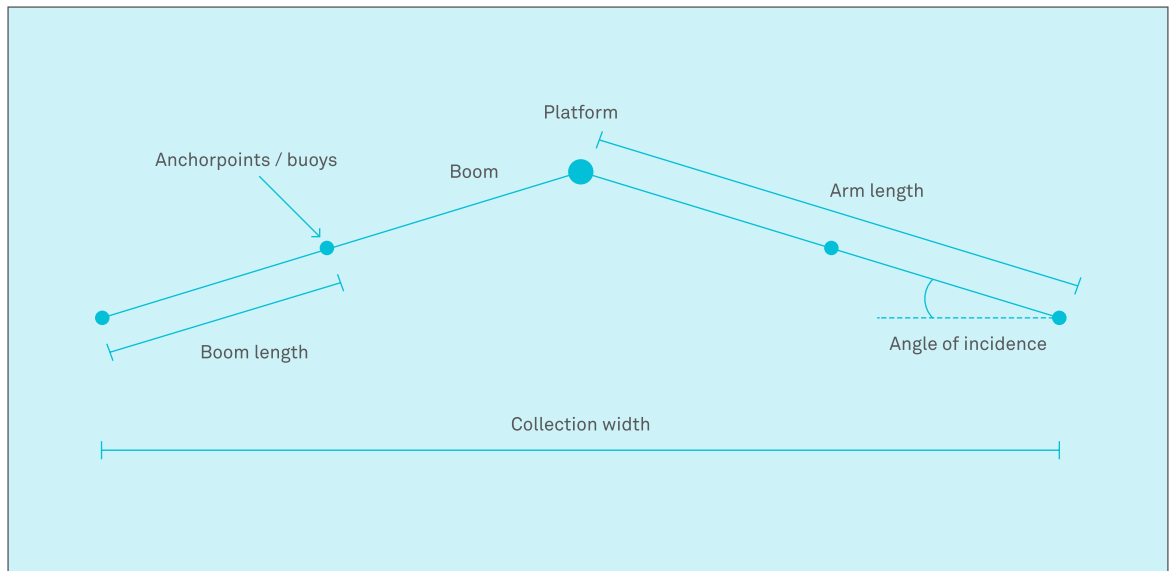
Figure 3.2 Concept terminology

The floating structure is V-shaped with an opening perpendicular to the current. It is composed of two long booms (Figure 3.2), in front of which the plastic is captured, and a collection platform, where the plastic is removed and stored until it can be transported to land. The number of platforms is a consideration between collection efficiency and costs, but for simplicity a configuration containing just a single platform has been chosen for this feasibility study. The boom angle, measures the angle between one arm of the boom and the direction perpendicular to the mean current and wind. Each arm of the V will have a determined boom length, and is divided into many smaller boom sections, the repeating unit of the booms. There will be moorings at various points along the boom length to maintain the array's position and shape, while also serving to limit the forces endured by the floating barriers. The distance between mooring points may vary based on the seabed geography. The total collection width of the structure is defined as the width over which plastic is captured by the booms, equal to the distance between the outer ends of the V.

Each boom section is composed of three elements (Figure 3.3). The buoyancy element / freeboard remains over the sea surface and provides buoyancy. It also serves to funnel floating plastic towards the collection platform. It is designed to help prevent overtopping, when water passes over the top of the structure and leads to likely loss of trapped plastics. The bottom weight element / ballast is used as a ballast for the boom, keeping it upright and in position. The skirt is a non-permeable but flexible sheet, which spans the distance between the freeboard and ballast and serves to direct plastic towards the collection platform. In the final concept a tension member is used to provide required axial stiffness.

The structure is kept in place by moorings, permanent structures attached to the seabed using anchors. The mooring lines are connected to the boom via submerged buoys.
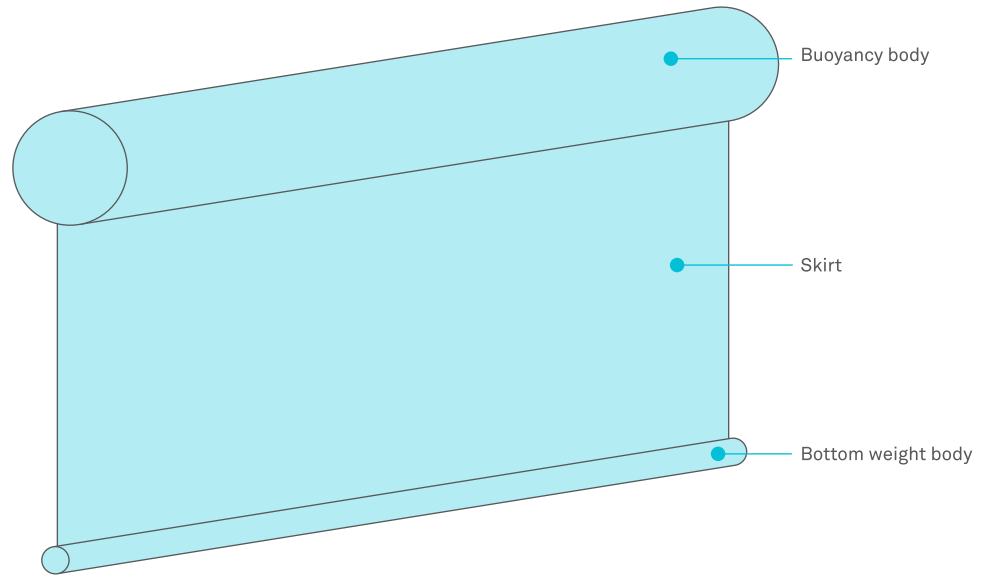
Figure 3.3 Boom's main components

3.1.3. INPUT PARAMETERS

In this chapter the decisions made in chapter 2 will continue to be used, including the skirt depth of 2-3 meters, 95 percent operational time, a placement at 30° N, 138° W, a significant wave height of 5.5 meters at 95 percent conditions, a total collection width of 100 kilometers and a minimum operational time of 10 years.

BOOM CONCEPTS

JOOST DE HAAN • STEFAN VAN RUYVEN • SAM VAN DER HORST • EMILE ARENS • BOYAN SLAT

The floating barrier functions as a structure to intercept and concentrate plastic debris, and can be considered the most important element of the array. It is also the most challenging element, in terms of surviving the environmental conditions, as it is in the splash zone of the ocean. This subchapter will briefly go over the design process performed to get to the most suitable boom design concept, and consists of three main parts. First, a selection of the most relevant design requirements is presented. Second, with these requirements in mind, conceptual ideas are briefly described. Finally, concluding remarks on the preliminary concepts will be given, and the supporting studies will be introduced.

3.2.1. DESIGN REQUIREMENTS

Concept development is guided by the design requirements. Note that not all requirements are included below; only the most relevant ones are discussed here, as they relate to the boom.

BUOYANCY

Buoyancy is required for the structure to float at the ocean surface. It must compensate for the deadweight of the structure, as well as possible vertical loads introduced by a mooring system. The required amount of buoyancy can be created by the structure itself or by using attached buoyancy elements.

CAPTURE EFFICIENCY

For the booms to collect substantial amounts of plastic debris, the capture efficiency must be considered. This efficiency depends on geometry, and structural response to environmental loads. Structural response depends on several physical properties described below.

THE ABILITY TO TRANSPORT PLASTIC

Besides capturing the plastic particles, the boom design should transport them in the direction of the collection platform. Hence, its shape should not stall fluid motion towards this platform. A smooth straight fluid stream is preferred. Furthermore, overtopping of waves should be prevented as much as possible.

BENDING STIFFNESS

Boom response to changes in water levels results in the requirement of limited bending stiffness. This requirement can be met by using flexible floating modules or rigid members with repeating flexible hinges. Ideally, the relative motion of the boom with respect to the water level is zero.

SKIRT ORIENTATION

Skirt response to waves and current impacts depends on factors such as skirt dimensions, bending stiffness and weight. To maximize efficiency, the skirt's orientation should remain close to vertical during operation.

In subchapter 3.5, multiple skirt weights and different amounts of ballast weight are simulated to give a first estimation on the influence of these properties.

STRUCTURE'S AXIAL STIFFNESS

Axial stiffness of the structure is required to limit its deflection under load. At maximum capture efficiency, environmental loads act (near) perpendicular to the boom's longitudinal direction. Under load, when seen from above, the boom will look like an arc, rather than the ideal straight shape. With the arc shape becoming too large, plastic transport towards the collection platform can be disturbed significantly. Plastic will simply stay 'trapped' in the arc.

3.2.2. BOOM CONCEPTS

The boom concept is developed with the design requirements listed above in mind. The engineering software company Solidworks organized a contest among its users, which resulted in multiple suggested boom concepts. Two submitted designs are presented first. In addition, two in-house developed concepts are briefly explained. Using these concepts, computational models were built to gain more understanding of the structural response to the environment. Guided by the simulation results, the most promising concept was hence developed, and subsequently detailed and dimensioned in cooperation with Huisman Equipment, Schiedam (NL). This concept is outlined in section 3.6.

3.2.2.1. SOLIDWORKS CONTEST CONCEPTS

The design contest organized by Solidworks resulted in a dozen design proposals from around the globe. The two most promising concepts are outlined in the report. The winning concept (Figure 3.4) was submitted by Amir Sadjadpour from the USA.

The concept uses a series of identical, repeating, plastic floats partially filled with seawater. Each is a Z-shaped skew polyomino; two stacked horizontal dominoes with the top one offset to the left, much like the Z-shaped pieces in Tetris. This geometry allows each buoy to connect to its neighbors via a self-locking mechanism that runs through a vertical pin (see yellow highlights in the figure above). The proposed dimensions are 10 m x 5 m x 1.6 m. Every tenth module is bigger to allow for a mooring point, and the use of identical, detachable modules allows for easy manufacture, deployment, exchange and repair.

Another interesting concept was submitted by Jose Garcia (Figure 3.5). The concept is named Vortex boom. The boom is modularly formed as well. The draft can be adjusted by filling the caissons with water and sand. The upright position of the boom is ensured by the ballast weight. The designer expects that due to the shape, water forms a vortex that enhances flow of the fluid towards the platform.
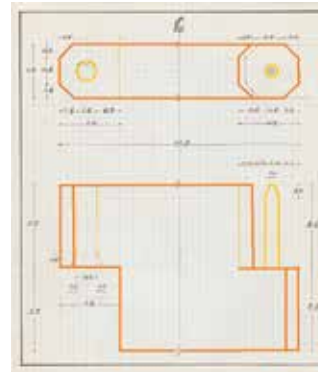
Figure 3.4 Sketches of the winning concept

Figure 3.5 Vortex boom render

Figure 3.7 Spherical bearing connection
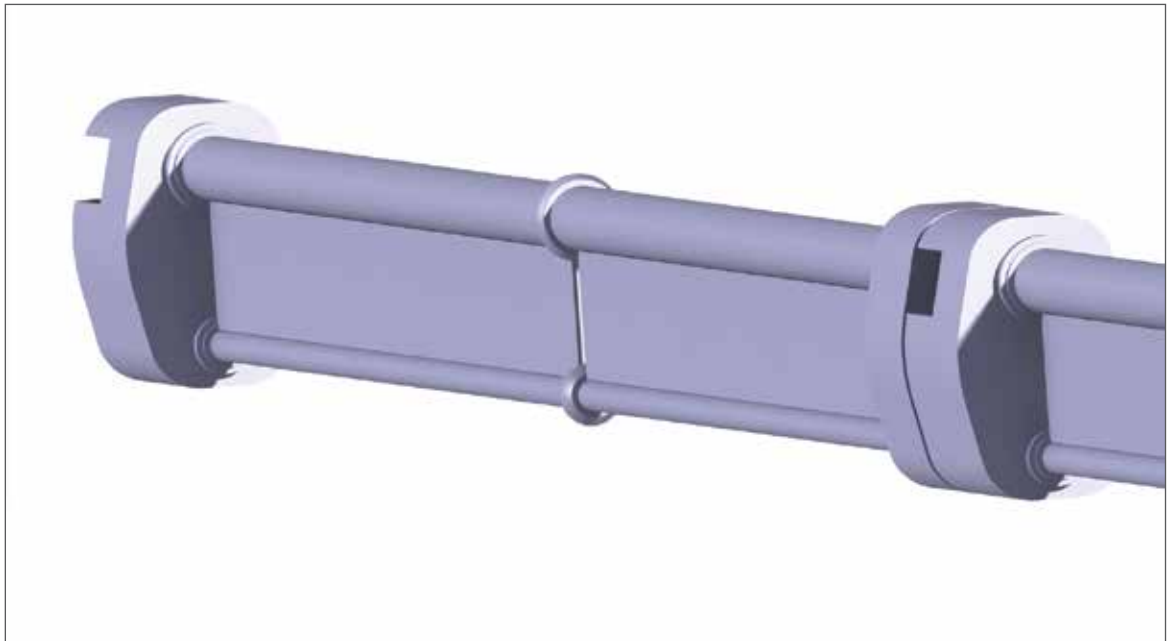
Figure 3.6 Rigid boom with flexible members - impression

3.2.2.2. RIGID STEEL BOOM

This concept's main structural part is a tubular steel boom, which acts as a buoyancy element. Due to the relatively high bending stiffness of the steel tube, flexible connecting elements or hinges are added to ensure operability when exposed to ocean waves. Obviously, a reduction in tube length increases the number of connecting elements and results in higher capital and operational expenditures.

To enhance collection of plastic debris, a skirt is placed below the buoyancy bodies. Ideally, the flexible skirt remains vertical during current and wave impact. To increase skirt stability, a chain or wire rope can be placed on the bottom of the skirt. A second option is to have lump weight mass placed at defined intervals. This allows for mass placement below the skirt via a rope element. Figure 3.6 shows an impression of the steel boom with flexible members. Dimensions are added for illustration purposes.

The connection elements are the main challenge when using a steel boom. The first concept consists of eyed plates placed between the pipe sections, which are connected by a pivot connection with spherical bearing (see Figure 3.7). The downsides of this concept are the high costs of the bearings, limited rotation angle and high service rate.

A variation of the concept uses a connection with universal joints (Figure 3.8). In the design two perpendicularly placed pivots replace the expensive bearing. The concept is partially inspired by the Pelamis® wave power project where a steel floatation boom is placed in the ocean to generate electricity from waves.
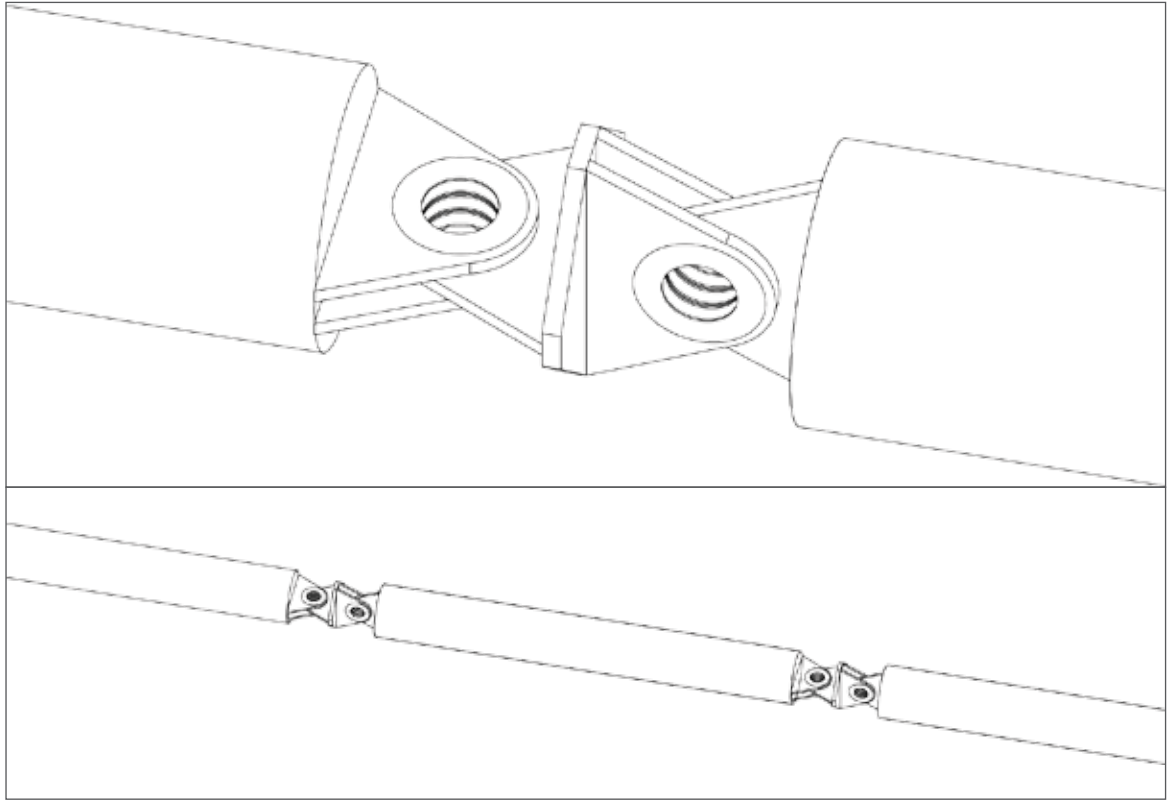
Figure 3.8 Universal joint concept

The third option that was considered to connect the steel tubes involves using rubber flanges (Figure 3.9). The rubber flanges are normally used to deal with expansion of steel pipe. However, rubber joints will likely not survive long, due to fatigue and other environmental influences.

3.2.2.3. FLEXIBLE POLYMER BOOM
This concept is almost identical to the steel boom. The main difference is that all elements are able to move along with the motion of the waves, similar to how oil containment booms work. The flexible boom concept allows for deformation to follow the wave elevation. The buoyancy body is made out of an elastic material. Below the body, a skirt is attached. Due to the low bending stiffness, this concept does not require hinges (Figure 3.10).

Figure 3.9 Rubber flange connection
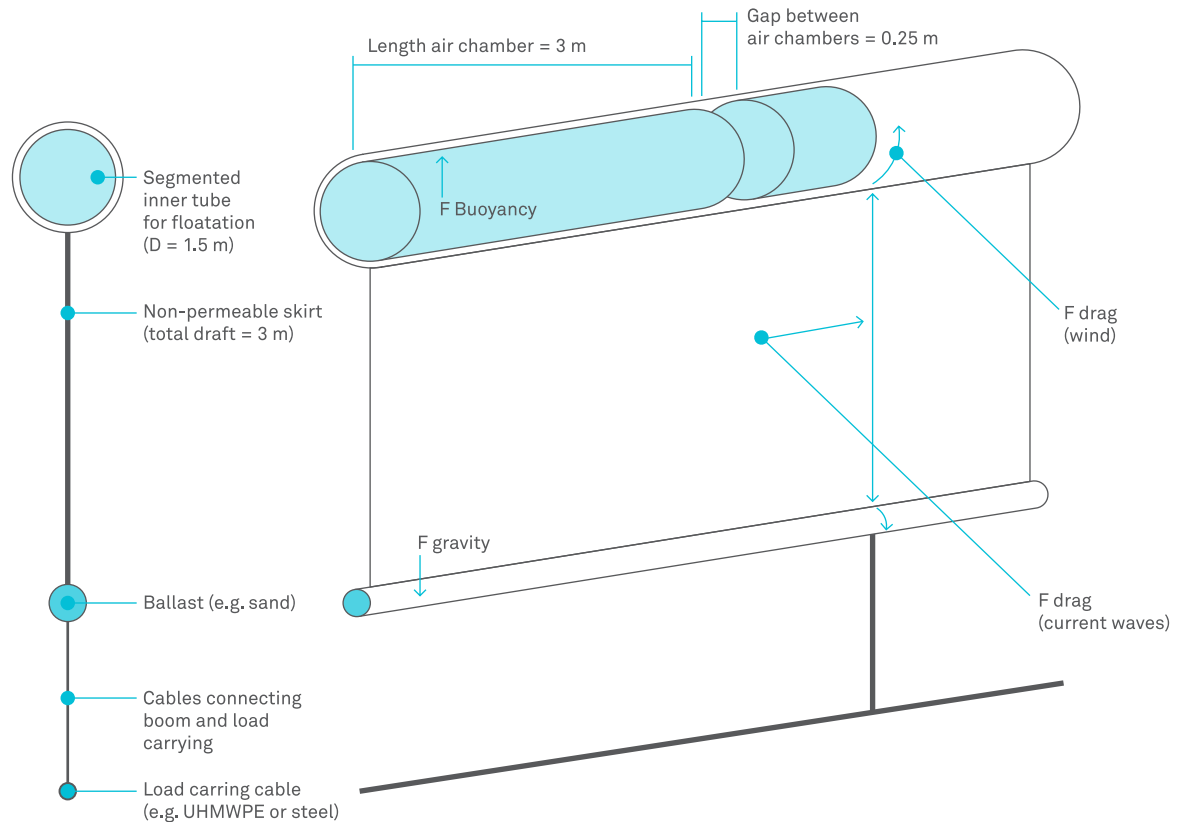
Figure 3.10 Flexible boom concept

3.2.3. CONCLUSIONS

The concepts presented thus far can be seen as the first iteration step in concept development. Because of the lack of further technical details, the Solidworks contest concepts have not been further developed in this feasibility study. Furthermore it's unknown how the first concept would be able to follow the waves, because of the hinges used as integral part of the concept, while the second concept does not seem to incorporate any hinging parts.

More promising concepts are the rigid and flexible booms discussed in the second part of the subchapter. The rigid steel boom and flexible polymer boom concepts are both modeled using the computer program Orcaflex, as can be seen in Chapter 3.5. The program is considered to be the world's leading package for dynamic analysis of marine offshore systems. The final concept and its properties will be covered in Chapter 3.6.

In order to confirm the essential properties of a boom (its plastic capture and transportation abilities), a generic boom cross-section will be used in the next two chapters.

BOOM CAPTURE EFFICIENCY

BRUNO SAINTE-ROSE • JAN DE SONNEVILLE

AGNES ARDIYANTI • LEONID PAVLOV

The aim of this part of the study is to determine the efficiency of the boom capture. This capture efficiency is used to quantify the amount of plastic caught (efficiency of the system), for the debris rate that is determined in chapter 4. The boom capture efficiency can be defined as the probability of a plastic particle flowing towards a boom to be captured. The study is performed by modeling the behavior of plastic micro-particles in the flow of water flowing under the boom with Computational Fluid Dynamics (CFD).

One important aspect to address, in order to analyze the efficiency of the boom configuration, is the flow dynamics around it. When a flow hits the skirt, it is deviated downwards and the intensity of the suction force created by the presence of the skirt can lead to the escape of some less-buoyant plastic debris.

In the following CFD study, two problems were addressed: first, the flow dynamics around the submerged part of a buoyancy body (a boom) was simulated in two dimensions in the plane perpendicular to the span of the boom for different velocities. Second, the velocity fields obtained in the first part allowed the numerical simulation of the trajectories of plastic debris of different sizes and buoyancy, and their interaction with the skirt. Finally, based on the input parameters stated in section 3.3.2.1 (see below), the boom capture efficiency can be estimated.

Ocean surface with large plastic
pieces floating partially submerged

Buoyancy body

Plastic particles of various sizes
and buoyancy flowing in the water

$V_{current}$

3m

Streamlines

Skirt
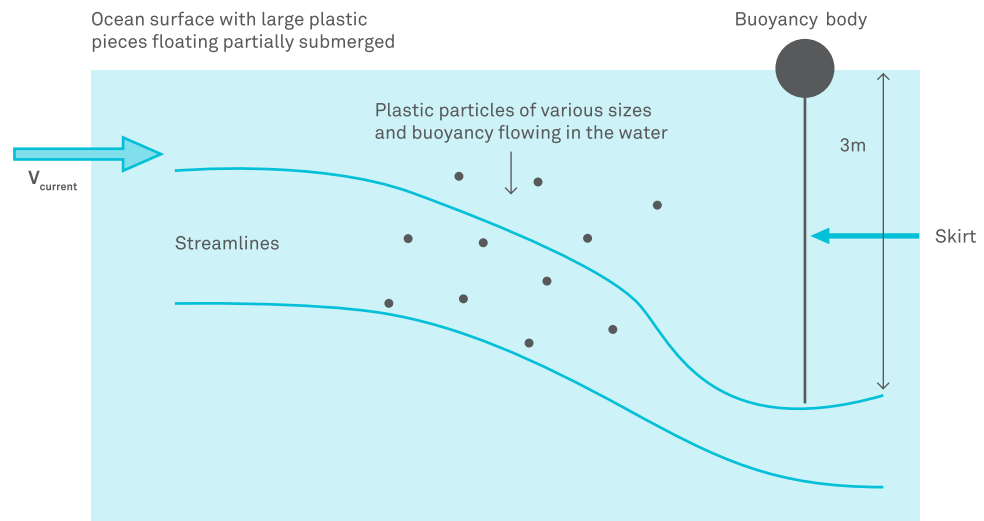
Figure 3.11 Sketch of the problem considered

3.3.1 PROBLEM DESCRIPTION

The problem and geometry considered are sketched in Figure 3.11. The boom is represented by a half disk of radius R of 0.5 m, which corresponds to a rough value of the submerged section of the buoyancy body in the plane perpendicular to the boom span. A thin obstacle of 2.5 m depth corresponds to the skirt, thus yielding a total draft H of 3 m. In the simulation, a skirt thickness of 1 cm is used. This results in a 1/250 aspect ratio for the skirt. No ballast representation was included in the simulation.

In the simulation, the skirt and buoyancy body are fixed. This means that neither the rigid motion induced by the current nor the elastic deformation of the skirt is taken into account. Moreover, the effect of waves and wind on the flow is not taken into account. Two angles are considered with respect to the vertical, first a 0° angle (the skirt is entirely vertical), and a 10° deflection of the skirt downstream.

The capture efficiency of the boom depends on the size of the plastic particles, the buoyancy and the local flow velocity.

PARTICLE TRANSPORT AND INTERACTION WITH SKIRT

In order to simulate the trajectory of particles that would mimic the behavior of plastic debris of a given size and buoyancy, the trajectory of spherical particles are considered in order to simplify the problem as a first assumption without a deeper knowledge of realistic debris characteristics. These particles are injected at a fixed distance (10 m) from the boom and barrier arrangement.

One-way coupling between the particle and the flow is considered and the equation of motion for the center of gravity (CoG in Figure 3.12) is solved. A description of the forces in free stream and wall interaction conditions is given in Figure 3.12
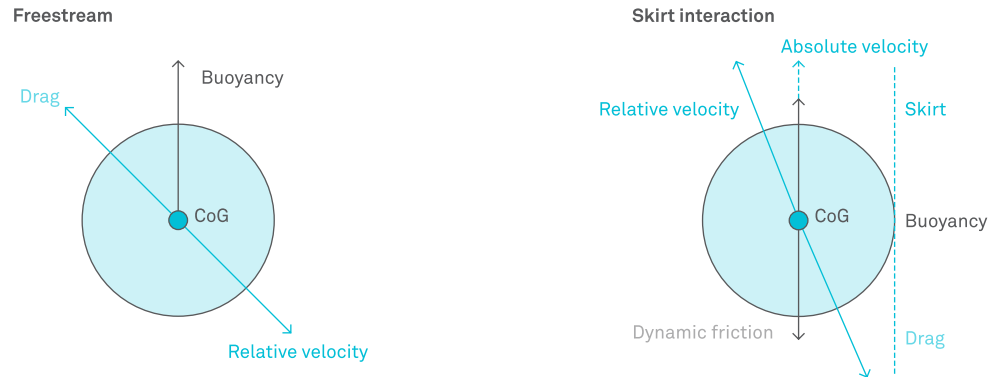
Figure 3.12 Sketch of forces on particle in free stream (left) and with wall interaction considering equilibrium of stream-wise forces (force of the fluid on the particle + barrier reaction) (right). CoG = center of gravity.

As the drag force depends on the particle's relative velocity with respect to the water flow (relative velocity), a water velocity field around the boom must be established first. The buoyancy force depends on the particle size and material. Based on oceanographic measurements, an input range of particle sizes can be chosen that are representative for the ocean gyres. As these measurements are relatively sparse, an interpolation model is used to estimate the particle properties. Lastly, the skirt interaction, reaction force, and dynamic friction are estimated based on general knowledge.

The factors affecting the forces acting on a plastic particle are particle diameter (D, m), current speed (U_0, cm/s), particle friction coefficient (C_f, dimensionless), and particle drag coefficient (C_d, dimensionless).

3.3.2. SIMULATION METHODS

The numerical simulation of the current around the submerged buoyancy body and skirt is carried out with a 2D CFD approach. This simulation uses oceanographic weather data, as well as measured particle sizes, to simulate the flow and the virtual particle behavior in this flow. In addition, interactions with the boom are taken into account as well.

3.3.2.1. SIMULATION MODEL

The simulations are carried out using the ANANAS code (team, 2013) developed by LEMMA, which solves the incompressible Navier-Stokes equations. Given the velocities considered and the characteristic dimension of the problem (the height of the obstacle), the Reynolds numbers that are at stake correspond to fully turbulent flows. As a consequence, beside the mass and momentum equations, the code also solves the two equations of the k-ε turbulence model (Launder & Spalding, 1974) in order to take into account turbulence. In addition, a law for the wall is applied to account for the non-slip condition at the wall. However, regarding the particle-skirt interaction, a friction coefficient (C_f) between 0.04 and 0.1 is considered. The algorithm used for space integration is of third order accuracy.

COMPUTATIONAL MODELING: BOUNDARY CONDITIONS

The computational domain is a rectangular box of dimensions [-20 m, 60 m] x [0 m, -40 m] in the XY plane with Y being the depth, and the center of the domain being located at the center of the buoyant body. These dimensions were chosen to allow the flow to be fully established, but at the same time to assure that the inlet and outlet boundaries would not be so close as to influence it. Indeed, downstream of the skirt, it is important that the computational domain is long enough for the flow to reattach before the outlet section.
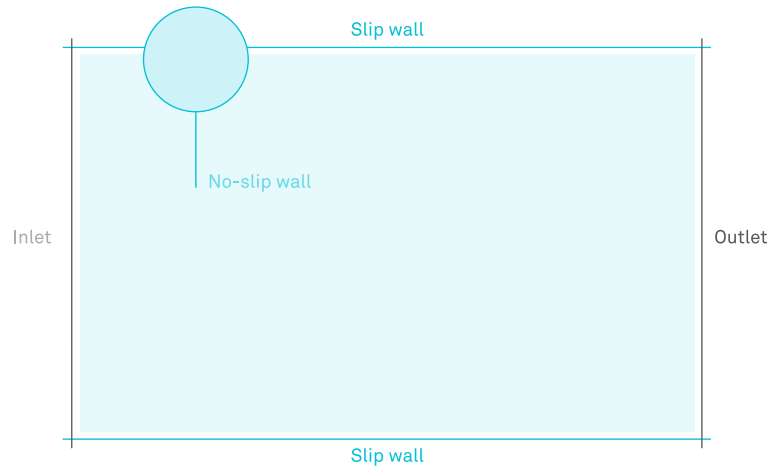
Figure 3.13 Location of the boundary conditions

The boundary conditions are defined as described in Figure 3.13. At the inlet, the flow velocity is imposed and hydrostatic pressure is imposed at the outlet. The following current velocities are used in the different computations U_0 = 5 cm/s, 7.5 cm/s, 10 cm/s and 15 cm/s (see also section 3.3.2.1)

Both the far field and water surface are considered as slip walls. A no-slip condition is set at the submerged buoyant body and skirt surface in order to impose zero velocity at the wall.

COMPUTATIONAL MODELING: MESH
For computational modeling, the computational domain is divided into elements of simple geometry, also called mesh. The meshing strategy aims at capturing the evolution of the quantities resolved by the algorithm (velocity, pressure). This is done within each cell, for each time-step of the simulation. Smaller cells allow for smaller, more detailed changes, and higher accuracy. A sufficient small change across a cell, i.e. small cell size, is required for the algorithm to give a correct result.

Therefore, a finer mesh is required to accurately distinguish the velocity gradients appearing near the skirt. The mesh considered in the computation is unstructured fully triangular as depicted in Figure 3.9. The mesh size ranges from 5 mm near the walls to 0.8 m in the far field. A fine grid resolution is compulsory to capture the velocity gradients in the boundary layers and early separation whereas a coarser mesh is sufficient in the far field.

Figure 3.14 below represents how the mesh cells are arranged within the boundary conditions and several zzoom-levels of the mesh are given below
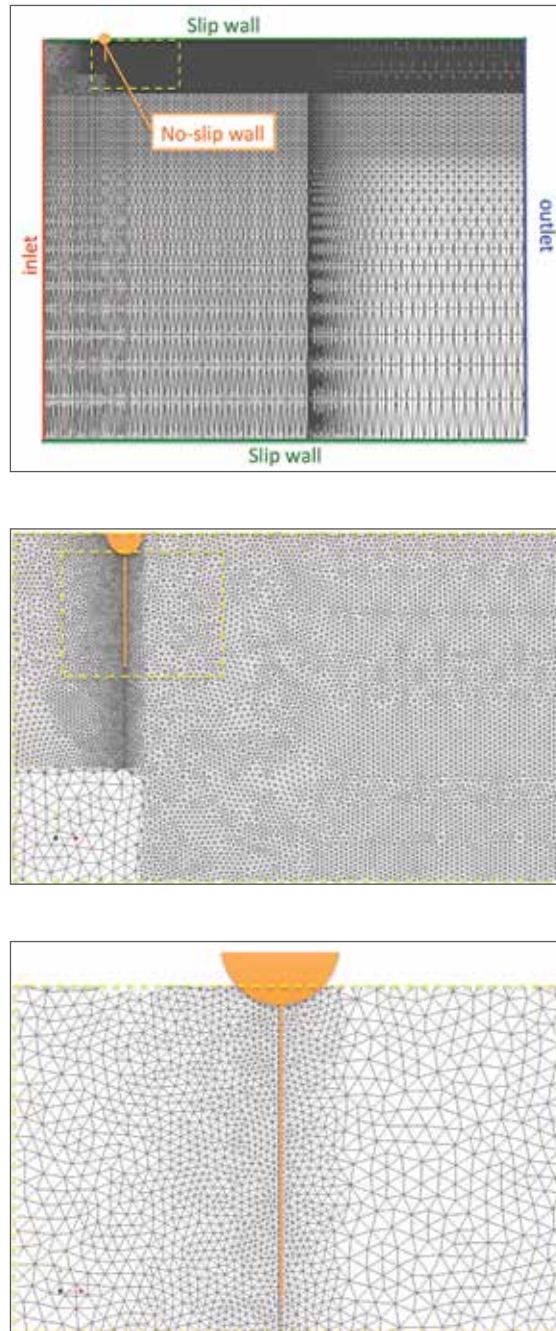
Figure 3.14 Views of the mesh with a progressive zoom on the plastic barrier from top to bottom for the vertical case

Computation procedure and algorithm characteristics
First, the steady state velocity flow field is interpolated on a Cartesian grid of dimensions [-10 m, 0 m] x [0 m, -10 m] and 1cm mesh size in order to simplify the numerics and optimize the accuracy of the interpolation. Then the time integration of the equation of motion is carried out using a Runge-Kutta first order scheme with a CFL number below 0.2. At each time-step, the velocity of the surrounding fluid is interpolated on the Cartesian grid with the neighboring cells. The algorithm source and input parameters are free to use and modify.

3.3.2.2. INPUT VALUES FOR THE MODEL
As a consolidation of the knowledge obtained from the 2D CFD analyses, a total CFD capture efficiency figure was computed. The computation was based on certain assumptions, listed below:

- The plastic particles are spherical.

- The vertical distribution of the plastic particles can be estimated using the approach provided in Kukulka, Proskurowski, Morét-Ferguson, Meyer, & Law (2012).

- For the approach given in Kukulka (2012), median values for the significant wave height and wind velocity at height 10 m above sea surface are used to representatively estimate the capture efficiency.

- Weight distribution of the plastic class sizes as measured and given in Section 2.3 is representative and applicable to the investigated location in the gyre.

- Normal velocity component (perpendicular to the array skirt) of the incoming plastic particles is approximately equal to the current speed (see Section 2.5).

Quantity	Value
Wind velocity at height 10 m	6.05 m/s
Significant wave height	2.09 m
Current speed	0.13 m/s

Table 3.1 Median values of applicable parameters in the selected location (31°N – 142°W) used in the calculation of capture efficiency. More details are given in section 2.4.

MEDIAN VALUES
The median values corresponding to the selected location (31°N – 142°W) are given in Table 3.1. More details of the location selection can be seen in section 2.4.

Based on the median value of the current speed in Table 3.1, the current velocities U_0 ranging from 5 cm/s to 15 cm/s are applied for the computations.

PARTICLE SIZE DISTRIBUTION ACROSS THE DEPTH
A similar definition of plastic size scales as in Section 2.2.3 is adopted here. An average rise speed (w_b) of 0.01 m/s for microplastics and 0.07 m/s for small to large-scale plastics is applied. The average rise speed for microplastics is assumed based on estimation of the buoyant rise velocity given by Kukulka et al. The rise speed level for small up to large scale was estimated based on multiple experiments featuring two plastic coupons from the small plastic size range. This figure was further taken as applicable rise speed for the plastics in the small to large scales.

Using the two different rise speeds and climate data applicable to the selected locations, the height-wise distributions of plastic were generated. These are given in Figure 3.15.

MicroPlastic concentration as a function of depth w_b=0.01m/s

Meso/macroPlastic concentration as a function of depth w_b=0.07m/s
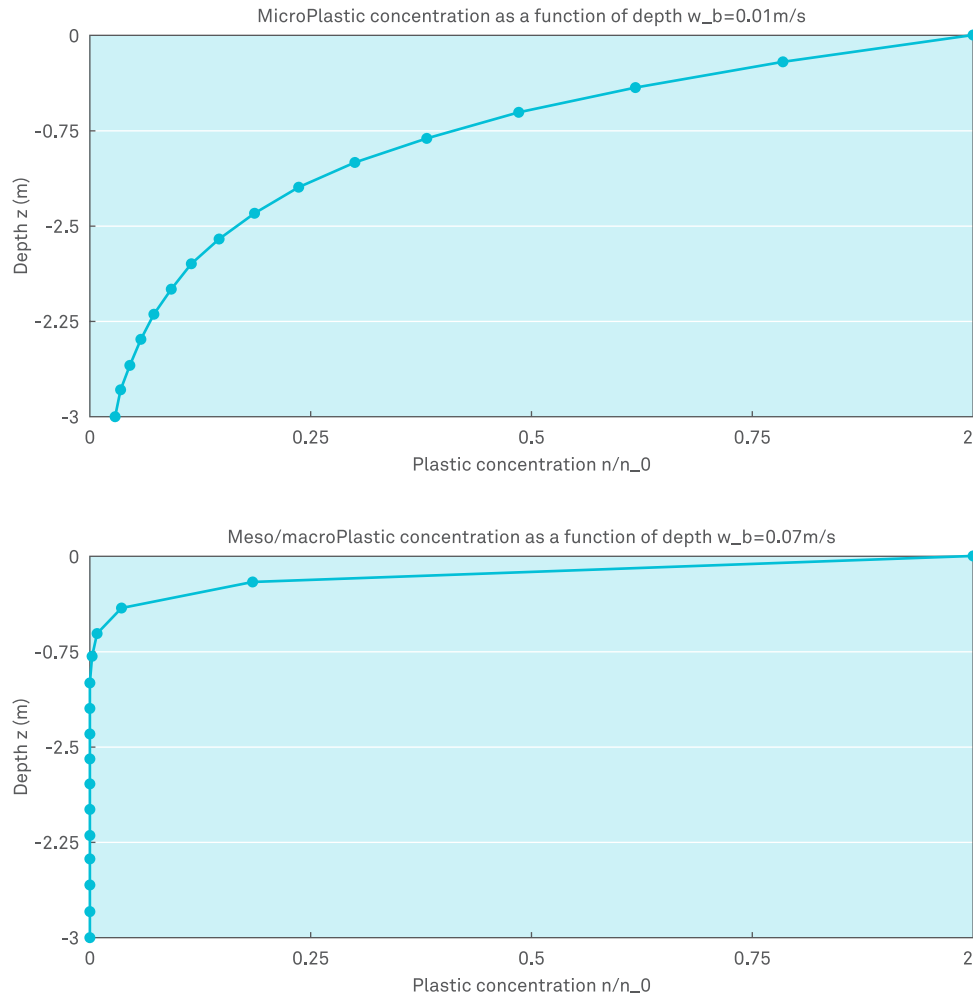
Figure 3.15 Estimated height-wise distribution of floating plastic using the approach from (Kukulka et al. 2012). w_b = average rise speed, n = number of plastic particles at a certain size and depth, n_0 = total number of plastic particles.

Following the distribution calculations, these results can be integrated to obtain the total amounts of plastic contained within a certain range of depths. The results of this integration are given in Table 3.2. In the table and in the text further the size classes from Section 2.2.3 are adopted. The large plastics class is defined as particles of sizes >30 cm. The medium size class is formed by particles of sizes in the range 10-30 cm and the particles of the size 2-10cm form the small size class. All sizes below are defined as microplastics.

As can be seen in the case of small plastics, there is a significant amount of particles distributed throughout a 2-meter water column. In the case of medium and large plastics, however, almost all particles are concentrated above the depth of 0.5 m. Combining the depth-wise distribution of the particles with the information on the particle densities and sizes, conclusions on the capture efficiency of the array can be drawn based on the results of the conducted 2D CFD study.

Depth range	Small plastic (2-10 cm) and microplastics (<2 cm)	Medium and large plastics (10-30 cm and >30 cm)
0 – 0.25 m	26.10%	87.90%
0.26 – 0.5 m	19.30%	10.60%
0.51 – 1 m	24.80%	1.40%
1.1 – 2 m	20.90%	0.02%
Below 2 m	8.90%	0.00%

Table 3.2 Total calculated plastic distribution per depth range for the different plastic sizes. Distributions are given in percentage of the total weight of the plastic.

Particle type	Particle size range (D, mm)	Contribution by weight to the total plastic content (%)
Microplastics	<20	15.1
Small plastics	20-100	33.2
Medium plastics	100-300	22.4
Large plastics	>300	29.3

Table 3.3 Contribution of the plastic size groups to the total mass of plastic in the world ocean (Section 2.2.3). Total mass of particles in the NPSG is estimated at 140,546 metric tons.

For the computation of the CFD efficiency values, the results from the simulations with the barrier tilted at 10° were used. Given that the median current speed at the selected location (31°N – 142°W) is 0.13 m/s, the data obtained from the simulations with 0.10 m/s and 0.15 m/s was used to obtain (and interpolate) the corresponding capture efficiencies.

SEA WATER PHYSICAL PROPERTIES
The physical properties of the fluid considered (sea water) (density, viscosity and far field turbulent quantities) are given in Table 3.1, which corresponds to 10 percent velocity fluctuations for k and to a turbulent length of H/10 for ε.

The input parameters used in this 2D CFD study are summarized in the Table 3.4 below.

Density (kg/m³)	Dynamic viscosity [Pa·s]	k^0 (m²/s²)	E_0 (m²/s³)
1025	$1*10^{-3}$	$2.5*10^{-5}$	$3.75*10^{-8}$

Table 3.4 Physical properties of sea water considered in computations

Notation	Parameter	Value range	Dimension
D	Particle diameter	<5 (micro) and >5 (meso and macro)	mm
ρ	Particle density	920 - 1000	kg/m³
c^f	Particle friction coefficient	0.04 and 0.1	-
u^0	Current speed	5/1/2015	cm/s
	Skirt tilt	0 and 10	°
	Sea water density	1025	kg/m³
	Sea water dynamic viscosity	$1*10^{-3}$	Pa.s
k^0	Sea water turbulent kinetic energy	$2.50*10^{-5}$	m²/s²
ε^0	Sea water turbulent energy dissipation	3.7510^{-8}	m²/s³

Table 3.5 Summary of input parameters for 2D-CFD modeling of the plastic particle movement around the boom and skirt.

3.3.3. RESULTS AND DISCUSSION
3.3.3.1. VELOCITY FLOW FIELDS

Figures 3.16 and 3.17 depict flow velocities around the skirt and boom, as represented by longitudinal velocity flow fields, streamlines, and velocity iso-lines, for vertical and 10o tilt cases.

These figures show that there is no significant difference between the flow pattern encountered for 5 cm/s and 15 cm/s cases. At these viscosities, the Reynolds numbers considered are highly turbulent, hence the only difference comes from the length of the downstream recirculation bubble, which is longer as the velocity rises. Further calculation (see supplemental information) proved that Reynolds number weakly affects the forces around the buoyancy body and skirt. Moreover, the tilt angle has a very weak influence on the flow characteristics as well.
It also appears that the recirculating region is very long in comparison with the skirt length and that the velocity upstream of the skirt starts decreasing well upstream.
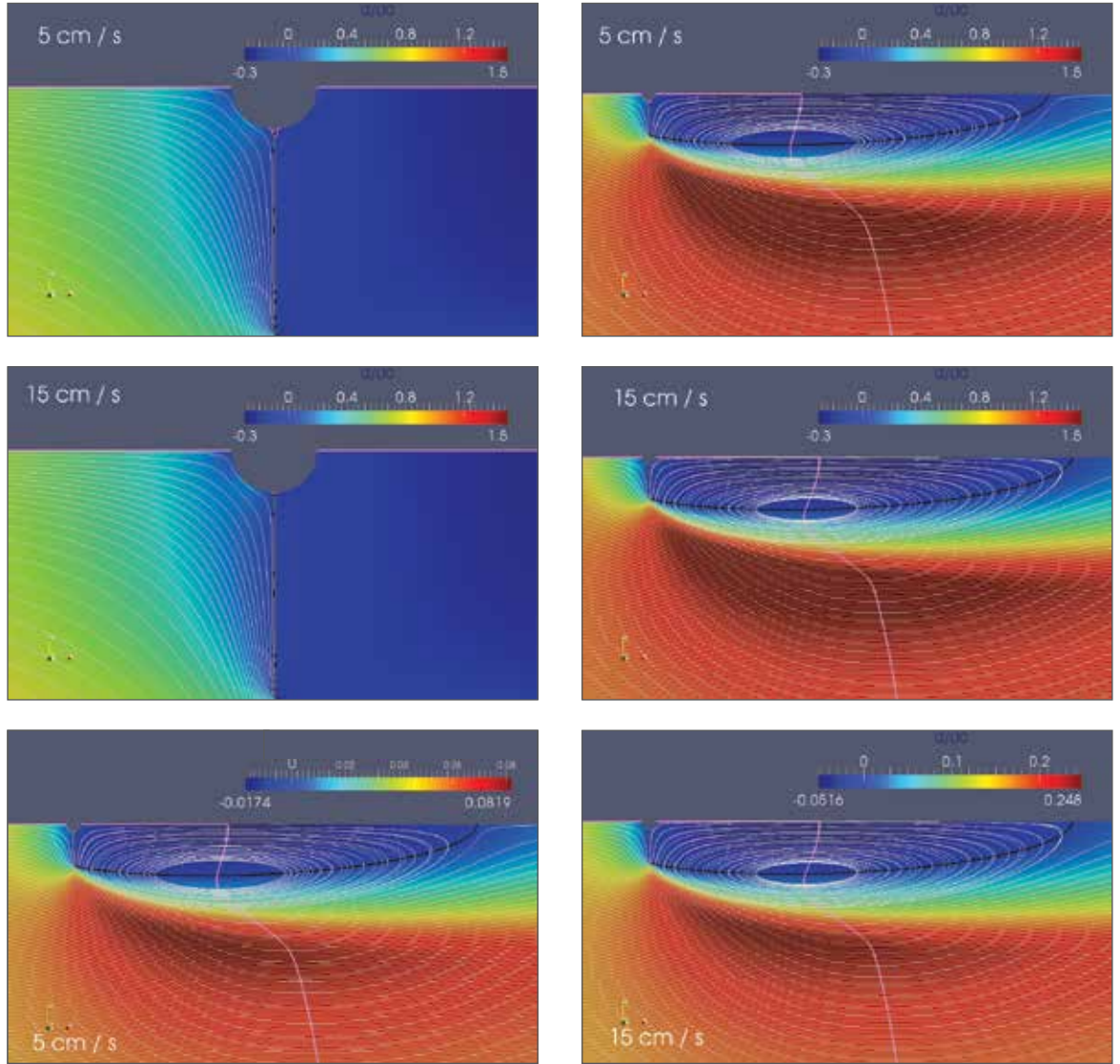
Figure 3.16 Longitudinal velocity flow fields normalized by U_0 the current velocity, streamlines (grey) and longitudinal (black) and vertical (pink) velocity iso-contours for 5 cm/s (top) and 15 cm/s (bottom), view of the boom vicinity (left) and global view of the flow field (right)
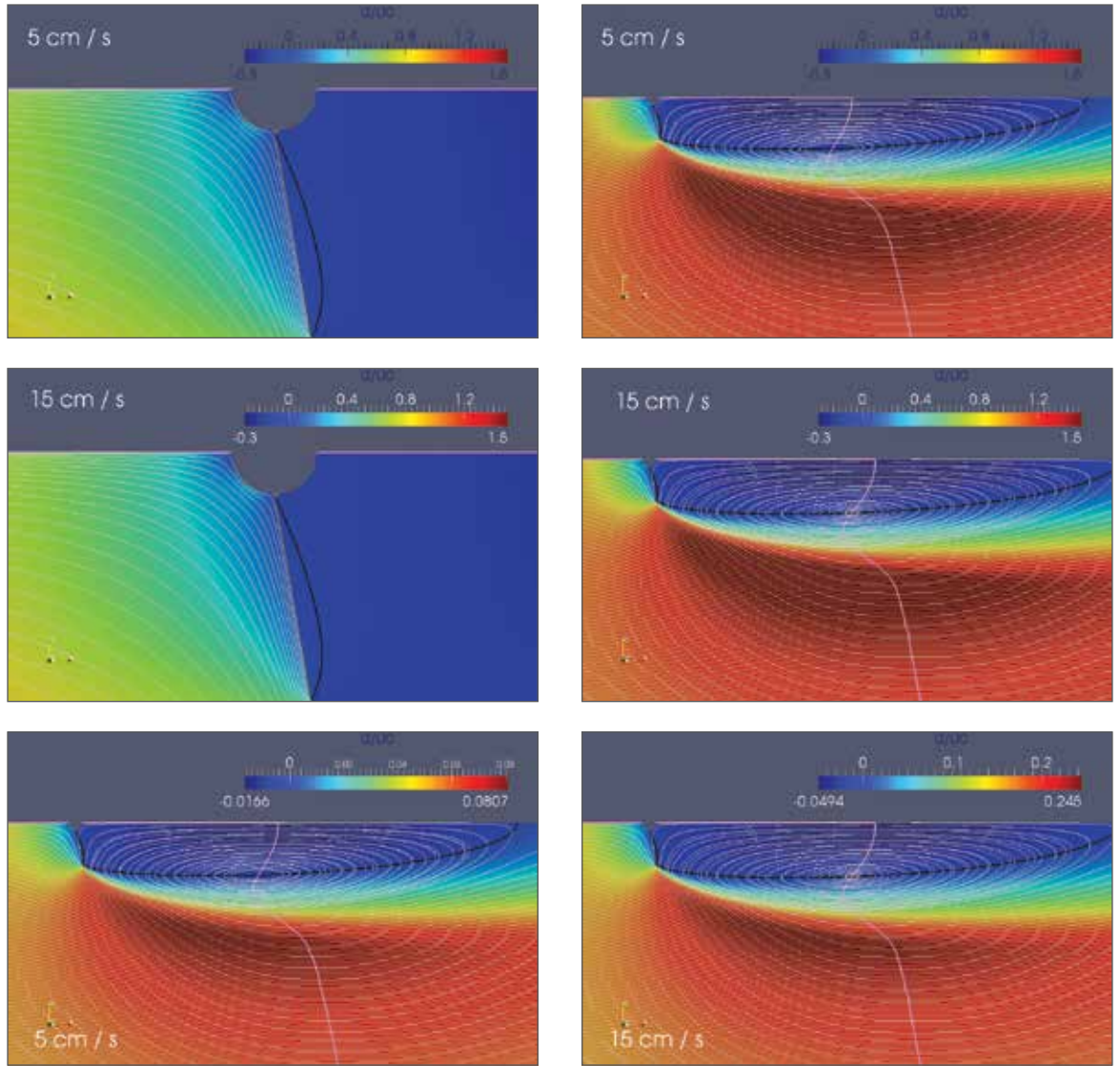
Figure 3.17 Longitudinal velocity flow fields normalized by U_0 the current velocity, streamlines (grey) and longitudinal (black) and vertical (pink) velocity iso-contours for 5cm/s (top) and 15cm/s (bottom), view of the boom vicinity (left) and global view of the flow field (right)
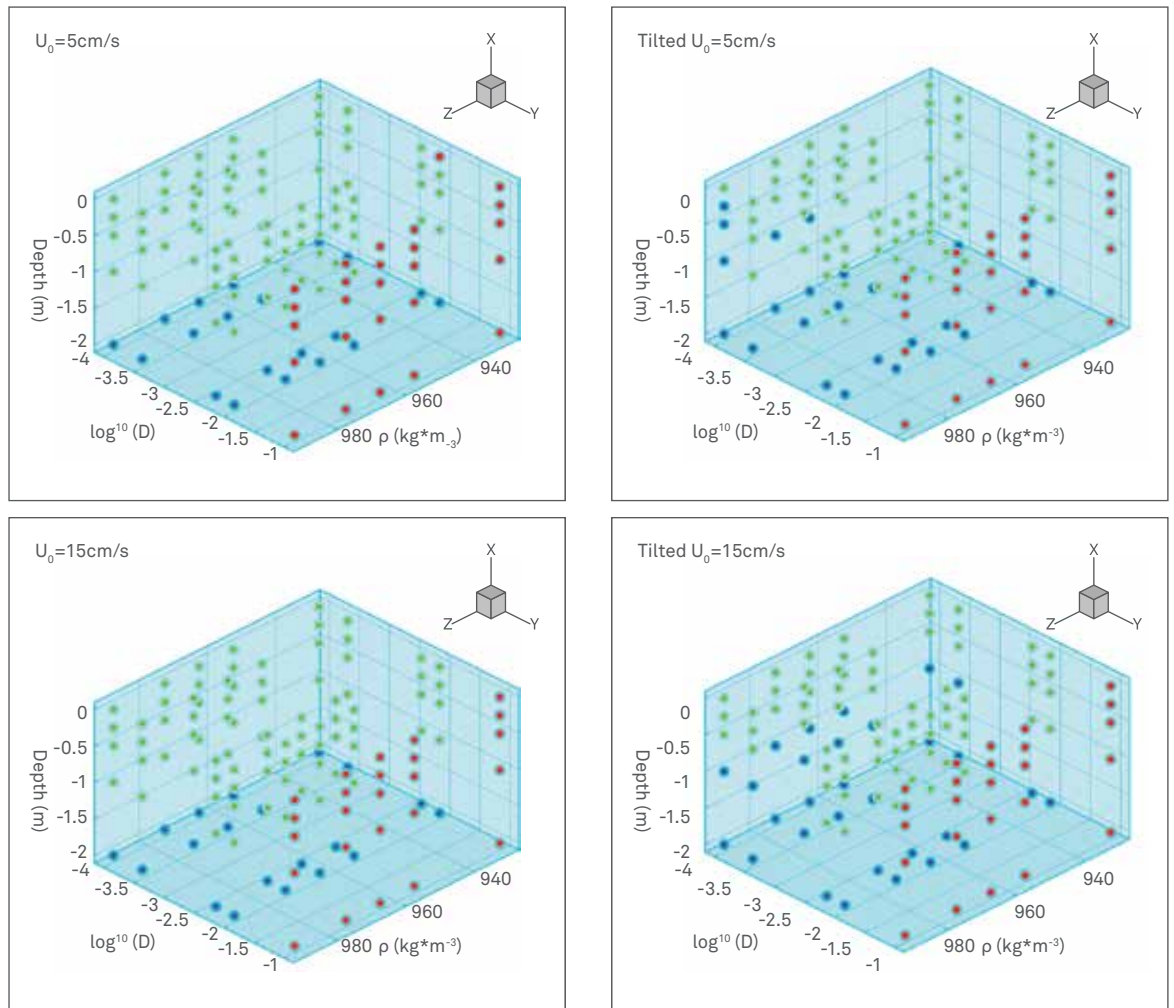
Figure 3.18

3.3.3.2. PARTICLE TRANSPORT AND WALL INTERACTION

In this first series of trajectory simulations 5 densities ρ (930 kg/m³, 955kg/m³, 965 kg/m³, 975 kg/m³ and 990 kg/m³), 5 diameters D ($1*10^{-4}$ m, $3*10^{-4}$ m, $5*10^{-3}$ m, 0.01 m and 0.1 m) and 5 initial depth h (-2 m, -1 m, -0. 5 m, -0.25 m and 0 m), for 5 cm/s and 15 cm/s current velocity and vertical and tilted skirt.

The issues of the trajectory simulations for the 5x5x5x2 cases are depicted in Figure 3.18 This figure is read as fol-lows: each triplet (D, ρ, h) corresponds to a point on the graph with the color code blue for the particles which are sucked underneath the skirt without touching it, green for those who reach the skirt but which still escape, and red for the trapped particles.

From Figure 3.18 it appears that for all diameters and density, all the particles reach the skirt for the vertical case between -1 m and 0 m depth and most of them for the tilted case. However, it appears that only the particles of 0.1 m are completely trapped (from the sizes shown in Figure 3.18). A further investigation in the transition re-gion is given further. It also appears that the density and velocity do not significantly affect the simulation results (for the interval scrutinized). In the following paragraph, the influence of the parameters on particle trajectories is further addressed.
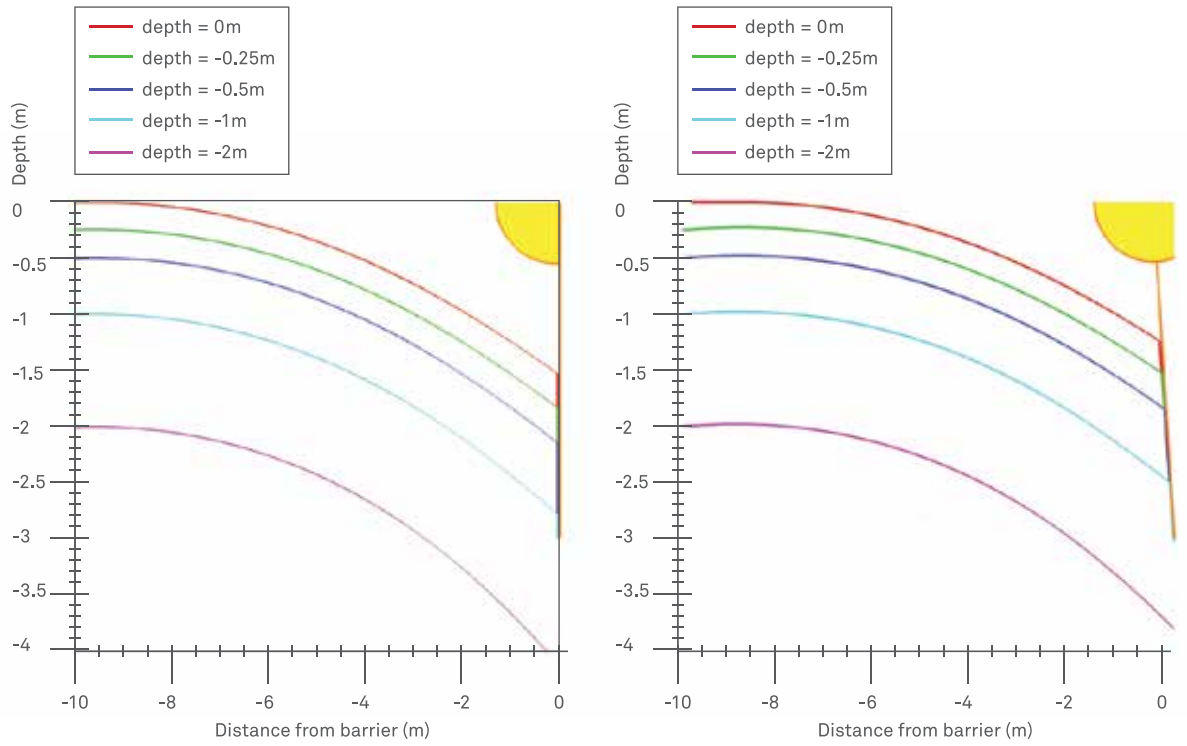
Figure 3.19 Influence of depth on particle trajectory for U_0 = 5 cm/s, D=0.01 m, p = 960 kg/m³
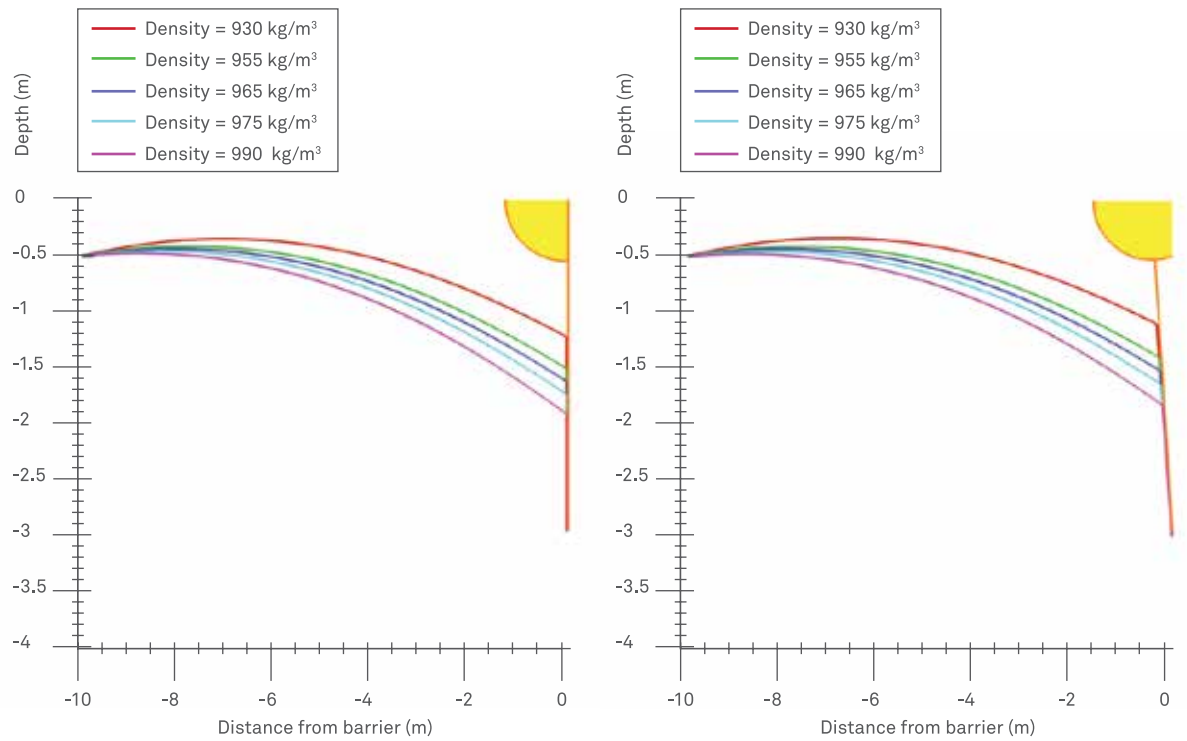
Figure 3.20 Influence of density on particle trajectory for U_0 = 5 cm/s, D = 0.01 m, Z (depth) = -0.5m

3.3.3.3. INFLUENCE ON PARAMETERS ON PARTICLE TRA-JECTORIES

The influence of initial depth on the particle trajectory is showed in Figure 3.19. In this, figure it appears that the particles follow parallel tracks, if they do not reach the surface. It is also important to notice that even though the particle hits the skirt at mid-height (red line for instance) it will still escape from the skirt.

The influence of density on the particle trajectory is showed in Figure 3.20 and appears to be of minor influence on the interval considered

The influence of diameter is illustrated in Figure 3.21. For a given combination of [depth, density] one can estimate a "buoyancy limit" when the particle is not buoyant enough to go up when it reaches the skirt. It appears that the "buoyancy limit" is located between D = 1.2 cm and D = 1.3 cm, which is when the particles start moving up as they touch the barrier. An equivalent effect can appear by varying the density with a given combination of [depth, diameter].

From the results shown in Figure 3.18, it can be seen that particles with diameter of 10 – 35 mm lay in the transition area as part of these articles are trapped, and the rest escaped the skirt after touching it. Therefore, and additional trajectory simulations in the diameter D range of 10 mm and 35 mm range are conducted for the 4 velocities on the tilted case and depicted in Figure 3.20. In this figure, the effect of density and current velocity are highlighted. This has been done to accurately identify at which particle size exactly the transition to caught/non-caught is happening to allow for further easier capture efficiency calculations.
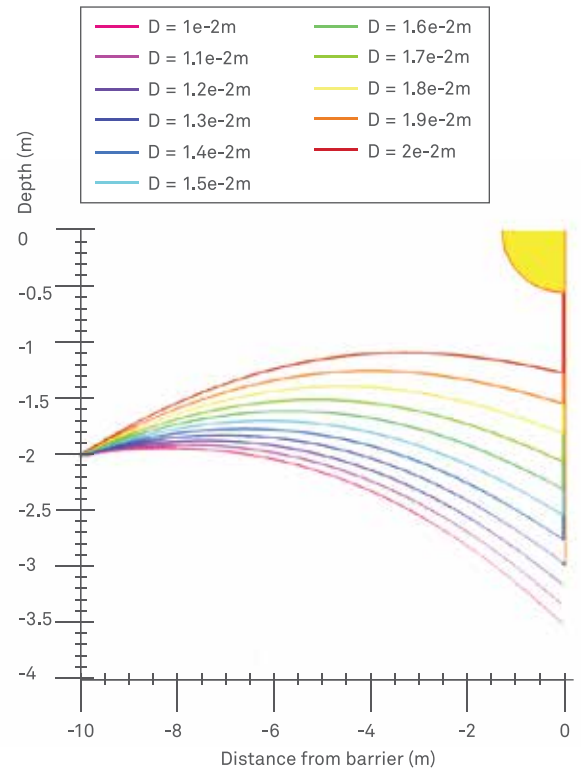
Figure 3.21 Illustration of the "buoyancy limit" for U_0 = 5 cm/s, p = 960 kg/m^{-3}

The trajectory simulation of the particles in the transition area (D = 10 – 35 mm) as given in Figure 3.22 shows that the particle movement in this diameter region are significantly influenced by the U_0 and ρ. Difference in the number of particles trapped is obvious when the current speed increases from 5 to 15 cm/s. Large difference in the number of particles trapped is also observed between particle density of 930 and 990 kg/m³. These observations suggest that for the range of diameters 10 – 35 mm within the investigated range of densities and current speed the buoyant forces become dominant over the viscous ones. The particle catch probabilities obtained from this range of particle sizes is defining the catch probability for the small plastics group.

INFLUENCE OF THE FRICTION COEFFICIENT

The coefficient that characterizes the dynamic friction between the particle and the skirt has a great influence on the outcome of the particle trajectories simulation. The influence of the friction coefficient (by changing C_f=0.04 to C_f=0.1 on the results is given in Figure 3.23. Where the results from the computation with C_f=0.04 are reminded. The objective was in fact to show that by using a higher value of the friction coefficient some particles that would have escaped with a lower value of C_f are now trapped. The accurate estimation of this friction coefficient will be required for most advanced studies. In particular given the surface state of the skirt and the plastic debris that will be considered. From this figure it appears that with a higher friction coefficient most of the 0.01 m particles are trapped whereas it is not the case for C_f=0.04.
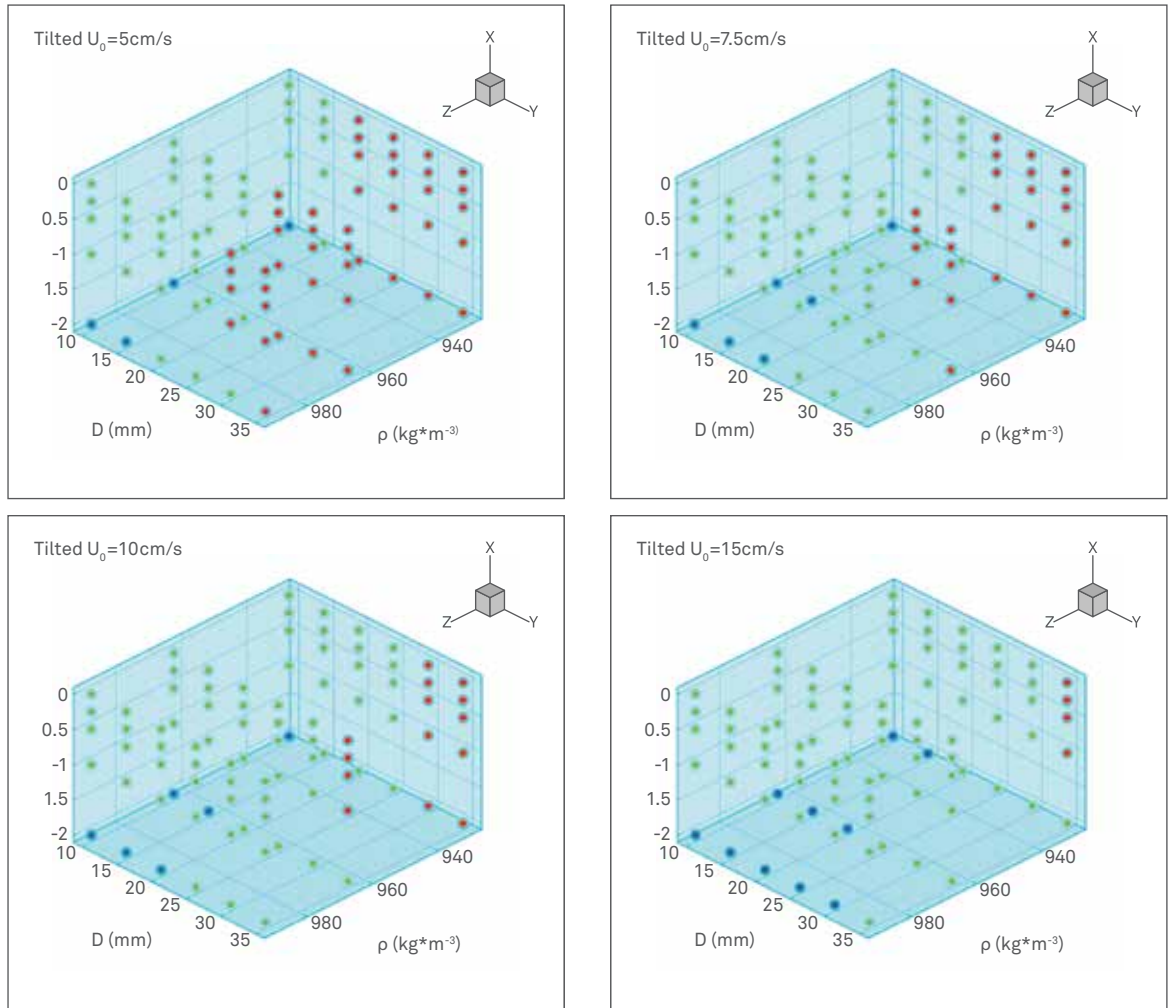
Figure 3.22 Trajectory simulations in the transition area (D = 10 – 35 mm)
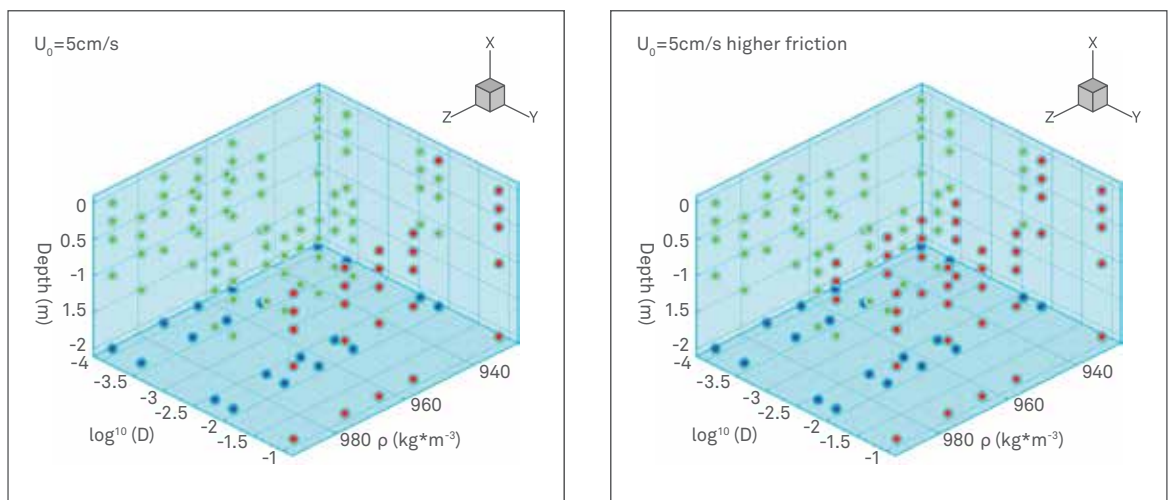
Figure 3.23 Comparison of the particle trajectory outcome with C_f = 0.04 (left) and C_f = 0.1 (right) on the vertical skirt

Figure 3.24 is an illustration of a case where for the same particle characteristics (in that case D = 0.01 m, ρ = 960 kg/m³ and a depth of -1 m) a higher friction coefficient will prevent the particle from escaping.

Given the findings of the previous trajectory simulations a last analysis is made considering U_0 = 10 cm/s for a density range of [960,1000] in the [10mm, 100mm] diameter range and is depicted in Figure 3.25 and for a friction coefficient C_f of 0.1.

One important remark that has to be made is first that the friction coefficients employed in this study are rather small and consider lubricated conditions. Second, the particle-particle interaction is not considered, nor the particle accumulation. Third, no ballast nor protuberances are considered in the bottom part of the skirt. The addition of these features should allow fewer particles to escape from the skirt.
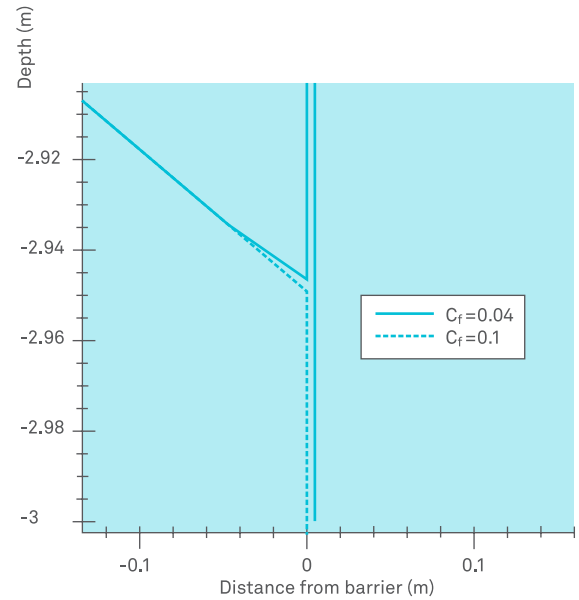
Figure 3.24 Zoom on particle trajectory when it hits the barrier for C_f=0.04 and C_f=0.1 for the vertical skirt
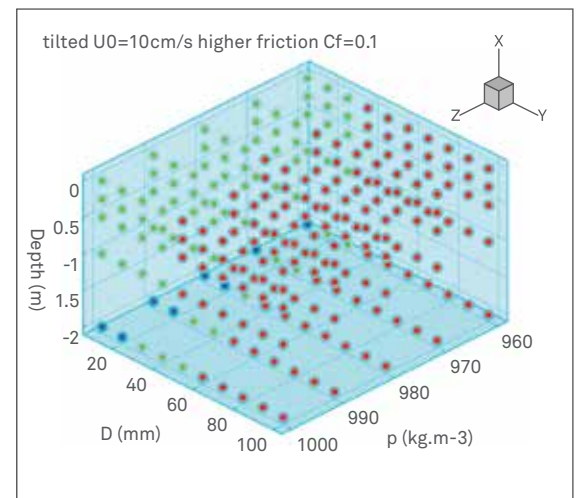
Figure 3.25 Trajectory simulations for U_0=10 cm/s [10mm, 100mm] range

3.3.4. CONCLUSIONS

Based on the densities and depths of the particles and the conclusions on whether the particles were caught or not the CFD capture efficiency was estimated.

The following generic conclusions can be drawn about the particle catch probability:

- No microplastics (particles < 2 cm) can be caught with the proposed solution irrespective to any variations in friction coefficient of the barrier, particle density or re lease depth.

- Most of the small sized plastics can be caught; depending on the particle density the size threshold above which the particles will be caught is around 35mm.

- All medium and large size plastics (irrespective of the depth wise position) are caught

Combining the results from the distribution of the plastic particles on scales of depth, density and sizes with the results obtained from the CFD simulation a total CFD capture efficiency of 78.6 percent was obtained.

The large and medium scale plastics contribute 51.7 percent to the efficiency since all of them are captured.

Due to the limited amount of simulation data available certain assumptions about the catch probability of small plastics were taken:

- It was assumed that mass of the particles is evenly distributed between across the entire range of sizes of the small plastics group. That is: the total mass of particles in the range 20-30 mm is the same as the total mass of particles in the range 30-40 mm

- It was assumed that the catch threshold for plastic particles for the current speed of 13 cm/s and skirt tilt angle of 10° is 35 mm. Simulations have confirmed that most of the 35 mm particles are caught, however in some specific simulation cases this did not hold. On the other hand this is counteracted by the fact that some of the smaller particles (30 mm) were caught under certain conditions.

Therefore, all particles in the range of 35-100 mm are assumed to be caught which constitutes 81.25 percent of the small plastics range and thus 27 percent of the total plastic content.

MODELING OF BOOM ANGLE

This part of the study can be seen as an extension to the 2D CFD Model. The 2-dimensional CFD model study is performed to investigate the fluid and particle flow perpendicular to the boom sections. The presence of the boom barrier will direct some portion of the ocean flow downwards. This creates a drag force on the plastic particles, which can lead to the escape of the particles that are not buoyant enough. Results showed the capture efficiency for different flows, particles and skirt angles.

The current chapter shows the investigation into the of fluid and particle flow in 3 dimensions. This allows for showing the relation between the ocean current flow and transport of plastic particles towards the sink. Here, the sink is the location where plastic debris is collected and separated from the water.

The main focus of this study was to investigate the transportation rate of the particles along the boom towards the sink. In addition, the capture efficiency was investigated in a 3D setup.

However, fewer parameters are varied compared to the 2D study. Three questions addressed are:

- How is the flow of the ocean current affected by a barrier/boom? What is the velocity distribution in steady-state condition?

- How do parameters such as barrier angle and the interaction of the flow with the barrier influence the transportation rate of the plastic particles along the boom towards the collection station?

- What is the catch probability of the plastic as a function of particle size, density and array geometry?

For solving this problem, two models were set up using two distinct commercial software packages: Comsol Multiphysics 4.4 and ANSYS CFX. Both problems featured the same simplified problem setup, but the assumptions taken and the ways in which the models were set up were different in the two cases. The differences mostly relate to the use of periodic and open boundary conditions as well as model locations where particles were released and the way velocity calculations were performed. Periodic boundary conditions model an infinite long barrier, whereas open boundary conditions can only model a fraction of the final barrier length, in our case 100 m.

One of the main limitations of the both models, however, is that wind and waves are not taken into account. Furthermore, the rigidity of the Ocean Cleanup Array is neglected. Simulations including wind and waves, or where the array could be made flexible in either direction have proven require more than the available amount of time. Due to the significant differences in size scales between thickness or draft of the boom on the one hand and the entire array on the other hand, the 3D volume was significantly reduced to look at a small part of the array. It was estimated, however, that the scaled down computational volumes would allow for capturing the behavior of the array and the flow in an adequate manner.

The conclusions regarding catch probability obtained during the 3D CFD modeling in both cases support the findings of the 2D CFD models. The results do not match perfectly, but within the range of the highest significance (macroplastics); partially for mesoplastics, the results of the 2D and 3D CFD studies are in agreement. Since the 2D CFD study covered a wider range of simulation setups, the results of the 3D CFD catch efficiency were used for reference, benchmarking and comparison, but not in the catch efficiency calculations.
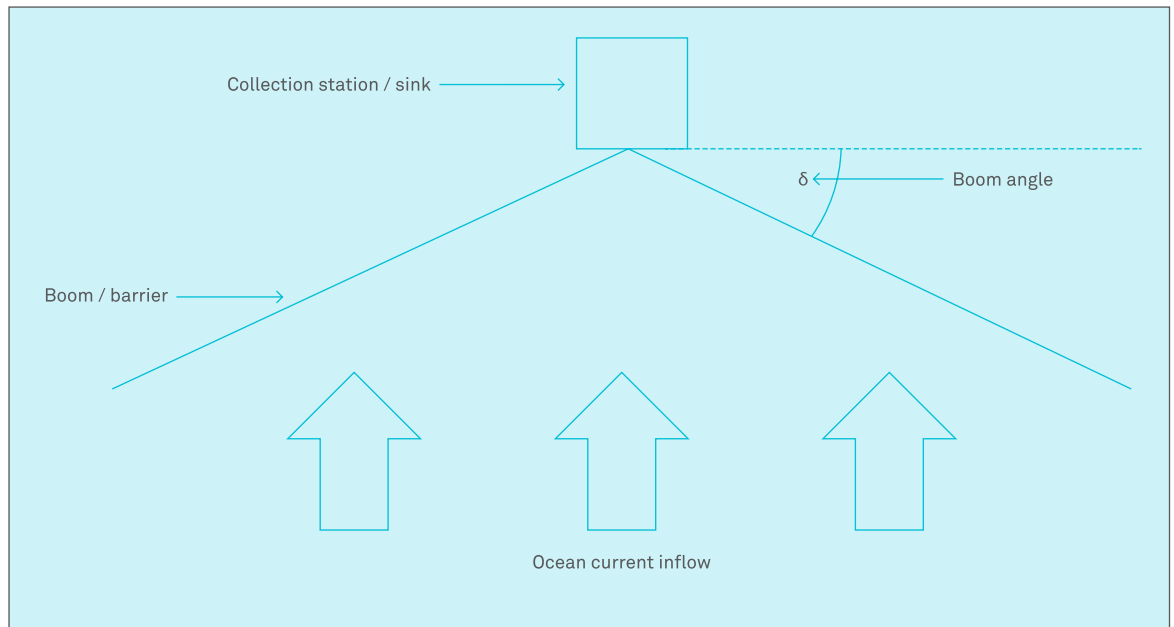
Figure 3.26 General structure layout – top view

3.4.1. COMSOL MULTIPHYSICS 4.4 3D CFD MODEL
NIKLAS WEHKAMP • DAVID KAUZLARIC • BOYAN SLAT
JAN DE SONNEVILLE • LEONID PAVLOV

3.4.1.1. MODEL SUMMARY
The program used for modeling is Comsol Multiphysics 4.4. Two different geometric setups were used to analyze the catch probability and the transportation rate of the particles. The catch probability indicates the probability of a particle to stay in front of the boom for the duration of the experiment. The transportation rate is calculated by taking the mean velocity of 5 particles for 300 seconds as they are drifting in proximity to the barrier. The general setup is shown in Figure 3.26. The figure shows a top view of the system. Figure 3.27 shows the created mesh, with axis convention.

The boom angle is defined as the angle between the boom and the direction perpendicular to the ocean current inflow. Next, the two setups are briefly explained.

3.4.1.1.1 GEOMETRY FOR CATCH PROBABILITY
The first setup models the behavior of particles located close to the collection station. This setup is used to calculate the capture probability for different particles. For this purpose, a "small" setup with a simulation domain of 50 x 6 x 20 m³ is used. The small setup makes computation faster, allowing for more parameter variations. The setup is displayed in Figure 3.28. The V shape of the barrier close to the collection station is modeled by the use of symmetry. The boundary on the right side of the flow box is mirrored, resulting in a V like structure for the barrier when looking at it from the top. The boom (or barrier) is modeled with a 3 m height.

3.4.1.1.2 GEOMETRY FOR PARTICLE TRANSPORT SIMULATION
The second geometric setup is used to model the particle speed in front of the barrier. Because the portion of the flow toward the sink will add up as the barrier gets larger, a simulation domain 100 x 100 x 20 m³ is used. The final boom length is expected to be larger, but this setup should allow to investigate how the boom angle affects the particle speed in front of the barrier. The geometrical setup is displayed in Figure 3.29.
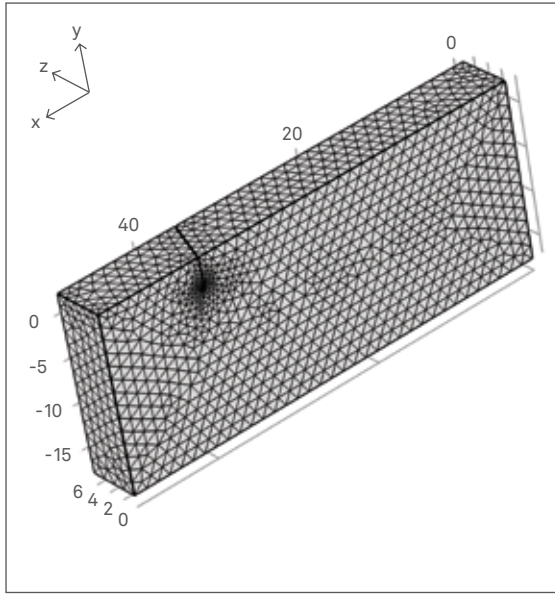
Figure 3.27 Mesh with axis convention
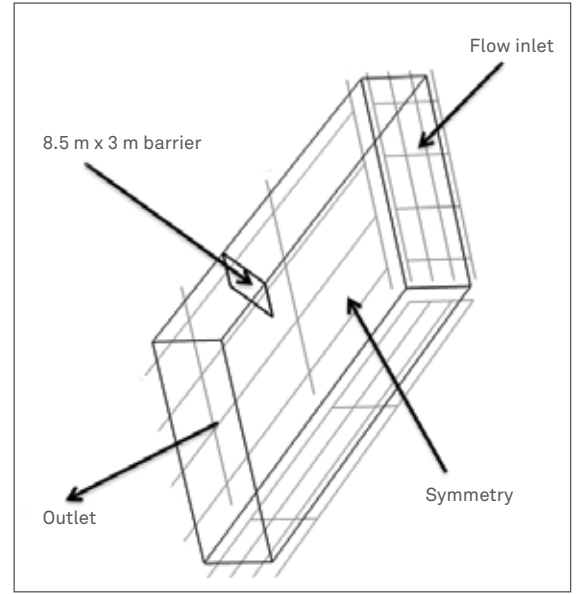
Figure 3.28 Geometric setup 1, the closed V Experiment (6m)
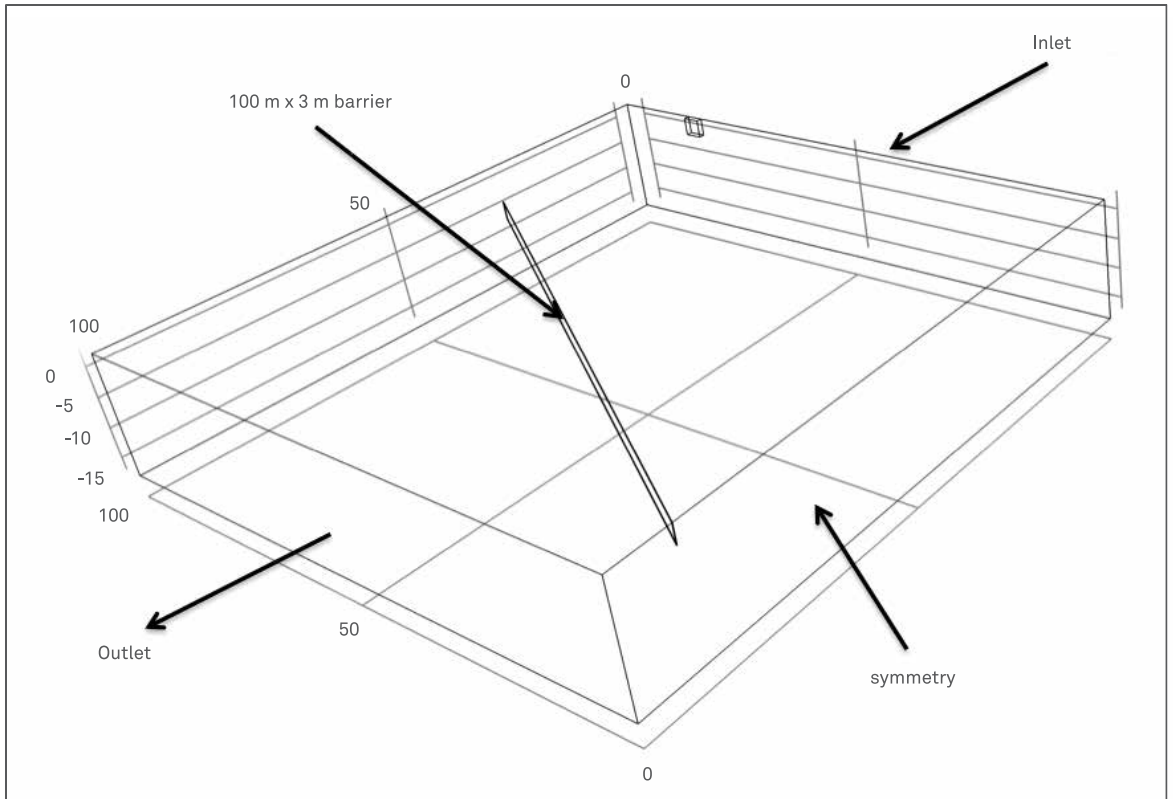
Figure 3.29 Geometry setup 2, the closed V Experiment (100 m)

3.4.1.1.3 TURBULENT FLOW MODEL TECHNIQUE

The flow acts as a drag force on the plastic particles that are distributed in the ocean. This drag force moves the particles towards the barrier. In front of the barrier, some portion of the water flow is directed downwards. The result is that the plastic particles are also pulled downwards, if the buoyancy force of the particle is smaller than the drag force.

The flow of the ocean in this study is simulated by the turbulent flow k-ε model, which is often used in industrial applications.

In the k- ε model, the k stands for the turbulent kinetic energy and ε stands for the turbulent dissipation rate. More information on the used modeling technique for turbulent flow can be found in Wilcox (1998). This model is both relatively robust and computationally inexpensive compared to more advanced turbulence models. One major reason to why the k-ε model is computationally inexpensive is that it employs wall functions to describe the flow close to walls instead of resolving the very steep gradients there.

3.4.1.1.4 FLUID PROPERTIES AND BOUNDARY CONDITIONS

The parameters below provide the model's main conditions.

The inlet velocity for all experiments in this study is defined as U_{in} = 0.1 m/s. Furthermore, the inflow turbulent intensity is set to IT= 0.05.

Resulting k and ε values are:
$k = 3.75 \cdot 10^{-5}$ [m²/s²]
$\varepsilon = 2.70 \cdot 10^{-6}$ [m²/s³]

Due to limited available time, wave and wind forces are not taken into account in the model.

For the outlet the boundary condition is defined by pressure p_0 = 0 and no viscous stress.

In order to model the ocean depth, an open boundary condition is set for the bottom.

For the walls of the barrier and the top of the flow box, the "slip wall" boundary condition is applied.

As already mentioned above, the V-shape of the barrier is modeled by the use of symmetry. The boundary on the right side of the flow box is mirrored, resulting in a V-like structure for the barrier when looking at it from the top.

3.4.1.2. RESULTS AND DISCUSSION
3.4.1.2.1. THE FLOW VELOCITY DISTRIBUTION IN STEADY-STATE CONDITION

An example for the streamlines of the flow is depicted in Figure 3.30. The streamlines illustrate how the barrier affects the flow of the ocean current. In the figure, the streamlines indicate that some part of the flow is directed downwards under the barrier.
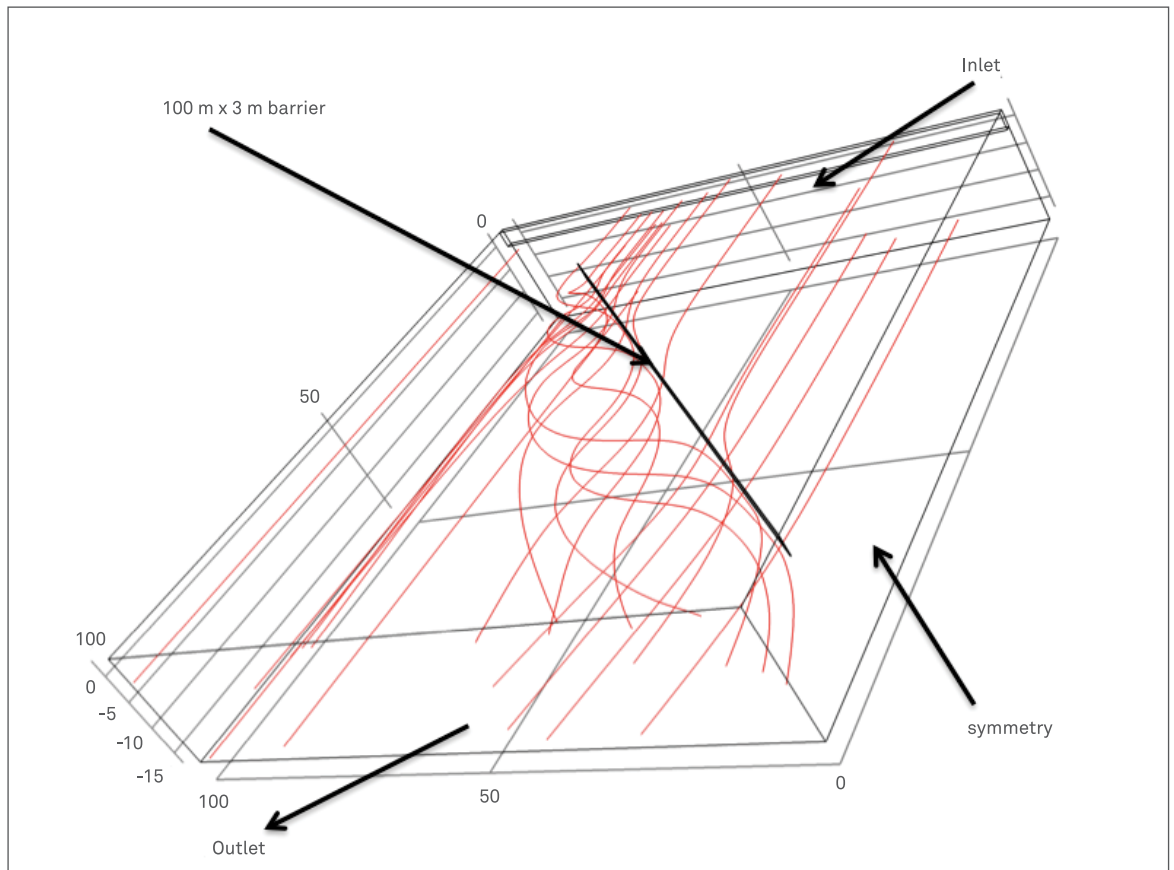
Figure 3.30 Streamlines for a 100 m barrier with 40° barrier angle

The following 3 figures (Figures 3.31, 3.32 & 3.33 illustrate how the velocity field changes with the barrier angle. A change in velocity is indicated by a change in color as indicated by the color scale on the right side of the graph.
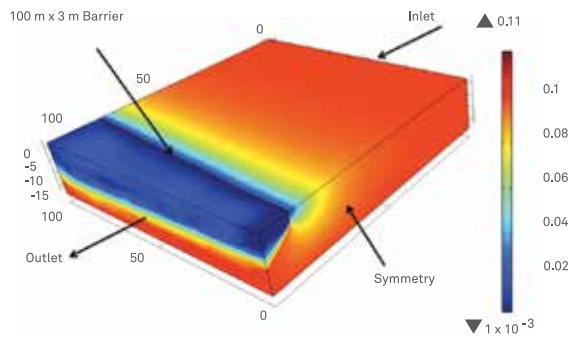
Figure 3.31 Velocity field at 5° barrier angle
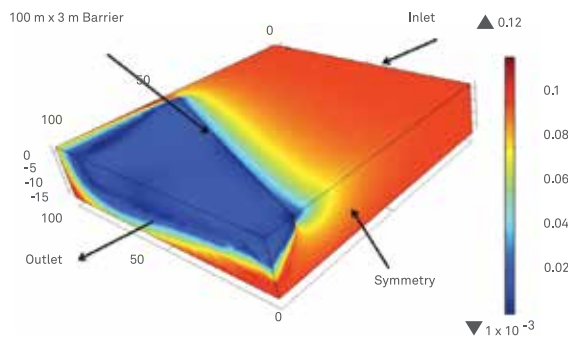
Figure 3.32 Velocity field at 20° barrier angle
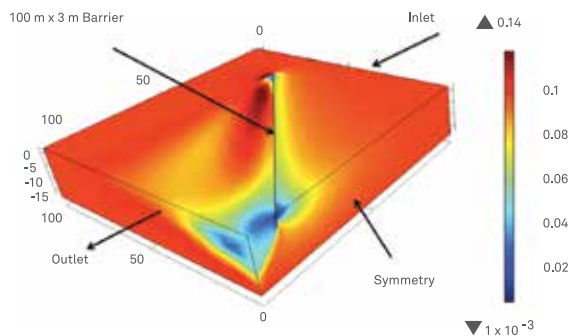
Figure 3.33 Velocity field at 45° barrier angle

It can be concluded from figures 3.31 – 3.33 that for increasing boom angles, the velocity in front of the barrier increases. Furthermore, it is interesting to see how far the barrier affects the flow field of the oceanic current. At a boom angle of 45° it becomes visible that at the outer tip of the V shape the flow rushes in the area behind the barrier.

3.4.1.2.2 CATCHING EFFICIENCY

The simulation is performed for geometric setup 1: Closed V Experiment (6 m) with long distance particle release.

The presented simulations give information on the particles that are very unlikely to be caught due to their lack of buoyancy. Particles lacking buoyancy cannot withstand the drag forces of the ocean water rushing downwards in front of the barrier. First, the simulation is run for varying particle sizes and densities. The following section shows the influence of boom angle on catching probability. The results of this study show the catching efficiency for an idealized case. Wind and waves, for example, are not taken into account. Please note that from the simulations we can see which particles are very unlikely to be caught. The simulations cannot give quantitative values for the particles that are caught, because wind and waves are not taken into account.

Catch probability vs. Particle size for different densities (closed V, angle 45°, flow speed 0.1m/s)
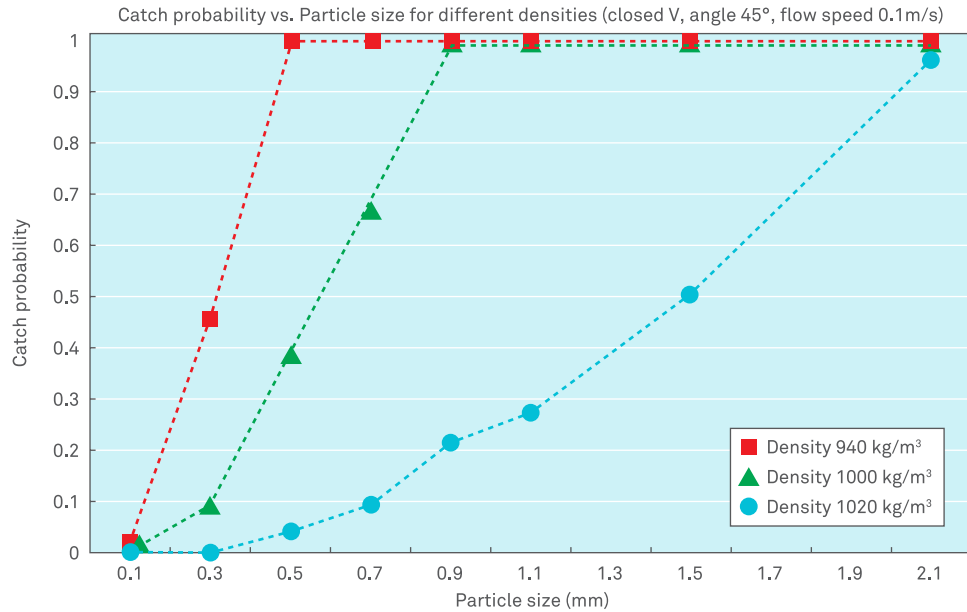
Figure 3.34 Catch probability as function of particle size and -density

PARTICLE SIZE AND DENSITY

Figure 3.34 illustrates the catch probability as a function of particle size for different particle densities. The catch probability in this study indicates the probability of a particle to remain in front of the boom for the duration of the experiment.

For this experiment, the closed V setup with a boom angle of 45° and flow speed 0.1 m/s was used. In the experiment the particle behavior was simulated for 15 minutes. During each experiment, 100 particles were released. The particles are randomly distributed from the surface down to 3 m depth at a distance of 35 m from the boom.

The results show that it will be very unlikely to catch a particle with a diameter of less than 0.1 mm, because even with the lowest density of 940 kg/m³ almost all particles escape the barrier. With increasing particle size, the catch probability increases as well. For all simulated densities, particles with a diameter of larger than 2 mm show a catch probability close to 1. They seem to have enough buoyancy to withstand the drag forces of the ocean that pull them downwards.

BOOM ANGLE

The graph below (Figure 3.35) illustrates the change in catch probability when changing the barrier angle. Again, the small setup of closed V with 6 m flow box is used. The particles are released at a 35 m distance to the barrier. Particle density is set at 1000 kg/m³ and particle size is 0.5 mm.

From simulations with barrier angles of 10, 20 and 45 degrees, it can be seen that the catch probability slightly increases for increasing barrier angle.

Catch probability vs. Barrier Angle (closed V, Particle size 0.5mm, flow speed 0.1m/s)
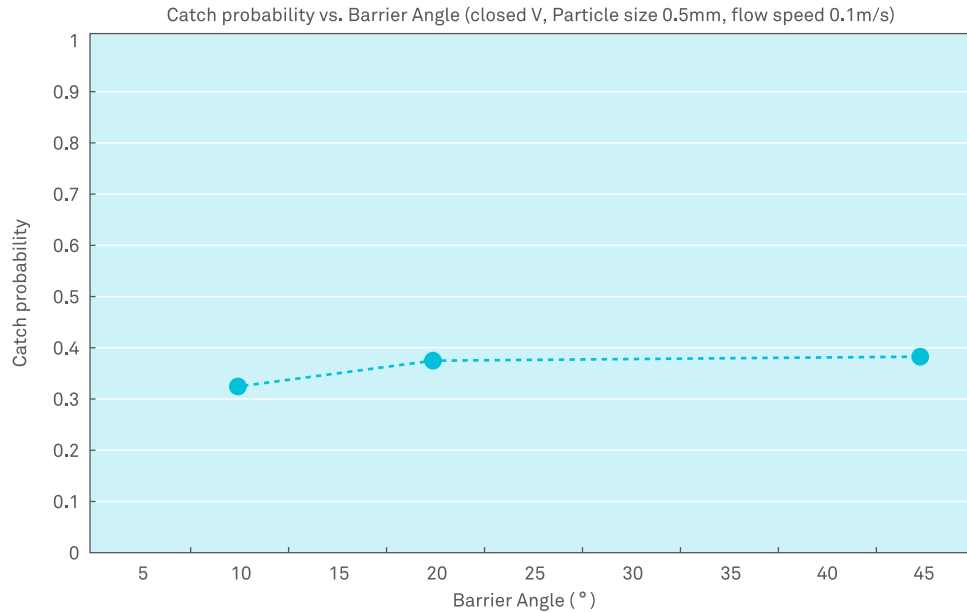
Figure 3.35 Catch probability as function of barrier angle

3.4.1.2.3 TRANSPORTATION RATE TOWARDS THE COLLECTING STATION

For this simulation, geometric setup 2 (closed V, 100 m) is used. The transportation rate is calculated by taking the average of the speed of 5 particles. The particle velocity magnitude is calculated every 0.5 seconds for 300 seconds as the particles are drifting close to the barrier. These values are then averaged.

The particle diameter was set to 1 mm whereas the current flow speed was kept at 0.1 m/s and the simulation time was set at 25 minutes.

In Figure 3.36, the particle velocity in the direction of the collection platform is plotted. The graph illustrates the increase of particle speed with increasing boom angle.

The relation between the z component of the particle velocity and the boom angle approximately follows the shape of a sin(2x) function. For small angles up to 20° the relation is approximately linear. At 45° the curve reaches the maximum value for the z-component of the particle velocity. This means that the highest transport rates in z direction can be reached with a barrier angle of 45 °.

Theoretically the transport rate in z direction will drop back to zero, when increasing the barrier angle further up to 90°. In order to find the optimal barrier angle it should be noted that increasing boom angles require increased boom lengths for equal frontal area.

3.4.1.3. SUMMARY AND RECOMMENDATIONS

In the final design, the boom angle is a key parameter when considering plastic particle transport towards the collecting platform.

Simulations show increasing particle speeds for increasing boom angles. The relation is quasi-linear up to angles of approximately 20° (note that this is the particle speed in the z-direction, the actual particle speed along the boom is faster).

From the extraction point of view, a larger barrier angle (up to 45°) is beneficial, because the simulations show a higher particle speed in front of the barrier for increased barrier angle (up to 45°). Furthermore the calculated catch probability is slightly higher for a larger barrier angle.

Particle velocity z-component vs. barrier angle (closed V, particle size 1 mm, flow speed 0.1 m/s
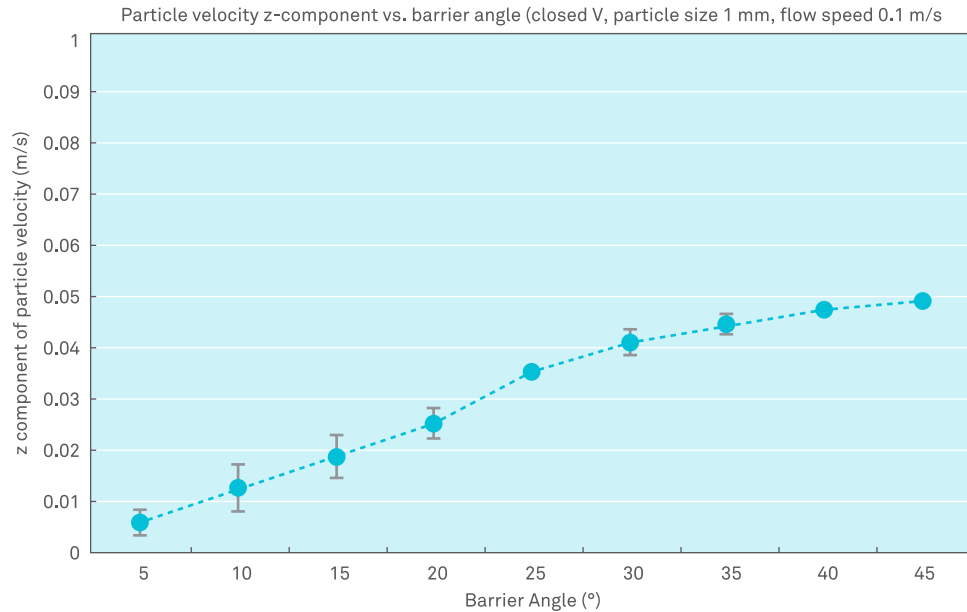
Figure 3.36 Particle velocity in the direction parallel to the array; towards the collecting platform.

Since the velocity in sink direction does not increase much for angles that are larger than 35° it is probably better to choose a barrier angle between 25° and 35°. This will still give a relatively high particle velocity in sink direction, but on the other hand the construction costs and the overall size of the structure will be smaller.

The study presented in subchapter 3.5 shows that the barrier will also tilt like a pendulum as a result of current and waves hitting the barrier. For simplicity the tilting is neglected in this report, even though it is expected that the tilting will have s strong effect on the particle behavior around the boom, especially on the catch probability. With relatively little additional computational effort it would be possible to tilt the barrier statically in order to investigate the influence this will have on the catch probability.

Since it is not clear yet how strong the influence of waves and wind is on the catch probability, this should be investigated first. This could be done on the one hand with more sophisticated simulations that take waves and wind into account or on the other hand with comparing the simulated results to experiments in reality.

Nevertheless the presented results in this study give a good estimate on the particle size that will not be catchable with the barriers.

3.4.2. ANSYS CFX 3D CFD MODEL
NANDINI SIVASUBRAMANIAN • DAVID KAUZLARIC
BOYAN SLAT • JAN DE SONNEVILLE • LEONID PAVLOV

3.4.2.1. MODEL SUMMARY
The numerical approach implemented for both computing the flow behavior around the boom and the transportation of the plastic particles along the boom is performed with ANSYS-CFX. To formulate the model of the boom and the ocean set up, assumptions and approximation were made in order to reduce computational efforts, time and also to achieve reasonable conclusions from the project in a short time.

- The Fluid structure interaction (FSI) analysis has been carried out on a scaled down version of the boom span with appropriate dimensions instead of taking the whole structure in to account.
- The length of the boom designed in the simulation is 10m whereas the real booms may be extended over several kilometers. Hence, our reduced simulation do main is intended to analyze the flow behavior far away from the collection station by implementing periodic boundary conditions.
- The boom is considered a fixed object with no degrees of freedom. As a consequence, the motion or deformation of the boom influenced by the flow behavior is not taken into account.
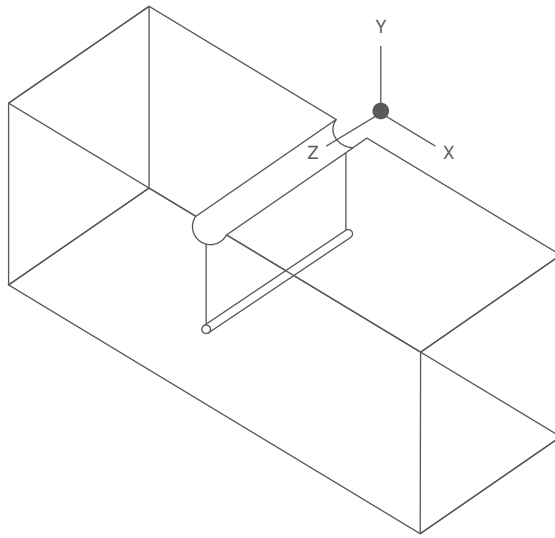
Figure 3.37 Simulation domain with boom connecting the two opposite translationally periodic boundaries.
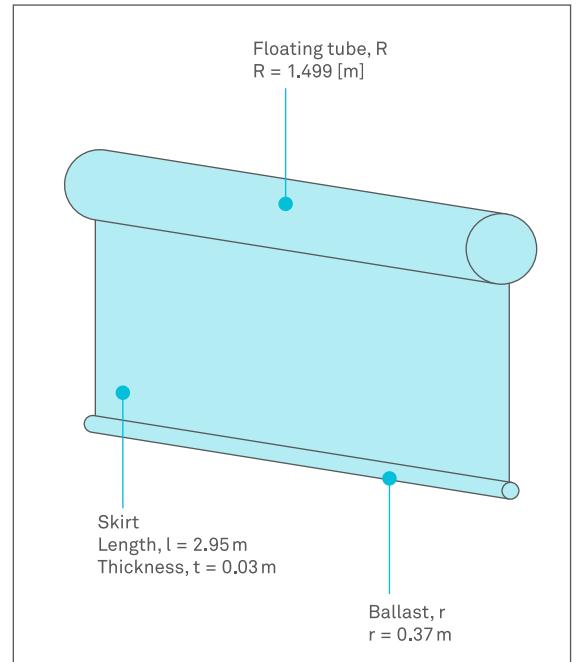
Figure 3.38 Closer view of the boom with its relevant dimensions

3.4.2.1.1 PHYSICAL MODELING

The fluid model consists of a single medium (water), where the fluid domain is made as a rectangular box of dimensions 25x10x10 m³ (see Table 3.6). Figure 3.37 shows a closer view of the boom fixed at the translational periodic boundaries of the fluid domain. Figure 3.38 shows a closer view of the boom.

The dimensions of the barrier used in the simulations are based on preliminary design drawings where the boom consists of three parts (the top floating tube, middle skirt, and the bottom ballast). The provisional values available at the time the simulations were carried out were used for setting up the model. These values, however, did not change significantly as the feasibility study progressed.

In the actual situation, the booms have to be buoyant in seawater and will be partially submerged due to the weight hanging from the skirt. Hence, the top tube is of 1.499 m diameter that is half submerged in the fluid domain of the simulations. The middle skirt is of the length 2.95 m and thickness 0.03 m. The bottom ballast has a diameter of 0.37 m (Figure 3.38).

Property	Value
Type	Design modeler
Length X	25 m
Length Y	10 m
Length Z	10 m
Fluid volume	2489 m³

Table 3.6 Dimensions of fluid box used for 3D CFD

3.4.2.1.2 TURBULENCE MODELING

Fluid flow is governed by basic conservation principles such as conservation of mass, momentum and energy. All these conservation principles are solved according to a fluid model given by a set of partial differential equations, representing the governing equations of the fluid motion.

Turbulent flow is a type of fluid flow characterized by fluctuating and chaotic property changes.

In this work, the RANS (Reynolds averaged Navier-Stokes) approach is used to model the effects of turbulence. A two-equation RANS-turbulence model is used as it offers a good compromise between numerical effort and computational accuracy. The so-called velocity scale and length scale are solved using separate transport equations – hence the term two equation model. This model holds two transport equations, one for turbulent kinetic energy (k) from which the turbulence velocity scale is computed and one for turbulent dissipation rate (ε), therefore the name k-ε model [5].

For the standard k-ε turbulence model, the turbulence parameters are also to be specified at the inlet boundary.

k value calculation [4] (Ansys, 2010a)
$k = 3/2*(\text{inflow velocity} * \text{Turbulent intensity})^2 = 3.75*10^{-5}$
$= 3/2*(0.1*0.05)2 = 3.75*10^{-5}$, where the turbulent intensity is set to 0.05

Eddy length scale calculation [4] (Ansys, 2010a)
Eddy length scale,(l)= 0.07* characteristic length
The characteristic length for our model is 10m, hence
l   = 0.07*10 = 0.7

The turbulence parameters are summarized in Table 3.7.

Parameter	Value
Turbulence model	standard k- E model
Method	k and length scale
k	$3.75*10^{-5}$ ($m^3* s^{-2}$)
Eddy length scale	0.7 (m)

Table 3.7 Summary of turbulence parameters for the k- E model
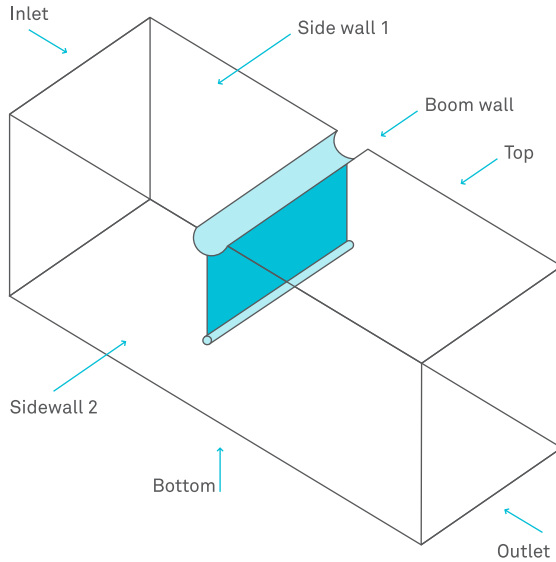
Figure 3.39 Boundary conditions and mesh of the model

Parts of the domain	Type of boundary condition
Inflow	Velocity inlet
Outflow	Pressure- outlet
Top	Wall (free slip)
Bottom	Opening
Side wall 1 & side wall 2	Translational periodic
Boom	Wall (No slip)

Table 3.8 Boundary conditions of the model

3.4.2.1.3 BOUNDARY AND INITIAL CONDITIONS

Figure 3.39 shows the boundary conditions used in the simulations. The inlet boundary condition (BC) for all the simulations here is specified to be 10 cm/s. representing the ocean current inflow (Figure 3.26).

Since the simulation is concerned with the flow behavior in an oceanic environment, the bottom of the model is considered to be an open type boundary condition (BC). At the surface opposite to the inlet, we specify an outlet BC, where the flow leaves the computational domain. The top BC is considered a free slip wall where the flow perpendicular to the boundary is neglected and only the parallel forces are considered. At the boom surface, a nonslip condition is specified, which means the velocity is zero. At sidewalls 1 and 2, periodic boundary conditions are applied, which reinject the material on the opposite domain boundary by preserving its velocity. This allows to mimic a large or infinite simulation domain with the only error introduced being the neglect of wavelengths larger than the actually simulated domain. Table 3.8 summarizes the applied boundary conditions.

The computational mesh of the entire domain is created with the help of the ANSYS meshing tool. For the implementation of the periodic boundary conditions, first identical surface meshes at the corresponding opposite side walls 1 and 2 were created. These surfaces were then used to create a tetrahedral volume mesh. A side-view on the mesh on sidewall 2 is shown in Figure 3.40, and the used number of elements, nodes, and faces is given in Table 3.9.

Property	Value
Elements	316866
Nodes	59800
Faces	27116

Table 3.9 Number of elements, nodes, and faces in the mesh
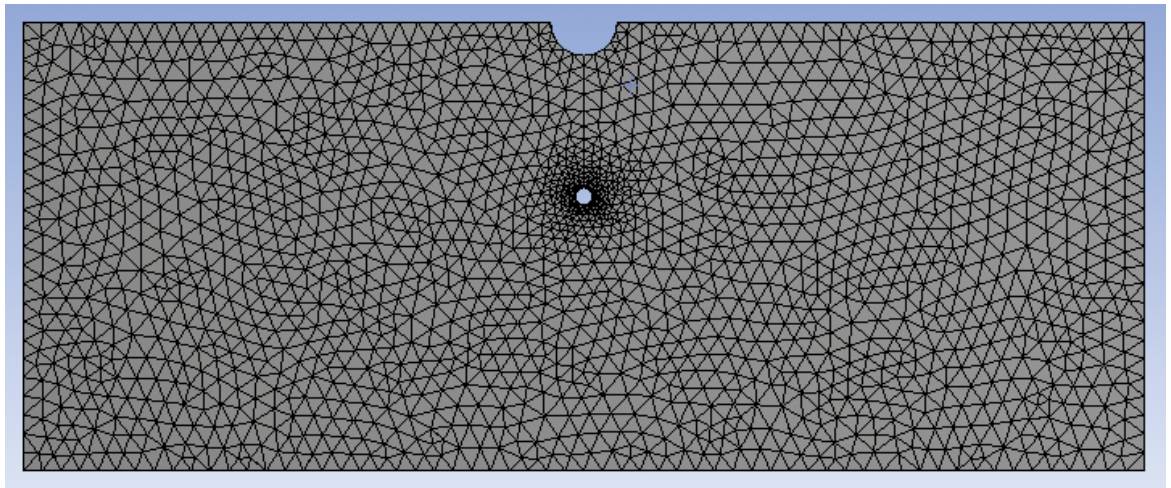
Figure 3.40 Side view on sidewall 2 of the mesh.

3.4.2.1.3 PARTICLE TRANSPORT MODELING

The plastic particles are tracked through the flow in a Lagrangian way by modeling a sample of individual particles. The Lagrangian modeling framework is one that moves with the flow, and is carried out by integrating a set of ordinary differential equations in time for each particle, for the particles' positions and velocities.

MATERIAL PROPERTIES

In order to reproduce the correct buoyant behaviour of the plastic particles, the correct mass densities have to be assigned, to both plastic and water. They are given in Table 3.10.

The mass density for the plastic particles was chosen as a worst-case scenario in accordance with the measured range of densities given in Chapter 9. Since the buoyancy forces are expected to support the catch of plastic particles at the boom and in particular to counteract the suction and escape of particles underneath the boom, the worst-case scenario is a low difference in mass density between plastic and water.

PARTICLE TRANSPORT EQUATIONS

Several forces affect the motion of a particle in a fluid: viscous drag (F_D), buoyancy force (F_B), virtual mass (F_{VM}), pressure gradient forces (F_P) and the centripetal and Coriolis forces (F_R) in rotating reference frames. The equation of motion is given by

$$m_p \frac{dU_p}{dt} = F_D + F_B + F_R + F_{VM} + F_P + F_{BA}$$

Where m_p is the particle mass, and U_p is the particle velocity variable. In this study, we consider the effect of the drag and the buoyancy forces and neglect the others.

Computation of the drag force and buoyancy forces is done using the typical formulas and is not explained in this report.

Phases	Density (kg m^{-3})
Water	1025
Plastic Particle	1000

Table 3.10 Densities of water and plastic particles
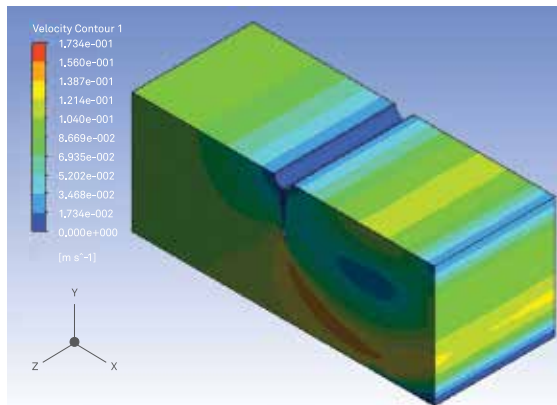
Figure 3.41 Magnitude of the flow velocity at a 10° barrier angle
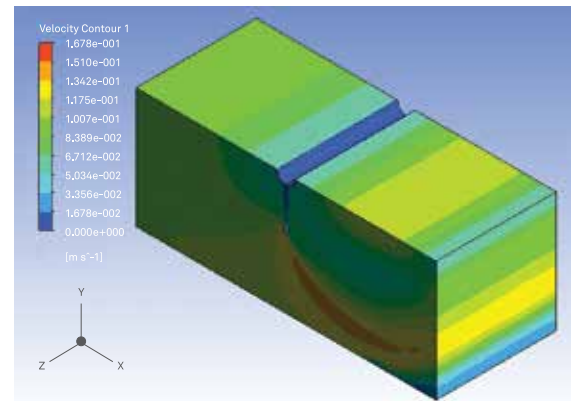
Figure 3.42 Magnitude of the flow velocity at a 30° barrier angle

3.1.1.1.5 SIMULATION SETUP

From the fluidic simulations we would like to determine the behaviour of the flow and the plastic particles as they approach the collection station. The flow simulations are performed as steady state. This reduces the computational effort and cross checking of these steady state results can be done by considering the flow transient and by integrating in time until a steady state solution is reached. Due to time constraints, transient simulations were not performed in this study. Apart from modelling steady state flow, we also need to analyse which percentage of particles travels along the boom, and which percentage escapes underneath, and whether the intended set up allows for efficient particle transportation along the boom.

Three different values for the barrier angle α of 10°, 20° and 30° were tested. Please refer to Figure 3.26 for the definition of the barrier angle. This tilt in the barrier angle is actually achieved by tilting the inflow velocity and keeping the geometry unchanged with a boom perpendicular to sidewalls 1 and 2 (cf. Figure 3.37 above). This allows easy implementation of periodic boundary conditions at the sidewalls 1 and 2 to mimic the flow and particle transport far away from the collection station.

3.4.2.2. RESULTS AND DISCUSSION
3.4.2.2.1 CONTOURS OF FLOW VELOCITY MAGNITUDE AT VARIOUS BARRIER ANGLES

The changes in the velocity magnitude of the flow field with respect to the barrier angle are presented in this section. Figures 3.41 & 3.42 show velocity contour plots for two different angles of 10° and 30°. It can be observed that in the set up with a barrier angle of 10°, the flow velocity magnitude along the boom does not exceed 2 cm/s within the distance of 1 m to the boom. It increases considerably for the set up with 30° angle with more than 5 cm/s within the first 1 m. Therefore, it can be said that the velocity magnitude of the flow in front of the boom increases with increased barrier angle.
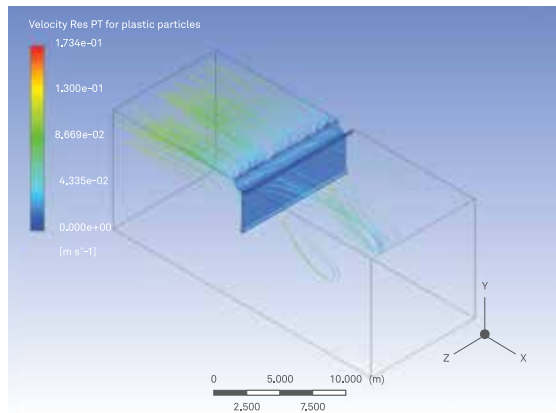
Figure 3.43 Particle trajectories at 10° barrier angle
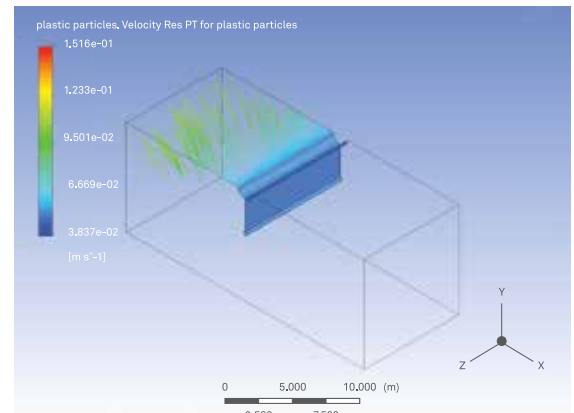
Figure 3.44 Particle trajectories at 30° barrier angle

3.4.2.2.2 PARTICLE TRAJECTORIES AT VARIOUS ANGLES

For computational convenience, the plastic particles are considered to have spherical shape. As stated above, their density is set to 1000 kg/m³. The particles are characterized by their diameter and are always injected at a distance of 12.5 metres from the boom. As mentioned earlier, in order to simplify the model, these simulations are done considering the booms to be rigid and immovable. Apart from neglecting any turbulence caused due to the winds and waves in a realistic ocean environment, the particle-particle interactions and the back action of the particles on the fluid are ignored.

Figures 3.43 and 3.44 show the particle trajectories for particles of diameter 3 mm. One hundred particles are injected, distributed randomly in the inlet region down to a depth of 4 m. During average weather conditions the majority of the floating plastics in the ocean environment are found to be distributed within this depth (Chapter 2.3)

When comparing the results for the tilting angles of 10° and 30°, it becomes clear that the particle velocities along the boom increase with increasing angle. At a boom angle of 10°, there are some particles that escape the boom and travel underneath, not able to stay on the surface by withstanding the ocean's drag force, whereas all 100 particle trajectories seem to travel along the boom indicating that the catch probability is 1 in the flow field with barrier angle 30°. This catch probability is quantified in the following paragraph.

Catch probability vs. boom tilt angle

Inflow velocity = 0.1 m/s   Particle density = 1000 kg/m³
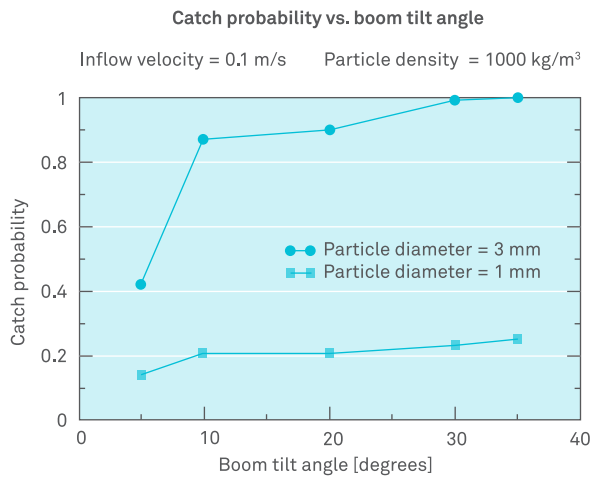
Figure 3.45 Particle transportation along the boom for various barrier angles

Catch probability vs. particle size

Barrier angle = 10°   Particle density = 1000 kg/m³
Flow velocity = 0.1 m/s
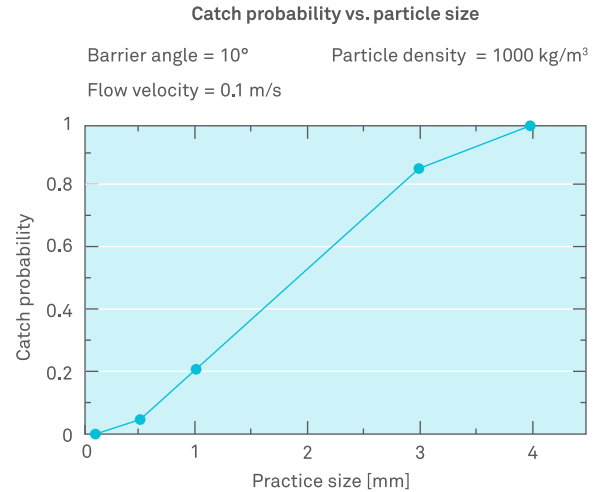
Figure 3.46 Particle transportation probability along the boom for various particle sizes

3.4.2.2.3 CATCH PROBABILITY VS. BOOM TILT ANGLE FOR VARIOUS DIAMETERS

With an inflow velocity of 0.1 m/s, Figure 3.45 is again obtained by injecting 100 plastic particles of sizes 1 mm and 3 mm. The catch probability can be defined as the ratio of particles transported along the boom to all particles (including the escaped ones). It can be seen that the catch probability increases with increasing boom angle from 5 to 35o for both considered particle sizes, but the absolute difference in the probabilities for the two particle sizes 1 and 3 mm is dramatic. The size dependence is further illustrated in the following plot.

3.4.2.2.4 CATCH PROBABILITY VS. PARTICLE SIZE FOR A BARRIER ANGLE OF 10°

The probability of particle transportation along the boom increases with increased particle size obviously. The bigger the particle size, the better is its buoyancy behaviour.

3.4.2.2.5 PARTICLE VELOCITY VS. BOOM TILT ANGLE

The velocity of the captured particles in front of the boom is calculated by recording the velocity of a single particle for 100 seconds along the boom and taking the time-average. The experiment is repeated for five different angles as shown in the figure below. The net particle velocity towards the collection station (i.e., perpendicular to the inflow) is calculated using the cosine-component of the total particle velocity in front of the barrier, for the respective tilt angle. Figure 3.47 shows the results.

The inflow velocity is 0.1 m/s and the size and density of the particle is 1 mm and 1000 kg/m³, respectively. From the information provided in Figure 3.47 it can be concluded that the particle speed in front of the barrier increases with increasing angle.

3.4.2.3. CONCLUSIONS AND RECOMMENDATIONS

In summary, the main question about the efficiency of the particle-catch can be answered as follows: First of all, it is obvious that even at a tilt angle of 10°, more than 85 percent of the particles with diameter larger than or equal to 3 mm are caught according to the results obtained in this study. This can be improved to more than 97 percent at a tilt angle of 30°. The caught particles are transported with a velocity of 1.7 to 4.1 cm/s along the boom towards the collection station, depending on the tilt angle (10° - 30°) and the current velocity (here taken as 10 cm/s).

For particles of sizes smaller than 3 mm, the catch probability decreases significantly, far below a satisfactory value, irrespective of the tilt angle, which leads to the conclusion that The Ocean Cleanup Array cannot efficiently catch particles smaller than this size.
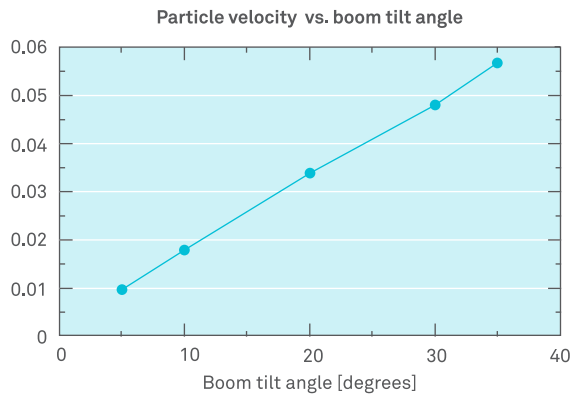
Figure 3.47 Particle transportation rate perpendicular to the inflow for various barrier angles

It has been observed that the catch probability strongly depends on initial particle depth , which investigated in the future work.

In addition, it is recommended to introduce realistic waves and buoyant motion of the boom, and to perform transient simulations.

3.4.3. BOOM ANGLE MODELING CONCLUSIONS

The conclusions regarding catch probability obtained during the 3D CFD modeling in both cases support the findings of the 2D CFD models. The results do not match perfectly, but within the range of the highest significance (macroplastics) and partially for mesoplastics the results of the 2D and 3D CFD studies are in agreement. Since the 2D CFD study covered a wider range of simulation setups, the results of the 3D CFD catch efficiency were used for reference, benchmarking and comparison, but not in the catch efficiency calculations.

The results related to the interaction of the flow with the array and the movement of plastic particles along the array are in good agreement between the two 3D CFD studies. Even though the way of modeling this particular part of the problem was different in the case of the two studies the results are similar. In the case of Comsol modeling, the computational domain was increased significantly in order to be able to capture particle velocities in the far field away from the sink.

In the case of ANSYS CFX periodic boundary conditions were implemented in order to measure the particle transportation rate towards the sink.

The particle velocities in the direction parallel to the array for array angles ranging from 5 to 35 degrees show similar behavior and reach average values of 0.55 cm/s – 4.4 cm/s (Comsol) and 1.0 cm/s – 4.7 cm/s (ANSYS CFX). Both particle velocity ranges correspond to a current velocity of 10 cm/s. The deviation in the results can be explained by the different geometric setups used in the simulations. The Comsol simulation uses a 100 m barrier while the ANSYS simulation uses a quasi-infinite barrier modeled by periodic boundary conditions. The length of the barrier affects the current velocity that builds up in front of the barrier.

The obtained values serve as a solid basis for defining the array angle and length. They also define the achievable plastic collection rate as a function of the array angle. The results of the 3D CFD study strengthen the findings of the 2D CFD investigation and confirm the weak points about the uncertainties currently associated with setting up CFD simulations of the particle collection efficiency problems.

BOOM LOAD MODELING

SEBASTIAAN VAN ROSSUM • JOOST DE HAAN

JAN DE SONNEVILLE • BOYAN SLAT

In previous subchapters, the boom model was reduced to a line or plane, whereby waves, currents and winds do not affect the shape and position of the boom. This simplification was made to get a first estimate of the performance and capture capability of the boom. The result of this model is a set of geometric properties such that the boom can catch and transport plastic to the platform. The determined properties are boom length, skirt depth and the effect of skirt orientation.

During operation under environmental loads, additional parameters become relevant. Subchapter 3.5 models the system under environmental loads to determine exerted forces on the boom and mooring system. Using the results, a feasible boom segment length is determined. Additionally, a study was performed to predict the movement of the skirt and ballast to identify potential problems regarding water flow during plastic collection.

This subchapter is divided into five parts. Before describing the model, an introduction to the simulation program is given. Second, the environmental loads are discussed, and the relevant loads are determined which serve as inputs for the model. Third, the structural part of the boom model is presented, including two boom concepts and the mooring system. The performance of the boom is determined using wave conditions and ocean currents in a number of different simulations. The resulting forces are presented in the fourth part. Further simulation work on the skirt is discussed in in the final part. More information on the Orcaflex model and parameters can be found in Appendix 4.
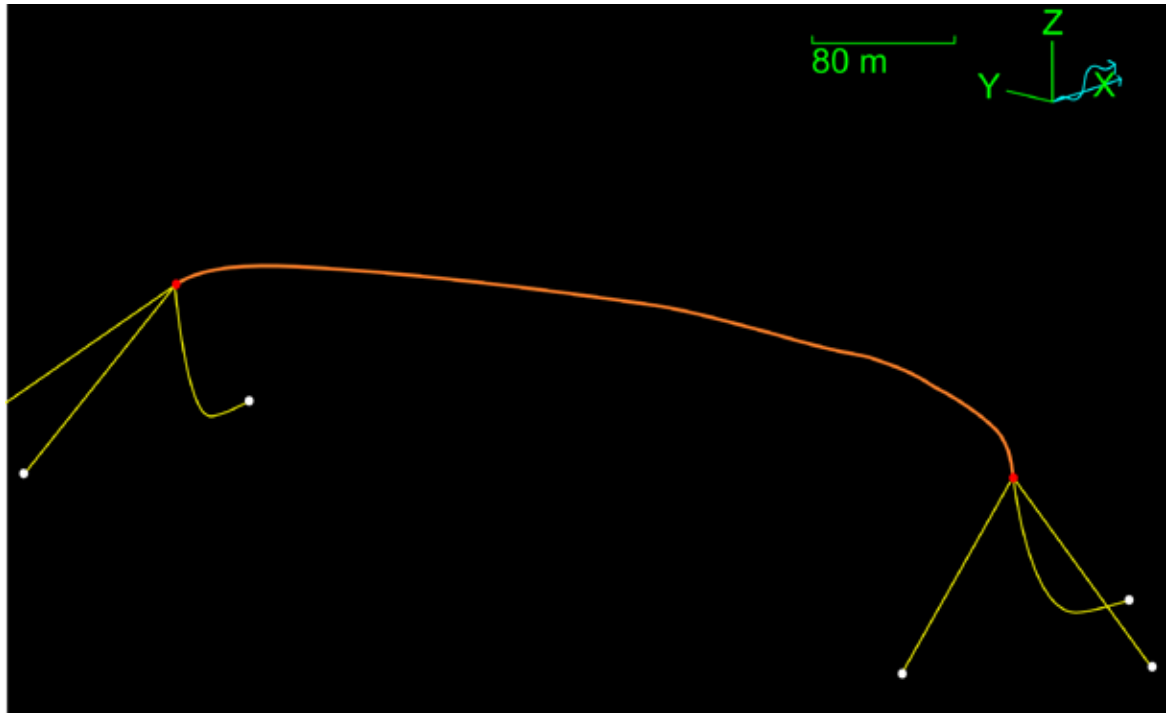
Figure 3.48 Boom model overview

3.5.1. THREE-DIMENSIONAL MODELING USING ORCAFLEX

Orcaflex software was used by Vuyk Engineering Rotterdam to perform the desired simulations. In this program, a model of the boom was drawn and placed in a simulated ocean and then a time-series of behavior of the boom to currents and waves was captured in six degrees of freedom. The model allows for quick alterations of the boom geometry and/or material for comparison.

In Orcaflex, a simulation starts by placing a model in a sea environment, after which the currents and waves build up according to a predefined wave/current model.

Figure 3.48 shows the overview of the final Orcaflex model under load.

The next section discusses the adjustments that were implemented due to computation time limitation.

MODEL LIMITATIONS

Due to the nature of this feasibility study, the available modeling time was shorter that than what will be used during the detailed design phase. The Orcaflex model was adjusted in several ways to limit the computation time. Adjustments were made regarding water depth, incoming waves and modeling of the skirt.

The water depth for the model was limited to 100 m. Experiments and common practice show that this water depth is sufficient to neglect the effects of the seafloor on the wave-boom model. Water depths for the chosen locations are in the order of kilometers and would have significantly increased computation time.

For further modeling time reduction, a combination of significant wave height (H_s) and wave period (T_z) was chosen rather than assessing the performance for the full range of sea states. The graphical representation of these parameters can be seen in Figure 3.49. More elaboration on this can be found in the section 3.5.2.1. Here, the full series of measured sea states is presented in form of a wave scatter diagram.

SIGNIFICANT WAVE HEIGHT
This height is commonly used as a measure of the height of ocean waves. The significant wave height (H_s or $H^{1/3}$) is the mean wave height (which is the distance from trough to crest, see picture below) of the highest third of measured/simulated waves.

WAVE PERIOD
The wave period (T_z) is defined as the average time between two up crossings of a wave. This is commonly used to define a sea state together with the significant wave height. A longer wave period equals higher wavelength and decreases steepness at equal wave height.
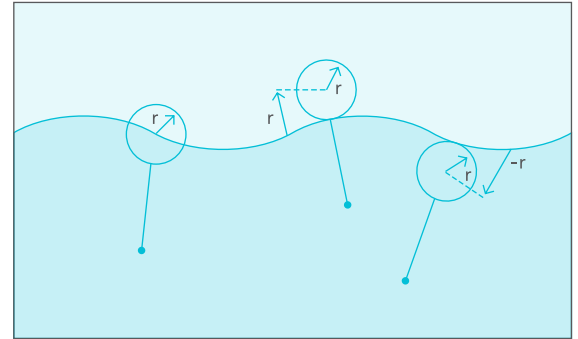
Figure 3.49 Explanation on significant wave height (H_s) and wave period (T_0)

Figure 3.50 Sea surface clearance definition

The computation time was further limited by removing the skirt geometry for models where the skirt´s orientation relevance is minimal. To compensate for the removal of the skirt geometry, the drag and mass of the boom were increased in these models.

3.5.2. ENVIRONMENTAL LOADS
The modeled structure was exposed to environmental forces due to waves and currents. Wind forces were not incorporated in the present model.

The sections below explain the process of determining the input for the Orcaflex model. As stated in the previous section, a critical sea state is preferred over the full range of occurring sea states to reduce computation time. This sea state can be seen as the most severe sea state during 95% of the time. In this section, the selection of the critical sea state is discussed.

3.5.2.1. OPERATIONAL LIMITS
The Ocean Cleanup uses a required uptime of 95 percent for the feasibility study (see Chapter 2). During this percentage of time the system's structural integrity is assured and collected plastic is sufficiently contained.

For this study, it was assumed that the operational limits are directly related to the extent to which the boom submerges and emerges. This value is obtained in OrcaFlex by recording the output of sea surface clearance. The sea surface clearance was defined as the distance between the centerline and the sea surface. Figure 3.50 shows this definition. The left boom has a sea surface clearance of 0, the middle boom has a clearance of the radius r and the right boom's position is at a clearance of −r.

A fully submerged or emerged boom will obviously cause an efficiency loss. Since plastic collection is the main purpose of the boom, sea surface clearance is an important design property. This parameter is therefore used for determining the critical sea state[1] for plastic collection. The extended model uses this sea state for simulation.

1 The sea state with highest fluctuation of sea surface clearance.
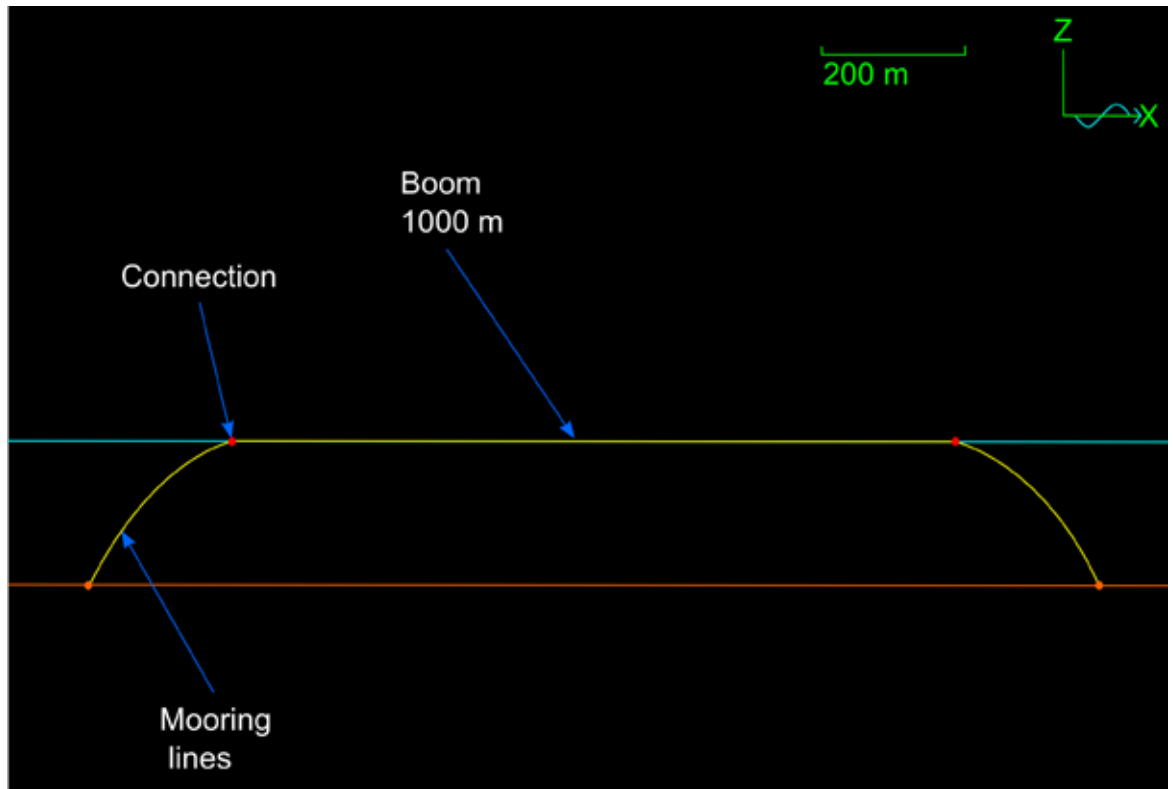
Figure 3.51 Side view of boom and mooring model configuration in Orcaflex

3.5.2.2. DETERMINATION OF THE CRITICAL SEA STATE

In this section, a simplified model of the boom and mooring system is used for determining the most critical sea state. Using the more extensive boom model would result in long computation times.

BOOM AND MOORING

The 1,000 m long boom is connected to the sea bottom by means of two mooring lines. The chosen water depth is 200 m; the lines' horizontal offset with respect to the boom end is 200 m as well. The polypropylene mooring line material is buoyant, which can be seen in Figure 3.51, the mooring line shows a reverse catenary.

ENVIRONMENTAL CONDITIONS

Multiple sea state simulations were run containing a current and a dominant significant wave height and period. The current was kept constant for all simulations while the combination of wave height and period was changed for each simulation.

As a result of acquired environmental data, presented in Chapter 2, the input for current speed was set at 0.15 m/s and it was directed perpendicular to the boom. The perpendicular direction is an operational requirement to collect the plastic.

Since the sea surface is in fact a summation of different wave components, the sea state is described by a spectrum representation. Each combination of wave height and period is represented in a JONSWAP spectrum. The wave direction was modeled both perpendicular and parallel to the boom. The full range of sea states is shown in Table 3.11 below.

HS/TZ	5	5.5	6	6.5	7	7.5	8	8.5	9	9.5	10	10.5	11	11.5	12
10	0.00%	0.00%	0.00%	0.00%	0.00%	0.00%	0.00%	0.00%	0.00%	0.00%	0.00%	0.00%	0.00%	0.00%	0.00%
9.5	0.00%	0.00%	0.00%	0.00%	0.00%	0.00%	0.00%	0.01%	0.01%	0.01%	0.01%	0.01%	0.01%	0.00%	0.00%
9	0.00%	0.00%	0.00%	0.00%	0.00%	0.00%	0.01%	0.01%	0.01%	0.02%	0.02%	0.01%	0.01%	0.01%	0.01%
8.5	0.00%	0.00%	0.00%	0.00%	0.00%	0.01%	0.01%	0.02%	0.02%	0.03%	0.03%	0.02%	0.02%	0.01%	0.01%
8	0.00%	0.00%	0.00%	0.00%	0.00%	0.01%	0.02%	0.03%	0.04%	0.05%	0.04%	0.04%	0.03%	0.02%	0.01%
7.5	0.00%	0.00%	0.00%	0.00%	0.01%	0.02%	0.04%	0.06%	0.08%	0.08%	0.07%	0.06%	0.04%	0.03%	0.02%
7	0.00%	0.00%	0.00%	0.01%	0.02%	0.04%	0.08%	0.11%	0.12%	0.13%	0.11%	0.09%	0.07%	0.04%	0.03%
6.5	0.00%	0.00%	0.00%	0.01%	0.04%	0.08%	0.13%	0.18%	0.20%	0.19%	0.17%	0.13%	0.09%	0.06%	0.04%
6	0.00%	0.00%	0.01%	0.03%	0.07%	0.14%	0.22%	0.28%	0.30%	0.29%	0.24%	0.18%	0.13%	0.08%	0.05%
5.5	0.00%	0.00%	0.02%	0.05%	0.13%	0.24%	0.35%	0.43%	0.45%	0.41%	0.34%	0.25%	0.17%	0.11%	0.06%
5	0.00%	0.01%	0.03%	0.10%	0.22%	0.39%	0.54%	0.63%	0.63%	0.56%	0.44%	0.32%	0.21%	0.13%	0.08%
4.5	0.00%	0.01%	0.06%	0.18%	0.37%	0.61%	0.80%	0.89%	0.86%	0.73%	0.56%	0.39%	0.25%	0.16%	0.09%
4	0.00%	0.03%	0.11%	0.30%	0.59%	0.90%	1.13%	1.19%	1.10%	0.90%	0.66%	0.45%	0.29%	0.17%	0.10%
3.5	0.01%	0.06%	0.21%	0.50%	0.90%	1.28%	1.51%	1.51%	1.32%	1.04%	0.74%	0.49%	0.30%	0.17%	0.10%
3	0.02%	0.12%	0.36%	0.79%	1.30%	1.72%	1.89%	1.78%	1.48%	1.11%	0.76%	0.48%	0.29%	0.16%	0.09%
2.5	0.05%	0.22%	0.60%	1.17%	1.77%	2.15%	2.20%	1.94%	1.53%	1.09%	0.71%	0.43%	0.25%	0.13%	0.07%
2	0.11%	0.39%	0.94%	1.63%	2.21%	2.45%	2.31%	1.90%	1.40%	0.94%	0.58%	0.34%	0.18%	0.10%	0.05%
1.5	0.22%	0.67%	1.36%	2.06%	2.48%	2.47%	2.11%	1.59%	1.08%	0.67%	0.39%	0.21%	0.11%	0.05%	0.03%
1	0.15%	0.35%	0.59%	0.75%	0.77%	0.67%	0.50%	0.34%	0.21%	0.12%	0.06%	0.03%	0.01%	0.01%	0.00%

Table 3.11 Wave scatter diagram

Table 3.11 shows 95% of the most frequently occurring waves in red, hence the sea states in which the system must remain operational. Yellow plus red text represent 99% of the sea states. The black percentages represent sea states that were not existent during the measurements. To fit in the report, the table was obtained by style modifications from a wave scatter diagram made with Octopus at the coordinates 138°W 30°N (Chapter 2).

The sea states indicated with black borders are the ones that were simulated to determine the most critical sea state. The selection includes the shortest five wave periods at each significant wave height within the red area. When the shortest 5 wave periods in the red area are the same for several significant wave heights (for example the H_s of 2 m versus the H_s of 2.5 m), only the highest waves were simulated, as they are more critical.

For validation purposes, less extreme wave climates from the 99% most occurring climates were also chosen. They may be less critical due to their longer wave period. It is hypothesized that due to the relatively long wave period, these sea states will result in the structure being able to follow the waves properly.

3.5.2.3. RESULTS

The boom assessed here is 1,000 meters long. In order to assess the results for each wave climate, sea surface clearance data was recorded at 3 points along the length of the boom (Figure 3.52). One at 250 meters from the mooring at one side, one in the middle at 500 meters from the mooring and a point at 250 meters from the mooring at the other side. The dots in Figure 3.52 indicate the locations of measurement.

To obtain the most probable sea surface clearance with a 3-hour return period, the simulation data is assumed to be Rayleigh distributed. The average of the maxima and minima at the three measuring points is used to compare the simulated wave climates. It should be noted that the extremes of the sea surface clearance are actually not Rayleigh distributed. Therefore, these maxima and minima should not be used for other purposes than for current comparison.

Tables 3.12 - 3.15 below show the results. The values indicate the sea surface clearance. The 5 highest results in Table 10 and 5 lowest results in Table 3.13 are shown in red.
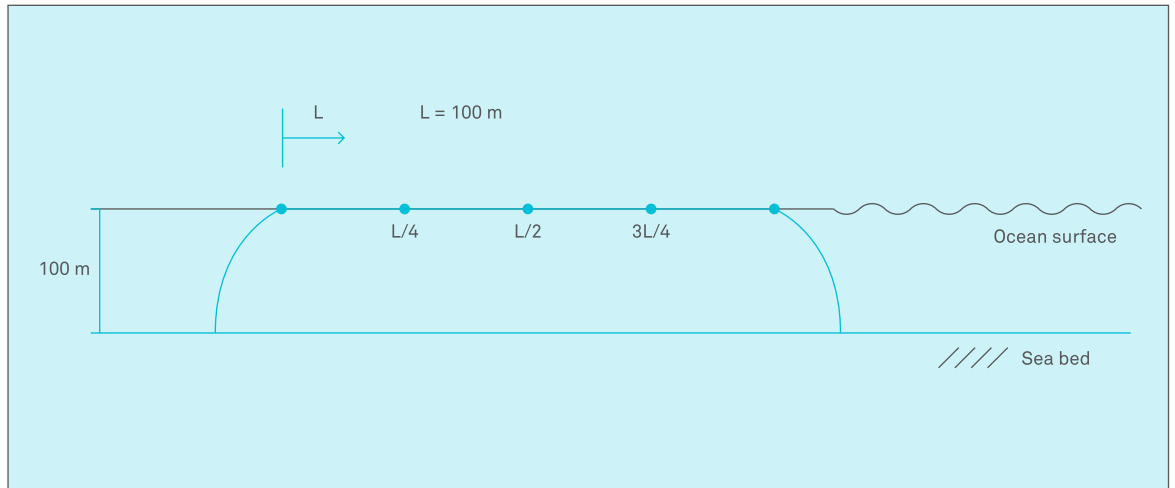
Figure 3.52 Boom model overview

HS / TZ	5	5.5	6	6.5	7	7.5	8	8.5	9	9.5	10	10.5	11	11.5
1.50	0.34	0.31	0.26	0.23	0.20									
2.50			0.43	0.38	0.34	0.33								
3.50			0.70	0.58	0.48	0.46	0.44							
4.00				0.66	0.56	0.51	0.48	0.46						
5.00					0.78	0.68	0.59	0.54	0.48					
5.50					0.72	0.65	0.61	0.55	0.54					
6.00						0.72	0.66	0.60	0.57	0.55				
6.50							0.64	0.58	0.57	0.56	0.53			
7.00								0.63	0.62	0.62	0.59	0.58		
8.00									0.70	0.65	0.65	0.63		

Table 3.12 Most probable sea surface clearance maxima with a 3-hour return period and parallel waves

HS / TZ	5	5.5	6	6.5	7	7.5	8	8.5	9	9.5	10	10.5	11	11.5
1.50	-0.34	-0.32	-0.27	-0.23	-0.20									
2.50		-0.51	-0.44	-0.39	-0.35	-0.34								
3.50			-0.75	-0.61	-0.50	-0.48	-0.45							
4.00				-0.70	-0.58	-0.53	-0.49	-0.48						
5.00					-0.84	-0.71	-0.62	-0.56	-0.49					
5.50					-0.77	-0.67	-0.63	-0.56	-0.56					
6.00						-0.76	-0.69	-0.62	-0.59	-0.57				
6.50							-0.66	-0.60	-0.59	-0.58	-0.56			
7.00								-0.65	-0.66	-0.66	-0.63	-0.61		
8.00									-0.73	-0.69	-0.67	-0.67		

Table 3.13 Most probable sea surface clearance minima with 3-hour return period and parallel waves

Tables 3.12 - 3.13, showing the sea surface clearance with parallel waves, illustrate that the most critical wave climate is the one with a significant wave height of 5 m and a mean wave period of 7 s. Critical here means that the structure was not being able to directly follow the ocean wave surface. The sea surface clearance ranges from -0.84 m to 0.78 m. This simulation has the highest maximum and lowest minimum value for the sea surface clearance and thus the biggest range between minimum and maximum.

HS / TZ	5	5.5	6	6.5	7	7.5	8	8.5	9	9.5	10	10.5	11	11.5
1.50	0.49	0.47	0.39	0.32	0.24									
2.50		0.75	0.64	0.57	0.46	0.40								
3.50			0.92	0.82	0.71	0.60	0.58							
4.00				0.96	0.82	0.74	0.64	0.57						
5.00					1.04	0.98	0.87	0.72	0.69					
5.50						1.07	0.95	0.81	0.77	0.72				
6.00							1.05	0.91	0.91	0.83	0.79			
6.50									0.99	0.91	0.81	0.74	0.63	
7.00										0.96	0.88	0.79	0.69	0.63
8.00											1.01	0.92	0.80	0.70

Table 3.14 Most probable sea surface clearance maximum with 3-hour return period and perpendicular waves

HS / TZ	5	5.5	6	6.5	7	7.5	8	8.5	9	9.5	10	10.5	11	11.5
1.50	-0.55	-0.51	-0.42	-0.34	-0.25									
2.50		-0.87	-0.73	-0.64	-0.51	-0.43								
3.50			-1.09	-0.95	-0.81	-0.67	-0.64							
4.00				-1.14	-0.95	-0.85	-0.72	-0.63						
5.00					-1.23	-1.15	-0.99	-0.82	-0.77					
5.50						-1.26	-1.11	-0.92	-0.87	-0.81				
6.00							-1.24	-1.06	-1.03	-0.92	-0.87			
6.50									-1.14	-1.04	-0.90	-0.82	-0.70	
7.00										-1.10	-0.98	-0.87	-0.77	-0.69
8.00											-1.15	-1.04	-0.89	-0.78

Table 3.15 Most probable sea surface clearance minimum with 3-hour return period and perpendicular waves

Tables 3.14 and 3.15, presenting the sea surface clearance with perpendicular waves, show that in this case the most critical wave climate is the one with a significant wave height (H_s) of 5.5 m and a mean wave period (T_z) of 7.5 s with a sea surface clearance reaching from -1.26 m to 1.07 m. This range is larger than what was found for the parallel propagating waves. At increasing wave periods, the extreme values for the sea surface clearance decrease.

From the above tables it can also be seen that a lot of the sea states with higher waves can result in lower extremes of the sea surface clearance at longer mean wave periods. When the boom cannot operate in a sea state with relatively short waves, it may be able to operate in an environment with relatively long but higher waves.

From the computations above, it can be concluded that for a sea state with the main wave direction perpendicular to the boom, a significant wave height of 5.5 m and a mean wave period of 7.5 s turns out to give the highest movements relative to the wave surface. This state is assumed to be the most critical one among the previously defined sea states. This combination was used for further simulations.

3.5.3. STRUCTURAL MODEL
The simplified structural model used in the previous section was no longer used for further simulation. For further simulation, a 6 line mooring system and more extensive boom model were applied.

Initially, two concepts were selected for modeling the boom. These are described in the next section. A skirt and ballast were connected to the boom for the purpose of capturing plastic material.

wall thickness:
0.025 m

0.5 m

7.5 m

1.5 m

wall thickness:
0.1 m

2.0 m

Skirt thickness:
$5.0*10^{-3}$ m
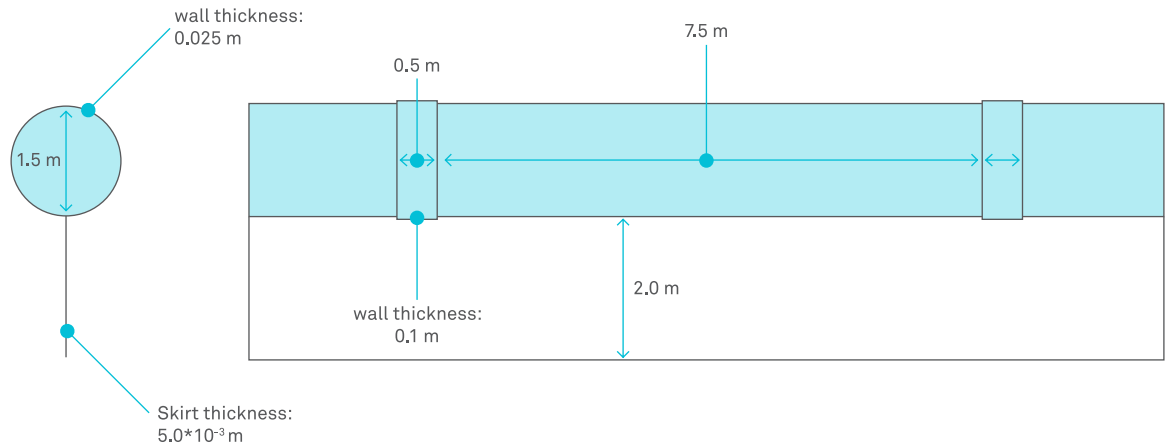
Figure 3.53 Physical interpretation rigid boom

3.5.3.1. BOOM

The Orcaflex boom model was built from three main structures. The required buoyancy was achieved by the floating boom elements. The two boom concepts included a flexible boom and a stiff boom with flexible connecting elements, to enhance the capability of the boom to follow the waves. The selection of these concepts was based on a concept study explained in subchapter 3.2.

RIGID BOOM

The stiff boom model has a hinge every 8 meters, which can be seen in Figure 3.53. The left side of the figure shows the cross section and right shows the side view of part of the boom. The stiff sections are the 7.5 m long sections in the figure.

For the hinges, links were used (The 0.5 m long sections which are drawn a bit wider than the other parts in Figure 3.53). The skirt was hanging beneath the boom, shown in white with a black outline. Compared with the CFD simulations presented in subchapters 3.3 and 3.4, the boom buoyancy element and skirt geometry is slightly different. This is due to parallel engineering activities.

As for materials, steel was used for the rigid parts, and for the links, neoprene is used. Steel was chosen because it is one of the main materials used in the offshore industry and neoprene has good environmental resistance, yield strength and other properties to use as flexible material

in the boom. Please note that this is a first selection of materials for this design phase. During detailed design phase, a thorough material selection will be included.

The length of a steel section (7.5 m) selected was based on 1/10 of the mean wavelength of the most occurring sea state. Longer steel sections tend to bridge waves. When a steel section bridges a wave, this results in wave crests going over the boom and reduced draft from the skirt, preventing the possibility to capture plastics.

FLEXIBLE BOOM

The flexible boom outer geometry is equal to the steel boom without the stiff sections. A flexible tube can follow the waves without the need for hinges. The tube now has the properties that have been given to the links between the steel sections in the stiff boom. The initial material is chosen as neoprene with an outer diameter of 1.55 m and an inner diameter of 1.35 m.

During actual simulations, an adjusted type of flexible boom was introduced. For this type the axial stiffness is equal to a neoprene material boom with a Dyneema cable running through the boom. In the model, the geometry is equal for both materials.
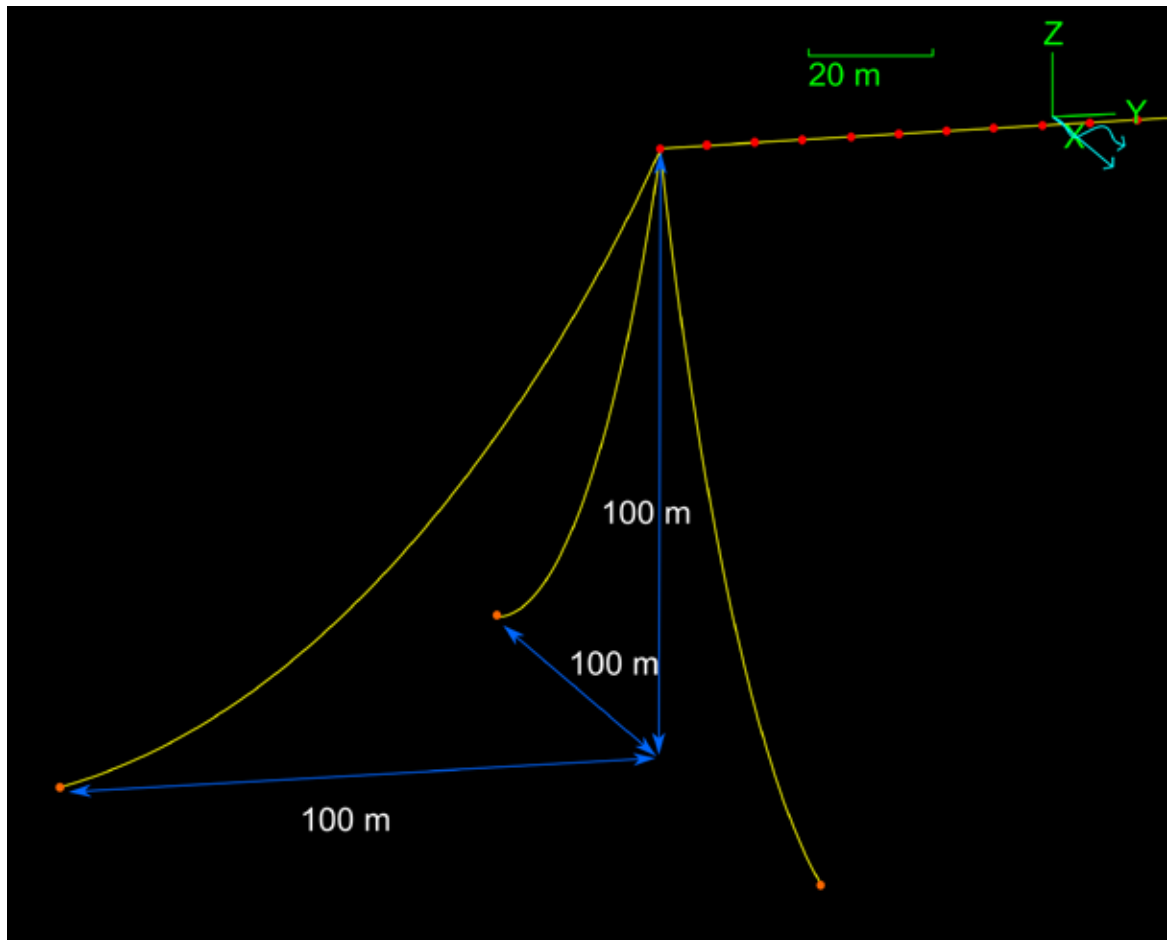
Figure 3.54 Mooring configuration in model

3.5.3.2. SKIRT AND BALLAST

A skirt was attached to the boom and oriented vertically. To reduce the loss of captured plastics, a ballast weight is likely to be attached to the bottom of the skirt. This ballast was part of the computation as well. The skirt was the same in both models, as well as the ballast weight underneath the skirt. In Section 3.5.5, the skirt and ballast weights are varied for design optimization purposes. More details on modeling of the skirt and ballast can be found in Appendix 4 where the Orcaflex model and its parameters are described in further detail.

3.5.3.3. MOORING CONFIGURATION

Placing mooring lines in the model was important to allow the model to reach equilibrium over time under the influence of the effects of waves and currents in a relatively constant direction. An estimate of the mooring system configuration was made since mooring design was not final during simulations. The mooring lines are shown in Figure 3.54.

The mooring system was modeled using 6 lines, 3 lines on each side of the boom. When seen from the top at each side of the boom, one line is attached parallel to the boom and the other 2 lines are placed perpendicular to the boom in both directions. The parallel mooring lines transfer the initiated tension in the boom to the seabed while the perpendicular mooring lines transfer the loads from incoming waves and current.

The lines are fixed to the seabed at a horizontal distance of 100 m from the boom end. The vertical distance from the boom end is also 100 m as this is the water depth of the model. All mooring lines are approximately 145 m long.
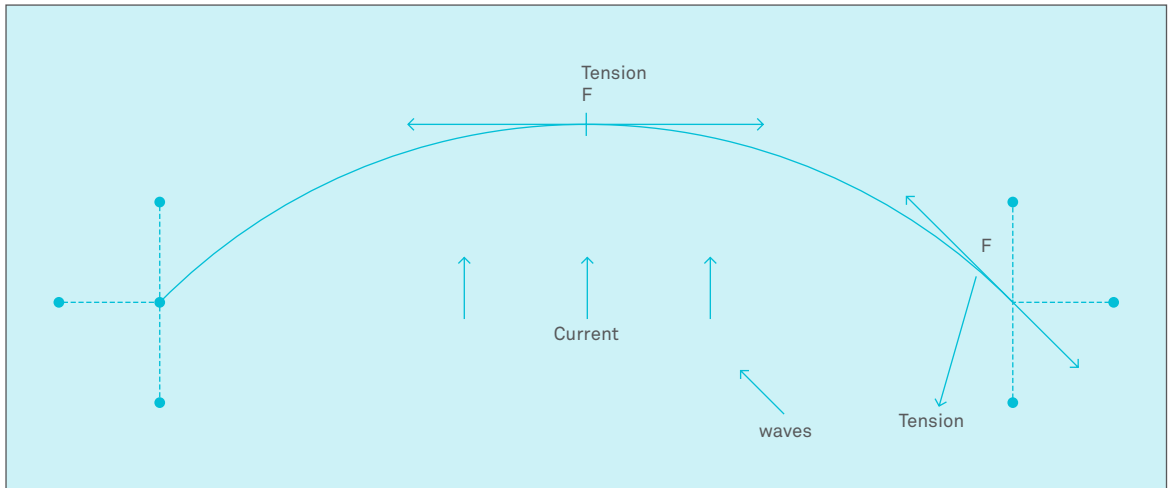
Figure 3.55 Wave and current condition during simulations

3.5.4. RESULTING FORCES

One of the main goals of the Orcaflex model is to obtain the initiated forces in the mooring system and tension in the boom. This result gives a better understanding of the relation between boom length and resulting forces.

STRUCTURAL MODEL

The structural model described in section 3.5.3 was used for this simulation. Note that the skirt was not included. Compensated drag and mass values were used to save computation time. In section 3.5.5, optimization of the skirt and ballast is discussed; here, the skirt and ballast are modeled. The forces are determined according to the scheme in Figure 3.55.

3.5.4.1. MODELED END FORCES

The resulting end force can be thought of as the total force that needs to be transferred to the sea bottom by the mooring system.

For the forces in the boom, it is important to know the highest occurring forces; therefore, the 3-hour return values of forces from dynamic simulations are shown. They are obtained from Generalized Pareto distributions. The results that will be shown are:

- The force at the end of the boom due to waves and current
- The force at the end of the boom due to current

WAVES AND CURRENT LOAD

In Figure 3.56, the differences in resulting end force can be seen for the steel-, neoprene- and Dyneema booms. The graph gives the impression that a linear correlation exists between the length of the boom and the forces. The formula of this trend is added.

Note that the parts in the structural model have the following yield strength:

- Steel sections $30*10^3$ kN
- Neoprene links/boom $1.5*10^3$ kN
- Dyneema cable $2.0*10^3$ kN

When forces exceed this value, unwanted plastic deformation occurs. Note that the steel boom has the neoprene links as weak part. The actual design of the boom is not the purpose of this part of the study; just an indication of the forces is given.

CURRENT LOAD

The force as a result of water current (which was modeled as 0.15 m/s perpendicular to the boom) is plotted in Figure 3.57. The calculation time allowed for longer lengths when only the static calculation is done.

$y = 0.591x + 279$

$y = 0.2587x + 191.58$

$y = 1.4195x + 360.58$
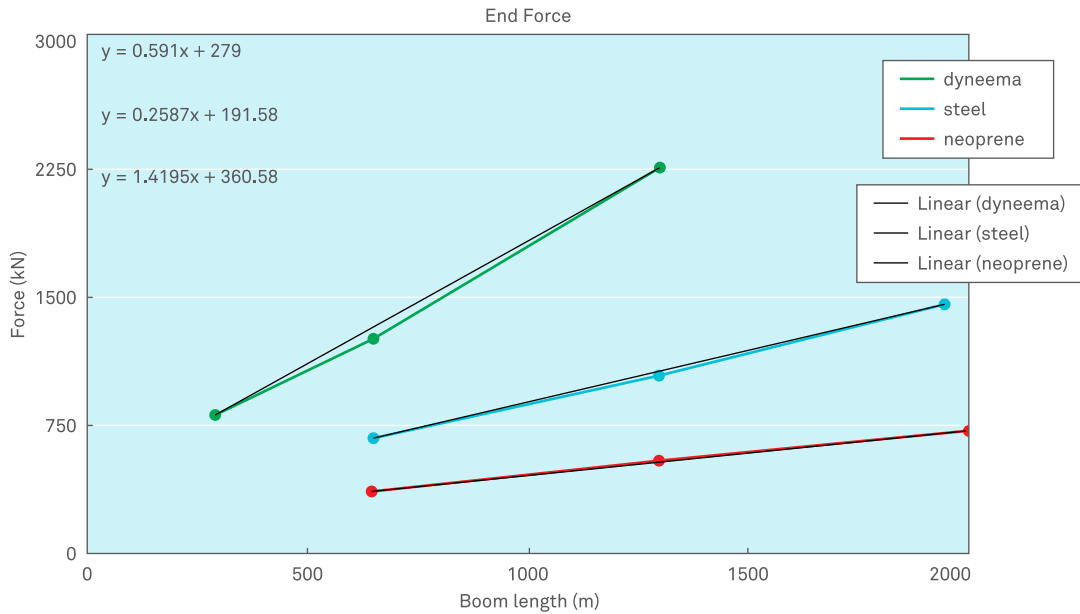
Figure 3.56 Resulting end force as function of boom length (current/waves)
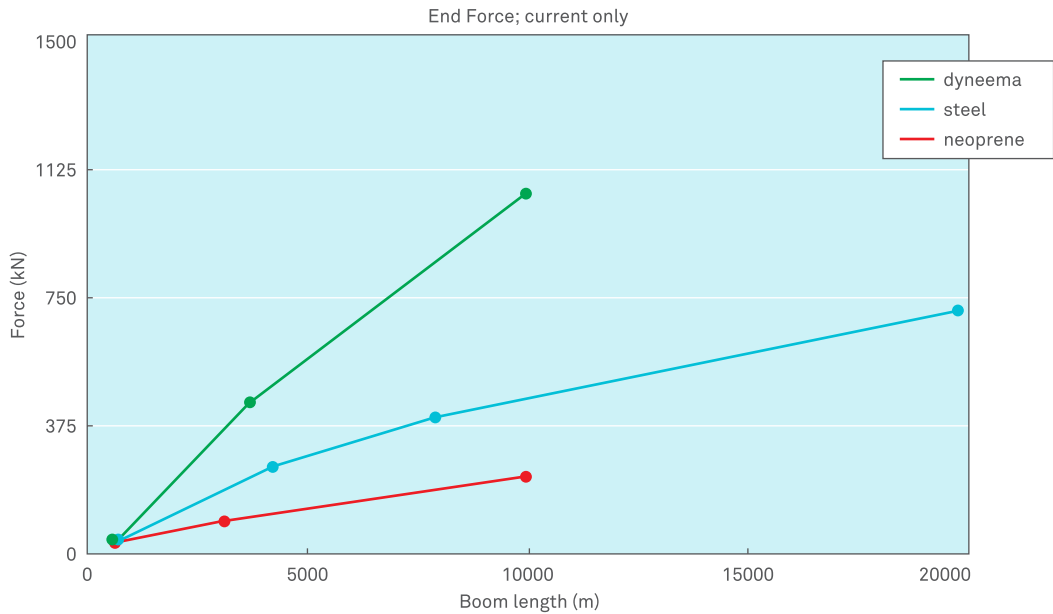
Figure 3.57 Resulting end force as function of boom length (current)

At increasing lengths, the curve tends to become less steep. It is expected that this is due to the arc-like shape of the boom under perpendicular load. When the boom has this shape, a smaller part of the current is directed perpendicular to the boom. This may cause the current to flow underneath the boom more easily. The same effect may occur with waves, however, for that simulation the boom length was set lower.

The results for the current can be reflected back to the waves, where longer models were not possible. They show the possibility to extrapolate the forces in Figure 3.56 above to longer boom lengths. This extrapolation may even be a conservative estimate of the force.

$y = 0.2147x + 168.77$

$y = 1.1012x + 252.71$
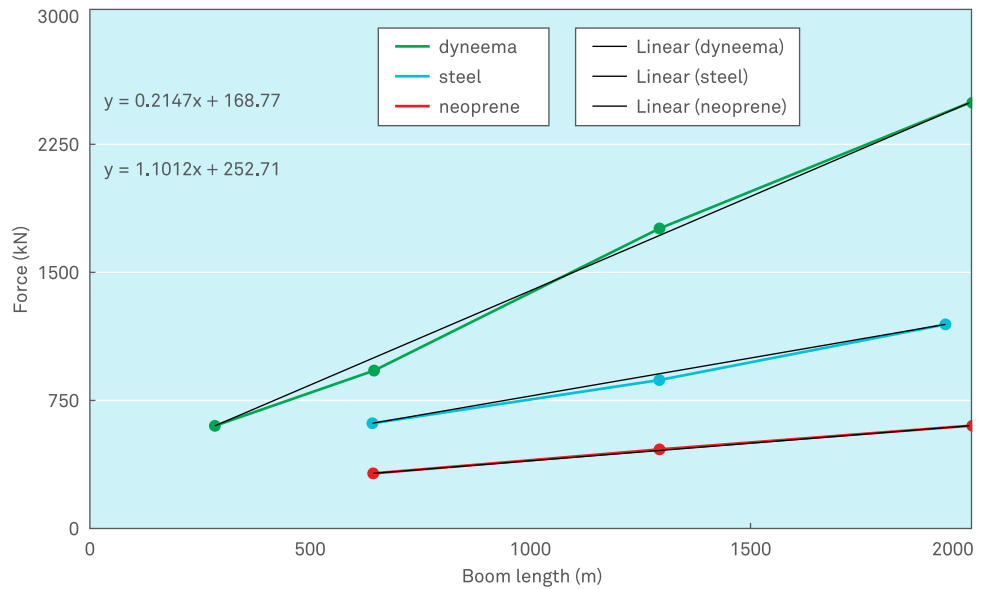
Figure 3.58 Mid effective tension as function of boom length

3.5.4.2. MODELED EFFECTIVE TENSION FORCES

In Figure 3.58, effective tension forces at mid-point of the booms are plotted. This is the force in axial direction of the boom. Forces in other than axial directions are negligible at this point and only occur near the mooring where the boom ends are limited in vertical and horizontal movements. The graph shows the mid effective tension for waves and current load only.

For boom lengths used in the simulation, the relation is fairly linear. The fact that for the Dyneema tensioned boom the tension is higher than both neoprene and steel boom is due to its high axial stiffness compared to the other options. The steel boom has neoprene links, which lower the stiffness significantly.

3.5.4.3. TENSION LIMITED BOOM LENGTH

High axial tension in the boom can result in the boom not being able to follow the wave surface. This effect is shown in Figure 3.59, where the tension force will cause wave overtopping and 'bridging' of the structure. This phenomenon did not happen in most of the simulations, but it is possible that the boom will be designed for longer lengths than used in the current model.
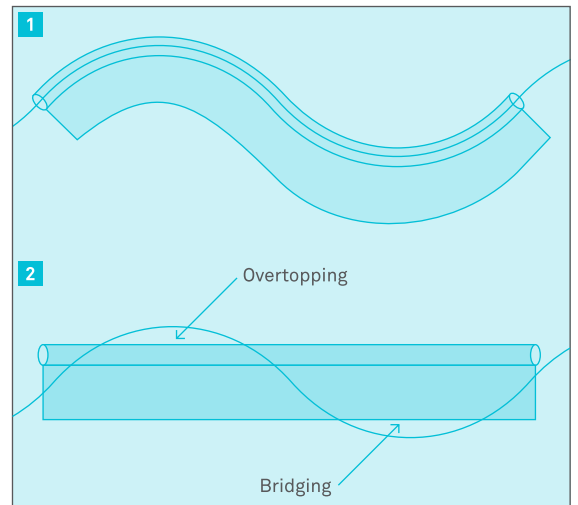
Figure 3.59 Effect of a too high tension force along the boom: in the top image, the boom can follow the shape of the wave, but in the bottom image, the tension force spans the boom in such a way that it remains straight
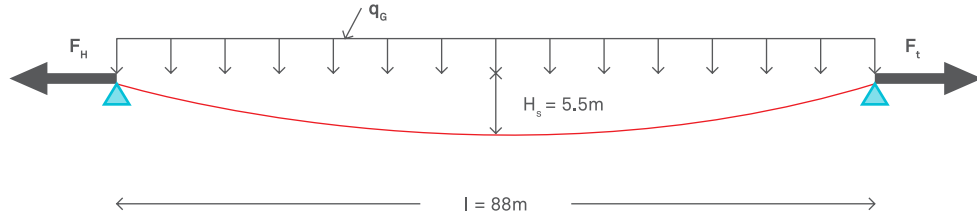
Figure 3.60 Schematic force overview

A structural mechanics analysis of this occurrence follows. The forces that explain this effect are illustrated in Figure 3.60. With the selected mean wave period T_z of 7.5 s and elevation H_s of 5.5 m, assume a wave length of 88 m and a boom that is positioned on top of the wave crests. The top of the wave crests is shown as supports. The boom should then be able to deflect at mid-section, which is 5.5 m lower in order to be able to follow the shape of the wave.

Due to the tension force F_t, the deflection is restricted to a certain extent; this is reached when the moment around the mid-point is zero due to combining F_t and q_G only. It is required that the possible deflection is greater than the wave height.

$$\frac{1}{8} * q_G * l^2 - F_t * H_s = 0 => F_t = \frac{\frac{1}{8} * q_G * l^2}{H_s}$$

Because the wave height (H_s = 5.5 m), wave length (l = 88 m), and the weight (q_G= ~10 kN/m) of the boom are known, the theoretical limit tension force in the boom at which this deflection is still possible can be estimated with the formula above.

$$F_t = \frac{\frac{1}{8} * 10 * 88^2}{5.5} = 1.8 * 10^3 \text{ kN}$$

Some assumptions that should be taken note of:
- Under the given length and forces, the moments are large with respect to the bending stiffness of the boom such that it behaves like a rope, having no bending stiffness.
- The boom floats on top of the wave crests and therefore the middle deflection needs to be equal to the full wave height.

When the boom floats at wave trough level instead of wave crest level, the boom section between the troughs deflects upwards due to buoyancy force. This buoyancy force is assumed similar to the gravitational force q_G and will thus come to the same result with the used formula.

When looking back at Figure 3.58 (3.5.4.2), this theoretical limit tension force F_t of $1.8*10^3$ kN can be linked to a boom length with the formula given in this figure for the Dyneema boom.

$$F_t = 1.1012x + 252.71$$

In which x is the boom length in m and F_t the limit tension force in kN. Solving for x:

$$x = \frac{1.8 * 10^3 - 252.71}{1.1012} = 1405 m$$

Before the modeled tension, the force in the boom becomes so large that it is not able to follow these waves anymore. For the steel boom this point is at:

$$F_t = 0.48383x + 308; x = \frac{1.8 * 10^3 - 308}{0.4383} = 3404 m$$

It should be noted that the links between the steel sections of this boom are as flexible as the neoprene boom and they are the main reason the steel boom has a relatively low force in it

The correlation of the 3 hour return value of the sea surface clearance and boom length for a Dyneema tensioned boom is shown in Figure 3.61.
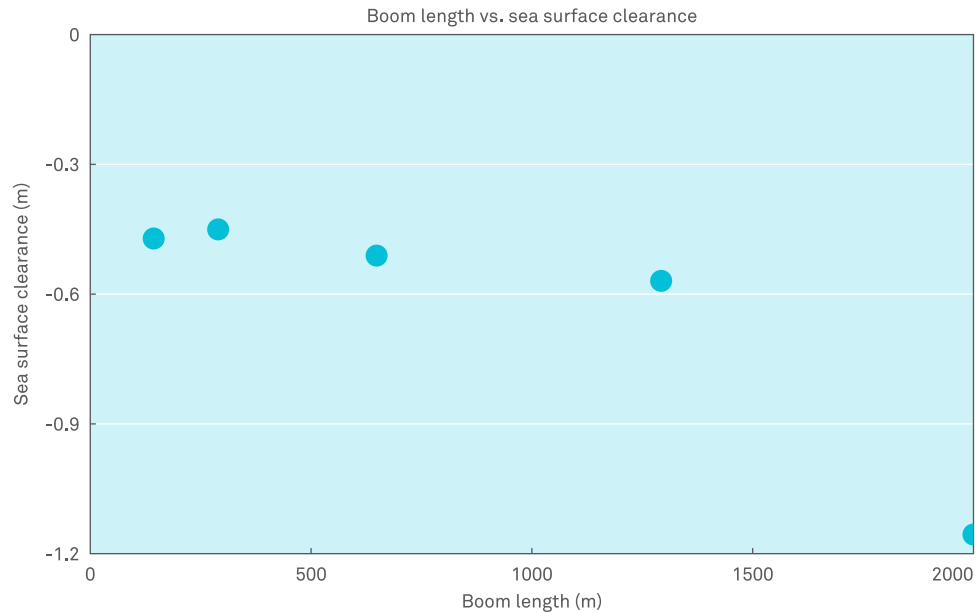
Figure 3.61 Boom length versus sea surface clearance

It is shown that up to a boom length of approximately 1 km, the sea surface clearance stays approximately equal. However, for longer booms, the sea surface clearance value reaches a much lower minimum. At 2 km the force is above the theoretical limit tension force.

This confirms the theory that the boom is less able to follow the waves when high tension forces are reached within it. By increasing the volume and mass of the boom, the q_G estimate in the calculations above will increase. Higher tension is then allowed before the limit tension force is reached where the boom is unable to follow the shape of the waves.

For a design with equal properties as the models in this study, it is advised not to use independently moored boom lengths longer than 1,400 meters.

3.5.5. OPTIMIZING SKIRT AND BALLAST WEIGHT
Besides obtaining loads acting on the system, simulations were run with the purpose of achieving other results. This section discusses simulations with different skirts and ballast weights to investigate the influence of these properties.

The skirt can move relative to the boom because the boom is attached to the mooring at its ends and is restricted in its movements while the skirt hangs underneath it without any obstruction. This causes the skirt to deviate from its vertical orientation as shown in Figure 3.62. If the angle is too big, captured plastics can easily flow underneath it. This is both due to a reduced draft and because fluid flow passes an inclined wall more easily than a vertical wall.

Figure 3.62 shows the boom at a moment where the horizontal wave forces in the boom are compensated by its restriction at the ends due to mooring, Fh; Boom. The ballast can still move in wave direction until Fh; Ballast caused by the tension force Fballast is equal to the horizontal wave forces.

Hanging ballast under the skirt can, in this way, help to keep the skirt in a vertical position. Properties of the skirt itself can have an influence on the movements too. The purpose of this section is to give a rough estimation of the combination of skirt and ballast that work best.

In the refined concept described in section 3.6, a different skirt attachment is proposed. This type is not included in this section due to parallel engineering activities.
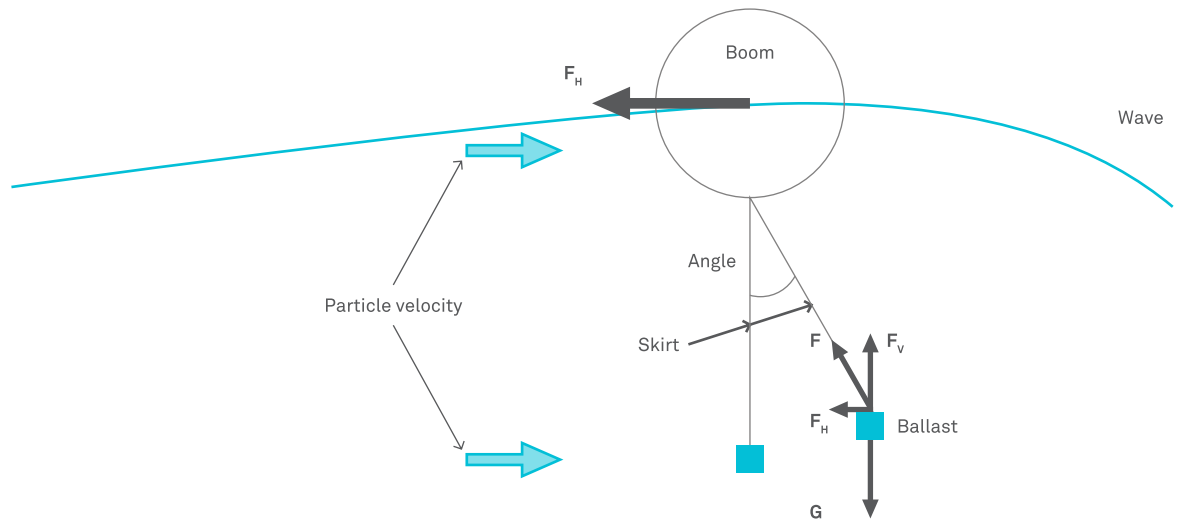
Figure 3.62 Skirt motion relative to the boom

Variable	Minimum (°)	Maximum (°)	Mean (°)	Standard Deviation(°)
Ballast: 10 kg/m; Heavy skirt	–52.67 (43.9)	51.50 (60.3)	–8.81	18.22
Ballast: 50 kg/m; Heavy skirt	–47.22 (41.7)	44.04 (49.6)	–5.53	15.70
Ballast: 100 kg/m; Heavy skirt	–40.02 (36.1)	45.05 (49.0)	–3.94	13.03
Ballast: 10 kg/m; Light skirt	–62.68 (40.1)	34.74 (57.3)	–22.59	17.57
Ballast: 50 kg/m; Light skirt	–40.21 (32.8)	34.93 (42.3)	–7.37	12.45
Ballast: 100 kg/m; Light skirt	–32.06 (28.4)	32.93 (36.6)	–3.63	10.46

Table 3.16 Skirt angles

SIMULATION TIME

The skirt movements relative to the boom started to show effects from the boom being held in position by the mooring after 200 s of simulation time. At 450 s of simulation time and after, some of the simulations became unstable. Therefore, the comparison is made using a simulation time range of 200 s to 450 s. This is a relatively short time because the boom had not fully moved into position yet. It is expected that longer simulation time will not cause a different conclusion on the ballast to be used. For each simulation, the angle, the sea surface clearance of the boom, and the sea surface clearance of the bottom of the skirt are obtained at the middle of the boom length.

They are shown through their maxima, minima, mean and standard deviation. The number between brackets is the difference between the minimum respectively maximum and the mean.

SKIRT ANGLE RESULTS

The skirt angles are determined for three different ballasts and two skirt weights. The resulting angles are shown in Table 3.16. As stated earlier, the angle is with respect to the vertical plane. Here, a negative value indicates the ballast weight position downstream.

Notable is the effect that the maximum and minimum angles of the light skirt are less significant than those of the heavy skirt at ballast masses of 50 kg/m or more. Figure 3.63 shows the reduced angle of the light skirt caused by the ballast tending to bend the skirt back to a vertical orientation at its end. This is more effective for the more flexible light skirt. In reality, even the stiffness of the heavy skirt is lower than the modeled stiffness for the light skirt in this direction.
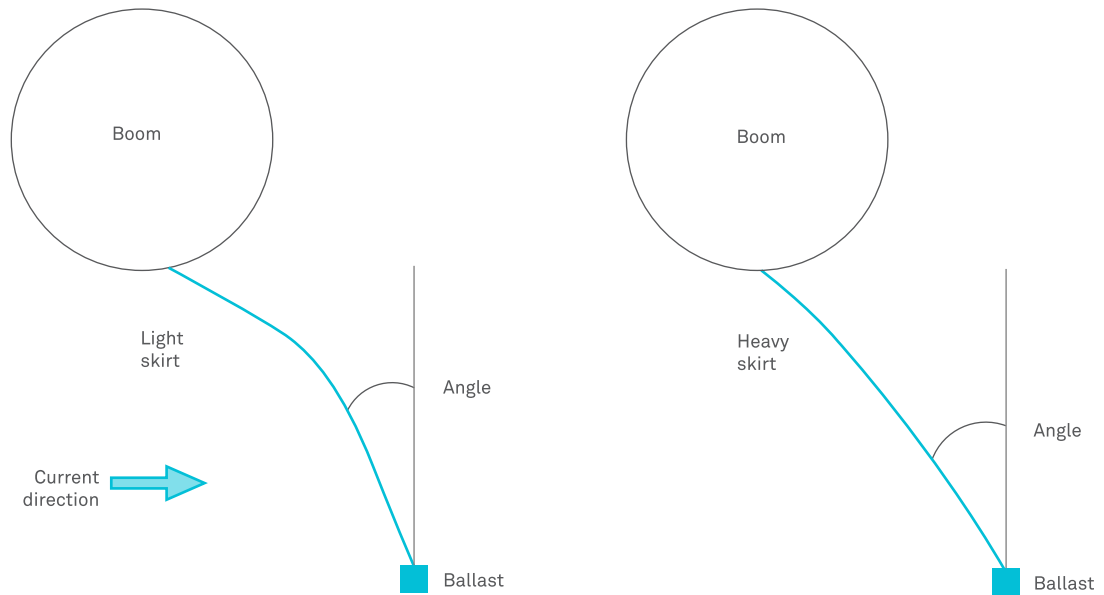
Figure 3.63 Angle on light versus heavy skirt

Table 3.16 shows that a ballast of 10 kg/m results in a mean angle of -23°, with a minimum angle of -63°. No further research has been done yet but it is expected that these angles will result in a significant loss of plastics. In comparison, the mean angle of 7° and the maximum of 40° as listed in the table with a ballast of 50 kg/m are likely to be sufficient for keeping plastics behind the boom. With a 100 kg/m ballast the angles are even less.

For now, the limit is set at a ballast of 50 kg/m as increasing ballast weight would require the skirt to be stronger, and the volume of the boom to increase if a certain amount of freeboard is required causing the expenses to go up.

STIFFNESS OF THE SKIRT VERSUS SEA SURFACE CLEARANCE
The resulting sea surface clearances are shown in Table 3.17 below. The increase in mean sea surface clearance with increasing ballast can be linked to the boom becoming less buoyant with increasing ballast and the axial stretching of the skirt due to the increased weight on it. These results show that with the chosen ballast, the draft of the skirt varies between 1.73 m and 4.35 m, with a mean of 2.97 m. Also this will for the time being, be assumed as reasonable for the trapping of plastics in front of the boom.

Figure 3.64 shows the difference between the maximum and minimum and gives a graphic representation of what is in the table. It can be seen that with increased weight, the deviations become larger. This may be caused by the increased weight having a larger effect on the relatively elastic skirt.

The resulting sea surface clearances are shown in Table 3.18. Figure 3.65 below also shows the difference between the maximum and minimum.

Variable	Minimum (m)	Maximum (m)	Mean (m)	Standard Deviation(m)
Ballast: 10 kg/m; Heavy skirt	-4.19 (1.40)	-1.74 (1.05)	-2.79	0.35
Ballast: 50 kg/m; Heavy skirt	-4.13 (1.27)	-1.84 (1.02)	-2.86	0.35
Ballast: 100 kg/m; Heavy skirt	-4.39 (1.45)	-1.63 (1.31)	-2.94	0.37
Ballast: 10 kg/m; Light skirt	-3.79 (1.19)	-1.36 (1.24)	-2.60	0.46
Ballast: 50 kg/m; Light skirt	-4.35 (1.38)	-1.73 (1.24)	-2.97	0.42
Ballast: 100 kg/m; Light skirt	-4.81 (1.51)	-2.01 (1.29)	-3.30	0.44

Table 3.17 Skirt bottom sea surface clearance
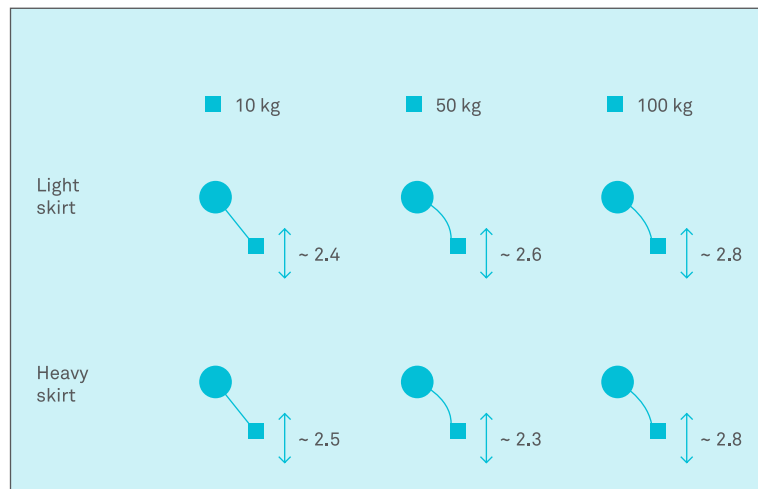
Figure 3.64 Deviation between maximum and minimum sea surface clearance of the ballast

Variable	Minimum (m)	Maximum (m)	Mean (m)	Standard Deviation(m)
Ballast: 10 kg/m; Heavy skirt	-1.92 (1.65)	0.60 (0.87)	-0.27	0.37
Ballast: 50 kg/m; Heavy skirt	-1.90 (1.59)	0.55 (0.86)	-0.31	0.37
Ballast: 100 kg/m; Heavy skirt	-1.94 (1.59)	0.61 (0.96)	-0.35	0.37
Ballast: 10 kg/m; Light skirt	-1.68 (1.46)	0.60 (0.82)	-0.22	0.35
Ballast: 50 kg/m; Light skirt	-1.77 (1.21)	0.56 (0.82)	-0.26	0.36
Ballast: 100 kg/m; Light skirt	-1.81 (1.52)	0.51 (0.80)	-0.29	0.35

Table 3.18 Skirt top sea surface clearance
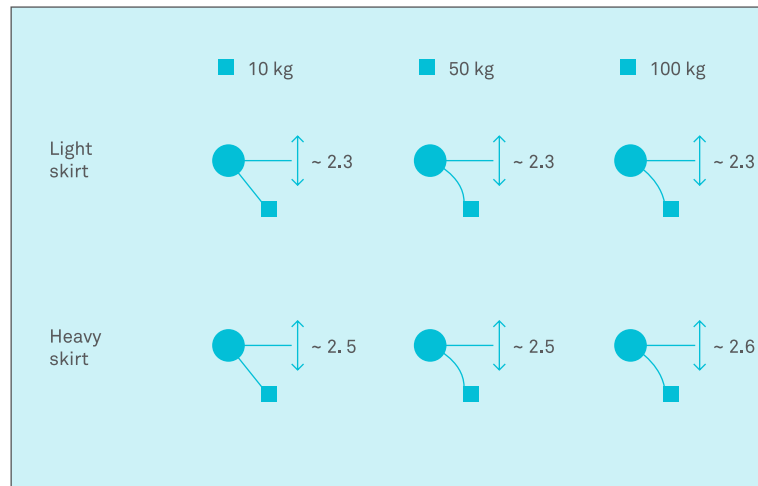
Figure 3.65 Deviation between maximum and minimum sea surface clearance of the boom

The increase in mean sea surface clearance with increasing ballast can be linked to the boom becoming less buoyant with increasing ballast. For this, less ballast will be slightly better as a wave going over the boom could take plastics with it.

Increased weight does not show a significant difference between the differences between the maximum and the minimum as shown in the figure above. This corresponds with the expectation that the increased ballast has greater effects on the stretching of the skirt as opposed to it having a lot of effect on the deviations of the boom.

Especially noticeable here is the difference between the minimum and the mean relative to the difference between the maximum and the mean. This means that the boom is more prone to submerging than to emerging in waves. This can be assigned to gravity forces and the boom at its ends being attached to the bottom.

Because the boom has a diameter of about 1.5 meter and thus a radius of 0.75 meter, every time a sea surface clearance of -0.75 meter is reached, the boom is overtopped by the wave. This means that the given sea surface clearance of minus 1.77 meter as a minimum at the chosen ballast, will negatively influence the plastic collection.

For now it is only important to know that heavier ballast does not have a lot of effect on the buoyant properties of the boom itself. Except that the mean and, with that, the minimum and maximum sea surface clearance drop a bit due to the structure as a whole becoming heavier.

3.5.6. SUMMARY AND CONCLUSIONS

During simulation, a number of aspects of the boom were determined by doing a series of simulations.

The design sea state is determined through a series of simulations by comparing sea states that are expected to result in the structure not being able to properly follow the water surface. The selected sea state is characterized with a significant wave height H_s of 5.5 m and mean wave period T_z of 7.5 s.

The boom and skirt model is simulated with 3 different ballast masses and 2 different skirt thicknesses. The skirt behavior is compared and the maximum skirt angle value is compared with a subjectively estimated limit. This resulted in the preference for a ballast weight of 50 kg/m and skirt thickness of 0.05 m. While the ballast has almost no effect on the draft of the boom, it does have a larger effect on the draft of the ballast, which is located at the bottom of the skirt. This is because the skirt is stretched significantly by the weight.

The skirt is removed from the model for force calculation due to computational time limitation and model instability. The model is adjusted with increased drag area and coefficient, resulting in a conservative estimate of the forces.

The relation between tension and high frequency flexibility was modeled. The limit tension force was estimated at 1,800 kN per 1,500 m of boom.

The boom will shape like an arc under wave and current load. Large horizontal excursion can have a negative influence on guiding plastic towards the collection terminal, so the booms must be placed under a tension where a positive angle of the booms still exists.

Results not presented in the report show that for the current floater diameter wave overtopping could occur frequently. It is advisable to investigate the result of a higher freeboard on overtopping and boom tension.

The simulations led to a better understanding of the boom behavior under wave load. Axial stiffness is required to limit the horizontal offset under load, while the bending stiffness should be limited to allow the boom to follow the waves.

BOOM CONCEPT REFINEMENT

JOOST DE HAAN • STEFAN VAN RUYVEN • SAM VAN DER HORST • EMILE ARENS • JAN DE SONNEVILLE • BOYAN SLAT

As a result of the design criteria mentioned in section 3.2.1 and simulation results in section 3.5, the most promising concept is the combination of a flexible boom and tension member. This concept allows the boom to follow the ocean surface, while preventing extreme horizontal excursions because of the connected tension member.

The design exists of buoyancy elements covered by a skirt, which blocks and transfers the plastic to the platform. At the bottom of the skirt a steel cable will be applied to guarantee enough down force for the skirt to remain in a vertical orientation.

The simulations in chapter 3.5 showed that if booms became too long, they would not be able to follow the waves any more, due to the tension in the boom. Hence, it was advised keeping the booms shorter than 1400 m. And since a total distance of approximate 100,000 m has to be bridged, we propose a new type of mooring system, where the tension cable and boom have been separated.

This cable will be connected to a steel cable (tension cable), which is located 30 meter under the water surface. This tension cable will be connected to the mooring cables. See Figures 3.66, 3.67 and 3.68.
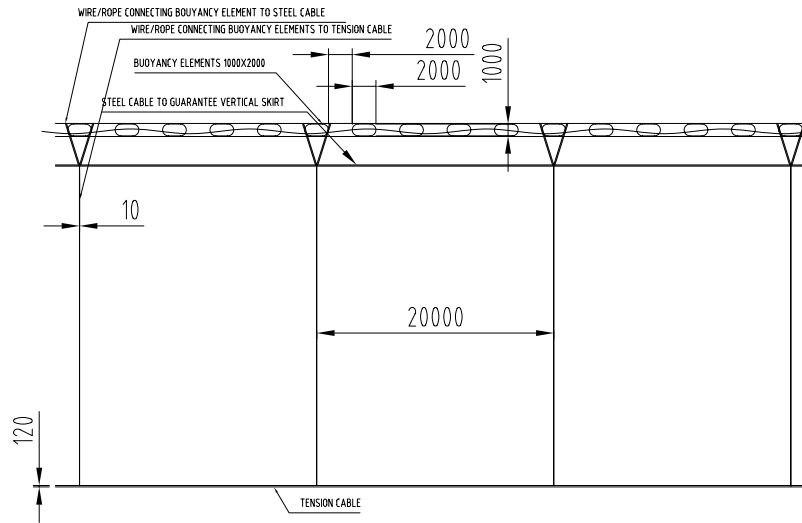
Figure 3.66 Boom section and tension cable – front view
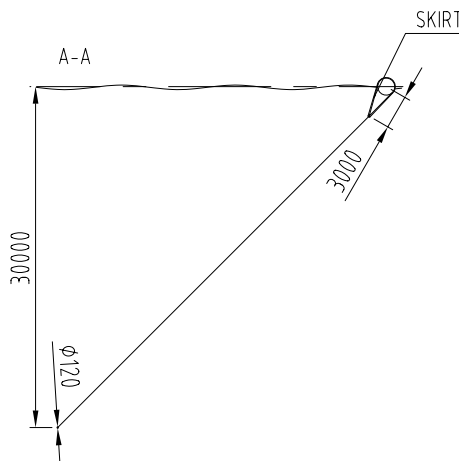
Figure 3.67 Left: Boom section and tension cable – side view.
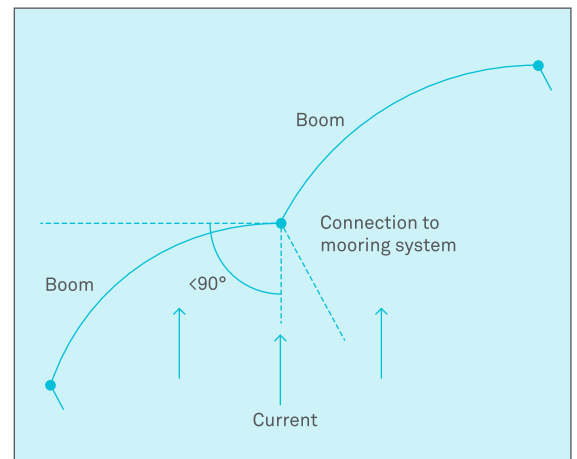
Figure 3.68 Top view of the boom.

Before explaining the concept more detailed, relevant boundary conditions are outlined.

MAIN CONDITIONS

- The fixed connection points for the tension cable will be applied with an interval of 4 km (see boom length optimization in chapter 3.7).
- The boom is installed with an angle of 45 degrees with respect to the (horizontal) tension member. Due to the arc shape, this angle increases towards the midsection between moorings, see also the top view of the boom in Figure 3.68
- The total width covered by the boom must be at least 50 km to both side of the platform.

- With current dimensions, the maximum tension in the tension cable between the mooring cables is 465 MT. This requirement results from a calculated lateral force of 600 N/m.
- The depth of the tension cable will be 30 m, for it to not be harmed if a ship accidentally crosses it.
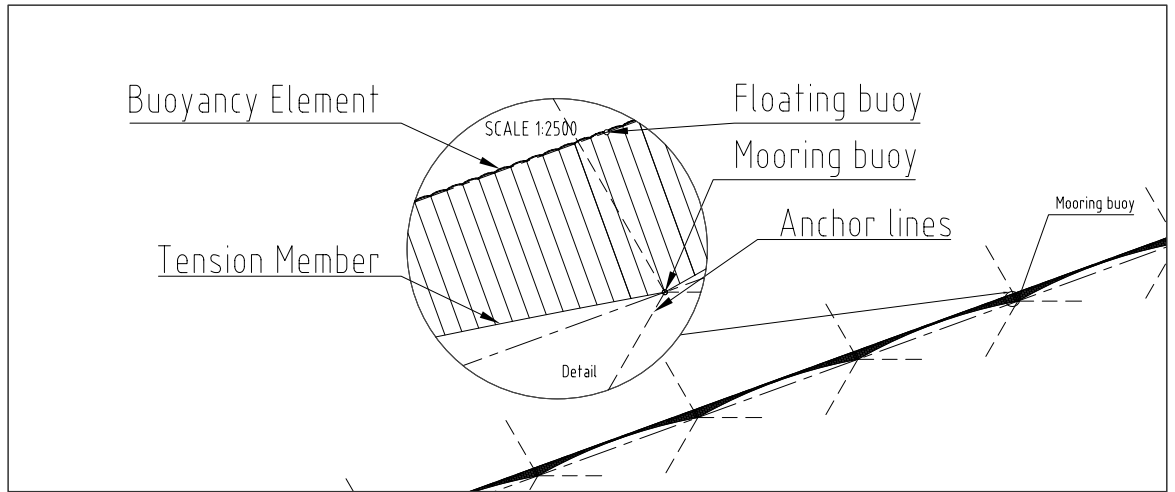
Figure 3.69 Tension cable impression

3.6.1. TENSION CABLE

The tension cable is the part of the design that will transfer the loads on the boom to the mooring cables. It is connected to the boom every 60 meters allowing the 54 km long boom to transfer its forces to the tension cable, see the impression in Figure 3.69. This way, large forces on the flexible boom are prevented.

The weight of the tension cable and cable connecting it to the boom combined should be lower than the booms buoyancy. Otherwise, the boom would be pulled under the water surface. Under current dimensions, the tension cable has a weight of 70 kg/m. To avoid the boom being lower in the water where the connection cables are attached to the boom, extra buoyancy is added to these places by adding buoys. Treatment against the environmental conditions is crucial for this cable as the cable is constantly submerged, exposed to sea water and ocean life.

The boom should be designed for at least 10 years of operation time. This results in the demand for a fatigue study. Due to wave frequency load, cyclic loading in the order of millions is present. For fatigue analysis, the expected loads and probabilities are used for determining the fatigue life. However, for the tension cable a steel cable of 120 mm is chosen which has a safety factor of 2.5, which is higher than the industry standard of 1.82 for mooring lines, thereby making fatigue-induced failure unlikely. Alternatively, a creep-resistant DM²0 Dyneema cable could also be used for this application, saving on weight and required buoyancy.

3.6.2. CONNECTION CABLE

A steel cable (see Figure 3.70) will be applied to connect the boom to the tension cable. This cable will be 20 mm in diameter; this is with taking a conservative safety factor of 3.3 into consideration as well. The cable length is such that the skirt will not have an angle along the current so the plastic cannot escape.
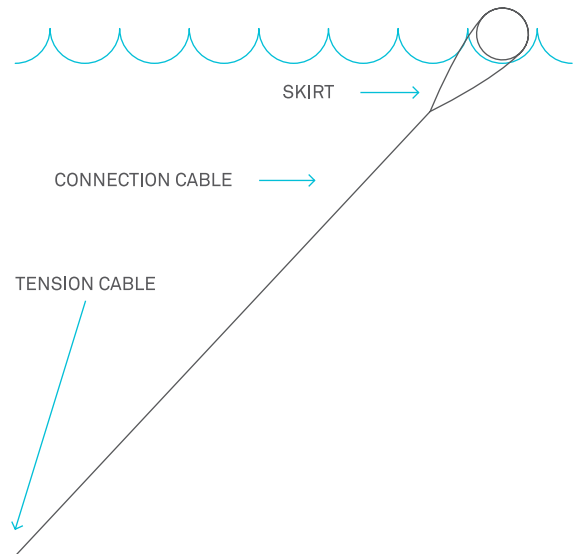
Figure 3.70 Connection cable impression
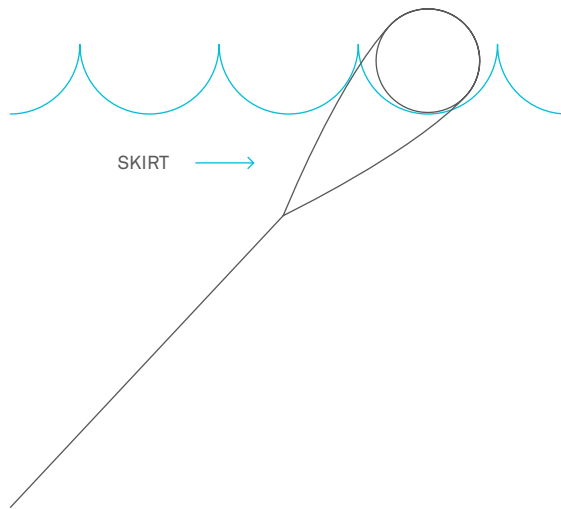
SKIRT ⟶

Figure 3.71 Boom skirt
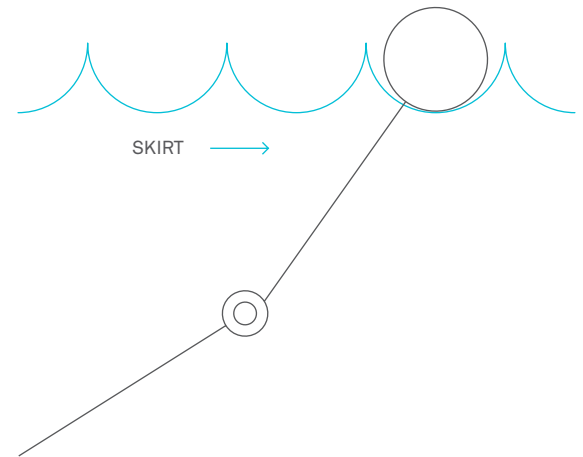
SKIRT ⟶

Figure 3.72 Boom skirt 2

3.6.3. SKIRT

The skirt (see Figure 3.71) is applied to collect and transfer the plastic to the platform. It will be applied around the buoyancy element and steel cable. This way there is no need for an additional connection between the skirt and the buoyancy element to carry the load of the skirt. However, some connection is required to prevent the buoyancy elements to travel in the boom's axial direction leaving the skirt not lifted by buoyancy elements at certain areas. Furthermore the positive slope of the skirt may negatively affect the fluid dynamics.

It can also be considered to apply the skirt as shown below, with a skirt around and closed at the buoyancy element. This would save material for the skirt but will require an extra connection. Because of the uncertainties the boom shown in 3.71 creates, the skirt shown in Figure 3.72 has been selected for the final concept.

External layer of ORCA® Chlorosulfonated Polyethylene CSM gives:
- Weatherproof resistance (fading and aging)
- Chemical resistance
- Abrasion resistance

Interlayer Neoprene® (CR) between the CSM and textiles gives:
- Optimal adhesion to textile and rubber

Neoprene inner layers gives:
- Perfect air & water tightness
- Excellent adhesion to textile and rubber
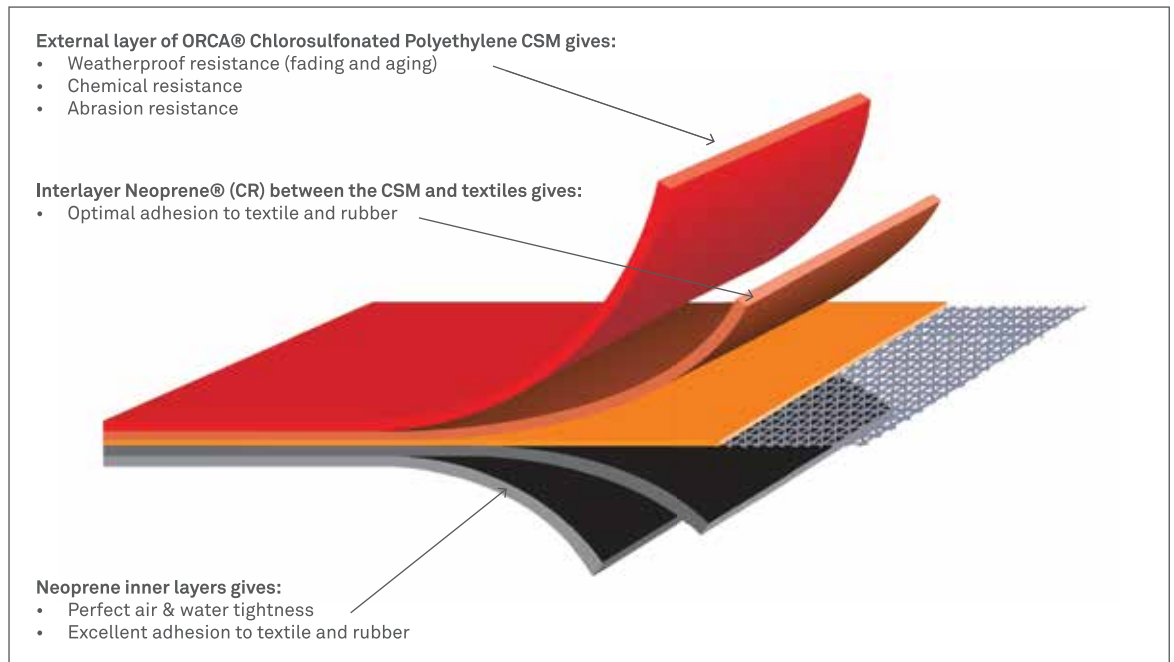
Figure 3.73 Orca fabric layers

MATERIAL

The skirt material will be exposed to all occurring environmental conditions for a period of 10 years. The material must be resistant for exposure to sea water, uv-light and mechanical abrasion. This combined with the flexibility of the skirt results in a limit amount of suitable materials. The material consists of multiple layers of high strength texture and non-permeable coating.

Proven technology materials that should be further investigated for use as skirt:

TREVIRA POLYESTER

The material is constructed from high tensile Trevira polyester base cloth, (pattern weaved) with heavy duty UV-stabilized PVC or polyurthane coating. This material is selected for use in buoyancy elements and ballast bags used in crane testing. The actual desired skirt structure is not for sale currently, but the company Seaflex can provide this material for the skirt.

ORCA® FABRIC

This fabric is often used for inflatable tubes in motorboats. Figure 3.73 shows the distinct layers that make the fabric. The base fabric is made from high tenacity polyester. Neoprene is highly suitable to give the skirt its non-permeability, and synthetic rubber could give the skirt its durability for UV and abrasion.

No data on fatigue behavior of the materials is available. In the subsequent design phase, manufacturers will be contacted to provide information on fatigue properties.
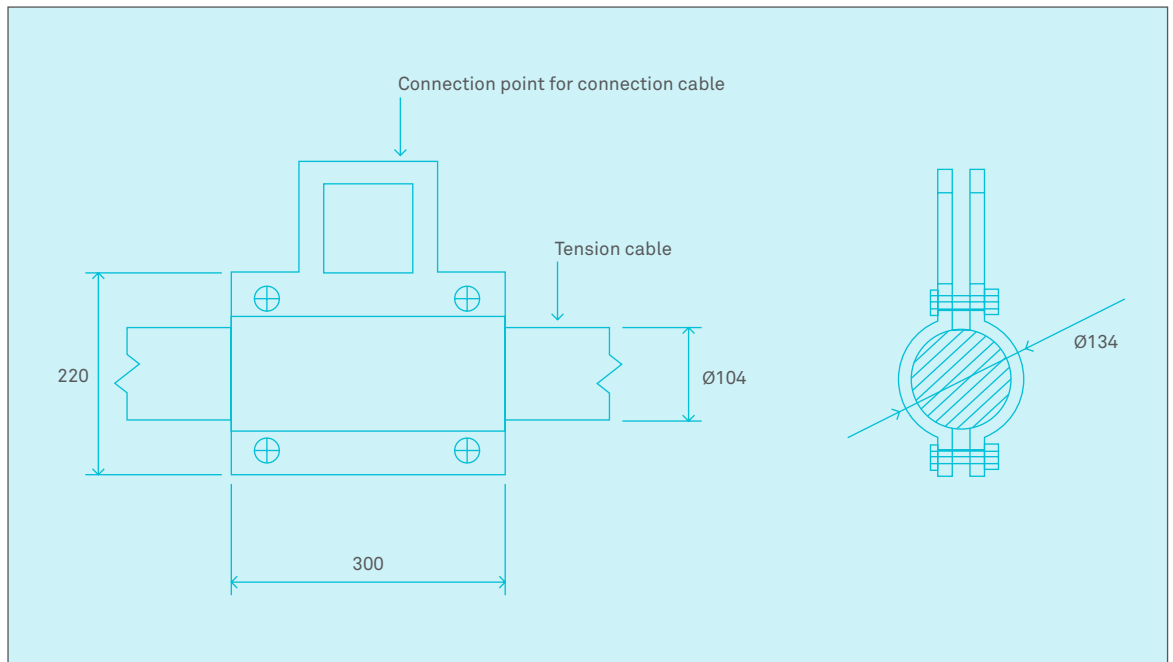
Figure 3.74 Connector for tension cable

3.6.4.CONNECTORS

CONNECTION CABLE TO TENSION CABLE

As can be seen in the next chapter it is most favorable for installation to have a quick and easy connection between these two cables. Therefore the next concept is suggested.

A connection piece will be mounted to the end of the connection cable. Then it can be bolted around the tension cable with pretension in order to prevent the connection to slide along the tension cable. In Figure 3.74 a sketch is shown of the concept.

The bolted connections could be replaced by another connection. At the connection cable side it can be chosen to make the connection piece hinged for example. As mentioned before, fatigue at this point might be an issue, for this reason this connection will require extra attention in the next phase. The bolted connection could also be welded, but when this has to be done on the vessel it is less favorable.

CONNECTION CABLE TO BOTTOM OF SKIRT

This concept is similar to the one described above. The difference is that now a connection is added for a cable/rope going to the buoyancy element (See Figure 3.75). The advantage for this connection is that more time is available to mount it since it can be done in advance.
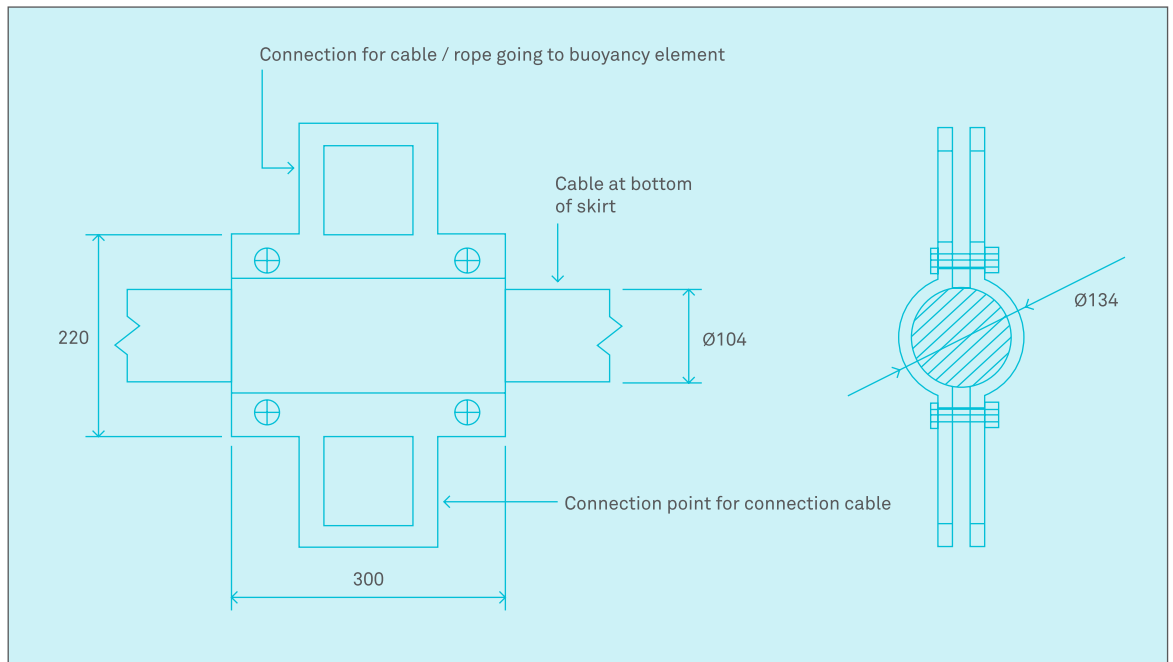
Figure 3.75 Connector for skirt bottom

Attention should be given to the skirt that has to be applied around the connection, which means a small opening should be made in the skirt for the connection cable. Again the bolted connection could be replaced by a welded connection as long as a pretension on the connection can be guaranteed so the connection won't slide along the cable at bottom of the skirt.

3.6.5. BUOYANCY ELEMENTS
To keep the boom floating, buoyancy elements will be applied. First a variant was investigated with steel pipes but this variant was found not suitable due to the wave movements at the surface will more easily lead to overtopping (waves going over the boom). Therefore a flexible boom concept was preferred over a stiff one. For the buoyancy elements there are multiple options.

Off the shelf buoyancy elements are preferred. Simple buoyancy elements can be applied. These elements are designed to last in marine environment and capable to take wave and wind impact. Other use of these elements is as fender for ships, preventing the ships to bump against quay walls.

Another option is to apply dredging pipes that are very flexible and suitable to apply in marine environment. This option however will be rather expensive compared to the buoyancy elements. Three options are outlined below.

OPTION 1
The first option is to use foam filled or pneumatic fenders. These fenders will be placed every 4 meters. The skirt is placed around the fenders. The advantages and disadvantages of the fenders are briefly described below.

Figure 3.76 Foam fender impression

Figure 3.77 Pneumatic fender impression

FOAM FILLED FENDERS

Foam filled fenders (Figure 3.76) require little to no maintenance, in comparison to air-filled fenders. Those have a chance of deflation, and according to its manufacturer a yearly inspection of the valves is recommended.

PNEUMATIC FENDERS (SEE FIGURE 3.77)

- Cheaper than foam filled fenders
- More environmental friendly than foam based fenders
- More compact to transport

OPTION 2

The second option is to use pipes as uses in dredging industry. The pipe used there consists of a rigid pipe piece made from HDPE connected with flexible rubber hoses (Figure 3.78) to ensure the flexibility of the pipe to follow the waves. To ensure floatation of the pipe special floatation buoys are placed around the pipe.

PROS

- Proven technology, used in offshore dredging operations
- Little to no maintenance required

CONS

- Expensive
- Non flexible pipe used, suitability for flexible booms should be investigated

Figure 3.78 HDPE pipe with buoyancy elements

OPTION 3

The third option uses floaters made out of an UV protective shell filled with unsinkable foam (Figure 3.79). The barrier has a freeboard of 1 meter above the water line, below the waterline a skirt can be attached to the barrier. The floatation pieces are bolted together which enables the option to place the skirt between them.

PROS
- Rigid floaters
- Skirt can be attached to the buoys relatively easy

CONS
- Expensive compared to fenders
- Time consuming installation

CONCLUDING REMARKS

Based on the input from multiple fender manufacturers, the reliability of pneumatic is uncertain for a deployment time of 10 years. Hence, we will now assume foam-filled fenders in this feasibility study. However, considering the benefits in terms of transportability, deployment time and recyclability, the suitability of pneumatic fenders, it is still recommended to further investigate the suitability of pneumatic fenders in a later phase.

Figure 3.79 Floaters with connectable skirt

3.6.6. COSTS

Table 3.19 shows the estimation for the production cost of the boom concept.

3.6.7. SUMMARY AND CONCLUSIONS

By reconsidering the preliminary concepts with the help of studies presented earlier in this chapter, the most promising design is presented. The design consists of a flexible floater connected to a tension member to avoid excessive horizontal excursions. The model is dimensioned using the results of the Orcaflex study. For now two types of skirt material are investigated, in both cases the material consists of multiple layers of high strength texture and non-permeable coating. Buoyancy elements are connected to the skirt allowing the structure to follow the wave surface elevation.

The presented concept is the first step in the design of a structure that can operate well at harsh environmental conditions for the design life of at least 10 years.

Part name	Cost per piece	# of pieces	Total cost	Source
Fender, diameter 150 cm, length 200 cm	€880	28,868	€25,403,840	Huisman Equipment b.v.
Skirt fabric, synthetic rubber, 1 cm thickness	€ 24 per m² (extrapolated from 2.5 cm plate)	885,500 m² (7.7 m * 115,000 m)	€21,252,000	ERIKS b.v.
Ballast cable, 40 mm diameter, steel	€ 29.25 per m	115,000 m	€3,363,750	Huisman Equipment b.v.
Tension cable, 113 mm diameter, steel, MBL 1200 MT	€ 227,49 per m	115,000 m	€26,161,350	Huisman Equipment b.v.
Connection cable, 20 mm, steel, MBL 24 MT	€ 7,63 per m	86,625 m	€660,949	Huisman Equipment b.v.
Navigation light	€ 145	319 (one every 360 m)	€46,255	Alibaba (estimation)
Manufacturing	€ 16.66 / m (based on assembly speed of 1 m/min, 10 people at €100/h)	115,000 m	€1,916,000	Estimation

Table 3.19 Cost calculation of the boom concept

In the subsequent project phase, the design will be further evaluated and detailed. This will result in the most cost efficient and technically feasible design.

''For the Ocean cleanup feasibility study Huisman equipment B.V. was involved in the design of the so called floating collecting boom and underwater placed tension member. Although the design of a collecting boom of this scale is a unique concept, can't be compared with anything ever build and doesn't fall within our field of expertise, Huisman believes the concept is feasible and executable with the use of existing floating barriers. Concerning the tension member we believe the internal forces that can be generated by the boom will be transferred through the cables and guided to the mooring lines. We find three important recommendations, which may strongly influence the final design, feasibility and costs:

a) To investigate the installation method
b) To investigate the dynamic behavior in extreme weather and wave conditions and, if necessary, to investigate an abandonment and recovery system of the floating boom concept.
c) To investigate the dynamic behavior of the floating boom either by scale or computer models.''

Eric Romeijn
Technical Manager, Huisman Equipment B.V.

STATION KEEPING

JOOST DE HAAN • SENOL OZMUTLU • CHRISTOPHE LIMOUZIN • JAN DE SONNEVILLE • BOYAN SLAT

Station-keeping capability during operation is an integral part of the Ocean Cleanup Array concept. Throughout the feasibility study, the selected location is the Northern Pacific Ocean (30° N, 138° W). Furthermore, water depths range from approximately 1,800 to 4,800 meters. Station keeping is challenging, because of the extreme water depths and also because the length of the moored structure is two orders of magnitude greater than anything that has been deployed offshore in the past.
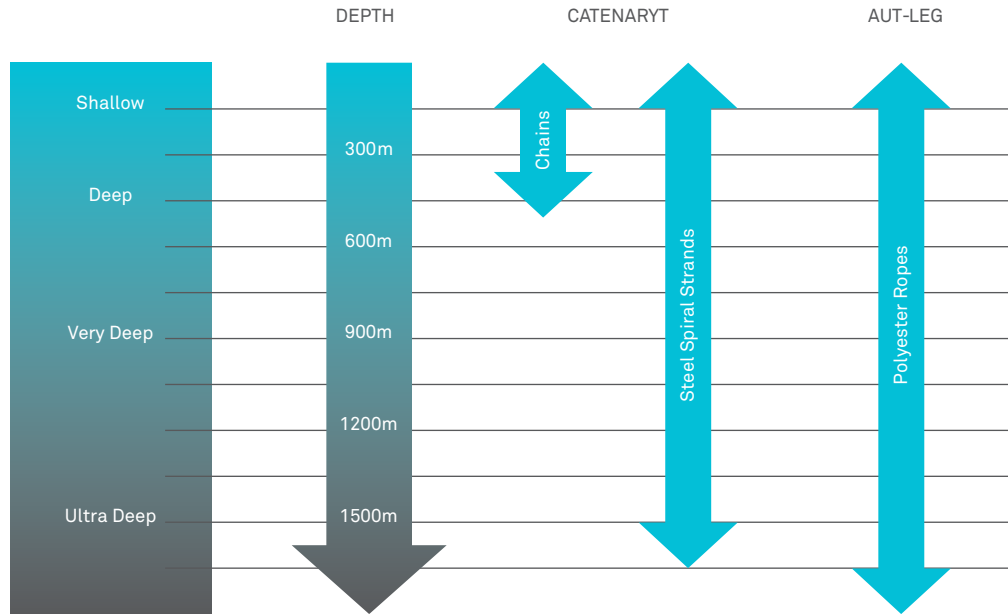
Figure 3.80 Typical mooring configurations and line type by water depth. Courtesy of Bridon.

3.7.1. CONCEPTS

Station keeping in open water can be done either actively or passively. Active station keeping is commonly done using a Dynamic Positioning (DP) system. The system consists of multiple propellers or thrusters, for which the thrust and direction are controlled. In this study no further elaboration is given on active station keeping. Although capital expenditures may be lower, the continuous power requirement is high in operational costs and impacts the environment negatively. This is especially the case because of the large drag forces created by the 100 km of floating barriers.

Passive systems typically consist of mooring line, anchoring and connectors. The mooring configuration and line type are highly dependent on duration of operation and water depth. Figure 3.80 depicts the typical mooring configurations and line types by water depth.

3.7.1.1. MOORING CONFIGURATIONS AND ROPE TYPES

It can be seen that the water depths of 3-5 km are not incorporated in the graph. Current water depth record for offshore structure mooring is about 2,400 m water depth (Shell Perdido Spar). Furthermore, in deep water environments steel wire rope or chain cannot be used, because the line's deadweight results in line tension exceeding the breaking strength.

The lower density of polyester rope makes it useful for deep water mooring systems. It is advisable to use chain or steel wire rope at the lower part of the mooring lines. At the touchdown point abrasion of the fiber rope impacts the rope's integrity. Even with a jacket for abrasion protection wear is expected. The touchdown point is shown in the picture below. This is the point in between number 13 and 14.

Components in a typical mooring line

1. wire rope
2. wire rope socket
3. swivel
4. pearlink
5. shackle
6. H-link
7. polyester rope
8 H-link
9. shackle
10. pearlink
11. swivel
12. pearlink
13. chain
14. shackle
15. anchor point
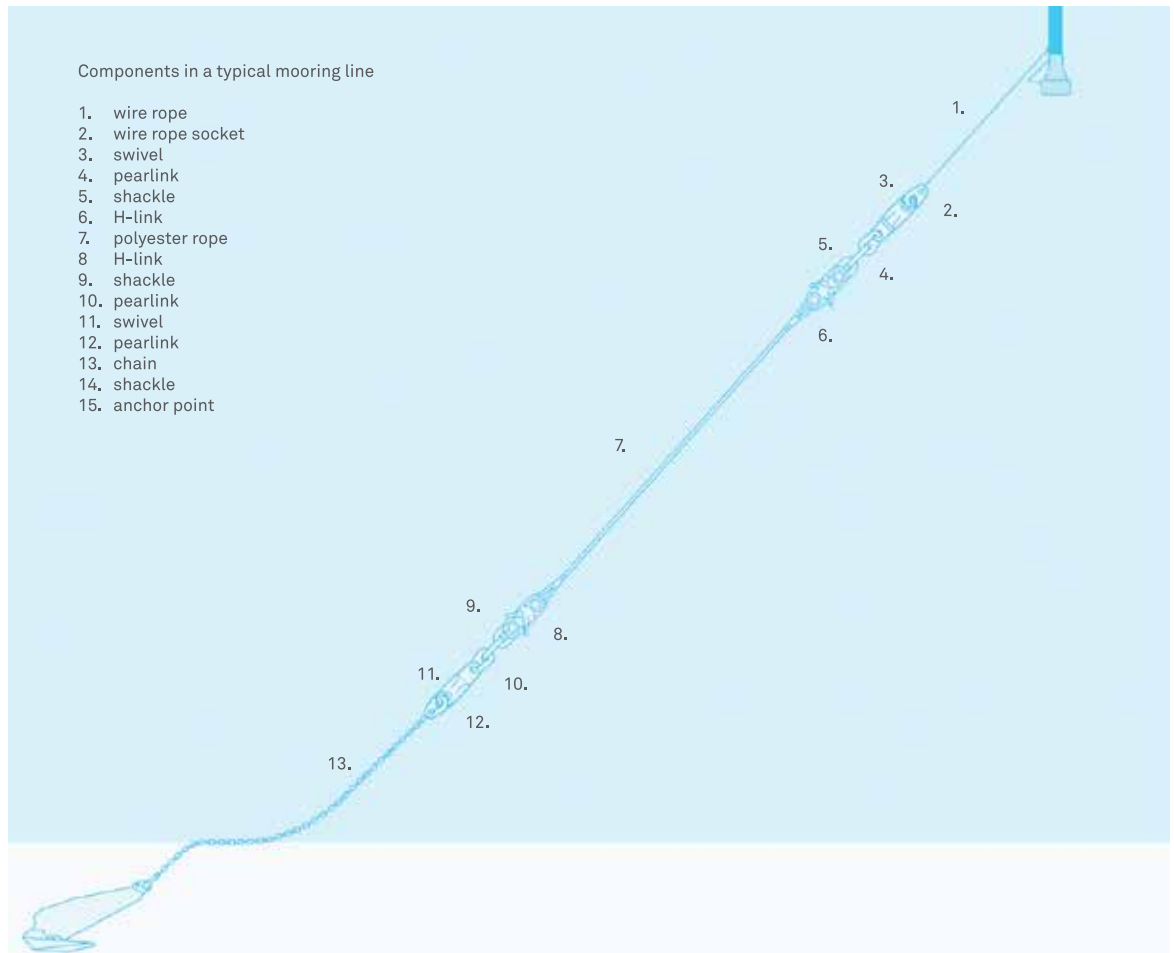
Figure 3.81 Components in a typical mooring line. Courtesy of Vryhof Anchor.

Polyester ropes are commonly used in taut leg configuration (Figure 3.82). Taut leg mooring has smaller footprint and requires less rope length at equal mooring capacity. Recent study showed that a combination of taut leg and catenary mooring results in smaller movement of the moored structure. Furthermore, this mooring system is also compatible with the characteristics of catenary mooring system, which eliminates the requirement of anti-uplift capacity of the anchors.

3.7.1.2. ANCHORING

Deep-water anchoring in taut leg (or semi taut leg) configuration is performed using three proven methods. These are the Vertical Load Anchor (VLA), suction pile and the fairly new penetrating torpedo anchors.

Figure 3.82 Catenary and taut leg configuration. Courtesy of C-leg media

3.7.2. CONCEPT OF CHOICE

In the current concept, the Stevmanta VLA is chosen (Figure 3.83). This is a product of collaboration partner Vryhof Anchors. It allows uplift at the anchor point, present at taut leg mooring systems. The anchor can be installed from one anchor handling vessel (AHV). No ROV is required, cutting installation costs. The figure below shows a front and side view of the anchor. The required size for the concept should follow from mooring system calculations. It is available for anchor areas ranging from 5 to 20 square meters. The area of choice depends on the load, anchor line arrangement and soil conditions.

Main dimensions Stevmanta VLA (dimensions in mm, area in m²)

Area	5	8	10	12	15	17	20
B	3143	3975	4445	4869	5443	5795	6286
C	2976	3765	4209	4611	5155	5488	5953
D	1945	2460	2750	3013	3368	3586	3890
E0	3075	3890	4349	4764	5326	5670	6150
E1	3371	4264	4767	5222	5839	6216	6742
F	172	217	243	266	298	317	344
H	1459	1845	2063	2260	2527	2690	2918
T	639	809	904	991	1107	1179	1279
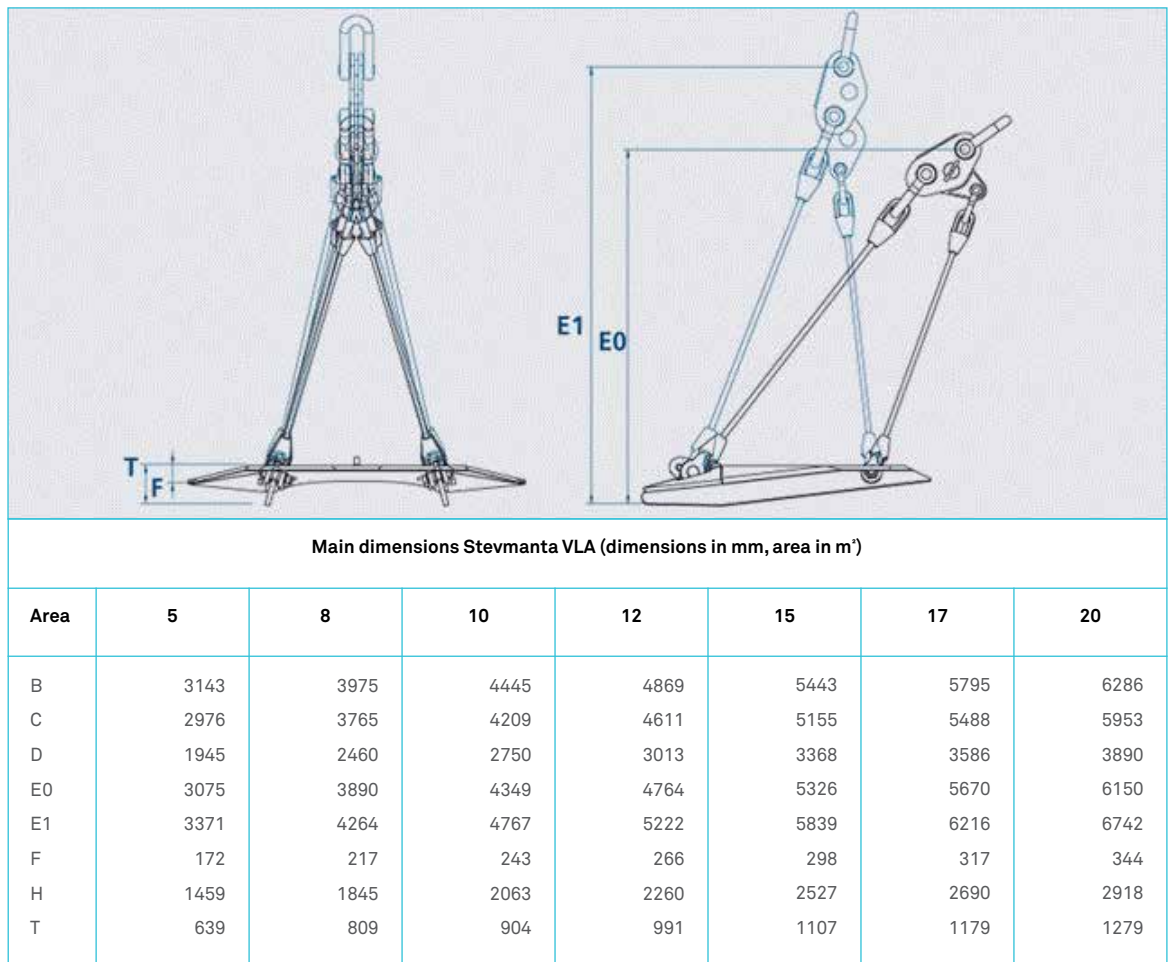
Figure 3.83 Stevmanta VLA, Courtesy of Vryhof Anchor

	Undrained shear strength (kPa)	Submerged unit weight (kN/m³)	Averaged soil sensitivity (St)
Lower Bound	1.2 x z	4	4
Upper Bound	1.4 x z	4	4
z is the depth below mudline in meters			

Table 3.20 Upper and Lower bound soil properties
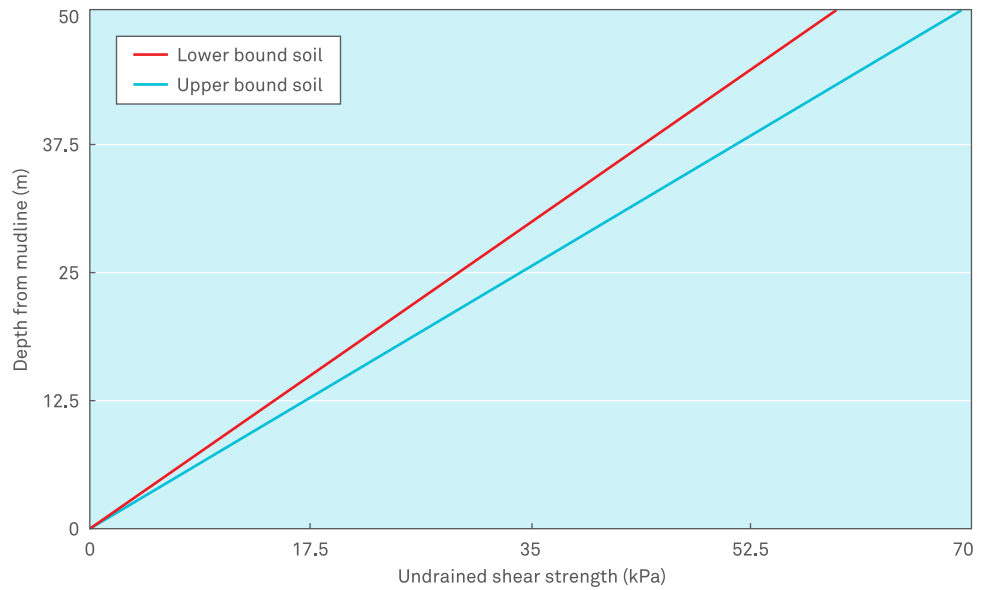
Figure 3.84 Lower and Upper Bound soil design profiles

SOIL CONDITIONS

At this preliminary phase, the site and soil conditions at/around the planned anchor locations are not known. Based on Vryhof's experience at deep water mooring locations 2000 – 3000 meters depth, the soil is assumed to be very soft clay. The assumed soil properties for Lower and Upper Bound design are tabulated below (Table 3.20). The Lower and Upper Bound soil design profiles are shown in Figure 3.84.

ANCHOR LINE ARRANGEMENT

There will be 29 nodes (submerged buoy elements) in the system. Every node (submerged buoy) will be moored by using three mooring lines. Each mooring leg, from mud-line to buoy, is comprised of: a bottom chain segment, a polyester rope segment, and a top chain or wire rope segment. The mooring lines shall be selected based on the preliminary design load of 3600 kN. The average angle between each mooring line and the vertical axis is 20 degrees.

For the anchor forerunner (i.e. the line segment in the soil from anchor shackle to the mud-line) a spiral strand wire rope is selected. The use of wire rope forerunner instead of chain will have positive influence in anchor penetration depth thus the required Stevmanta VLA size will be smaller. Per API RP 2SK or class regulations the MBL of the line should be 1.67 x the maximum intact load (calculated from dynamic analysis). Considering the maximum line load of 3600 kN, a spiral stand of 70 mm with 8 mm sheathing thickness is selected. The Minimum Braking Load (MBL) of the selected forerunner is 6012 kN.

	LB Soil	UB Soil
Anchor size used	14 m² Stevmanta VLA	14 m² Stevmanta VLA
Installation load at anchor shackle ($F_{ins@anchor}$) = shear pin size	1834 kN	1834 kN
Estimated tension at seabed 0° uplift ($F_{ins@mudline}$)	1971 kN	1956 kN
Penetration depth anchor shackle	32.8 m	27.9 m
Penetration depth center of area anchor	35.8 m	33 m
Estimated drag length	36 m – 51 m	33 - 47 m
N_c factor used	12	12
UPC	7209 kN	7209 kN

Table 3.21 A comparison between the upper and lower bound estimates in terms of soil conditions

DESIGN LOADS

The maximum mooring design load is specified by The Ocean Cleanup as 3,600 kN. The required ultimate pull-out capacity is doubled due to API RP 2SK recommended safety factor for plate anchors. Therefore, the UPC is 7200 kN

REQUIRED STEVMANTA VLA SIZE

For the upper and lower bound (UB and LB respectively) soil conditions the required anchor size and installation depth are calculated by Vryhof.

The proposed 14 m² Stevmanta VLA, when installed with an installation load of 187 tons at the anchor (i.e. shear pin break load), will obtain the required capacity under the assumed soil conditions. Table 3.21 summarizes the anchor installation, capacity, and performance values.

The estimated drag length refers to the horizontal distance between anchor drop points to the shear pin break point during installation stage. After the shear pin has broken there is no extra drag for the selected Stevmanta VLAs up to its UPC of 7,200 kN.

Diameter*		MBL		Approximate mass				Post installation drift stiffness		Intermediate stiffness		Storm stiffness	
				In air		Submerged							
in	mm	kN	kips	kg/m	lb/ft	kg/m	lb/ft	MN	10³ kips	MN	10³ kips	MN	10³ kips
4 15/16	126	3924	882	10.0	6.7	2.5	1.7	51.0	11.5	105.9	23.8	109.9	24.7
5 1/2	139	4905	1102	12.1	8.1	3.0	2.0	63.8	14.3	132.4	29.8	137.3	30.9
5 15/16	151	6180	1389	14.4	9.7	3.6	2.4	80.3	18.1	166.9	37.5	173.0	38.9
6 1/4	158	6959	1565	15.9	10.7	4.0	2.7	90.5	20.3	187.9	42.3	194.9	43.8
6 5/8	168	7848	1764	18.0	12.1	4.5	3.0	102.0	22.9	211.9	47.6	219.7	49.4
6 15/16	177	8829	1984	19.9	13.4	5.0	3.4	114.8	25.8	238.4	53.6	247.2	55.6
7 1/4	185	9810	2205	21.9	14.7	5.5	3.7	127.5	28.7	264.9	59.5	274.7	61.7
7 15/16	201	10987	2469	25.8	17.3	6.5	4.3	142.8	32.1	296.6	66.7	307.6	69.1
8 3/8	213	12263	2756	28.9	19.4	7.2	4.9	159.4	35.8	331.1	74.4	343.4	77.2
8 3/4	223	13734	3086	31.8	21.4	8.0	5.4	178.5	40.1	370.8	83.3	384.6	86.4
9	229	14715	3307	33.6	22.6	8.4	5.7	191.3	43.0	397.3	89.3	412.0	92.6
9 1/2	241	15696	3527	37.2	25.0	9.3	6.3	204.0	45.9	423.8	95.2	439.5	98.8
9 3/4	247	16677	3748	39.2	26.3	9.8	6.6	216.8	48.7	450.3	101.2	467.0	104.9
10 1/8	257	17858	3968	42.4	28.5	10.6	7.1	232.2	51.6	482.2	107.1	500.0	111.1
10 3/8	263	18639	4189	44.4	29.8	11.1	7.5	242.3	54.5	503.3	113.1	521.9	117.3
10 9/16	268	19620	4409	46.4	31.2	11.6	7.8	255.1	57.3	529.7	119.0	549.4	123.5
10 13/16	274	20601	4630	48.5	32.6	12.1	8.2	267.8	60.2	556.2	125.0	576.8	129.6
11 1/16	281	21582	4850	50.7	34.1	12.7	8.5	280.6	63.1	582.7	131.0	604.3	135.8
11 1/4	286	22563	5071	52.6	35.3	13.2	8.8	293.3	65.9	609.2	136.9	631.8	142.0
11 7/16	291	23544	5291	54.7	36.8	13.7	9.2	306.1	68.8	635.7	142.9	659.2	148.1
11 5/8	296	24525	5512	56.7	38.1	14.2	9.5	318.8	71.7	662.2	148.8	686.7	154.3

Figure 3.85 Specification sheet Bridon Polyester mooring rope

MOORING ROPE

As stated earlier, the mooring rope material selected is Polyester. The material is not natural buoyant, increasing the required buoyancy. In the boom concept, a surface floater (boom element) is connected to the subsurface buoy. The subsurface buoy is located at about 30 meters below the waterline.

From calculations the required MBL can be found. Figure 3.85 shows specifications at various diameters.

The factors influencing the MBL are stated in section 3.7.4. After outlining the environmental conditions that must be taken into account, analysis steps are summed. In current stage no extensive calculations are completed. This should be further investigated
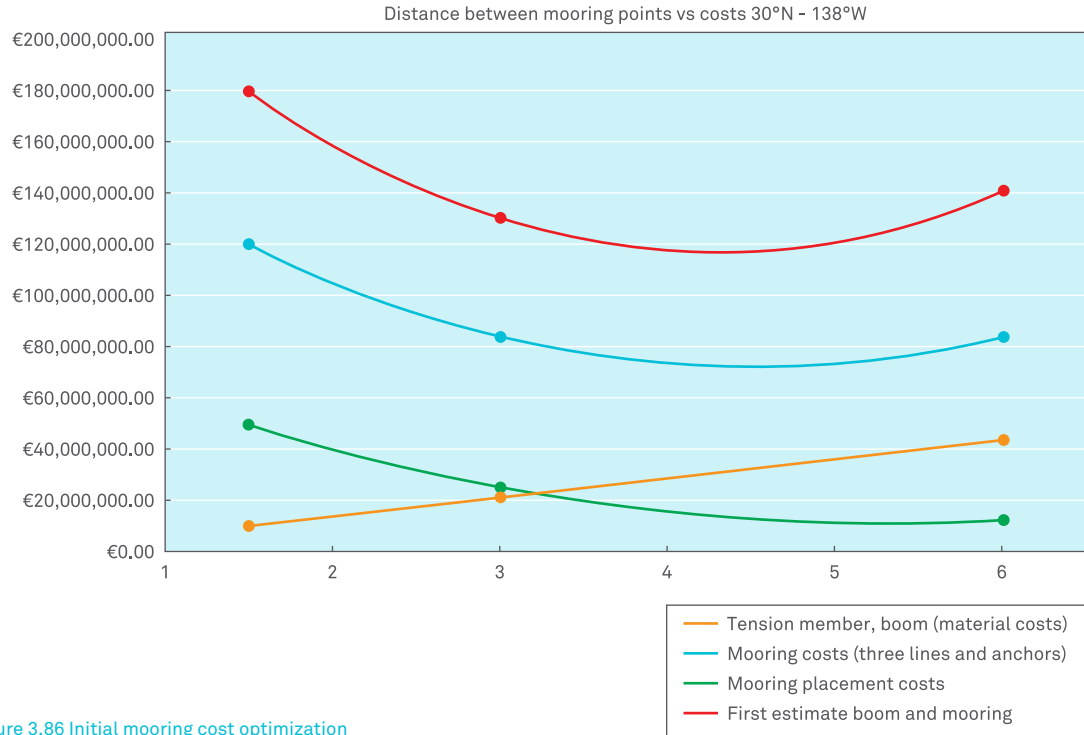
Figure 3.86 Initial mooring cost optimization

Distance between mooring points vs costs 30°N - 138°W

Tension member, boom (material costs)
Mooring costs (three lines and anchors)
Mooring placement costs
First estimate boom and mooring

3.7.3. COST OPTIMIZATION

While designing the boom and mooring system, one has to deal with many decisions that all influence both price and the design.

To solve this, an iteration has been made on the distance between mooring points. In Figure 3.86 the costs of major components are plotted, calculated for different distances between moorings.

One can see that the distance has an almost linear effect on the tension member costs, because the tension cables between moorings have to become thicker to support the boom, when the distance is increased.

On the other hand, with a larger distance between moorings, the placement becomes cheaper as less cables have to be connected to the ocean floor.

In addition the cables themselves are thicker, but in lesser amount still less expensive than more, thinner cables. In total the costs have an optimum for a distance of about 4 km between moorings (bottom of top line in the graph), en hence this distance has been used to dimension the tension cable (see chapter 3.6), and the mooring equipment.

3.7.4. MOORING CONFIGURATION DESIGN CONSIDERATIONS

When evaluating mooring system strength, the maximum design condition and maximum operating condition are used.

Maximum design condition is the most severe weather condition. For permanent mooring, structures are designed to survive at 100 year return period storm conditions. This is the condition for a storm occurring once every 100 years at that location. This statistical sea state is extrapolated from long term in situ measurements.
As the term announces, the maximum operating condition is the limit for operation. In case of the array, this means that for more severe weather conditions plastic collection cannot continue.

WIND

For the final design of permanent moorings, fluctuating wind should be modeled. This is usually based on the 1 hour average velocity, plus a time-varying component calculated from a suitable empirical wind gust spectrum.

WAVES

In situ measurements allow for accurate determination of the wave height versus wave period relationships. The period can significantly affect the wave drift forces and array motions. Therefore a range of wave periods should be examined. Fatigue analysis uses the long-term joint distribution (often presented as scatter plot)

CURRENT

Most common categories of currents are tidal currents, circulation currents (loop/eddy), storm generated currents and soliton currents.

In certain geographic areas, current force can be the governing design load. The selection of appropriate current profile requires careful consideration.

SOIL AND SEAFLOOR CONDITIONS

Bottom soil conditions should be determined for the intended site to provide data for the anchoring system design. Sea floor shape should be accounted for in the mooring analysis. Also, a bottom hazard survey should be performed. Currently no data is available in house for the selected location.

MARINE GROWTH

Type and accumulation rate of marine growth is unknown currently. Growth may affect weight, hydrodynamic diameters and drag coefficients of the mooring lines and moored array.

STRENGTH ANALYSIS

The design should be modeled to obtain responses such as line tensions, anchor loads and array offsets under the design environment. The responses are checked against allowable values to ensure adequate strength. Simulation exists of dynamics of the boom, coupled with mooring line dynamics. API's recommended practice is used for writing this section.

Combined time and frequency domain simulation is often applied. The combined method reduces complexity and the computational effort associated with full time domain simulation. Mean and low frequency responses are simulated in the time domain while the wave frequency responses are solved separately in the frequency domain. Regarding mooring line response, dynamic analysis is required. Here: mass, damping and fluid acceleration is accounted for as well. Four nonlinear effects can have important influence on mooring line behavior:

- Nonlinear stretching behavior of the line
- Changes in geometry
- Fluid loading
- Bottom effects

Additionally, low frequency motion determination is uncertain due to damping. Low frequency damping consists of:

- Viscous damping of the array (wind, wave and current drag)
- Wave drift damping
- Mooring system damping.

Here, the wave drift damping and mooring system damping are sometimes neglected because of a lack of understanding in these damping components. Under conditions these can be higher than the viscous damping, leading to significant over-estimation of low frequency motions.

Analysis conditions can include damaged mooring systems. Most important outcomes are mean and maximum offset, and line tension.

Analysis in short:

1 Determine environmental criteria
2 Determine mooring pattern, characteristics of wire and initial tension
3 Determine the mean environmental loads acting on the boom
4 Using static mooring analysis, determine the mean offset
5 Determine low frequency motions
6 Determine significant and maximum wave frequency motions
7 Determine maximum offset, tension and anchor loads
8 Compare results with the design criteria

FATIGUE ANALYSIS

Mooring system fatigue analysis compares the long-term cyclic loading in a component with the resistance to fatigue damage of that component. A T-N approach is normally used. The T-N curve used shows a number of cycles to failure for a component as function of the constant normalized tension range. The Miner's Rule is used to calculate the annual cumulative fatigue damage ratio D.

Analysis in short:

1 Represent the long term environmental events by a number of discrete environmental states. In general 8 to 12 reference directions provide a good representation of the directional distribution of a long term environment. The required number of sea states is normally in the range of 10 to 50.
2 For each state, a strength analysis should be performed.
3 Compute the annual fatigue damage for one sea state in one direction due to both the low frequency and wave frequency tension.
4 Repeat for all states and compute the total annual fatigue damage D and fatigue life L using the probability of occurrence for each sea state.
Note that L = 1/D.

3.7.5. OPERATIONS

Please refer to Chapter 5 for more information on operational aspects including installation. Inspection and maintenance is not considered, since the mooring system is placed to remain operational during the 10 years the boom is put into place.

3.7.6. COSTS

The total length has been derived based on the depth profile of a straight line across the pre-determined location as seen in chapter 2.4, resulting in a mean depth of 3,915 m (minimum: 2,000 m, maximum: 4,900 m). The used mooring angle is 70° relative to the seabed.

Part name	Cost per piece	# of pieces	Total cost	Source
14 m² Stevmanta VLA	€108,250	90	€9,742,500	Vryhof Anchors B.V.
150m Common link bottom chain, grade 3, dia. 84 mm, MBL 5886 kN	€54,338	90	€4,890420	Vryhof Anchors B.V.
Polyester rope, 120 mm diameter, MBL 600 MT, spooled onto steel transportation reel	€107 / m	344,794 m*	€36,892,958	Vryhof Anchors B.V.
Underwater buoy	€120,622	29	€3,498,038	Lange Machinery Group Ltd.

Table 3.22 Cost calculation for the mooring system

3.7.7. CONCLUSIONS

Keeping the array in position at all times will place substantial demands on a passive mooring system. At the given water depths, a fiber rope mooring system is the only option to use. To ensure integrity of the system, chain and wire rope is used at the bottom and top ends. A Stevmanta Vertical Load Anchor (surface area 14 m²) is sufficient to withstand the design loads including the safety factor.

"Although it is a new type of floating concept, the size and weight of the object as well as the potential risks (environmental as well as commercial) are less severe than the majority of offshore structures in oil and gas. The tools and methods that are available to offshore engineering world can readily be applied for the realization of this project. It is Vryhof's professional opinion that with the current knowledge and technology, the mooring of the objects at the given water depths is feasible. The mooring configuration and deployment procedures are similar to proven solutions at 2500 m water depth. The concept is executable regarding anchor and mooring line installation and load transfer from the tension member to the seafloor."

Senol Ozmutlu, PhD
Projects Director, Vryhof Anchors

CHAPTER 4

PLATFORM, EXTRACTION AND TRANSPORT

Once plastic has been concentrated using the moored floating barriers, the plastic will need to be physically extracted from the seawater, pre-processed, transshipped, and transported to shore. This chapter explores the possibilities for using existing solutions, including the platform, processing equipment, and transport vessel.
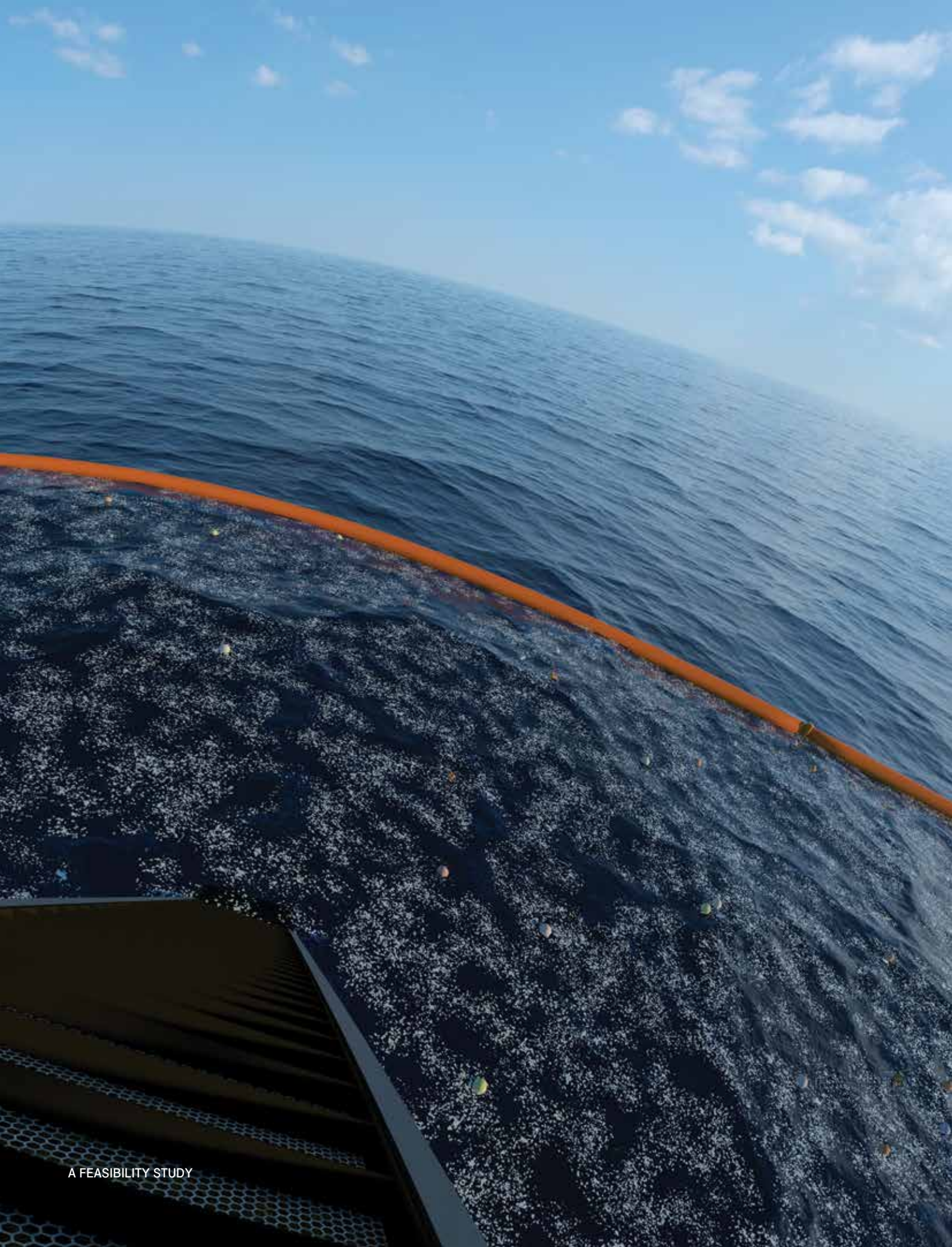
DEBRIS COLLECTION RATE

SJOERD DRENKELFORD • BOYAN SLAT

To determine the required dimensions for machines, transport capacities and power requirements, a baseline for the material flow needs to be established. This baseline is calculated based on external research and multiple efficiency factors.

The total amount of plastic in the North Pacific garbage patch is estimated to be 140,546 metric tons (see Chapter 2.2). This amount will be the basis of the material flow calculations.

4.1.1 CALCULATIONS

Multiple efficiency factors are used in the material calculation:

(F)
Field efficiency: the Array's length will be shorter than the radius of the gyre, so some debris will flow past the barriers. A field efficiency of 0.5 was found by using computational modeling (see Chapter 2.6).

(U)
Underflow efficiency: some debris will have too little buoyancy and will follow the current of the ocean underneath the booms. The value of this efficiency was found to be 79 percent. This was determined by performing a 2-dimensional computational fluid dynamics analysis (see Chapter 3.3).

(T)
Time efficiency: the platform is presumed to be able to be operational 95 percent of the time. The remaining 5 percent of the time the weather conditions will be too rough, and hence the equipment will not operate.

(C)
Collection efficiency: there will always be an amount of debris that finds its way around the extraction equipment. Since this cannot be determined before tests are done, this parameter is set to 100 percent.

(COM)
Composition efficiency: in addition to floating plastic there will be some organic material collected, such as pieces of wood and small organisms. The Ocean Cleanup is not aware of any studies undertaken to determine the ratio of plastic and non-plastic marine debris for the location focused on. However it is commonly estimated that 50 to 80 percent of marine debris is made up of plastic (Barnes, 2009), reflecting results of beach surveys. For example, on West European coasts, 63-81 percent of garbage consists of plastic, with an average of 75 percent across all surveyed beaches (OSPAR, 2007). This 75 percent value will be used for the material flow calculations.

With these efficiencies and the total amount of plastic debris in the North Pacific gyre, the total amount of theoretically collectable plastic can be determined by the following formula:

This results in 70,320 tons of collectable material in the North Pacific gyre. It is assumed that this amount will be collected in 10 years. This running time comes from the computational modeling performed by The Ocean Cleanup. More information about this computational modeling can be found in Chapter 2.7. This results in the following material flows:

- 7032 tons per year
- 586 tons per month
- 1.20 tons per hour

Due to ecological issues the extraction equipment will not operate at night. The hourly material flow presented above is based on an assumed eight-hour night, leaving 16 working hours per day for the collection.
Measurements on small fragments of the plastic samples collected in Hawaii have shown the plastic to have a bulk density of 300 kg/m³. Volume-wise, the flow of material will be:

- 23,440 m³ per year
- 1,953 m³ per month
- 4.01 m³ per hour

A material flow of 1.20 tons or 4.01 m³ per hour can be expected for 16 operating hours per day and a running time of 10 years. Note that the flow of material is taken as a constant function, although it will probably vary over time.

PLASTIC EXTRACTION FROM SEAWATER

SJOERD DRENKELFORD • BOYAN SLAT

The booms accumulate plastic in front of the platform where it can be extracted. In this chapter the method of extraction and processing is selected based on functional requirements and prerequisites. After that, concepts are assessed to determine the optimum solutions. These optimal concepts are then finalized and conclusions are drawn.

Plastic debris
in ocean   →   The Ocean
                                                  Cleanup   →   Plastic debris
                                                                                      at destination

Figure 4. 1 First level scheme of The Ocean Cleanup's process

Plastic debris
in ocean   → | Collection | Treatment | Buffer | Transport | →   Plastic debris
                                                                              at destination

Figure 4. 2 Functions of the process

4.2.1 SYSTEM REQUIREMENTS

To be able to generate and assess different solutions for collection and processing, system requirements are needed. These are based on the functional requirements and prerequisites.

4.2.1.1 FUNCTIONAL REQUIREMENTS

The goal of The Ocean Cleanup is to remove floating plastic contaminants from the world's oceans. The operation can be described as a process to move from a current state to a desired state. The current state is that plastic debris is floating within the gyres. At the end of the process, the plastic should be at its destination, which is probably a processing plant. The process is schematically shown in Figure 4.1. Although the cycle is not completed until the plastic is processed, this last step is not considered in this section, since it will probably be performed at established industries. It is therefore not a step in the design process.

When zooming in on this operation, four basic functions can be identified: collection, treatment, storage and transport (see Figure 4.2).

These four basic functions can be further expanded to describe the whole process. This is shown in Figure 4.3., where the scope of the research of subchapter 4.2 is shown. The gathering of the material is not discussed, since the floating booms do that step. They guide the floating material to the platform, where the collection stage begins. The last three functions are not reviewed, since they can be done by existing industries.
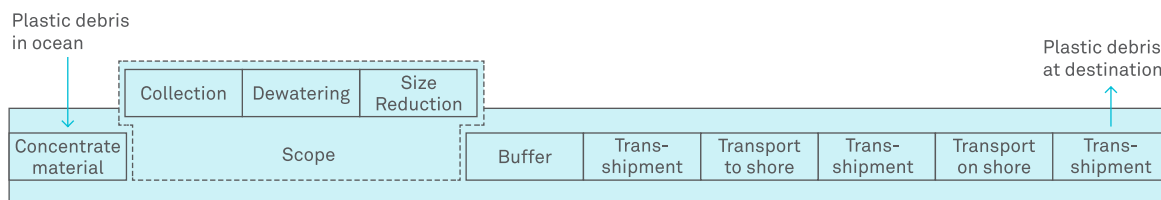
Figure 4.3 Scheme of total process, split into basic functions, including extraction scope

The three process steps within the scope each have their own function(s):

COLLECTION

The main function of the collection step is to remove the floating debris from the ocean and to transport it to a working location on the platform.

DEWATERING

To decrease the water content of the collected debris.

SIZE REDUCTION

To reduce the maximum particle size of the collected material. This is required for more efficient storage, transshipment and transportation.

4.2.1.2 PREREQUISITES

Apart from the direct functions that are implied by the process of The Ocean Cleanup, prerequisites have to be stated. Some of these requirements, like safety, cannot be compromised. Others can be used as guidelines to assess the generated solutions.

SAFETY

The solution provided by The Ocean Cleanup has to be safe for humans.

DURABILITY

The presented solution will consist of a platform in the middle of the Pacific Ocean and all of the systems must be durable enough to withstand the environmental conditions of wind and waves that are specified in Chapter 2.

MAINTENANCE-FRIENDLY

Due to the environmental conditions as described in Chapter 2, maintenance can be a difficult task. Ease of maintenance needs to be taken into account when generating and assessing solutions.

BLOCKAGE

Blockage can cause the transshipment to come to a halt and this would delay the transport. More importantly, blockage can damage the equipment. Therefore, it must be prevented. Blockage can be caused by, for example, plastic parts that are too large for the equipment or by mechanical failure.

SPILLAGE

Spillage of the plastic has to be minimized to optimize the efficiency of the project.

POWER

From a practical and sustainable viewpoint, the platforms need to be as energy efficient as possible.

COSTS

The solution has to be cost efficient so as to make the Ocean Cleanup economically acceptable.

BULK DENSITY

Measurements taken from the samples collected from Hawaii have produced a mean bulk density of 300 kg/m³. This was determined by Norbert Fraunholcz, of Recycling Avenue, who examined the samples. More information on this subject can be found in Chapter 9.

COLLECTION DEPTH

A multi-level trawl was created and used by The Ocean Cleanup in the North Atlantic gyre. Analysis of the samples resulted in an optimal collection depth of three meters (Chapter 2.5).

MATERIAL FLOW SPECIFICATIONS

The calculations in Chapter 4.1 have shown that a material flow of 1.20 tons per hour can be expected.

4.2.1.3 RESULTING SYSTEM REQUIREMENTS

The system requirements for the logistical systems are a combination of the functional requirements and the prerequisites.

FUNCTIONAL REQUIREMENTS

- Remove floating plastic debris from the ocean:
  1.20 tons per hour
- Up to a depth of 3 meters
- Of a particle size range of 1 mm to 3 m
- Treat the collected debris:
  Reduce the water content as much as possible
  Decrease the particle size to one that the equipment can handle

PREREQUISITES

- Durable and maintenance-friendly
- Safe for humans
- Low risk of blockage
- Low spillage
- Low energy consumption
- Cost efficient

4.2.2 CONCEPTS

To be able to create concepts for the entire operation, the basic functions that are presented in the system requirements are used. Multiple solutions are presented for each of these functions, along with their advantages and disadvantages.

4.2.2.1 COLLECTION

The plastic debris is caught by the booms, and accumulates where they converge, in front of the platform. In this zone, the debris is collected as it floats into a semi-protected area through large holes. Due to the size range of the debris, the collection needs to be done in multiple steps, to ensure that all the debris is picked up and to prevent clogging. This choice was made in consultation with Norbert Fraunholz (Fraunholcz, 2014) of Recycling Avenue.

The first step will catch debris larger than 1 meter. The second step will collect medium-sized debris, from 10 mm to 1 meter and the last step will extract particles smaller than 10 mm. These values have been selected as starting boundaries and might need later adjustment to meet equipment sizes. The proposed solutions will be assessed for each size range.

SCOOPS

By using scoops that are made out from a meshed material, debris can be collected from the water. The principle is very simple and can be found in lots of applications on many scales. The simplest being a children's fishing net. Depending on the size of the scoop related to the material flow, one scoop or a cascade of scoops might be used. The cascade would work like a bucket chain excavator.

ADVANTAGES

Since the scoop also collects the entire body of water that surrounds the plastic particles, even the smallest particles are collected without washing away.
Depending on the size of the scoops, all particles sizes can be collected from the ocean.

DISADVANTAGES

These buckets typically displace a lot of water during the scooping action, which leads to higher energy consumption.

POCKET BELT CONVEYOR

A pocket belt conveyor (See Figure 4.4) has corrugated sidewalls running along the length of the belt and straight walls running across the belt. Due to this geometry it forms pockets, which can capture debris along with some of the water. This solution ensures that even the smallest particles are collected, since the entire batch of water that they float in is picked up. It does however require a preliminary step that collects the larger particles, since the belt pockets would otherwise have to be very large to be able to collect the largest particles. Depending on the acceptable water amount, a dewatering step is required.

ADVANTAGES

- Similar to the scoops, the entire body of water that surrounds the plastic particles is collected, which ensures that even the smallest particles are caught.

- Depending on the depth of the pockets, the angle of the conveyor can become steeper, which makes it shorter and thus will require a smaller support structure.

DISADVANTAGES

- If plastic parts are larger than the pockets, they might fall off the conveyor.

- A body of water is always collected, which will lead to higher energy consumption.

Figure 4.4 Pocket belt conveyor. Courtesy of Loibl Allen-Sherman-Hoff GmbH

MESH CONVEYOR

A mesh conveyor has a belt made out of meshed material. The mesh acts like a sieve to filter out particles. Depending on the desired minimum particle size and the available mesh, an additional dewatering stage might not be necessary.

ADVANTAGES

- Since the excess water goes through the conveyor, no energy is wasted to lift extra water

DISADVANTAGES

- Depending on the size of the holes in the belt, the small particles cannot be collected.

- The holes in the belt can get clogged, due to particles of a critical size or flexible particles. Belt cleaning is therefore required to ensure the dewatering properties of this belt type.

CLEATED BELT CONVEYOR

A cleated belt conveyor (Figure 4.5) has rubber strips on its carrying side, called cleats. These cleats can have a lot of shapes, like straight lines, arrows and V-shapes. The cleats reduce or prevent the material from rolling down the conveyor. Depending on their height, they can collect the smaller particles, along with some water.

This solution can be used for all of the particle sizes, depending on the height and spread of the cleats. The shape of the cleats determines how much water is collected along with the plastic debris. Smaller particles can be washed off when water is removed, and therefore caution is required.

ADVANTAGES

- Since the belt has no holes, it cannot get clogged.

- Depending on the size of the cleats and the distance between them, this belt type can handle large parts.

DISADVANTAGES

- Small particles can wash off the sides of the belt.

Figure 4. 5 Example of a cleated belt conveyor. Courtesy of The Knotts Company

SUCTION PIPE

In the dredging industry suction pipes are widely used to collect slurries of clay, sand and water. A similar system could be used in this case. The inlet of the pipe should be located near or on the water surface, to enable it to suck up all of the floating debris. This technique also collects water, so the slurry of water and debris needs to be dewatered on the platform.

ADVANTAGES

- This method has proven its durability in the dredging industry.
- Even the smallest particles are collected, since the entire body of surrounding water is sucked up.

DISADVANTAGES

- Depending on the size and design of the pump, the maximum particles size is limited. If parts are too large, the pump could get clogged or jammed.

- To be able to collect the smallest particles, a large body is displaced, which leads to a higher energy consumption.

Collected debris must be dewatered to reduce transportation weight and therefore fuel consumption and cost, as well as to minimize storage space.

FILTERS

Filters can be used to separate water from solid particles. Typically, the filter has the shape of a screen or a bag. When the filter is full, it needs to be replaced with a new one.

ADVANTAGES

- Filters are available with very small mesh sizes, so the smallest particles can easily be extracted from the water.

DISADVANTAGES

- A filter is only suitable for a certain size range, depending on the mesh size. Larger parts could clog the filters or even tear it apart.
- Filters are not suitable for large quantities of material and might need to be replaced often, depending on the material flow.

HYDROCYCLONE

A hydrocyclone (Figure 4.6) is a device in which a mixture is separated by using the differences in density of the entering materials. The incoming stream is forced into a conical shaped chamber, in which a cyclone is generated. This cyclone promotes the natural segregation of the various materials. The heavy fragments flow out through the lower end, while the lighter ones will pass through a pipe in the center of the topside.

ADVANTAGES

- The hydrocyclone has no moving parts, which makes it very durable.

DISADVANTAGES

- Since the high pressure of the incoming flow generates the vortex that promotes the segregation, a pump is required to add this pressure.
- Since the inner core of the vortex is forced out of the widest section of the cone, there will always be some water with this exit flow. A completely dry exit flow is therefore not possible.

Figure 4. 6 Example of a hydrocyclone.

VORAXIAL SEPARATOR

A voraxial separator is basically an improved version of a hydrocyclone. Similar to a hydrocyclone it uses centrifugal forces to remove lighter and heavier masses from a main stream. The difference between the two machines is that the voraxial separator uses an impeller to accelerate the stream of material into a vortex, instead of a conical chamber, causing the fractions to segregate. The vortex makes the heaviest matter move to the outside of a large tube. The lighter material – in this case, plastic – is at the same time forced into the center of this tube, where it flows into a smaller tube and is removed. Contrary to a hydrocyclone, a voraxial separator does not require a large pressure drop, since pressure is not the source of the vortex.

ADVANTAGES

• Since an impeller generates the separation vortex, a high incoming pressure is not required.

DISADVANTAGES

• Since the working principle is similar to that of a hydrocyclone, it has the same disadvantage that it cannot produce a completely dry product flow.

SCREW CONVEYOR

Screw conveyors are used in sink-float tanks to skim the floating particles from the surface. The particles are caught between the screw blades and are pushed up through a tube. The principle was invented by Archimedes to lift water. In this application, the central axle is placed under a small inclination angle, to ensure little water enclosure, as can be seen in Figure 4.7.

ADVANTAGES

• The screw conveyor moves the parts with a low speed, which enables the collection of small parts with only a small body of water.

DISADVANTAGES

• A steady water surface is required to operate efficiently, or else the waves will wash out the parts.

Figure 4. 7 Example of a dewatering screw conveyor. Courtesy of Nordic Water

ROTARY DRUM SCREEN

A rotary drum screen is a rotating filter. The incoming stream passes through one side of the drum; the solid particles stick to the screen and are deposited on the other side of the tank. A scraper cleans the drum when it passes the waste collection screw conveyor.

ADVANTAGES

- Depending on the size of the mesh, the smallest particles can be removed from the water stream.

DISADVANTAGES

- Since material can be washed over the drum, large rolling angles of the platform pose a problem.

4.2.2.2 SIZE REDUCTION

Reducing the maximum particle size of the material allows for more efficient storage and transportation, and reduces the chance that the debris clogs machines.

SHREDDER

In a shredder, material is torn apart by large rollers which have cutters to tear up the material and pull it into the machine until it is small enough to be discharged. Other types of size reduction equipment are available, like granulators and grinders, and all work in the same way as the shredder. The difference between these machines is the input size, output size and material flow. Which specific machine should be used will be decided in the final concept.

ADVANTAGES

- Storing the material is more efficient when it is shredded, since less empty space is trapped between the parts.
- If the material is shredded to a smaller maximum size, this makes it easier to handle during transshipment.

DISADVANTAGES

- Shredding material requires a large energy input, which is not desired.

4.2.3 DISCARDED DESIGN CHOICES

Several design choices can be discarded before the final assessment. These are design choices whose operational parameters are clearly unsuitable to the task at hand, or that have been seriously discouraged by field experts.

DEWATERING SOLUTION: SCREW CONVEYOR

Screw conveyors can only dewater properly if the water surface is smooth. Since this condition is infrequent in open water, this solution is discarded.

COLLECTION: LARGE PARTS

Due to the low number of large parts of floating plastic, it is assumed that an active mechanical collection system would be a waste of material and energy. Instead, a passive screen in front of the collection equipment will collect these parts. As required, large debris can then be removed by a small vessel and fed to the processing equipment manually.

4.2.4 ASSESSMENT

In this section the best solutions are determined for each of the basic functions. First, possible solutions are shown in a morphological scheme (Table 4.1), then, the most promising concepts are assessed for the applicable criteria.

Four promising concepts are selected from the morphologic scheme. Each of these concepts is split into two variants, denoted by the letters A and B. The A-variants are based on a SWATH vessel platform, the B-variants on a Spar buoy platform. These promising concepts and their basic functions are presented in Table 4.2.

Basic function	Possible solutions				
Collection small parts	Scoops	Pocket Belt conveyor	Mesh conveyor	Cleated belt conveyor	Suction pipe
Collection medium parts	Scoops	Pocket Belt conveyor	Mesh conveyor	Cleated belt conveyor	Suction pipe
Size reduction	Shredder				
Dewatering	Filters	Hydro-cyclone	Voraxial separator	Rotary drum screen	

Table 4.1 Morphological scheme

	Solution 1A	Solution 1B	Solution 2A	Solution 2B
Collection small parts	Scoops	Scoops	Pocket Belt conveyor	Pocket Belt conveyor
Collection medium parts	Scoops	Scoops	Pocket Belt conveyor	Pocket Belt conveyor
Size reduction	Shredder	Shredder	Shredder	Shredder
Dewatering	Filters	Filters	Hydro cyclone	Hydro cyclone
	Solution 3A	Solution 3B	Solution 4A	Solution 4B
Collection small parts	Suction pipe	Suction pipe	Suction pipe	Suction pipe
Collection medium parts	Mesh conveyor	Mesh conveyor	Cleated belt conveyor	Cleated belt conveyor
Size reduction	Shredder	Shredder	Shredder	Shredder
Dewatering	Voraxial separator	Voraxial separator	Rotary drum screen	Rotary drum screen

Table 4.2 Selected promising solutions

Criterion	Weighing factor	1A	1B	2A	2B	3A	3B	4A	4B
Safety	3	3	3	3	3	4	4	4	4
Durability	3	2	1	2	1	5	5	5	5
Maintenance	2	4	3	3	2	3	3	3	3
Blockage	3	4	4	4	4	3	3	3	3
Spillage	2	3	3	3	3	5	5	5	5
Power	1	3	2	3	2	4	3	4	3
Costs	1	2	1	2	1	5	5	5	5
Total	-	46	39	44	37	61	60	61	60

Table 4.3 Criteria for collection of small particles

The selected concepts are assessed for each of the remaining basic functions. The criteria on which they are assessed come forth from the prerequisites. Not every criterion is used for every assessment, since they do not always apply. Weighing factors are applied to represent the relative importance of the criteria:

• Less important
• Normally important
• Very important

The concepts will receive grades for each criterion, varying between 1 and 5:

• Bad
• Poor
• Average
• Good
• Excellent

See Table 4.3 for the assessment. There is no assessment for the size reduction function, since there is only one solution.

For this assessment the most important factors are safety, durability and blockage, since these factors cannot be compromised. Spillage and maintenance have been graded as normally important, since they are unwanted, but can be dealt with. Power and costs have been rated as less important, but may act as final decision criteria.

For the assessment of the collection of medium-sized particles (Table 4.4), the same weighing factors have been applied as for the assessment collection of small particles.

For the assessment of the dewatering (Table 4.5), the same weighing factors have been applied as for the assessment collection of small particles.

The resulting assessment is presented in Table 4.6.

From this assessment it is clear that concept 3A is the most promising concept. This is based on a SWATH vessel platform. The most promising concept regarding a Spar buoy platform is concept 3B. In the next section, concept 3 is finalized for both platform types and practical realizations presented.

Criterion	Weighing factor	1A	1B	2A	2B	3A	3B	4A	4B
Safety	3	3	3	3	3	4	4	3	4
Durability	3	2	1	2	1	5	4	3	2
Maintenance	2	4	3	3	2	3	2	4	3
Blockage	3	4	4	4	4	3	3	4	4
Spillage	2	3	3	3	3	5	5	3	5
Power	1	3	2	3	2	4	3	4	3
Costs	1	2	1	2	1	5	4	3	4
Total	-	46	39	44	37	61	54	51	53

Table 4.4 Collection of medium-sized particles

Criterion	Weighing factor	1A	1B	2A	2B	3A	3B	4A	4B
Safety	3	3	3	3	3	4	4	5	5
Durability	3	3	3	4	4	4	4	4	4
Maintenance	2	1	1	4	4	3	3	3	3
Blockage	3	1	1	5	5	5	5	3	3
Spillage	2	3	3	3	3	3	3	2	2
Power	1	3	3	3	3	4	4	5	5
Costs	1	4	4	4	4	3	3	3	3
Total	-	36	36	57	57	58	58	54	54

Table 4.5 Criteria for dewatering

Basic function	1A	1B	2A	2B	3A	3B	4A	4B
Collection small particles	46	39	44	37	61	60	61	60
Collection medium particles	46	39	44	37	61	54	51	53
Dewatering	36	36	57	57	58	58	54	54
Total	128	114	145	131	180	172	166	167

Table 4.6 Resulting assessment

4.2.5 FINAL CONCEPT

In collaboration with Dutch national and international companies, suitable machines are selected for each of the basic functions, whilst considering costs, dimensions, weights and power consumption.

COLLECTION OF SMALL PARTICLES: SLURRY PUMP

The slurry pump to collect small parts of plastic has been selected in consultancy with the Dutch company Deltapompen B.V. (Deltapompen) it was chosen together with the slurry pump that will perform the transshipment function, explained in Chapter 4.4. The material flow to be pumped by this second slurry pump was the basis of the pump capacity. Deltapompen have specified that plastic material flow of 1.20 tons or 4.01 m³ per hour must be accompanied by a water flow of 300 m³/h. The first slurry pump needs to supply this body of water, so the capacity of this pump was also set to 300 m³/h. Deltapompen has selected a centrifugal slurry pump that can handle particles with a maximum size of 50 mm and that uses 22 kW of electrical power. The costs of this pump, the motor and the mounting are €10,500. Since the pump will be operating in a salt-water environment, it will be made from a material called super duplex, which is a type of steel with high corrosion resistance.

For a pump to be able to transport slurry, it needs to be below the water surface, since it requires an incoming pressure. Self-priming pumps exist, but due to the multiple suction chambers, solid particles would get stuck in the pump. To be below the water requires the pump to be placed in one of the submerged parts of the platform, or for the entire pump to be submerged.

It is assumed that this slurry pump can be applied in both platform types.

COLLECTION OF MEDIUM-SIZED PARTICLES: MESH CONVEYOR

Due to the vertical distribution of the plastic particles, the conveyor needs to reach 3 meters below the water surface. To discharge the debris into the hopper of the shredder, the conveyor needs to reach up to 2 meters above the deck. For a SWATH vessel platform this comes down to a total height of 9 meters and for the Spar Buoy platform this is 18 meters. An angle of 45 degrees was chosen, so the lengths of the two conveyors are 13 meters and 26 meters. The belt speed was chosen to be 1 meter per second for both platforms.

In collaboration with the Dutch company Ammeraal Beltech, a plastic mesh conveyor was selected (Beltech). This belt type is frequently used in apparatus for washing heavy fruit and potatoes and is therefore impact resistant, a favorable property in an environment with continuous waves. A belt width of 1,371 mm was selected to be able to handle debris up to 1 meter in size. Ammeraal Beltech has specified the costs of this conveyor to be €6,064 for a SWATH vessel platform and €12,127 for a Spar buoy platform.

The selected conveyor includes cleats that will prevent the material from sliding down the conveyor. Ammeraal Beltech has also provided an engineering manual to be able to calculate tensile strengths and required motor power.

Component	Description	Costs (€)
Belt	Uni-SNB-M²-50%	6,064
Electric motor	ML 71A4, 1500 rpm, 230V, 0,25 kW	115
Worm wheel redactor	CM 30, Gear Ratio = 10	163
Frequency controller	Fuji Frenic Mini, 0.4 kW	236
Total		**6,578**

Table 4.7 Components and costs of the mesh conveyor for a SWATH vessel platform

Component	Description	Costs (€)
Belt	Uni-SNB-M²-50%	12,127
Electric motor	ML 71B4, 1500 rpm, 230 V, 0,37 kW	125
Worm wheel redactor	CM 30, Gear Ratio = 10	163
Frequency controller	Fuji Frenic Mini, 0.4 kW	236
Total		**12,651**

Table 4.8 Components of the mesh conveyor system for a Spar buoy platform

For a SWATH vessel platform, the calculated tensile strength was 80 N and the required motor power was 190 W. For a Spar buoy platform, these values are 160 N and 220 W respectively. Both of the required motor powers include the power required to lift the collected material. Drive chains were selected to power these conveyor belts. Their components and the costs of the two systems are shown in Table 4.7 for a SWATH vessel platform and in Table 4.8 for a Spar buoy platform. Frequency controllers have been selected along with the drive chains to ensure smooth starting and stopping, which is beneficial for the life of the belts.

It must be noted that the required power consumption is very low. As can be seen from the two tables above, the drives have therefore been overpowered. Since these calculations do not take the required power for water displacement of the cleats and the conveyor into account, tests will need to be done to determine the actual required power in Phase 2 of the project.

SIZE REDUCTION

Since the majority of the collected plastic is medium-sized particles, the assumption is that all the weight needs to be shredded. The pieces of debris too large for the mesh conveyor will be manually removed from the water and fed to the shredder.

A shredder has been found that is capable of handling this material flow from the American company Granutech-Saturn Systems Corporation: the Roto-Grind 110H (Corporation). This machine is capable of handling the required material flow and consumes 90 kW. It shreds the material to a maximum size of 20 mm. This is more than the desired 10 mm maximum size, but is not a problem since the slurry pumps, which are the bottlenecks for the particle size, can handle particles with a maximum of 50 mm. The costs for this machine are $225,000, which is approximately €165,000. The rotor length is approximately 1.25 meters, so this confirms the size boundary choice of 1 meter that was specified in the system requirements.

DEWATERING

In collaboration with the Dutch company Auxill Neder-land B.V., the Voraxial Separator 8000, which can handle flows from 225 m³/h to 1150 m³/h, was selected (Auxill). This machine costs €190,000 and consumes 37.5 kW. Two transport vessels will be required as determined in Chapter 4.4. Both of these vessels will receive a Voraxial Separator, so the total costs will be €380,000. Since these machines can handle flows much larger than the 300 m³/h that they will encounter in this project, the required power will probably be lower than 37.5 kW, although tests are required to confirm this. The Ocean Cleanup Array cannot produce a completely dry material flow and for now it is assumed that the flow will be 50 percent material and 50 percent water, and that tests are needed to confirm this. These tests will need to be performed in the second phase of the project.

4.2.6 CONCLUSIONS

The optimal solution is a slurry pump and mesh conveyor for the extraction of the plastic, and a grinder to reduce the particle size. The total costs and the maximum power consumption of this equipment for both platform types are shown in Table 4.9. The last row represents the costs per ton of collectable plastic, calculated using the total amount of collectable plastic in the North Pacific gyre; 70,320 tons (see Chapter 4.1). This result will be used in the total costs analysis in Chapter 10.

Secondary equipment and supporting constructions will be designed in the second phase of the project. This will include apparatus to connect the equipment presented above and the structures that support the mesh conveyor and the inlet of the first slurry pump. Due to the uncertainty of the costs, the costs for all of the equipment have been increased by 50 percent for both platforms.

This section will describe the design of the plastic collection platform. The focus will mainly be on the structural aspect of the platform and less on the processing equipment that will be onboard. First the functions the platform has to fulfill and the requirements that follow from these functions will be discussed, as well as possible design solutions that can fulfill the requirements. Thereafter the two most promising solutions will be elaborated further. Finally the two alternatives will be compared and one will be chosen as the concept that will be used in the final design.

Function	Costs (€)	Maximum platform power consumption (kW)	Costs (€)	Maximum platform power consumption (kW)
Collection of small particles	10,500	22	10,500	22
Collection of medium-sized particles	6,578	1	12,651	1
Shredder	165,000	90	165,000	90
Dewatering	380,000		380,000	
Secondary equipment and supporting constructions	281,039		284,076	
Total costs	843,117	113	852,227	113
Total on-platform processing costs per ton of collected plastic	11,99	-	12,12	-

Table 4.9 Total costs extraction and processing equipment for both platform types

CHOICE OF PROCESSING PLATFORM

MARIJN DEKKER • SJOERD DRENKELFORD

JABE FABER • BOYAN SLAT

This section will describe the design of the plastic collection platform. The focus will mainly be on the structural aspect of the platform and less on the processing equipment that will be onboard. First the functions the platform has to fulfill and the requirements that follow from these functions will be discussed, as well as possible design solutions that can fulfill the requirements. Thereafter the two most promising solutions will be elaborated further. Finally the two alternatives will be compared and one will be chosen as the concept that will be used in the final design.

4.3.1 ASSESSMENT OF REQUIREMENTS AND POSSIBLE SOLUTIONS

The platform has three functions that together form a part of the handling of the plastic from gyre to new use. The first function of the platform is to extract the plastic from the ocean, as discussed in Section 4.2. The next is to perform some initial processing of the plastic. The platform has to host the equipment necessary for the retrieval and processing of the plastic, which means that there has to be sufficient space onboard of the platform and the platform has to be able to carry the weight of the equipment. The platform also has to provide the right conditions for the equipment to operate. Most machinery has an operational limit with regard to the accelerations it can undergo. This puts restrictions on the motions of the platform.

Finally the platform has to store the plastic until it is retrieved for transport to shore. This buffer function either requires a large amount of space available for storage onboard the platform or the use of an additional vessel for the storage, for instance a barge.

During the operations the platform has to stay in position and connected to the booms, as it has to be at the place where the plastic is collected. Exactly how much movement is allowed depends on the characteristics of the extraction method, which is described in Section 4.2. There are two possible solutions to keep the platform in position. Either a connection to the sea bed (mooring) or a propulsion system that counters the environmental loads (Dynamic Positioning or DP) can be used. Given the long operational period of the platform the latter is not feasible, since the energy consumption would be tremendous. During the operational life time of the platform, there will be many storms and other severe weather events.

The plastic collection will be discontinued during these events but the platform should be able to survive without any damage to the platform itself or the onboard equipment, as it should be possible to restart the operations afterwards without any issues. The need for maintenance after survival conditions should be avoided as much as possible. Normal operation maintenance should also be limited, since the platform will be located in a remote location and mobilization costs for repair operations will thus be significant.

To summarize the aforementioned requirements are listed below. The platform should:

- have sufficient space available for processing equipment and plastic storage
- be able to carry the equipment and plastic
- provide workable conditions for the equipment, i.e. regarding the motions of the platform
- stay in position both during normal operations and survival events
- require as little maintenance as possible, both during normal operations and after survival events.

4.3.2 DESIGN ALTERNATIVES

In the following paragraphs a short description of the various design alternatives that meet the requirements is given.

Figure 4. 8 Examples of an FPSO vessel and a barge used for transport.

4.3.2.1 CONVENTIONAL MONOHULL

Monohull vessels are widely used in the offshore sector, for instance as floating production, storage and offloading (FPSO) vessels, or floating barges (Figure 8). These vessels are designed to be sail for a significant part of their life and are thus optimized to have a low resistance during transport. Therefore the length of the vessel is usually significantly larger than the draught or breadth, resulting in a small ratio of frontal area over displacement.

The optimization for transport comes at a cost, as monohulls are vulnerable to environmental loads on the vessel coming from the side. This can lead to large roll motions, which is not desirable for the machinery onboard the vessel. FPSO's can avoid the large roll motions on location by weathervaning (rotating) around a central turret.

Since the platform must stay connected to the booms and the plastic will be cumulated at one side of the platform, weathervaning will only be possible to a limited extent. This means that significant side loads are still possible and large motions are to be expected. Therefore a vessel-shaped monohull is not a suitable option for the platform.

4.3.2.2 SWATH VESSEL

An alternative design that gives a higher stability than a monohull vessel for the same dimensions is the Small Water Area Twin Hull (SWATH). Similar to a catamaran this hull design has two separate areas that penetrate the waterline, as is shown in Figure 4.9. The distance between the areas gives a high roll stability. The difference with a catamaran is that a SWATH vessel has a much smaller cross-sectional area at the waterline, hence the name. The required buoyancy is provided by two bulges that are fully submerged. A similar hull design used in the offshore sector is the semisubmersible (Figure 4.10), which consists of one or multiple submerged pontoons that are connected to the topside by a series of columns. The waterline cross-section only consists of the columns, which gives an area that is much smaller than the total area of the topside.

The small waterline area means a SWATH attracts only little wave loads, which further increases the stability and allows for an economic design. The mooring system of the platform also can be designed for smaller loads in this case.

The downside of the small waterline area is that a small change in weight leads to a large change in the draught of the vessel. This makes a SWATH design less suited for the storage of variable amounts of plastic. Since the storage space onboard is also limited an external barge for the plastic storage would be required.

Figure 4. 9 Example of a 25 m SWATH vessel

Figure 4. 10 Example of a semisubmersible crane platform

4.3.2.3 SPAR BUOY

A spar buoy is a slender vertical buoy with a large submerged volume that provides the buoyancy for the topside that is located on top of the buoy (S. Chakrabarti, 2005). The stability is provided by a low center of gravity, which is achieved by ballasting the lower end of the buoy. A spar buoy is characterized by its high stability (R. Gianville et al., 1991). This makes it very suitable for the use of sensitive equipment onboard. For this reason a spar buoy is used for the Hywind floating wind turbine developed by Statoil, shown in Figure 4.11. Another benefit of the use of a spar buoy as basis for the platform design is that the large hull has sufficient volume to store the collected plastic before it is transported to shore.

The large hull construction also means that a relatively large amount of material is required however, resulting in higher construction costs. The wave and especially current forces on the platform are also relatively large due to the large submerged volume, resulting in large mooring loads and thus an extensive mooring system.

Another point of concern is the transportation to location. The large draught of the spar buoy means that it is usually not possible to transport it in upright position near shore. Therefore the buoy needs to be transported horizontally and upended at location. This requires a rather complex installation using controlled buoyancy tanks and furthermore means that the topside of the platform either needs to be transported on its side and in contact with water or connected to the buoy afterwards, both options posing some problems for the design.

Figure 4. 11 Artist's rendering of the Statoil Hywind spar turbine platform

4.3.2.4 TLP

A spar buoy is a slender vertical buoy with a large sub-merged volume that provides the buoyancy for the topside that is located on top of the buoy (S. Chakrabarti, 2005). The stability is provided by a low center of gravity, which is achieved by ballasting the lower end of the buoy. A spar buoy is characterized by its high stability (R. Gian-ville et al., 1991). This makes it very suitable for the use of sensitive equipment onboard. For this reason a spar buoy is used for the Hywind floating wind turbine developed by Statoil, shown in Figure 4.11. Another benefit of the use of a spar buoy as basis for the platform design is that the large hull has sufficient volume to store the collected plastic before it is transported to shore.

The large hull construction also means that a relatively large amount of material is required however, resulting in higher construction costs. The wave and especially current forces on the platform are also relatively large due to the large submerged volume, resulting in large mooring loads and thus an extensive mooring system.

Another point of concern is the transportation to location. The large draught of the spar buoy means that it is usually not possible to transport it in upright position near shore. Therefore the buoy needs to be transported horizontally and upended at location. This requires a rather complex installation using controlled buoyancy tanks and further-more means that the topside of the platform either needs to be transported on its side and in contact with water or connected to the buoy afterwards, both options posing some problems for the design.

Figure 4. 12 Artist's rendering of a Tension Leg Platform

4.3.2.5 PRELIMINARY COMPARISON

The four concepts discussed in the previous section are compared below. Both the SWATH and the Spar Buoy look promising, whereas the monohull and the TLP are less suited as a basis for the platform. Therefore only the SWATH and Spar Buoy concepts will be elaborated further in the following sections. Subsequently, the final choice for a preferred concept will be presented.

Platform types	Monohull	SWATH	Spar Buoy	TLP
Advantages		High stability Small wave loads	High stability Storage room for plastic	Very stiff for vertical and roll motions
Disadvantages	Small roll stability	Sensitive for change of weight No storage room for plastic	Large environmental loads Complex transportation	High tensile load in anchors required to prevent large horizontal motions. Expensive anchors due to tensile loads. Risk of breaking anchors

Table 4.10 Preliminary comparison between platform types

	Mass	Buoyancy
Submerged volume 4236 m³		4342 t
Topside incl. equipment	1000 t	
Hull incl. equipment	2000 t	
Plastic 3000 m³	900 t	
Ballast	442 t	
Total	**4342 t**	**4342 t**

Table 4.11 Preliminary comparison between platform types

4.3.3 SPAR BUOY CONCEPT

The second concept is a spar buoy design. This design consists of storage for the collected plastic in the hull of the spar with a deck on top of it. As the hull of the spar buoy is needed to store the plastic, the outer shell of the hull will be solid and no lattice structures are used. An impression of the spar is given in Figure 4.13.

The hull is a cylindrical shape with a diameter of 11.4 m and a height of 57.5 m, of which 41.5 m will be submerged. The hull will mainly be used for the storage of plastic. For this, a volume of 3000 m³ - situated as a cylinder with 8.4 m diameter and 54.5 m - is reserved. Although for transport a volume of 6000 m³ has been reserved, this includes the added water necessary to pump it from platform to ship. To reduce the size of the buffer, water will be added to the mixture while pumping, by means of a seacock. As discussed in Section 4.1 the plastic collection rate will total 65 m³/day, which means the plastic has to be collected every 45 days.

The inlet pump for small plastic and the voraxial separator will be located just below the water surface to avoid pumping the plastic flow to a higher point. The pump and the separator will be accessible by a staircase located at the side of the storage area. The bottom of the hull will be filled with steel ballast to provide the required stability for the spar. The exact mass of the ballast has to be determined from buoyancy and stability calculations, but based on designs of other spar buoys a mass of approximately 500 tons filling the lowest meter of the hull over the full diameter has been estimated. A preliminary buoyancy calculation is given in Table 4.11.

The deck area will be a square area of 11.5 by 11.5 meters. The deck will be placed directly on top of the hull, 16 meters above the water surface, to give clearance for waves in extreme conditions. The deck will be used for the processing equipment (as determined in Chapter 4.2): the shredder for larger plastic particles; the connection to the mesh conveyer and (likely) a structure used to haul it in case of severe weather; a maintenance area; the main switch board; a diesel generator; an entrance to the staircase into the hull; a 50 ton crane to lift spare parts and other equipment; and an entrance to the boat landing. A sketch of the preliminary deck lay-out is given in Figure 4.13.
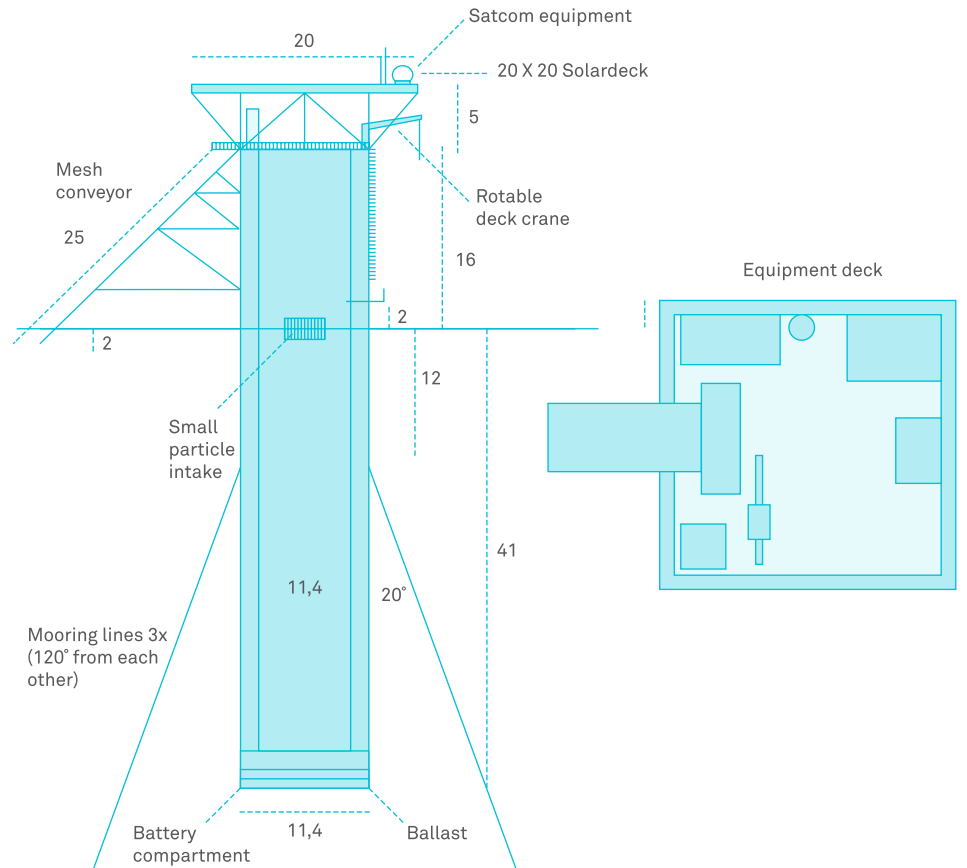
Figure 4.13 Preliminary design of a classic spar as a processing platform (left), and a possible deck arrangement (right). Dimensions are in meter.

The maintenance area will have an area of 4 by 3 m. It will only be suited for visits during maintenance operations and not for overnight stays. In the case of maintenance that requires more than one day the crew can stay on-board the support vessel overnight. The platform has explicitly been designed to be unmanned, since a manned platform requires a separated water supply and waste storage, living quarters and emergency evacuation, which would induce significant costs. Instead, periodical maintenance would be performed by crew of a service vessel. A Platform Supply Vessel (PSV) is likely suitable for such purpose. During these visits, the crew would also be able to inspect the booms and moorings, as well as perform small-scale repairs on the floating barriers when necessary.

On top of the main deck there will be a roof filled with PV panels for the platform's power supply. As discussed in Section 4.5 the platform's average power demand is 60 kW, which requires 400 m² of solar cells. Since the deck area is only 132 m², the roof with PV panels will extend from the main deck at an angle of approximately 45 degrees. It will be located 5 m above the main deck. The electricity generated by the solar cells will be stored in a battery located in the bottom of the hull. Because of the significant weight of the battery pack, it will be placed at the bottom of the platform, contributing to the ballast weight.

In terms of cost, based on a processed steel price of € 4 to € 6 per kg, and a total weight of the steel structure of 2800 t (which excludes plastic and equipment), we estimate the cost of this platform (excluding equipment and mooring) to be between € 11,200,000 and € 16,800,000.

4.3.4 SWATH CONCEPT

The SWATH vessel that is used for the platform is based on a design by Abeking & Rasmussen with a length of 60.5 m, width of 24 m and draught of 5 m. This design consists of two water-piercing bodies that provide the required buoyancy and stability for the platform. On top of this, a large open deck space is placed, with a three story structure on the front half of the vessel. In this structure, the area needed to accommodate maintenance can be situated, as well as a control room containing the main switch board for the onboard machinery and communication devices for contact with nearby ships and the mainland.

USG engineering has developed two different deck layouts to place the processing equipment on the hull design. As described in Section 4.2.3 the processing equipment consists of a mesh conveyor belt, shredder for the large plastic parts, a suction pipe with pump, and voraxial separator for dewatering for the small plastic parts. A small container will also be placed on the deck for temporary storage of the processed plastic. A support vessel is required for the bulk storage of the plastic however, since the SWATH design lacks both the required storage space and additional buoyancy to store the plastic directly on the platform. Therefore a second pump is placed on the platform to transport the plastic to the storage vessel.

In the first layout concept. the conveyor belt and intake pipe are placed at the bow of the ship, as shown in Figure 4.14. The other equipment is placed on the open deck on the aft of the platform, where there is sufficient space to place a 60 m³ container for temporary storage. The second layout has the conveyor belt and intake for small plastic located at the aft of the platform, near the other equipment. This layout is shown in Figure 4.15. In this case, the overall length of the pipes connecting the equipment, as well as the required pump capacity, can be reduced. Therefore this concept is preferable to the first layout option.

The SWATH vessel is usually equipped with 4 diesel-electric engines that have a total capacity of 2400 kW and consume 600 kg of fuel per hour at full power (Nils Olschner, Abeking & Rasmussen, personal communication). The power requirements for the platform will be much smaller, in the order of 100 kW. Therefore it can be equipped with smaller engines in order to decrease costs and fuel.

The usage of an additional vessel for the storage of the plastic influences the operational window of the platform. In extreme weather conditions, the storage vessel will have to disconnect from the platform and move to a sheltered area. Since the booms will also disconnect in severe weather (wave heights of 5.5 m and larger), the disconnection of the storage vessel from the platform does not reduce the operational window as such. However the movement of the storage vessel to and from the sheltered area will require some additional time, depending on the distance from the deployment location. As shown in Chapter 4.4, the storage vessel will most likely have a sailing speed of 10 to 11 knots. The platform itself can remain at its position during a storm, as the SWATH hull is in principle designed to withstand any weather conditions (Nils Olschner, Abeking & Rasmussen, personal communication). We estimate the capital expenditures of a SWATH vessel to be around € 50 million.

4.3.5 CHOICE OF CONCEPT

Because of its superior stability and beneficial capital and operational costs, the decision has been made to use a spar platform concept as the preliminary platform type of choice.

Although detailed engineering is needed to design the most suitable platform, this chapter has demonstrated that there are several readily available solutions for a sea-worthy floating body to house plastic extraction and processing equipment, as well as the optional in-platform plastic buffer. Basic dimensioning has also given us a sense of the order of magnitude the costs would be expected.

In terms of cost, Iemants Steel Constructions NV has quoted a base case of € 14,000,000 (based on a mean steel and manufacturing cost of € 5 per kg). The best-case scenario was estimated to be € 11,200,000, while the worst-case scenario was € 16,800,000.
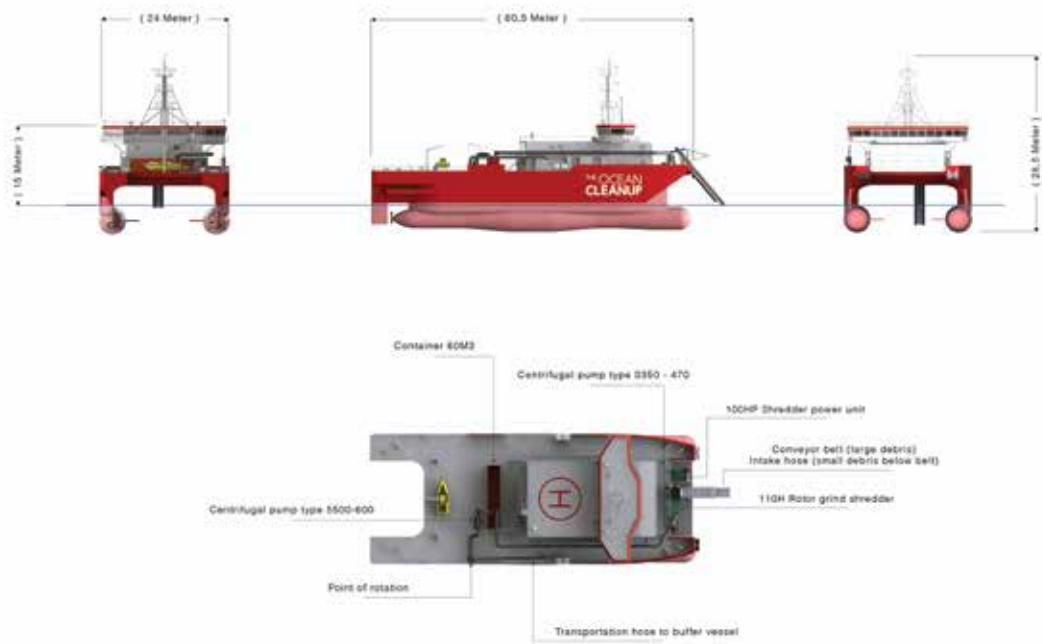
Figure 4. 14 Artist's renderings showing a possible equipment arrangement on an existing 60 m SWATH vessel
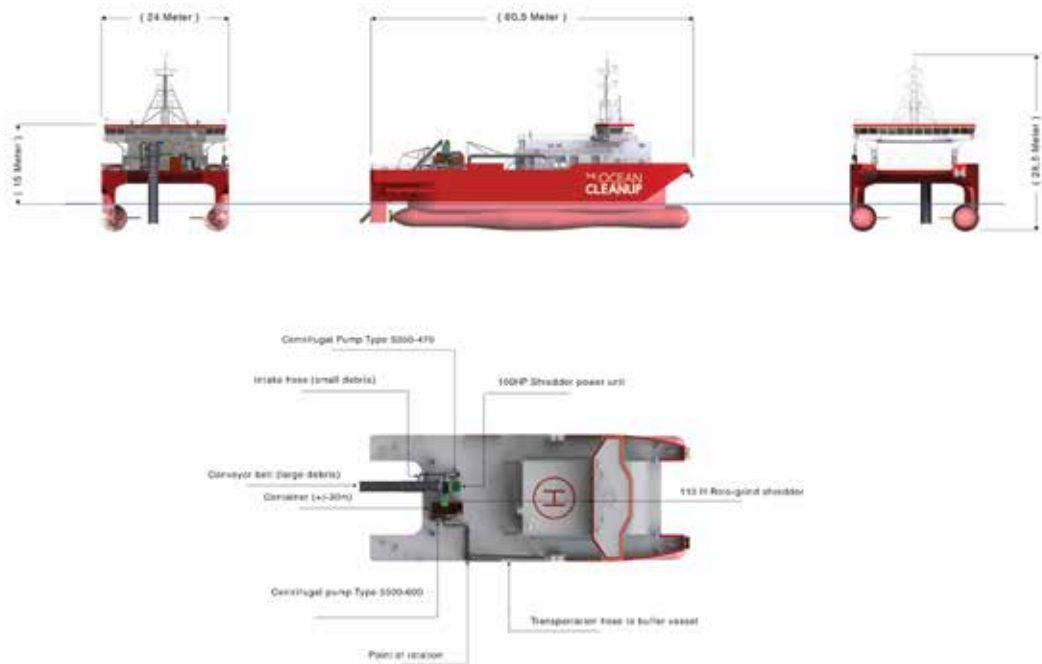
Figure 4. 15 Artist's renderings showing another possible equipment arrangement on an existing 60 m SWATH vessel

PLASTIC TRANSSHIPMENT AND TRANSPORT

SJOERD DRENKELFORD

Completely processing the material on the platform is not desirable since the rolling motion of the platform poses a problem for the chemical processes as proposed in Chapter 9. Therefore, the collected and size-reduced material needs to be transshipped from the platform and shipped to shore. This section discusses the methods for this: first, the system of requirements is created; second, concepts for the basic functions are presented. In the assessment that follows, these are reviewed, the best concept is selected and the final conclusions are presented.
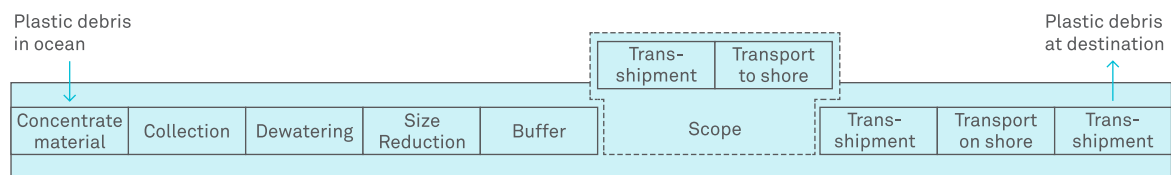
Figure 4. 16 Scheme of total process with scope on transshipment and transport

4.4.1 SYSTEM REQUIREMENTS

To be able to generate and assess different solutions for the collection and processing, system requirements are needed. These are based on functional requirements and prerequisites.

FUNCTIONAL REQUIREMENTS

In Chapter 4.2 the system requirements are presented for the entire Ocean Cleanup system. In Figure 4.16 the scheme of the total process is repeated, but with a different scope that is here limited to the relevant areas.

The process steps within this scope have their own function(s):

TRANSSHIPMENT

To move the collected material from the buffer to a transport medium.

TRANSPORT

To transport the collected debris from the collection platforms to the mainland and to protect the material from the environment during the trip to shore.

PREREQUISITES

Apart from the direct functions that are implied by the process of The Ocean Cleanup, prerequisites have to be stated. Some of these requirements cannot be compromised, like safety. Others can be used as guidelines, to assess the generated solutions.

SAFETY

The solution provided by The Ocean Cleanup has to be safe for humans.

DURABILITY

The presented solution will consist of a platform in the middle of the Pacific Ocean and all of the systems must be durable enough to withstand the environmental conditions of wind and waves that are specified in Chapter 2.

MAINTENANCE-FRIENDLY

Due to the environmental conditions described in Chapter 2, maintenance can be a difficult task. Ease of maintenance needs to be taken into account when generating and assessing solutions.

BLOCKAGE

Blockage can cause the transshipment to come to a halt and this would delay the transport. More importantly, blockage can damage the equipment. Therefore, it must be prevented. Blockage can be caused by, for example, plastic parts that are too large for the equipment or by mechanical failure.

SPILLAGE

Spillage of the plastic has to be minimized to optimize the efficiency of the project.

POWER

From a practical and sustainable viewpoint, the platforms need to be as energy efficient as possible.

COSTS

The solution has to be as cost efficient as possible to make The Ocean Cleanup economically acceptable.
Bulk density: Measurements taken from the samples collected from Hawaii have produced a mean bulk density of 300 kg/m³. This was determined by Norbert Fraunholcz, of Recycling Avenue, who examined the samples. More information on this subject can be found in Chapter 9.
Material flow specifications: The calculations in Chapter 4.1 have shown that a material flow of 1.20 tons per hour can be expected.

RESULTING SYSTEM REQUIREMENTS

The system requirements that apply to the logistical systems are comprised of the functional requirements and the prerequisites.

FUNCTIONAL REQUIREMENTS

- Transship the collected plastic into a transport vessel
- Transport the collected plastic to shore

PREREQUISITES

- Durable and maintenance-friendly
- Safe for humans
- Low risk of blockage
- Low spillage
- Low power consumption
- Cost efficient

4.4.2 CONCEPTS

To be able to create concepts for the entire operation, the basic functions that are presented in the system requirements are used. Multiple solutions are presented for each of these functions, along with their advantages and disadvantages. It should be noted that the plastic will be shipped as bulk cargo, or large quantities of unpacked material, due to the volume of the material flow as calculated in Chapter 4.1.

4.4.2.1 TRANSSHIPMENT

When the buffer is full or has reached a certain capacity, the plastic will be shipped to shore. One of the most critical steps in this process is the transshipment of the debris from the buffer to the transport medium, because the conditions at sea can be very rough. High waves and wind can hamper the operation and have a serious potential to put strain on mechanical components. The following transshipment options were considered:

GRAB CRANES

Grab cranes are used around the world in bulk solids handling. In many ports they are used to load and unload ships. An example of a typical bulk handling grab crane is shown in Figure 4.17.

ADVANTAGES

• Relatively low capital investment.

DISADVANTAGES

• Since the grab can only reach material that is directly underneath it, the entire floor surface of the buffer needs to be reachable for the grab. This implies that either the entire roof coverage of the buffer can be opened or removed, or that an internal conveying system is required, to transport the material to a location where the grab can reach it.
• As can be seen in Figure 2, a grab crane is a high structure with a heavy grab that is hanging on steel cables. This high structure and the grab are very sensitive to the rolling movement of the platform and can cause the grab to swing uncontrollably, posing a threat to the safety of workers and equipment.

Figure 4.17 Typical grab crane. Courtesy of Pim Stouten

BELT CONVEYOR SYSTEM

A frequently-used solution for the transshipment of bulk solid materials is a belt conveyor system. A schematic view of such a system is shown in Figure 4.18. A truss structure is used to position the end of a conveyor belt directly above a vessel's cargo hatches. The material (drawn in blue) is fed from the platform and carried by the conveyor belt to the end of the truss structure and is discharged into the vessel.

ADVANTAGES

• A belt conveyor system is a continuous loading system, which ensures a very stable and controllable trans shipment regime.

DISADVANTAGES

• As can be seen in Figure 4.18, the range of this system is limited by the supporting structure. The transport vessel needs to be within the range of the belt convey or and, while within this range, it is vital that the transport vessel and platform do not collide.
• The belt conveyor system is positioned above the transport vessel. Therefore, to avoid potential damage, it needs to be high enough so that it does not make physical contact with the transport vessel due to weather conditions presented in Chapter 2.
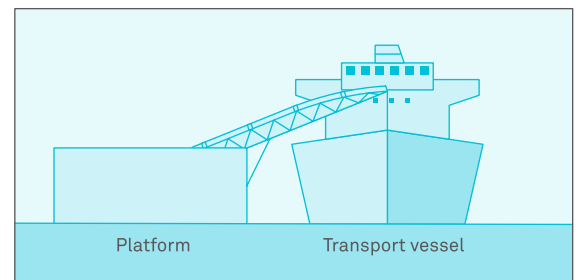
Figure 4.18 Schematic view of a belt conveyor system

BUFFER EXCHANGE

The previous methods imply a stationary buffer integrated or attached to the platform. Here, a mobile buffer such as a barge or a large floating container, is discussed. An example of such a system can be seen in the pictures of the early concept in Chapter 1. When the buffer is full, it is removed and replaced with an empty one. The buffer can then be transported to shore.

ADVANTAGES

- This method makes the transshipment move fast, since only one storage unit needs to be replaced with an empty one. This results in short changeover times.

DISADVANTAGES

- Similar to the belt conveyor system solution, the buffer needs to be in close range of the equipment that fills it, but it also must be prevented from crashing into the platform.

SLURRY PUMP

If the plastic debris is small enough, it can be mixed with water and pumped from a buffer to a transport medium. The pumps that are used for this are centrifugal pumps, which use an impeller to provide the pressure to force the slurry through the pipes. This method of transshipment has been successfully applied to petroleum products in the oil industry.

In the oil industry, large pumps are used to transport oil and other petroleum products from one container into another. These pumps employ centrifugal forces using the same principles that could be applied for the plastic parts here. These parts have to be shredded to below a certain maximum size and mixed with water. This slurry can then be pumped through a pipe to the transporting vessel. On board the ship the water can then be removed by one of the dewatering solutions presented earlier in Chapter 4.2.

ADVANTAGES

- Since a retractable hose can be used to connect them, the distance between the platform and the transport medium is not limited by a solid structure.
- A slurry pump does not require high structures, since \ pipes or hoses do not need to be lifted to a high point above the transport vessel, but can be forced upwards through the same hose or pipe.

DISADVANTAGES

- This method pumps water with the plastic, which results in higher energy consumption.

One of the most important processes is the transportation of the collected debris to shore. Due to the location of the Ocean Cleanup Array (a distance of approximately 1852 km to the US coast), it is essential that the transportation is done efficiently. The following transport options were considered:

BULK CARRIER

Bulk carriers are the world's backbone when it comes to the transportation of dry bulk. The transported material is stored in multiple cargo holds, each one reachable through its own hatch on the deck. The hatch covers are clearly visible in Figure 4.19.

ADVANTAGES

- The large hatches on the deck of a bulk carrier enable fast transshipment, since there can be a high volume flow of material.
- Bulk carriers are designed to withstand naval environments, so they are suited for the conditions at the preliminary location in the North Pacific Ocean, as described in Chapter 2.

DISADVANTAGES

- The transshipment through the hatches on deck would be dependent on the weather conditions, since high waves could cause the transshipment equipment to crash into the transport vessel.

Figure 4.19 An example of a bulk carrier. Courtesy of Pacific Carriers Limited

PUSH BOAT

Push boats can transport push barges to and from the platform. These barges can be used as a buffer; an empty barge would be delivered and a full one collected in a single trip.

ADVANTAGES

- Since it would be already filled, transshipment only requires time to exchange the full with the empty buffer.

DISADVANTAGES

- To be able to safely cross the ocean without flooding, hatch covers need to be designed, along with a method of applying and storing them.
- Push barges and boats have a slow sailing speed (approximately 5 knots), which will result in a longer sailing time to shore than for example a bulk carrier, which typically sails at 10 to 15 knots.
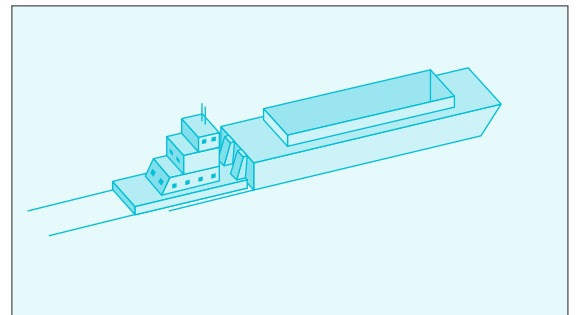

Figure 4.20 Drawing of a push barge

PRODUCT TANKER

Product tankers, or oil tankers, are used to transport all kinds of liquids around the world. Their holds are closed and they are filled through a manifold on deck. A manifold is a piping system that uses valves to redirect the material flow to the desired destination.

ADVANTAGES

- Product tankers are designed to withstand naval environments, so they are suited for the conditions at the preliminary location in the North Pacific Ocean.
- The manifold on deck enables transshipment without having to reattach the transshipment hoses or pipes to fill different cargo holds.

DISADVANTAGES

- Plastic needs to be mixed with a liquid (water) to create a slurry that can be pumped. This implies extra volume displacement and therefore higher energy consumption. It also limits the possibilities for trans shipment. Depending on the size of the transport vessel, it might be required to dewater this slurry on the vessel.

Figure 4. 21 Example of a product tanker. Courtesy of the Irish Marine Development Office.

4.4.3 DISCARDED DESIGN CHOICES

Several design choices can be discarded before the final assessment.

TRANSSHIPMENT SOLUTION: GRAB CRANE

A grab crane requires a high structure and large moving parts. This creates a very hazardous working environment for both people and machinery. This method would also require that a large vessel is moored onto a relatively small platform, which is actively discouraged by a field expert (Mammoet Salvage). This method was therefore discarded.

TRANSSHIPMENT SOLUTION: BELT CONVEYOR SYSTEM

This solution was discarded for the same reasons as those for the grab crane.

TRANSPORT PROBLEM: PUSH BOAT

Push boats and barges have been actively discouraged by a field expert (Mammoet Salvage). These combinations are just not suited for use on large open waters, due to the large impact forces that occur between the pusher and the barge. This solution is therefore discarded for safety and durability reasons.

4.4.4 ASSESSMENT

In this section the best solutions are determined for the basic functions. First, all of the presented concept solutions are shown in a morphological scheme (Table 4.12). After that, promising concepts are set up and assessed for the applicable criteria.

Since a SWATH vessel platform cannot hold a buffer, it always requires an external vessel to act as a buffer. Although the buffer is exchanged when it is full, the transshipment to the buffer can only be done safely by using a slurry pump. For each platform type, two possible solutions can be selected.

The chosen concepts are assessed for each of the remaining basic functions, which are drawn from the prerequisites. Not every criterion is used for every assessment, since they do not always apply. Factors are weighted to represent the relative importance of the criteria:

- Less important
- Normally important
- Very important

The concepts will receive grades for each criterion, varying between 1 and 5:

- Bad
- Poor
- Average
- Good
- Excellent

Since all of the solutions share the same transshipment basic function, no assessment is required for this function. The only remaining assessment is that of the transport function, which is shown in Table 4.14

Basic function	Possible solutions	
Transshipment	Slurry pump	Buffer exchange
Transport	Bulk carrier	Product tanker

Table 4.12 Morphological scheme

	Solution 1A SWATH	Solution 1B Spar	Solution 2A SWATH	Solution 2B Spar
Transshipment	Slurry pump	Slurry pump	Slurry pump	Slurry pump
Transport	Bulk carrier	Bulk carrier	Product tanker	Product tanker

Table 4.13 Selecting promising solutions

For this assessment the most important factors are safety, durability and blockage, since these cannot be compromised. Spillage and maintenance have been graded as nominally important, since they are unwanted, but they can be dealt with. Power and costs have been rated as less important and may act as final decision criteria.

From this assessment it is clear that Concept 2 is the most promising. In the next section, this concept is finalized for both platform types and practical realizations are presented.

4.4.5 FINAL CONCEPT

In collaboration with Dutch and international companies, suitable machines were selected for each of the basic functions and information regarding costs, dimensions, weights and power consumptions were provided.

4.4.5.1 TRANSSHIPMENT

The Dutch company Deltapompen B.V. was consulted for the selection of the slurry pumps. For the transshipment slurry pump they selected a pump with a capacity of 300 m³/h, which uses 90 kW of electrical power. This pump will cost € 19,000, including the motor and the mounting. Similar to the slurry pump that extracts the small particles from the ocean, this pump will be made from the corrosion resistant material super duplex and is able to pump slurries with a maximum particle size of 50 mm. This pump is suitable for both platform types.

4.4.5.2 TRANSPORT

There are two options for the transportation of the collected debris: buying or chartering a vessel. Which is the most economical depends on the type of platform to be used.

SWATH VESSEL

For a SWATH vessel platform, which cannot hold a buffer, the constant nearby mooring of a vessel is required to perform continuous processing. This also implies that two vessels are required, due to the transportation time. This would result in very high costs when a vessel is chartered. For this platform type, the only practical economic option is to buy a vessel.

The SWATH vessel platform needs to be supplied with marine gas oil every 14 days to keep its generators running. It makes sense to synchronize the transport vessel periods, so that they can also transport fuel and other supplies. In 14 days, the Ocean Cleanup Array would collect approximately 899 m³ of plastic debris. Since the Voraxial Separator produces a 50-50 mix of plastic and water, as explained in Section 4.2, twice the amount of cargo capacity is required. Thus, required cargo capacity of the transporting vessels is 1,798 m³.

To calculate the order of magnitude of the costs of transportation, a tanker vessel of sufficient size has been chosen as a baseline. The specifications of this vessel are stated in Table 4.15. It should be noted that this vessel does not have a bow thruster, so it is not capable of using Dynamic Positioning (DP), necessary for the continuous mooring of the vessel during the 14-day loading period. A calculation based on actual data is not possible, so the fuel consumption of dynamic positioning is assumed to be 50 percent of the fuel consumption of sailing. An example given to support this assumption is the MSV Fennica, which uses 30 MT of fuel at normal sailing speed and 15 MT of fuel for dynamic positioning (Offshore).

Criterion	Weighing factor	1A	1B	2A	2B
Safety	3	4	4	5	5
Durability	3	5	5	5	5
Maintenance	2	4	4	3	3
Blockage	3	5	5	4	4
Spillage	2	4	4	5	5
Costs	1	2	2	4	4
Total	-	60	60	62	62

Table 4.14 Criteria for transport

Cargo capacity	2,538 m³
Length	75 m
Sailing speed	10 knots
Fuel consumption	3.5 MT heavy fuel per day
Price	€ 1,258,000

Table 4.15 Specifications example vessel for a SWATH vessel platform, taken from www.maritimesales.com on 24-2-2014

Cargo capacity	8,664 m³
Length	118 m
Sailing speed	12 knots
Fuel consumption	6.1 MT heavy fuel per day
	0.7 MT MGO per day
Price	€ 1,000,000

Table 4.16 Specifications of an example vessel for a Spar buoy platform[2]

For the vessel needed, the Spliethoff Group has indicated that a crew of 6 people is required, which would cost approximately € 350 per day. For two vessels with a running time of 10 years, this results in a total ship crew cost of € 2,548,200.

The example ship consumes 3.5 MT of heavy fuel oil per day. The price of heavy fuel oil is € 424 per Metric ton[1]. The total fuel costs are calculated by using the total sailing time of 100 hours (8.4 days) and a mooring time on site of 14 days, during which dynamic positioning is used. Two days are allowed for loading and unloading. The remaining days are uncertain, but in the worst case scenario, the vessel would be required to use dynamic positioning, which is also accounted for in the fuel calculations. The resulting fuel cost of one journey for one vessel is € 22,854. Multiplying this with the number of cycles that are implied with a running time of 10 years and two vessels, the total fuel costs are € 5,941,936. It has to be noted that this estimate does not account for inflation and changes to the price of oil.

As mentioned before, two ships are required to ensure continuous operation. The costs for the ships themselves are therefore € 2,516,000. The total costs for the transportation of the plastic debris for a SWATH vessel platform, involving two ships, their fuel and their crew, are therefore € 11,005,936.

SPAR BUOY PLATFORM
For the Spar buoy, either chartering or buying a vessel is realistic, since this platform type is able to hold a buffer. The costs for buying a vessel have been calculated with the same method as was used for a SWATH vessel platform. The specifications of the example ship are shown in Table 4.16. The same assumption was made about the fuel consumption of dynamic positioning as for the example vessel for a SWATH vessel platform.

[2] taken from maritimesales.com on 1-4-2014 (Bunkerworld.com).

It is assumed that this vessel constantly needs a crew on board for the full running time of the project and that they cost the same as the crew for the transport vessel for the SWATH vessel platform, which is € 350 per day. The crew costs are therefore calculated to be € 1,277,500.

The example ship consumes 6.1 MT heavy fuel oil and 0.7 MT of marine gas oil per day with prices of € 424 per Metric ton and € 862 per Metric ton[3], respectively. With a sailing time of 8 days and an on-site time of 32 days, the fuel costs for a 10 year period are € 7,794,559. Inflation and oil price variation are not taken into account in this calculation.

With the ship's purchase cost at € 1,000,000, the total costs for buying a ship will result in transportation costs of € 10,072,059.

For chartering a vessel, the Spliethoff Group has indicated that the cost to transport 6,000 m³ of plastic over the required distance would be € 210,000. At the collection rate of 1953 m³ per month, such a journey would be needed every 1.5 month (assuming a volume of water equal to the collected plastic). With a running time of 10 years, this results in the total transportation costs of € 16,800,000. The presented chartering costs are based on dry bulk vessels, which cannot transport wet cargo without capsizing. It is assumed that the costs of product tankers of similar size are similar to those of bulk carriers.

Buying a vessel will be less expensive than chartering one. There is another reason to prefer to buy a vessel and that is the supply regime of the platform. This can be easily facilitated with an owned vessel, but it is much more complicated when chartered ships are used. For these two reasons, the optimal solution is to buy a vessel.

4.4.6 CONCLUSIONS

The optimal solution for the transshipment and transport of the collected debris will be to use a slurry pump and owned product tankers. The total costs and the maximum power consumption of this equipment for both platform types are shown in Table 8. The last rows represent the costs per ton of collectable plastic, which is calculated using the total amount of collectable plastic in the North Pacific gyre; 70,230 tons (see Chapter 4.1). This result will eventually be used in the total costs analysis in Chapter 10.

Similarly to the extraction equipment, the secondary equipment and the supporting constructions will be designed in the second phase of the project. Therefore, the costs for all of the equipment have been increased by 50 percent for both platforms.

[3] fuel price in the Rotterdam harbor on 24-02-2014 (Bunkerworld.com).

Function	SWATH vessel		Spar Buoy	
	Costs (€)	Maximum platform power consumption [kW]	Costs (€)	Maximum platform power consumption [kW]
Transshipment	19,000	90	19,000	90
Secondary equipment and supporting constructions	9,500	-	9,500	-
Transport	11,005,936	-	10,072,059	-
Total costs	11,034,436	90	10,100,559	90
Total transport costs per ton of collected plastic	157.12	-	143.82	

Table 4.17 Total costs transshipment and transport for both platform types

PLATFORM POWER GENERATION

REMKO LEINENGA • HERBERT PEEK

Electricity is required for the platform to operate. The great distance from shore makes visits for maintenance and refueling very expensive. For this reason, it is assumed that the system should be as autonomous as possible, and can be monitored from a distance.

Function	Estimated platform power consumption [kW]	Estimated operational time
Collection of small particles	22	8h/day
Collection of medium-sized particles	2	8h/day
Shredder	90	4h/day
Transshipment	90	13.5h/month
Dewatering	37.5	8h/day
Lighting, communication, autonomy	5	24h/day

Table 4.18 Consumption of processing equipment and support equipment on the platform

4.5.1 REQUIREMENTS

Because The Ocean Cleanup aims to improve the environment, a sustainable solution for electricity generation is preferred to minimize the carbon footprint of the operation. The levels of energy required must be understood in order to find possible solutions for power generation. Estimated electrical consumption on the platform is listed below in Table 4.18.

As can be seen from Table 4.18, the two most energy-intensive processes are shredding and transshipment, with each consuming 90 kW. Additionally, since each process occurs for a relatively short time period, operating only for a few hours per day or per month, presents a problem. Sustainable energy sources, such as wind or solar power, would deliver too much energy when the equipment is turned off and probably too little when it is on. The use of a battery could solve this problem; however, the technical aspects involved in integrating a complex battery pack would not only make the system more expensive, but would also reduce the array's flexibility by restricting it to a timetable.

For these reasons it has been decided that the more constant electricity required for the passive cleanup, 66.5 kW (22+ 2 + 37.5 + 5),will be generated by means of solar and possibly wind power, and that the 180 kW for the shredder and transshipment will be generated using a diesel generator. This means that the system will work 20 hours per day on the battery and 4 hours per day on a combination of diesel and solar power.

4.5.2 POWER GENERATION

To ensure a constant supply of power the total consumption of the system in different situations must be assessed. The situations considered were: emergency, normal sea conditions, and transshipment.

Using the outcome of this analysis, the various energy generating options can be assessed. As shown in Table 4.19, 66.5 kW will not be needed at all times: an average load factor of 0.9 is enough to ensure continuous operation. This means that a total of more than 60 kW must be generated using solar panels on the platform to provide power for normal sea conditions. With an average of 160 Watt/m², a solar panel field of around 400m² would be required.

Description	#	kW	Load factor	U	Preferences	Emergency?		SEA Normal (time)		Trans- shipment	
				V	Ind. Loading	%	kW	%	kW	%	kW
Total load		247			247		11		28		86
Deck equipment Collection of small particles	1	22.00	0.9	400	v		0.00	35	6.93		0.00
Collection of medium-sized particles	1	2.00	0.9	400	v		0.00	35	0.63		0.00
Shredder	1	90.00	0.9	400	v		0.00	5	4.05	100	0.00
Transshipment	1	90.00	0.9	400	v		0.00		0.00		81.00
Dewatering	1	37.50	0.9	400	v	20	6.75	35	11.81	100	0.00
Lighting,						100	4.50	100	4.50		4.50
communication,							0.00		0.00		0.00
autonomy	1	5.00	0.9	400	v		0.00		0.00		0.00

Table 4.19 Different situations of use

4.5.3 POWER STORAGE

BATTERY
A Lithium Ion battery in a DC grid is preferred for its weight, compact nature, long life and energy storage stability. A battery pack able to deliver 40 kW would require 40 cells with each weighing 200 kg.

FUEL TANK
Total fuel consumption would be at a rate of 0.2 dm³/kW. For the generator calculated this will result in a consumption of +/- 28 dm³ diesel fuel per hour. Based on a 4 hour run time per day the consumption will be 100 dm³ a day.

The current configuration will use 3 m³ of gasoline a month. An appropriately sized fuel tank would need to be installed to meet this level of consumption.

4.5.4 RESULTS

WEIGHT
The total weight of:
- Switchboards and cables is estimate at 2.5 ton.
- Solar panels 10 ton. (250x25 kg)
- Battery pack including chargers: 12 ton

Not including: fuel, plastic, etc.

DIMENSIONS
- Switchboard: HxLxD 2x3.6x0.5 m
- Generator: HxLxD 1.5x2x1.5 m
- Solar panels: 400 m²

Not including: fuel tank etc.
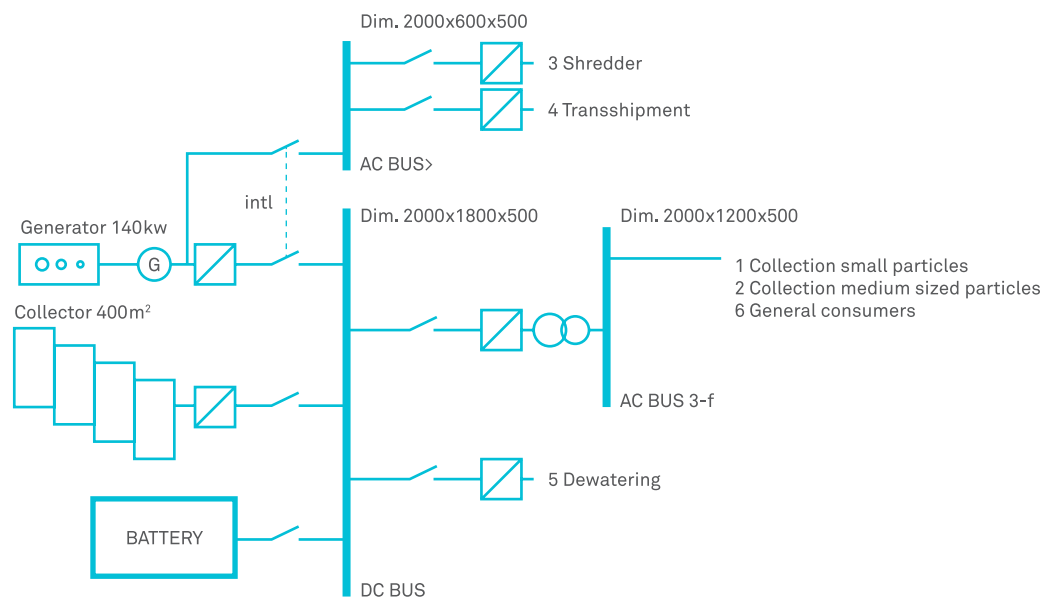
Figure 4.22 A schematic view of the electricity grid on the platform

COSTS

These prices are based on the services provided by eL-Tec elektrotechnologie. Since not all the technical specifications are currently known, changes in design can have financial consequences:

Battery pack	€ 40,000	Redundancy bus system / managed switch	
Battery charge system	€ 80,000	Double PLC witch redundancy	
Solar panels	€ 100,000	I/O redundancy	
Switchboards and cable	€ 150,000	On site location	
Starters / remote monitoring and control		Visualization	
Conveyor belt inlet		Sensors/transmitters	€ 50,000
Slurry pomp		Camera system	€ 30,000
Shredder		Fire detection	€ 5,000
Separator		Communication	€ 20,000
Conveyor outlet		Generator (140 kW)	€ 100,000
Control equipment		Illumination & basic alarms	€ 15,000
Light		**Expectation for the total**	
Monitoring and control		**electrical installation will be**	**€ 790,000**
including hard and software	€ 200,000		

OPERATIONS

Chapter 5 gives an overview of procedures during operation of the array. These procedures are described for the entire life cycle of the structure. Once fabricated, the structure must be transported to the chosen location, where installation of mooring, boom and collection platform will take place. After placement, maintenance is required due to degradation and incidents. More information on bio fouling is discussed after the maintenance subchapter. The chapter closes with final remarks about decommissioning. It is expected that decommissioning costs will be equal to or less than than the installation costs.

A FEASIBILITY STUDY
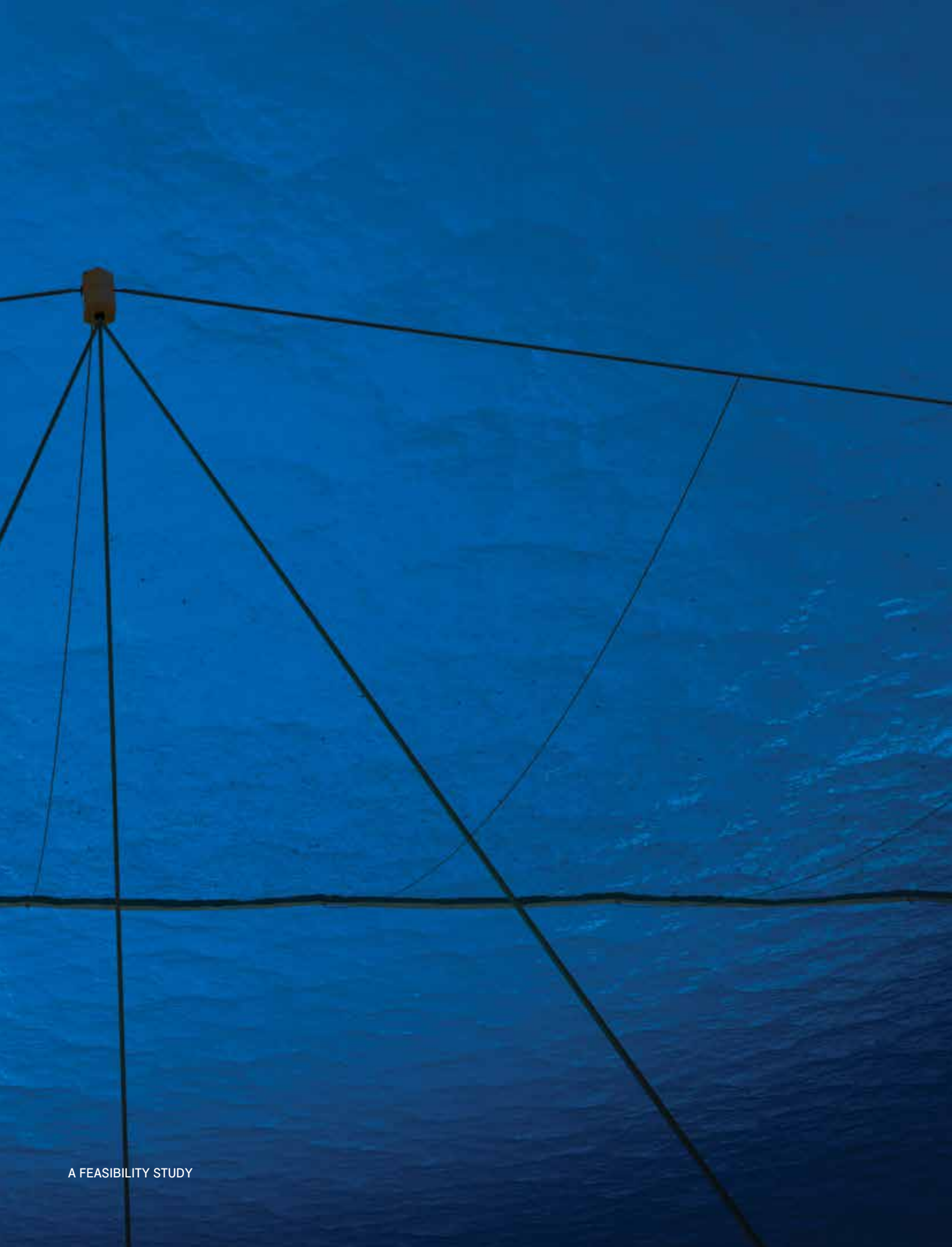
PLACEMENT

JOOST DE HAAN • BOYAN SLAT • JAN DE SONNEVILLE

The array's installation is an enormous operation. First estimations are that placing the mooring and structure will take several months to complete. This section briefly outlines the installation of mooring, booms and the collection platform.

PENETRATION MODE   VERTICAL MODE
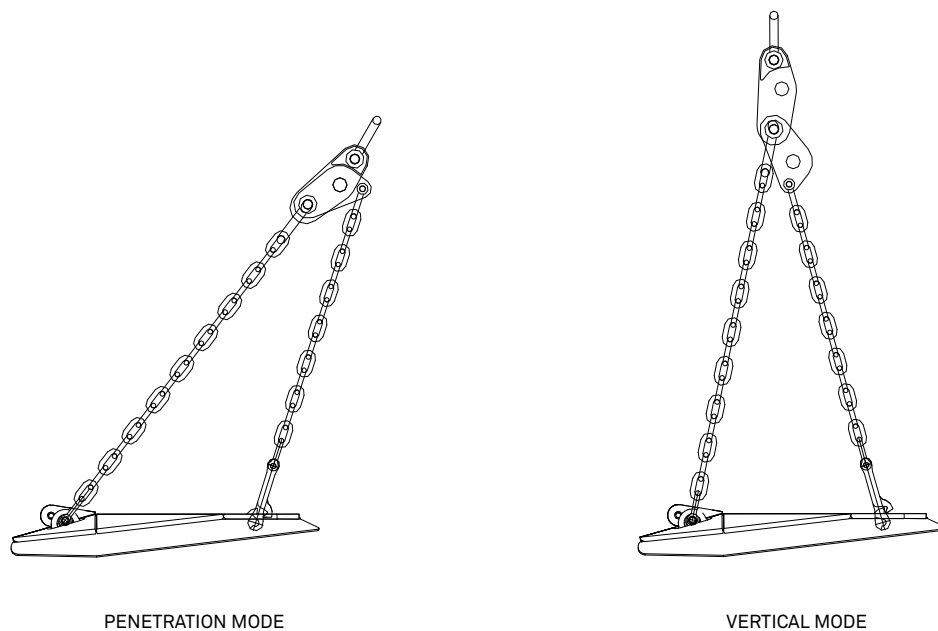
Figure 5.1 Stevmanta VLA (permanent version) in installation (left - shear pin in angle adjuster is still intact) and normal loading mode (right - after the shear pin in angle adjuster is broken)

5.1.1. MOORING INSTALLATION

In the concept, the mooring consists of a single vertical polyester rope connected to the seabed using a vertical load anchor (VLA).

The Stevmanta VLA allows for single line installation using the shear pin angle adjuster, see Figure 5.1. During installation, the installation line is the same polyester line as the one used for the mooring.

Installation can be performed using one anchor-handling vessel (AHV). A typical AHV, with around 200 tons of Bollard Pull, will be able to install and retrieve the anchor. Typical day rate of deep-water AHV is in the order of $80,000 USD, and an additional $20,000 USD will be calculated for a barge carrying and storing the large volume of mooring lines and anchors. The mode of the anchor changes when the shear pin breaks at a load equal to the required installation load.

For Stevmanta VLA, there is no setup time required. Therefore, the anchor can be connected to the floating unit immediately after the installation.
A brief introduction to the required installation steps follows.

STEPS

1   Optional: attach the tail to the anchor.
    This tail assists in orientation on the seabed.
2   Connect the mooring line to the angle adjuster on the AHV.
3   Lower the anchor overboard, descend tail first. Please note that multiple rope elements are required to obtain the required length.
4   After touchdown, the AHV pays out the line while it slowly sails away from the anchor.
5   Increase line tension, the anchor will start to embed into the seabed.
6   The shear pin will fail when the predetermined installation load has been reached with the AHVs bollard pull.
7   The anchor is now in normal loading mode; tension can be increased for proof loading.
8   Attach submerged buoy to the polyester line end and overboard.
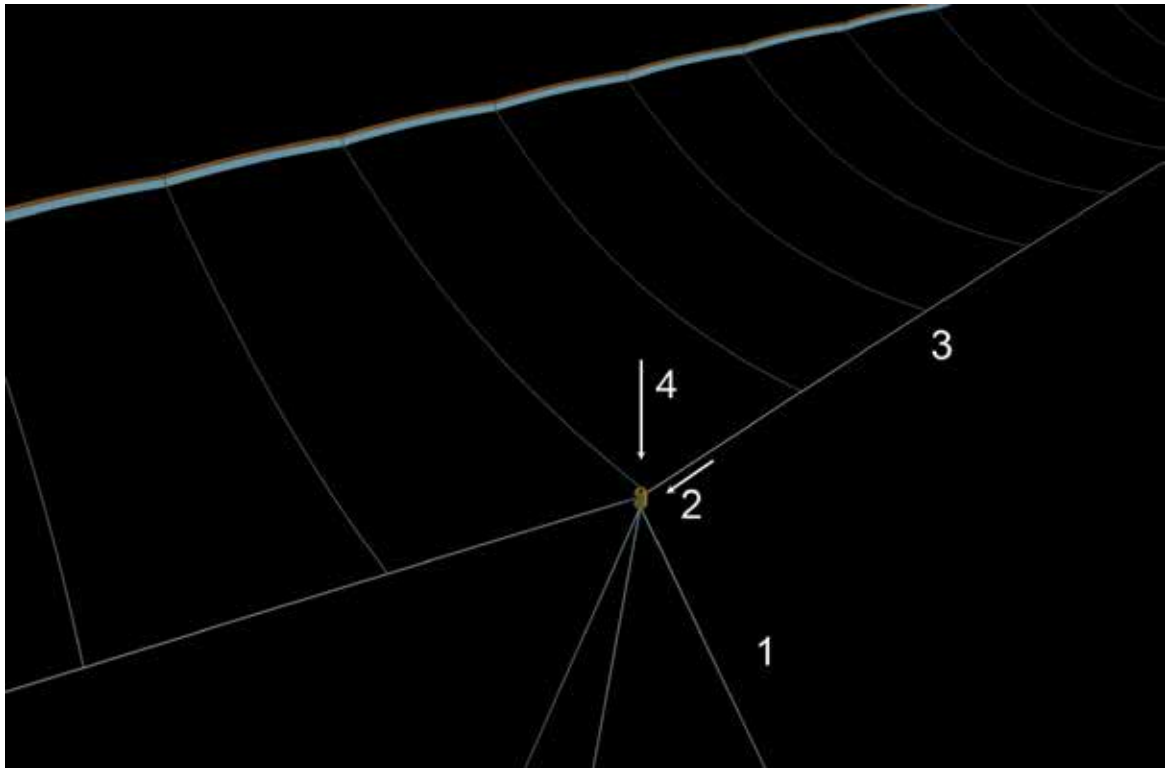
Figure 5.2 The installation process, where first the mooring would be installed under low tension (1), the tension cable would be attached to the underwater mooring, while still at the surface (2), the boom would be rolled out and attached to the next mooring point (3). When the booms have been coupled to both sides of the underwater buoy, the mooring would be tensioned, pulling the buoy to a depth of 30 m.

CHALLENGES

The AHV must carry rope lengths exceeding 4000 meters. Available deck space should be considered.

Mooring dynamic calculations are not included in the feasibility study. At the chosen location, severe weather conditions are of great influence.

The project-specific installation details and procedures shall be developed in the detailed design phase.

5.1.2. BOOM AND TENSION CABLE INSTALLATION

The installation of the tension cable and connection cables can all be performed from deck (without requiring the use of expensive ROVs) following these steps:

1 The underwater buoys are connected to the mooring lines, but tension is not applied, meaning that these buoys will be floating initially.
2 While connecting the tension cable to the underwater buoys, the connection cables are attached and connected to buoyancy elements, to keep these connection cables available and prevent the tension cable from sinking under its own weight
3 The mooring lines connected to the underwater buoy are pulled through the buoy until the desired tension is reached; this applied tension will position the buoys at a depth of 30 m.
4 The boom segments are connected to the connection cables.

Figure 5.2 above gives an impression of the components, when installed. The more detailed steps of installing the tension cable are:

1 One side of the tension cable which is on a reel will be connected to the mooring point.
2 While the boat sails to the next mooring point the tension cable will be unrolled.
3 While unrolling the tension cable the connection cables and buoyancy elements will be connected to it.
4 When the next mooring point is reached, the tension cable will be connected to the mooring point.
5 The boom is installed to the connection cables.

Alternatively, the booms can be connected to the tension cable onshore, creating long sections of 4 km long that can be tugged with a transport vessel to the site.

In this case, the installation steps would be:
1 The underwater buoys are connected to the mooring lines, but tension is not applied, meaning that these buoys will be floating initially.
2 For each section the tension cable and boom are connected to the underwater buoys
3 The mooring lines connected to the underwater buoy are pulled through the buoy until the desired tension is reached. This applied tension will position the buoys at a depth of 30 meter.

This alternative makes installation offshore quicker, but the transport will be less efficient if only one boom segment can be pulled by one boat at a time (reducing the risk of booms entangling with each other).

CHALLENGES
• The 4 km long tension cable will be transported on a reel. So when one side of the tension cable is connected to the mooring point and the boat sails to the next mooring point, the connection cables have to be connected to the tension cable on deck while the tension cable is unrolled from its reel. Since this has to be done often, a quick connection process has to be created on board so the tension cable can be un rolled continuously.
• When the tension cable is installed the boom has to be installed to the connection cables. In order to do so, first the buoyancy element at the connection cable has to be removed which is extra work. However, the buoyancy element can also be used by connecting the boom to it. In this case the buoyancy element should be provided with a connection for the boom to be connected to, making the installation of the boom easier and faster.

A more detailed investigation into the installation of booms and tension cables should be done in a later phase of the project.

Figure 5.3 Spar buoy tugged

5.1.3. PLATFORM TRANSPORTATION AND INSTALLATION

The chosen spar buoy concept for the platform is not equipped with self-propulsion, which would only be required for transportation to the destination location. For that reason, the platform must be transported by other vessels. Two options are considered.

TUGBOATS

Usually used for low to medium distance transport, tugs are relatively broad available and widely used; therefore, they might be economically more feasible than using a heavy transport vessel. Tugboat sailing speeds are slightly lower than that of a transport vessel. The image below shows an example. Please note that the dimensions of spars shown in this section are larger than the collecting platform concept. The illustrated spars are used for offshore oil and gas development projects.

SEMI-SUBMERSIBLE HEAVY TRANSPORT VESSEL

Depending on the availability, a heavy transport vessel can be economical as well. The vessel submerges by filling the ballast tanks. In submerged position it can sail underneath the spar. It is lifted again and can then be transported by the supporting vessel. The company Dockwise is a leader in transport using this method. Cruise speeds of 12 knots and over are realizable.

INSTALLATION

Installation depends on the actual transport price:

1 In case of the semi-submersible transport vessel the draft is increased, after which the vessel floats away from the barge again.
2 The spar is put in upright position by filling its ballast tanks with sea water.
3 Mooring is applied as described in section 5.1.1. Multiple polyester ropes are connected to the spar instead of the single vertical line for the booms. The lines are in taut configuration to minimize the rope length.

Figure 5.4 Spar transport using a heavy transport vessel

5.1.4. INSTALLATION COSTS
5.1.4.1. MOORING

Mooring will require one day per cable line, based on an estimation by Vryhof. The mooring can be done using a large anchor-handling vessel, costing approximately $80,000 USD per day as of 2012 (Overview of the Offshore Supply Vessel Industry, 2012), while a large ocean-going barge is estimated to be around $20,000 USD. Since the steel transportation reels of the mooring ropes have a diameter of 5 m, and a flange diameter of 4 m (for a 2000 m rope), a large barge with a deck area of at least 2250 m² (e.g. 32 by 70 m) will be sufficient to store all mooring lines. However, it may be more cost-effective to use multiple smaller barges instead. The total mass of the cables is around 7200 MT, which is well in limits of large ocean barges.

In terms of operation time, it has been estimated by Vryhof Anchors that it takes one day to install a single mooring lime. A total of 30 mooring points are required for The Ocean Cleanup Array (29 for the booms, and 1 for the platform), meaning a total deployment time of 90 days. However, transportation time to and from location must also be taken into account.

For decommissioning these costs are assumed to be the same as for installation.

OPERATION	TIME PER OPERATION	TOTAL AMOUNT REQUIRED	TOTAL CUMULATIVE TIME (1 VESSEL)	VESSEL DAY RATE	FUEL COSTS PER DAY	SOURCE
Scenario 1 **Deployment from barge** Boom deployment off-shore (AHTS)	5 m / min	115,000 m	22 days *	€12k (€10k - €23k)	€2,160	Marinemoney. com
Boom transport, 8000 m boom capacity, 9.26 km / hour (AHTS + Barge)	16.6 days back and forth	14 trips	233 days	€26.5k (€24.5k - €37.5k)	€5,184	Marinemoney. com
Scenario 2 **Deployment from land** Tugging of 4 km boom sections (AHTS)	16.6 days	29 sections	481 days	€12k (€10k - €23k)	€5,184	Marinemoney. com
Installation time of boom section (AHTS)	1 day	29 sections	35 days *	€12k (€10k - €23k)	€2,160	Marinemoney. com

Table 5.1 Cost calculation of boom installation, in two scenarios

Total costs	Base	Best	Worst
Scenario 1	€ 7,693,892	€ 7,183,892	€ 10,498,892
Scenario 2	€ 7,447,392	€ 6,415,392	€ 13,123,392

* includes 6 days travel time, based on 23 km/h

Table 5.2 Operation cost estimations for boom installation

5.1.4.2. BOOM AND TENSION MEMBER

Based on the cost calculations given in Table 5.1 and 5.2, Scenario 2 is likely cheaper (3% difference in base case). However, due to the uncertainties this dragging operation also adds new risks and uncertainties, for this feasibility study we choose for scenario 1, and will be using those numbers for the cost calculations in chapter 10.

For decommissioning, these costs are assumed to be the same as for installation.

5.1.4.3. PLATFORM

Tugging the Spar platform will require a specialized ship, the estimated day-rate for such a ship is 400,000 euro per day. Sailing for 7 days this comes to an estimated 2,800,000 euro.

The swath vessel can just sail itself to the required location, the marine fuel required for this is negligible relative to the scope of this project.

These costs are assumed to be the same for decommissioning as for installation.

MAINTENANCE

JOOST DE HAAN • BOYAN SLAT

The location of the array is remote compared to other offshore structures. It is located approximately 1,000 nautical miles from land. For maintenance, it is important to store sufficient amounts of spare parts offshore. Possible locations for storage are the collection platform or on the maintenance vessel.

A more complete formulation of required maintenance will be acquired after identifying the involved risks during operation. This requires a thorough risk assessment. In the feasibility study, only part of the required maintenance is included.

Scenario	Operational days	Total cost per year
Best	5 days per month (1 operation per 2 months)	€ 1,149,167
Base	11 days per month (1 operation per month)	€ 2,298,333
Worst	29 days per month (permanent presence, back-and-forth once per month)	€ 6,066,667

Table 5.3 Cost calculation for vessel maintenance

5.2.1. TYPES OF MAINTENANCE

In the selected concept, the boom and skirt are made from a flexible material. No data is currently available on the required maintenance interval of these materials when subjected to long term mid ocean conditions. In collaboration with the manufacturer, the required repeating maintenance interval will be determined. Due to possible unforeseen incidents, additional unscheduled maintenance may be required.

Maintenance tasks include:

- Removal of debris and salt from solar panels
- Mechanical removal of biofouling
- Recoupling boom sections after storm
- Replace boom sections after collision or storm
- Replacement of electrical components (lights, radar) and mechanical components (shredder blades, pump impellers)

5.2.2. MAINTENANCE VESSEL AND COST

Multiple options for vessel type can be considered. For minor maintenance, a monohull, catamaran or SWATH type vessels are suitable. Monohulls provide relatively high cruising speeds (approx. 25 knots) whereas catamaran type vessels normally cruise at 20 knots and SWATH vessels at 15 knots. SWATH vessel operational limits allow for wave heights of up to 60% higher than that for monohull vessels. However, since SWATH day rates are unknown to us, we chose a monohull AHTS for this scenario. For major maintenance operations, heavy lift vessels might be required.

Based on an average AHTS vessel with a day rate of € 12,000, and fuel costs of € 4,500/day (based on a consumption of 10 tons/day), and a cost of € 1,000 per day for crew, the costs of 3 scenarios were calculated in Table 5.3.

PREVENTION AND FIGHTING OF BIOFOULING

GABRIELLE S. PRENDERGAST

Biofouling, or biological fouling, is the accumulation of microorganisms, plants, algae, or animals on wet surfaces, typically barnacles, seaweeds and mussels. Biofouling can damage the performance of floating, submerged, fixed or mobile structures in contact with the sea because of the following:

- Deformation of the shape of a surface – the resulting reduced hydrodynamic efficiency requires more power to propel a vessel. It can also clog up moving parts of mechanical structures.

- Weighing down a structure - impacts performance due to the level at which it sits in the water. Typically the design of 1 floating structures are optimized based upon water level.

- Degradation of structures - some organisms bore into wood or other organic materials. Others may interfere with the efficacy of a surface's coating, putting salt water in direct contact with the metal beneath resulting in corrosion.

At the time of writing, the design of the Ocean Cleanup Array has not been finalized. Furthermore, the number of species that could foul the array is unknown. The aim of this chapter is not to describe the species that will colonize the array, when or how quickly biofouling will occur, nor the specific physical attributes of the biofouling accumulation such as its weight or effect on hydrodynamics. Instead, the chapter aims to describe at a high level: the problem, its source and progression, its probable high-level effects on the Array and to make recommendations for its mitigation.

5.3.1. INTRODUCTION TO BIOFOULING

Biofouling refers to unwanted life growing attached to an interface, such as between seawater and the surface of the Ocean Cleanup Array. Biofouling can be separated into two functional categories; microfouling and macrofouling, but the size range is in fact a continuum that ranges from micrometers, such as bacteria, to meters, such as kelp. Many species considered macrofoulers may begin life as microfoulers. Species vary enormously worldwide based on factors such as season, geographic location, depth, current speed, light, temperature, salinity, food availability, surface type, surface texture, and presence of mates. Some accumulations are highly biodiverse and others are dominated by a single species. Some are temporary and precondition the surface for the next wave of colonization, while others are considered 'mature' and 'stable' communities. Within an accumulation a bare patch can appear, perhaps by the action of a storm or a predator. These patches may become colonized by an entirely different pattern of life than its surroundings. For the small number of organisms that cause the greatest problems in industry - typically shipping - a large amount of research exists. Much less information is available for the larger population of species and locations which do not cause issues,

The first phase of biofouling (after chemical conditioning of the surface upon introduction to seawater) is the accumulation of a biofilm. A biofilm is a microbial layer composed of a variety of microscopic species enmeshed in a slimy polysaccharide matrix. Marine bacteria, photosynthetic microalgae and cyanobacteria are typical kinds of organisms found here. They are the first to form because of their ubiquity in the marine environment in addition to their short generation time. A biofilm thickness ranges from about 50 micrometers to about 2 millimeters, but can be highly heterogeneous. Microbes in a biofilm are able to create an environment very different to that of the surrounding water. For instance, they may increase the oxygen content (in the presence of photosynthesisers) to 300% saturation, but become anoxic in the dark and increase the pH to 10. Biofilm formation can begin within hours of a surface being introduced into the marine environment.

After the biofilm has formed, a succession of algal and animal macrofoulers develops. The specific species comprising the macrofouling community can be highly unpredictable, as is their rate of arrival, spread and growth. Most animal fouling species are fixed to the surface as adults and therefore the larval stages are responsible for the spread of fouling communities. Algal spores can be only a few microns in size on arrival but grow and spread to form large mats or fronds. Similarly, animal larvae tend to be on the order of hundreds of microns, but can grow to be very large.

WHERE IT COMES FROM AND HOW IT GROWS

There are various ways that marine fouling organisms reproduce and spread. Some release their eggs and sperm into the ocean where fertilization takes place. Others may brood their larvae and release them locally. Some spread clonally: one individual buds genetically identical sisters and spreads out to colonize a surface. When larvae and spores are released into the environment, most can only survive for a very short period of time unless they find a place to settle. The amount of time they can survive affects how far they can travel - if carried by currents - to colonize a new area. Algal dispersal tends to be limited from meters to hundreds of meters, but for animal larvae the range of dispersal potential spans many orders of magnitude - from tens of meters to thousands of kilometers. An example of this is seen in the islands of the Pacific where groups with high dispersal potential are better represented.

The attachment of only one individual organism can potentially spread and colonize large areas. Sponges, corals, ascidians, bryozoans and algae are examples of species that commonly colonize a surface by clonal growth or the release of larvae or gametes (eggs and sperm). Coastal waters host fouling communities because there are so many solid structures in a habitable zone. For instance, the sea floor is shallower, manmade coastal structures abound, rocks and the intertidal zone are all solid surfaces that are easily encountered by marine organisms.

Because they live there, their offspring are released locally and are more likely to find a suitable place to settle. They can have very high densities in the coastal waters and competition for space to settle can be fierce as most spaces are already colonized.

Within the open ocean, it is difficult to track the source of fouling organisms, so how species get to where they are found is often very poorly understood. The only solid structures are transient passing vessels or the surfaces of larger animals. The hulls and ballast tanks of shipping vessels passing the Array must therefore be considered as potential sources of fouling species.

It can be assumed that most of the plastic debris this project seeks to intercept came from a number of coastal sources, where it may have collected a fouling community, and therefore the number of potential species must be higher than for any one geographic region. Because of the intense competition for space to settle, it is reasonable to assume that the plastic will carry fouling organisms. Indeed, one study found a healthy adult barnacle growing attached to the tag ring on the leg of a migrating seabird. Barnacles often grow on oceanic species, such as turtles and whales. The Array will provide an attractive source of shelter for these species, where it would otherwise be unavailable. It is reasonable to assume that the array will be approached by a greater number of mobile species than an equivalent patch of open water. These mobile species could carry potential fouling recruits to the array. Additionally, it has been shown for many fouling species that biofilms can act as an attracting cue to settlement. Depending on how the Array is deployed, it may acquire organisms en route from the coast to its fixed location in the gyre. If towed it will likely carry its own potential fouling community with it.

Temperate coastal regions typically display strong seasonality of recruitment, growth and reproduction of fouling species. Many locations under the heaviest fouling pressure are located in tropical and subtropical regions. Because of their limited seasonality, they tend to have relatively constant temperatures and seasonal variations are dominated by differences in precipitation only. As the Array is initially intended for deployment in a subtropical region, effects of seasonality can be expected to correlate well with this.

5.3.2. LIKELY EFFECTS ON THE ARRAY
WEIGHT

One of the largest problems presented by fouling on a floating structure is that of increased weight. The structure will be designed to sit at an optimal position on the surface. But if the weight is significantly increased, it could float below the surface or even sink entirely. As the Array's booms are estimated to be tens to hundreds of kilometers in length, the potential for fouling weight problems is substantial. Under optimal conditions the mass of biofouling can reach tens to hundreds of kilograms per square meter. The conditions in the open ocean are far from optimal, but this value may serve as a useful worst case scenario for designers.

STRUCTURAL DAMAGE

The amount of structural damage depends on the materials used for construction. The material must be protected from the corrosive properties of salt water and will require a coating to perform this function. The open ocean environment is often referred to as a desert and any solid structure within it may be likened to an oasis because it offers shelter normally unavailable. They become fouled by photosynthesising algae and by animals. The fouling assemblage will attract grazing species as the microcosm develops. Grazing species may significantly damage any coatings that protect the surface. Once the underlying surface is exposed, the seawater may quickly cause serious structural damage.

DIFFERENTIAL FOULING

At least four distinct niches, or ecological habitats, are expected to emerge on the array.

The first is the surface that is not submerged, but is periodically splashed and sprayed, in direct sunlight and exposed to fresh water when it rains. This will be the most hostile environment to species as it fluctuates from wet to dry, from hot to cold, and from hypersaline (through evaporation) to freshwater conditions will be the most extreme on the Array. Consequently, minimal fouling is expected in this niche and will most likely limited to biofilm or to monospecies accumulations of particularly hardy macrofoulers.

The next niche is the underside of the Array which, if flat and broad, will be shaded from direct sunlight. This area is most likely to be dominated by biofilm and animal communities. It is possible that current flow will be sufficient to dislodge species from this surface if the design permits the flow to pass over this surface in such a way as to maximize surface shear.

The third niche is that of the immersed vertical sides facing into the flow of currents. This area is capable of supporting biofilm, algal and animal assemblages of species. Depending on the angle of incidence of the current with the boom arms of the Array and the quality of the antifouling measures applied, this area also has the possibility for fouling to be removed by water flow. This niche has the most functional importance to the operational performance of the Array, and possible effects of fouling in this area are discussed further below, under 'fluid dynamics'.

The fourth niche comprises the vertical surfaces of the Array that are not exposed to the current and are sheltered from flow. This area, like the third niche, is also capable of supporting mixed assemblages of species. However, their chances of being dislodged by flow are minimal and likely limited to effects of rough seas. Fouling on this aspect of the Array is unlikely to interfere with the plastic

accumulating capacity. However, as with all fouling, the potential for weight increase and other damage to the underlying structure is not trivial.

Further niches may or may not be present on the Array. These include:

Indentations, which offer a microclimate different to that of the surrounding niche, are more likely to become heavily fouled. These areas are also less likely to have flow to remove the fouling, due to shelter from shear. If the Array is constructed from composite parts, special attention must be given to the joints.

Surface texture and roughness can be optimized for fouling reduction; for example, the fine structure of shark skin has antimicrobial qualities based on its texture. A commercial product called "Sharklet" is available which covers a surface in this type of microstructure and has antibacterial effects. Research is currently being funded to assess this material's anti-macrofouling potential, but it is not yet available on the scale required for this project. Submerged moving parts, intake pipes, filters and nets, are also likely to become destructively fouled unless optimized for flow to shear off any organisms (by coating with a 'foul-release' coating, see table below), or coated with toxic antifoulants.

Anchoring mechanisms must also be considered at risk to fouling. The depth to which photosynthetically active light can penetrate the marine environment is greater in the open ocean, so the fouling community is likely to be mixed biofilm, animal and algal up to a depth of around 200 meters, below which animals will dominate. As food availability is so low in the open ocean, and decreases with depth, the density of fouling organisms that can be supported is likely to be very low. However, any solid structure in an almost dark, three dimensional liquid environment has great potential to act as a magnet for life.

FLUID DYNAMICS

The third niche described above, that of the immersed vertical sides facing into the flow of currents, was cited as most likely to impact the plastic collecting performance of the Array.

There are two major factors to consider: first, whether the booms are fouled with a biofilm or with macrofouling; and second, the size distribution of the plastic particles being gathered. In the case of only a biofilm being present, the slimy polysaccharide matrix that houses the microbes can be very sticky and will pose a larger problem than the smaller particles of plastic. It is very possible that even in the absence of macrofouling, sufficient small particles of plastic will clump and stick to the biofilm, subsequently becoming biofilmed themselves. A macrofouled Array will have greater potential to entrap larger plastic particles. The plastic may become integrated with the fouling assemblage and increase the surfaces available for colonization and affect its structural integrity. Instead of plastic debris smoothly progressing with the current along the smooth surface of the boom in the direction of the capture apparatus, it will accumulate on surface features created by marine life and/or become 'stuck' to a biofilm. The shear strength of flow across the array will be related to the incidence angle of the boom arms to the prevailing current flow. Of course, all marine fouling assemblages are different and exist in different oceanographic conditions, but a general estimate is that the critical current velocity for many species to reach their maximum biomass is 0.2 to 0.5 meters per second. If this critical limit is exceeded the biomass tends to decrease rapidly. This is a generalization, as many fouling species prefer shelter from flow while others require flow to feed, for example.

5.3.3. POSSIBLE COMBAT STRATEGIES

The two best strategies to combat fouling are antifouling coatings and cleaning. These approaches work best when used together and both have significant cost implications.

The author knows of no unmanned open ocean structures. Manned structures in shallower waters, such as oil rigs, are able to be cleaned by divers and mobile structures are able to move to locations where they can more easily be accessed for cleaning. Mobile structures are designed to cut through the water with hydrodynamic efficiency. The hydrodynamics of a vessel are very well understood and are factored into the design of antifouling coatings. The flow velocities experienced by a ship's hull are likely to be far greater than those passing across the Array. As such, the Array will be an experiment to reveal how a fouling assemblage might develop on a fixed position, unmanned, open ocean structure. Limited nutrients may constrain algal growth and too few larvae may encounter the surface for a fouling community to grow. Animal life may not be able to acquire sufficient appropriate food to grow and reproduce. It is possibe that growth will be slow enough to be manageable, flow will be able to dislodge all attached species, or that a sustainable cleaning regime will allow the Array to function. However these are best-case scenarios and are improbable. A good design will necessarily allow for a range of scenarios to ensure that the project is not lost.

ANTIFOULING COATING OPTIONS

There are three solutions, each with pros and cons. The table below summarizes these solutions and estimates of average prices. However, these prices are for marine vessels and may differ depending on the structure being coated and the customer (for instance, a shipping company is likely to get lower prices with a fleet of vessels than for a single project). The data also assumes that the structure would be made from metal, as data is mostly available from the shipping industry.

Coating Type	Pros	Cons	Cost (in Euros)
No coating	Anticorrosive ('A/C') primer only	Likely structure will become heavily fouled, rate of which will depend on fouling intensity in that area. Regular cleaning necessary to keep the fouling off (maybe every 2-3 months)	A/C primer is around €5 / l and one liter covers about 4 m³ at the recommended dry film thickness (150 μm). Coating one square meter would cost about €1.25.
Fouling Release ('F/R') coatings - (these coatings rely on flow to dislodge, or 'release', the fouling)	Environmentally friendly. Easy to clean (Some owners have started to use it on stationary marine structures as it's easy to clean compared to biocidal coatings). Recoat options are easy, if existing finish is in good condition, another finish coat can be simply sprayed on top.	This type of coating will foul quickly if not cleaned regularly (approximately every 2 - 3 months). If the fouling challenge is low, the time between cleans can be extended. If cleans are not done properly, and the surface is scratched, performance will drop off and more frequent cleaning will be necessary. F/R coatings are soft, so likely to be easily damaged by sharp pieces of plastic. Will likely require sufficient flow across the structure to slough off the fouling (i.e. comparable to shipping speeds)	Scheme is: Foul-release Top Coat (2 options, A or B (B is top quality performance and longevity)) – 1 coat x 150μm A/C primer – 2 coats x 150 μm Intermediate (attaches the primer to the top coat) – 1 coat x 100μm Primer costs around €33/l and 1l covers 5.7 m³ Intermediate costs around the same and covers 4.8 m³ Top coat costs around €50/l and 1l covers around 4.9 m³ The 'A' scheme would cost €14 /m³ The high performance 'B' scheme, would cost €18 /m³
Biocidal coatings	Cheaper than F/R coatings. Likely to work for longer on static structures.	For re-coat options, three coats of finish need to be applied. Harder to clean. Leaches biocides into the sea.	Scheme is: A/C primer – 2 coats x 150μm Intermediate – 1 coat x 100μm Biocidal top coat – 3 coats x 125μm. This is biocidal technology that has been established for years. The outlook is simple, the more biocidal coating that is applied, the longer it lasts. Three coats should be enough for five years. Intermediate paint costs around €4/l and covers 5.7 m³ Top coat costs around €14/l and covers 4.3 m³ Total cost is therefore approximately €11 /m³.

Table 5.4 Antifouling coating options

This table does not include the cost of application, which must be performed by professionals in appropriate facilities. Each coating of paint has a specific application process and needs time to cure before subsequent coatings can be applied. Application costs will vary with location due to labor costs, the costs of land to accommodate a large scale project, and any applicable customs fees.

SURFACE CLEANING

The best antifouling strategies combine coatings with cleaning. Ships are typically cleaned with brush carts or jet sprays, close to the shore in dry docks and/or by divers. Cleaning ships can cost tens of thousands of US dollars even in an accessible location, because of the professional employees and facilities necessary. It is unknown whether cleaning companies would consider travelling to a remote location to clean the Array in situ, but this would significantly increase the cost. A cleaning rotation could be added to the procedure for the collection of plastic gathered by the Array.

If not in situ, the Array would need to be detached and returned to a shipyard, harbor or other facility for professional cleaning before redeployment. This would be very costly.

Another option is to use a robot to continuously groom the Array surface. Such machines exist and are designed to deploy on the sides of large metal ships that are staffed. They can be monitored, collected during bad weather and cleaned when moving parts stop working due to fouling. This approach is therefore not considered viable for the Array.

5.3.4. CONCLUSIONS

An effective and cost-efficient solution to biofouling needs to be designed and deployed as part of the project to avoid later problems with structural damage, additional weight, mechanical blockage etc. In terms of costing, € 14/m² will be used as a base case, while the best-case scenario will be set at € 11/m², and the worst-case scenario at € 18/m².

STORMS AND IMPACT

JOOST DE HAAN • BOYAN SLAT

The array is designed for operation at 95% up-time; hence, design loads have been based on a significant wave height of 5.5 m. This is based on the wave climate data produced by BMT Argoss, which is more conservative than the data calculated in chapter 2 (which indicated an H_s of 4.5 m in more than 95% of the time). In the first part of this chapter, two examples of storm condition management are illustrated. Later, a short note on collision impact during operation is included.

UNCOUPLED

60 M STRIP
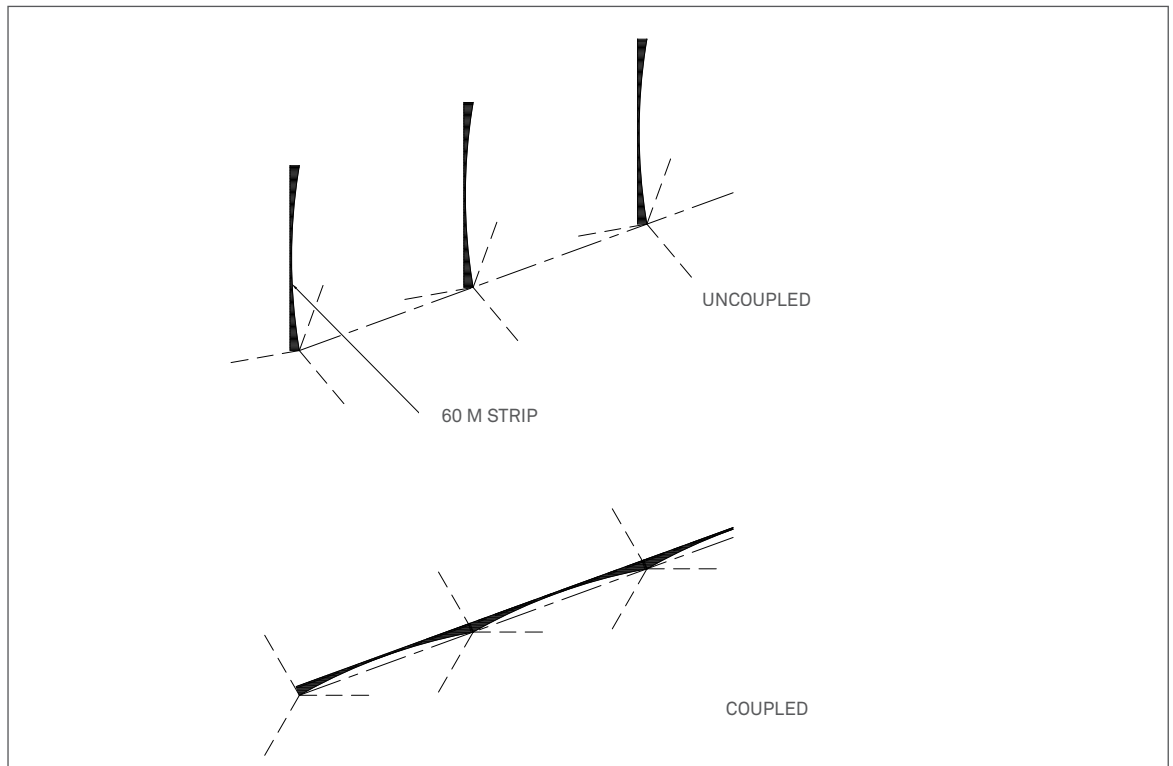
COUPLED

Figure 5.5 Boom sections, uncoupled during storm (above) and coupled in normal condition.

5.4.1. STORM CONDITIONS

For the structure to survive the amount of axial loads in extreme conditions, it could either be dimensioned for the forces it will have to endure during a 100-year storm (H_s = 12.2 m), or strategies could be implemented which would compromise the primary function of the device while reducing the amount of forces on the structure. Since we expect the capture efficiency to be low in extreme conditions due to the expanded vertical distribution, it has been decided that the device will not operate in these conditions. The two force-reducing strategies that have been identified are:

- Sinking the booms to a depth at which they are less affected by the waves
- Semi-decoupling the booms, so that they are able to orient in the direction of the waves and winds, reducing dynamic loads

Because the first strategy would involve a major redesign of the booms, and would likely require complex systems to flood and re-inflate the barriers, we further investigated the second strategy in this chapter, divided into two options:

OPTION 1
The boom sections will be installed with an attachment to the tension cable every 60 m. During a storm these individual booms could be disconnected from the connection cable (attached to the tension cable) at one side of the boom (see Figure 5.5). This disconnection is initiated by a breaking pin, designed to fail when the booms' maximum design load has been crossed, causing it to uncouple. This way, the decoupling procedure can be executed without any human interference. Furthermore, the connection cable will always stay at the water surface and the boom section is free to float along the wave direction, reducing loads on the booms, and therefore also reducing loads on the tension cable and connection cables.

WIRE TO PULL BACK
STRIP AFTER STORM
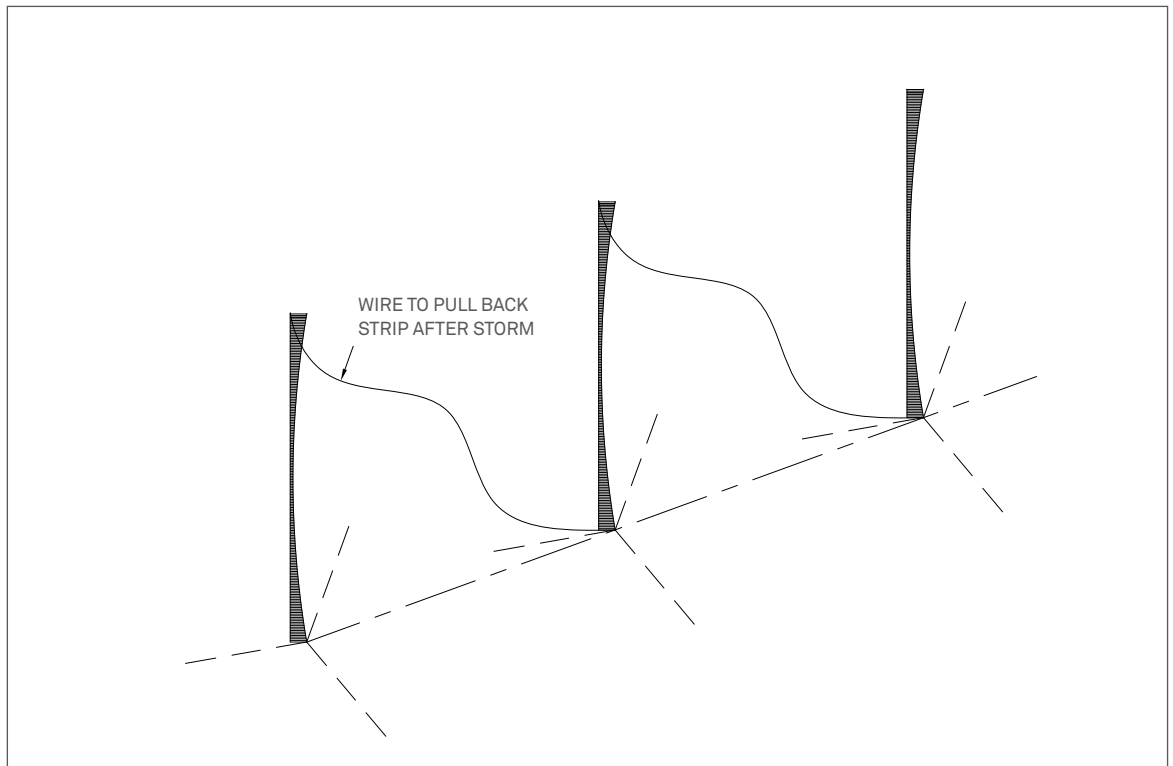
Figure 5.6 Boom configuration option with rope connecting the free end of a strip to the beginning of the adjacent rope

However, assuming the recoupling of the booms would not be done automatically, the challenge would be to recouple the over 1900 boom segments in a matter of days. Another option is to apply a winch which pulls the strip to its original position again but this is also unfavorable since it would require many winches, resulting in greater power consumption and more intensive maintenance.

Another variant could be a wire/rope which connects the free end of the strip to the beginning of the strip next to it, long enough for the strip to still move along the wave direction (Figure 5.6). This rope can be pulled from a boat to bring the strip back to its original position. In this variant, the boat does not have to sail the strip to its correct position since it will be pulled automatically to its correct position. An additional advantage is that no ROV is required for this operation.

OPTION 2

The second option would be similar to the first one, but instead of decoupling individual booms, entire 4000 m-long mooring-to-mooring segments would be decoupled. This still reduces the loads on the structure, but would reduce the amount of time needed to recouple, since it would now only constitute 29 elements that would have to be recoupled. The disadvantage would be that more force would be necessary to pull the boom back into its position.

The required bollard pull can be limited by the forces caused by the current and waves, by first dragging the boom against the current while the boom has a small surface area, followed by pulling the boom in the direction of the buoy to which it should be recoupled.

To recouple, the underwater buoys attached to the moorings could be jacked up to the sea surface, the tension cables could then be attached to the buoys without the need of ROVs, after which the buoys could be jacked down again to a depth of 30 m.

COLLISION IMPACT

The Array will be equipped with visual beacons, as well as radar reflectors, to increase its chances of being detected by vessels in its vicinity. Additionally, an active system (Automatic Identification System and/or radio) can be used to broadcast the Array's position.

Even though measures will be taken to prevent conflicts, a crossing by a vessel cannot be ruled out entirely. In the current concept, the tension member and submerged buoy are placed at about 30 m below the water surface, preventing any damage to the most expensive part of the boom. The modular structure ensures that only a limited length of boom would need replacement. If such an incident occurs, it is expected that a maximum of 120 m of floating barrier (two 60 m sections) would have to be replaced.

5.4.2. CONCLUSIONS

Events such as collision or operation in storm conditions require solutions that reduce the amount of resulting downtime. In this chapter several potential solutions have been described. The concepts presented here will significantly lower the chance of severe loss in structural integrity.

Additional research on this can be done during the following project phases, with particular focus on optimizing the costs between engineering for more extreme conditions (increasing capital expenditures), or requiring more operations to recouple sections (increasing operational expenditures).

ENVIRONMENTAL IMPACTS

For the project to be a worthwhile venture, contributing to a better environment, the benefits should naturally significantly outweigh the costs of the project. The removal of plastic from the oceans using nets would likely harm the aquatic ecosystem and emit vast amounts of carbon dioxide. The Ocean Cleanup hypothesizes this could be avoided by using the passive system described in Chapter 3. This chapter aims to quantify the impact of the array on the environment.

INTRODUCTION

ROBBERT ZUIJDERWIJK • KATHERINE SCHMIDT MARK VAN DIJK

Plastic pollution has a profound impact on sea life (Chapter 1). There are benefits to sea life from removing some of this plastic, however it is necessary to look holistically at the impact of the cleanup operation on the environment as well. The solution to the plastic problem should not be worse than the problem itself and therefore, in this chapter, an analysis of the impact of The Ocean Cleanup Array on the oceanic ecosystem is included. It is estimated that although The Ocean Cleanup Array can have a significant influence on local ecologic properties, precautions have been taken to ensure that biomass removal is limited.
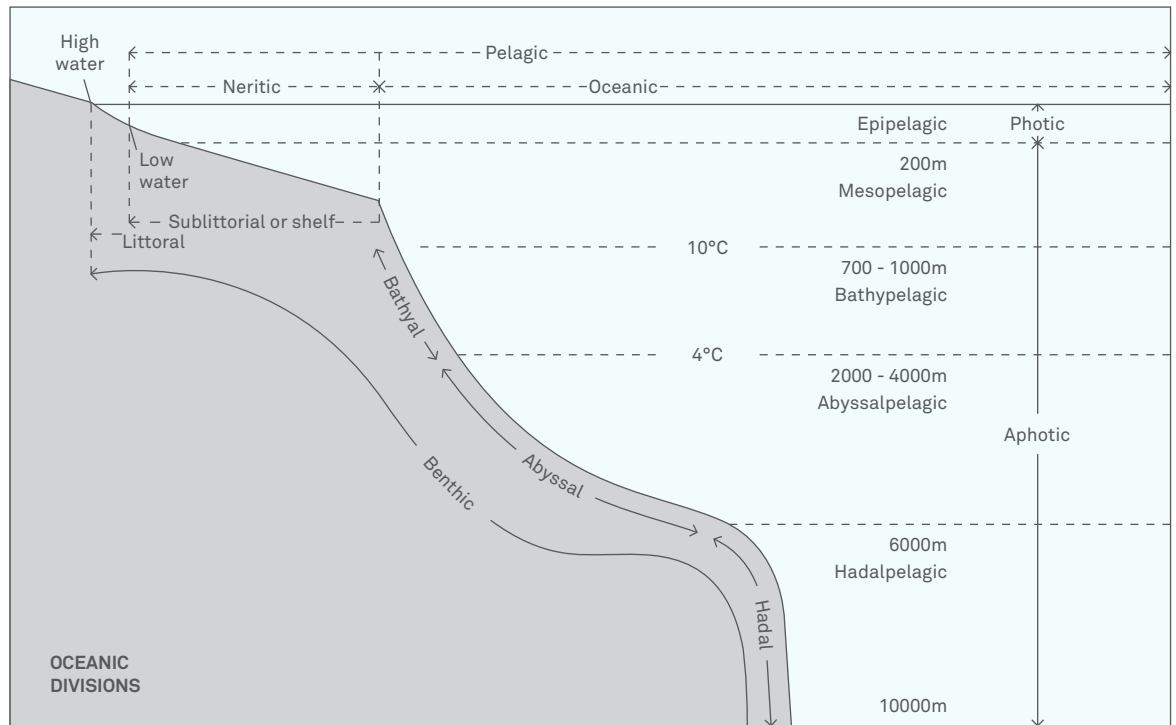
Figure 6.1 Overview of oceanic divisions. The Ocean Cleanup Array will float on the surface, affecting the photic zone (0 - 200 m) directly. Image from Wikipedia.

6.1.1 ECOLOGY OF THE OCEAN

The world's oceans cover about 71% of the surface of the Earth and contain 97% of the planet's water (NOAA). The largest portion of the ocean consists of the pelagic zone and can reach depths of over 10 km (Figure 6.1). Most oceanic research however is focused on the upper 200 meters of the water column, known as the euphotic or epipelagic zone, where enough light penetrates the water to enable photosynthesis. The mesopelagic zone stretches from 200 to 1,000 meters below the surface. Together these zones are home to the ocean's primary producers, phytoplankton, which are estimated to fix 40% of the atmospheric carbon through photosynthesis (Falkowski, 1994). They are the foundation of the oceanic food web and play an important role in the structure of the pelagic system (Adjou, Bendtsen, & Richardson, 2012). Therefore, phytoplankton bycatch by the Ocean Cleanup Array, which will interact with the surface part of the epipelagic zone, has the potential to have an effect on other marine organisms. Additionally, removal of larger animals would also impact their populations and local ecology in a more direct way.
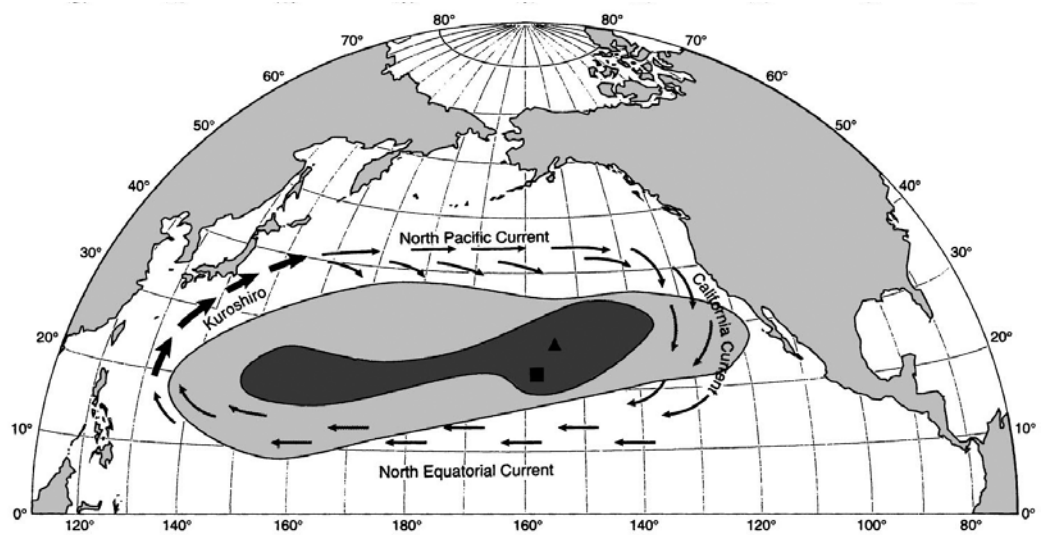
Figure 6.2 Map of the North Pacific Ocean showing several important features of the NPSG. Major circulation patterns define the approximate boundaries of the NPSG. Redrawn from (McGowan, 1974) and (D. M. Karl, 1999). Sampling stations ALOHA ( ) and CLIMAX ( ) are nearest to the proposed location for The Ocean Cleanup Array ( ) and therefore serve best to estimate the ecologic impact of the array.

6.1.2 THE NORTH PACIFIC SUBTROPICAL GYRE

The Ocean Cleanup Array will be placed within the North Pacific Subtropical Gyre (NPSG), in what is known as 'The Great Pacific Garbage Patch'. The NPSG is the largest ecosystem on the planet and extends from approximately 15°N to 35°N latitude and 135°E to 135°W longitude (Sverdrup, 1942). Due to the size of the NPSG, it exhibits physical, chemical, and biological variability on a variety of time scales (D. M. Karl, 1999). The NPSG is characterized as an oligotrophic or nutrient-poor area, and primary production is thought to be strongly nutrient limited (Hayward, 1987). Furthermore, global climatic phenomena such as ENSO (El Niño / Southern Oscillation (Stenseth et al., 2003)) and PDO (Pacific Decadal Oscillation (Mantua & Hare, 2002)) have profound effects on the abundance of primary producers (Bouman et al., 2011). These phenomena change sea surface temperature (SST) and cause eddies and fronts, inducing horizontal and vertical mixing of cold and warm waters. This forcing has implications for the distribution and abundance of primary producers in the NPSG (Polovina, Howell, Kobayashi, & Seki, 2001). These are factors that should be taken into account when assessing the influence of The Ocean Cleanup Array on marine life.

Efforts to make repeated measurements of key parameters in the same area within the NPSG resulted in the founding of the Hawaiian Ocean Time-Series (HOT), situated at Station ALOHA (A Long-term Oligotrophic Habitat Assessment, 22°45'N, 158°W) (D. M. Karl & Lukas, 1996) and measurements in the CLIMAX-area (28°N, 155°W) (Venrick, McGowan, Cayan, & Hayward, 1987). The passive cleanup of the NPSG's plastic will take place at approximately 31°N, 142°W (Figure 6.2). As these locations are all situated in roughly the same ecological area, HOT and CLIMAX data might be used to predict faunal composition at the site of The Ocean Cleanup Array. Furthermore, remote sensing of photosynthetic pigments using satellites can provide accurate data on the concentration of phytoplankton in the ocean (Peloquin et al., 2012).

PHYTOPLANKTON

ROBBERT ZUIJDERWIJK • NATHAN WALWORTH

KATHERINE SCHMIDT • TADZIO HOLTROP

Most of the phytoplankton present in the NPSG consist of autotrophic bacteria (cyanobacteria) that obtain their energy through photosynthesis; around 90% of the photosynthetic pigment chlorophyll a present in the NPSG is contributed by these bacteria (Li, M., Letelier, & Church, 2011). These species vary in size from 0.2 to 2 μm, with species of Synechococcus measuring ~1.0 μm (Johnson & Sieburth, 1979) and Prochlorococcus spp. ~0.6 μm (Chisholm et al., 1988). Samples taken during HOT cruises found Prochlorococcus spp. cells to account for 98% of total phytoplankton cell count (Campbell & Vaulot, 1993). In nutrient poor areas, smaller organisms tend to dominate biomass because of their larger surface-to-volume ratio (Raven, 1998). Cells larger than 8 μm were seldom observed in samples taken at Sta. ALOHA (Andersen, Bidigare, Keller, & Latasa, 1996).

Cyanobacteria are present all year, but satellite, ship, and mooring data also reveal recurring phytoplankton blooms during summer (Dore, Letelier, Church, Lukas, & Karl, 2008; Wilson, 2003). These blooms can stretch out over an area of 350,000 km² and persist for up to 4 months (Wilson, 2003). The blooms are distinct from the seasonal chlorophyll cycle in time and magnitude and are consistently centered around 29 - 31°N, although variability in longitudinal positioning was observed. Because of its natural buoyancy, population densities are greatest at depths of between 20 and 40 m. However, during low wind regimes extensive surface blooms of Trichodesmium spp. can occur (Capone, Zehr, Paerl, Bergman, & Carpenter, 1997). During surveys near 28°N and Sta. ALOHA, blooms were observed that primarily contained Rhizosolenia spp. diatoms, hosting nitrogen-fixing endophytes, and Trichodesmium spp. (Dore et al., 2008; D. Karl et al., 1997; Wilson, 2003). Mats of these species can become up to several centimeters in length. Blooms provide an input of organic and inorganic nutrients as well as a habitat for other phytoplankton, (cyano) bacteria, protozoa, fungi, hydrozoans and copepods (Capone et al., 1997). It is estimated that nitrogen fixation provides more than half the nitrogen demand in the NPSG ecosystem and can account for a net sequestering of CO_2 (Capone et al., 1997; Church et al., 2009; Dore et al., 2008; D. Karl et al., 1997).

ORGANISM CONDITION	CELL CONCENTRATION (10^6 CELLS.ML^{-1})	CARBON*	NITROGEN*	PHOSPHORUS*
Prochlorococcus MED4				
P-replete	110 (5)	45.8 (4.0)	9.4 (0.9)	0.98 (0.19)
P-limited	56 (4)	60.9 (1.8)	9.6 (0.07)	0.34 (0.08)
Student's t	-	$p < 0.01$	NS	$p < 0.01$
Synechococcus WH8012				
P-replete	54 (11)	92.4 (13.3)	20.0 (2.7)	1.84 (0.13)
P-limited	49 (10)	132 (6.2)	20.6 (2.0)	0.46 (0.17)
Student's t	-	$p < 0.01$	NS	$p < 0.01$
Synechococcus WH8103				
P-replete	11 (0.6)	213 (7.3)	50.2 (1.8)	3.34 (0.51)
P-limited	31 (4)	244 (20.7)	39.8 (3.8)	0.81 (0.01)
Student's t	-	$p < 0.1$	$p < 0.05$	$p < 0.01$

* in fg.cell^{-1} | NS = Not significant ($p > 0.1$)

Table 6.1 Cellular carbon, nitrogen, and phosphorus in axenic cultures of Prochlorococcus marinus MED4 and Synechococcus WH8012 and WH8103 in P-replete or P-limited conditions (Bertilsson et al., 2003)

6.2.1 PHYTOPLANKTON ABUNDANCE

There are two ways to calculate the amount of biomass present in the water of the NPSG; extrapolation of chlorophyll a measurements obtained from satellite data, or by using the rate of carbon incorporation: the primary production. These methods are described below as Method 1 and Method 2, respectively.

METHOD 1

The MAREDAT dataset has been used to estimate the phytoplankton abundance in the top 5 meters of the water column. According to this dataset, chlorophyll a concentrations in the top 5 meters was on average 0.107 mg m^{-3} (Peloquin et al., 2012). HOT program data suggests that the amount of chlorophyll a in the water column changes with seasons and with depth. There are two different reasons; increased chlorophyll a per cell to capture more light in winter, and increased total chlorophyll a as a result of more cells during spring (D. M. Karl, 1999). Estimating photoautotrophic biomass from chlorophyll a is rather inaccurate, even with remote sensing techniques (D. M Karl & Dobbs, 1998). To estimate the amount of biomass present in 0.107 mg m^{-3} chlorophyll a, this value can be converted to bacterial cell count with the formula postulated by Bird & Kalff:

log AODC = 5.867 + 0.776 * log chlorophyll a (Bird & Kalff, 1984)

AODC (Acridine Orange Direct Count) is the number of bacteria per milliliter and chlorophyll a is in micrograms of chlorophyll a per liter:
5.867 + 0.776 * log 0.107 = 5.11, then
log 5.11 = 0.708 bacteria per milliliter in the top 5 meters of the water column.

Bacterial cellular content has been determined previously for Prochlorococcus MED4 and Synechococcus WH8012 and WH8103 in a phosphorus-limited environment (Table 6.1) (Bertilsson, Berglund, Karl, & Chisholm, 2003), similar to the current state of NPSG waters (D. M. Karl et al., 1995).

METHOD 2

Another option to assess the influence of The Ocean Cleanup Array on phytoplankton abundance is to determine the net reduction in primary production. Primary production is considered to be the rate at which inorganic carbon is incorporated into organic compounds. Because phototrophic organisms also use some of these compounds for their own metabolic processes, the primary production mentioned here is the net primary production. During a 9 year monthly observation period performed at Sta. ALOHA, primary production varied between 219 and 1055 mg $C.m^{-2} d^{-1}$ for a water column of 200 meters depth (D. M. Karl, 1999). Using a production of approximately 6 mg $C.m_{-2} \cdot d^{-1}$ (Figure 6.3) and a mean carbon flux of 14.5 mol $C.m^{-2}$ annually (Table 6.1, Karl,1999) or 476 mg $C.m^{-2} d^{-1}$ it is calculated that approximately 6 percent of total primary production takes place in the top 5 meters of the ocean's surface.

6.2.2 PHYTOPLANKTON BYCATCH ESTIMATIONS

The world's oceans are estimated to produce 48.5 petagrams ($Pg=10^{15}$ g) carbon annually (Field, Behrenfeld, Randerson, & Falkowski, 1998). The total size of the Pacific Ocean is $165*10^6$ km² (Encyclopedia Britannica) with the NPSG making up approximately $20*10^6$ km² (12.1% of the Pacific Ocean) (Sverdrup, 1942). The total width of The Ocean Cleanup Array is 100 km, the average speed of the water current in this part of the gyre is estimated at 0.14 m / s^{-1} (Chapter 2.4.3) and the booms extend up to 3 meters below the surface. The area of water flowing through The Ocean Cleanup Array per day equals the array width times the ocean surface current speed ($m \cdot d^{-1}$): $1.0*10^5$m * 0.14 $m.s^{-1}$ * 3,600 sec * 24 hours = $1.21*10^9$ m² day^{-1}, or 1210 km² day^{-1}.

Relative to the total NPSG surface, this area equals: 1210 km² d-1 / $20*10^6$ km² * 100% = $6.05 *10^{-3}$ % of total NPSG surface water each day, or 2.21% annually.

A conservative estimate of the amount of water that flows through the entire array per day equals the array's width times the array's depth times the ocean surface current speed ($m.d^{-1}$): $1.0*10^5$ m * 3 m * 0.14 $m.s^{-1}$ * 3,600 seconds * 24 hours = $3.63*10^9$ m³ d^{-1}

Phytoplankton bycatch can be estimated by at least two methods, as explained below:

METHOD 1

According to the remotely sensed chlorophyll a value of 0.107 mg m^{-3}, the top 5 meters of NPSG waters contain on average 708 bacteria per liter. Multiplying with the amount of water passing through the platform gives the amount of bacteria that come into contact with the array: $708*10^3$ bacteria m^{-3} * $3.63*10^9$ m³ $d.^{-1}$ = $2.57*10^{15}$ bacteria / day.

98% of picoplankton cells from samples taken at station ALOHA were found to be Prochlorococcus spp. (Campbell & Vaulot, 1993). Multiplying the amount of this bacterium with its elemental constitution (Table 6.1) gives an estimate of the total amount of cyanobacterial phytoplankton biomass that comes into contact with The Ocean Cleanup Array for the elements C, N, and P per day in both femtograms and grams. The results of the calculation can be found in Table 6.2.

To estimate annual cyanobacterial bycatch daily flow of this species is multiplied by 365 days:

For carbon (C), this is 156.52 * 365 = 57.13 kg
For nitrogen (N), this is 24.67 * 365 = 9.00 kg
For phosphorus (P), 0.87 * 365 = 0.32 kg
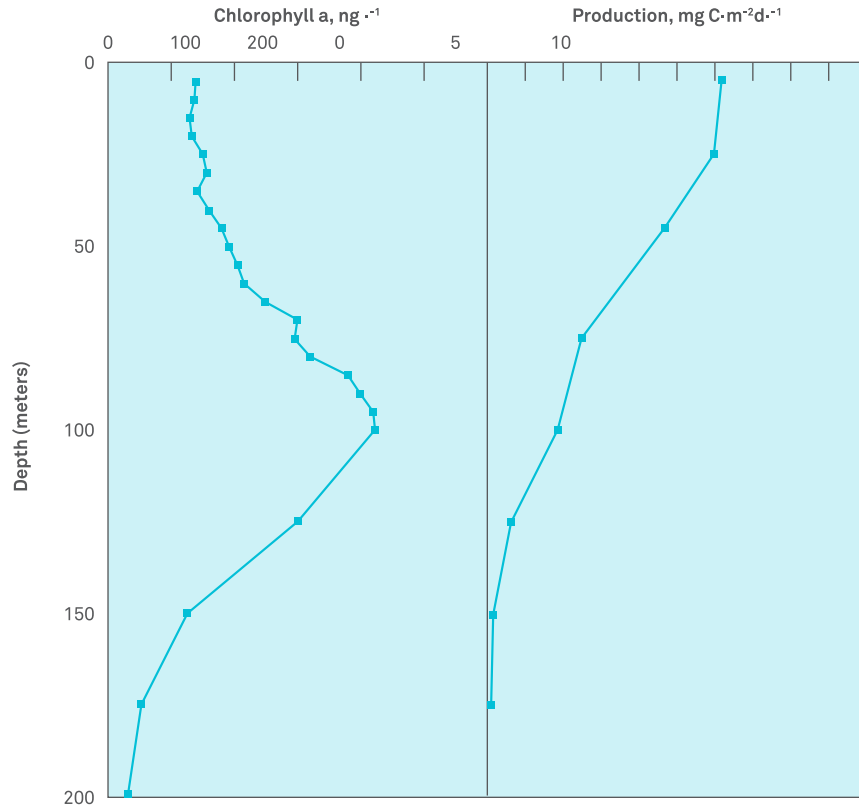
Figure 6.3 Left: Chlorophyll a (ng·l⁻¹) vs. depth; right: primary production (mg C·m⁻²·d⁻¹) vs depth. In the top 5 meters the primary production is about 6 mg C·m⁻²·d⁻¹. Image from Karl, 1999.

METHOD 2

Under the previously explained assumption that 6% of the total primary production in NPSG euphotic zone occurs in the first 5 meters of the water column, the part of the primary production that comes into contact with the array equals the daily water flow times the net primary production in the top 5 meters:

Primary production of 219 mg $C*m^{-2}*day^{-1}$ equals $219*10^6$ mg $C*km^{-2}*day^{-1}$.

Therefore, the daily primary production of water flowing through The Ocean Cleanup Array equals:

Minimum: 1210 km² / day * $219*10^6$ mg C / km² / day * 6% = $15.9*10^9$ mg C, or $15.9*10^3$ kg carbon daily

Maximum: 1210 km² / day * $1055*10^6$ mg C / km² / day * 6% = $76.6*10^9$ mg C, or $76.6*10^3$ kg carbon daily

Therefore annually, a body of water with a net primary production between $58.0*10^5$ and $280*10^5$ kg carbon flows through The Ocean Cleanup Array.

PROCHLOROCOCCUS, P-LIMITED		BACTERIAL CELL COUNT	TOTAL BIOMASS (fg)	TOTAL BIOMASS (g)
Carbon content*	60.9	$2.57*10^{15}$	$1.57*10^{17}$	156.52
Nitrogen content*	9.6	$2.57*10^{15}$	$2.47*10^{16}$	24.67
Phosporus content*	0.34	$2.57*10^{15}$	$8.74*10^{14}$	0.87

* in fg*cell $^{-1}$

Table 6.2 Calculation of the mass of C, N, and P captured daily by The Ocean Cleanup Array

WORST CASE SCENARIO

Assuming a total loss of all phytoplankton that comes into contact with The Ocean Cleanup Array, estimated phytoplankton biomass loss is 66.4 kg (C+N+P) annually. The primary production achieved by this amount of biomass is estimated between $58.0*10^5$ kg and $280*10^5$ kg annually.

When expressed as a percentage of total oceanic production within the NPSG, this is:

$58*10^5$ kg / $48.5*10^{15}$ g * 100% = $1.19*10^{-5}$ % minimum
$280*10^5$ kg / $48.5*10^{15}$ g * 100% = $5.77*10^{-5}$ % maximum

BEST CASE SCENARIO

Because the boom skirts are designed to generate a downward current, most phytoplankton is expected to escape capture by the booms. The fraction of phytoplankton captured in front of the booms might also be consumed by zooplankton, leading to a (partial) recycling of nutrients within the ecosystem. However, the phytoplankton that is drawn directly into the platform by the slurry pump is assumed to be removed from the ecosystem entirely.

The slurry pump in the design has a capacity of 300,000 l*h-1, and is expected to be in operation 8 hours per day. The amount of water drawn in by the pump then equals:
300,000 L*h-1 * 8h *d^{-1} = 2,400,000 L*d^{-1}

The fraction of contact water that passes through the processing platform equals the 8 hour pump capacity divided by total water flow through the array:
2,400 m³ d^{-1} / $36.29*10^8$ m³ d^{-1} = $6.61*10^{-7}$

Where $36.29*10^8$ m³*d^{-1} is the total daily volume that comes in contact with the array.

Multiplying the estimated biomass loss with this factor gives the biomass losses caused by the platform's pump:
For carbon, this is 57.13 kg * $6.61*10^{-7}$ = $3.78*10^{-5}$ kg
For nitrogen, this is 9.00 kg * $6.61*10^{-7}$ = $5.96 * 10^{-6}$ kg
For phosphorus, 0.32 kg * $6.61*10^{-7}$ = $2.11 * 10^{-7}$ kg

Multiplying this factor with the net primary production of the water passing through the platform gives the annual loss of primary production caused by the pump:
Minimum $58.0*105$ kg C $* 6.61*10^{-7} = 3.8$ kg carbon per year

Maximum $280*105$ kg C $* 6.61*10^{-7} = 18.5$ kg carbon per year

As mentioned, phytoplankton blooms of Rhizosolenia spp. and Trichodesmium spp. temporarily increase primary production during summer. Because of their temporary nature, bycatch of these producers is difficult to predict, however, the effects of their presence should not be underestimated. One mediating factor in bycatch during bloom conditions is that Rhizosolenia spp. mats show extensive vertical migration in the central North Pacific gyre during which they acquire nitrate at depth and resurface for photosynthesis (Dore et al., 2008; Singler & Villareal, 2005). This would allow them to pass under the booms unscathed. Trichodesmium spp. is also capable of vertical migration through ballasting with dense carbohydrates accumulated during photosynthesis at the surface (Capone et al., 1997). Accumulation of Trichodesmium spp. in front of the booms might attract other pelagic life such as zooplankton grazers, and in this way impact the food web indirectly. The impact of The Ocean Cleanup Array on zooplankton species will therefore be assessed in the next paragraph.

ZOOPLANKTON

**MARLEEN ROELOFS • MORITZ SCHMID
ROBBERT ZUIJDERWIJK**

Plankton (singular plankter) is a diverse group of organisms that live in the water column and have limited ability to swim against a current. This definition encompasses many species from bacterial phytoplankton and fish larvae to mollusks and crustaceans. In this paragraph, size classes as defined by Omori (1985) (Omori & Ikeda, 1985) will be used (Table 6.3).

There are three factors related to zooplankton that need to be taken into consideration when estimating the amount of bycatch by the Ocean Cleanup Array. These are the species diversity, their biomass and the vertical distribution of the zooplankton.

TYPE	SIZE	EXAMPLES		SOURCE
Picoplankton	0.2 - 2 µm	Bacterial phytoplankton		wikimedia.org
Nanoplankton	2 - 20 µm	Small Diatoms; algae		botanyjohn.org
Microplankton	20 - 200 µm	Protozoa; Rotifera		wikimedia.org
Mesoplankton	0.2 - 2 mm	Cladocera, Ostracoda		wikimedia.org
Macroplankton	2 - 20 mm	Euphausiacea (krill); salps		wikimedia.org
Megaplankton	> 20 mm	Jellyfish		wikimedia.org
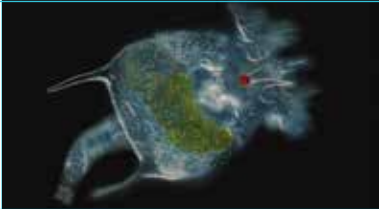
6.3.1 ZOOPLANKTON ABUNDANCE

Two important representatives of zooplankton occur in the top 7 meters of the water column (PICES); Euphausiacea, or krill (10 – 20 mm; macrozooplankton), and Copepods (1- 2 mm; mesozooplankton). Abundances of these groups vary considerably over the years (Figure 6.4)

The experimental site Sta. ALOHA at 22.45°N, 158°W is currently the best available predictor of the ecological environment at the location of the array placement. In recent years, an increase in mesozooplankton biomass has been reported there (Sheridan & Landry, 2004). A continuation of this trend would imply current biomass amounts of 1.7 g(dry)/m² for night tows and 1.15 g(dry)/m² for daytime tows (Figure 6.5).
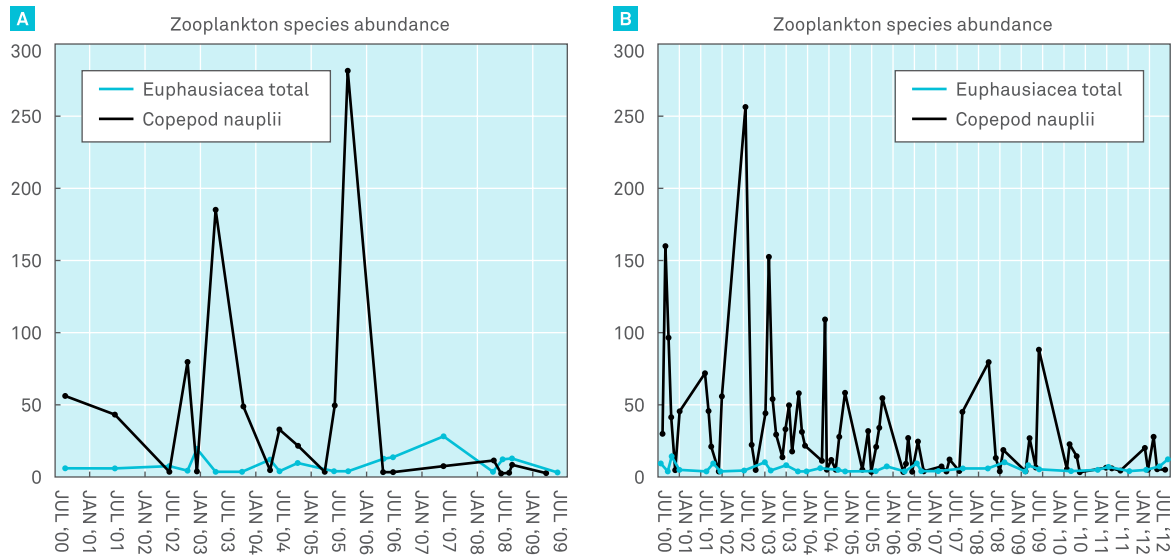
Figure 6.4 Population densities of euphausiacea and copepoda in samples taken at Western North Pacific, 165°E, 50°N (A) and offshore British Columbia, 140°W, 55°N (B). ("The Continuous Plankton Recorder Survey of the North Pacific,") Source: http://www.pices.int/projects/cpr ; Pacific CPR data collection is supported by a consortium for the North Pacific CPR survey coordinated by the North Pacific Marine Science Organisation (PICES) and comprising the North Pacific Research Board (NPRB), Exxon Valdez Oil Spill Trustee Council (EVOS TC), Canadian Department of Fisheries and Oceans (DFO) and the Sir Alister Hardy Foundation for Ocean Science (SAHFOS).

However, the results shown were obtained from oblique tows to the base of the euphotic zone (for methods, see (Landry, Al-Mutairi, Selph, Christensen, & Nunnery, 2001)), and do not represent the upper 3 meters of the ocean. Older studies have reported higher zooplankton standing stocks, ranging from 1.5 g/m² in winter to 30 g/m² in summer, with near shore waters found to have a very high standing stock of up to 1,600 g/m² in summer and fall for a water column up to 500 m deep (Cooney, 1986). Due to natural variations in zooplankton over time and large differences in abundance between coastal waters (where most zooplankton biomass measurements take place) and the oligotrophic ocean, bycatch estimations for The Ocean Cleanup are difficult to generate.

6.3.2 ZOOPLANKTON DIVERSITY

The North Atlantic species Calanus finmarchicus winters in deep water and returns to the surface in the spring to feed and reproduce, while the Pacific species N. cristatus, N. plumchrus and E. bungii, mature near the end of the winter. The growth rates of these copepods are strongly correlated with the blooming of phytoplankton. The coupling between grazers and phytoplankton is so intense that for large portions of the North Pacific Ocean, the evidence for the annual phytoplankton bloom is a sizeable increase in zooplankton rather than the phyto-plankton itself (Cooney, 1986). Recently, microzooplankton grazing was estimated to be as high as 60-75% of daily phytoplankton production (Landry & Calbet, 2004).

6.3.3 ZOOPLANKTON VERTICAL DISTRIBUTION

Zooplankton range in size from several microns up to a few centimeters, and have size specific adaptations to ensure their survival. Plankton size largely determines their ability to swim in a specific direction or their confinement to passive drifting with oceanic currents*. Most zooplankton is negatively buoyant and therefore has to swim in order to avoid sinking (Haury & Weihs, 1976). Other species such as chaetognaths employ specialized oil sacks to increase buoyancy (Kapp, 1991). It is conceivable that larger organisms such as jellyfish are able to deal with the viscous forces and swim away from the array, but smaller plankton might not. This microzooplankton might be swept under the booms, potentially suffering damage from contact with the array, while larger organisms are able to successfully swim away from potential harm.

Lastly, zooplankton migrates vertically in the water column following a circadian rhythm, a process known as Diel Vertical Migration, or DVM. Together, these processes are of major influence to bycatch by The Ocean Cleanup Array.
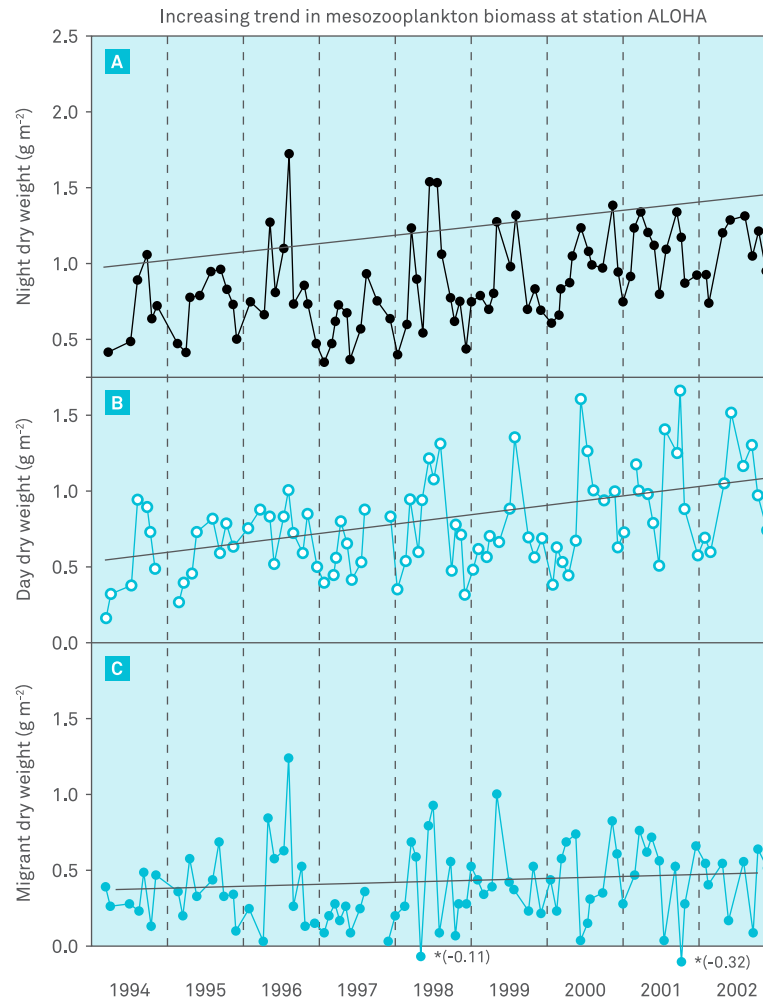
Figure 6.5 Mesozooplankton dry weight biomass measured at Sta. ALOHA from 1994 to 2002. Mean biomass for mesozooplankton collected during the night (A), day (B), and biomass of migrating mesozooplankton (night-day, C) are shown. Linear regressions for each plot (dashed lines) in g(dry)/m² are: (A, night): 1.62×10^{-4} *d + 0.458; (B, day): 1.23×10^{-4} *d + 0.204; (C, migrant): 3.92×10^{-5} *d + 0.257. Insets are the unstandardized residuals from each regression (g*DW*m^{-2}) vs. time (days). Image from Sheridan, 2004.

*Apart from gravity and buoyancy, a body moving in water experiences two forces: inertial forces and viscous forces. Inertial forces are related to momentum and viscous forces are related to the tendency of the fluid to resist deformation. In hydrodynamics, this is the Reynolds number (Stokes, 1851).

L is the length of the body (along the flow direction), the speed of the body, the fluid density and μ the fluid viscosity. The Reynolds number for small organisms is low (small L) and therefore they experience high viscosity in seawater, whereas larger organisms with higher Reynolds numbers experience mainly inertial forces, and thus continue to move after exercising the swimming motion. Most zooplankton live at the transition between viscous and inertial forces, coping with the advantages and drawbacks of both regimes.
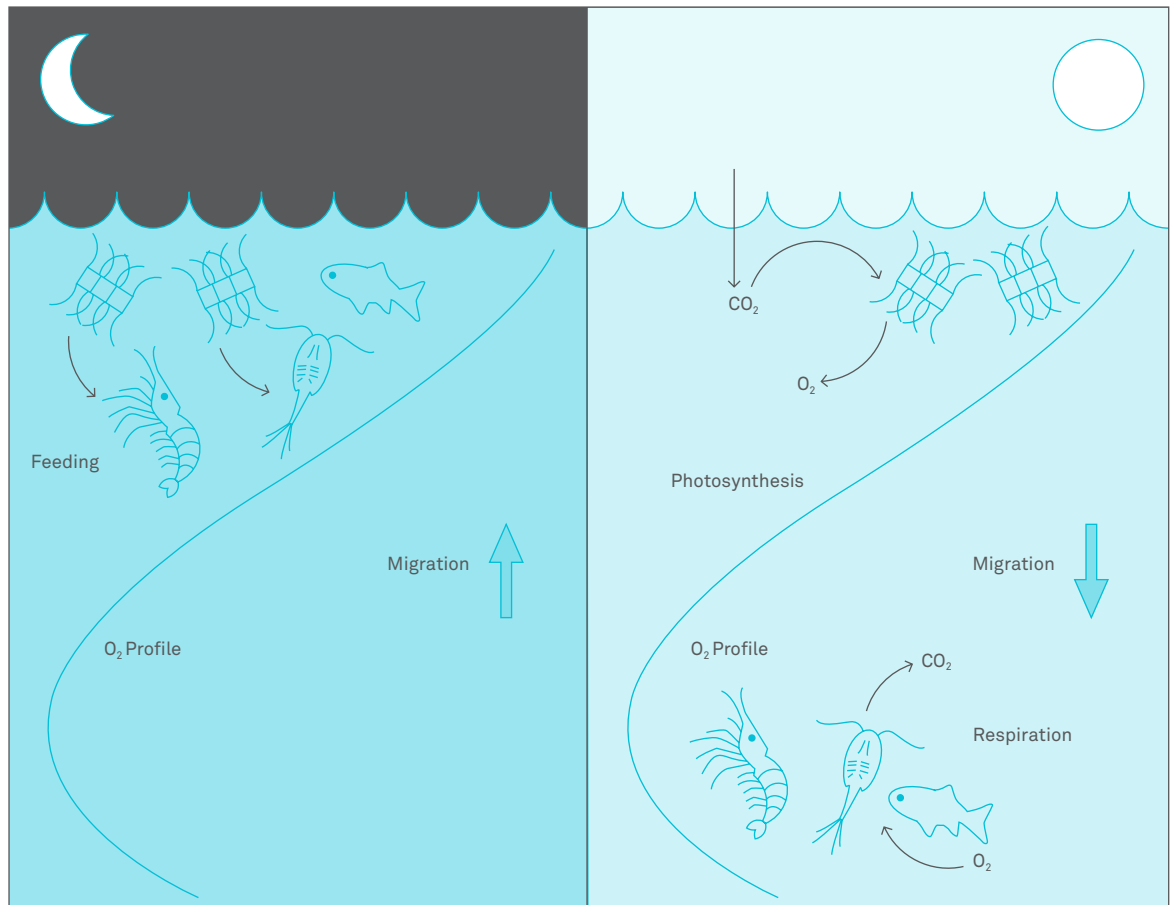
Figure 6.6 Diel Vertical Migration. Image from (Doney & Steinberg, 2013)

6.3.4 DIEL VERTICAL MIGRATION (DVM)

DVM is the largest synchronized migration of biomass on a global scale (Berge et al., 2009) and has been investigated thoroughly (Liu & Sun, 2010; Lo, Shih, & Hwang, 2004). It describes the vertical redistribution of zooplankton species during the day-night cycle and can be cued by different triggers (e.g. light intensity (Cottier, Tarling, Wold, & Falk-Petersen, 2006)). A generally accepted hypothesis is the predator-avoidance hypothesis, which states that zooplankton graze at the food-rich surface during night but remain at a greater depth during the day to avoid predation by organisms that hunt by sight (Hays, Harris, & Head, 2001) (Figure 6.6).

The pattern of DVM (e.g. depth, surfacing time) varies between zooplankton species (Lo et al., 2004) and with different developmental stages (Liu & Sun, 2010). Timed samples taken at different depths suggest that migration extends to the surface of the ocean, with zooplankton density highest between 9 PM and 2 AM (Figure 6.7). A study on the dynamics of Euphausia pacifica demonstrated that certain developmental stages rise to the top 5 meters of the water column at around 3 AM (Liu & Sun, 2010). It should be noted that these surveys were carried out in March and May, possibly omitting any changes in migration time and depth due to seasonality.
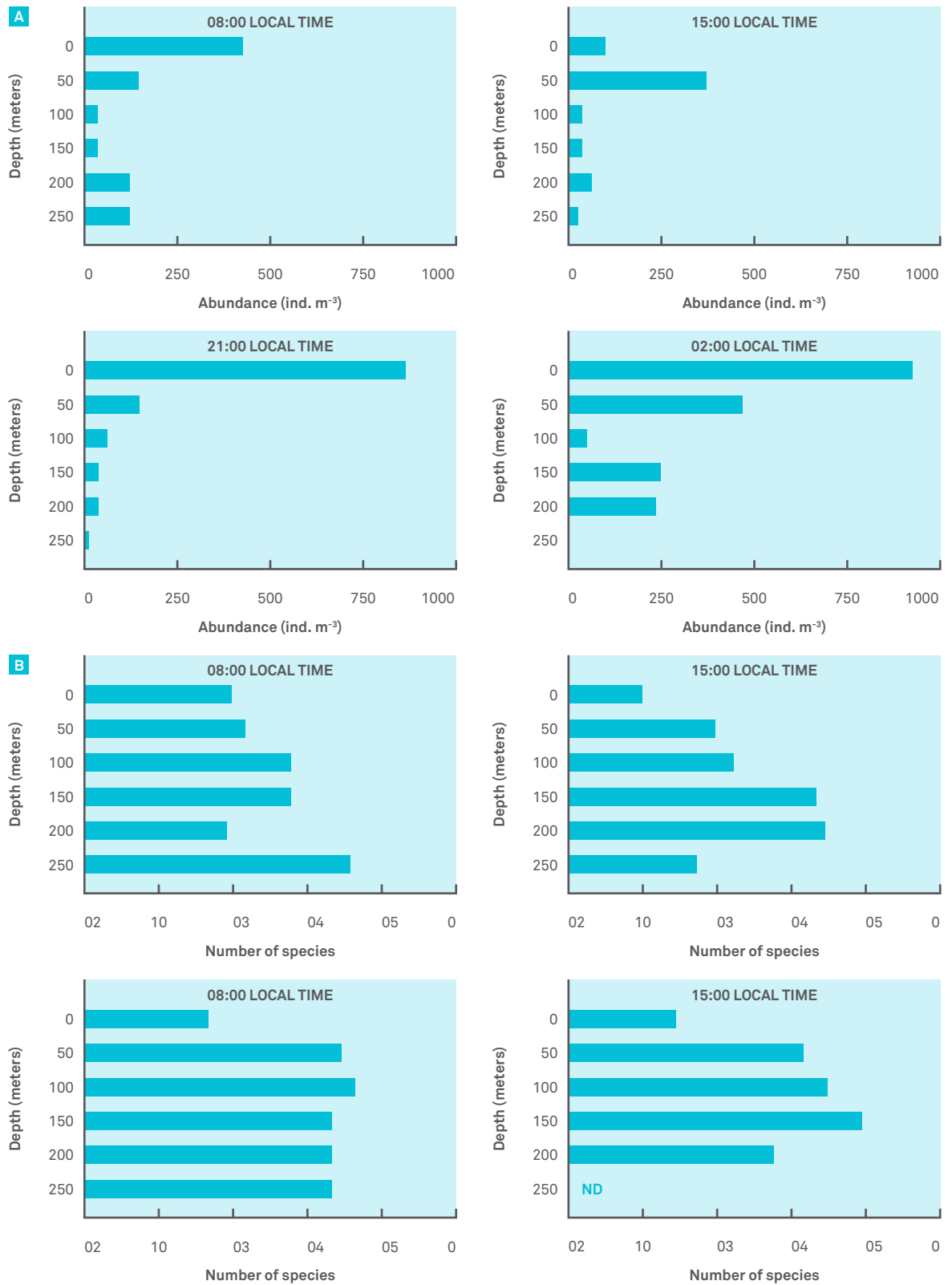
Figure 6.7 Diel Vertical Migration of zooplankton. Box A: Species abundance (individuals m⁻³) at different time steps. Box B: Number of species at different time steps; ND = no data (Lo et al., 2004).

6.3.5 ZOOPLANKTON BYCATCH ESTIMATIONS

Zooplankton bycatch estimations are difficult to generate. One way of estimating zooplankton abundance is by correlating zooplankton biomass with phytoplankton biomass. Data analysis of plankton assemblages from 12 globally distributed areas suggests that in areas with low phytoplankton biomass (such as the NPSG during non-blooming conditions), microzooplankton (2-200 μm) biomass is on average 20% of phytoplankton biomass (Irigoien, Huisman, & Harris, 2004). Following the phototrophic biomass estimations of 380 μmol $C*m^{-3}$ posed by Karl, 1999 (D. M. Karl, 1999):

380 μmol $C*m^{-3}$ * 0.20 = 76 μmol $C*m^{-3}$ for zooplankton ranging between 2 and 200 μm in size.

The amount of water that flows through the entire array per day equals the array's width times the array's depth times the ocean surface current speed ($m*s^{-1}$):
$1.0*105$ m * 3 m * 0.14 m s-1 * 3,600 seconds * 24 hours $= 3.63*10^9$ $m^3 *d^{-1}$

$3.63*10^9$ m^3*d^{-1} * 76 $μmol*Cm^{-3} = 2.76*10^{11}$ μmol C, or $2.76*10^5$ mol C

Multiplying this number with the molar weight of carbon gives the total amount of carbon biomass:
$2.76*105$ * 12.011 g / mol $= 3.31*10^6$ g carbon, or $3.31*10^3$ kg carbon.

Assuming that carbon makes up 40% of total zooplankton dry weight (Omori, 1969), this amounts to a total biomass of:
$3.31*10^3$ kg / 0.40 $= 8.28*10^3$ kg (dry) of microzooplankton biomass that flows under The Ocean Cleanup Array daily. Annually, this amounts to $3.02*10^6$ kg biomass.

This calculation does not take into account plankton larger than 200 μm, so these have to be estimated in a different way. Surface trawls performed using a manta trawl with an opening of 0.9 m * 0.15 m and a mesh size of 333 μm within the NPSG found a mean dry weight biomass of 841 g/km² zooplankton (Moore, Moore, Leecaster, & Weisberg, 2001). Samples taken were evenly distributed between day and night-time hours in August. Biomass variation due to seasonality is therefore not taken into account.

The amount of surface water flowing through the platform in km² multiplied by the concentration of plankton in the surface trawls gives an estimate of surface plankton dry weight mass that might be collected daily:
1210 km² * 841 g(dry)/km² $= 1.02*10^6$ gram (dry), or $1.02*10^3$ kg (dry) daily

The plankton concentrations were obtained using a mantra trawl with an opening height of 0.15 m. The booms of The Ocean Cleanup Array will extend 3 meters into the water. Assuming an equal concentration of plankton in the top 3 meters of the ocean surface, the amount of biomass that might be caught equals:
$1.02*10^3$ kg * (3/0.15) $= 2.03*10^4$ kg (dry) biomass daily, or $7.43*10^6$ kg annually

Combining the zooplankton fractions together, the estimated amount of zooplankton biomass that comes into contact with The Ocean Cleanup Array is:
$3.02*10^6$ kg + $7.43*10^6$ kg $= 1.04*10^7$ kg

WORST CASE SCENARIO

Assuming that all zooplankton that comes into contact with either the booms or the platform will perish, most of it will sink to the ocean floor and become available for pelagic recycling or benthic organisms instead of being pumped into the platform. So even though they are themselves killed in the process, nutrient removal from the food web is limited to the fraction of zooplankton that is sucked into the slurry pump. As a result, The Ocean Cleanup Array will likely cause a local shift in deep sea benthic processes as more planktonic remains fall to the seabed. Biomass removal by the Array will then be limited to the fraction of the amount of water that comes into contact with the array that is pumped into the platform:

$2,400 \ m^3 \cdot d^{-1} / 36.29 \cdot 10^8 \ m^3 \cdot d^{-1} = 6.61 \cdot 10^{-7}$ (daily pump volume / daily water flow through Array)
$6.61 \cdot 10^{-7} \cdot 1.04 \cdot 10^7 \ kg = 6.91 \ kg$ (dry) zooplankton biomass

6.3.6 REDUCTION OF ZOOPLANKTON BYCATCH BY THE OCEAN CLEANUP ARRAY

The amount of bycatch will be highest during the night when zooplankton surfaces to graze on phytoplankton (Lo et al., 2004). To reduce bycatch, platform pumps could operate 8 hours a day and be switched off at night. This enables the zooplankton to surface during the night, forage on phytoplankton and afterwards sink below boom depth.

Lastly, recent studies on plastic transfer between trophic levels showed that microplastics can enter the food chain through ingestion by microzooplankton and can then be transferred to higher trophic levels (Setälä, Fleming-Lehtinen, & Lehtiniemi, 2014). Considering these observations and the likelihood of increased concentrations of microplastics in the NPSG, zooplankton bycatch might even serve to remove plastic-laden organisms from the food web.

VERTEBRATES

ROBBERT ZUIJDERWIJK

After array deployment, plastic concentrations near the platform will increase until equilibrium has been reached; where the influx of plastic particles equals particle removal by the array. Inherent to this equilibrium state is a higher density of plastic in front of the booms and near the platform. As the plastic has been in the ocean for some time, at least some of the plastic will be colonized by microorganisms (Carson, Nerheim, Carroll, & Eriksen, 2013). Furthermore, a percentage of positively buoyant phytoplankton and zooplankton (pleuston/neuston organisms) will accumulate in front of the array. This will create an oasis in the middle of a nutrient-starved oceanic desert, attracting other oceanic life.

The first group that might be attracted to the platform-associated nutrient gradient is the group of filter feeders. This could include species of fish, sharks and/or whales, which are known to feed near the surface (Bannister, 2008; McKinnell & Dagg, 2010; Sims, 2000). The presence of these filter feeders near the platform could have a recruiting effect on other marine organisms.

The booms will also trap ghost nets, fishing lines and other large (>50 cm) pieces of plastic, in which other types of prey species might be entangled. Entrapment in these floating bodies usually contributes to an early death of the entrapped animal, but the trapped animal thereby also serves as a potential food source for other, free-swimming predators. These predators could include fish, sharks, whale species, as well as marine birds, dolphins and sea turtles. Seals are excluded from this assessment as they inhabit coastal areas, and the array will be too far from the mainland to be reached by these animals.

Data on the prevalence of marine vertebrates in the North Pacific Subtropical Gyre is scarce. Therefore, all vertebrates known to inhabit the North Pacific are assumed to come into contact with the platform. The platform might serve them as shelter from the wind, by providing shadow or as a nutritional Walhalla. The novelty and area of platform placement make it impossible to estimate the ecological impact, and therefore its impact can only be assessed after the array is in operation. However, laws dictate that bycatch of fisheries should be reduced as much as possible (see Chapter 8 of this report).

According to these definitions, all vertebrates collected by The Ocean Cleanup Array are considered bycatch, and efforts should be made to prevent this. A small amount of bycatch is inherent to the platform's operation, for instance when animals trapped in a ghost net enter the platform and subsequently perish. Vertebrates present close to the platform pose the biggest problem. Here, they run the risk of injury or death from the moving parts of the conveyer belt or the slurry pump. Furthermore, because plastic particles are concentrated in front of the platform, the risk of plastic consumption is also highest in this area.

STUDY	OCEAN REGION	SPECIES	REDUCTION IN BYCATCH (%)*
Kraus et al. 1997	Gulf of Maine	Harbor porpoise (Phocoena phocoena)	92
Trippel et al. 1999	Bay of Fundy	Harbor porpoise	68-85
Larsen 1999	North Sea	Harbor porpoise	93
Gearin et al. 2000	Washington State	Harbor porpoise	90-93
Bordino et al. 2002	Argentina	Franciscana dolphin (Delphinus franciscana)	85
Barlow & Cameron 2003	California	Short-beaked common dolphin (D.delphis)	85

* Change in bycatch between nets with and without pingers.

Table 6.4 Results of experiments to determine marine mammal bycatch reduction in set and drift gill nets (Cox, 2007).

6.4.1 BYCATCH SOLUTIONS

Currently there is no solution available to harvest ghost nets weighing several hundred kilograms while simultaneously locking out vertebrates larger than ~50 cm, and therefore vertebrates must be deterred from the platform in a different way. In the past, a scientific approach was taken to bycatch reduction in commercial fisheries. This has resulted in the use of nets fitted with turtle exclusion devices (TEDs), acoustic devices ("pingers"), and changes in hooks and bait, resulting in significant bycatch reduction (Table 6.4) (Cox et al., 2007). Other means might be effective as well (Southwood, Fritsches, Brill, & Swimmer, 2008).

Accidental bycatch of marine vertebrates by The Ocean Cleanup Array might be reduced in the same way. Bycatch reducing devices (BRDs) are mostly used to deter a specific species of fish, mammal or bird. Because a variety of animals is expected to accumulate in front of the platform, the BRDs should incorporate an equal variety in signals used to repel these animals, with an emphasis on repelling the species listed in the ESA. Companies such as SaveWave, that provide custom solutions for ecologic problems, will be employed to reduce vertebrate bycatch.

MOORING

The Ocean Cleanup Array will be moored to the ocean floor by Stevmanta VLA anchors from the company Vryhof Anchors. These anchors are designed to penetrate the ocean floor and cause minor disturbance to environment. On removal of the array, these anchors can be extracted from the ocean floor. As a result, no significant ecologic impact is expected from the mooring.

CARBON FOOTPRINT ANALYSIS

EVELIEN BOLLE

The main aim of the proposed project is to benefit the environment; therefore a clear requirement must be that there is no net negative impact to the environment (as mentioned in section 1.8). Inevitably, during the operations to remove, transport and treat the ocean plastics, emissions will be created and energy will be consumed. In order to get a sense of the order of magnitude of these negative effects, a carbon footprint analysis has been included in this feasibility study.

6.5.1 METHOD

6.5.1.1 DEFINING 'CARBON FOOTPRINT'

A 'carbon footprint' is a term used to describe the amount of greenhouse gas (GHG) emissions which arise from the life cycle of a product. It involves the greenhouse gases; carbon dioxide (CO_2), methane (CH_4), and nitrous oxide (N_2O), together with families of gases including hydrofluorocarbons (HFCs) and perfluorocarbons (PFCs). The use of CO_2 equivalent (CO_2 e) as a standard unit allows for the impacts from this wide range of gases to be quantified (British Standards Institution, 2008).

A 'life cycle' can be defined as the "consecutive and interlinked stages of a product system, from raw material acquisition or generation of natural resources, to end of life, inclusive of any recycling or recovery activity" (British Standard Institution, 2011; ISO, 2006).

A 'life cycle assessment' (LCA) can be defined as a "compilation and evaluation of inputs, outputs and potential environmental impacts of a product throughout its life cycle" (ISO, 2006).

A further distinction can be made between life cycle assessments which are performed 'cradle-to-gate' or 'cradle-to-grave'. A cradle-to-grave life cycle is calculated from the extraction or acquisition of raw materials to recycling and disposal of waste. A cradle-to-gate life cycle on the other hand stops at the point at which the product leaves the organization undertaking the assessment (British Standard Institution, 2011).

Carbon footprinting is a special form of a life cycle assessment. During a full LCA the climate change, social, economic and environmental impacts are assessed, whereas a carbon footprint only looks at the impact category of climate change (ISO, 2011).

This study is based on the framework set out by the BSI Publicly Available Specification (PAS) 2050. PAS 2050 is built on existing life cycle methods (BS EN ISO 14040 and BS EN 14044). The PAS 2050 framework gives requirements specifically for the assessment of greenhouse gas (GHG) emissions within the life cycle of goods and services (British Standard Institution, 2011). The method provides a powerful way for companies to incorporate emission impacts into decision making and to demonstrate environmental/corporate responsibility leadership (British Standards Institution, 2008).

The calculation of the carbon footprint consists of five steps:

Step 1: Building a process map of the product's life cycle, including all material, energy and waste flows;
Step 2: Checking boundaries and prioritization;
Step 3: Collecting data on material amounts, activities and emission factors across all life cycle stages;
Step 4: Calculating the footprint;
Step 5 (optional): Checking uncertainty to assess the precision of the footprint analysis (British Standards Institution, 2008);

6.5.1.2 GOAL AND FUNCTIONAL UNIT

The goal of this study was to perform a streamlined carbon footprint to determine the emissions associated with the removal of plastics from the ocean and the production of oil through pyrolysis out of this end-of-life plastic. Different scenarios were compared.

The functional unit is the reference unit used for the calculation of the carbon footprint (British Standard Institution, 2011). The aim of this study was to look specifically at the removal of plastics from the ocean and the treatment of the recycled plastic. The functional unit in this case was therefore taken to be the weight of 1 ton (MT) of plastic.

6.5.1.3 DEFINING THE PROCESS MAP OF PRODUCT'S LIFE CYCLE

The scope of this streamlined carbon footprint was from 'cradle to gate', which included the life cycle stages related to the plastic removal, transport, treatment of the removed plastic and the disposal of the residue (refer to Figure 6.8). These stages are summarized below:

PASSIVE CLEANUP OF THE OCEAN
Activities of The Ocean Cleanup Array to remove plastic waste out of the ocean.

LOADING/TRANSSHIPMENT
Charging of the vessel which transports the plastic to land.

MARINE TRANSPORT
Fully laden vessel sails from The Ocean Cleanup Array to land.

DISCHARGE/TRANSSHIPMENT
Offloading the cargo from the vessel.

PYROLYSIS
The end-of-life plastic is transformed into oil and residue.

DISPOSAL
Transport to dispose the residue.

No transport was taken into account after the discharge of the vessel as the pyrolysis plant was assumed to be situated in the port of arrival of the vessel.

PROCESS FLOW

| Plastic in the ocean |
| Platform Ocean Cleanup |
| Loading of the vessel |
| Marine transport |
| Discharge in harbour |
| Pyrolysis |
| Disposal of residue |
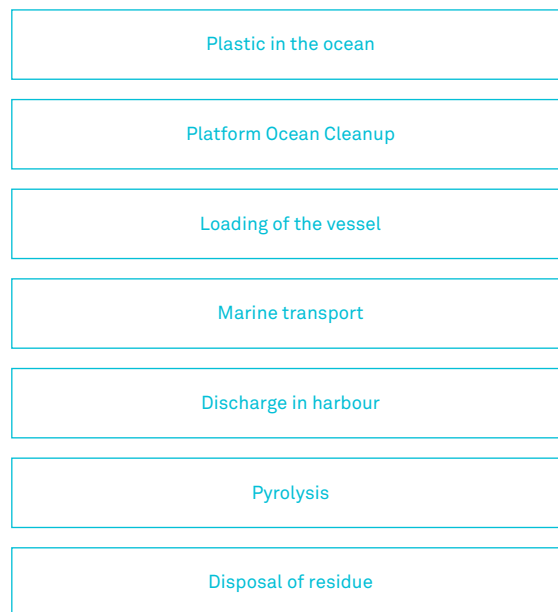
Figure 6.8 Life cycle stages

The carbon footprint is calculated using primary activity data and secondary data. Primary activity data is defined as quantitative measurements of activity from a product's life cycle that, when multiplied by the appropriate emission factors, determines the greenhouse gas emissions arising from a process (British Standard Institution, 2011).

Secondary data is defined as data obtained from sources other than direct measurement of the emissions from processes included in the life cycle of the product (British Standard Institution, 2011).

6.5.1.4 BOUNDARIES

The start point of the study was the removal of plastic from the ocean by The Array. The impact of: all activities performed on the array, transshipments, transport, final treatment of the plastic and the disposal of the residue were included.

The effect of the recovery of energy and plastics was taken into account by including the impacts avoided as a result of not having to produce these from other sources.

The startup of a pyrolysis production plant requires some external energy. This external energy was not taken into account. The production plant was assumed to be working 24h/24h and only a negligible part of the feedstock of the plant was anticipated to be plastic from The Ocean Cleanup.

No impacts were accounted for the manufacturing and the disposal of the equipment. The carbon footprint analysis focused on the process of removal and treatment of ocean plastic debris.

6.5.1.5 AVOIDED IMPACTS

The calculation of avoided burdens due to the production of fuel by the pyrolysis process was carried out on the basis of taking into account the avoided emissions of not having to extract this fuel from the ground. As stated by Khoo and Than, 2006, the estimated energy required to extract the fossil fuel from the ground was assumed to be 138 kWh/ton of oil.

6.5.2 CARBON FOOTPRINTING SCENARIOS

Eight scenarios were assessed. A distinction in the scenarios was based on the type of platform used for The Array. The first (1) type of platform considered was the SWATH Vessel platform (section 4.3.1.2.2). The second (2) type of platform considered was the Spar Buoy platform (section 4.3.1.2.3).

The carbon footprint of the Spar Buoy platform scenario was assessed once for a chartered general cargo with a transported volume of 6,000 m³ and once for a purchased vessel with a transport capacity of 8,664 m³. For the purchased vessel two different scenarios were investigated. These scenarios did have a minimum or a maximum onsite time.

The SWATH Vessel platform scenario and the four Spar Buoy platform scenarios each had two included scenarios. Two pyrolysis plants analyzed the plastic samples of The Ocean Cleanup. Each plant had its own results.

The six scenarios studied were:

1A	SWATH Vessel Platform and pyrolysis plant A;
1B	SWATH Vessel Platform and pyrolysis plant B;
2A	Spar Buoy Platform, 6,000 m³ chartered vessel and pyrolysis plant A;
2B	Spar Buoy Platform, 6,000 m³ chartered vessel and pyrolysis plant B;
2C	Spar Buoy platform, 8,664 m³ purchased vessel, minimum onsite time and pyrolysis plant A;
2D	Spar Buoy platform, 8,664m³ purchased vessel, minimum onsite time and pyrolysis plant B;
2E	Spar Buoy platform, 8,664 m³ purchased vessel, maximum onsite time and pyrolysis plant A;
2F	Spar Buoy platform, 8,664 m³ purchased vessel, maximum onsite time and pyrolysis plant B;

A presentation with the inputs of the scenarios can be seen in Figure 6.9 and Figure 6.10.

As oil is produced through the pyrolysis process, the data was compared to the emissions due to a fossil fuel reference system. For this comparison, the functional unit was taken as 1 MT of oil produced.

SWATH Vessel Platform Inputs

PROCESS FLOW

	Plastic in the ocean
Platform power generation: photovoltaic + generator (28 L/h)	Platform Ocean Cleanup
Transshipment included in platform power consumption	Loading of the vessel
Cargo capacity: 3,385m³ Fuel consumption: Sailing:3,5 MT/day DP: 1,75 MT/day 1 cycle = 28 days, 14 days plastic removal	Marine transport
Transshipment: 90 kW	Discharge in harbour
No heat input required	Pyrolysis
HVG (17 MT) transport for residue Distance 40km (20 km loaded, 20 km unloaded)	Disposal of residue

Figure 6.9 SWATH vessel platform scenario

SPAR Buoy Platform Inputs

PROCESS FLOW

|	
	Plastic in the ocean
Platform power generation: photovoltaic + generator (28 L/h)	Platform Ocean Cleanup
Transshipment included in platform power consumption	Loading of the vessel
Cargo capacity: 6,000m³ or 8,664m³ Fuel consumption: Sailing: 12 m³/day or 17 m³/day DP: 6 m³/day or 8,5 m³/day 1 cycle = 39 days or 42 days	Marine transport
Transshipment: 90 kW	Discharge in harbour
No heat input required	Pyrolysis
HVG (17 MT) transport for residue Distance 40km (20 km loaded, 20 km unloaded)	Disposal of residue

Figure 6.10 SPAR buoy platform scenario

6.5.3 CALCULATING THE FOOTPRINT

The equation used to obtain a carbon footprint is the sum of all materials, energy and waste across all activities in a product's life cycle, multiplied by their emission factors (British Standards Institution, 2008).

The emission factors and the fuel properties (density) were obtained on the website 'Greenhouse Gas Conversion Factor Repository' of the UK Department of Environment, Food and Rural affairs and are represented respectively in Table 6.5 and 6.6 (DEFRA, 2013).

The Platform's proposed power sources were through renewable energy (photovoltaics) and a diesel generator (see also section 4.5). In normal circumstances, the generator was assumed to be turning for one hour a day and was supposed to use 28 L/h. The generator was also supposed to provide the energy for the transshipment. The estimated time for the transshipment was taken as 13.5 hours/month.

When bad weather and cloud cover occurs, the generator was assumed to function as the principal power source. Accordingly, an average of three days of bad weather per month was taken into account and on each day the generator was assumed to run for three hours a day.

The fuel consumption of the vessels required for the transport of collected plastic debris was also taken into account. The fuel consumption estimated the time involved sailing and the dynamic positioning involved on-site. The fuel consumption during dynamic positioning was supposed to be half of the consumption during sailing.

The energy involved for discharge in the harbor was supposed to be provided by electricity. The harbor was assumed to be in the United States and the transshipment was supposed to make use of the same slurry pump as used for the transshipment between The Ocean Cleanup Array and the vessel. As a consequence, an equal amount of time was assumed to be needed for the transshipment.

The products of the pyrolysis obtained in the two plants were (see also Chapter 9 Processing of removed plastic debris):

1. Plant A: 17% syngas, 15% light fraction, 62% diesel fraction, 5% char, 1% water;
2. Plant B: 15% syngas, 77% marine fuel, 7% char, 1% water;

The syngas, water and light fraction obtained through the pyrolysis were recycled in the process (Fraunholcz, 2014). The produced gases that escaped and were emitted to the air were assumed to be negligible.

The transport distance between the pyrolysis plant and the disposal facilities for the char residue were estimated to be 20 km. The transport trip was assumed to be made by heavy goods vehicle (HGV) with a capacity of 17 MT. The whole capacity of the truck was supposed to be used for the char waste produced by the pyrolysis process of The Ocean Cleanup plastic debris.

6.5.3.1 ASSUMPTIONS FOR THE SWATH SCENARIOS 1A AND 1B

In both scenarios, the generator of The Ocean Cleanup Array was supposed to work for 23.75 hours in 14 days. This was the sum of one hour a day, 3 hours accounting for bad weather (1.5 days) and 7.75 hours needed for the transshipment of the plastic. As a consequence the transshipment to shore was also supposed to take 7.75 hours. As stated in 'section 7.1 the example vessel used had a capacity of 2,538 m³. The sailing speed of the vessel found on www.maritimesales.com was 10 knots, with a daily fuel consumption of 3.5 MT of heavy fuel. During dynamic positioning the vessel was supposed to use 1.75 MT of heavy fuel.

The transport of the char residue was supposed to take place in a HGV with 17 MT. A truck will only transport char originating from the pyrolysis of The Ocean Cleanup plastic debris. If the char produced due to the pyrolysis of one cycle of recycled plastic debris is less than 17 MT, the transport for disposal of the char will still take place in a 17 MT truck.

ACTIVITY	FUEL	UNIT	CO² EMISSION
			kg CO$_{2 e}$
Liquid Fuels	Diesel (100% mineral diesel)	tonnes	3188.5
	Fuel oil	tonnes	3232.7
	Petrol (average biofuel blend)	tonnes	3005.8
	Gas oil	tonnes	3427.2
	Diesel (average biofuel blend)	litres	26.0
	Diesel (100% mineral diesel)	litres	26.7
Electricity generation (US, 2013)		kWh	0.522

ACTIVITY	TYPE	UNIT	CO² EMISSION	
			kg CO$_2$ e, 0% Laden	**kg CO$_2$ e, 100% Laden**
HGV (all diesel)	Rigid (>3.5 - 7.5 tonnes)	km	0.548	0.642
	Rigid (>7.5 tonnes-17 tonnes)	km	0.655	0.840
	Rigid (>17 tonnes)	km	0.789	1.131
	All rigids	km	NA	NA
	Articulated (>3.5 - 33t)	km	0.732	1.093
	Articulated (>33t)	km	0.708	1.172
	All artics	km	NA	NA
	All HGVs	km	NA	NA

NA = Data not available

Table 6.5 Emission factors (DEFRA, 2013).

	Net CV GJ/tonne	Gross CV GJ/tonne	Density kg/m³	Density Litres/tonne
Diesel	42.90	45.70	837.52	1.194,00
Fuel Oil	40.70	43.30	985.22	1.015,00

Table 6.6 Fuel properties (DEFRA, 26/02/2013). CV = calorific value

6.5.3.2 ASSUMPTIONS FOR THE SPAR SCENARIOS 2A, 2B, 2C,2D, 2E AND 2F

The scenarios 2A, 2B, 2C and 2D supposed a transport frequency of 1.25 months. This was approximated be 39 days.

The scenarios 2E and 2F supposed a longer cycle time due to a longer on-site time (See also Chapter 4.4.5 Final concept (Plastic transshipment and transport)). The cycle time was taken as 42 days or 1.5 months. Although a longer cycle time was used, the transported amount of plastic remained the same as in the scenarios 2A, 2B, 2C and 2D. This is due to the maximum storage capacity of the SPAR buoy platform which is 6,000 m³. Half of the 6,000 m³ storage capacity is occupied by plastic and half by water.

In all scenarios the generator of The Ocean Cleanup Array was supposed to work for 63.38 hours in 39 days. This is the sum of one hour a day, 7.5 hours accounting for bad weather (3.5 days) and 16.88 hours needed for the transshipment of the plastic.
As a consequence the transshipment to shore was also supposed to take 16.88 hours.

The scenarios 2A and 2B supposed using a chartered vessel with a transported volume of 6,000 m³. The on-site time per cycle was 1 day.

The heavy fuel consumption of the proposed vessel was 12 m³/day at 12 knots sailing speed (Hupkes Wijnstra, 2014). During transshipment on-site, the vessel was supposed to only make use of dynamic positioning. A heavy fuel use of 6 m³/day was taken into account for this on-site time.

The scenarios 2C, 2D, 2E and 2F make use of the purchased vessel with a transport capacity of 8,664 m³. The purchased vessel uses 6.1 MT/day heavy fuel oil (HFO) and 0.7 MT/day marine gas oil (MGO). A heavy fuel use of 3.05 m³/day was supposed during dynamic positioning.

The scenarios 2C and 2D supposed the sailing time to be 8 days and the on-site time per cycle to be 1 day. This on-site time is supposed to be the minimum time. The vessel is supposed to anchor or have a berth in the harbor in between the cycles.

The scenarios 2E and 2F supposed the sailing time to be 8 days and the on-site time per cycle to be 32 day. This on-site time is supposed to be the maximum time. During one cycle, the ship is supposed to be sailing for 8 days, to be on-site for 32 days and to be in the harbor for discharge and loading for 2 days. Because of the maximum storage capacity of the SPAR buoy platform only 39 days of plastic removal were accounted for. The on-site dynamic positioning of the vessel is not supposed to be next to the platform as in the SWATH platform scenarios 1A and 1B. This scenario is taken into account because of economic reasons from a logistics point of view. An anchored ship or a moored ship costs a lot. It is supposed to be more economical to let the ship sail all the time (See also Chapter 4.4.5 Final concept (Plastic transshipment and transport))

Emission source	Emission (kg CO^2 e/MT plastic)							
Scenario	1A	1B	2A	2B	2C	2D	2E	2F
HFO used	547,93	547,93	323.52	323.52	213.55	213.55	642.47	642.47
Diesel (platform)	5.58	5.58	5.35	5.35	5.35	5.35	5.35	5.35
Energy used for transshipment	1	1	0.9	0.9	0.9	0.9	0.9	0.9
Transport (40 km total)	0.11	0.12	0.09	0.12	0.09	0.12	0.09	1.12
Avoided emission	-44.7	-55.5	-44.7	-55.5	-44.7	-55.5	-44.7	-55.5
Total	**-38.01**	**499.13**	**285.16**	**274.39**	**175.19**	**164.42**	**604.11**	**594.34**

Table 6.7 Carbon Footprint results for the different scenarios and the different stages.

6.5.4 RESULTS AND ANALYSIS

The carbon footprints for the different scenarios 1A, 1B, 2A, 2B, 2C, 2D, 2E and 2F are respectively 509.94 kg CO^2 e, 499.14 kg CO^2 e, 285.17 kg CO^2 e, 274.39 kg CO^2 e, 175.19 kg CO^2 e, 64.42 kg CO^2 e, 604.11 kg CO^2 e and 593.34 kg CO^2 e.

The carbon footprint of the marine transport life cycle stage accounts for the largest part of the total carbon footprint for each of the scenarios. The scenarios making use of the SPAR buoy platform and with a maximum on-site time (2E and 2F) do have the biggest carbon footprint. This is due to the continuous use of a vessel during the whole collection and transportation process. The large carbon footprint of the SWATH platform scenarios (1A and 1B) can be explained by the same cause.

The carbon footprint gives an indication of the vessels energy efficiency. The difference between the SPAR buoy platform scenarios 2A, 2B and 2C, 2D indicates that the purchased vessel is more energy efficient than the chartered vessel.

A small amelioration of the carbon footprint of the scenarios 2E and 2F can be obtained by using the whole storage capacity of the used vessel. This is possible through using the vessel on-site in the same way as in the SWATH platform scenarios. In this way a cycle time of 57 days can be used and a total amount of 1295 MT of plastic debris can be transported in one cycle.

The avoided emissions are due to the fuel produced during the pyrolysis process. Almost no difference can be observed between pyrolysis plant A and B. The tests conducted on the recycled plastic of The Ocean Cleanup re-vealed an average calorific value of 45 MJ/kg. Fraunholcz N. explained that this calorific value could be kept as an average for the produced oil true pyrolysis created from the plastic debris. It should be kept in mind that this is not exact; it depends on the water content and oxygen content in the fuel next to the carbon content (Fraunholcz, 2014). As a consequence the environmental impact due to the avoided emissions depends on the composition of the recycled plastic debris.

The carbon footprint of the platform's power consumption can still be ameliorated by making use of wind energy. When wind turbines are implemented on the platform, the use of the generator in bad weather conditions could be limited.

6.5.4.2 CARBON FOOTPRINT FOSSIL FUEL SCENARIO

The estimated energy required to extract the fossil fuel from the ground was assumed to be 138 kWh/ton of oil. Solid waste was reported as 4.97 kg/ton of oil (Khoo & Tan, 2006). The required energy was supposed to be provided by electricity. The case study was assumed to be in the United States.

The transport distance between the fossil fuel plant and the disposal facilities for the solid waste were estimated to be 20 km. The transport trip was made by a heavy goods vehicle (HGV) with a capacity of 4 MT. The whole capacity of the truck was supposed to be used for solid waste, produced by extracting fossil fuel. The carbon footprint of the extraction of oil from the ground and the disposal of the produced waste is 72.1 kg CO^2 e.

Carbon Footprint in kg CO$_2$ e per MT
removed plastic for the different scenarios
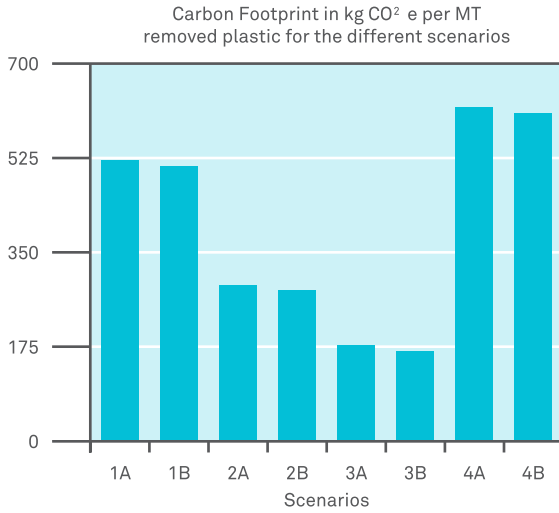
Figure 6.11 Visualization of the carbon footprint of the different scenarios and the contribution of each life cycle stage.

Contribution of each life cycle stage to the Global Warming Potential in kg CO$_2$ e per MT removed p
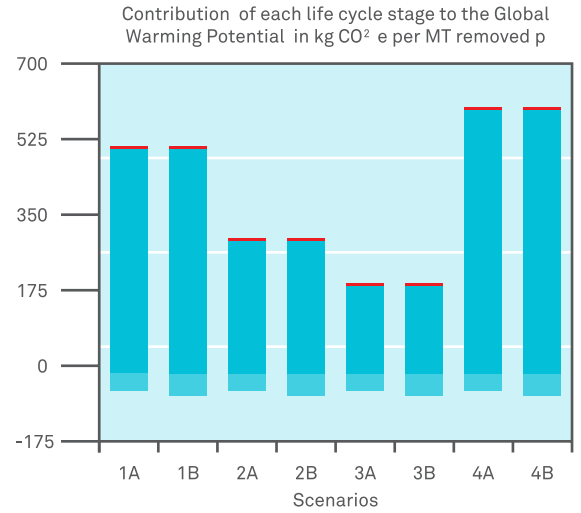
Figure 6.12 Visualization of the carbon footprint of the different scenarios

For comparison, the carbon footprint of the fossil fuel system and the different scenarios of The Ocean Cleanup are presented in Figure 6.13. It should be noted that the functional unit of the scenarios of The Ocean Cleanup was taken to be 1 MT of produced oil.

The SPAR buoy vessel scenarios with a long on-site time (2E and 2F) and the SWATH platform scenarios result in the largest carbon footprint. The SPAR buoy platform scenarios with the purchased vessel and the minimum on-site time result in the smallest carbon footprint compared to the fossil fuel scenario.

With the functional unit taken as 1 MT of oil produced, a difference can be observed between pyrolysis plant A and pyrolysis plant B. When the other input parameters are the same Pyrolysis plant A (scenarios 1A, 2A, 2C and 2E) always leads to a higher carbon footprint than Pyrolysis plant B (1B, 2B, 2D and 2F).

Carbon footprint per MT oil produced
for the different scenarios
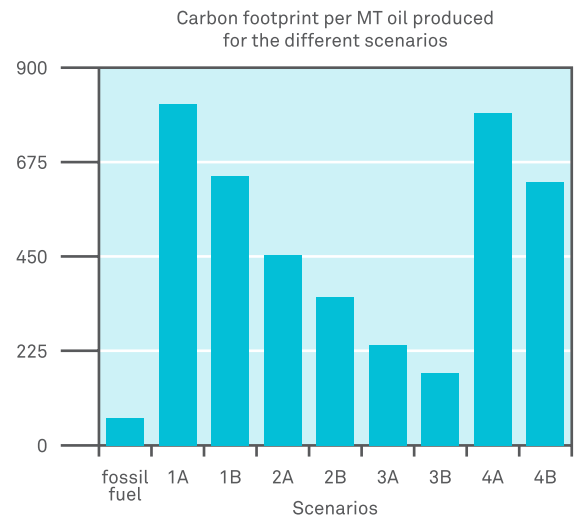
Figure 6.13 Carbon Footprint of the fossil fuel scenario and The Ocean Cleanup scenarios with functional unit 1 MT produced oil

CONCLUSIONS

ROBBERT ZUIJDERWIJK • MARK VAN DIJK

Even though most phytoplankton likely passes under the booms without touching the boom itself, assuming that in an attempt to rid the Pacific Ocean from its plastic The Ocean Cleanup Array harvests all the plankton it comes into contact with, this would annually constitute a maximum loss of $1.04*10^7$ kg of planktonic biomass. Given the immense primary production of all the world oceans ($48.5*10^{12}$ kg), it would take less than 7 seconds to reproduce this amount of biomass. However, these numbers do not incorporate the possibility of blooming conditions. Phytoplankton blooms occurring in front of The Array can have larger ecologic impact due to their size, persistence and role in the NPSG ecosystem. As zooplankton production is directly related to phytoplankton production, it is assumed that also impact on the amount of zooplankton will be negligible.

In terms of vertebrates, although harm caused by the barriers seems unlikely, there may be some bycatch where plastic is physically extracted from the water. Due to the low water volumes that are being affected in this process, this effect is likely negligible. To prevent the possible impact on vertebrates at the collection platform, active deterrents should be used near the extraction equipment, where the intake of plastic and seawater takes place. Since some of the animal deterrents have only been tested on moving ships, it is therefore advised to test these systems on a stationary platform, while carefully monitoring vertebrate presence close to this platform.

The smallest carbon footprint was obtained for the SPAR platform scenarios with a minimum on-site time. The largest carbon footprint was obtained by the SPAR buoy platform scenarios with a long on-site time. The calculation of the carbon footprint revealed that the life cycle stage 'Marine Transport' has the largest environmental impact. This impact can be reduced by limiting to a minimum the on-site time of the vessel and by using a vessel with high energy efficiency. The transportation of more plastic per vessel and per cycle could lead to a longer cycle time and a smaller carbon footprint. As the storage capacity of the SPAR buoy platform is limited, attention should be paid to the processes dewatering and size reduction.

The carbon footprint of the platform's power consumption can still be ameliorated by making use of renewable energy. Given that most carbon is produced during marine transport of the plastic (and is the only part of the process that prevents The Ocean Cleanup Array from being a carbon-negative process), local processing should be considered in the next phase.

PRELIMINARY TESTING

BOYAN SLAT • WART LUSCUERE
EZRA HILDERING VAN LITH • JAN DE SONNEVILLE

In order to validate the basic concepts that have been described in chapter 3, The Ocean Cleanup deployed a 40 m boom segment near the Azores, Portugal. Methods and observations are described in this chapter.

METHODS
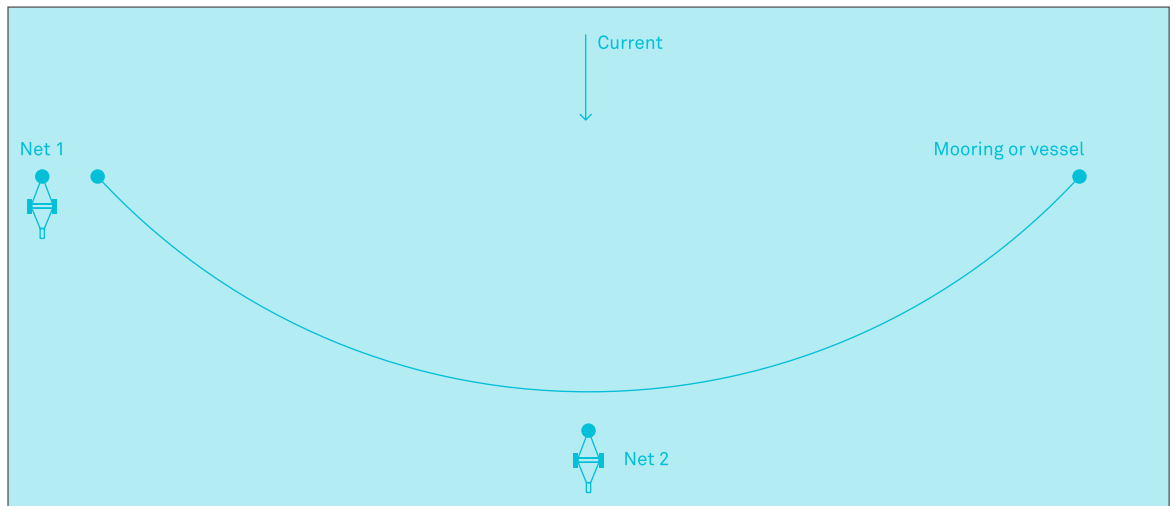
Figure 7.1 A schematic drawing of the test set-up. The large curved line represents the floating barrier, and the red dots are points where the materials are being attached to a vessel or mooring

The large scale test served as a proof-of-concept, demonstrating the interaction between a boom, plastic and zooplankton in the North Atlantic gyre. This was the largest test of a series performed by The Ocean Cleanup during the feasibility study research.

A floating barrier segment was moored in oceanic conditions, perpendicular to the prevalent current, see Figure 7.1. A large trawl (or 'net') was placed behind the barrier to capture what flowed past the barrier (net 2). A second net (a copy of the first net) was placed alongside the barrier (net 1), serving as a control. With a mesh size of 220 μm, these nets can trap zooplankton and plastics larger than this, while smaller particles such as phytoplankton would pass through. To evaluate the influence of the barrier, the measured results were then compared.

The test aimed to serve as a validation for the Computational Fluid Dynamics model (CFD). Here however, the boom and particles were subjected to variable ocean conditions that were not included in the simulations due to time constraints. Therefore, these test results improve the reliability of software-based determinations.

By measuring the volume of zooplankton caught by the floating barrier, the impact on sea life could be investigated. In chapter 6, calculations could only be made using two scenarios. In the best case scenario, the concentration of zooplankton found at the mouth of the nets would be equal to the concentration of zooplankton found in an undisturbed environment (i.e. the background concentration). In the worst-case scenario, all plankton in the top 3 m of the water column that flows through the array would be captured. By measuring the zooplankton capture efficiency it was possible to see whether the worst-case scenario was applicable. To measure zooplankton only, a mesh size was chosen that was too large to capture phytoplankton.

To conclude, a number of hypotheses were formulated to be assessed during this test:

- **HYPOTHESIS 1**
  Plastic gets trapped in front of the floating barrier.
- **HYPOTHESIS 2**
  Plastic accumulates in the center of the barrier.
- **HYPOTHESIS 3**
  Zooplankton does not get trapped in front of the floating barrier.

To confirm hypothesis 1, there must be less plastic in net 2 than in net 1.

To confirm hypothesis 2, the movement of plastic along one side of the barrier towards the center must be observed.

To confirm hypothesis 3, there must be an equal amount of zooplankton in net 1 and net 2.

FLUID DYNAMICS TOBSERVATIONS
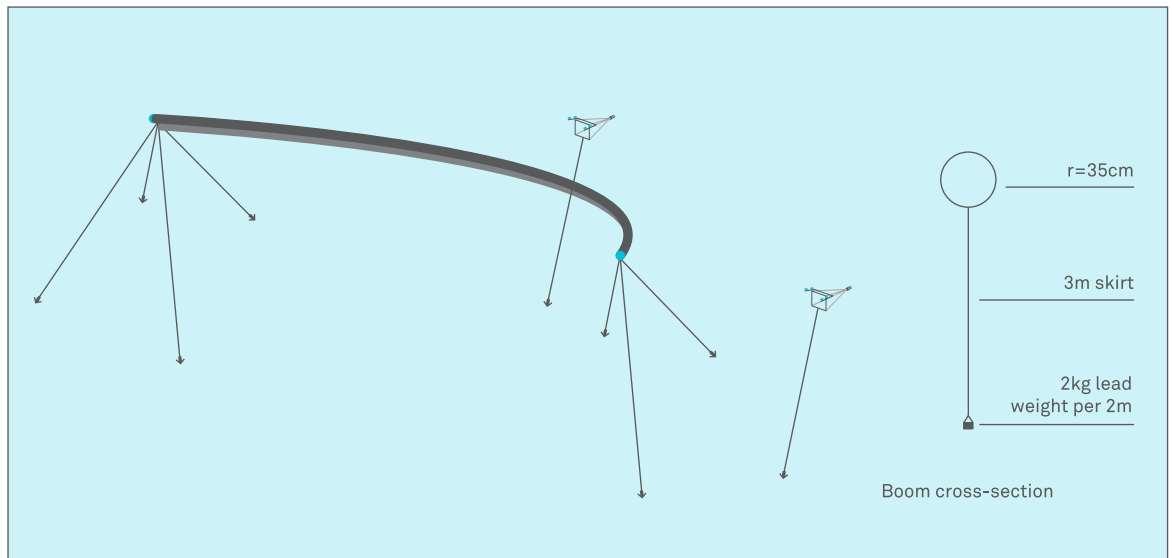
Figure 7.2 – Mooring configuration. Schematic drawing of the planned mooring configuration of the booms and trawls

The boom used in the test consisted of two segments, each 20 m in length, and featured a skirt with a draft of 3 m, and a 70 cm freeboard to provide flotation and prevent over-topping. The skirt was made of PVC-coated fabric, floatation was provided by filling the top of the boom with beach balls (70 cm diameter), and to keep the skirt vertical a 2 kg dive weight was fitted to the bottom of the skirt every 2 m. The two segments were joined together in a watertight manner (using a piece of PVC fabric, duct tape and shackles) to make one 40 m boom, which was attached to a mooring point at both sides.

The mooring points were distanced 35 m between each other, at a depth of ~25 m. As can be seen in Figure 7.2, four lines were attached to each mooring point, these were secured to the sea bed using steel grappling anchors. Both mooring points were fitted with a 0.5 m diameter buoy to compensate for the downward pulling force caused by the boom's drag force.

The samples were collected using two trawls consisting of a rectangular frame (constructed out of aluminum pipes and steel couplings) with an effective opening width of 202 cm, and an effective opening height of 356 cm (of which 300 cm is below the water line), see Figure 7.3a. The trawl net opening extended 56 cm above the water line to prevent over-topping. At the water line, fenders were attached to cross-bars of the frame for floatation and stability. Thin steel wire ropes spanned across the opening of the trawl for stiffness. The trawls were fitted with 220 micrometer nets (polyester, Top7even, the Netherlands), each measuring 8 m in length. The nets connected to a PVC cod end (30 cm diameter), fitted with a 150 x 30 cm² collection bag. Both trawls were fixed to the sea bed using a single 40 m polypropylene rope and a rock.

Figure 7.3 Trawl: a) Computer rendering of the trawl design, showing the metal frame, to which a net and fenders have been attached, b) deployment of trawl.

The boom used in the test consisted of two segments, each 20 m in length, and featured a skirt with a draft of 3 m, and a 70 cm freeboard to provide flotation and prevent over-topping. The skirt was made of PVC-coated fabric, floatation was provided by filling the top of the boom with beach balls (70 cm diameter), and to keep the skirt vertical a 2 kg dive weight was fitted to the bottom of the skirt every 2 m. The two segments were joined together in a watertight manner (using a piece of PVC fabric, duct tape and shackles) to make one 40 m boom, which was attached to a mooring point at both sides.

The mooring points were distanced 35 m between each other, at a depth of ~25 m. As can be seen in Figure 7.2, four lines were attached to each mooring point, these were secured to the sea bed using steel grappling anchors. Both mooring points were fitted with a 0.5 m diameter buoy to compensate for the downward pulling force caused by the boom's drag force.

The samples were collected using two trawls consisting of a rectangular frame (constructed out of aluminum pipes and steel couplings) with an effective opening width of 202 cm, and an effective opening height of 356 cm (of which 300 cm is below the water line), see Figure 7.3a. The trawl net opening extended 56 cm above the water line to prevent over-topping. At the water line, fenders were attached to cross-bars of the frame for floatation

and stability. Thin steel wire ropes spanned across the opening of the trawl for stiffness. The trawls were fitted with 220 micrometer nets (polyester, Top7even, the Netherlands), each measuring 8 m in length. The nets connected to a PVC cod end (30 cm diameter), fitted with a 150 x 30 cm² collection bag. Both trawls were fixed to the sea bed using a single 40 m polypropylene rope and a rock.

The Azores were chosen as the test site for the following reasons: they are located on the edge of the North Atlantic gyre and experience similar ocean conditions, while the plastic and plankton composition (but not concentration) are comparable to the chosen preliminary Pacific site. The setup was moored in Baía do Canto (near Santa Amaro on the island of Pico, Azores, Portugal), at the red dot on Figure 7.4. Specifically, this area was chosen for its depth of less than 30 meters, near absence of fishing activities, and easy access.

Figure 7.4 Pico map. Map of testing location, 38°27'13" N, 28°8'19" W

During testing, wind and waves were low (wave height H_s <1 m, whereas mean H_s North Pacific is 2.6 m), but the current was relatively strong due to the full moon. The current reversed approximately every 6 hours because of the tides (at 1 am, 7 am, 1 pm, and 7 pm). Samples were collected in periods when the current came from the correct direction (East to West), as can be seen in Figure 7.5a with the moored barrier.

The same barrier was also towed in another experiment to create an artificial current of about 30 cm s^{-1}, about double the speed of the mean current in the North Pacific gyre, see Figure 7.5b. From the boat, one buoy, one bottle, one mesoplastic fragment and one microplastic fragment were released. Visual observations of the movement of plastic particles in front of the boom were made from the boat. This plastic was later recovered by a diver, who also witnessed the plastics' behavior from under the water.

Figure 7.5 Moored barrier and pulled barrier: a) Left side, a photo of the floating barrier, moored to the seabed, b) on the right side, a photo of towing of the boom to create an artificial current using boats.

BY-CATCH OBSERVATIONS

All released plastic particles were intercepted by the boom. The plastic items deployed at the side of the boom, showed that the plastic was transported along the boom towards the center. Although no measurements could be taken of the velocity of the plastic along the boom, the plastic was already moving along the barrier with small boom angles of less than 20° (estimated).

On the 16th and 17th of March 2014, a single 21 hour trawl session was performed with both trawls. The time taken between the emptying of each cod end was less than 15 minutes and was always done in the same order.

A visual comparison of the zoo plankton found in the cod net in the lee of the barrier and the control at the side of the barrier found approximately the same amount in both nets Figure 7.6. Furthermore, no increase of zooplankton in front of the barrier was observed. This suggests that the barrier did not interfere with zooplankton popula- tions. However, changes in the direction of the current may have resulted in differing orientations of the trawls as well as interference from the boom on the control trawl's inflow. It was also assumed that turbulence from the wake of the boom did not result in vertical mixing of zooplankton. Overall this results in lower reliability of the data, the effects of which cannot be easily quantified.

Figure 7.6 Cod ends. Cod ends with its zooplankton contents, low- er or bottom one as control, and the top one from behind the boom

MOTION OBSERVATIONS

CONCLUSIONS

The influence of the environment on the shape and motion of the boom was studied and the following observations were made:

1   Under the influence of currents and waves, the boom flexed into a curved shape as expected.

2   Even in waves with a short wavelength, the boom followed the waves. No over-topping of water was observed.

3   While in the moored position, the ballast attached to the boom skirt was sufficient to maintain the vertical orientation of the skirt. However, during the towing (with speeds estimated to be between 30 and 60 cm/s), the skirt surfaced, indicating that at those speeds the amount of ballast was insufficient.

CHAPTER 7.5

The large-scale test validated the capture and concentration potential of a floating barrier with a skirt depth of 3 m, in moderate environmental conditions, and for plastic sizes ranging from large microplastics upwards.
In addition, qualitative data suggests that zooplankton does not get caught by the barrier.

The flexible floating barrier was shown to be able to follow the motion of the sea surface, thereby preventing efficiency losses of plastic due to over-topping in the tested conditions, although the wave height was significantly smaller than the average conditions in the North Pacific Gyre. During towing of the boom, the skirt surfaced at higher current speeds. Per chapter 2.6, those current conditions are rare, however it seems that the ~1 kg/m ballast is not sufficient and should be higher during real-life deployment, such as the 10 - 100 kg/m tested in chapter 3.

An experiment that excludes the effects of variable currents, such as within a river delta, is required to experimentally validate the hypothesis that the boom does not catch plankton. Furthermore, scale model tests of a floating barrier exposed to the spectrum of real environmental and mooring conditions are required to help determine a suitable amount of ballast for the barrier.

LEGAL CHALLENGES

Besides the technical and environmental requirements of The Ocean Cleanup Array, several legal topics that should also be considered. Obviously the potential for conflict with shipping traffic should be taken into account, as well as the legal designation of the platforms, and potential bycatch regulations. Interestingly, the entire operation takes place in international waters. This chapter will investigate whether any major legal hurdles should be overcome before implementation can take place.
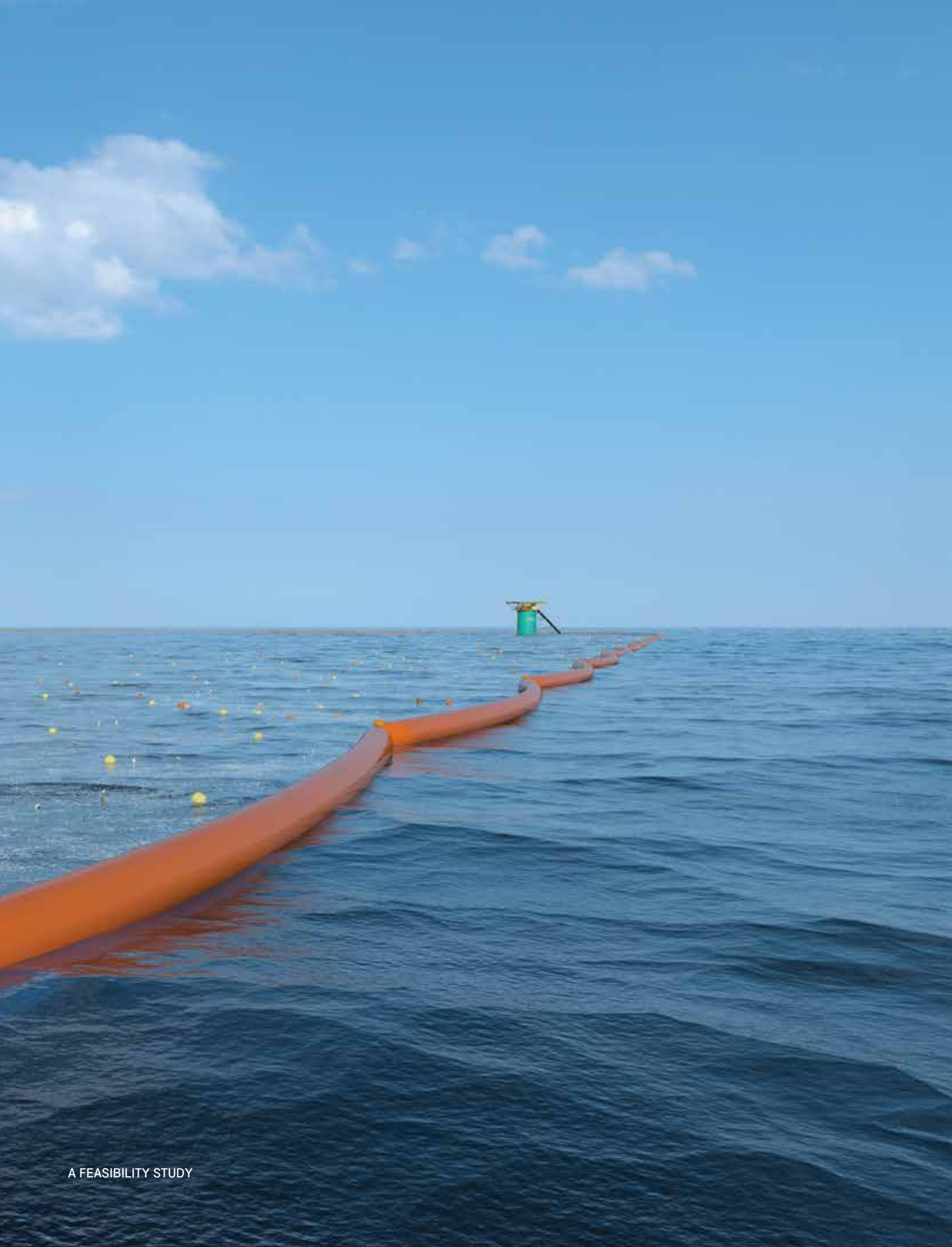
In this chapter we analyze and discuss the legal challenges of a cleanup of plastic in the North Pacific Gyre. For this we formulate many of the legal issues and provide solutions that will prevent states with major ocean interests (USA, Canada, Russia, China, India etc.), international organizations (UNCLOS, EU) and business (shipping companies, cruise lines) from opposing The Ocean Cleanup Project. Our vision from a legal perspective must be to anticipate and solve problems, assess vested interests, and create a scenario that allows players to buy in and support The Ocean Cleanup Project.

The five issues addressed in this chapter are as follows:

ISSUE ONE
WHO OWNS THE PLASTIC IN THE OCEANS?
What are the legal issues that would prevent the Ocean Cleanup from collecting plastic on the high seas? Is there any issue of ownership of the plastic? Does the law or customary practice of salvage apply?

Once it is collected and processed by The Ocean Cleanup platforms (thus transformed into pellets or ground plastic) does the processed plastic belong to The Ocean Cleanup?

ISSUE TWO
OBSTRUCTION OF SEA TRAFFIC
Given that the deep-sea platforms will potential lay across recognized and established sea passages used by commercial traffic is there any legal issue preventing us from posing an impediment to such traditional passages? Is there any international law that applies and relates to the blockage of sea-lanes?

As impeding deep-sea traffic may impose higher costs on ocean shipping lines (i.e., going around The Ocean Cleanup platforms) how do we get the commercial entities to buy into our project and be prepared to support what we do?

ISSUE THREE

WHAT SHOULD BE THE LEGAL DESIGNATION OF OUR PLATFORMS?

Simply put do we register these platforms as a ship under a nation state flag or seek some other designation?

Do we seek some nation designation as a deep-sea platform and does that make our project subject to diplomatic concerns that the platforms may be used by the enabling nation state for military or spying (listening) purposes? One concern is that if we seek flag state protection do we risk becoming an extension of that state? Should we seek special status from the UN under UNCLOS? What status should we seek and how?

There are also liability and insurance issues and any eventual investor may wish to see the platform or array insured.

ISSUE FOUR

BYCATCH

What happens when The Ocean Cleanup Array accidentally catches a sea turtle or other protected species as bycatch? Is there liability for such by-catch? What national and international laws and treaties do we need to be aware of?

ISSUE FIVE

TRANSPORT OF PROCESSED PLASTIC TO SHORE

The entire idea of collecting and processing the plastic is to make it a recyclable product that has a commercial value. In order words, our focus is on the ability of the Ocean Cleanup to become a commercially viable project. There is likely to be national legislation that applies the moment we bring the processed plastic ashore into a national state port for processing and land-based discharge. What kind of laws might we encounter for such landing of the "plastic product" in key states where we would likely land the plastic? What international treaties and bilateral treaties would govern such transportation from the high seas into territorial water of the plastic pellets? What would they be considered a hazardous good? If not what designation would they be given? Would the pellets also be subject to tax as an imported good?

The chapter finishes with a review of possible legal frameworks that could provide a legal foundation for ocean rehabilitation projects like The Ocean Cleanup.

PLASTIC OWNERSHIP

NICHOLAS P. KATSEPONTES

It is estimated that 80 percent of all marine debris originates from land-based sources (Sheavly & Register, 2007). Likewise 80 percent of all marine debris is plastic (Weisman, 2007). The plastic that has found its way to the high seas comprises a variety of forms outlined in Section 1.1 of this Feasibility Study. What is important to note for issues of legal ownership is that for the vast majority of the plastic in the oceans its very nature makes it impossible to ascertain and attribute any ownership rights. Who owns a water bottle or plastic bags, or six pack rings? In such instances is ownership even an issue? There are certain types of plastics that may have characteristics or identification marks that allow for a determination of ownership such as fishing nets, shipping and other containers that allow for identification of their originating owner.

Plastic that has found its way to the high seas can be categorized as: i) lost by accident, ii) peril at sea, iii) intentionally dumped, or, iv) abandoned. Each may have it own legal implications dependent upon the ability to identify a possible owner.

8.1.1 LAW OF SALVAGE

The law of salvage is a concept practiced as part of maritime law that, in the most general terms, provides that a party that recovers another party's ship or cargo as a result of a peril or loss at sea shall be entitled to a reward or compensation determined in part by the value of the property salvaged (Curfman, 2008). A primary concern of motivation of salvage law is the preservation and protection of property on the high seas (Schoenbaum, 2004). The right to be rewarded for salvage at common law is derived from equitable principles and a public policy motivation. There is no contractual basis for traditional salvage rights. Historically, salvage is a right in law, when a person, acting as a volunteer (that is, without any pre-existing contractual or other legal duty so to act) preserves or contributes so to preserving at sea any vessel, cargo, freight, or other recognized subject of salvage from danger.

There are three elements that must be present for salvage law to apply: i) a marine peril or risk, ii) voluntary service by salvor, and iii) a successful outcome where the vessel is salvaged or property recovered (Curfman, 2008). In the case of defining what property be the subject of salvage, the traditional definition would cover only a ship or craft ("vessel"), the cargo on board, freight payable, and bunkers carried on board.

It is interesting to note that the 1989 Salvage Convention has expanded the concept of property. Article 1 (c) defines property as "property means any property not permanently and intentionally attached to the shoreline and includes freight at risk." (IMO, 1989) The definition is therefore quite broad and in a practical sense further defined by Article 14 that allows for Special Compensation when an act of salvage protects or prevents "damage to the environment" (IMO, 1989). The term "damage to the environment" is a defined term in Article 1 of the Convention and states: "... substantial physical damage to human health or to marine life or resources in coastal or inland waters or areas adjacent thereto, caused by pollution, contamination, fire, explosion or similar major incidents."

While this section does not specifically mention the high seas, "areas adjacent thereto" suggests in the broadest scope areas outside of waters coming under national jurisdiction. Further, the nature of pollution and how it spreads on water requires consideration of the fact that plastic pollution on the high seas originates from land and can impact territorial waters. Thus a salvage of plastic on the high seas that prevents pollution that impacts coastal waters can be covered by the Convention. There is precedent for the prevention of oil pollution that could cause damage to the environment constituting a valid basis for salvage and such salvage service constituting "a valuable service to the community" ("Semco Salvage & Marine Pte Ltd. v. Lancer Navigation (The Nagasaki Spirit)," 1995). Thus the concept of preventing pollution in this case plastic that is established as physically harmful to human health could give rise to a right of salvage in instances of property clearly identified to an owner.

This concept may apply to scenarios where plastic is discarded from a ship due to accident or to peril at sea with the owner (the ship) having no intention of relinquishing ownership of the plastic in question. In practical terms one must consider such instances as rare given the nature of the majority of plastic in the oceans as being "anonymous plastic" which no defining characteristics allowing for the establishment of ownership. This may apply in instances of plastic containers or their contents washed or thrown overboard in a storm or to preserve the safety of a vessel. Likewise fishing nets bearing identity marks establishing ownership that were lost or abandoned to preserve the safety of the fishing vessel may attract salvage rights. In this regard The Ocean Cleanup could be entitled to salvage rights over clearly identifiable plastic where owners still express an interest in achieving possession of their property.

8.1.2 THE LAW OF ABANDONMENT

The plastic that is categorized as "anonymous" and has found its way into the oceans has for all intents and purposes been abandoned by its owners. Abandonment is a term of ownership and possession. In a legal sense there are two key elements that must be present or satisfied in order to effect an abandonment of property. "Abandonment occurs when there is a giving up, a total desertion and relinquishment of private goods by the former owner." ("Simpson v. Gowers," 1981)

The legal act of abandonment may arise when the owner with the specific intent of desertion and relinquishment casts away or leaves behind his property…" ("Simpson v. Gowers," 1981) In addition, to the act of abandonment there must exist an intended action or motivation on the part of the owner to relinquish all rights of ownership and in this regard to have no concern or interest in who may take subsequent possession of the property (Saw, 2011). Plastic garbage disposes of by its owner whether thrown in the garbage or from the window of a car would appear to be subject to this legal definition of abandonment.

There are however competing views amongst jurisdictions as to the law of abandonment.

CANADA AND THE UNITED STATES

In the United States and Canada the same legal standard of abandonment has evolved. The Canadian standard has been previously described in Simpson v. Gowers ("Simpson v. Gowers," 1981). The American case law states: "abandonment refers to an owners voluntary and intentional relinquishment of a proprietary interest in property to the extent that another person may take possession of that property and assert a superior right to it." ("United States v. Shelby,") The case law largely addresses examples of disposal of property in trash bins and generally a property owner who places garbage in a trash bin "renounces the key incidents of ownership – title, possession, and the right to control." ("Ananda Church of Self-Realization v. Massachusetts Bay In. Co.," 2002) The key term under the American and Canadian law is that of "divesting abandonment" defined as the party abandoning his or her property consciously divesting their future interest in that property. As such possession by the next party creates a new title interest in the abandoned property (Saw, 2011).

AUSTRALIA AND NEW ZEALAND

Australian courts did not initially accept the concept of divesting abandonment whereby abandonment was not deemed to divest an owner of his title to his property comparing abandonment to that of property that is lost and found by another party. The owner is still the original owner and the funder of the property simply has possession not ownership ("Johnstone v. Wilmot Pty Ltd. v Kaine," 1928). Ownership was thus a chain of title that could not be broken by abandonment unless consciously done so by the owner by transferring title. Subsequent cases while endorsing the results of the Johnstone case established and accepted the "possibility" that there was "no reason in principle why title to property could not be extinguished by an act of abandonment" ("Moorhouse v. Angus & Robertson (No1) Pty Ltd.," 1981). Finally, in one case a person scavenging at a public trash dump was deemed to have the ability to acquire title to goods found at the trash dump and deemed abandoned by its owners (" Leonard George Munday v. Australian Capital Territory," 1998).

ENGLAND

The English courts take a more narrow view of the legal concept of abandonment. The concept of unilateral divesting abandonment is not consistent with the concept of property law and the complete right of ownership cannot be abandoned simply by losing possession (Saw, 2011). Thus a party who simply finds abandoned property could not establish title or ownership of property. Similar to the "garbage cases" that emerged in the United States and Canada, English courts have ruled that the act of leaving one's garbage outside for the local municipal authorities to pick up is not an act of abandonment. Until such time as it is taken away by the local authority it still belongs to the owner. When the local owner takes the garbage away from the curb it belongs to the local authority. Thus title or a form of ownership has passed (" Long v. Dilling," 1999). English law would appear to require a conscious and deliberate act by the owner in elation to unilaterally divesting his ownership to the property that unequivocally show the intent to abandon as in the case of the trash left at the curb.

The varying views of the legal concept of abandonment may vary with a more favorable view to The Ocean Cleanup existing in Canadian and American law. English and Australian law appear to take a narrower view making less clear who would own garbage found on the high seas. Central to any jurisdiction is the concept of enforcement of rights to property and in this regard how can any property owner provide or make a better claim that the party having taken possession of plastic found on the high seas.

8.1.3 LAW OF FINDS

The law of finds is primarily focused upon title to found property. The common law of finds views property that is abandoned as returned to a state of nature much as would apply to fish, ocean plans and other species that belong to no one. Courts have been reluctant to apply this concept in relation to shipwrecks or salvage claims and have rarely done so except where the vessels in question are clearly deemed abandoned by their owners or in relation to treasure at sea ("R.M.S. Titanic, Inc. v. Wrecked & Abandoned Vessel,"). The preference has been to apply salvage law, as it is more applicable to the commercial realities of maritime trade and to the policy perspective of providing incentives for volunteer salvors to undertake salvage operations of vessels, property and protection of the environment ("Henen v. United States," 1981).

In a historical setting the law of finds has been applied in the context of shipwrecks ("Henen v. United States," 1981). However, the necessary elements for its application can have a wider application to other property situated in the oceans including plastic. In order for the law of finds to apply there must be present: i) intent of the finding party to establish possession over the property in question; ii) actual possession as in exerting physical control over the property; and iii) a determination that the property has been abandoned by the owner ("R.M.S. Titanic, Inc. v. Wrecked & Abandoned Vessel,"). The first two elements are easy enough to establish as physical acts of taking possession or in the case of The Ocean Cleanup collecting the plastic would satisfy these elements. In the case of the third element, a level of proof is required to establish abandonment. By implication applying the concept of abandonment means that the owner cannot be ascertained. If an owner can be ascertained them courts have deferred to and applied the law of salvage. (Curfman, 2008)

Pursuant to the law of finds the establishment of abandonment requires evidence that is clear and convincing that the owner has abandoned the property (Curfman, 2008). In the case of shipwrecks where the concept has been applied, abandonment has been deemed to be present where there is an express statement or action that the owner is abandoning the shipwreck or an absence of any party intervening when a shipwreck is found to claim ownership (Schoenbaum, 2004). This may include where the passage of time has made it impossible to ascertain the owner or the owner does not exist any more as a legal entity (i.e., company as owner no long exists).

There are real benefits to the law of finds as relating to The Ocean Cleanup and ocean based plastic. The application of the principles of the law of finds can be projected outside of the historical application of shipwrecks to other forms of property. The fact that it will be impossible to ascertain the ownership of the vast majority of ocean borne plastic satisfies the requirement of abandonment. This is supported again by the very nature of the plastic in the oceans, which in part comprises discarded waste and thus implies a conscious decision of its owners to relinquish title, as they would land based garbage. If you knew who discarded the plastic water bottle would they want it back? Not likely – thus further evidence of abandonment. Inherent to the application of the law of finds is that the owner will not look for the property lost or in this case plastic in the oceans.

Court have also commented upon the societal benefits of the law of finds in the context of creating different a set of incentives than those created by the law of salvage, which seeks to return property to owners and get compensation for so doing. This implies there is a value to the owners of the property worthy of undertaking the salvage efforts. This is not the case of ocean borne plastic, to which the individual owners attribute little or no value. The maritime law of finds creates a form of title to persons who reduce to their possession objects which are abandoned in or find their way into the oceans ("Odyssey Marine Explorations, Inc. v. Unidentified, Shipwrecked Vessel or Vessels," 2006).

One of the policy benefits of applying the law of finds to abandoned property such as plastic is that it creates an incentive to put lost property back to productive use. (Curfman, 2008) The incentive of creating title by taking possession of ocean borne plastic is a critical element to the commercialization of The Ocean Cleanup as a pure profitable business of cleaning the oceans.

OBSTRUCTION OF SEA TRAFFIC

REBECCA RUSHTON • HOLLY CAMPBELL • PAULA WALKER
RICHARD G. HILDRETH

The planned area for testing and operation of The Ocean Cleanup arrays will likely encounter commercial shipping traffic between the continental United States and Hawaiian ports (see Figure 8.1-3 indicating where common shipping routes intersect The Ocean Cleanup's proposed array site). Two treaties governing sea traffic on the high seas apply here. The United Nations Convention on the Law of the Sea (UNCLOS) permits freedom of operation of vessels on the high seas and guarantees every State the right to sail ships. Additionally, the Convention on the International Regulations for Preventing Collisions at Sea (COLREG) prescribes the rules of operation for "vessels" on the high seas.

Figure 8.1 GeoCommons: The Global Shipping Lane Network. Source: (geocommons, 2014). Horizontal and vertical lines indicate longitude and latitude; other lines indicate common shipping routes

PORT HAWAI'I'S MID PACIFIC LOCATION
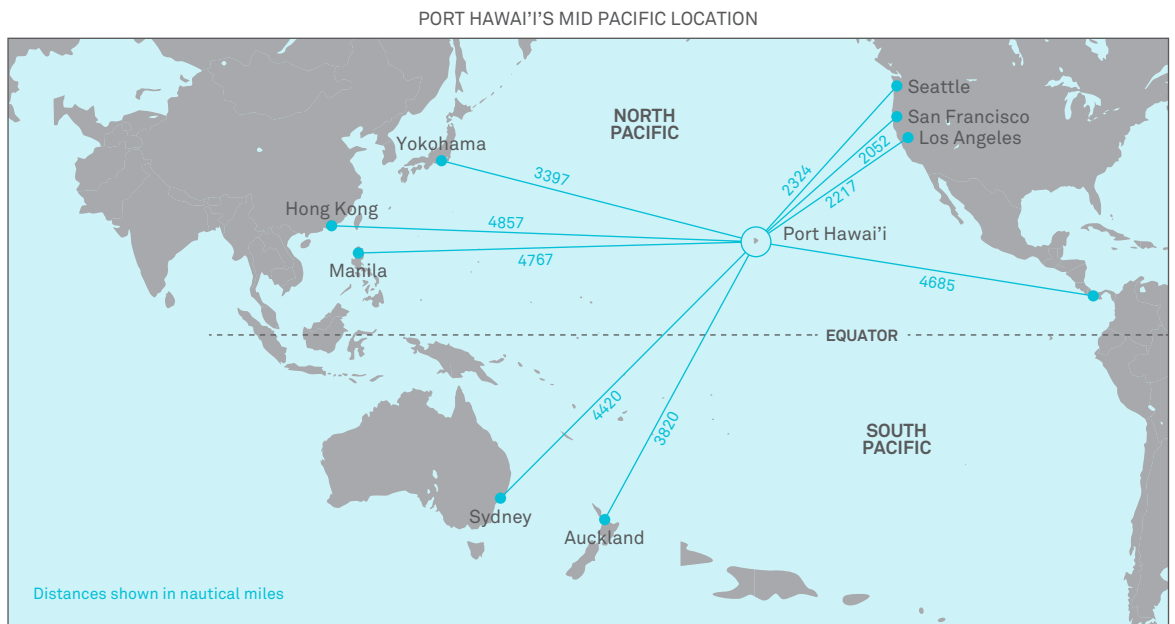
Figure 8.2 Hawaii Dept. of Transportation, A Guide to Port Hawai'i 11. Source: (A Guide to Port Hawai'i 11, 2012). Lines indicate common shipping routes; numbers indicate the distance in miles.

1. Shanghai 2. Hong Kong 3. Yantian 4. Lazaro Gardenas 5. Miami 6. Savannah 7. Norfolk 8. New York

1. Pusan 2. Shanghai 3. Mingao 4. Hong Kong 5. Dachan Bay 6. Halifax 7. New York 8. Savannah 9. Kingston

1. Pusan 2. Qingdao 3. Shanghai 4. Ningbo 5. Charleston 6. New York
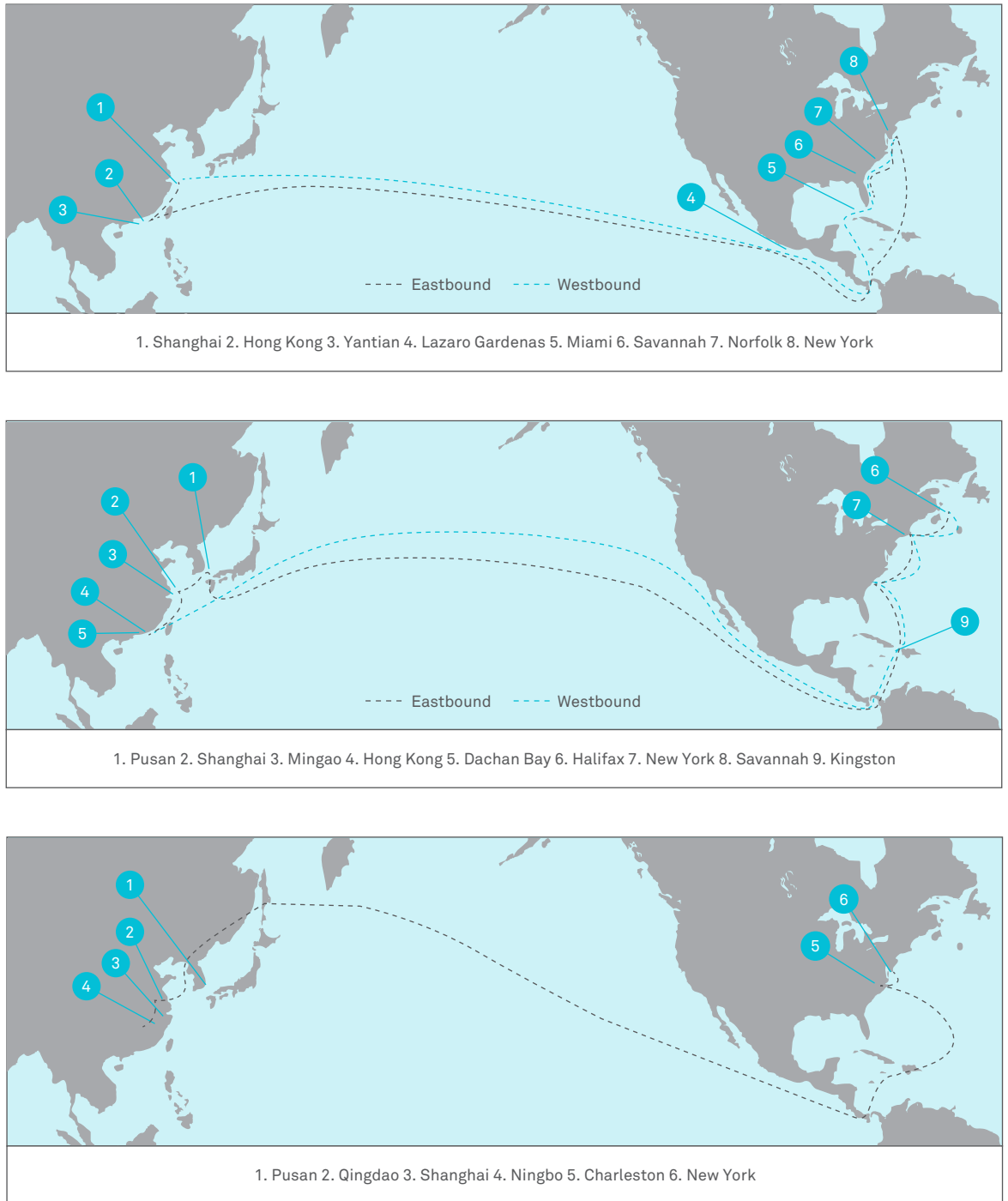
Figure 8.3 China Shipping Container Lines Co, Ltd., America Line. Source: (China Shipping Container Lines Co, 2014). Top middle and bottom image show three common shipping lanes for container transport from Asia to the US.

UNCLOS Legal Regime & State Enforcement Jurisdiction

Ocean
Cleanup
Platform

Shore

Territorial Sea
11nm

Contiguous
Zone
24nm

Exclusive
Economic
Zone
200nm

High Seas
+200nm

Nm = nautical miles

Costal states have exclusive enforcement
jurisdiction for all matters.

Costal states have jurisdiction for customs,
immigration and sanitary matters.

Costal states have limited jurisdiction in areas of pollution, marine natural
resources (fishing etc.) and other issues that may impact national security.

Subject to UNCLOS & other international treaties but freedom of high seas applies.
Vessel are subject to the jurisdiction of the flag they fly even on the high seas.

8.2.1 INTERNATIONAL LAW: UNCLOS

SIGNATORY STATES

Thailand, European Union, Japan, China, and Canada.
(U.S. recognizes as customary international law.)

- Article 87: Freedom of navigation on the high seas may be exercised by any State, including landlocked States, and includes the "freedom to construct artificial is lands and other installations."

- Article 90: Every State has the right to sail ships on the high seas

ISSUE

The Ocean Cleanup activities may impinge traditional navigation of commercial vessels by obstructing ships' routes due to the estimated size of The Ocean Cleanup array.

APPLICATION

While every state has the right to sail ships, and ships have the right of freedom of navigation, UNCLOS does not proscribe specific routes for ships on the high seas. Since states also have the right to construct artificial islands, navigational freedom seems to apply more to the act of sailing than to the route or physical barriers on the high seas.

8.2.2 COLREG

SIGNATORY STATES
Canada, China, Russia, United States, South Korea, and Japan

- Rule 1(a): Rules apply to all ships operating on the high seas

- Rule 2(b): compliance with the Rules includes ac counting for limitations of vessels that may require a departure from the Rules to prevent immediate danger

- Rule 3(a): The word "vessel" includes every description of watercraft . . . used or capable of being used as a means of transportation on water.

- Rule 7(d)(ii): the risk of collision may exist if approaching a very large vessel, even if an appreciable bearing change is evident

- Rule 8(c): if there is sufficient sea room, alteration of course may be the most effective action to avoid collision and pass at a safe distance

- Rule 8(e)(iii): even vessels with priority of passage must comply with the Rules when they risk being involved in a collision

- Rule 14(a): When two vessels risk a head-on collision, each shall alter their course starboard and pass on the portside of the other

- Rule 15: when crossing routes risks collision, the vessel that has the other on the starboard side shall avoid crossing ahead of the other vessel

ISSUE
The size of The Ocean Cleanup arrays may present a safety hazard to other vessels operating on the high seas. COLREGs apply to all "vessels" capable of being used for transportation on water. COLREG does not apply to platforms, such as oil drilling or LNG platforms. COLREG probably does not include The Ocean Cleanup arrays because they are likely platforms not "vessels" used for transportation. Whether or not the arrays are classified as "vessels" and subject to COLREG, the arrays should be equipped with safety features to assist ships in avoiding collisions with the arrays for the safety of shipping traffic and preventing damage to the arrays.

APPLICATION
COLREG applies to vessels "capable of being used as transportation." If The Ocean Cleanup arrays were attached to the sea floor as platforms, then COLREG would probably not apply to the arrays, but would apply to ships transporting material from the arrays. Rule 8(c) suggests that ships alter their course to avoid collision with other vessels if there is sufficient sea room. This rule may be the most applicable to commercial vessels that will have to avoid The Ocean Cleanup arrays, and may require that commercial vessels take less direct routes from the United States mainland to Hawaii in order to avoid possible collisions with the arrays.

COLREG probably does not apply to The Ocean Cleanup arrays because the arrays do not meet the definition of "vessel" if they are attached to the sea floor as platforms. Though neither UNCLOS nor COLREG prevents the array from operating, because it presents a unique situation that poses questions regarding shipping right-of-ways and hazards to shipping traffic, the array may have to abide by additional safety regulations from either the flag-state or IMO.

Officially established shipping lanes and route measures do not extend beyond a State's Exclusive Economic Zone (EEZ) into the high seas. However, most ships follow either customary shipping routes between ports or the Great Circle route travelling East-West around the Pacific Ocean. Ships following the Great Circle route in opposite directions meet regularly, but abide by COLREG to avoid collisions. Additionally, ships use Automatic Identification Systems (AIS) and radar collision avoidance facilities (ARPA) to change course or speed in order to avoid collisions.

Initial research of COLREG indicates that The Ocean Cleanup arrays are probably not considered "vessels" under the COLREG definition. The arrays are more similar to "platforms" that are excluded from COLREG. They may nonetheless be expected to abide by COLREG requirements for preventing collisions on the high seas. Regardless, to protect its investment, The Ocean Cleanup will likely need to take measures to ensure that the arrays can be detected and avoided by passing ships. This could include equipping the arrays to be detected by ships' AIS and ARPA systems, and/or equipping them to be detected by outfitting them with reflectors, audio devices and/or lights.

LEGAL DESIGNATION OF OUR PLATFORMS

REBECCA RUSHTON • HOLLY CAMPBELL • PAULA WALKER
RICHARD G. HILDRETH

8.3.1 UNCLOS (LOSC)

SIGNATORY STATES

There are 162 nations that are signatories to the Law of the Sea Convention so far. These include the North Pacific gyre neighboring states Mexico, Japan, China, Russia and Canada. The United States has not approved UNCLOS (although in 2012 only 34 US Senators said they would not approve the treaty; it takes 67 senators to overcome a filibuster).

The United States recognizes most of the LOSC as customary international law, except for the 1994 provisions relating to the International Seabed Authority and seabed mining.

- Article 87(1): LOSC Article 87 lists the ability to construct artificial islands and to conduct scientific research as two of the six "freedoms of the high seas." The High Seas, beyond the continental shelves and EEZs of neighboring countries, are not subject to the jurisdiction of any state, unless a country flags the vessels or platforms. See discussion in By-catch paper submitted by the IOLSI.

"[C]onstruction of artificial islands or installations on the high seas does not acquire for the relevant state any form of sovereignty over that area such as a capacity to generate maritime claims nor does it impact upon the delimitation of maritime boundaries. States may also elect to construct artificial islands for the purposes of marine scientific research, in which case provisions found in Part XIII of the LOSC would also be applicable."

The International Law of the Sea, Donald R. Rothwell and Tim Stephens, 2010 ed., p. 157.

If the platforms and vessels were flagged by a state or states they would be subject to the laws of that state or states. An assumption for this feasibility study at this point, for the sake of analysis, is that platforms will not be flagged by a state.

The question then is whether the UN would have some role in jurisdiction over the platforms, either by flagging or otherwise.

8.3.2 CAN THE UNITED NATIONS FLAG VESSELS OR PLATFORMS?

Possibly. While the UN International Law Commission (ILC), in preparing the draft of what became the High Seas Convention, rejected the flagging of vessels by the UN and other international organizations, the 1958 Geneva Conference inserted Article 7 in the High Seas Convention stating that the provisions of the Convention "do not prejudice the question of ships employed on the official service of an intergovernmental organization flying the flag of the organization." The Law of the Sea, R.R. Churchill and A.V. Lowe, 1985 ed., pp. 182-3. However, the LOSC (UNCLOS) Article 93 allows the UN, its specialized agencies and the IAEA (International Atomic Energy Agency), to flag UN vessels.

Examples: In 1956 the UN flagged some of its own ships responding as part of the 1956-7 UN Emergency Force in Egypt. See discussion of this and other examples at UNCLOS I, Official Records, Vol. IV, p. 138.

8.3.3 WILL THE PLATFORMS BE SUBJECT TO THE INTERNATIONAL SEA BED AUTHORITY (ISA)?

Probably not. The ISA, which is not binding on the United States, is the body through which states subject to UNCLOS are to control all resource-oriented uses of the sea bed beyond national jurisdiction, when resources are considered the "common heritage of mankind" and thus beyond any state's jurisdiction. Although the Ocean Cleanup arrays will likely be anchored in the high seas seabed, they will not be subject to the authority of the UN ISA since (1) the activity is not considered to be resource extraction from the seabed and therefore should not be regulated by the ISA, and (2) even if the activity itself were to be considered resource extraction, it is likely to be considered a non-governed use excluded from ISA jurisdiction (such as pipeline and cable laying and scientific research unconnected with the exploitation of seabed resources). (Churchill & Lowe, 1988)

However, if the activity (e.g. plastic mining) was subject to the UN ISA under UNCLOS, then the IGA "Enterprise" (a part of the United Nations) could manage it and engage in "mining" activities itself, and could enter into joint ventures with commercial operators. The proceeds would be distributed among the signatory states.

8.3.4 CAN THE UNITED NATIONS, OUTSIDE OF ITS AUTHORITY FOR FLAGGING OR THE ISA, SOMEHOW TAKE RESPONSIBILITY FOR THE OCEAN CLEANUP ARRAYS?

Possibly. There is some precedent for the United Nations regulating large scale floating arrays on the high seas. Before the 1990s there were large-scale pelagic drift nets for fishing (primarily for squid) floating in the high seas, some of which were 48 kilometers (30 miles) long. Although placed for an entirely different purpose, many of these were similar in some ways to the proposed plastic cleanup arrays. Many of these drift nets were on the ocean surface in large arrays extending long distances on the surface, and several meters under the surface (some were suspended under the ocean surface). They were held in place by floats and weights, rather than anchored. The United Nations, in recognition of the large impact the drift nets had on fishing and living marine resources of the world's oceans and seas, banned them by a UN Resolution. Applying the precautionary principle, the United Nations, through the General Assembly, adopted several resolutions doing so (McDorman, Bolla, Johnston, & Duff, 2005). Therefore, there is some precedent for the UN to take action when there are large-scale impacts on the oceans. This time, however, the action would be to clean up the plastics using large-scale ocean arrays, rather than to prohibit fishing on high seas using large ocean drift-net arrays.

BYCATCH

REBECCA RUSHTON • HOLLY CAMPBELL • PAULA WALKER RICHARD G. HILDRETH

There are many definitions of "bycatch," but bycatch is generally considered any non-target species caught during operations at sea. The United Nations estimated that more that 20 million tons of bycatch was caught in 2010. (FAO, 2010) Unmanaged bycatch threatens the sustainability of fisheries, continued existence of endangered species, and the economic viability of individuals and countries that depend on the oceans. Though bycatch from The Ocean Cleanup will likely be minimal, The Ocean Cleanup should be aware of international treaties and domestic laws governing by-catch that may affect cleanup operations. The most applicable international treaties include the Law of the Sea Convention, Convention on Migratory Species, and Inter-American Convention for the Protection and Conservation of Sea Turtles. Additionally, even when operating on the high seas domestic laws of the flag state will apply The Ocean Cleanup operation procedures, and individuals working on The Ocean Cleanup array are subject to their States' domestic laws.

The United Nations Convention on the Law of the Sea (UNCLOS) is the primary international treaty governing actions concerning the oceans. While UNCLOS does not directly address by-catch, it does apply to other international treaties concerning by-catch and includes provisions that may be interpreted as encouraging States to mitigate the effects of their activities on by-catch. Specifically, Article 117 discusses the duty of States to adopt measures for conservation of living resources on the high seas (UN, 1982). These measures apply to all nationals and ships operating under a State's jurisdiction.

Many international treaties defer to UNCLOS for consistency in their basic goals and principles. In 1995, the Food and Agriculture Organization created the 1995 Code of Conduct for Responsible Fisheries (The Code), which adopted UNCLOS's basic principles and was endorsed by all FAO Members. The Code calls for the sustainable use of aquatic ecosystems and includes minimizing fisheries impacts on non-target species as a primary objective (FAO, 1995). Even after its implementation, by-catch continued to be a pressing concern forcing the FAO to enact species-specific plans (FAO, 1995). These plans included the 1999 FAO International Plan of Action for Reducing Incidental Catch of Seabirds in Longline Fisheries (IPOA-Seabirds), the 1999 FAO International Plan of Action for the Conservation and Management of Sharks (IPOA-Sharks), and the 2009 FAO Guidelines to Reduce Sea Turtle Mortality in Fishing Operations (FAO, 1995).

When the FAO's species-specific plans failed to sufficiently address by-catch, it created the first global guidelines for by-catch management and reduction (FAO, 1995). The Guidelines' objectives include minimizing by-catch, improving management, and increasing reporting of by-catch. These objectives are to be implemented by States through national laws and policies consistent with UNCLOS, the 1995 Code, and the 1995 Fish Stocks Agreement. However, it is unclear at this time whether the Guidelines would apply to the pollution reduction technology. The Guidelines' scope covers all "fishing activities" in all oceans but does not further define "fishing activities." As the Ocean Cleanup Project has the objective of passive collection of floating plastic wastes, it would not qualify as a fishing activity.

While it does not use the term "by-catch," the Convention on Migratory Species (CMS) prohibits any "taking" of an endangered migratory species. CMS addresses the effects of maritime activities on all migratory species, but primarily focuses on migratory species that are currently endangered or are at risk of becoming endangered (CMS, 1983). In order to protect endangered migratory species, CMS prohibits any Party from "taking" an endangered species. "Taking" is defined as fishing, capturing, or attempting to engage in such activities. Again, as per above, the Ocean Cleanup Project activities would not be considered as "taking" of migratory species. Though CMS mainly addresses activities occurring within national jurisdiction boundaries, it also directs states to protect migratory species during activities on the high seas. Article III states that Parties engaged in activities outside of national jurisdictional boundaries that may result in the taking of migratory species shall endeavor to prevent, remove, or minimize the adverse effects of activities or obstacles that seriously impede or prevent the migration of species.

The different laws and treaties will be addressed in more detail in the subsections below, including who are signatory, key provisions and issues, and their application to The Ocean Cleanup project.

8.4.1 INTERNATIONAL LAW: UNCLOS

SIGNATORY STATES

62 nations including Russia, the European Union, Japan, China and Canada. (U.S. recognizes as customary international law.)

• Article 117: Issue: indirectly implicates prevention of by-catch and could be used as legal justification for other by-catch related treaties.

APPLICATION

States have a duty to adopt measures for conservation of living resources on the high seas, so The Ocean Cleanup's flag state probably has by-catch laws it must follow.

• Article 56: Limits foreign vessel operations in EEZs without that State's permission and applies domestic laws that affect by-catch.

APPLICATION

Within their EEZ, States have sovereign rights and jurisdiction to, among other things, protect and preserve the marine environment. The Ocean Cleanup needs permission to operate in an EEZ and would need to adhere to the State's by-catch laws.

• Article 73: Subjects The Ocean Cleanup to a State's domestic by-catch laws.

APPLICATION

Within their EEZ, States may enforce laws/regulations adopted in conformity with UNCLOS.

8.4.2 1995 CODE OF CONDUCT FOR RESPONSIBLE FISHERIES (THE CODE)

SIGNATORY STATES

Thailand, Russia, Korea, China, Japan, and U.S.

ISSUE

incorporates UNCLOS principles that could be applied to The Ocean Cleanup by-catch; does not specifically apply to planktonic species but does include "non-fish" species.

APPLICATION

Code is voluntary and, itself, non-binding.

• 1.1: The Code is voluntary, but includes binding measures from other treaties.

• 6.5: Absence of information should not be used to fail to protect non-target species.

• 7.2.2(g): Protective measures should include minimization of non-target species catch, both fish and non-fish species. Plankton may be considered "non-fish" species but are not specifically addressed under any international laws.

8.4.3 INTERNATIONAL PLAN OF ACTION – SEABIRDS (IPOA - SEABIRDS)

Only focuses on incidental catch from longlines; probably not of concern to The Ocean Cleanup.

8.4.4 INTERNATIONAL PLAN OF ACTION - SHARK (IPOA - SHARKS)

ISSUE

Language is sufficiently broad to encompass The Ocean Cleanup's operations.

APPLICATION

The plan seems to be directed at States with vessels that target sharks for commercial fishing.

- 11: Shark catch includes by-catch.
- 17: Applies to sharks caught on the high seas.

8.4.5 GUIDELINES TO REDUCE SEA TURTLE MORTALITY IN FISHING OPERATIONS

ISSUE

The Pacific Ocean is considered a high-risk area for leatherback turtles and loggerheads.

APPLICATION

Guidelines are voluntary, based on a best-practices model, so they only apply if the Guidelines have been adopted in some form by the flag state.

8.4.6 2010 GUIDELINES ON BYCATCH MANAGEMENT AND REDUCTION OF DISCARDS (GUIDELINES)

ISSUE

Voluntary Guideline to reduce by-catch in "fishing activities."

APPLICATION

Unclear whether it applies to The Ocean Cleanup's activities because there's no definition of "fishing activities."

- 2.3: Objective includes minimizing by-catch.

8.4.7 CONVENTION ON MIGRATORY SPECIES

ISSUE

Prohibits the take of any endangered migratory species (Art. II(1))

APPLICATION

Large Pacific States, including Canada, U.S., and Japan, are not parties to the convention but may be parties to other agreements.

8.4.8 CONVENTION ON INTERNATIONAL TRADE OF ENDANGERED SPECIES (CITES)

Does not apply to The Ocean Cleanup; only applies to international trade (import/export).

8.4.9 1995 FISH STOCKS AGREEMENT

ISSUE

Because this project rests in the high seas, straddling stocks (species that migrate between one or more exclusive economic zone and the high sea) as well as highly migratory species (including tuna and tuna-like species, pomfrets, marlin, sailfish, swordfish, saury, cetaceans, and sharks) will be implicated.

APPLICATION

States shall highly monitor the stocks and species in order to review their status and the efficacy of conservation and management measures, and then revise such measures as needed. Enhanced reporting of vessel locations and catch and by-catch rates are also required. The U.S. publishes an annual report entitled the U.S. National By-catch Report.

8.4.10 INTER-AMERICAN CONVENTION FOR THE PROTECTION AND CONSERVATION OF SEA TURTLES

RELEVANT SIGNATORIES

U.S., Ecuador, Mexico, The Netherlands (relevant to flagging), Panama, Guatemala, Costa Rica, Peru, and Chile.

ISSUE

Sea turtles are a highly protected, high-migratory species. Any kind of "take" of any turtle is to be mitigated.

APPLICATION

Signatories to the Convention agree to undertake efforts, working with the best available scientific data, to decrease the amount of sea turtle catch on their flagged vessels. The United States implements a monitoring program and closes fisheries after the fisheries have made a cap number of interactions with turtles (quotas established in Biological Opinions).

8.4.11 WESTERN AND CENTRAL PACIFIC FISHERIES COMMISSION

ISSUE

Highly migratory species will be highly affected by this project. Swordfish, marlin, sailfish, sharks, tuna-like species are all highly susceptible to being caught in the holding tanks, and possibility diverted by the booms into the platform.

APPLICATION

Highly migratory or straddling fisheries are regionally managed by cooperating countries. Both (or all) countries assume responsibility for proper fishery management. This convention applies to all species of highly migratory fish stocks within the convention area.

Areas affected (thus countries affected): waters surrounding Hawaii, American Samoa, Guam, U.S. Pacific Remote Island areas, and the Northern Marianas Islands. By-catch was approached here on a mostly jurisdictional basis, asking which laws and treaties cover those areas of the northern Pacific Ocean where The Ocean Cleanup may operate. This approach is not a catchall. As an accompanying question (#2) notes below, the reach of some laws is not restrained by national boundaries. While concluding that The Ocean Cleanup's by-catch will likely be minimal, the mere prospect of by-catch does bring The Ocean Cleanup into the realm of regulatory oversight. By-catch will be but one of several regulatory matters facing The Ocean Cleanup. Should The Ocean Cleanup seek additional legal analysis of by-catch issues, continued work would develop the regulatory process and where components of The Ocean Cleanup qualify within that process.

Acronym	Full name
C.F.R.	Code of Federal Regulations
CITES	Convention on the International Trade of Endangered Species
CMS	Convention on the Conservation of Migratory Species of Wild Animals
EEZ	Exclusive Economic Zone
ESA	Endangered Species Act
FAO	U.N. Food and Agriculture Organization
IPOA-Seabirds	1999 International Plan of Action for Reducing Incidental Catch of Seabirds in Longline Fisheries
IPOA-Sharks	1999 International Plan of Action for the Conservation and Management of Sharks
MMPA	Marine Mammal Protection Act
MSA	Magnus0n-Stevens Fishery Conservation and Management Act
NEPA	National Environmental Policy Act
NOAA	National Oceanic and Atmospheric Administration
U.N.	United Nations
UNCLOS	United Nations Conventen on the Law of the Sea
UNEP	United Nations Environment Programme
U.N.T.S.	United Nations Treaty Series
U.S.	United States
U.S.C.	United States Code

TRANSPORT OF PROCESSED PLASTIC TO SHORE

REBECCA RUSHTON • HOLLY CAMPBELL • PAULA WALKER RICHARD G. HILDRETH

Our preliminary research suggests that there will likely be regulations and legal constraints facing The Ocean Cleanup in transporting the plastic to shore. It also suggests that because the reuse and recycling of plastic is favored over manufacturing new plastics, there may also be regulatory incentives providing The Ocean Cleanup some advantage in transporting plastics to shore to render in some fashion for reuse or disposal. (DePaolo, 1995)

Transport to shore requires deep and extensive scientific, policy and legal research. What is presented in this chapter is intended to merely skim the surface of what may confront The Ocean Cleanup. The following eight areas, while not an exhaustive list, give a broad scope of the necessary considerations and the potential scientific, policy and legal matters involved. This is intended to point the way for The Ocean Cleanup to conduct further detailed legal and policy analysis investigation pending decisions to actually deploy the arrays.

We based our research on United States laws, policy and regulation. We assume that The Ocean Cleanup will face similar issues in any of the developed western nations. We assume as well that The Ocean Cleanup's commitment to improving the environment in performing this clean up of the ocean, indicates that it intends to hold itself to the highest standards possible in rendering the marine debris collected to some benign form for reuse or disposal.

8.5.1 TOXICITY

Many plastic products are a source of toxic substances due to chemicals added during manufacturing like polychlorinated biphenyls (PCBs) (EPA, 2012b). Additionally, plastics act as a sink for toxic substances and may absorb PCBs or dioxins from the surrounding environment (Engler). Many countries, including the United States, require special permits for handling, cleaning up, and disposing of toxic products, such as those containing PCBs.

8.5.2 RADIOACTIVITY

Radioactive material is naturally occurring in the environment in small amounts ("ABCs of Radioactivity – Radioactivity 101: Emissions," 2013). Because plastic absorbs substances from the surrounding environment and does not breakdown easily, there is a possibility that plastics in the Pacific Ocean could be radioactive. Though some may worry about increased radiation from the Fukushima nuclear power plant due to the Japanese Tsunami, this is unlikely because radionuclides dissolve in seawater, disperse, and decay over time ("Mistake Triggers False Alarm about Ocean Radioactivity," 2013).

8.5.3 BACTERIA

Scientists recently discovered that plastics in the ocean host microbes, as many as 1,000 different species, some of which are known to cause diseases in animals and humans ("Microbes on Floating Ocean Plastics: Uncovering the Secret World of the 'Plastisphere," 2014). Research indicates that some forms of harmful bacteria actually favor plastics over other available sources. Additionally, plastic debris from medical or personal hygiene products may already contain and transmit bacteria and other pathogens (NOAA, 2012). This may present legal and policy issues related to protection of human health.

8.5.4 INVASIVE SPECIES

If debris is transported to shore, it may facilitate the movement and survival of invasive species (EPA, 2012a). Marine debris contributes to the movement of species from one area to another. Floating debris can carry invasive species long distances, including across the Pacific Ocean. Invasive species threaten native species through competition, crowding, and predation (Wildlife, 2013). Current debris management and policy have evolved since the Japanese Tsunami in 2011, and include contacting both state and federal wildlife officials.

8.5.5 WASTE FROM PROCESSING

Waste from processing recycled plastic can be either beneficial or detrimental. On one hand, plastic waste is a potential resource for fuel production(UNEP, 2009). Companies are exploring technology to turn recycled plastic into oil (Romanow, 2014). However, only certain types of plastics are effective resources. On the other hand, wastewater produced from the plastic recycling process is corrosive (Beckart Environmental). Potential recyclers may have to implement new technologies for high volume processing. Recyclers may also have to be concerned about regulations concerning wastewater and other waste products from the recycling process.

8.5.6 EMISSIONS

Plastic manufacturing of virgin materials contributes to at least 100 million tons of CO_2 emissions and about 14 percent of toxic releases into the atmosphere every year ("Ecotextiles, Plastics – Part 2: Why recycling is not the answer,"). These numbers could be reduced if more plastic was recycled (EPA). Maximum achievable reductions in greenhouse gas emissions from recycled plastic material compared to virgin plastics are about 60 percent (Recovery, 2012). While the emissions are reduced when recycling plastic, a plant that renders plastic will be subject to numerous emissions regulations (Recycling).

The fact that the plastics gathered would be an un-separated assortment of plastics from various sources may pose some real challenges to recycling and disposing (DePaolo, 1995). In particular, the fact that this plastic may come 'burdened' with 'unwanteds'—such as bacteria, toxins (in addition to original manufacture PCBs), invasive species—may pose additional challenges to recycling for reuse (DePaolo, 1995).

8.6.7 MARKET

For manufacturers, it is still more economically efficient to use virgin materials than recycled plastics. However, there is an increasing trend to use recycled plastic as technology improves and cost decreases. There is an ongoing effort to recycle more types of plastic, such as lids and buckets, to create new equipment for automobile parts, playground equipment, and carpet (EPA).

8.5.8 DISTRIBUTION OF ORIGINAL AND PROCESSED MATERIAL

As mentioned earlier, plastics harvested from the ocean may contain toxic substances. Distribution of raw plastic material for treatment or recycling in the United States will be limited to companies with special permits from the EPA (EPA, 2012b).

PROPOSAL FOR A LEGAL FRAMEWORK FOR INTERNATIONAL OCEAN REHABILITATION PROJECTS

NICHOLAS HOWARD • NICHOLAS P. KATSEPONTES

International ocean pollution agreements fail to provide for or encourage the rehabilitation of ocean ecologies already affected by plastic accumulation. However, the necessary foundation for ocean rehabilitation projects already exists. Emerging international laws of general application[1] could form political and legal frameworks to define the status of ocean rehabilitation projects and states' obligations to such projects.

In the context of ongoing feasibility assessments for The Ocean Cleanup, this section seeks to aggregate recent developments in international environmental law to demonstrate the existence of novel legal frameworks, which are capable of supporting ocean rehabilitation projects such as The Ocean Cleanup. Although this analysis is specific to ocean environments, the basic international legal principles could support application to other environmental issues. The goals of this section are threefold, and are in order of subsections: 1) to analyze the relevance of current international maritime legal frameworks in the context of ocean rehabilitation; 2) to extract relevant principles from international maritime agreements and laws of general application, particularly related to pollution; and 3) to suggest a possible legal framework to define and support environmental rehabilitation efforts.

This chapter will address the most fundamental legal question: can international law define and support the existence of ocean cleaning platforms in international waters? What obligations or responsibilities, if any, would states have toward the platforms? It is worth noting that this analysis assumes that the purpose of the platforms is for environmental rehabilitation, not primarily for commercial purposes or profit. In order to define and understand the status of the platforms under international law, it is necessary to look to maritime treaty law. The question of states' obligations requires an analysis of principles outside of treaty law.

8.6.2 CURRENT OCEAN POLLUTION FRAMEWORKS AND THE STATUS OF THE OCEAN CLEANUP IN INTERNATIONAL LAW

The numerous international agreements dealing with ocean pollution focus on prevention by regulating dumping by ships at sea and states' obligations in preventing the movement of land-based wastes into the oceans. No single agreement addresses all sources of plastic pollution and most have been widely criticized for broad exemptions and vague requirements (Hagen, 1990). Many frameworks are specialized, dealing only with particular oceans or types of pollution[4]. This section will briefly review several agreements relevant to plastic pollution. Though these frameworks provide little direct support for rehabilitation efforts on the high seas, they are helpful to provide context and enumerate certain basic principles and weaknesses under the current system.

In addition to the exclusive focus on prevention of further pollution, the agreements, which expressly include plastics as prohibited waste, deal primarily with dumping or pollution from ships. Dumping causes a relatively small minority of the plastic pollution problem, with a vast majority of plastics coming from land-based sources. The London Dumping Convention, for instance, covers only land-based materials, which are loaded onto ships for dumping at sea (IMO, 1972).[5] The United Nations Convention on the Law of the Sea ("UNCLOS") appears to provide stronger enforcement mechanisms by subjecting disputes over ocean pollution to compulsory dispute resolution. However, land-based pollution under article 207 is mainly subject to "best effort" clauses; states must adopt laws to prevent pollution and endeavour to harmonize legislation through regional and/or global rules. Conversely, dumping is prohibited except in accordance with standards specified by the International Seabed Authority. The enforcement mechanisms in UNCLOS are effectively limited to dumping since even the most ineffective legislation would meet the requirements under article 207.

[1] For the purposes of this paper, international laws of general application include custom and general principles included under Article 38 of the Statute of the International Court of Justice and as defined in judicial decisions.

Annex V to the MARPOL Convention is most often cited for the prevention of ocean plastics pollution since it addresses the problem of plastic expressly. Annex V imposes a complete ban on the disposal of all forms of plastic at sea

(IMO, 1972). However, MARPOL, like UNCLOS, has created a complex permitting system to allow for certain types of dumping at sea and leaves the enforcement through fines and fees to individual states. Unlike UNCLOS, MARPOL does not afford dispute resolution mechanisms unless the states have agreed to particular fora outside MARPOL. The trend of avoiding the land-based pollution problem also continues in MARPOL.

Rehabilitation projects like the Ocean Cleanup provide an option for rehabilitation that can supplement prevention regimes in an attempt to fully mitigate the problem of ocean plastics. Finding room for rehabilitation projects among prevention-focused regimes poses difficult definitional questions, some of which can be solved through a broad and constructive reading of UNCLOS.

LAW OF THE SEA

UNCLOS is the only international framework that deals directly, though not in depth, with installations on the high seas. UNCLOS is the most authoritative and extensive maritime treaty and speaks to general principles for activities in international waters. The convention is generally considered to reflect customary international law. According to UNCLOS article 87, no state may exercise sovereign rights over the high seas; all states are free, inter alia, to navigate, construct installations, and conduct scientific research in international waters. Though installations are not explicitly defined in UNCLOS, the Drafting Committee of the Third UN Conference on the Law of the Sea understood them to include artificial (i.e. manmade) structures and islands (Nordquist, Nandan, & Kraska, 2011).

The few provisions in UNCLOS applying to installations in international waters are largely independent of a particular purpose (i.e. installations are not restricted to issues of shipping, research or any particular field). However, UNCLOS pays consistently special attention to the freedom of scientific research on the high seas, such that installations for scientific research are provided their own section (Part XIII, section 4). Marine scientific research, like any scientific research seeks to "observe, explain, and eventually to understand sufficiently well how to predict and explain changes in the natural (marine) world." (Wegelein, 2005) It would be difficult to argue that the ocean cleaning platforms' dominant purpose is scientific research.

As discussed above, their purpose appears to be largely environmental and rehabilitative, a purpose that remains undefined and unregulated in international maritime law. Part XIII section 4 serves generally to limit the scope of scientific installations, rather than to regulate activity, placement, longevity or any other of the myriad concerns with installations on the high seas. It provides, inter alia,

[2] The terms "international waters" and "high seas" are used synonymously to refer to the mare liberum or trans-boundary waters outside of national jurisdiction. This paper adopts the definition from the United Nations Convention on the Law of the Seas – waters outside the EEZ (and the territorial and contiguous zones) of any state and any extended continental shelf claims under Article 76.

[3] Land-based sources of plastic account for 60 to 80 percent of ocean plastic UCLA report

[4] e.g. the Cartagena Convention which deals primarily with pollution from ships in the Caribbean Region

[5] London Dumping Convention "Convention on the Prevention of Marine Pollution by Dumping of Wastes and Other Matter 1972",

[6] OTEC on high seas

that installations do not have EEZs or territorial waters and that they do not possess the status of islands. It is important to note, however, that article 264, section 6 Part XIII deals with the settlement of disputes regarding the conduct of marine scientific research and/or installations. The procedure involves conciliation and, failing that, binding adjudication by the International Tribunal for the Law of the Sea, the International Court of Justice, or an arbitral tribunal (article 287). It is unclear whether the ocean cleaning platforms would fall under the framework set out for research installations, since their dominant purpose is not research. It is possible that environmental purposes could be equated with scientific research. However, the derivation of economic benefit, even indirectly, from the activities could make the conduct too commercial to fall under the research framework or create a convincing parallel.

In distinguishing "installation" from "equipment" (another UNCLOS term from Article 258), the former takes on a sense of longevity (i.e. permanency) and purpose. This inference is supported by certain limitations on the purpose of installations under UNCLOS, demonstrating that installations are structures constructed for a particular purpose, some of which are prohibited: they must be peaceful (i.e. non-military) and their use must be reasonable with due regard for the interests of other states.

Specific to installations, Article 87 provides states with the "freedom to construct... installations permitted under international law". The language of this provision subjects it to other customary or treaty law that may further limit the types of installations or their uses. No such explicit law exists. The freedoms in article 87 are limited in 87(2) by the requirement that they be exercised with "due regard for the interests of other states" and their rights to the seabed. At its most fundamental, due regard requires that installations refrain from unreasonably restricting traffic (in known shipping lanes, for instance) and blocking states' ability to explore and make use of minerals under the seafloor. The permanency of installations, as mentioned above, may conflict with the requirement for due regard. Some authors have suggested that long

term mooring of platforms in international waters (particularly if they span large areas) could be unreasonable as they may prevent the establishment or exploration of new shipping lanes or other novel endeavours.6 However, since treaties must be construed to be internally consistent, it is necessary to read the freedom to construct installations harmoniously with the requirement of reasonableness.

Read in context of the whole convention, provisions relating to installations also suggest that they are not used for loading or unloading ships (distinct from ports, specifically deep-water ports) nor are they are naturally formed areas of land (Wegelein, 2005). Given this definition and the foundational status of UNCLOS, the ocean cleaning platforms would likely be considered installations under international law. Whether they are subject to the framework in Part XIII depends on their dominant purpose or whether environmental rehabilitation is a reasonable equivalent to marine scientific research for the purposes of UNCLOS. This topic will be dealt with more in the section on common heritage.

ATTRIBUTION OF THE PLATFORMS TO A STATE OR INTERNATIONAL ORGANIZATION UNDER UNCLOS

UNCLOS article 92 requires that ships sail the flag of one state only, though article 93 preserves the right for ships "employed on the official service of the United Nations" to fly the UN flag or the flag of a UN organization. No such requirement is expressly provided for installations. Article 93 suggests that the freedoms enumerated in article 87 are enjoyed by any ship or installation flying a state flag (thereby attributed to a particular state and its jurisdiction under article 92), by clarifying that ships flying the flag of the United Nations enjoy the same freedoms.

Several provisions appear to contemplate the registration of installations by a state. Article 109, for example, allows prosecution of persons who illegally broadcast signals from an installation in the high seas by "the state of registry of the installation". Other provisions allow the enforcement of the flag requirement by providing that warships possess a "right of visit" if a ship is without nationality or refuses to show its flag (article 110). This provision, read in the context of UNCLOS Part VII High Seas, particularly article 109, suggests that the right of visit would also apply to installations. Therefore, it is advisable that installations fly either a national or organizational flag.

Attribution could provide easier coordination and access to information, particularly if an international organization with significant state representation is able and agrees to register the platforms. However, if attributed to a state, jurisdiction over the platforms would become clear – the attributing state gains full jurisdiction. Given the international nature of ocean pollution, single-state or even regional attribution could create issues with ownership, monitoring and control. If a UN organization agreed to register the platforms, jurisdiction could be dealt with through an instrument issued by the administrative branch of the organization. That instrument would define issues of jurisdiction, including any dispute resolution mechanisms. UNCLOS provides no guidance on which UN organizations are competent for attribution of installations or ships, suggesting only that ships must be "employed on the official service" of the organization.

Two UN Programmes would provide ideal forums for attribution, but may not possess adequate independence or agency. UN-Oceans is a coordination organization established by the Administrative Committee on Coordination pursuant to Agenda 21, Chapter 17 of the United Nations Conference on Environment and Development, 1992. Since UN-Oceans is an Oceans and Coastal Areas Network, it does not possess the status of "specialized agency" mentioned in article 93 of UNCLOS and may not be able to provide attribution. Like the United Nations Environment Program, it is a program rather than an agency of the UN. Conversely, the International Maritime Organization ("IMO") is a specialized agency of the UN that has a mandate to promote safe, secure, environmentally sound, efficient and sustainable shipping. Though shipping is its primary mandate, it has been instrumental in numerous environmental treaties on ocean pollution and its member states have adopted many pollution-focused agreements. Attribution through the IMO is more likely to fall within the meaning of UNCLOS article 93, but may fall outside the organization's mandate. It is also notable that the IMO has almost universal membership.

GENERAL ENVIRONMENTAL PRINCIPLES IN INTERNATIONAL LAW – STATES' OBLIGATIONS
Even if the Ocean Cleanup arrays could be defined under UNCLOS as installations and receive some form of legal status through attribution, whether state or organization, UNCLOS is not equipped to deal with the sui generis nature of rehabilitation projects on the high seas. UNCLOS primarily deals with states' ships and the use of international waters, particularly commercial uses such as shipping or resource extraction. The rehabilitation of ocean environments necessarily extends beyond the pragmatic state-centric approaches to shipping and resource extraction in UNCLOS. It is highly unlikely that an individual state would be willing to accept the burden of

---

[7] UNCLOS article 302 specifically preserves the right of a state not to disclose information about its activities on the high seas.

[8] Though UNCLOS requires that states refrain from use or threat of force on the seas (article 301), there is no prohibition on other activities, including use of platforms for spying.

ocean rehabilitation. As mentioned above, rehabilitation projects by a single state raise issues with control and monitoring, since the state would have complete control over the platforms.[7] Ensuring effectiveness and accountability would also be difficult; UNCLOS does not distinguish between activities, so the platforms could also be used for other, less communitarian purposes.[8] Since rehabilitation lies outside the range of activities described in UNCLOS and other treaties, it is also unclear whether non-participating states would have any obligation toward the platforms and rehabilitation projects generally.

8.6.3 POSSIBLE LEGAL FRAMEWORKS TO DEFINE AND SUPPORT ENVIRONMENTAL REHABILITATION EFFORTS

As stated above, the international nature of ocean pollution and the high seas requires international governance. An international system of governance for pollution mitigation projects is a novel suggestion, but could provide opportunities for increased cooperation and scalability. When dealing with international commons, such as the high seas, the success of an international governance model is supported by political and social science research . Two international legal principles provide further support and a basis for international governance of the Ocean Cleanup: the common heritage of mankind principle, and the precautionary principle.

8.6.3.1 COMMON HERITAGE OF MANKIND

As stated above, the international nature of ocean pollution and the high seas requires international governance. An international system of governance for pollution mitigation projects is a novel suggestion, but could provide opportunities for increased cooperation and scalability. When dealing with international commons, such as the high seas, the success of an international governance model is supported by political and social science research . Two international legal principles provide further support and a basis for international governance of the Ocean Cleanup: the common heritage of mankind principle, and the precautionary principle.

States' responsibilities for the prevention of ocean pollution are clearly enumerated in numerous global agreements, though many commentators question the laws' effectiveness and strength. The extent of states' obligations in rehabilitation projects on the high seas depends on current agreements and developing laws of general application. The unique political and legal context of the high seas introduces the concept of "common heritage of mankind" into ocean rehabilitation projects. Developed from a long history, the common heritage principle has found a home in international maritime and environmental agreements. Recent academic work and decisions from the International Court of Justice ("ICJ") and international arbitrations have begun to recognize new environmentally focused international legal principles. The precautionary principle has received particular attention for its evolution as an international law of general application, outside the context of particular treaties. Some commentators and decision-makers have hypothesized the precautionary and common heritage principles as general principles of law or as novel customary international laws ("CIL") under Article 38 of the Statute of the International Court of Justice. New and developing environmental principles of general application may provide an argument in favour of limited state responsibility for ocean rehabilitation efforts.

The common heritage of mankind ("CHM") principle has emerged as a foundational principle in international law, equivalent to erga omnes obligations and jus cogens rules.[9] As such, CHM serves as a standalone principle derived not by induction from domestic legal systems, or by deduction from international agreements, but from natural law as a universal right or obligation.10 States' interests in preserving their rights in common resources (access, benefit, preservation etc.) are self-evident. The CHM principle ensures that states retain rights to commons spaces, subject to certain limitations. CHM has also been formulated as a general principle of law or customary international law under Article 38 of the Statute

of the International Court of Justice (Baslar, 1998). Regardless of the source of its authority, the CHM principle is clearly applicable to all states, leaving only the question of the contexts to which it should be applied. Applied to international waters, the CHM principle could provide an effective minimum standard for states' obligations toward rehabilitation projects like the Ocean Cleanup. Extending CHM to international waters is not a significant leap from its currently accepted applications. President Bedjaoui in the ICJ's Nuclear Weapons Advisory Opinion demonstrated the flexibility and dynamism of international legal principles, including the CHM, in dealing with important issues. At the time, nuclear weapons were at the top of the agenda; today environmental issues dominate the list. This section will discuss the scope of the CHM principle, its applicability to the high seas and its impact on states' responsibilities toward rehabilitation projects, particularly The Ocean Cleanup.

Simply because the CHM principle finds its source in natural law does not mean that the concept is anchored to the context in which it was first developed; it continues to develop through application to new contexts. General principles of international law are "an authoritative recognition of a dynamic element in international law, and of the creative function of the courts which may administer it." (Voigt, 2009) The first conceptualization of the CHM principle was in the Antarctic Treaty signed in 1959, which required that, the Antarctic "be used for peaceful purposes only", "in the interests of...the progress of all mankind." ("The Antarctic Treaty," 1959) The CHM concept took hold in the numerous discussions, UN resolutions, and agreements about seabed use leading up to the creation of UNCLOS. The CHM principle was also included in the Outer Space Treaty, concluded at the same time as the discussions regarding the seabed intensified.

In 1982, the CHM principle was included in the final text of UNCLOS under article 136, stating that the seabed and ocean floor under international waters are the CHM. More recently, the CHM principle has been invoked in environmental contexts, most famously in the UN Educational, Scientific and Cultural Organization (UNESCO) Declaration on the Responsibilities of the Present Generations Towards Future Generations.[11] Each application of the CHM principle has four common attributes:

[9] In a declaration on the ICJ's Advisory Opinion on the Legality of the Threat or Use of Nuclear Weapons, 1966, President Bedjaoui spoke to the status of the CHM principle: "Witness the proliferation of international organizations, the gradual substitution of an international law of co-operation for the traditional international law of co-existence, the emergence of the concept of "international community" and its sometimes successful attempts at subjectivization. A token of all these developments is the place which international law now accords to concepts such as obligations erga omnes, rules of jus cogens, or the common heritage of mankind." http://www.icj- cij.org/docket/files/95/7499.pdf#view=FitH&pagemode=none&search=%22common heritage%22

[10] In locating the source of general principles of international law, Christina Voigt suggested three sources – 1) induction from general acceptance in many domestic legal systems; 2) deduction from general acceptance in international legal frameworks; or 3) natural law. These three sources have generally been accepted as the appropriate analysis for the determination of general international legal principles. http://www.retfaerd.org/gamle_pdf/2008/2/Retfaerd_121_2008_2_s3_25.pdf

- The area must be outside national jurisdiction such that universal use is permitted;
- Benefits should be actively shared among all states;
- Any uses should be exclusively peaceful; and
- The area should be conserved, both in form and usability, for future generations. (Pardo, 1983)

UNCLOS only expressly declares the seabed and ocean floor the CHM in article 136. The laissez-faire approach of the free-access model to the high seas was not expressly replaced by the CHM in UNCLOS. When taken together, the principles governing international waters in UNCLOS essentially amount to the equivalent of the CHM, but lacking the preservation requirement.

Continuing developments in our understanding of ocean ecosystems combined with the UNESCO Declaration and similar instruments suggest that preservation is becoming increasingly central to ocean governance. Ultimately, international waters meet all four criteria and are often viewed as the CHM. Furthermore, article 155 permits the UNCLOS Review Conference to determine "the legal status of the waters superjacent" to the seabed. The Review Conference is also tasked with the maintenance of the CHM principle. If international waters are not already the CHM, the argument will be increasingly difficult to repel as damage to the oceans continues. A subsequent section on "Grotian Moments" will discuss the theory describing the rapid development of generally applicable international laws. Application of the CHM principle to international waters is certainly a candidate for rapid expansion in response to evolving circumstances.

One of the most common criticisms of the CHM principle is the lack of precise definition of its contents and effect. Given the breadth of its possible application, it is likely to be interpreted conservatively to impose constraints on the concept. If the CHM applied to international waters, ocean rehabilitation projects could receive international status and create obligations on states. Since projects like the Ocean Cleanup would be fulfilling the CHM principle's conservation requirement, creation of a novel "common heritage conservation" status for such projects is conceivable under international law. States would be obligated not to interfere with or oppose the project. However, such negative obligations are not unlike the current laissez-faire system in UNCLOS.

It is conceivable, though significantly more controversial, that the CHM principle applied to international waters would generate positive obligations on states. This conclusion is supported by current applications of the CHM principle to the seabed; states must actively share the benefits derived from use of the area, the second of the CHM attributes. A similar argument could apply based on the fourth attribute of the CHM: preservation or conservation, where the costs of actions taken to meet the preservation requirement should be shared between states. Costs could be interpreted broadly, including financial support of new projects. More likely, a narrow positive obligation would be preferred, such that states would share the costs of non-interference. For example, shipping lanes may have to be moved or new lanes could not be created if rehabilitation projects were underway in the same space. Where one state bears the burden of a particular instance of non-interference, this burden could be redistributed among all states sharing in the common heritage of the ocean. The existence of even limited positive obligations is further supported by another novel development in customary international law: the precautionary principle.

[11] UNESCO Declaration See specifically articles 4 and 8 which speak to the use of commons by present generations subject to their continued existence and usability for future generations. Though the declaration is not binding, similar instruments are often cited in the development of new international legal principles. The UNESCO declaration certainly contributes to our understanding of the CHM principle and how its content may evolve.

8.6.3.2 PRECAUTIONARY PRINCIPLE

The precautionary principle has been discussed as a customary international norm or a general principle of law for more than two decades. Recent appearances in ICJ decisions and arbitrations suggest that a broader acceptance is beginning to take hold. First developed in the 1960s and 1970s in response the increasing complexity and uncertainty of environmental scientific data, the precautionary approach requires proportionate action in the face of uncertain data. The principle accepts that scientific data may be incapable of accurately determining the capacity of an environment to absorb disturbances like pollution before effects are irreversible. It creates a bias in favor of caution. Most environmental legislation and international agreements implement a precautionary approach to varying degrees. However, the principle is most important in the governance of international commons, where the current costs of pollution are almost non-existent.

Like the CHM principle, the precautionary approach has generally been applied to require non-interference when states' interests conflict with environmental interests. However, like the prevention-focused regimes discussed above, a preventive application assumes that the current state of an environment, the ocean for instance, is environmentally sound. In the case of plastic pollution, it is abundantly clear that ocean environments are not ecologically sound. While the CHM principle may impose obligations on states not to interfere with ocean rehabilitation projects, the precautionary principle may create a foundation for greater positive obligations on states to contribute to rehabilitation.

In the Nuclear Tests (1974), Gabcikovo-Nagymaros (1997) and Pulp Mills (2006) ICJ cases, judges wrote separate opinions urging the majority to find new environmental norms, either as customary international law or general principles. They provided substantial reasoning to justify the place of certain environmental principles in international law, including the requirement for environmental impact assessments (EIAs), the principle of sustainable development and the precautionary principle. They proposed, based on state practice, science, and academic writing that the precautionary principle had reached the status of custom or general principle. The ICJ has played a major role in "developing customary rules in a number of fields". (Lowe & Fitzmaurice, 1996) It is likely because CIL's elements—i.e. state practice and opinio juris—are extensively explored by the International Law Commission, the International Law Association, the ICJ, and distinguished publicists. (Akehurst, 1976; Lepard, 2010; UN, 1950, 2006; Wood, 2013) Indeed, CIL has been developed recently in human rights law, (Simma & Alston, 1988) environmental law, (Birne, Boyle, & Redgwell, 2009; Bodansky, 1995; ICJ, 2010) maritime law, (Lauterpacht, 1950) and international humanitarian law (Meron, 1989).

Judge Weeramantry, in his separate opinion in the Gabcikovo-Nagymaros case, took an exploratory approach to the precautionary principle. He began with the conclusion that environmental damage imposes obligations erga omnes.[12] In response to such damage, he found that states were required by customary international law to conduct EIAs and adhere to sustainable development practices. He found that those two instruments had received widespread acceptance in domestic legislation and were generally viewed as legal obligations (opinio juris). Though he spent less time with the precautionary principle, Weeramantry did suggest that EIAs and sustainable development are merely applications of the precautionary principle, thereby suggesting that the principle is also customary international law.[13]

[12] Weeramantry at p 115

[13] Ibid 91

[14] Trindade at para 90

[15] Ibid at para 191

In the Pulp Mills case, Judge Cançado Trindade, wrote a lengthy and convincing separate decision in favour of the precautionary principle, which largely incorporated Weeremantry's decision. In discussing the principle, Judge Trindade emphasized its "inter-temporal" dimension, the same concept that forms the basis of the CHM principle in the UNESCO Declaration – precaution is necessary to fulfill states' responsibilities toward future generations.[14] He found that the precautionary principle, made up of the responsibility to conduct EIAs and adhere to sustainable development principles, "reflect the opinio juris, which, in turn, lies as the basis of the formation of law."[15] The distinction between general principles and customary is unclear in Judge Trindade's decision, since opinion juris is a facet of customary law, though his discussion frequently references general principles. For the purposes of this study, the difference is irrelevant; whether general principle or custom, it is clear that the precautionary principle is quickly becoming a central tenet of international environmental law. As ocean plastic continues to accumulate with the possibility of irreversible effects, the precautionary principle can play a greater role in defining states' obligations. Some publicists have argued that custom can develop rapidly when a "Grotian Moment" occurs. Grotian Moments, or times of rapid legal development catalyzed by crisis, will be further explored in the following section.

The CHM principle, as discussed above, suggests that commons must be preserved for future generations and universal use. However, the vagueness of these requirements has generated conflict over its exact content. The precautionary principle could be used to fill the practical gaps left by the CHM principle. Significantly more precision has been used in describing the content and effect of the precautionary principle. At the very least, the ICJ cases discussed above suggest that EIAs and sustainable development practices are inherent in a precautionary approach to new activities. However, these practices are used to assess proposed activities and to mitigate the environmental damage they cause. The inherent assumption is that prevention is a sufficient precautionary step to achieve the goal of conservation or preservation set out in the CHM. The reality of ocean pollution suggests that some rehabilitation is necessary to make any development sustainable.

Read together, the precautionary principle and the CHM may create obligations for states to actively contribute to ocean rehabilitation projects such as the Ocean Cleanup. The CHM sets a minimum theoretical standard for the conservation of a particular commons resource, such as international waters, based on use for future generations. The precautionary principle suggests that any reasonable evidence that international waters may not meet the standard set by the CHM principle will require active rehabilitation. The strength of the precautionary principle's impetus toward action is likely to increase if the damage caused to the oceans is or may become irreversible.

8.6.3.3 GROTIAN MOMENTS

The CHM and precautionary principles are candidates for rapid development through a "Grotian Moment". The foundations of the two principles have already been laid by state practice, judicial discussion and academic analysis, as discussed above. A "Grotian Moment" occurs when "new rules and doctrines of customary international law emerge with unusual rapidity and acceptance." (Scharf, 2010) They typically arise after moments of crisis including after World War II, the September 11th attacks on the United States, and the invention and use of nuclear weapons (Scharf, 2010). Although the term "Grotian Moment" was not coined at the time, in the ICJ's 1969 North Sea Continental Shelf Cases, the Court ruled that a short timeframe does not prevent finding new CIL (ICJ, 1969).

But can a "Grotian Moment" occur with limited state practice and opinio juris? The ICJ appears to be flexible in concluding when CIL has crystallized. For example, in the Nicaragua case, the ICJ put great weight on opinio juris without much emphasis on state practice (ICJ, 1986; Kirgis, 1987). Judge Weeramantry adopted a similar approach in his separate opinion in the Gabcikovo-Nagymaros case. Conversely, writers have noted that state practice alone can imply a belief that the practice is required or permitted by law if no evidence to the contrary exists from the relevant actors (Brownlie, 2008; Lauterpacht, 1958). Certainly, the ICJ has relied solely on state practice.[16] Frederic Kirgis observes the ICJ is much more flexible in assessing when CIL has crystallized when the stakes are high (Kirgis, 1987). As he noted:

On the sliding scale, very frequent, consistent state practice establishes a customary rule without much (or any) affirmative showing of an opinio juris, so long as it is not negated by evidence of non-normative intent. As the frequency and consistent of the practice decline in any series of cases, a stronger showing of an opinio juris is required. At the other end of the scale, a clear demonstrated opinio juris establishes a customary rule without much (or any) affirmative showing that governments are consistently behaving in accordance with the asserted rule... (Kirgis, 1987)

The "sliding scale" and "Grotian Moment" theories may demonstrate international courts' willingness to apply, use and even create CIL and general principles of law. The two legal frameworks (CIL and general principles) are still considered "obscure" and it can be hard to determine when to differentiate the two concepts. Often, as was the case in most instances referenced in this paper, general principles and CIL emerge from the same issues and evidence (Charlesworth, 2012). The confusion is particularly prevalent in international environmental law where many concepts are based not on implicit or express state concept through general acceptance, practice or opinion juris, but on natural law and necessity (jus necessitatis). Until the ICJ, ILC, or distinguished publicists clarify the matter, it will be possible to categorize various norms as both CIL and general principle, under the broad heading of generally applicable international law. Since both are considered equally valid sources of law under Article 38 of the ICJ Statute, the effect of any difference is irrelevant for the purpose of this paper.

---

[16] The SS Wimbledon, 1923 PCIJ, ser A, No 1 at 25; Nottebohm Case (Liechtenstein v Guatemela), Second Phase, 1955 ICJ Rep 4 at 22 (Judgment of April 6).

8.6.3.4 CONCLUSION

The volume of plastic in the world's oceans is already cause for concern. Our understanding of its devastating effects on water quality, ecology, and human and marine life appears to only have scratched the surface. The permanency of plastic demands more than preventative measures, though prevention is certainly fundamental to mitigation. The Ocean Cleanup may provide the first effective method to begin rehabilitation efforts in international waters. This opportunity should not be hindered by ineffective and narrowly interpreted legal regimes. The foundation for international cooperation on environmental issues already exists, in international agreements and, particularly in generally applicable legal principles. It is worth emphasizing, however, that the CHM and precautionary principles are precariously placed as international environmental law. Invoked narrowly and sporadically in international agreements and disputed vociferously as custom or general principles, their applicability, content and force are by no means certain. Most likely, some form of state action, either through declarations or agreement, would be necessary to solidify the place of CHM and precautionary principles in international law. However, the increasing rate of ocean plastic pollution, the development of our understanding of its devastating impact, and the expansion of the principles through recent judicial decisions suggest that the CHM and precautionary principles may soon play a significant role in ocean rehabilitation projects. Hopefully states, decision-makers, and commentators will recognize the opportunity for mitigation presented by these broad foundational concepts and will attempt to build workable frameworks around them.

PROCESSING OF COLLECTED PLASTIC DEBRIS

Although the focus of this study is the feasibility of extracting plastic from the oceans, a valid question is what The Ocean Cleanup would do with the plastic once this process has been completed. It is often said that the quality of plastic found in the ocean is too low to be converted into a product with value. This chapter will investigate this statement.
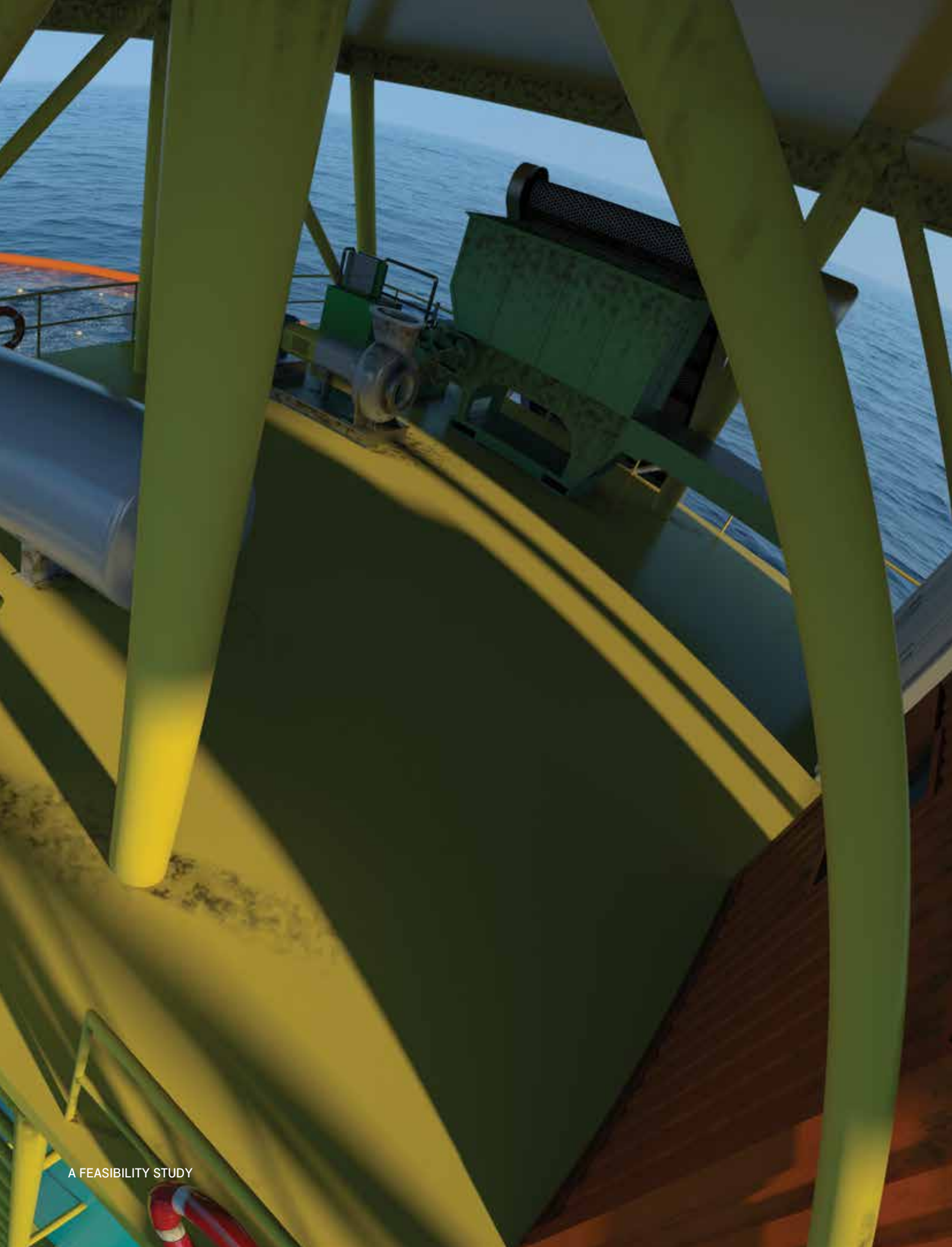
COLLECTION AND CHARACTERIZATION OF REPRESENTATIVE PLASTIC SAMPLES

NORBERT FRAUNHOLCZ • JOCHEM JONKMAN

KAUÊ PELEGRINI • BOYAN SLAT

Figure 9.1: Molecular structure of thermoplastics (a) and thermosets (b)

Synthetic polymers can be divided into thermoplastics and thermosets. Thermoplastics are referred to as plastics. Plastics consist of large polymeric molecules, see Figure 9.1. At room temperatures, the individual molecules are condensed to a solid phase due to intermolecular cohesion forces. By increasing the temperature beyond a critical value – which lies in the range of 180–260 °C for most plastic types – plastics will melt. This property makes them suitable for recycling into new plastic products. Examples of major plastic types are polyethylene (PE) and polypropylene (PP), polystyrene (PS), polyethylene terephthalate (PET) and polyvinyl chloride (PVC).

Objects made of thermoset material can be regarded as a single giant molecule, see Figure 9.1. This three-dimensional network of covalent bonds breaks down into smaller molecules at elevated temperatures, i.e., heating will destroy the original thermoset material without melting first. Consequently, recycling options of thermosets are limited to energy recovery or to use as filler in new polymer products after grinding to powder. Examples of thermosets are polyurethane (PUR) and most types of rubber (e.g. car tyres). All types of thermosets are heavier than water, except for foamed materials, such as PUR foam, which therefore may occur in floating marine litter.

The density of polymers depends on both the atomic weight of the constituting atoms – e.g. carbon (C), hydrogen (H) and oxygen (O) – and the spatial structure of the macromolecules, i.e. how densely the molecules are packed in the material. The latter mainly depends on the strength of the interaction forces between the macromolecules and their shape (i.e. linear or branched). Since heavy elements in the macromolecules also tend to generate strong interaction forces that pull the molecules closer together, all common polymer types containing elements other than carbon and hydrogen are heavier than water.

Consequently, pure hydrocarbons are the only group of polymers potentially lighter than water. Although polystyrene (PS) is a pure hydrocarbon, it is slightly heavier than water. This is because PS contains benzene rings in its macromolecule, which generate substantial interaction forces making PS relatively densely packed. PS comes with densities of 1040 kg/m³ or slightly higher. Since the density of seawater lies in the range of 1030 to 1045 kg/m³ for all open seas and oceans, PS just floats or just sinks in seawater. Therefore, PS has to be considered as possibly present in floating marine litter.

Polyolefins are also pure hydrocarbons, but unlike PS, they are relatively loosely packed due to their linear but branchy molecules and the absence of benzene rings. As a result, all pure polyolefins are lighter than water (1000 kg/m³) and therefore float on seawater as well. Exceptions are polyolefin materials in which fillers are used, such as chalk or glass fibre. Such filled materials may be heavier than water depending on the filler content.

Polyolefins are the largest group of plastics, with a share of approx. 40 percent of global production, and can be divided into the following major sub-groups: polypropylene (PP), low-density polyethylene (LDPE), linear low-density polyethylene (LLDPE) and high-density polyethylene (HDPE). The density of pure polyolefins lies in the range of approx. 900 – 960 kg/m³. As polyolefins are essentially built of linear chains of C and H only (i.e. $-CH_2-$ and $-CH_3$ groups), differences in density within this group are a result of differences in their spatial structures, as shown in Figure 9.2.

|			
			960
		955	
			940
	935		
915	910		
		905	
<880			
PP	**LDPE**	**LLDPE**	**HDPE**
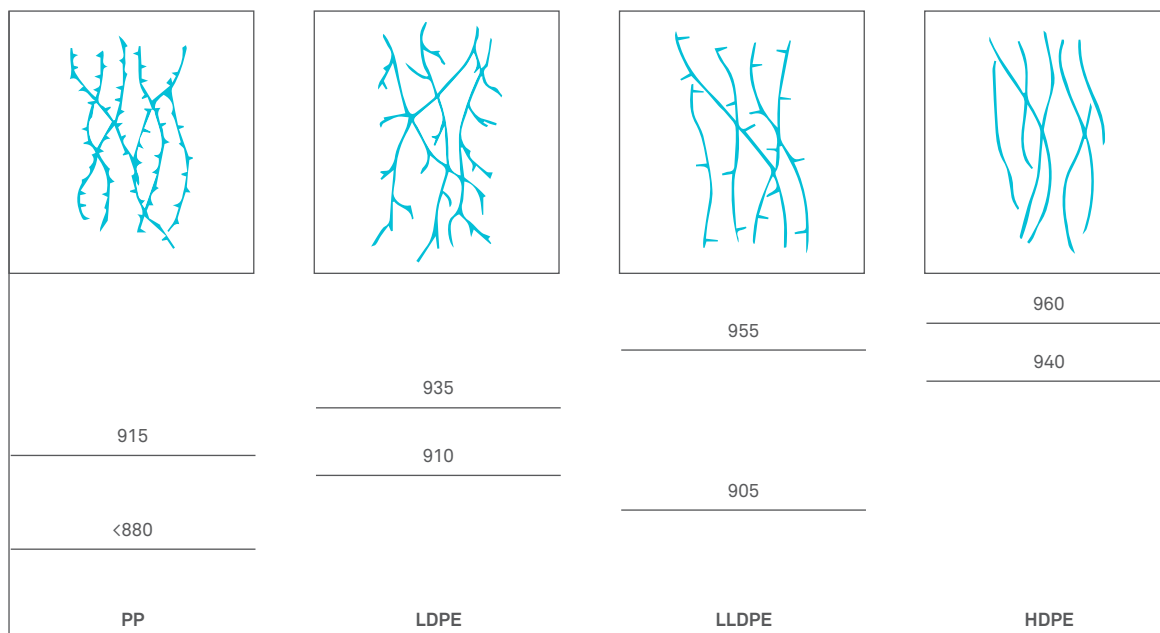
Figure 9.2: Density of different types of polyolefins as a function of their spatial structure (Fraunholcz). Polypropylene is the lightest polyolefin type due to its large amount of side branches ($-CH_3$)

All polymeric materials degrade under the influence of heat, UV light and oxidation in general, which results in the loss of mechanical properties and makes them brittle (see section Degradation analysis below). Therefore, the recyclability of plastics is limited to about six return cycles under normal conditions, whereas it can drop to zero when plastics are exposed to oxidative environments for substantial periods of time.

9.1.1 RECOVERY OPTIONS FOR WASTE PLASTICS

Plastics are complex materials for which the optimal way of treatment after their useful service life is not always obvious due to the combined influence of quality, raw material prices and legislation. Few experts would argue on the need and usefulness of recycling metals; however, the question as to whether polymers from a given waste source should be recycled as a material or whether the energy should be recovered, is much more complex. The main reason is that waste plastics can be used both as a material and as a fuel, except for halogenated plastics, such as PVC. In addition, plastics can be recycled as a material a limited number of times due to degradation, as outlined above.

Figure 9.3b:, a map showing the two coves in Hanalua bay (C2 and C3) and the two coves in (C4 and C5). The volunteers collected debris between C2 and C5 (image courtesy of Google Earth)
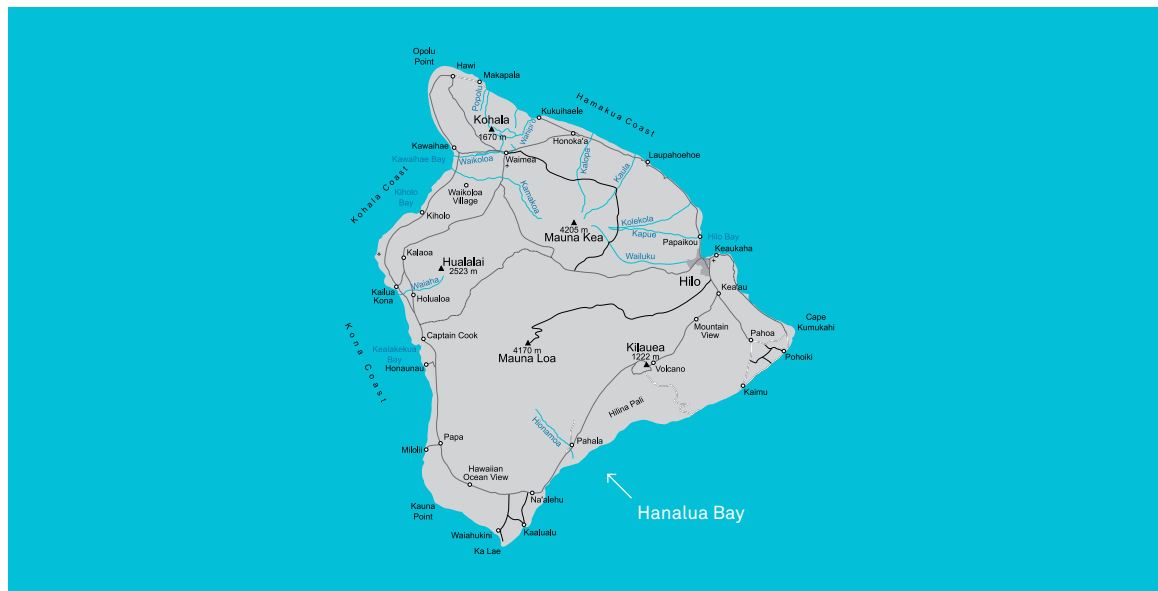
Figure 9.3a: a map showing Hanalua bay in relation to other stretches of coastline near South Point, Island of Hawaii, Hawaii.

There are several options to deal with waste plastics (reuse and incineration without energy recovery are not regarded as recycling options here):

• Recycling (high value-added material recovery)
• Down-cycling (low value-added material recovery)
• Back to feedstock recycling
• Energy recovery

Back to feedstock recycling describes thermal or chemical processes in which plastics are broken down to monomers or even further, e.g. to CO and H_2 (syngas). These substances can be used again as a feedstock in the synthesis of new polymers. Pyrolysis and gasification are processes that can be used for both producing raw materials for feedstock recycling or for producing fuel (oil or gas).

9.1.2 SAMPLE COLLECTION

In order to collect a sample that is large enough to be subject to a range of analysis, a beach sampling was commissioned. To make the sample's consistency as representative of the North Pacific Gyre marine debris as possible, the sampling took place on the Hawaiian island chain, which is located in the North Pacific Gyre. Since islands are a sink to marine debris, we assumed the consistency of washed-up debris to be similar to the consistency of marine debris.

On July 13th, 2013, a crew of 35 volunteers collected a total of 780 kg of marine debris, as part of a three-hour long beach clean-up conducted by the Hawai'i Wildlife Foundation (HWF). Of the collected debris, 91 kg was derelict netting. The volunteers were instructed to only collect plastic, and avoided sampling other natural or non-floating materials (including wood, glass, metal and rocks).

The sampling took place near the South Point of the Island of Hawai'i (Hawai'i), on a stretch of coastline measuring over 3 km, covering 4 coves (See Figures 9.3a and 9.3b). Two of these coves are in Hanalua bay, and the other two coves are at Ka'ahue bay. The last time a clean-up had been performed was on November 17th, 2012. During the previous clean-up, a total of 1,994 kg of marine debris was collected, of which 454 kg was derelict netting. The length of Hanalua beach is approximately 400 meters, while the 2 coves were each approximately 30 meters in length. The width of the sample area ranged between approximately 5 and 15 meters.

The sampling took place on a remote and uninhabited location (See Figure 9.4), reducing the possibility of contamination from direct land-based sources of debris, including tourism.

Figure 9. 4 Volunteers collecting beached debris (Image courtesy of Megan Lamson/HWF).

While most of the coastline was rocky, the 4 coves were partly sandy. Due to gaps between the rocks, the clean-up crew was not able to retrieve particles from the rocky parts of the coastline smaller than approximately 5 cm. Micro plastics up to approximately 0.5 cm were collected by hand on the sandy parts of the coves.

Due to transport size constraints, objects larger than 50 cm were omitted from the sample, including nets. The leftover debris was then randomly split, creating a sub-sample of 313 kg, which was then sent to The Ocean Cleanup.

Concluding, we assume to have collected a representative North Pacific gyre plastic sample, apart from:

- An underrepresentation of debris smaller than approximately 5 cm
- Not having included debris larger than approximately 50 cm
- The possibility of (small amounts of) land-based contamination
- The possibility of the presence of non-floating and natural debris within the sample.

9.1.3 SAMPLE ANALYSIS

Upon arrival at The Ocean Cleanup in The Netherlands, the Hawai'i sample was subjected to several analyses and tests, in order to identify feasible ways of treatment of this type of debris for maximum recovery of its intrinsic material value. The Dutch company Recycling Avenue BV has carried out a general characterization including size and density distribution as well as material composition. Subsequently, several analyses were performed to determine to what extent the polyolefin plastics in the sample are degraded due to weathering (e.g. UV radiation and bacterial activity). The degradation tests were carried out at the Laboratório de Polímeros, Universidade de Caxias do Sul, Brasil. In addition, SITA Benelux and the Hungarian company PowerEnergykft carried out tests to produce pyrolysis oil from the polyolefin plastics.

Fraction (mm)	Total mass (kg)	Percentage of sinks* (ma-%)	Total mass excl. sinks** (ma-%)	Mass distribution excl. sinks** (ma-%)
<200	153.7	7.7	141.9	57.1
>200	57.9	0	57.9	23.3
Rope	48.8	0***	48.8	19.6
Total	**260**		**248.6**	**100**

** Sinking in water (1000 kg/m³)

*** Assumed, not measured

Table 9.1: Mass balance of the master sample after manual sorting

COMPOSITION AND SIZE DISTRIBUTION ANALYSES
Sample preparation

First, the master sample was subjected to tailored preparation steps in order to facilitate the characterization work and subsequent tests and analyses. The sample preparation consisted of the following steps:

1 Manual sorting of the whole master sample into three fractions:
   1   Ropes and fishing nets
   2   Non-rope objects larger than 200 mm (visually estimated)
   3   Non-rope objects smaller than 200 mm (visually estimated)

2 Taking sub-samples from all fractions from Step 1 according to the quartering rules of sampling where possible. If required, the quartering procedure was repeated a number of times until a suitable sample amount for the characterization was obtained

3 Determination of the mass balance of the manually sorted fractions

Due to the apparent homogeneity of the rope fraction regarding object shape, size and material composition (i.e. no wood, stones, etc.), characterization work focused on the non-rope fractions. The following analyses were carried out on sub-samples of these non-rope fractions:

1 Determination of size distribution by screening
2 Float-sink analysis in water (1000 kg/m³)
3 Composition analysis of all size fractions by manual sorting after float-sink analysis
4 Density fractionation of the lighter-than-water material by float-sink analysis at different densities in the range of 880 – 1000 kg/m³
5 Determination of plastic types in several fractions by FTIR (Fourier Transform InfraRed spectroscopy) analysis

MASS BALANCE OF THE MASTER SAMPLE
According to Table 9.1, 80 percent of the plastics in the sample were non-rope objects, 70 percent of which were smaller than approx. 200 mm.

Sieve fraction (mm)	Mass (kg)	Mass distribution (ma-%)	Percentage of sinks** (ma-%)	Weighted average of sinks** (ma-%)
<2	834	4.8	25***	1.19
2-11,2	860	4.9	8.70	0.43
11,2-31,2	6726	38.4	6.05	2.32
31,2 - 46,5	5218	29.8	7.17	2.14
46,5 - 200	3862	22.1	7.13	1.57
Total	17500	100.00		7.65

** Sinking in water (1000 kg/m³)

*** Estimated

Table 9.2: Particle size distribution of the <200 mm fraction obtained by sieve analysis using standardized laboratory sieves. The weighted average content of heavier-than-water (1000 kg/m³) material of the <200 mm fraction was calculated using float-sink analysis data from Table 9.3.

Table 9.2 shows the particle size distribution of the <200 mm fraction. The average content of the <200 mm fraction on heavier-than-water material (1000 kg/m³) is 7.7 weight percent (wt%) (or mass percent ma%) as indicated in this table. The heavier-than-water objects mainly consisted of organics (e.g. wood) and inert materials (e.g. stones and batteries), the majority of which clearly got into the sample unintended during collection on the beach. These components were, therefore, excluded from further tests and analyses.

According to Table 9.2, the contamination level of organics and heavier-than-water material in the sample increases with reducing particle size. The size fraction 200-400 mm contained only plastics floating on water (PP and PE).

Size fraction (mm)	Fraction F=Float S=Sink	Material type	Mass (g)	Mass distribution in size fraction (ma-%)	Material sub type	Mass (g)	Percentage in size fraction (ma-%)	Re-marks
2 - 11.2	F	plastic	733.7	86.7	other plastic fishery plastic foam	733 0 0.5	87 0 0.1	
	S	rope organics plastic non plastic** Total	13 26 7 67 846	1.5 3.1 0.8 7.9 100				
11.2 - 31.5	F	plastic	6020	89.50	other plastic fishery plastic foam	5389 628 3	80.1 9.3 0.04	
	S	rope organics plastic non plastic** Total	174 125 16.9 390 6726	2.6 1.9 0.3 5.8 100				
31.5 - 46.5	F	plastic	4760	90.6	other plastic fishery plastic foam	3890 867 2	74 17 0.05	
	S	rope organics plastic non plastic** Total	90 29 46 331 5255	1.7 0.5 0.9 6.3 100				
46.5 - 200	F	plastic	3518	90.7	other plastic fishery plastic foam	3336 103 79	86 3 2	
	S	rope organics plastic non plastic** total	84 0 276 0 3878	2.2 7.1 100				
200 - 400	F	plastic	5981	100	other plastic fishery plastic foam floating PET bottle	4841 917 87 137		
	S		0	0				

**: mainly inorganics, such as stones and batteries

Table 9.3. Float sink analysis of individual size fractions from Table 9.2 in water (1000 kg/m³) followed by composition analysis by manual sorting

Remarkably, 60 wt% of the lighter-than-water material is heavier than 960 kg/m³, as indicated in Table 9.3. Note that polyolefins, such as PP, LDPE and HDPE, typically lie in the density range of 900-960 kg/m³. Apart from foamed resins, polyolefins are the only solid plastics that are lighter than water. Therefore, two reasonable explanations come to mind for the above finding: (1) the majority of the objects in the sample contain a small amount of fillers, such as chalk, or (2) the plastic objects are oxidized due to weathering, which shifts their original density to higher values. The latter phenomenon seems more likely after a visual inspection and from indicative rigidity tests of individual pieces from the sample. This assumption is also supported by the data in Table 9.4, which shows very little material in the density range of <940 kg/m³. Degradation analyses were carried out to ascertain these issues, see below.

Infrared spectroscopy showed that approximately 90% of the sample was PE as shown in Table 9.5 below. This finding is consistent with the results obtained by (Rios, Moore, & Jones, 2007).

Density fraction (kg/m³)	Mass (g)	Percentage (wt-%)	
<880	0	0	
<881	0	0.0	
<882	2.4	0.5	
<883	13.5	3.0	
<884	10.2	2.3	5.8
<885	6	1.3	
<886	17	3.8	
<887	49.2	11.0	
<888	79.7	17.8	33.9
<889	103.1	23.0	
<890	153.3	34.2	
<891	11.8	2.6	
	1.7	0.4	60.3
Total	447.9	100.00	

Table 9.4: Density distribution of lighter-than-water (1000 kg/m³) material of the 11.2-31.2 mm fraction from Table 9.2. Analysis method: float-sink analysis in ethanol-water mixtures of different densities.

Sample RAV PV2 1.0 F	Fraction	P.O. (PE, PP)	Mass (g)	Mass % of fraction (m%)	# of pcs. (#)
Plastic (plastic)	2 - 11.2	PE	12.1	91.7	73
		PP	1.1	8.3	13
	11.2 - 31.5	PE	166.2	80.6	69
		PP	40	19.4	24
	31.5 - 46.5	PE	448.9	91.1	45
		PP	43.9	8.9	11
	46.5 - 200	PE	435.3	90.8	23
		PP	44.3	9.2	5

Table 9.5: IR analysis on samples taken from each 1.0 F plastic(plastic) fraction to determine the PE/PP ratio distribution within the sample

9.1.4 DEGRADATION ANALYSIS

Degradation of polymers is a result of chemical attacks, mainly oxidation, leading to loss of mechanical properties, such as tensile and impact strength, strain, and also fading of color. In addition, strong oxidation may also lead to shortening of the chain length of the polymer, which can be observed as cracks on the surface of a degraded object and which make the material brittle. Degradation occurs due to one or more environmental factors such as heat, (UV) light, oxidative chemicals (e.g. acids, bases and some types of salt) or bacterial and fungal activity. Although degradation is an essential process to clean up plastic waste in the natural environment by biodegradation, it is clearly undesirable if the polymeric material is to be recycled (material recovery) or is to be converted to oil for use as a fuel (pyrolysis). On the other hand, other recovery options are much less affected when degraded plastic waste is used as an input, such as gasification (converting plastics to syngas) or energy recovery by incineration.

Degradation under atmospheric conditions (which is the case for floating or even submerged plastic pieces in the ocean), generally involves - but is not limited to - chemical absorption of oxygen atoms in the polymer chain in the form of ketones (C=O), hydroxyl (OH) or carboxylic (COOH) groups. Due to this oxygen uptake, advanced degradation leads to an increase of material density, which we indeed observed in our samples from Hawai'i (see section Composition and size distribution analyses).

If waste plastics are to be recycled as a material, the negative influence of degradation is obvious. The reason that degradation also affects the quality of pyrolysis oil lies in the fact that the chemically bound oxygen from the degraded polymer chains is carried over into to the pyrolysis oil. As a result, the oil becomes acidic and attacks the inner walls of combustion engines and fuel pipes. In addition, chemically bound oxygen reduces the heating value of the oil (i.e. the amount of heat released during combustion of a given amount of oil, e.g. 1 kg).

As material recycling and pyrolysis are preferred recovery options for plastics recovered from marine debris in this project, knowledge on the degree of degradation of these plastics is important. Therefore, we performed analyses to determine the degree of degradation due to oxidation of the sample. The degradation tests were carried out at the Laboratório de Polímeros, Universidade de Caxias do Sul, Brasil.

PREVIOUS FINDINGS

Sudhakar et al., (2007) studied the loss of mass of synthetic plastics in seawater due to (bio)degradation. To this end, they immersed samples of HDPE, LDPE and PP in the Bay of Bengal near Chennai Port (Port) and Fisheries Survey of India (FSI) for a period of six months with a monthly sample withdrawal. This study indicated maximum losses of mass of 1.5-2.5% for LDPE, 0.5-0.8% for HDPE and 0.5-0.6% for the PP after 6 months of exposure. In studies of Albertsson & Karlsson (1990) it was found that the LDPE buried in soil lost 3.5% of its mass in 10 years. This low rate of decomposition is in accordance with studies of (Otake, Kobayashi, Asabe, Murakami, & Ono, 1995), in which it was found that 10 years is a relatively short period of time for biodegradation of synthetic polymers, such as polyethylene [3]. The same study reports a mass reduction of 2.5% in LDPE and a decrease in tensile strength of 24 to 20 MPa in 6 months in tropical conditions. The formation of carbonyl groups was found to help microorganisms in the process of degradation. Note that under tropical conditions, higher levels of biodegradation can probably be expected due to the higher levels of temperature, oxygen and microorganisms.

Figure 9.5: Ground mixture of PP and HDPE from marine debris before washing

SAMPLE PREPARATION

For the analysis, we selected polyolefin objects >2 mm from the Hawai'i sample. Ropes and fishery objects were excluded from this analysis. The sample was prepared by mixing polyolefins from all size fractions from Table 9.3 (see section Composition and size distribution analyses) according to their mass ratio in the original raw sample. The sample was then ground in a cutting mill to <20 mm and washed in a neutral detergent solution and dried in an oven at 90 °C for 72 hours (see Figure 9.5). Subsequently, the prepared polyolefin mixture was separated into pure fractions of PP and HDPE using the float-sink method in a water-ethanol mixture of density 920 kg/m³. This is because the applied method of degradation analysis by infrared spectroscopy required mono-plastic type fractions. Finally, the ground samples were subjected to cryogenic milling to obtain fine powders, which were subsequently dried for 72 hours in a desiccator.

The resulting dry polymer powders were mixed with KBr and pressed to tablets of defined dimensions suitable for the infrared spectrophotometer used (see next section).

INFRARED (FTIR) SPECTROSCOPY

PP and HDPE samples were analysed separately by spectrophotometry using the Fourier transform infrared (FTIR) method. A spectrophotometer of the type Nicolet, model Impact, with a measurement range of 400 to 4000 cm^{-1} was used. This spectrophotometer required the samples be ground to powder and pressed to tablets of defined dimensions in a potassium bromide (KBr) matrix. The measurements were carried out in threefold for all samples.

For the present purpose of FTIR analysis of polyolefins, the following bands are characteristics:

Polyethylene (HDPE): 1465 and 731 cm^{-1}
Polypropylene (PP): 840, 1166, 1455 and 2720 cm^{-1}

For the evaluation of the degree of degradation, the carbonyl index (CI) derived from the obtained spectrometric graphs was used. In this work, the CI was calculated as the ratio between the areas of peaks belonging to oxidized components to those belonging to the natural characteristic components of the polymer.

For polyethylene, the area of the peaks at 1780 and 1700 cm-1 was used for the oxidized components (carbonyl forming bands) and the area of the peak at 1465 cm-1 was used to represent the natural component of PE. For polypropylene, the same area of 1780 and 1700 cm-1 was used for the oxidized components, whereas the area belonging to the peak at 2720 cm-1 was used to represent the natural component of PP.

RESULTS

The carbonyl index is a useful and broadly used measure to quantify the degree of degradation of polymers. Yet, it is not an absolute measure of degradation and it can, therefore, not be directly translated to the loss of mechanical properties of the given polymer. Hence, we compared the data of our measurements with studies in which degradation was induced under controlled laboratory conditions and in which the carbonyl index was defined in the same way as in our study.

Figure 9.6 and Figure 9.7 show the obtained FTIR spectra for PE and PP, respectively, showing the formation of the carbonyl groups at 1720 cm-1, which is characteristic for the oxidation of the material. Table 9.6 shows the calculated values of the carbonyl index (CI) for the studied PE and PP samples. Higher values of CI indicate stronger oxidation. Note that CI values of PE and PP cannot directly be compared to each other, because the basis of calculating the CI value is different for both polymers (i.e. the area belonging to the peak that represents the natural component of PE and PP are different).
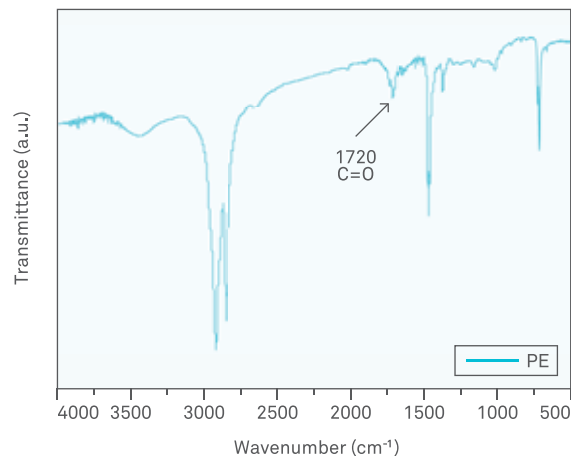
Figure 9.6. FTIR spectrum of the studied PE sample recovered from marine debris at the beaches of Hawai'i
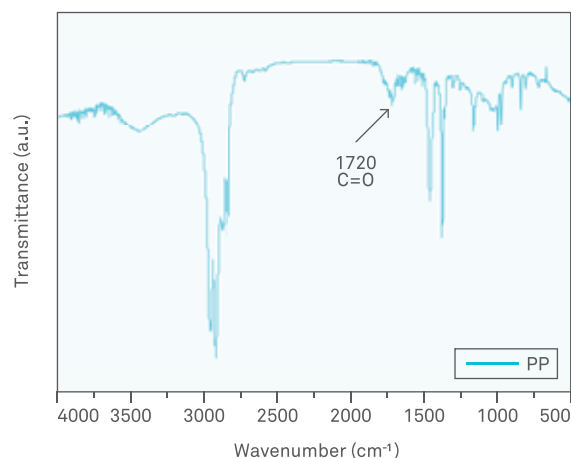
Figure 9.7. FTIR spectrum of the studied PP sample recovered from marine debris at the beaches of Hawai'i

Gulmine, Janissek, Heise, & Akcelrud, (2003) measured the carbonyl index of LDPE (low density polyethylene) and HDPE (high density polyethylene) using the same comparison bands which were used in this study. They exposed the samples to UV light of an intensity of 0.35 W/m², and to an elevated temperature of 50 °C for 16 days (LDPE) and 67 days (HDPE) respectively. They obtained CI values close to 0.5 for both LDPE and HDPE, which closely match our data. Further, in a study carried out at the University of Caxias do Sul, Brasil, the carbonyl index was measured for PE that was exposed to accelerated aging by UV light (according to ASTM G154-00) for 2 days and by heat in an air-circulated oven at 55°C for 113 days. The resulting carbonyl indices were 0.86 for UV exposure and 0.05 for heat exposure, respectively.

(Rabello & White, 1997) obtained carbonyl index values of between 9.1-9.3 for polypropylene that was exposed to UV light with an intensity of 2.2 W/m², at a temperature of 30 °C, for 63 days. They used the same comparison bands as in our study.

Samples	Carbonyl
PE1	0.48
PE2	0.49
PE3	0.48
PP1	9.14
PP2	9.49
PP3	9.26

Table 9.6. Carbonyl index of the PE and PP samples of this study as determined by FTIR spectrophotometry. The indicated figures represent repeated measurements

CONCLUSIONS

From the above degradation tests so far it can be concluded that the polyolefin samples originating from marine debris from the beaches of Hawai'i were less degraded than expected. The degree of degradation of HDPE appears particularly mild both when compared to studies of accelerated ageing under controlled conditions and when compared to the degradation found for PP from the same sample origin.

Due to the characteristics of its chemical structure, polypropylene (PP) is more susceptible to degradation than polyethylene (PE). In turn, low-density polyethylene (LDPE) is more susceptible to degradation than high-density polyethylene (HDPE) at the same amount of exposure. HDPE has the greatest resistance to degradation among polyolefins due to the low number of branches in its chain when compared to LDPE and PP. In addition, PP presents tertiary carbon atoms in its macromolecules, in which hydrogen is easily attacked generating a free radical, which triggers the degradation process (crosslinking in the case of PP). Among the different types of influences leading to degradation, irradiation by UV light is probably the strongest, especially when compared to exposure by heat and other environmental influences for the same period of time. The degradation effect of UV light begins on the surface of the attacked material, but at extended exposure it also affects deeper layers leading to the formation of cracks, fissures, brittleness, colour change and fracture. For both PP and PE, which are non-polar polymers, a marine environment does not accelerate degradation significantly when compared to polar polymers, in which water uptake can promote hydrolysis, indicative of degradation. This is an aggressive environment not only due to the presence of salts but also due to wind and sea currents.

In this work, we evaluated the carbonyl index, which is a quantitative parameter that can be used to compare the degree of oxidation of materials. Higher values of the carbonyl index indicate more advanced degradation. However, due to the difficulty of defining exposure time and intensity in marine environments, we compared the results with laboratory degradation tests, in which these parameters were carefully controlled.

The degradation analysis in this work was carried out on plastic samples from marine debris collected along the coast of Hawai'i (see sections above). It should be noted that there might be significant differences in the degree of degradation between samples collected on the coast and those collected directly from the sea, depending upon the residence time of the objects in both environments and weather conditions. There are indications that the coast is a more aggressive environment with respect to degradation than the open sea, especially when objects are completely submerged in water. First, objects lying on the coast show stronger build-up of heat due to sun irradiation than objects floating in sea, which are cooled by the water. As a result, objects on the coast may reach significantly higher temperatures than the surrounding air resulting in an acceleration of light-induced and thermo-oxidative degradation.

Further, all materials submerged in seawater invariably undergo fouling. The initial stages of fouling result in the formation of a biofilm on the surface and gradual enrichment of the biofilm leads to a rich algal growth. Consequently, the biofilm becomes opaque, which reduces the light intensity reaching the object surface. Hence, the rate of photo-degradation at sea appears to be partly determined by the rate of fouling. Advanced stages of fouling are characterized by the colonization by macrofoulants, such as bryozoans, on the affected plastic surfaces.

The excess weight of the macrofoulant might cause the colonized plastic object to become submerged. As the ultraviolet portion of sunlight is strongly attenuated in seawater, submerged plastics will show a slower rate of photo-degradation. On the other hand, microbe-rich foulant film tends to accelerate biodegradation.

(Pegram & Andrady, 1989) reported on tests, in which samples of PP, PE, rubber and fishing nets were exposed to different natural environmental conditions for one year. They found that the most favourable environment for degradation for all samples was in open air, while the underwater conditions inhibited degradation due to the cooling effect of samples exposed to seawater. Biofouling of the sample surface leading to reduced light exposure may also have decreased the rate of weathering.

PYROLYSIS TESTS

NORBERT FRAUNHOLCZ • JOCHEM JONKMAN

Polyolefin plastics (PP and PE) strongly resemble aliphatic (linear-chain) components of crude oil. From that point of view, polyolefins can be regarded as petrified oil. The goal of the pyrolysis process is to convert waste plastics into oil at the highest possible yield to replace fossil fuel. Pyrolysis involves thermal decomposition of the long macromolecular chains of plastics, with the chains becoming liquid at room temperature when their lengths drop below approximately 20 carbon atoms. Pyrolysis is usually carried out in the temperature range of approximately 450 - 550 °C. However, as it is very difficult to control where exactly the macromolecular chains are broken by the thermal process, pyrolysis invariably yields decomposition products with a wide range of chain lengths. As a result, gasses and liquids (oil) as well as solids (char) are produced in different ratios, mainly depending on the process parameters and catalysts used. Gases produced during pyrolysis are usually combusted on-site to maintain the required process temperature, so that pyrolysis does not depend on external energy sources except when starting the process.

Raw pyrolysis oil is a mixture of many different hydrocarbon components and can be compared to crude oil. Therefore, refinement of the raw oil is necessary for many applications, such as to produce gasoline for combustion engines. On the other hand, large ship engines can take a broad range of oil qualities and unrefined pyrolysis oil can meet quality requirements for marine fuel. As the refinery step involves additional costs and converts only part of the raw oil input into the target product (e.g. gasoline), marine fuel appears a very attractive application for pyrolysis oil despite its somewhat lower market price when compared to refined products.

At the time of writing of this report, Companies A and B have already reported on their results whereas the tests at Company C are still underway. Both companies A and B have reported that the pyrolysis oil obtained with our samples originating from marine debris met their quality standards and was comparable to the quality of oil derived from their regular plant input, which usually represents mixtures of PP, HDPE and LDPE from different waste sources. Both companies stated that they would be able to take such marine debris as an input material without restriction in their plants when the material is pre-treated in the way similar to our sample. Note that the quality of pyrolysis oil was in both tests evaluated by visual inspection. Chemical composition analyses were not performed at this stage.

9.2.1 TEST SETUP

Three companies, either users or suppliers of pyrolysis equipment, were requested to test our plastic samples from marine debris and report on the quality of the obtained pyrolysis oil. In order to have a basis of reference, we sent samples from the very same batches for these tests as used for the degradation analyses (see paragraph on Degradation analysis above). Due to the relatively small amount of available samples (approx. 5-10 kg per test), all tests were carried out on a laboratory scale.

9.2.2 SAMPLE PREPARATION

For the pyrolysis tests, we selected polyolefin objects >2 mm from the Hawai'i sample, from which ropes and fishery objects were excluded. The samples were prepared by mixing polyolefins from all size fractions from Table 9.3 (section Composition and size distribution analyses) according to their mass ratio in the original raw sample. The samples were then ground in a cutting mill to <12 mm in order to arrive at a fairly narrow particle size distribution and subsequently shipped to the test facilities. These samples represented mixtures of PP and HDPE and contained a few percent of non-polyolefins, such as wood and foamed plastics, but the samples were free from heavier-than-water plastics (e.g. PET).

9.2.3 RESULTS

The companies involved in the pyrolysis tests preferred not to be mentioned by name at this stage in this report. Therefore, the results below are referred to as originating from Company A, B and C.

9.2.4 MASS BALANCE OF PYROLYSIS

Companies A and B provided us with the mass balance of their full-scale pyrolysis plants when processing their regular input material (all figures in wt%):

Company A producing gasoline:

- 17% syngas
- 15% light fraction for internal use in the plant
- 62% gasoline fraction
- 5% char
- 1% water

The gasoline fraction is further treated by column distillation that yields the mass balance:

- 1% light oil fraction
- 86% gasoline fraction suited for diesel engines of road vehicles
- 7% kerosene suited for power generators
- 7% heavy fraction to be returned to the pyrolysis process

Company B producing marine fuel:

- 15% syngas
- 77% marine fuel
- 7% char
- 1% water

Depending on the intended mixing ratio, the pyrolysis oil can be directly blended into the regular marine fuel for lower percentages in the fuel or refined first for higher percentages. There is no data at this point on the ratio of mixing where refining becomes necessary, or on the mass balance of the refinery with this type of pyrolysis oil.

9.2.5 CONCLUSIONS

The results of pyrolysis tests are very encouraging. According to the companies involved, the quality of the pyrolysis oil obtained from the polyolefin fraction of marine debris is comparable to that obtained with the regular input of their pyrolysis plants. It appears from the results that the process producing marine fuel is more attractive due to its substantially higher yield of 77% for the target fraction when compared to the gasoline producing process with a final yield of 53% for the gasoline fraction. In addition, the less strict quality requirements on marine fuel are an advantage in an actual application of this recovery route.

FINANCIALS

**BERND VAN DIJK • DARIO GRASSINI • JAN DE SONNEVILLE
BOYAN SLAT**

The focus of this chapter is to provide insight into: (i) the estimated required investment in capital expenditures; and (ii) an indication of the estimated annual operating expenses. This also allows for comparison to alternative cleanup solutions that are currently being utilized.

Section 10.1 presents the investment in capital expenditures; Section 10.2 presents the estimated operating expenditures and decommissioning costs; Section 10.3 inspects various scenarios to provide an indication of the break-even costs/price. This is in combination with the mass of plastic removed assumptions. The chapter then concludes with section 10.4 cost conclusions and a comparison to alternative solutions.

The costs and prices are attained from information presented in the appropriate chapters within the feasibility report. In assessing the accuracy of the estimated costs, we look at three broad possible results: base case, best case, and worse case cost. The case price sensitivity is calculated using quotes received from potential suppliers, Internet research, intuitive calculations, and various assumptions. These unit cost results were applied to three different array lengths (50, 100, and 200 kilometres); each length with its own determined field efficiency (63 percent, 100 percent, and 200 percent relative to the 100 km value of 45 percent).

The scope of this report does not cover multiple periods or valuations. It focuses on the initial capital outlay and the annual costs of platform operation. Prospective future costs and valuations will be examined in detail during the next phase when additional information regarding the masses of plastic to be captured over the years and sales prices of relevant plastic quality will be gathered to assist in those calculations. From there we will be able to more accurately predict the potential cash flows from sales and any return on investment.

Capital and operating expenditures do not include amounts for insurance, harbour costs, transport, or installation. In calculating the costs, certain assumptions are made by using exchange rates and approximate costs of fuel. Hedging against currency exchange, inflation, and fuel price fluctuations, as well as accounting for professional service fees, will be considered in more detail during the coming phases.

CAPITAL EXPENDITURES

Maintenance
€ 2,167

Platform
equipment
€ 1,722

Platform
€ 18,795

Mooring
€ 61,781
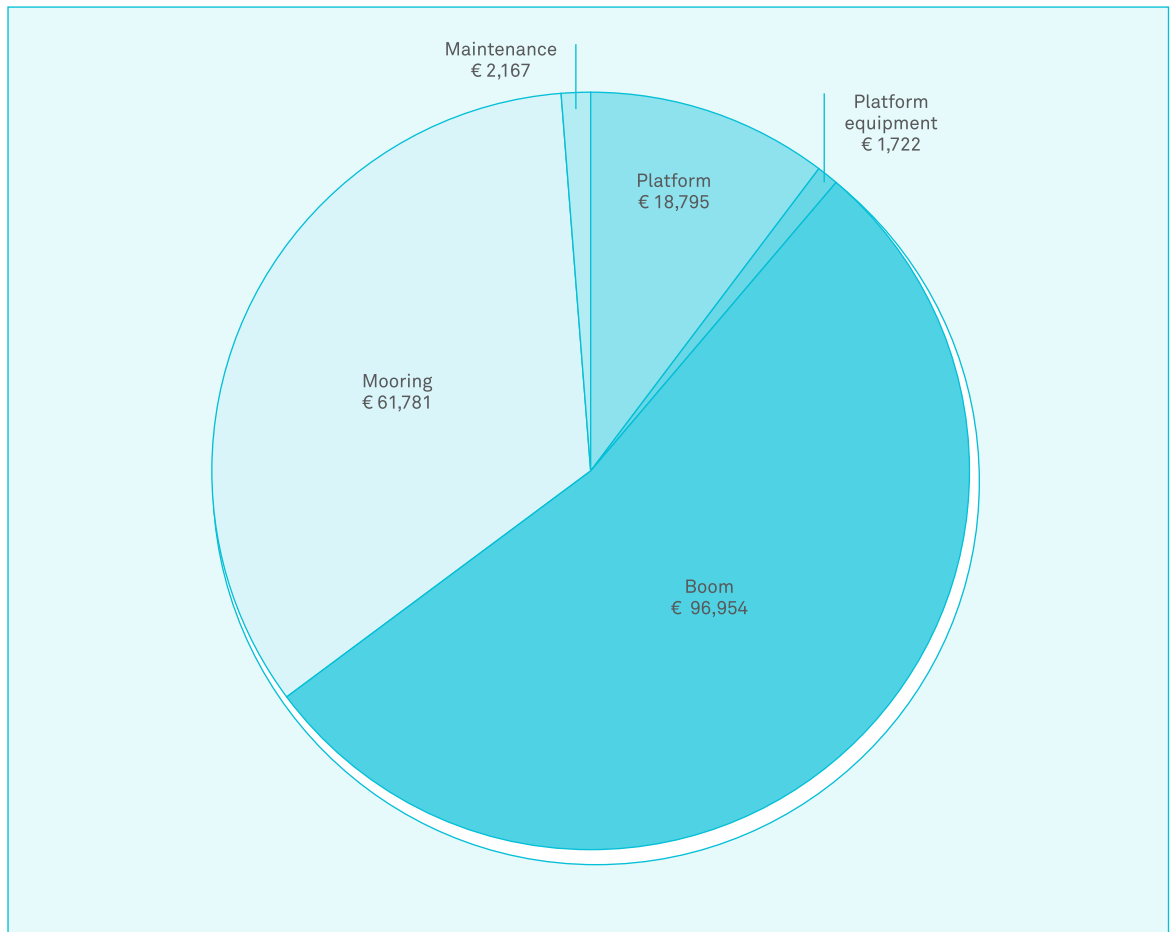
Boom
€ 96,954

Figure 10. 1 Estimated initial Base Capital Expenditure in euro '000s

10.1.1 COMPONENTS OF CAPEX

TOC has categorised CapEx into five main cost components: the platform, platform equipment, boom, mooring, and maintenance (after year 1). These include a variety of items with the required minimum mass of units at current market rates (in euro). A detailed breakdown of the costs can be found in Figure 10.8. For a base-case scenario where a 100 km Array is being utilized, the total initial estimated capital expenditure is approximately €180,193,050. Figure 10.1, shows the breakdown of the main categories.

10.1.2 MAIN CAPITAL EXPENDITURES

Table 10.1 below shows the estimated cost per unit of the Top 5 items and other significant items. These relate to different categories and take into consideration a base-, best-, and worst-case cost scenario for an Array length of 100 kilometres.

As can be seen from the top sheet, the five main cost-drivers of the capital expenditures are the mooring lines, tension cable, buoyancy elements, boom fabric, and spar platform.

One significant item to note is the cost of the selected platform. For this feasibility study, The Ocean Cleanup (hereafter referred to as TOC) assumes to be using a custom-built spar platform with an estimated cost of € 14 million. This cost is based on quotes received from credible platform manufacturers. This selection was also determined to be more effective with regards to our mission. In comparison to the other option, a SWATH Vessel with a cost of € 50 million, the spar platform is € 36 million less expensive.

	Category	Base	Best	Worst
Total CapEx		**180,193**	**147,984**	**202,685**
Mooring lines	Mooring	36,893	25,825	40,582
Cable	Boom	26,161	22,237	30,085
Buoyancy elements	Boom	25,404	22,864	27,944
Fabric	Boom	21,252	19,127	23,377
Spar buoy	Platform	14,000	11,200	16,800
Top 5 total		123,710	101,252	138,789
% of total CapEx		68,65%	68,42%	68,48%
Other significant CapEx costs				
Anchoring	Mooring	9,743	8,769	10,717
Antifouling coating	Boom	9,660	6,859	11,689
Bottom chain	Mooring	4,890	4,401	5,379
Ballast	Boom	3,364	3,028	3,700
Mooring	Mooring	1,995	1,397	2,195
Manufacturing	Boom	1,916	958	2,299
Vessel, fuel & crew	Other	1,000	900	1,100

Table 10.1 Top 5 CapEx cost items (not considering installation costs); in euro '000 for a 100 km Array. Table also shows 'Other significant CapEx costs'.

10.1.3 UNCERTAINTIES AND SPREAD OF CAPEX

There are a number of assumptions, uncertainties, and different quotes that cause a spread from the base cost. For the desired scenario consisting of: a 100 km Array with a 10 year limited life, geared to capture 7,000 tons of plastic with a 45 percent efficiency rate, each item on the list of capital expenditures deviates from the base cost by its own percentage to provide a best/worst case. These can also be seen in Figure 10.8. For the total initial CapEx, the outlay of € 180.2 million is estimated to range between € 147.9 million (best-case) and € 202.7 million (worst-case). This is a spread consisting of an 18 percent decrease and 12 percent increase, respectively. from the base cost which attempts to demonstrate the range of the anticipated costs.

CHAPTER 10.2

OPERATING EXPENDITURES

Staff
€ 800

Transport of plastic
€ 907

Maintenance
€ 3,268

Platform operations
€ 25
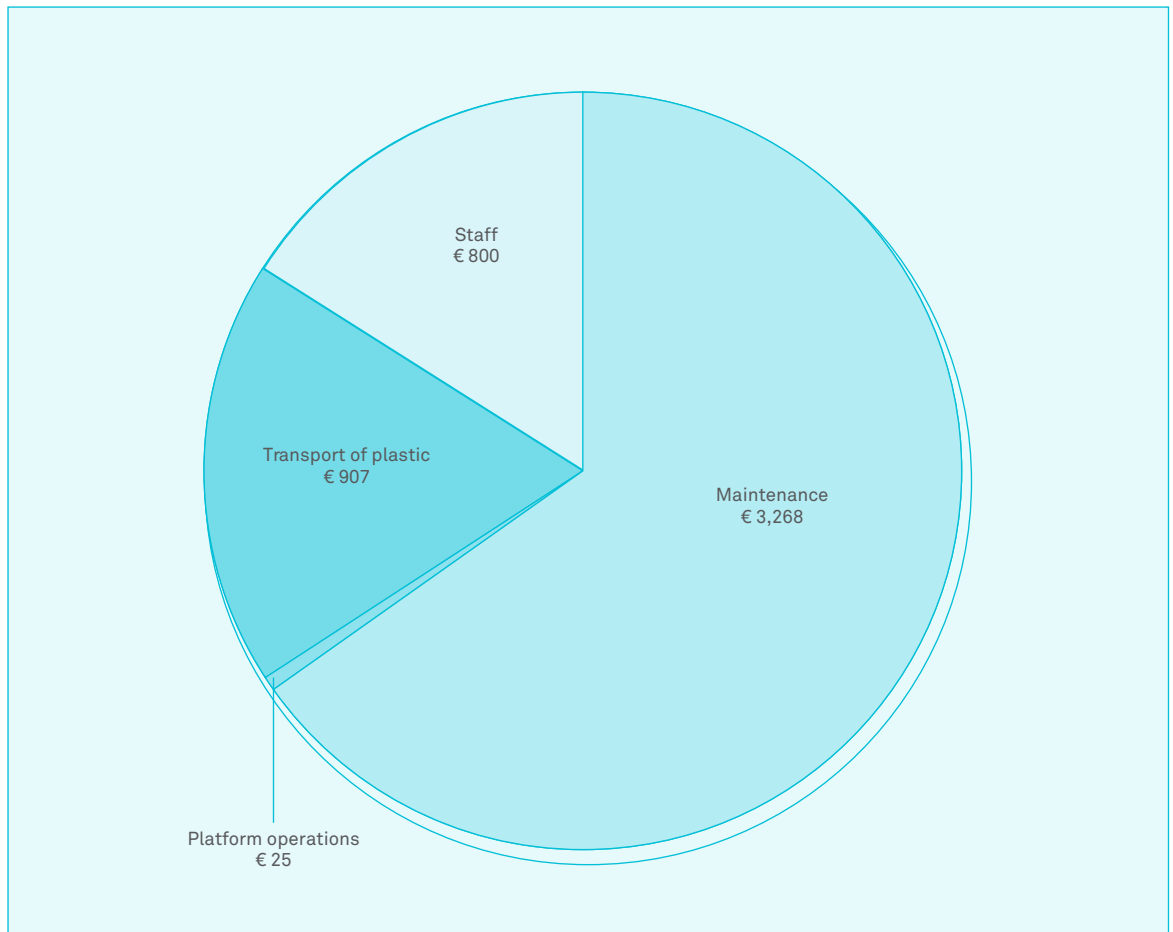
Figure 10.2 Estimated annual base operating expenditure in euro '000s for a 100 km Array

10.2.1 COMPONENTS OF OPEX

Operating expenditures have been classified into four main categories: maintenance, platform operations, transport of plastic, and staff. These also include a variety of items with the required minimum volume of units at a current market rate in euro. A detailed breakdown of the OpEx costs can be found in Figure 10.8. For a base-case scenario where a 100 km Array is being utilized, the total annual estimated operating expenditures is approximately € 3,304,000.

Not included in the OpEx are decommissioning costs. These will be incurred when removing the platform, moorings, and booms from the ocean. The current base-decommissioning estimate is € 16.8 million (6.3 + 7.7 + 2.8 million respectively).

	Category	Base	Best	Worst
Total OpEx		**5,000**	**3,428**	**6,886**
Maintenance vessels, fuel, crew	Maintenance	2,298	1,149	3,769
Spare parts	Maintenance	970	727	1,212
Onshore staff	Staff	800	720	880
Fuel transport	Transport of plastic	779	702	857
Crew transport	Transport of plastic	128	115	141
Top 5 total		4,975	3,413	6,859
% of total OpEx		99.50%	99,56%	99,60%

Table 10.2 Top 5 OpEx cost items; in euro '000 for a 100km Array

10.2.2 MAIN OPERATIONS EXPENSES

To generate an indication of the cost price and comparison to alternative cleanup methods, annual operating expenses have been calculated. Table 10.2 below shows the Top 5 Operating Expenses in which TOC also factors into consideration the best- and worst-case costs. Figure 10.8 shows a total overview including: maintenance labour costs, platform operation fuel, and chartering the plastic transit vessel.

10.2.3 UNCERTAINTIES AND SPREAD OF OPEX

As with CapEx, in the scenario where TOC is able to obtain a 45 percent field efficiency using a 100 km Array to collect a mass of 7,000 tons annually, there are uncertainties and spreads associated with the operating expenses. The total annual OpEx base is € 5.0 million and is estimated to range between € 3.4 million (best-case) and € 6.9 million (worst-case) allowing for a 31 percent decrease and 38 percent increase respectively from the base cost. Uncertainties in this area can be a function of the capital expenditures and on-going expenses required to run the operations such as: staff costs, the number of times per year the transport vehicle needs to extract plastic from the platform, the required spare parts (estimated at 0.6 percent of CapEx) and the maintenance vessel, fuel, and crew administered.

BREAK-EVEN COSTS/PRICES

To determine a first important indication of the financial feasibility of the project, a break-even analysis is performed. This analysis compares total costs (capital depreciation and operational costs) in relation to the total mass of plastic extracted from the ocean. The result is the minimum price The Ocean Cleanup would have to sell each kilogram of plastic to "stay above water" - i.e. the break-even price (euro / kg).

Breakeven analysis: price per kg
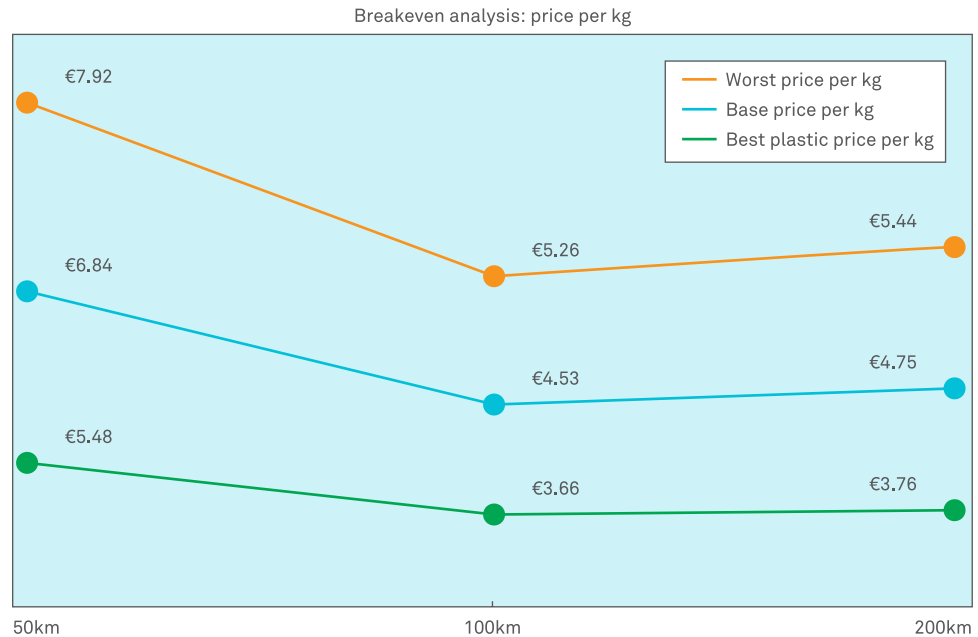
Figure 10.3 Break-even analysis in price per kilogram for each Array length in kilometres

10.3.1 METHOD (FOUR VARIABLES) AND ASSUMPTIONS

In performing the break-even analysis, four variables and certain assumptions are considered. The four variables are: scenario (base-, best-, worst-case cost), length of the Array (50 / 100 / 200 km), the lifetime of the project in years (20 years (economic) or 10 years (limited)), and lastly the total mass (7,000 / 15,000 / 45,000) in tons per year of plastic extraction. A field efficiency rate of 63 percent, 100 percent and 200 percent (relative to the field efficiency of a 100 km array) has been used for the three array lengths respectively.

Utilizing a financial model that tests the cash (Capex and Opex) as well as cost (depreciation and operation) outlook over the project's period, one can determine the break-even price considering the above variables, assumptions, and costs per unit of CapEx and OpEx. For instance: In a base case scenario, utilizing an Array length or 100 km, with an limited life (10 years), to capture a mass of 7,000 tons per year, the break-even price is € 4.53 / kg.

In the calculations, a limited lifetime of 10 years is applied instead of a general economic lifetime (for most equipment 20 years). This is because projections indicate the mean amount of plastic mass will decrease with time. Thus, the average mass of plastic that will be collected per year will likely be lower than what has been calculated using the 10-year deployment time. Lastly, the resale value of any capital infrastructure is conservatively assumed to be zero, as its sales price is too uncertain. However, any CapEx sales would reduce the total cost of the project. Resale revenue would also be applied against decommission expenses.

10.3.2 SENSITIVITY ANALYSIS

The below figures represent the results of the scenarios:

Array Length in kilometres ('000s)		50			100			200		
Field efficiency relative to the 100 km array		63%			100%			150%		
Total Cost (Euros '000 / yr) - P&L Outlook % Deviation from Base case		24,496	19,559 -20%	28,205 15%	25,068	19,436 -22%	28,863 15%	33.747	26,570 -21%	38,446 14%
	Volume	Breakeven price (€/kg)			Breakeven price (€/kg)			Breakeven price (€/kg)		
Ton/year (efficiency 100 km)	7,000	5.84	4.71	6.68	3.82	3.01	4.36	3.45	2.77	3.90
Ton/year (efficiency 100 km)	15,000	2.85	2.33	3.25	1.91	1.54	2.16	1.74	1.42	1.95
Ton/year (efficiency 100 km)	45,000	1.20	1.03	1.34	0.89	0.77	0.98	0.83	0.73	0.90

Table 10.3 Annual Costs - Economic life

Array Length in kilometres ('000s)		50			100			200		
Field efficiency relative to the 100 km array		63%			100%			150%		
Total Cost (Euros '000 / yr) - P&L Outlook % Deviation from Base case		28,894	22,953 -21%	33,171 15%	30,039	23,926 -20%	34,487 15%	47,396	36,976 -22%	53,654 13%
	Volume	**Breakeven price (€/kg)**			**Breakeven price (€/kg)**			**Breakeven price (€/kg)**		
Ton/year (efficiency 100 km)	7,000	6.84	5.48	7.82	4.53	3.66	5.16	4.75	3.76	5.35
Ton/year (efficiency 100 km)	15,000	3.32	2.69	3.78	2.24	1.84	2.54	2.35	1.88	2.62
Ton/year (efficiency 100 km)	45,000	1.36	1.15	1.51	1.00	0.87	1.10	1.04	0.88	1.13

Figure 10. 4 Annual Costs - Limited life

The preferred scenario includes: Base costs, an Array length of 100 km, a limited life of 10 years; the total cost is € 31.7 million per year. At a mass of 7,000 tons, this results in a break-even price of € 4.53 / kg.

COST CONCLUSIONS

	Best	Base	Worst
Initial Capital Expenditure	€ 147,984,453	€180,193,050	€202,684,608
CapEx Replacement Costs after 5 yrs	€ 61,035,640	€70,198,000	€ 78,191,390
Operating Expenditures over 10 yrs	€ 34,276,271	€ 49,997,283	€ 68,860,495
Decommissioning cost after 10 yrs	€ 12,607,500	€ 16,810,000	€ 18,491,000
Total Cost over 10 yrs Including Replacement & Decommissioning Costs	€ 255,903,864	€ 317,198,333	€ 368,227,492

Figure 10.4 OpEx in relation to CapEx, euro (best-, base-, and worst-case) over ten years.

10.4.1. SUMMARY OF ESTIMATED CAPITAL AND OPERATING EXPENDITURES

The below figure displays the: best-, base-, and worst-case cost scenarios in euro for (i) the total estimated required investment in capital expenditures; and (ii) an indication of the estimated operating expenses over ten years. It also includes the (iii) Replacement cost of equipment that has a useful life of 5 years and (iv) Decommissioning costs after 10 years.

As expected with the passive cleanup concept, capital expenditures outweigh the operating expenditures. The percentage deviation for the above amounts result in: (i) a 18 percent decrease (best) to a 14 percent increase (worst) from the base cost for capital expenditures; and (ii) a 16 percent decrease to 16 percent increase from the base cost for operating expenditures. The Ocean Cleanup will take the above figures into account in order to attain the necessary funding, develop a viable business model with the required infrastructure and personnel expertise, and ensure the financial sustainability of the project.

10.4.2 COMPARISON OF BREAK-EVEN PRICE WITH ALTERNATIVE CURRENT CLEANUP CONCEPTS

There have been numerous other cleanup concepts in the past, conducted by various organizations and public volunteers. Furthermore, cleanup efforts are currently being undertaken, mostly by means of beach cleanups. To be able to judge on the financial viability of the project, this section will compare the cost per kg to other proposed and present measures. Figure 10.6 compares The Ocean Cleanup's base price to alternative concepts. The figure is far from complete, since most concepts have not shared details like costs, deployments time and debris collection rates.

Annual cost per Kg
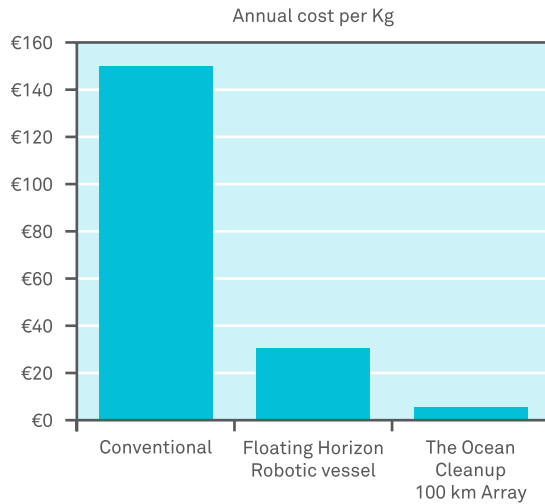
Annual cost per Kg

Figure 10.5 A comparison of cleanup costs per concept per kg
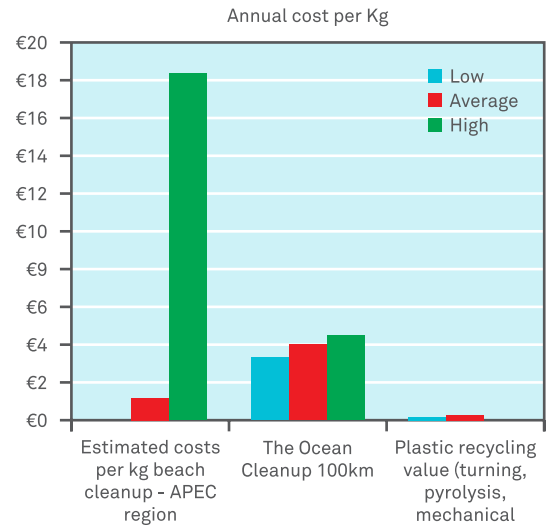
Figure 10.6 The Ocean Cleanup versus APEC beach efforts (voluntary cleanup cost, average cleanup cost in region, ghost net cleanup cost) and Plastic recycling value (total cost per kg)

Concluding, based on the costs outlined in Figure 10.8, The Ocean Cleanup Array is estimated to be 7x to 33x cheaper than conventional cleanup proposals per extracted mass of plastics. In order to extract 70,320,000 kg (42 percent) of garbage from the North Pacific gyre in 10 years, we calculated a total cost of € 317,198,333 (low: € 255,903,864, high: € 368,227,492). This means that in order for it to be profitable, a break-even cost of € 4.53 per kg (low: € 3.66, high: € 5.16) must be taken into account. This cost is comparable to beach clean-ups (€ 0.07 – 18.0 per kg).

All three cases are cheaper than the direct industry damage in the APEC region (€ 6.51, based on 1.265 billion USD per year, and 140,000 tons of plastic in the region). We have not included this number in the comparative graph (Figure 10.7) though, because first of all this estimation is an annual value, instead of a one-time cost. Secondly, most direct economic damage occurs in coastal areas, whereas The Ocean Cleanup targets pelagic marine debris.

Based on the current estimates of costs and the amount of plastic in the oceans, the costs outweigh the profits generated by high-volume solutions, like incineration or pyrolysis, but it is unknown what the financial prospective would be for mechanical recycling, and should be investigated in a later phase.

In terms of financial viability, as has been defined in chapter 1.8, we believe The Ocean Cleanup array has a medium to high financial viability.

CAPITAL EXPENSES	UNIT COST		VOLUME		BASE CASE EUR '000	BEST CASE % deviation -/-	WORST CASE % deviation +/+	ECONOMIC LIFE Years	LIMITED LIFE Years
Platform									
Spar buoy	14,000	EUR / unit	1	units	14,000	-20%	20%	20	10
Mooring	1,995	EUR / unit	1	units	1,995	-30%	10%	20	10
Installation	2,800	EUR / unit	1	units	2,800	-25%	25%	20	10
Equipment									
Capture and transshipment									
Mesh conveyor	9	EUR / unit	1	units	9	-25%	300%	5	5
Slurry pump A	11	EUR / unit	1	units	11	-5%	5%	5	5
Slurry pump B	29	EUR / unit	1	units	29	-5%	5%	5	5
Processing									
Shredder	165	EUR / unit	1	units	165	-5%	5%	5	5
Voraxial separator	380	EUR / unit	1	units	380	-5%	5%	5	5
Supporting construction / connection	280	EUR / unit	1	units	280	-20%	20%	5	5
Power generation									
PV installation	100	EUR / unit	1	units	100	-25%	5%	10	10
Battery	120	EUR / unit	1	units	120	-5%	5%	10	10
Generator	100	EUR / unit	1	units	100	-5%	5%	10	10
Electrical system	150	EUR / unit	1	units	150	-10%	10%	10	10
Control equipment	200	EUR / unit	1	units	200	-5%	5%	10	10
Sensors & transmitters	50	EUR / unit	1	units	50	-5%	5%	10	10
Camera system	30	EUR / unit	1	units	30	-25%	25%	10	10
Fire detection	5	EUR / unit	1	units	5	-25%	25%	10	10
Other (Engineering)	-	EUR / unit	1	units	-	-15%	15%	10	10
General									
Lighting	15	EUR / unit	1	units	15	-5%	5%	5	5
Communication	20	EUR / unit	1	units	20	-25%	25%	5	5
Boom									
Floating barrier									
Fabric	21,252	EUR / unit	1	units	21,252	-10%	10%	5	5
Buoyancy elements	25,404	EUR / unit	1	units	25,404	-10%	10%	5	5
Ballast	3,364	EUR / unit	1	units	3,364	-10%	10%	5	5
Antifouling coating	9,660	EUR / unit	1	units	9,660	-29%	21%	5	5
Manufacturing	1,916	EUR / unit	1	units	1,916	-50%	20%	5	5
Installation	7,694	EUR / unit	1	units	7,694	-4%	6%	5	5
Tension member									
Cable	26,161	EUR / unit	1	units	26,161	-15%	15%	20	10
Connection cables	661	EUR / unit	1	units	661	-10%	10%	20	10
Installation costs	796	EUR / unit	1	units	796	-10%	10%	20	10
Navigation lights	46	EUR / unit	1	units	46	-10%	10%	20	10
Mooring									
Anchoring	9,743	EUR / unit	1	units	9,743	-10%	10%	20	10
Mooring lines	36,893	EUR / unit	1	units	36,893	-30%	10%	20	10
Installation	6,316	EUR / unit	1	units	6,316	-25%	10%	20	10
Underwater buoy	121	EUR / unit	29	units	3,509	-15%	20%	10	10
Navigation buoys	15	EUR / unit	29	units	430	-15%	20%	10	10
Bottom Chain	4,890	EUR / unit	1	units	4,890	-10%	10%	10	10
Other									
Transport vessel and transshipment	1,000	EUR / unit	1	units	1,000	-10%	10%	10	10
TOTAL CAPEX					180,193.85	147,984	202,685		
						-18%	12%		
OPERATIONAL EXPENSES									
Maintenance									
Spare parts	0.6%	of CapEx	1	units	970	-25%	25%		
Maintenance vessels, fuel, crew	2,298		1	units	2,298	-50%	64%		
Platform operations									
Fuel	25	EUR / unit	1	units	25	-40%	10%		
Transport of plastic									
Fuel	779	EUR / unit	1	units	779	-10%	10%		
Crew	128	EUR / unit	1	units	128	-10%	10%		
Staff									
Onshore	80	EUR / unit	10	units	800	-10%	10%		
TOTAL OPEX					4,999.73	3,428	6,886		
						-31%	38%		
DECOMMISSIONING									
Moorings	6,316	EUR / unit	1	units	6,316	-25%	10%		
Booms	7,694	EUR / unit	1	units	7,694	-25%	10%		
Platform	2,800	EUR / unit	1	units	2,800	-25%	10%		
TOTAL DECOM	16,810				16,810	12,608	18,491		
TOTAL CAPEX per year (over 10 years)		Euro '000 / year			18,019	14,798	20,268		
TOTAL CAPEX + OPEX per year		Euro '000 / year			23,019	30,833	45,646		

Table 10.5 Line item break down of capital expenditure, operating expenditure, and decommission costs. Includes unit cost, mass, base-, best-, and worst-case, economic, and limited life.

CONCLUSIONS

BOYAN SLAT • FRANS RATELBAND • JAN DE SONNEVILLE
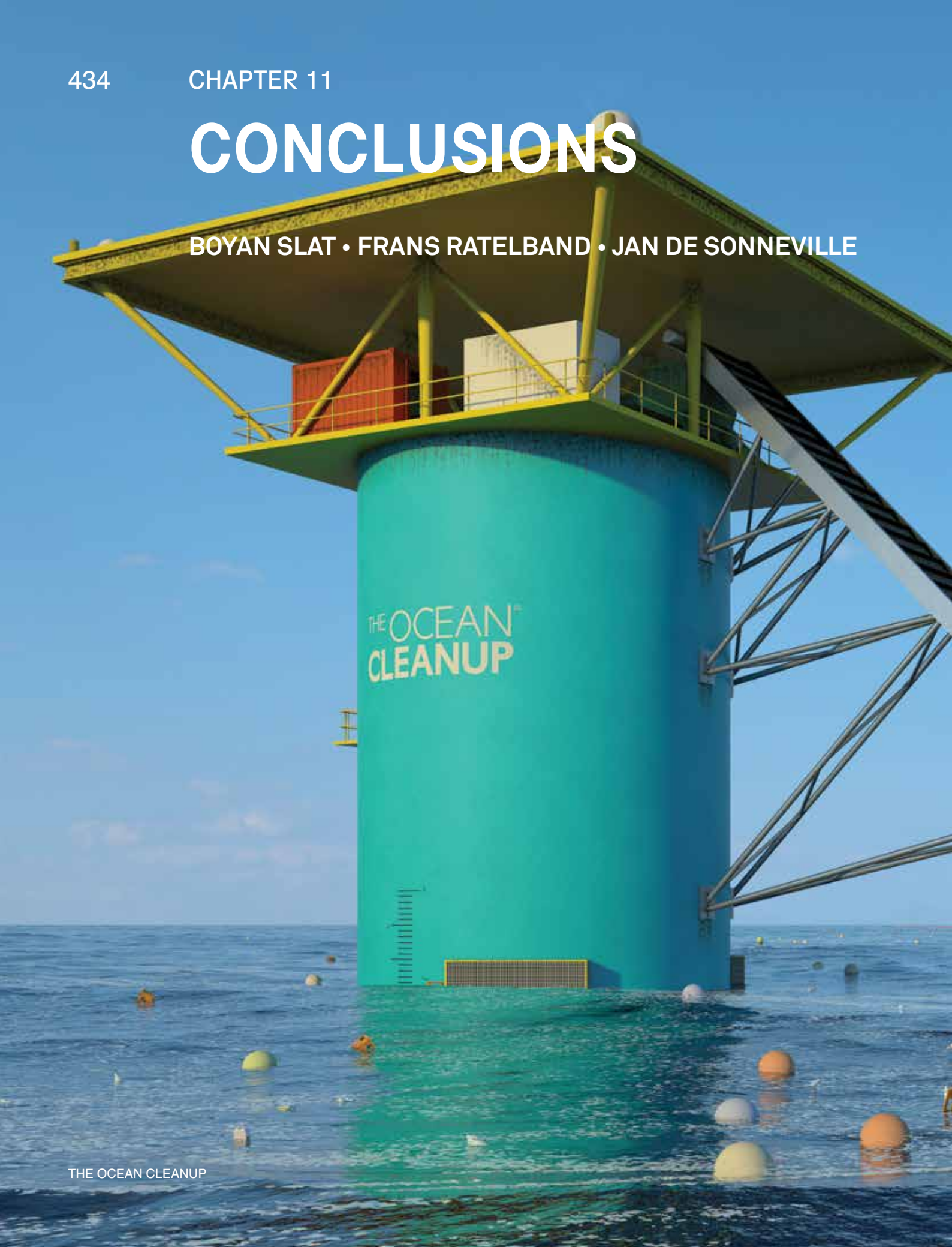
MAIN CONCLUSIONS

In this feasibility study, we have investigated the technical feasibility, financial viability and scalability of large-scale passive plastic removal from the North Pacific gyre using The Ocean Cleanup Array concept.

Plastic pollution is a major threat in terms of ecology, economics and ecotoxicology, and is likely to continue to increase in the next decades, amplifying its hazardous effects (chapter 1).

Using vertical distribution measurements, we have shown that most plastics can be found in reachable distances from the sea surface (section 2.3). At the selected preliminary location, a dominant wind and current direction has been identified (section 2.5). Using simplified computational methods, we have also shown that a passive cleanup array can, in theory, collect significant amounts of plastic, i.e. just under half the plastic in the Great Pacific Garbage Patch with a 100 kilometer span over 10 years (section 2.6).

Using CFD simulations, we calculated that the floating barriers are able to capture 79 percent of plastics by mass (section 3.2), and also showed that plastic gets transported along an angled barrier, thereby proving it is a suitable structure to concentrate plastic pollution (section 3.3).

We developed a boom suitable to withstand ocean conditions (section 3.6), and dimensioned mooring systems suitable for deployment at mid-ocean depths (section 3.7).

We have also shown that existing technology is likely suitable for the extraction, pre-processing and transport of plastics (chapter 4), as well as for the operations (chapter 5).

In terms of environmental impact, we have shown that the collection platform's primary energy source can be solar (section 4.5), and that the impact to sea life is negligible (chapter 6). The entire project would emit carbon emissions equal to 372-1,367 cars.

There are currently no major legal hurdles preventing the implementation of the project on the chosen preliminary location (chapter 8). Furthermore, we have shown there is at least one way to process ocean plastics into a usable and valuable product (chapter 9).

Based on this collected evidence, we conclude The Ocean Cleanup Array likely is a feasible and viable method for large-scale, passive and efficient removal of floating plastic from the North Pacific Garbage Patch.

In order to extract 70,320,000 kg (42 %) of garbage from the North Pacific gyre in 10 years, we calculated a total cost of € 329,180,000 (low: € 280,060,000, high: € 368,890,000). This means that in order for it to be profitable, a break-even cost of € 4.70 per kg (low: € 4.00, high: € 5.27) must be taken into account. This has been based on a conservative estimate of 140,546,000 kg of plastic within the North Pacific accumulation zone. These costs per kg within the range of beach cleanups (€0.07-18.0), and lower than the direct costs to industry in the APEC region per kg per year (€ 6.51).

Finally, for this project to be truly successful in reducing the amount of plastics in the Great Pacific Garbage Patch, it is essential for the influx of new plastic pollution into the oceans to be radically reduced (section 2.6).

RECOMMENDATIONS

The research undertaken has provided the basis not only for drawing conclusions of the concept's feasibility and financial viability, but also for recommending necessary future research before the project is executed in full scale. To summarize, the two essential elements of future in the second phase of the project are:

• The in-depth engineering and optimization of the structure; and

• Improving the plastic mass estimate, by taking spatial and temporal variability, as well as measured vertical distribution into account.

These and several other (secondary) recommendations for future work have been outlined in this chapter, separated into appropriate research fields.
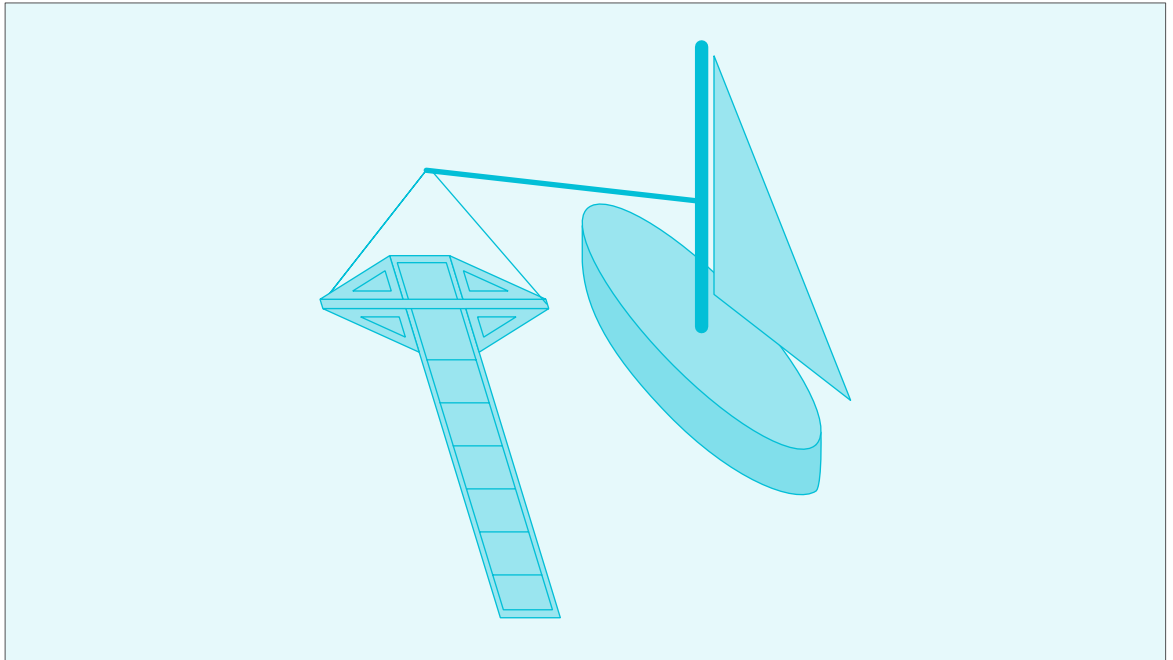
Figure 11.1 Measuring vertical distribution using a multi-level trawl

11.2.1 PHYSICAL OCEANOGRAPHY

DISTRIBUTION AND MASS

- To reduce the magnitude of uncertainties of the vertical distribution data, and its relation with environmental conditions, more multi-level trawl measurements need to be taken (see Figure 11.1). Preferably this should be done in the North Pacific gyre, as this is likely to be the primary target of this project.

- A large measurement-based dataset of plastic concentrations of different sizes - both micro and macro plastics - needs to be built in order to confirm the assumption others have made by extrapolating plastic concentration measurements over entire gyres. To avoid distortion caused by spatial variations in time, multiple parallel and simultaneous gyre transections could be measured (see Figure 11.2). Such a large-scale experiment could also study the assumption that the ratio between micro and macro debris is constant across the gyre. If so, by sampling a large volume of surface water using a large sampling device, a mass spectrum could then by obtained which can then be extrapolated to the gyre, creating a much more accurate mass estimate.
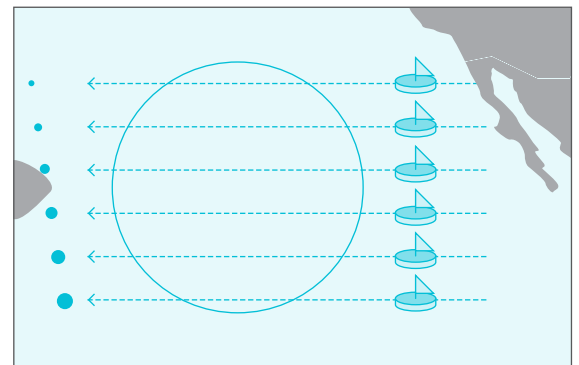
Figure 11.2 Simultaneous transections of an area could avoid inaccuracies caused by spatial and temporal variability

LOCAL CONDITIONS

- To be able to accurately scale the required processing equipment, accurate material flow data for the chosen location must be collected, including its fluctuations over time (see Figure 11.3). This could, for example, be achieved by developing and deploying a permanently moored sampling device.

- Before the project can be executed, detailed studies on the local wave and climate conditions as well as soil properties must be undertaken. Detailed measurement-based data for our area of interest is currently unavailable, due to its remoteness. Deploying a weather buoy apparatus, e.g. attached to the sampling device, could do this.

CURRENT MODELLING AND ARRAY INTERACTION

- To increase the accuracy of the field efficiency determination, the interaction between the floating barriers and current, as well as the interaction between the floating barriers and the plastics, should be taken into consideration. It is unknown what the influence of the barriers will be on the (local) currents. It could be, for example, that the surface velocity is lower during 'reverse-current events', since the barrier is absorbing part of that current's energy (see Figure 11.5).

- Laboratory tests should confirm the ratios between different driving forces of plastic in the ocean; wind, waves and surface currents
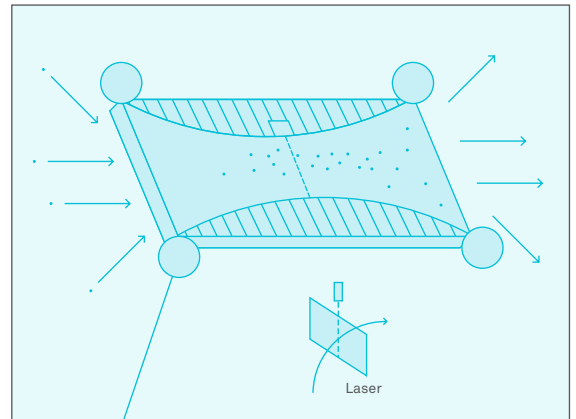
Figure 11.3 An example of a potential (permanently moored) sampling device, designed to optically measure plastic flux over time.
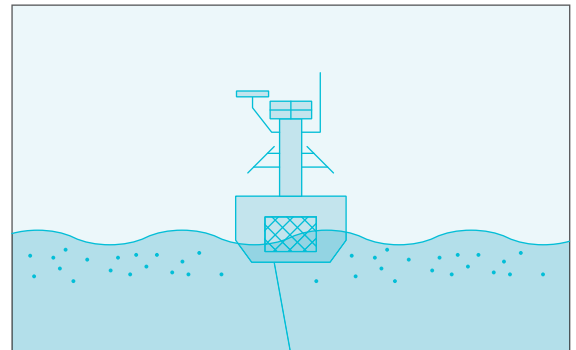
Figure 11.4 A Weather Buoy
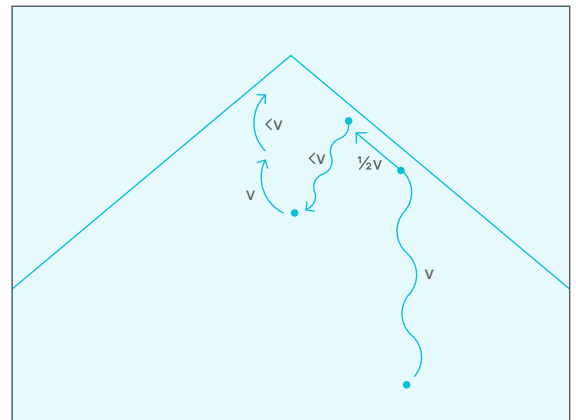
Figure 11.5 An example of a hypothetical trajectory of a particle in 2D, under influence of the array. The particle approaches the array with velocity v cm/s, moves along the barrier with velocity <v cm/s, gets transported away from the array due to a reverse-current event with a velocity that is likely smaller than v cm/s, etc.

11.2.2 ENGINEERING

DURABILITY

- Improving the quantification of the loads on the floating barriers and moorings using a series of up-scaling tests (see section 11.2), and refined designs.

- Experimentally investigate the sensitivity of structural elements for fatigue, which could result in a more efficiently dimensioned structure, reducing costs.

- Impact resistance of the booms for rare and exceptionally large debris (from fridges to shipping containers) should be investigated, to refine current judgments on maintenance and replacements requirements of boom sections.

- Investigating and developing alternative storm survival strategies, with the aim of possibly reducing costs.

- Validating the speed, impacts and coating effectiveness in terms of biofouling

ULTRA DEEP SEA MOORINGS

- Although there is most likely no difference between deep sea moorings currently in use and our ultra-deep sea moorings (see Chapter 3), detailed mooring analyses in terms of vibrations, loads and operations will be necessary to be able to more accurately estimate the costs of the moorings (see Figure 11.7).
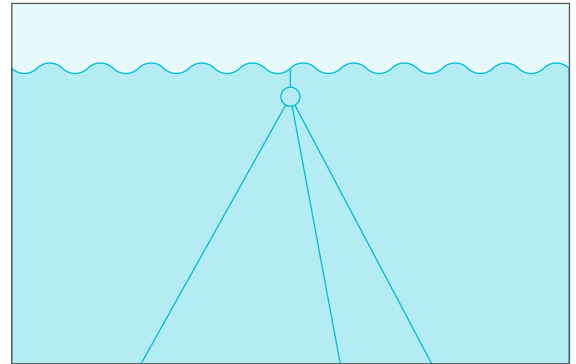
Figure 11.6 A mooring system

11.2.3 FLUID DYNAMICS

3D WAVE AND BOOM INFLUENCE ON PARTICLE TRAJECTORIES

- Investigating the effects of wind- and wave-induced turbulence on the boom capture efficiency.

- Including the interaction between particles and the structure in the CFD analyses.

- Quantifying the potential efficiency loss due to over-topping in high wave conditions.

11.2.4 ECOLOGY

LOCAL IMPACT

- Field tests should investigate whether plankton indeed survives after encountering the floating barriers, and these tests should also dictate whether any active deterrence of vertebrates at the extraction equipment is necessary.

11.2.5 MARITIME LAW

- Engagement of the United Nations is advisable, since the UNCLOS/Law of the sea currently does not provide full guidance for the concept that has been proposed in this feasibility study.
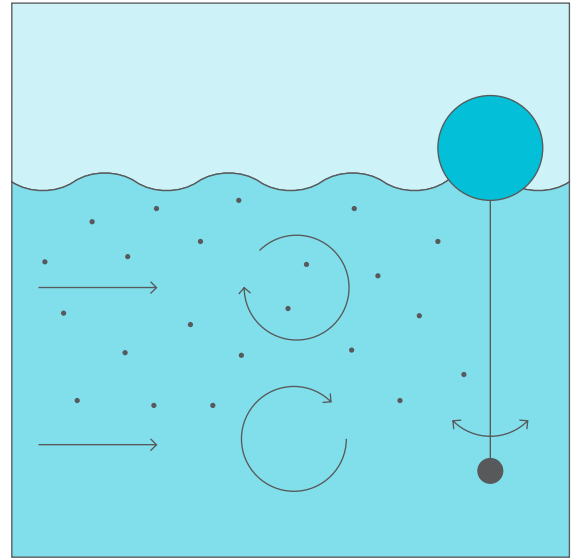
Figure 11.7 The trajectory of the plastic particle near the boom is not only decided by the (turbulent) current flow (left), but also by wave mixing (center) and the motion of the barrier under the influence of waves (right).

11.2.6 RECYCLING

- Processing tests should be repeated with samples directly coming out of a gyre, instead of a sample taken from a beach. This includes investigating the ratio between plastic and non-plastic debris (by mass) floating inside the North Pacific Gyre, across all particle sizes. At the moment, estimates of this ratio have only been based on beached debris, as well as micro-debris samples.

- Investigating the feasibility, advantages and implications of local (on-platform) processing.

- Investigating the feasibility and advantages of other processing options, including mechanical recycling, composites and plasma gasification.

- Investigating if persistent organic pollutants (POPs) have been decomposed, have settled in the pyrolysis' slack, or if pre-treatment of the plastics would be needed to exclude these compounds from the product.

11.2.7 FINANCE

- The added market value of ocean plastics should be investigated, should mechanical recycling be chosen as a processing method.

- Funding models for the 3rd phase (see Figure 13.7) should be explored, including philanthropic, corporate, governmental and inter-governmental means.

OUTLOOK AND NEXT STEPS

In order to address the uncertainties summarized in Chapter 11.1, the second phase of the project must serve to bridge the gap between the results of this feasibility study and the implementation of the technology. In this phase, we propose a series of up-scaling tests, working towards a large-scale operational pilot. To be more cost-efficient, The Ocean Cleanup acts as a facilitator for the research, outsourcing most of the fundamental research to institutes, and collaborating with offshore and engineering companies to cover most of the tests' costs. Figure 11.9 illustrates the step-by step relation between the project initiation phase (July 2012 to May 2013), the preliminary engineering phase (Phase 1 - May 2013 to May 2014), followed by phase 2, in which the engineering will undergo further iteration and validation steps (starting in 2014).
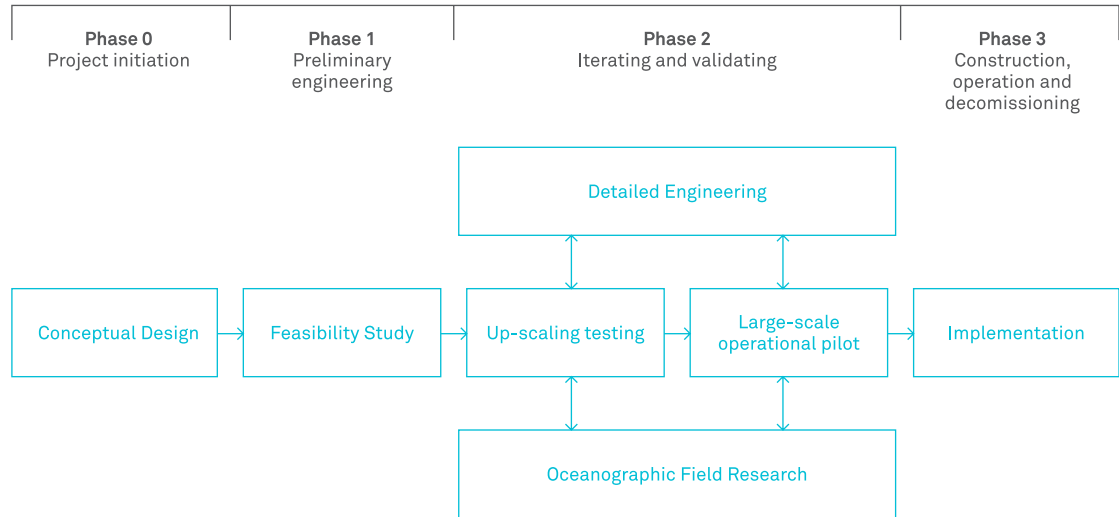
Figure 11.9 Phasing of The Ocean Cleanup project

The series of tests will generate new data in a range of structural and physical topics. Furthermore, these up-scaling tests will serve as a platform for the engineering and oceanographic research groups, enabling them to immediately implement newly developed technology or testing equipment in a real-life environment. This real-time feedback could rapidly increase the speed in which research takes place. As can be seen in Figure 11.10, the identified research topics can be roughly divided into two parts: oceanography and engineering. Each of these research topics can benefit from the results of the tests, while the tests can be improved thanks to the knowledge created in the research groups.

Ideally, the up-scaling tests illustrated in Figure 11.11 would be designed as a functional plastic collection device; the extracted plastic could then be used for the ocean plastic characterization and processing research.

The actual scale and function of each test will depend on the characteristics of the location and the results of detailed engineering and oceanographic research, as well as the output of the previous tests. The scale will likely range from ~100 m at the scale model test (1:1000) to ~10 km at the large-scale operational test (1:10).

PHASE II
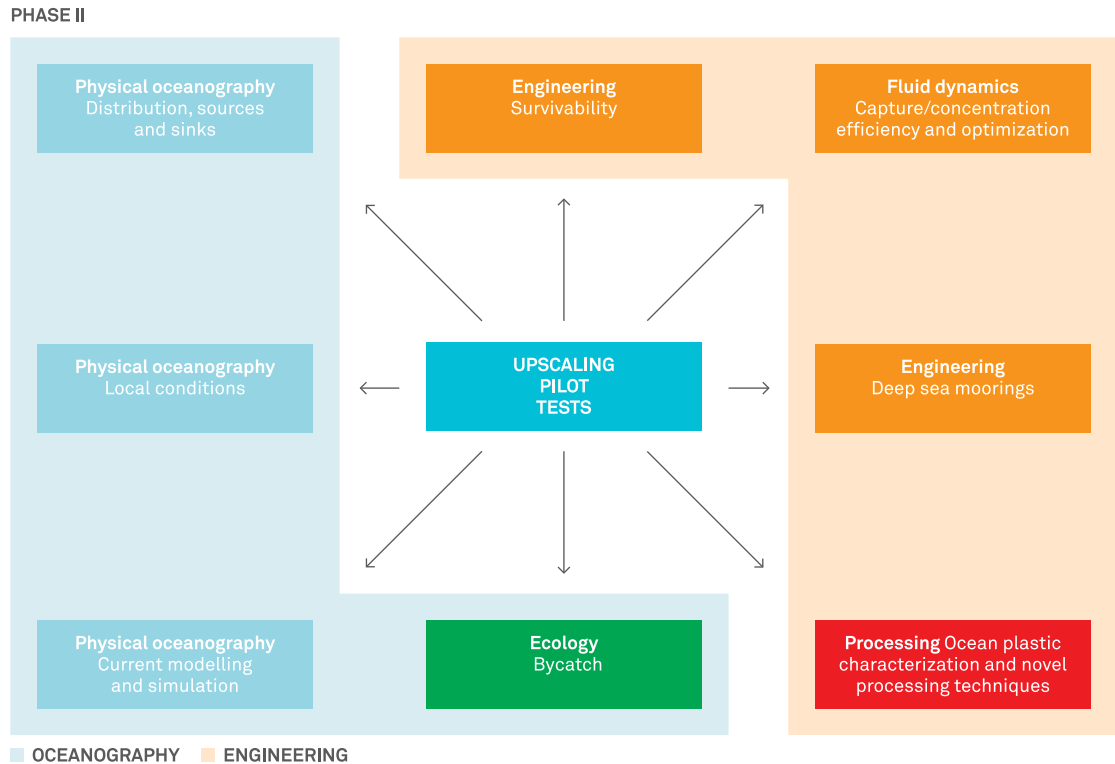
Figure 11.10 An illustration of the relation between the various in-depth research topics, and the series of up-scaling pilots

The majority of the oceanographic field research will be in the first 1-2 years, because many engineering topics require the oceanographic results as input parameters (environmental conditions, soil conditions, plastic flux, etc.). In addition to pre-defined research topics (including forces, boom-particle interaction, moorings, survivability, etc.), these tests also serve to uncover any unforeseen interactions between the structure and the environment, as well as practicing operational procedures.

As can be seen in Figure 11.11, a testing project is followed by another testing project. Depending on the available resources, the tests may or may not overlap. The mission control center will coordinate the other work throughout the phase, and will fulfill the managerial role in the testing projects.

We expect this phase to take 3-4 years. In terms of costs, the first phase required about € 100,000 in cash, and an estimated € 1-2 m of in-kind contributions. In this second phase of the project, we project a total cost of € 45 m, of which €40 m will most likely be covered thanks to collaborations, sponsorships and in-kind contributions.

Further notices on the future plans, and the execution of the work after the feasibility study can be found on www.theoceancleanup.com.

PHASE II OUTLINE

| | 2014 | 2015 | 2016 | 2017 |
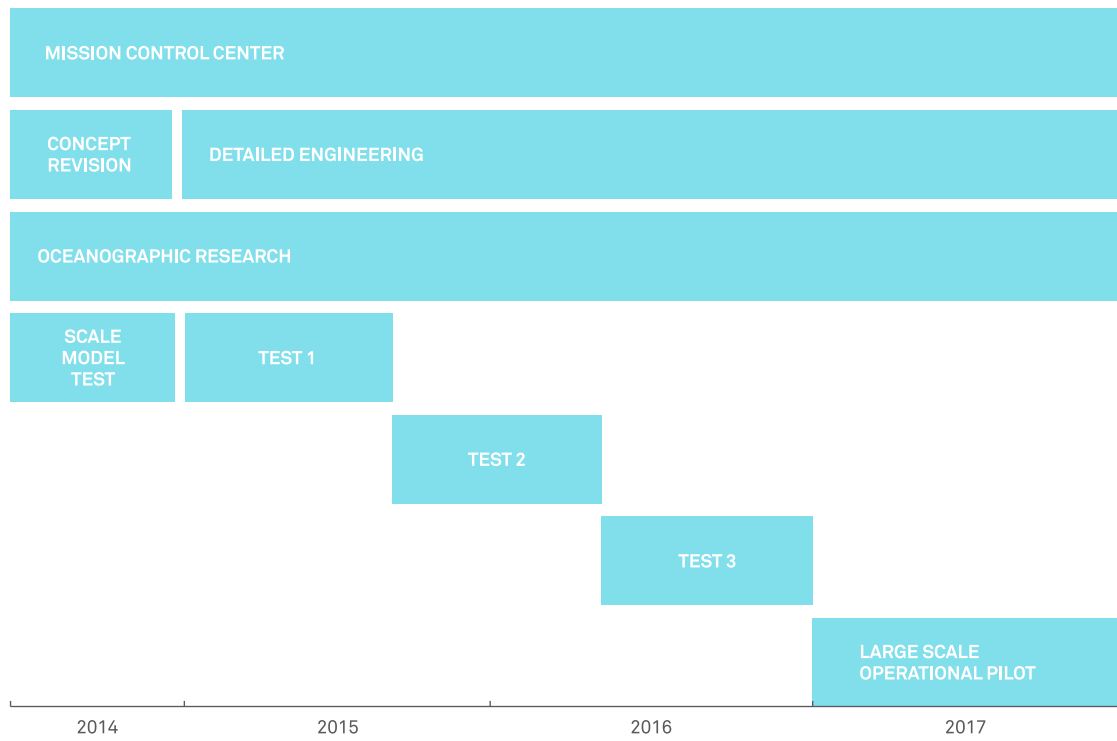
Figure 11.11 How work will be distributed in relation to time

REFERENCES
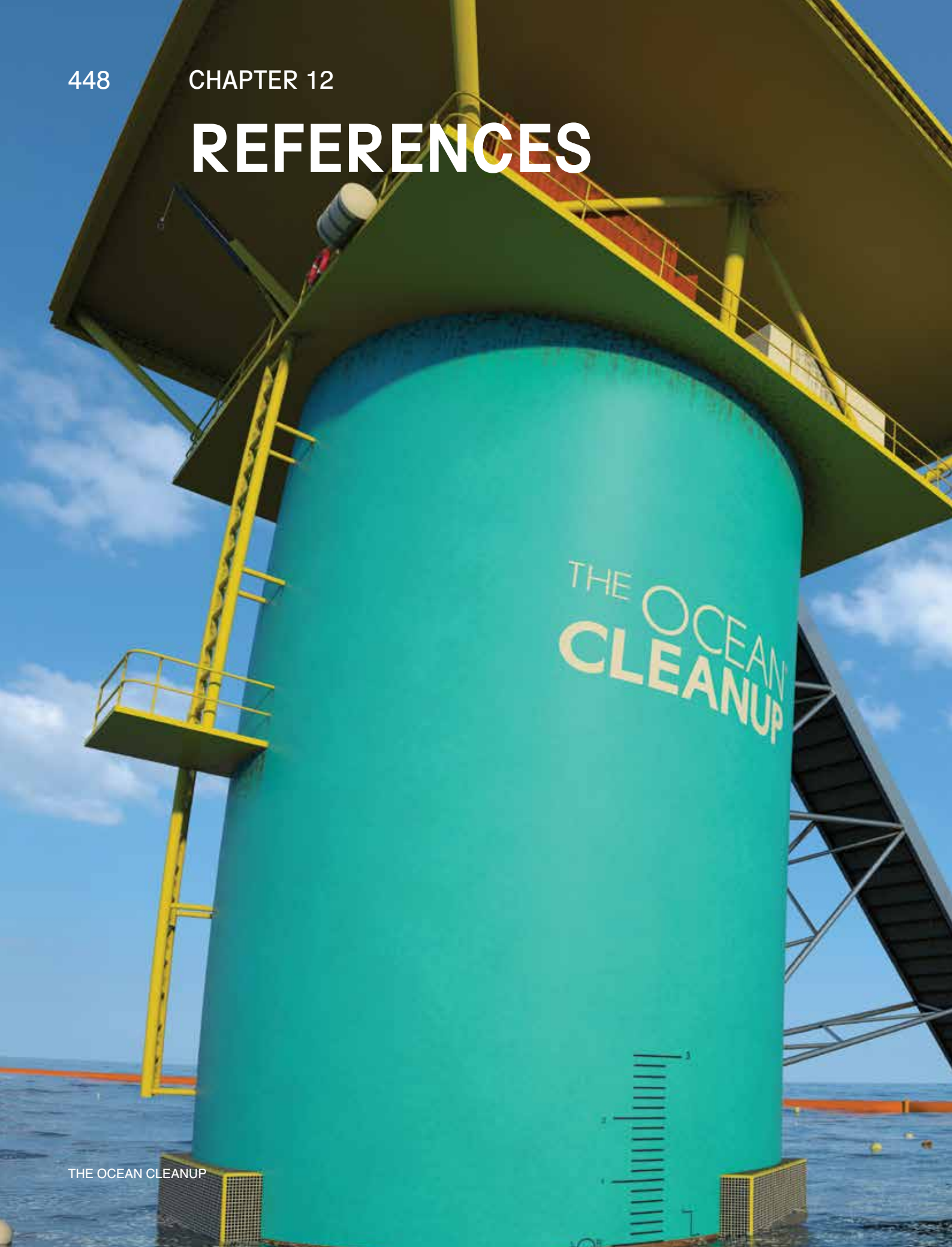
A Guide to Port Hawai'i 11. (2012). Retrieved from http://hidot.hawaii.gov/harbors/files/2012/10/A-Guide-To-Port-Hawaii.pdf.

ABCs of Radioactivity – Radioactivity 101: Emissions. (2013). from http://www.whoi.edu/oceanus/viewArticle.do?id=166969

Adjou, M., Bendtsen, J., & Richardson, K. (2012). Modeling the influence from ocean transport, mixing and grazing on phytoplankton diversity. Ecological Modelling, 225(0), 19-27. doi: http://dx.doi.org/10.1016/j.ecolmodel.2011.11.005

Akehurst, M. (1976). Custom as a Source of International Law. British Yearbook of International Law, 47(1), 1-53. doi: 10.1093/bybil/47.1.1

Albertsson, A.-C., & Karlsson, S. (1990). The influence of biotic and abiotic environments on the degradation of polyethylene. Progress in Polymer Science, 15(2), 177-192. doi: http://dx.doi.org/10.1016/0079-6700(90)90027-X

Aliani, S., Griffa, A., & Molcard, A. (2003). Floating debris in the Ligurian Sea, north-western Mediterranean. Marine Pollution Bulletin, 46(9), 1142-1149. doi: http://dx.doi.org/10.1016/S0025-326X(03)00192-9

Allsopp, M., Walters, A., Santillo, D., & Johnston, P. (2000). Marine Global Marine Debris Report. In GREENPEACE (Ed.): United Nations Environment Programme.

Allsopp, M., Walters, A., Santillo, D., & Johnston, P. (2007). Plastic Debris in the World's Oceans: Greenpeace International.

AMRF. (2010). The Algalita Marine Research Foundation. from http://www.algalita.org/

Ananda Church of Self-Realization v. Massachusetts Bay In. Co., 95 Cal App 4th 1273 C.F.R. (2002).

Andersen, R. A., Bidigare, R. R., Keller , M. D., & Latasa, M. (1996). A comparison of HPLC pigment signatures and electron microscopic observations for oligotrophic waters of the North Atlantic and Pacific Oceans. Deep Sea Research Part II: Topical Studies in Oceanography, 43(2–3), 517-537. doi: http://dx.doi.org/10.1016/0967-0645(95)00095-X

Andrady, A. L. (2003). Plastics and the Environment: Wiley.

Andrady, A. L. (2011). Microplastics in the marine environment. Marine Pollution Bulletin, 62(8), 1596-1605. doi: http://dx.doi.org/10.1016/j.marpolbul.2011.05.030

Andrady, A. L., Hamid, S. H., Hu, X., & Torikai, A. (1998). Effects of increased solar ultraviolet radiation on materials. Journal of Photochemistry and Photobiology B: Biology, - 46(- 1–3), - 103.

Annual Report (2013) Inter-American Convention for the Protection and Conservation of Sea Turtles- United States of America

ANSYS, I. (2010a Stationkeeping). ANSYS CFX-Solver Theory Guide Release 13.0.

ANSYS, I. (2010b). ANSYS CFX-Solver Theory Guide Release 13.0.

ANSYS FLUENT 6.3 documentation. (2008) 7.2.2., http://aerojet.engr.ucdavis.edu/fluenthelp/html/ug/node165.htm

The Antarctic Treaty (1959), http://www.ats.aq/index_e.htm.

Auman, H., Ludwig, J. P., Giesy, J. P., & Colborn, T. (1997). Plastic Ingestion by Laysan Albatross Chicks on Sand Island, Midway Atoll, in 1994 and 1995. Albatross Biology and Conservation, 239-244.

Auxill Nederland, B.V. from http://www.auxill.nl/

Avery-Gomm, S., O'Hara, P. D., Kleine, L., Bowes, V., Wilson, L. K., & Barry, K. L. (2012). Northern fulmars as biological monitors of trends of plastic pollution in the eastern North Pacific. Mar Pollut Bull, 64(9), 1776-1781. doi: 10.1016/j.marpolbul.2012.04.017

Bannister, J. L. (2008). Baleen Whales (Mysticetes). In W. F. Perrin, Würsig, B., Thewissen, J.G.M. (Ed.), Encyclopedia of Marine Mammals (pp. 80-89): Academic Press.

Bardach, J. E., Cotter, C. H., & Morgan, J. R. Pacific Ocean Encyclopaedia Britannica.

Barnes, D. K. A. (2002). Biodiversity: invasions by marine life on plastic debris. Nature, 416(6883), 808-809. doi: 10.1038/416808a

Barnes, D. K. A., & Fraser, K. P. P. (2003). Rafting by five phyla on man-made flotsam in the Southern Ocean. Marine Ecology Progress Series, 262, 289-291. doi: 10.3354/meps262289

Barnes, D. K. A., Galgani, F., & Thompson, R. (2009). Accumulation and fragmentation of plastic debris in global environments.

Barnes, D. K. A., & Milner, P. (2005). Drifting plastic and its consequences for sessile organism dispersal in the Atlantic Ocean. Marine Biology, 146(4), 815-825. doi: 10.1007/s00227-004-1474-8

Barron, C. N., Kara, A. B., Hurlburt, H. E., Rowley, C., & Smedstad, L. F. (2004). Sea Surface Height Predictions from the Global Navy Coastal Ocean Model during 1998–2001*. Journal of Atmospheric and Oceanic Technology, 21(12), 1876-1893. doi: 10.1175/JTECH-1680.1

Barron, C. N., Kara, A. B., Martin, P. J., Rhodes, R. C., & Smedstad, L. F. (2006). Formulation, implementation and examination of vertical coordinate choices in the Global Navy Coastal Ocean Model (NCOM). Ocean Modelling, 11(3–4), 347-375. doi: http://dx.doi.org/10.1016/j.ocemod.2005.01.004

Baslar, K. (1998). The Concept of the Common Heritage of Mankind in International Law: Martinus Nijhoff.

Baulch, S., & Perry, C. (2014). Evaluating the impacts of marine debris on cetaceans. Mar Pollut Bull, 80(1-2), 210-221. doi: 10.1016/j.marpolbul.2013.12.050

Beckart Environmental, I. On-site Wastewater Treatment Working for Ohio Plastics Recycler.

Beltech, Ammeraal from www.ammeraalbeltech.nl)

Berge, J., Cottier, F., Last, K. S., Varpe, O., Leu, E., Soreide, J., . . . Brierley, A. S. (2009). Diel vertical migration of Arctic zooplankton during the polar night. Biol Lett, 5(1), 69-72. doi: 10.1098/rsbl.2008.0484

Bergmann, M., Klages, M., Increase of litter at the Arctic deep-sea observatory (2012). Mar. Pollut. Bull., 64(12), 2734.

Bertilsson, S., Berglund, O., Karl, D. M., & Chisholm, S. W. (2003). Elemental composition of marine Prochlorococcus and Synechococcus: implications for the ecological stoichiometry of the sea. Limnol. Oceanogr(48), 1721-1731.

Bird, D. F., & Kalff, J. (1984). Empirical Relationships between Bacterial Abundance and Chlorophyll Concentration in Fresh and Marine Waters. Canadian Journal of Fisheries and Aquatic Sciences, 41(7), 1015-1023. doi: 10.1139/f84-118

Birne, P., Boyle, A., & Redgwell, C. (2009). Judgment, ICJ Reports 2010 International law and the environment: Oxford University Press.

Bisphenol A (BPA): Use in Food Contact Application (U. S. D. o. H. H. Services, Trans.). (2010). In U. S. F. D. Administration (Ed.).

Black, K. P., & Gay, S. L. (1990). A Numerical Scheme for Determining Trajectories in Particle Models. In R. Bradbury (Ed.), Acanthaster and the Coral Reef: A Theoretical Perspective (Vol. 88, pp. 151-156): Springer Berlin Heidelberg.

Bocio, A., Domingo, J. L., Falcó, G., & Llobet, J. M. (2007). Concentrations of PCDD/PCDFs and PCBs in fish and seafood from the Catalan (Spain) market: Estimated human intake. Environment International, 33(2), 170-175. doi: http://dx.doi.org/10.1016/j.envint.2006.09.005

Bodansky, D. (1995). Customary (and Not So Customary) International Environmental Law.

Bouman, H. A., Ulloa, O., Barlow, R., Li, W. K. W., Platt, T., Zwirglmaier, K., . . . Sathyendranath, S. (2011). Water-column stratification governs the community structure of subtropical marine picophytoplankton. Environmental Microbiology Reports, 3(4), 473-482. doi: 10.1111/j.1758-2229.2011.00241.x

Bravo, M., Astudillo, J. C., Lancellotti, D., Luna-Jorquera, G., Valdivia, N., & Thiel, M. (2011). Rafting on abiotic substrata: properties of floating items and their influence on community succession. Marine Ecology Progress Series, 439, 1-17. doi: 10.3354/meps09344

Brown, D. M., & Cheng, L. (1981). New Net for Sampling the Ocean Surface. Marine Ecology Progress Series, 5, 225-227.

Browne, M. A., Crump, P., Niven, S. J., Teuten, E., Tonkin, A., Galloway, T., & Thompson, R. (2011). Accumulation of microplastic on shorelines woldwide: sources and sinks. Environ Sci Technol, 45(21), 9175-9179. doi: 10.1021/es201811s

Browne, M. A., Crump P Fau - Niven, S. J., Niven Sj Fau - Teuten, E., Teuten E Fau - Tonkin, A., Tonkin A Fau - Galloway, T., Galloway T Fau - Thompson, R., & Thompson, R. Accumulation of microplastic on shorelines woldwide: sources and sinks. (1520-5851 (Electronic)).

Browne, M. A., Niven, S. J., Galloway, T. S., Rowland, S. J., & Thompson, R. C. (2013). Microplastic Moves Pollutants and Additives to Worms, Reducing Functions Linked to Health and Biodiversity. Current Biology, 23(23), 2388-2392. doi: http://dx.doi.org/10.1016/j.cub.2013.10.012

Brownlie, I. (2008). Principles of Public International Law: Oxford University Press.

Bugoni, L., Krause, L., & Petry, M. V. (2001). Marine debris and human impacts on sea turtles in southern Brazil. Mar Pollut Bull, 42(12), 1330-1334.

Bunkerworld.com.   Retrieved 4/24/2014, from http://www.bunkerworld.com/

Burke, W. (1991). The regulation of driftnet fishing on the high seas: legal issues, II The Law of the Sea Concerning Coastal State Authority Over Driftnets on the High Seas (pp. 13, 16).

Campbell, L., & Vaulot, D. (1993). Photosynthetic picoplankton community structure in the subtropical North Pacific Ocean near Hawaii (station ALOHA). Deep Sea Research Part I: Oceanographic Research Papers, 40(10), 2043-2060. doi: http://dx.doi.org/10.1016/0967-0637(93)90044-4

Camphuysen, K. (2001). Northern Gannets Morus Bassanus Found Dead in the Netherlands, 1970-2000: Dutch Seabird Group, Netherlands Institute for Sea Research (NIOZ).

Capone, D. G., Zehr, J. P., Paerl, H. W., Bergman, B., & Carpenter, E. J. (1997). Trichodesmium, a Globally Significant Marine Cyanobacterium. Science, 276(5316), 1221-1229. doi: 10.1126/science.276.5316.1221

Carpenter, E. J., Anderson, S. J., Harvey, G. R., Miklas, H. P., & Peck, B. B. (1972). Polystyrene spherules in coastal waters. Science, 178(4062), 749-750.

Carpenter, E. J., & Smith, K. L., Jr. (1972). Plastics on the Sargasso sea surface. Science, 175(4027), 1240-1241.

Carson, H. S., Nerheim, M. S., Carroll, K. A., & Eriksen, M. (2013). The plastic-associated microorganisms of the North Pacific Gyre. Marine Pollution Bulletin, 75(1–2), 126-132. doi: http://dx.doi.org/10.1016/j.marpolbul.2013.07.054

CBD (Convention on Biological Diversity) (2012). Impacts of Marine Debrison Biodiversity: Current Status and Potential Solutions. In S. o. t. C. o. B. Diversity (Ed.), CBD Technical Series.

Center, N. G. S. F. SeaWiFS Project. Retrieved 4/18/2014, 2014, from http://oceancolor.gsfc.nasa.gov/SeaWiFS/

Charlesworth, H. (2012). Law-making and sources. In J. Crawford (Ed.), The Cambridge Companion to International Law (pp. 190). Cambridge: Cambridge University Press.
Charnock, H. (1955). Wind stress on a water surface. Quarterly Journal of the Royal Meteorological Society, 81(350), 639-640. doi: 10.1002/qj.49708135027

Chelton, D.B., Schlax, M.G., Samelson, R. M. Global observations of nonlinear mesoscale eddies. (2011). Prog.

Oceanogr., 91(2), 167.

China Shipping Container Lines Co, (2014). America Line. http://www.cscl.com.cn/english/

Chisholm, S. W., Olson, R. J., Zettler, E. R., Waterbury, J., Goericke, R., & Welschmeyer, N. (1988). A novel free-living prochlorophyte occurs at high cell concentrations in the oceanic euphotic zone. Nature, 334(6180), 340-343. doi: 10.1038/334340a0

Church, M. J., Mahaffey, C., Letelier, R. M., Lukas, R., Zehr, J. P., & Karl, D. M. (2009). Physical forcing of nitrogen fixation and diazotroph community structure in the North Pacific subtropical gyre. Global Biogeochemical Cycles, 23(2), GB2020. doi: 10.1029/2008GB003418

Churchill, R. R., & Lowe, A. V. (1988). The Law of the Sea: Manchester University Press.

Clark, R. B. (1997). Marine Pollution (4th ed.): Clarendon.

Clift, R., Grace, J. R., & Weber, M. E. (1978). Bubbles, Drops, and Particles.

Cole, M., Lindeque, P., Halsband, C., Galloway, T. S., Microplastics as contaminants in the marine environment: a review. (2011). Mar. Pollut. Bull., 62(12), 2588.

Collignon, A., Hecq, J.-H., Glagani, F., Voisin, P., Collard, F., & Goffart, A. (2012). Neustonic microplastic and zooplankton in the North Western Mediterranean Sea. Marine Pollution Bulletin, 64(4), 861-864. doi: http://dx.doi.org/10.1016/j.marpolbul.2012.01.011

Colton Jr., J. B., Knapp, F. D., & Burns, B. R. (1974). Plastic Particles in Surface Waters of the Northwestern Atlantic. Science, 185(4150), 491-497. doi: 10.2307/1738284

Code of Conduct for Responsible Fisheries, pt. 6.5, 7.2.2(g), 8.5 (1995) C.F.R. (1995).

Commission, W. a. C. F. (2014). Conservation and Management Measures.

Committee on the Formation of Customary International Law, A. B. o. t. I. L. A. (1987-1988). The Role of State Practice in the Formation of Customary and Jus Cogens Norms of International Law. Paper presented at the Proceedings and Committee Reports of the American Branch of the International Law Association.

The Continuous Plankton Recorder Survey of the North Pacific. from https://www.pices.int/projects/tcprsotnp/default.aspx/

Convention on the Conservation of Migratory Species of Wild Animals § art. II(1) Nov. 1, 1983, 1651 U.N.T.S. 333 (1983).

Convention on the International Regulations for Preventing Collisions at Sea. (1972). London: Retrieved from http://www.admiraltylawguide.com/conven/collisions1972.html.

Convention on the Prevention of Marine Pollution by Dumping of Wastes and Other Matter (1972), London.

Cooney, R. T. (1986). The seasonal occurrence of Neocalanus cristatus, Neocalanus plumchrus, and Eucalanus bungii over the shelf of the northern Gulf of Alaska. Continental Shelf Research, 5(5), 541-553. doi: http://dx.doi.org/10.1016/0278-4343(86)90075-0

Cottier, F. R., Tarling, G. A., Wold, A., & Falk-Petersen, S. (2006). Unsynchronized and synchronized vertical migration of zooplankton in a high arctic fjord. Limnology and Oceanography, 51(6), 2586-2599.

Council, Pacific Fisheries Management (2012). Highly Migratory Species: Background. http://www.pcouncil.org/highly-migratory-species/background/

Council, Pacific Fisheries Management (2013). Highly Migratory Species: Fishery Management Plan and Amendments. http://www.pcouncil.org/highly-migratory-species/fishery-management-plan-and-amendments/#hms_fmp

Cox, A. T., & Swail, V. R. (2001). A global wave hindcast over the period 1958–1997: Validation and climate assessment. Journal of Geophysical Research: Oceans, 106(C2), 2313-2329. doi: 10.1029/2001JC000301

Cox, T. M., Lewison, R. L., Zydelis, R., Crowder, L. B., Safina, C., & Read, A. J. (2007). Comparing effectiveness of experimental and implemented bycatch reduction measures: the ideal and the real. Conserv Biol, 21(5), 1155-1164. doi: 10.1111/j.1523-1739.2007.00772.x

Cummings, J. A. (2005). Operational multivariate ocean data assimilation. Quarterly Journal of the Royal Meteorological Society, 131(613), 3583-3604. doi: 10.1256/qj.05.105

Curfman, D. (2008). Thar Be Treasure Here: Rights to Ancient Shipwrecks in International Waters – A New Policy Regime. Wash. U.L. Rev., 188-189.

Dahlberg, M. L., & R.H., D. (1985). Observations of man-made objects on the surface of the North Pacific Ocean Proceedings of the Workshop on the Fate and Impact of Marine Debris. Honolulu, Hawaii: National Marine Fisheries Service, Southwest Fisheries Center.

Darnerud, P. O. (2003). Toxic effects of brominated flame retardants in man and in wildlife. Environment International, 29(6), 841-853. doi: http://dx.doi.org/10.1016/S0160-4120(03)00107-7

Davison, P., & Asch, R. G. (2011). Plastic ingestion by mesopelagic fishes in the North Pacific Subtropical Gyre. Marine Ecology Progress Series, 432, 173-180. doi: 10.3354/meps09142

Day, R. H., & Shaw, D. G. (1987). Patterns in the abundance of pelagic plastic and tar in the north pacific ocean, 1976–1985. Marine Pollution Bulletin, 18(6, Supplement B), 311-316. doi: http://dx.doi.org/10.1016/S0025-326X(87)80017-6

Day, R. H., Shaw, D. G., & Ignell, S. E. (1990). The quantitative distribution and characteristics of neuston plastic in the North Pacific Ocean Proceedings of the Second International Conference on Marine Debris: 2-7 April, 1989, Honolulu, Hawai (pp. 182-211): U.S. Department of Commerce, National Oceanic and Atmospheric Administration, National Marine Fisheries Service.

DEFRA. (2013). Greenhouse Gas Conversion Factor Repository. from http://www.ukconversionfactorscar-bonsmart.co.uk/

Delegation of Management Responsibility for the Pacific Remote Islands Marine National Monument, Rose Atoll National Monument and the Marianas Trench National Monument, Order No. 3284 C.F.R.

Dellnitz, M., Froyland, G., Horenkamp, C., Padberg-Gehle, K., Gupta, A., Seasonal variability of the subpolar gyres in the Southern Ocean: a numerical investigation based on transfer operators. (2009). Nonlinear Process. Geophys., 16(6), 655.

Delta Pompen, B.V. from www.deltapompen.com

Denuncio, P., Bastida, R., Dassis, M., Giardino, G., Gerpe, M., & Rodríguez, D. (2011). Plastic ingestion in Franciscana dolphins, Pontoporia blainvillei (Gervais and d'Orbigny, 1844), from Argentina. Marine Pollution Bulletin, 62(8), 1836-1841. doi: http://dx.doi.org/10.1016/j.marpolbul.2011.05.003

DePaolo, A. R. (1995). Plastic Recycling Legislation: Not Just the Same Old Garbage. Boston College Environmental Affairs Law Review.

Derraik, J. G. (2002). The pollution of the marine environment by plastic debris: a review. Mar Pollut Bull, 44(9), 842-852.

Desforges, J.-P. W., Galbraith, M., Dangerfield, N., & Ross, P. S. (2014). Widespread distribution of microplastics in subsurface seawater in the NE Pacific Ocean. Marine Pollution Bulletin, 79(1–2), 94-99. doi: http://dx.doi.org/10.1016/j.marpolbul.2013.12.035

Diamanti-Kandarakis, E., Bourguignon, J. P., Giudice, L. C., Hauser, R., Prins, G. S., Soto, A. M., . . . Gore, A. C. (2009). Endocrine-disrupting chemicals: an Endocrine Society scientific statement. Endocr Rev, 30(4), 293-342. doi: 10.1210/er.2009-0002

Dixon, T. J., & Dixon, T. R. (1983). Marine litter distribution and composition in the North Sea. Marine Pollution Bulletin, 14(4), 145-148. doi: http://dx.doi.org/10.1016/0025-326X(83)90068-1

Doney, S. C., & Steinberg, D. K. (2013). Marine biogeochemistry: The ups and downs of ocean oxygen. Nature

Geosci, 6(7), 515-516. doi: 10.1038/ngeo1872

Dore, J. E., Letelier, R. M., Church, M. J., Lukas, R., & Karl, D. M. (2008). Summer phytoplankton blooms in the oligotrophic North Pacific Subtropical Gyre: Historical perspective and recent observations. Progress in Oceanography, 76(1), 2-38. doi: http://dx.doi.org/10.1016/j.pocean.2007.10.002

Duboise, T. (2014). Plastic Bag Ban Report. http://plasticbagbanreport.com

Dufault, S., & Whitehead, H. (1994). Floating marine pollution in 'the Gully' on the continental slope, Nova Scotia, Canada. Marine Pollution Bulletin, 28(8), 489-493. doi: http://dx.doi.org/10.1016/0025-326X(94)90522-3

Ecomare. (2010). De Vleet. from http://www.zeeinzicht.nl/vleet/

Ecotextiles, Plastics – Part 2: Why recycling is not the answer. from https://oecotextiles.wordpress.com/tag/toxic-emissions/

Endangered Species Act, 16 U.S.C. § 1531 C.F.R.
Engler, R. E. The complex interaction between marine debris and toxic chemicals in the ocean. (1520-5851 (Electronic)).

EPA (U.S. Environmental Protection Agency). Marine Debris: Trash on the Move, available at http://water.epa.gov/type/oceb/marinedebris/upload/Marine_Debris_Brochure_8-5x11.pdf.

EPA. Plastics 7 Exhibits 12-15, available at http://www.epa.gov/climatechange/wycd/waste/downloads/plastics-chapter10-28-10.pdf.

EPA Plastic Recycling: A Snapshot on Markets, Technology, and Trends. Retrieved from http://www.epa.gov/osw/conserve/smm/sfmr/webinar2-appr.pdf

EPA (2011). Marine Debris in the North Pacific: A Summary of Existing Information and Identification of Data Gaps. Pacific Southwest/Region 9 75 Hawthorne Street, San Francisco, CA: Retrieved from http://www.epa.gov/region9/marine-debris/pdf/MarineDebris-NPacFinalAprvd.pdf.

EPA (2012). Toxic Substances Control Act (TSCA) - Polychlorinated Biphenyls. http://www.epa.gov/epawaste/hazard/tsd/pcbs/pubs/stordisp.htm (last updated June 27, 2012).

EPA (2012a). Marine Debris Impacts: Invasive Species. http://water.epa.gov/type/oceb/marinedebris/md_impacts.cfm (last updated Mar. 6, 2012).

EPA (2012b). Toxic Substances Control Act (TSCA) - Polychlorinated Biphenyls. http://www.epa.gov/epawaste/hazard/tsd/pcbs/pubs/stordisp.htm (last updated June 27, 2012).

Eriksen, M., Lebreton, L. C. M., Carson, H. S., Thiel, M., Moore, C., Borrero, J. C., ... Reisser, J. (2014). Global Estimate of Plastic Pollution Floating in the World's Oceans.

Eriksen, M., Maximenko, N., Thiel, M., Cummins, A., Lattin, G., Wilson, S., . . . Rifman, S. (2013). Plastic pollution in the South Pacific subtropical gyre. Marine Pollution Bulletin, 68(1–2), 71-76. doi: http://dx.doi.org/10.1016/j.marpolbul.2012.12.021

Eriksson, C., & Burton, H. (2003). Origins and biological accumulation of small plastic particles in fur seals from Macquarie Island. Ambio, 32(6), 380-384.

Fact Sheet 6: Beaufort Scale, (2014), Met Office UK, from http://www.metoffice.gov.uk/media/pdf/b/7/Fact_sheet_No._6.pdf. Accessed 3/2/2014.

Falkowski, P., G. (1994). The role of phytoplankton photosynthesis in global biogeochemical cycles. Photosynthesis Research, 39(3), 235-258. doi: 10.1007/BF00014586

FAO. (2010). Technical Consultation to Develop International Guidelines on Bycatch Management and Reduction of Discards, Rome, Italy.

Faris, J., & Hart, K. (1994). Seas of Debris: A Summary of the Third International Conference on Marine Debris: Alaska Fisheries Science Center.

Field, C. B., Behrenfeld, M. J., Randerson, J. T., & Falkowski, P. (1998). Primary production of the biosphere: integrating terrestrial and oceanic components. Science, 281(5374), 237-240.

Fletcher, K. M., & O'Shea, S. E. (2000). Essential Fish Habitat: Does Calling it Essential Make it So? Environmental Law, 30(1).

Foundation, B. C. (2013). Disrupted Development: The Dangers of Prenatal BPA Exposure (pp. 20).

Fraunholcz, N. (2014). [Recycling Avenue BV]. http://www.recycling-avenue.nl

Froyland, G., Padberg, K., England, M., Teguler, A.M. Detection of coherent oceanic structures via transfer operators. (2007). Phys. Rev. Lett., 98(22).

Atlantic meridional overturning circulation and the Southern Hemisphere supergyre. (2007). Geophys. Res. Lett., 34(23).

Geocommons. (2014). The Global Shipping Lane Network. from http://geocommons.com/maps/5254

Goldstein, M. C., Rosenberg, M., & Cheng, L. (2012). Increased oceanic microplastic debris enhances oviposition in an endemic pelagic insect. Biology Letters, 8(5), 817-820. doi: 10.1098/rsbl.2012.0298

Goldstein, M. C., Titmus, A. J., & Ford, M. (2013). Scales of Spatial Heterogeneity of Plastic Marine Debris in the Northeast Pacific Ocean. PLoS One, 8(11), e80020. doi: 10.1371/journal.pone.0080020

Gordon, R. P. (2000). The Vertical and Horizontal Distribution of Microplastics in the Caribbean and Sargasso Seas Along the W-169 Cruise Track.

GRACE. (3/17/2014). Gravity Recovery and Climate Experiment (GRACE). Retrieved April 17, 2014, from http://www.csr.utexas.edu/grace/

Gramentz, D. (1988). Involvement of loggerhead turtle with the plastic, metal, and hydrocarbon pollution in the central Mediterranean. Marine Pollution Bulletin, 19(1), 11-13. doi: http://dx.doi.org/10.1016/0025-326X(88)90746-1

Granutech Corporation from http://www.granutech.com/

Gregory, M.R. (1977). Plastic pellets on New Zealand beaches. Marine Pollution Bulletin 8:82-84

Gregory, M.R. (1990). Plastics: accumulation, distribution, and environmental effects of meso-, macro-, and megalitter in surface waters and on shores of the southwest Pacific. Paper presented at the The Second International Conference on Marine Debris, Honolulu, Hawaii.

Gregory, M. R., Environmental implications of plastic debris in marine settings—entanglement, ingestion, smothering, hangers-on, hitch-hiking and alien invasions. (2009). Phil. Trans. R. Soc., 364(1526), 2013.

Grodsky, S.A., Lumpkin, R., Carton, J. A., Spurious trends in global surface drifter currents. (2011). Geophys. Res. Lett., 38(10). http://www.aoml.noaa.gov/phod/dac/Grodsky_etal11.pdf

Gulmine, J. V., Janissek, P. R., Heise, H. M., & Akcelrud, L. (2003). Degradation profile of polyethylene after artificial accelerated weathering. Polymer Degradation and Stability, 79(3), 385-397. doi: http://dx.doi.org/10.1016/S0141-3910(02)00338-5

Gustafsson, K., Björk, M., Bureau, S., & Gilek, M. (1999). Bioaccumulation kinetics of brominated flame retardants (polybrominated diphenyl ethers) in blue mussels (Mytilus edulis). Environmental Toxicology and Chemistry, 18(6), 1218-1224. doi: 10.1002/etc.562018062

Day, R. H., Shaw, D. G., & Ignell, S. E. (1989). The Quantitative Distribution and Characteristics of Neuston Plastic in the North Pacific Ocean, 1985-88.

Hagen, P. E. (1990). The International Community Confronts Plastics Pollution from Ships: MARPOL Annex V and the Problem That Won't Go Away. International Law & Policy, 5(2).

Halpern, B. S., Walbridge, S., Selkoe, K. A., Kappel, C. V., Micheli, F., D'Agrosa, C., . . . Watson, R. (2008). A Global Map of Human Impact on Marine Ecosystems. Science, 319(5865), 948-952. doi: 10.1126/science.1149345

Hammer, J., Kraak, M. H., & Parsons, J. R. (2012). Plastics in the marine environment: the dark side of a modern gift. Rev Environ Contam Toxicol, 220, 1-44. doi: 10.1007/978-1-4614-3414-6_1

Hanni, K. D., & Pyle, P. (2000). Entanglement of Pinnipeds in Synthetic Materials at South-east Farallon Island, California, 1976–1998. Marine Pollution Bulletin.

Harker, J. H., Backhurst, J. R., & Richardson, J. F. (2002). Chemical Engineering, Volume 2 (5 ed.): Butterworth-Heinemann.

Haury, L., & Weihs, D. (1976). Energetically efficient swimming behavior of negatively buoyant zooplankton,. Oceanography, 21(797-803).

Hays, G. C., Harris, R. P., & Head, R. N. (2001). Diel changes in the near-surface biomass of zooplankton and the carbon content of vertical migrants. Deep Sea Research Part II: Topical Studies in Oceanography, 48(4–5), 1063-1068. doi: http://dx.doi.org/10.1016/S0967-0645(00)00109-0

Hayward, T. L. (1987). The nutrient distribution and primary production in the central North Pacific. Deep Sea Research Part A. Oceanographic Research Papers, 34(9), 1593-1627. doi: http://dx.doi.org/10.1016/0198-0149(87)90111-7

Henen v. United States, 525 F. Supp. 350 (S.D.N.Y. 1981) C.F.R. (1981).

Hidalgo-Ruz, V., Gutow, L., Thompson, R. C., & Thiel, M. (2012). Microplastics in the Marine Environment: A Review of the Methods Used for Identification and Quantification. Environmental Science & Technology, 46(6), 3060-3075. doi: 10.1021/es2031505

Hinojosa, I. A., Rivadeneira, M. M., & Thiel, M. (2011). Temporal and spatial distribution of floating objects in coastal waters of central–southern Chile and Patagonian fjords. Continental Shelf Research, 31(3–4), 172-186. doi: http://dx.doi.org/10.1016/j.csr.2010.04.013

Hinojosa, I. A., & Thiel, M. (2009). Floating marine debris in fjords, gulfs and channels of southern Chile. Marine Pollution Bulletin, 58(3), 341-350. doi: http://dx.doi.org/10.1016/j.marpolbul.2008.10.020

Hoeksema, B. W., Roos, P. J., & Cadée, G. C. (2012). Trans-Atlantic rafting by the brooding reef coral Favia fragum on man-made flotsam. Marine Ecology Progress Series, 445, 209-218. doi: 10.3354/meps09460

Hoekstra, H. D., Spoormaker, J. L., Breen, J., Audouin, L., & Verdu, J. (1995). UV-exposure of stabilized and non-stabilized HDPE films: physico-chemical characterization. Polymer Degradation and Stability, 49(2), 251-262. doi: http://dx.doi.org/10.1016/0141-3910(95)87007-5

Hupkes Wijnstra, S. (2014, 3/22/2014).

ICJ (International Court of Justice), Fisheries Jurisdiction: United Kingdom v. Iceland, 1974 (1974).

Impacts of Marine Debris on Biodivesity: Current Status and Potential Solutions. (2012). CBD Technical Series: Secretariat of the Convention on Biological Diversity, with the Scientific and Technical Advisory Panel--GEF.

IPRC, Mistake Triggers False Alarm about Ocean Radioactivity. (2013). from http://iprc.soest.hawaii.edu/news/marine_and_tsunami_debris/debris_news.php

Nottebohm Case (Liechtenstein v Guatemela), Second Phase (1955).

ICJ (International Court of Justice). (2010). Pulp Mills on the River Uruguay (Argentina v. Uruguay) (pp. 14).

IMO, Convention on the Prevention of Marine Pollution by Dumping of Wastes and Other Matter (1972).

IMO Documentation - Convention on the International Regulations for Preventing Collisions at Sea, as amended (COLREG 1972).

Institute, American Petroleum. (2005). API RP 2SK : Recommended Practice for Design and Analysis of Stationkeeping Systems for Floating Structures Recommended practice 2SK. http://www.techstreet.com/products/22147

Institution, British Standards (2008). Guide to PAS 2050: How to assess the carbon footprint of goods and services. In L. BSI (Ed.), http://aggie-horticulture.tamu.edu/faculty/hall/publications/PAS2050_Guide.pdf

Institution, British Standards (2011). Specification for the assessment of the life cycle greenhouse gas emissions of goods and services. In L. BSI (Ed.) http://shop.bsigroup.com/upload/Shop/Download/PAS/PAS2050.pdf

IPCC (Intergovernmental Panel on Climate Change). Climate Change 2014: Mitigation of climate change: IPCC Working Group III Contribution to AR5. https://www.ipcc.ch/report/ar5/wg3/

The International Convention on Salvage, 1953 UNTS 194 C.F.R. (1989).

IPW. (2010). International Pellet Watch. from http://www.pelletwatch.org

Irigoien, X., Huisman, J., & Harris, R. P. (2004). Global biodiversity patterns of marine phytoplankton and zooplankton. Nature, 429(6994), 863-867. doi: http://www.nature.com/nature/journal/v429/n6994/suppinfo/nature02593_S1.html

ISO (International Standards Organization). (1998). Environmental management—life cycle assessment—life cycle impact assessment (Vol. 14042BS EN ISO 14042). Geneva: ISO.

ISO (2006). Environmental management – Life cycle assessment – Principles and framework (Vol. BS EN ISO 14040). Geneva.

ISO (2011). Carbon footprint of products — Requirements and guidelines for quantification and communication (Vol. BS EN ISO 14067).

Ji, C.-Y., Yuan, Z.-M., & Chen, M.-l. (2011). Study on a new mooring system integrating catenary with taut mooring. China Ocean Engineering, 25(3), 427-440. doi: 10.1007/s13344-011-0035-4

Johnson, A., Salvador, G., Kenney, J., Robbins, J., Kraus, S., Landry, S., & Clapham, P. (2005). Fishing Gear Involved in Entanglements of Right and Humpback Whales. Marine Mammal Science, 21(4), 635-645. doi: 10.1111/j.1748-7692.2005.tb01256.x

Johnson, H. K., Højstrup, J., Vested, H. J., & Larsen, S. E. (1998). On the Dependence of Sea Surface Roughness on Wind Waves. Journal of Physical Oceanography, 28(9), 1702-1716. doi: 10.1175/1520-0485(1998)028<1702:OTDOSS>2.0.CO;2

Johnson, P. W., & Sieburth, J. M. (1979). Chroococcoid cyanobacteria in the sea: a ubiquitous and diverse phototrophic biomass. Limnology and Oceanography, 24(5), 928-935. doi: 10.4319/lo.1979.24.5.0928

Johnstone v. Wilmot Pty Ltd. v Kaine, 23 Tas LR 43 C.F.R. (1928).

Kako, S., Isobe, A., Seino, S., & Kojima, A. (2010). Inverse estimation of drifting-object outflows using actual observation data. Journal of Oceanography, 66(2), 291-297. doi: 10.1007/s10872-010-0025-9

Kapp, H. (1991). Some aspects of buoyancy adaptations of chaetognaths. Helgoländer Meeresuntersuchungen, 45(1-2), 263-267. doi: 10.1007/BF02365646

Karl, D. M., Letelier, R., Tupas, L., DorKarl, D., Letelier, R., Tupas, L., . . . Hebel, D. (1997). The role of nitrogen fixation in biogeochemical cycling in the subtropical North Pacific Ocean. Nature, 388, 533-538.

Karl, D. M. (1999). A Sea of Change: Biogeochemical Variability in the North Pacific Subtropical Gyre. Ecosystems, 2(3), 181-214. doi: 10.1007/s100219900068

Karl, D. M., & Dobbs, F. C. (1998). Molecular Approaches to Microbial Biomass Estimation in the Sea. In K. Cooksey (Ed.), Molecular Approaches to the Study of the Ocean (pp. 29-89): Springer Netherlands.

Karl, D. M., Letelier, R., Hebel, D., Tupas, L., Dore, J., Christian, J., & Winn, C. (1995). Ecosystem changes in the North Pacific subtropical gyre attributed to the 1991-92 El Nino. Nature, 373(6511), 230-234.

Karl, D. M., & Lukas, R. (1996). The Hawaii Ocean Time-series (HOT) program: Background, rationale and field implementation. Deep Sea Research Part II: Topical Studies in Oceanography, 43(2–3), 129-156. doi: http://dx.doi.org/10.1016/0967-0645(96)00005-7

Kershaw, P., Katsuhiko, S., Lee, S., Samseth, J., & Woodring, D. (2011). Plastic Debris in the Ocean. In U. N. E. P. (UNEP) (Ed.), UNEP Year Book.

Khoo, H. H., & Tan, R. B. H. (2006). Environmental Impact Evaluation of Conventional Fossil Fuel Production (Oil and Natural Gas) and Enhanced Resource Recovery with Potential CO sub(2) Sequestration. Energy and Fuels, 20(5), 1914-1924. doi: 10.1021/ef060075+

Kirgis, F. L. (1987). Custom on a Sliding Scale. Nicaragua: American Society of International Law.

Koelmans, A. A., Besseling, E., Wegner, A., & Foekema, E. M. (2013). Plastic as a carrier of POPs to aquatic organisms: a model analysis. Environ Sci Technol, 47(14), 7812-7820. doi: 10.1021/es401169n

Kubota, M., A mechanism for the accumulation of floating marine debris north of Hawaii. (1994). J. Phys. Oceanogr., 24(5), 1059.

Kubota, M., Takayama, K., & Namimoto, D. (2005). Pleading for the use of biodegradable polymers in favor of marine environments and to avoid an asbestos-like problem for the future. Appl Microbiol Biotechnol, 67(4), 469-476. doi: 10.1007/s00253-004-1857-2

Kukulka, T., Proskurowski, G., Morét Ferguson, S., Meyer, D., & Law, K. (2012) The effect of wind mixing on the vertical distribution of buoyant plastic debris. Vol. 39. Geophysical Research Letters (pp. 1-6).

Laender, F. D., Hammer, J., Hendriks, A. J., Soetaert, K., & Janssen, C. R. (2011). Combining Monitoring Data and Modeling Identifies PAHs as Emerging Contaminants in the Arctic. Environmental Science & Technology, 45(20), 9024-9029. doi: 10.1021/es202423f

Laist, D. (1997). Impacts of Marine Debris: Entanglement of Marine Life in Marine Debris Including a Comprehensive List of Species with Entanglement and Ingestion Records. In J. Coe & D. Rogers (Eds.), Marine Debris (pp. 99-139): Springer New York.

Lalli, C. M., & Parsons, T. R. (1997). Chapter 1 - Introduction. In C. M. Lalli & T. R. Parsons (Eds.), Biological Oceanography: An Introduction (Second Edition) (pp. 1-15). Oxford: Butterworth-Heinemann.

Landry, M. R., Al-Mutairi, H., Selph, K. E., Christensen, S., & Nunnery, S. (2001). Seasonal patterns of mesozooplankton abundance and biomass at Station ALOHA. Deep Sea Research Part II: Topical Studies in Oceanography, 48(8–9), 2037-2061. doi: http://dx.doi.org/10.1016/S0967-0645(00)00172-7

Landry, M. R., & Calbet, A. (2004). Microzooplankton production in the oceans. ICES Journal of Marine Science: Journal du Conseil, 61(4), 501-507. doi: 10.1016/j.icesjms.2004.03.011

Launder, B., & Spalding, D. B. (1974). The numerical computation of turbulent flows Computer Methods in Applied Mechanics and Engineering (pp. 269-289).

Lauterpacht, H. (1950). Sovereignty over Submarine Areas International Law: Being the Collected Papers of Hersch Lauterpacht (Vol. 3).

Lauterpacht, H. (1958). The Development of International Law by the International Court: Cambridge University Press.

Law, K. L., Moret-Ferguson, S., Goodwin, D. S., Zettler, E. R., DeForce, E., Kukulka, T., & Proskurowski, G. (2014). Distribution of surface plastic debris in the eastern Pacific Ocean from an 11-year dataset. Environmental Science & Technology. doi: 10.1021/es4053076

Law, K. L., Moret-Ferguson, S., Maximenko, N. A., Proskurowski, G., Peacock, E. E., Hafner, J., & Reddy, C. M. (2010). Plastic accumulation in the North Atlantic subtropical gyre. Science, 329(5996), 1185-1188. doi: 10.1126/science.1192321

Lebreton, L. C. M., Greer, S. D., & Borrero, J. C. (2012). Numerical modelling of floating debris in the world's oceans. Marine Pollution Bulletin, 64(3), 653-661. doi: http://dx.doi.org/10.1016/j.marpolbul.2011.10.027

Legler, J. (2008). New insights into the endocrine disrupt-

ing effects of brominated flame retardants. Chemosphere, 73(2), 216-222. doi: 10.1016/j.chemosphere.2008.04.081

Leonard George Munday v. Australian Capital Territory, 146 FLR 17 C.F.R. (1998).

Lepard, B. (2010). Customary International Law: A New Theory with Practical Applications: Cambridge University Press.

Li, B., Karl, D.M., Letelier, R. M., Church, M. J. (2011). Size dependent photosynthetic variability in the North Pacific Subtropical Gyre. Mar. Ecol. Prog. Ser., 440, 27-40. doi: 10.3354/meps09345

Lithner, D., Nordensvan, I., & Dave, G. (2012). Comparative acute toxicity of leachates from plastic products made of polypropylene, polyethylene, PVC, acrylonitrile-buta-diene-styrene, and epoxy to Daphnia magna. Environ Sci Pollut Res Int, 19(5), 1763-1772. doi: 10.1007/s11356-011-0663-5

Liu, H.-L., Sun, S. (2010). Diel vertical distribution and migration of a euphausiid Euphausia pacifica in the Southern Yellow Sea. Deep Sea Research Part II: Topical Studies in Oceanography, 57(7–8), 594-605. doi: http://dx.doi.org/10.1016/j.dsr2.2009.10.009

Lo, W.-T., Shih, C.-T., & Hwang, J.-S. (2004). Diel vertical migration of the planktonic copepods at an upwelling station north of Taiwan, western North Pacific. J Plankton Res, 26(1), 89-97. doi: 10.1093/plankt/fbh004

Long v. Dilling, 705 N.E. 2d 1022 C.F.R. (1999).

Lowe, V., & Fitzmaurice, M. (1996). Fifty Years of the International Court of Justice.

Lumpkin, R., Decomposition of surface drifter observations in the Atlantic Ocean. (2003). Geophys. Res. Lett., 30(14), 1753.

Lumpkin, R., Maximenko, N., Pazos, M., Evaluating where and why drifters die. (2012). J. Atmos. Ocean. Technol., 29(2), 300.

Lumpkin, R., Johnson, G.C., Global ocean surface velocities from drifters: Mean, variance, El Niño-Southern Oscillation response, and seasonal cycle. (2013). Journal of

Geophysical Research: Oceans, n/a.

Magnuson-Stevens Fishery Conservation and Management Act, 16 U.S.C § 1801 C.F.R.

Mallory, M. L., Roberston, G. J., & Moenting, A. (2006). Marine plastic debris in northern fulmars from Davis Strait, Nunavut, Canada. Mar Pollut Bull, 52(7), 813-815. doi: 10.1016/j.marpolbul.2006.04.005

Mantua, N. J., Hare, S. R. (2002). The Pacific Decadal Oscillation. Journal of Oceanography, 58(1), 35-44. doi: 10.1023/A:1015820616384

Marine Mammal Protection Act, 16 U.S.C. § 1361 C.F.R.
Markov, A. (1971). Extension of the Limit Theorems of Probability Theory to a Sum of Variables Connected in a Chain. In R. Howard (Ed.), Dynamic Probabilistic Systems (Volume I: Markov Models) (pp. 552-577): John Wiley & Sons, Inc.

MARPOL, International Convention for the Prevention of Pollution from Ships (1973). International Maritime Organization Retrieved from http://www.imo.org/About/Conventions/ListOfConventions/Pages/International-Convention-for-the-Prevention-of-Pollution-from-Ships-(MARPOL).aspx.

Marxsen, C.S., Potential world garbage and waste carbon sequestration. (2001). Environ. Sci. Policy, 4(6), 293.

Mata, M. M., Wijffels, S. E., Church, J. A., & Tomczak, M. (2006). Eddy shedding and energy conversions in the East Australian Current. Journal of Geophysical Research: Oceans, 111(C9), C09034. doi: 10.1029/2006JC003592

Mato, Y., Isobe, T., Takada, H., Kanehiro, H., Ohtake, C., & Kaminuma, T. (2001). Plastic resin pellets as a transport medium for toxic chemicals in the marine environment. Environ Sci Technol, 35(2), 318-324.

Maxey, M. R., & Riley, J. J. (1983). Equation of motion for a small rigid sphere in a nonuniform flow. Physics of Fluids (1958-1988), 26(4), 883-889. doi: doi:http://dx.doi.org/10.1063/1.864230

Maximenko, N., Hafner, J., & Niiler, P. (2012). Pathways of marine debris derived from trajectories of Lagrangian drifters. Marine Pollution Bulletin, 65(1–3), 51-62. doi: http://dx.doi.org/10.1016/j.marpolbul.2011.04.016

Maximenko, N., Hafner, J., Niiler, P., Centurioni, L., Rio, M.-H., Melnichenko, O., . . . Galperin, B. (2009). Mean Dynamic Topography of the Ocean Derived from Satellite and Drifting Buoy Data Using Three Different Techniques*. Journal of Atmospheric and Oceanic Technology, 26(9), 1910-1919. doi: 10.1175/2009JTECHO672.1

McClain, C. R., Signorini, S. R., & Christian, J. R. (2004). Subtropical gyre variability observed by ocean-color satellites. Deep Sea Research Part II: Topical Studies in Oceanography, 51(1–3), 281-301. doi: http://dx.doi.org/10.1016/j.dsr2.2003.08.002

McConnell, B. J., Fedak, M. A., Lovell, P., & Hammond, P. S. (1999). Movements and foraging areas of grey seals in the North Sea. Journal of Applied Ecology, 36(4), 573-590. doi: 10.1046/j.1365-2664.1999.00429.x

McCormick, B. W. (1995). Aerodynamics, Aeronautics, and Flight Mechanics (2 ed.): Wiley.

McDermid, K. J., & McMullen, T. L. (2004). Quantitative analysis of small-plastic debris on beaches in the Hawaiian Archipelago. Mar Pollut Bull, 48(7-8), 790-794. doi: 10.1016/j.marpolbul.2003.10.017

McDorman, T., Bolla, A., Johnston, D., & Duff, J. (2005). Ocean Science and Technology Meets Ocean Law, Part B. The Driftnet Controversy International Ocean Law: Materials and Commentaries (pp. 353).

McGowan, J. A. (1974). The nature of oceanic ecosystems The biology of the ocean Pacific (pp. 9-28). Corvallis, Oregon: Oregon State University Press.

McIlgorm, A., Campbell, H. F., & Rule, M. J. (2011). The economic cost and control of marine debris damage in the Asia-Pacific region. Ocean & Coastal Management, 54(9), 643-651. doi: http://dx.doi.org/10.1016/j.ocecoaman.2011.05.007

McIlgorm, A., F., C. H., & J, R. M. (2009). Understanding the

Economic Benefits and Costs of Controlling Marine Debris In the APEC Region. In M. R. C. W. Group (Ed.), (pp. 95).
McKinnell, M., & Dagg, M. J. (2010). Marine Ecosystems of the North Pacific Ocean. IN PICES (Ed.), PICES Special Publication (Vol. 4).
Memorandum: National Policy for the Oceans, Our Coasts, and the Great Lakes, 74 Fed. Reg. 28,591 C.F.R. (2009).

Mendez, M. A., Plana, E., Guxens, M., Foradada Morillo, C. M., Albareda, R. M., Garcia-Esteban, R., . . . Sunyer, J. (2010). Seafood consumption in pregnancy and infant size at birth: results from a prospective Spanish cohort. J Epidemiol Community Health, 64(3), 216-222. doi: 10.1136/jech.2008.081893

Meron, T. (1989). Human rights and humanitarian norms as customary law. Oxford: Claredon Press.

Mezzetta, S., Cirlini, M., Ceron, P., Tecleanu, A., Caligiani, A., Palla, G., & Sansebastiano, G. E. (2011). Concentration of DL-PCBs in fish from market of Parma city (north Italy): estimated human intake. Chemosphere, 82(9), 1293-1300. doi: 10.1016/j.chemosphere.2010.12.028

Microbes on Floating Ocean Plastics: Uncovering the Secret World of the 'Plastisphere. (2014). In A. G. Union (Ed.)., http://www.sciencedaily.com/releases/2014/02/140224171658.htm

Military and Paramilitary Activities in and against Nicaragua (Nicaragua v United States) (1986).

Moore, C. J., Synthetic polymers in the marine environment: a rapidly increasing, long-term threat. (2008). Environ. Res., 108(2), 131.

Moore, C. J., & Phillips, C. (2011). Plastic Ocean: How a Sea Captain's Chance Discovery Launched a Determined Quest to Save the Oceans: Avery Books.

Moore, C. J., Moore, S. L., Leecaster, M. K., & Weisberg, S. B. (2001). A Comparison of Plastic and Plankton in the North Pacific Central Gyre. Marine Pollution Bulletin, 42(12), 1297-1300. doi: http://dx.doi.org/10.1016/S0025-

326X(01)00114-X

Moorhouse v. Angus & Robertson (No1) Pty Ltd., 1 NSWLR 700 C.F.R. (1981).

Morét-Ferguson, S., Law, K. L., Proskurowski, G., Murphy, E. K., Peacock, E. E., & Reddy, C. M. (2010). The size, mass, and composition of plastic debris in the western North Atlantic Ocean. Mar Pollut Bull, 60(10), 1873-1878. doi: 10.1016/j.marpolbul.2010.07.020

Morris, R. J. (1980a). Floating plastic debris in the Mediterranean. Marine Pollution Bulletin, 11(5), 125. doi: http://dx.doi.org/10.1016/0025-326X(80)90073-9

Morris, R. J. (1980b). Plastic debris in the surface waters of the South Atlantic. Marine Pollution Bulletin, 11(6), 164-166. doi: http://dx.doi.org/10.1016/0025-326X(80)90144-7

Moser, M., & David, S. L. (1992). A Fourteen-Year Survey of Plastic Ingestion by Western North Atlantic Seabirds. Colonial Waterbirds, 15(1)(83-94).

Mouat, J., Lopez, L. R., & Bateson, H. (2010). Economic Impacts of Marine Litter. In KIMO (Ed.).

Mynott, S. (2013). What makes plankton migrate. Saltwater Science. Retrieved 4/27/2014, from http://www.nature.com/sciTable/blog/saltwater-science/what_makes_plankton_migrate

NASA, Gridded Population of the World, Version 3 (GPWv3). (2005). Socioeconomic Data and Application, http://sedac.ciesin.columbia.edu/data/collection/gpw-v3

NASA. (2014). Ocean in Motion: Ekman Transport. from http://oceanmotion.org/html/background/ocean-in-motion.htm

National Wildlife Refuge System Administration Act,, 16 U.S.C. § 668dd C.F.R.

Ng, K. L., & Obbard, J. P. (2006). Prevalence of microplastics in Singapore's coastal marine environment. Marine Pollution Bulletin, 52(7), 761-767. doi: http://dx.doi.org/10.1016/j.marpolbul.2005.11.017

NOAA (National Oceanic and Atmospheric Association), Fisheries (2013). Critical Habitat. http://www.nmfs.noaa.gov/pr/species/criticalhabitat.htm

NOAA, Fisheries (2014). Endangered and Threatened Marine Species. from http://www.nmfs.noaa.gov/pr/pdfs/species/esa_table.pdf

NOAA. Ocean. Retrieved 1/7/2014, from http://www.noaa.gov/ocean.html

NOAA. (2011). U.S National Bycatch Report, Retrieved 3/1/2014 from, http://www.nmfs.noaa.gov/by_catch/bycatch_nationalreport.htm

NOAA. (2012). Marine Debris Solutions, What NOAA Says, from http://www.marinedebrissolutions.com/Main-Menu/Sources-of-Marine-Debris/What-NOAA-Says.html

NOAA. (2014). The Global Drifter Program. Satellite-tracked surface drifting buoys. Retrieved 4/17/2014, http://www.aoml.noaa.gov/phod/dac/index.php

NOAA. (2014). National Coastal Data Development Center, from http://ecowatch.ncddc.noaa.gov/thredds/catalog.html

Nordquist, M., Nandan, S. N., & Kraska, J. (2011). United Nations Convention on the Law of the Sea, 1982: A commentary.

North Sea Continental Shelf (FRG v Denmark; FRG v Netherland) § para 71, 73, and 74 (1969).
Northwestern Hawaiian Islands Marine National Monument, 71 Fed. Reg. 51,134, 51,141 C.F.R. (2006).

Odyssey Marine Explorations, Inc. v. Unidentified, Shipwrecked Vessel or Vessels, No. 8:06-cv-1685-T23TBM, 2006 WL 3091531 C.F.R. (2006).

Oehlmann, J., Schulte-Oehlmann, U., Kloas, W., Jagnytsch, O., Lutz, I., Kusk, K. O., . . . Tyler, C. R. (2009). A critical analysis of the biological impacts of plasticizers on wildlife. Philos Trans R Soc Lond B Biol Sci, 364(1526), 2047-2062. doi: 10.1098/rstb.2008.0242

Offshore, Arctia. MSV Fennica vessel specifications.

Okada, H., Tokunaga, T., Liu, X., Takayanagi, S., Matsushima, A., & Shimohigashi, Y. (2008). Direct evidence revealing structural elements essential for the high binding ability of bisphenol A to human estrogen-related receptor-gamma. Environ Health Perspect, 116(1), 32-38. doi: 10.1289/ehp.10587

Omori, M. (1969). Weight and chemical composition of some important oceanic zooplankton in the North Pacific Ocean. Marine Biology, 3(1), 4-10. doi: 10.1007/BF00355587

Omori, M., & Ikeda, T. (1985). Methods in Marine Zooplankton Ecology. xiii, 332 pp. John Wiley, 1984. Price £47.80. Journal of the Marine Biological Association of the United Kingdom, 65(02), 562-562. doi: doi:10.1017/S0025315400050669

Oregon Department of Fish and Wildlife. (2013). Marine Aquatic Invasive Species, Japanese Tsunami Debris. http://www.dfw.state.or.us/conservationstrategy/invasive_species/marine_aquatic_invasive_species.asp

Oros, J., Torrent, A., Calabuig, P., & Deniz, S. (2005). Diseases and causes of mortality among sea turtles stranded in the Canary Islands, Spain (1998-2001). Dis Aquat Organ, 63(1), 13-24. doi: 10.3354/dao063013

Orós, T., Calabuig, P., & Déniz, S. (2005). Diseases and Causes of Mortality among Sea Turtles Stranded in the Canary Islands, Spain (1998–2001). Dis Aquat Organ, 63, 13-24.

OSPAR. (2008). Background Document for the EcoQO on Plastic Particles in Stomachs of Seabirds. Biodiversity Series.

Otake, Y., Kobayashi, T., Asabe, H., Murakami, N., & Ono, K. (1995). Biodegradation of low-density polyethylene, polystyrene, polyvinyl chloride, and urea formaldehyde resin buried under soil for over 32 years. Journal of Applied Polymer Science, 56(13), 1789-1796. doi: 10.1002/app.1995.070561309

Overview of the Offshore Supply Vessel Industry. (2012). http://www.marinemoney.com/sites/all/themes/marine-money/forums/houston12/presentations/OSV_OUTLOOK%20Clarksons.pdf

Page, B., McKenzie, J., McIntosh, R., Baylis, A., Morrissey, A., Calvert, N., . . . Goldsworthy, S. D. (2004). Entanglement of Australian sea lions and New Zealand fur seals in lost fishing gear and other marine debris before and after Government and industry attempts to reduce the problem. Mar Pollut Bull, 49(1-2), 33-42. doi: 10.1016/j.marpolbul.2004.01.006

Palmer, J., Turney, C., Hogg, A., Hilliam, N., Watson, M., van Sebille, E., Cowie, W., Jones, R., Petchey, F., The discovery of New Zealand's oldest shipwreck – possible evidence of further Dutch exploration of the South Pacific. (2013). Journal of Archaeological Science.

Panel, Scientific and Technical Advisory (2011). Marine Debris as a Global Environmental Problem. In KIMO (Ed.). Pardo, P. (1983). Before and After. Law and Contemporary Problems, 46, 95-105.

Parker, L. (2014, April 14). The Best Way to Deal With Ocean Trash. 2014, from http://news.nationalgeographic.com/news/2014/04/140414-ocean-garbage-patch-plastic-pacific-debris/

PCCS. (2011). The Centre for Coastal Studies. from http://www.coastalstudies.org

Pedlosky, J. (1990). The Dynamics of the Oceanic Subtropical Gyres. Science, 248(4953), 316-322. doi: 10.1126/science.248.4953.316

Pegram, J. E., & Andrady, A. L. (1989). Outdoor weathering of selected polymeric materials under marine exposure conditions. Polymer Degradation and Stability, 26(4), 333-345. doi: http://dx.doi.org/10.1016/0141-3910(89)90112-2

Peloquin, J., Swan, C., Gruber, N., Vogt, M., Claustre, H., Ras, J., . . . Wright, S. (2012). The MAREDAT global database of high performance liquid chromatography marine pigment measurements. Earth Syst. Sci. Data Discuss., 5(2), 1179-1214. doi: 10.5194/essdd-5-1179-2012

Pichel, W. G., Churnside, J. H., Veenstra, T. S., Foley, D. G., Friedman, K. S., Brainard, R. E., Clemente-Colón, P. (2007). Marine debris collects within the North Pacific Subtropical Convergence Zone. Marine Pollution Bulletin, 54(8), 1207-1211. doi: http://dx.doi.org/10.1016/j.marpolbul.2007.04.010

Pichel, W. G., Veenstra, T. S., Churnside, J. H., Arabini, E., Friedman, K. S., Foley, D. G., . . . Li, X. (2012). GhostNet marine debris survey in the Gulf of Alaska – Satellite guidance and aircraft observations. Marine Pollution Bulletin, 65(1–3), 28-41. doi: http://dx.doi.org/10.1016/j.marpolbul.2011.10.009

Pister, B. (2009). Urban marine ecology in southern California: the ability of riprap structures to serve as rocky intertidal habitat. Marine Biology, 156(5), 861-873. doi: 10.1007/s00227-009-1130-4

Plastics Europe. (2013). Plastics - the Facts 2013: An analysis of European latest plastics production, demand and waste data. http://www.plasticseurope.org/Document/plastics-the-facts-2013.aspx?FolID=2

Polovina, J. J., Howell, E., Kobayashi, D. R., & Seki, M. P. (2001). The transition zone chlorophyll front, a dynamic global feature defining migration and forage habitat for marine resources. Progress in Oceanography, 49(1), 469-483. doi: 10.1016/S0079-6611(01)00036-2

Poulain, P-M., Gerin, R., Mauri, E. Wind effects on drogued and undrogued drifters in the eastern Mediterranean. (2009). J. Atmos. Ocean. Technol., 26(6), 1144.

Proclamation No. 5030, 48 Fed. Reg. 10,605 C.F.R. (1983). Proclamation No. 8031, 71 Fed. Reg. 36,443 C.F.R. (2006). Proclamation 8335 - Establishment of the Marianas Trench Marine National Monument (2009).

Rabello, M. S., & White, J. R. (1997). The role of physical structure and morphology in the photodegradation behaviour of polypropylene. Polymer Degradation and Stability, 56(1), 55-73. doi: http://dx.doi.org/10.1016/S0141-3910(96)00202-9

Ralph, E. A., & Niiler, P. P. (1999). Wind-Driven Currents in the Tropical Pacific. Journal of Physical Oceanography, 29(9), 2121-2129. doi: 10.1175/1520-0485(1999)029<2121:WDCITT>2.0.CO;2

Randall, J. E. (1992). Review of the Biology of the Tiger Shark (Galeocerdo Cuvier). Aust. J. Mar. Freshwater Res., 43, 21-31.

Raven, J. A. (1998). The twelfth Tansley Lecture. Small is beautiful: the picophytoplankton. Functional Ecology, 12(4), 503-513. doi: 10.1046/j.1365-2435.1998.00233.x Recovery, California Department of Recycling and (2012). Evaluation of Greenhouse Gas Emissions Associated Recycled-Content Products.

Recycling, Eureka. Recycling Plastics May Be Better Than Wasting, But Can Be Toxic Too. Retrieved April 24, 2014, from http://www.eurekarecycling.org/page.cfm?ContentID=126

Reisser, J., Hajbane, S., Rogers, S., Shaw, J., & Pattiaratchi, C. (2013). Plastic Debris in the North-west Marine Region, Australia.

Reisser, J., Shaw, J., Wilcox, C., Hardesty, B. D., Proietti, M., Thums, M., & Pattiaratchi, C. (2013). Marine plastic pollution in waters around Australia: characteristics, concentrations, and pathways. PLoS One, 8(11), e80466. doi: 10.1371/journal.pone.0080466

Richardson, P. L. (1997). Drifting in the wind: leeway error in shipdrift data. Deep Sea Research Part I: Oceanographic Research Papers, 44(11), 1877-1903. doi: http://dx.doi.org/10.1016/S0967-0637(97)00059-9

Rios, L. M., Moore, C., & Jones, P. R. (2007). Persistent organic pollutants carried by synthetic polymers in the ocean environment. Mar Pollut Bull, 54(8), 1230-1237. doi: 10.1016/j.marpolbul.2007.03.022

R.M.S. Titanic, Inc. v. Wrecked & Abandoned Vessel, 435 F. 3d 521 (4th Cir. 2006) C.F.R.

Robards, M. D., Piatt, J. F., & Wohl, K. D. (1995). Increasing frequency of plastic particles ingested by seabirds in the subarctic North Pacific. Marine Pollution Bulletin, 30(2), 151-157. doi: http://dx.doi.org/10.1016/0025-326X(94)00121-O

Rochman, C. M., Browne, M. A., Halpern, B. S., Hentschel, B. T., Hoh, E., Karapanagioti, H. K., . . . Thompson, R. C. (2013). Policy: Classify plastic waste as hazardous. Nature, 494(7436), 169-171.

Rochman, C. M., Hoh, E., Hentschel, B. T., & Kaye, S. (2013). Long-term field measurement of sorption of organic contaminants to five types of plastic pellets: implications for plastic marine debris. Environ Sci Technol, 47(3), 1646-1654. doi: 10.1021/es303700s

Rochman, C. M., Hoh, E., Kurobe, T., & Teh, S. J. (2013). Ingested plastic transfers hazardous chemicals to fish and induces hepatic stress. Sci Rep, 3, 3263. doi: 10.1038/srep03263

Rochman, C. M., Lewison, R. L., Eriksen, M., Allen, H., Cook, A. M., & Teh, S. J. (2014). Polybrominated diphenyl ethers (PBDEs) in fish tissue may be an indicator of plastic contamination in marine habitats. Sci Total Environ, 476-477, 622-633. doi: 10.1016/j.scitotenv.2014.01.058

Romanow, S. (2014). Industry associations form pact to recycle waste plastic into oil, Hydrocarbon Processing.

Rubin, B. S. (2011). Bisphenol A: an endocrine disruptor with widespread exposure and multiple effects. J Steroid Biochem Mol Biol, 127(1-2), 27-34. doi: 10.1016/j.jsbmb.2011.05.002

Ryan, P. G. (1988). The characteristics and distribution of plastic particles at the sea-surface off the southwestern Cape Province, South Africa. Marine Environmental Research, 25(4), 249-273. doi: http://dx.doi.org/10.1016/0141-1136(88)90015-3

Ryan, P. G. (1990). The Effects of Ingested Plastic and Other Marine Debris on Seabirds. Paper presented at the Second international Conference on Marine Debris, Honolulu, Hawaii.

Ryan, P. G. (2013). A simple technique for counting marine debris at sea reveals steep litter gradients between the Straits of Malacca and the Bay of Bengal. Mar Pollut Bull, 69(1-2), 128-136. doi: 10.1016/j.marpolbul.2013.01.016

Ryan, P. G. (2014). Litter survey detects the South Atlantic 'garbage patch'. Mar Pollut Bull, 79(1-2), 220-224. doi: 10.1016/j.marpolbul.2013.12.010

The S. S. Wimbledon, PCIJ, Ser. A,. No 1 C.F.R. (1923).

Sajiki, J., & Yonekubo, J. (2003). Leaching of bisphenol A (BPA) to seawater from polycarbonate plastic and its degradation by reactive oxygen species. Chemosphere, 51(1), 55-62.

Saw, C. L. (2011). Abandonment and Passing of Property in Trash. Singapore Acadamy of Law Journal.

Sax, L. (2010). Polyethylene terephthalate may yield endocrine disruptors. Environ Health Perspect, 118(4), 445-448. doi: 10.1289/ehp.0901253

Scharf, M. P. (2010). Seizing the 'Grotian Moment' Accelerated Formation of Customary International Law in Times of Fundamental Change. Cornell International Law Journal, 43(3).

Schlining, K., von Thun, S., Kuhnz, L., Schlining, B., Lundsten, L., Jacobsen Stout, N., . . . Connor, J. (2013). Debris in the deep: Using a 22-year video annotation database to survey marine litter in Monterey Canyon, central California, USA. Deep Sea Research Part I: Oceanographic Research Papers, 79(0), 96-105. doi: http://dx.doi.org/10.1016/j.dsr.2013.05.006

Schoenbaum, T. J. (2004). Admiralty and Maritime Law (4th ed.).

Schrey, E., & Vauk, G. J. M. (1987). Records of entangled gannets (Sula bassana) at Helgoland, German Bight. Marine Pollution Bulletin, 18(6, Supplement B), 350-352. doi: http://dx.doi.org/10.1016/S0025-326X(87)80024-3

Semco Salvage & Marine Pte Ltd. v. Lancer Navigation (The Nagasaki Spirit) (1995).

Sen, Z., Altunkaynak, A., & Erdik, T. (2012). Wind Velocity Vertical Extrapolation by Extended Power Law (Vol. 2012). Setälä, O., Fleming-Lehtinen, V., & Lehtiniemi, M. (2014). Ingestion and transfer of microplastics in the planktonic food web. Environmental Pollution, 185(0), 77-83. doi: http://dx.doi.org/10.1016/j.envpol.2013.10.013

Sharfstein, P., Dimitriou, D., & Hankin, S. (2005). The US-GODAE Monterey Data Server. Paper presented at the American Geophysical Union, Fall Meeting 2005.

Shaw, D. G. (1977). Pelagic tar and plastic in the Gulf of Alaska and Bering Sea: 1975. Science of The Total Environment, 8(1), 13-20. doi: http://dx.doi.org/10.1016/0048-9697(77)90058-4

Sheavly, S. B., & Register, K. M. (2007). Marine Debris & Plastics: Environmental Concerns, Sources, Impacts and Solutions. Journal of Polymers and the Environment, 15(4), 301-305.

Sheridan, C. C., & Landry, M. R. (2004). A 9-year increasing trend in mesozooplankton biomass at the Hawaii Ocean Time-series Station ALOHA. ICES Journal of Marine Science: Journal du Conseil, 61(4), 457-463. doi: 10.1016/j.icesjms.2004.03.023

Shiomoto, A., & Kameda, T. (2005). Distribution of manufactured floating marine debris in near-shore areas around Japan. Mar Pollut Bull, 50(11), 1430-1432. doi: 10.1016/j.marpolbul.2005.08.020

Shomura, R. S., & Yoshida, H. O. (1985). Proceedings of the Workshop on the Fate and Impact of Marine Debris. Paper presented at the Observations of man-made objects on the surface of the North Pacific Ocean, Honolulu, Hawaii.

Siedler, G., Church, J., Gould, J., Gould, W. J., The world ocean surface circulation. (2001). Ocean Circulation and Climate: Observing and Modelling the Global Ocean, 77, 193.

Simma, B., & Alston, P. (1988). The Sources of Human Rights Law: Custom, Jus Cogens, and General Principles.

Sims, D. W. (2000). Filter-feeding and cruising swimming speeds of basking sharks compared with optimal models: they filter-feed slower than predicted for their size. J Exp Mar Bio Ecol, 249(1), 65-76.

Simpson v. Gowers (1981), 121 D.L.R. (3d) 709.

Singler, H. R., & Villareal, T. A. (2005). Nitrogen inputs into the euphotic zone by vertically migrating Rhizosolenia mats. Journal of Plankton Research, 27(6), 545-556. doi: 10.1093/plankt/fbi030

Southwood, A., Fritsches, K., Brill, R., & Swimmer, Y. (2008). Sound, chemical, and light detection in sea turtles and pelagic fishes: sensory-based approaches to bycatch reduction in longline fisheries. Endang Species Res, 5, 225-238.

Stenseth, N. C., Ottersen, G., Hurrell, J. W., Mysterud, A., Lima, M., Chan, K.-S., . . . Adlandsvik, G. (2003). Studying climate effects on ecology through the use of climate indices, the North Atlantic Oscillation, El Niño Southern Oscillation and beyond. (270), 2087-2096.

Stokes, G. G. (1851). On the effect of the internal friction of fluids on the motion of pendulums. 9(Part II), 8-106. Suarez, S. (2008). The Outer Limits of the Continental Shelf: Legal Aspects of their Establishment New York: Springer.

Sudhakar, M., Trishul, A., Doble, M., Suresh Kumar, K., Syed Jahan, S., Inbakandan, D., . . . Venkatesan, R. (2007). Biofouling and biodegradation of polyolefins in ocean waters. Polymer Degradation and Stability, 92(9), 1743-1752. doi: http://dx.doi.org/10.1016/j.polymdegradstab.2007.03.029

Sverdrup, H. (1942). The Oceans - Physics, Chemistry and Biology: Prentice-Hall.

Talley, L. D., Pickard, G. L., Emery, W. J., & Swift, J. H. (2011). Descriptive physical oceanography: An introduction: Elsevier.

Taking of Marine Mammals Incidental to Operation and Maintenance of the Neptune Liquefied Natural Gas Facility off Massachusetts, 76 Fed. Reg. 34,157 C.F.R. (2011). Tanaka, K., Takada, H., Yamashita, R., Mizukawa, K.,

Fukuwaka, M. A., & Watanuki, Y. (2013). Accumulation of plastic-derived chemicals in tissues of seabirds ingesting marine plastics. Mar Pollut Bull, 69(1-2), 219-222. doi: 10.1016/j.marpolbul.2012.12.010

Taylor, P. K., & Yelland, M. J. (2001). The Dependence of Sea Surface Roughness on the Height and Steepness of the Waves. Journal of Physical Oceanography, 31(2), 572-590. doi: 10.1175/1520-0485(2001)031<0572:TDOSSR>2.0 .CO;2

team, L. (2013). ANANAS v3.2 reference manual.

Teuten, E. L., Rowland, S. J., Galloway, T. S., & Thompson, R. C. (2007). Potential for plastics to transport hydrophobic contaminants. Environ Sci Technol, 41(22), 7759-7764 .

Teuten, E. L., Saquing, J. M., Knappe, D. R., Barlaz, M. A., Jonsson, S., Bjorn, A., . . . Takada, H. (2009). Transport and release of chemicals from plastics to the environment and to wildlife. Philos Trans R Soc Lond B Biol Sci, 364(1526), 2027-2045. doi: 10.1098/rstb.2008.0284

The United Nations Convention on the Law of the Sea of 10 December 1982 Relating to the Conservation and Management of Straddling Fish Stocks and Highly Migratory Fish Stocks Paper presented at the United Nations Conference on Straddling Fish Stocks and Highly Migratory Fish Stocks, New York, NY.

Thiel, M., Hinojosa, I., Vasquez, N., & Macaya, E. (2003). Floating marine debris in coastal waters of the SE-Pacific (Chile). Mar Pollut Bull, 46(2), 224-231.

Thiel, M., Hinojosa, I. A., Miranda, L., Pantoja, J. F., Rivadeneira, M. M., & Vasquez, N. (2013). Anthropogenic marine debris in the coastal environment: a multi-year comparison between coastal waters and local shores. Mar Pollut Bull, 71(1-2), 307-316. doi: 10.1016/j.marpolbul.2013.01.005

Thompson, R. C., Olsen, Y., Mitchell, R. P., Davis, A., Rowland, S. J., John, A. W., . . . Russell, A. E. (2004). Lost at sea: where is all the plastic? Science, 304(5672), 838. doi: 10.1126/science.1094559

Thompson, R. C., Swan, S. H., Moore, C. J., & vom Saal, F. S. (2009). Our plastic age. Philosophical Transactions of the Royal Society B: Biological Sciences, 364(1526), 1973-1976. doi: 10.1098/rstb.2009.0054

Titmus, A. J., & Hyrenbach, K. D. (2011). Habitat associations of floating debris and marine birds in the North East Pacific Ocean at coarse and meso spatial scales. Mar Pollut Bull, 62(11), 2496-2506. doi: 10.1016/j.marpolbul.2011.08.007

Tomás, J., Guitart, R., Mateo, R., & Raga, J. A. (2002). Marine debris ingestion in loggerhead sea turtles, Caretta caretta, from the Western Mediterranean. Marine Pollution Bulletin, 44(3), 211-216. doi: http://dx.doi.org/10.1016/S0025-326X(01)00236-3

The United Nations Agreement for the Implementation of the Provisions of the United Nations Convention on the Law of the Sea of 10 December 1982 relating to the Conservation and Management of Straddling Fish Stocks and Highly Migratory Fish Stocks (1995), http://www.un.org/Depts/los/convention_agreements/texts/fish_stocks_agreement/CONF164_37.htm

UN (United Nations) (1950). Report of the International Law Commission to the General Assembly (Part II): Ways and Means of Making the Evidence of Customary International Law More Readily Available. In I. L. Commission (Ed.), 2 YBILC 367, ILC Doc A/1316.

UN Atlas of the Oceans: Straddling Stocks (2010), http://www.oceansatlas.org/servlet/CDSServlet?status=ND1maWdpczE0NzY5JjY9ZW4mMzM9KiYzNz1rb3M~.

UN Convention on the Law of the Sea, 1833 U.N.T.S. 3 C.F.R. (1982).

UN (2006). Guiding Principles applicable to unilateral declarations of States capable of creating legal obligations. In I. L. Commission (Ed.). http://legal.un.org/ilc/texts/instruments/english/draft%20articles/9_9_2006.pdf

UNEP (United Nations Environmental Programme) (2009). Marine Litter: A Global Challenge, http://www.unep.org/

pdf/unep_marine_litter-a_global_challenge.pdf
UNEP (United Nations Environmental Programme). (2009). Converting Waste Plastics into a Resource. http://www.unep.or.jp/Ietc/Publications/spc/WastePlastics-EST_Compendium.pdf

UNEP (2011). Year Book 2011: Emerging Issues in our Global Environment. http://www.unep.org/yearbook/2011/
United States v. Shelby Iron Company. 273 US 571 (Sup. Ct. 1927)

Van, A., Rochman, C. M., Flores, E. M., Hill, K. L., Vargas, E., Vargas, S. A., & Hoh, E. (2012). Persistent organic pollutants in plastic marine debris found on beaches in San Diego, California. Chemosphere, 86(3), 258-263. doi: 10.1016/j.chemosphere.2011.09.039

Van Cauwenberghe, L., Claessens, M., Vandegehuchte, M. B., Mees, J., & Janssen, C. R. (2013). Assessment of marine debris on the Belgian Continental Shelf. Mar Pollut Bull, 73(1), 161-169. doi: 10.1016/j.marpolbul.2013.05.026
Van Cauwenberghe, L., Vanreusel, A., Mees, J., & Janssen, C. R. (2013). Microplastic pollution in deep-sea sediments. Environ Pollut, 182, 495-499. doi: 10.1016/j.envpol.2013.08.013

van Franeker, J. A., Blaize, C., Danielsen, J., Fairclough, K., Gollan, J., Guse, N., . . . Turner, D. M. (2011). Monitoring plastic ingestion by the northern fulmar Fulmarus glacialis in the North Sea. Environ Pollut, 159(10), 2609-2615. doi: 10.1016/j.envpol.2011.06.008

van Sebille, E., Beal, L., Johns, W. E., Advective time scales of Agulhas leakage to the North Atlantic in surface drifter observations and the 3D OFES model. (2011). J. Phys. Oceanogr., 41(5), 1026.

van Sebille, E., England, M. H., & Froyland, G. (2012). Origin, dynamics and evolution of ocean garbage patches from observed surface drifters. Environmental Research Letters, 7 (4), 044040..

Venrick, E. L., Backman, T. W., Bartram, W. C., Platt, C. J., Thornhill, M. S., & Yates, R. E. (1973). Man-made Objects on the Surface of the Central North Pacific Ocean. Nature, 241(5387), 271-271.

Venrick, E. L., McGowan, J. A., Cayan, D. R., & Hayward, T.

L. (1987). Climate and Chlorophyll a: Long-Term Trends in the Central North Pacific Ocean. Science, 238(4823), 70-72. doi: 10.1126/science.238.4823.70

Voigt, C. (2009). Sustainable Development as a Principle of INternational Law: Martinus Nijhoff Publishers.

Wakata, Y., Sugimori,Y,, Lagrangian motions and global density distribution of floating matter in the ocean simulated using shipdrift data. (1990). J. Phys. Oceanogr., 20(1), 125.
Walker, W. A., & Coe, J. M. (1989). Survey Of Marine Debris Ingestion By Odontocete Cetaceans. Paper presented at the Second International Conference on Marine Debris.

Walpole, S. C., Prieto-Merino, D., Edwards, P., Cleland, J., Stevens, G., & Roberts, I. (2012). The weight of nations: an estimation of adult human biomass. BMC Public Health, 12, 439. doi: 10.1186/1471-2458-12-439

Wegelein, F. H. (2005). Marine Scientific Research: The Operation And Status of Research Vessels And Other Platforms in International Law.

Weisman, A. (2007). The World Without Us: St. Martin's Thomas Dunne Books.

Western Pacific Fisheries: Fishing in the Marianas Trench, Pacific Remote Islands, and Rose Atoll Marine National Monuments, 78 Fed Reg. 32996 C.F.R. (2013).

Wilber, R. J. (1987). Plastic in the North Atlantic. Oceanus.
Wilcox, D. C. (1998). Turbulence Modeling for CFD (2nd ed.): DCW Industries.

Williams, J. M. (1981). Limiting Gravity Waves in Water of Finite Depth. Philosophical Transactions of the Royal Society of London. Series A, Mathematical and Physical Sciences, 302(1466), 139-188. doi: 10.1098/rsta.1981.0159
Williams, J. M. (1986). Tables of Progressive Gravity Waves: John Wiley & Sons Australia, Limited.

Williams, R., Ashe, E., & O'Hara, P. D. (2011). Marine mammals and debris in coastal waters of British Columbia, Canada. Mar Pollut Bull, 62(6), 1303-1316. doi: 10.1016/j.

marpolbul.2011.02.029

Wilson, C. (2003). Late Summer chlorophyll blooms in the oligotrophic North Pacific Subtropical Gyre. Geophysical Research Letters, 30(18), 1942. doi: 10.1029/2003GL017770

Wood, M. (2013). First report on formation and evidence of customary international law. In U.-I. L. Commission (Ed.), UN Doc A/CN 4/663.

Wright, S. L., Thompson, R. C., & Galloway, T. S. (2013). The physical impacts of microplastics on marine organisms: A review. Environmental Pollution, 178(0), 483-492. doi: http://dx.doi.org/10.1016/j.envpol.2013.02.031

Yamamoto, T., & Yasuhara, A. (1999). Quantities of bisphenol a leached from plastic waste samples. Chemosphere, 38(11), 2569-2576.

Yamashita, R., & Tanimura, A. (2007). Floating plastic in the Kuroshio Current area, western North Pacific Ocean. Mar Pollut Bull, 54(4), 485-488. doi: 10.1016/j.marpolbul.2006.11.012

Zehr, J. P., Waterbury, J. B., Turner, P. J., Montoya, J. P., Omoregie, E., Steward, G. F., . . . Karl, D. M. (2001). Unicellular cyanobacteria fix N2 in the subtropical North Pacific Ocean. Nature, 412(6847), 635-638. doi: 10.1038/35088063

Zettler, E. R., Mincer, T. J., & Amaral-Zettler, L. A. (2013). Life in the "Plastisphere": Microbial Communities on Plastic Marine Debris. Environmental Science & Technology, 47(13), 7137-7146. doi: 10.1021/es401288x

Zhang, P. (2013). A Proposal of International Regulations for Preventing Collision between an Offshore Platform and a Ship Marine Navigation and Safety of Sea Transportation (pp. 175-178): CRC Press.

Zhou, P., Huang, C., Fang, H., Cai, W., Li, D., Li, X., & Yu, H. (2011). The abundance, composition and sources of marine debris in coastal seawaters or beaches around the northern South China Sea (China). Mar Pollut Bull, 62(9), 1998-2007. doi: 10.1016/j.marpolbul.2011.06.018

ACKNOWLEDGE-
MENTS
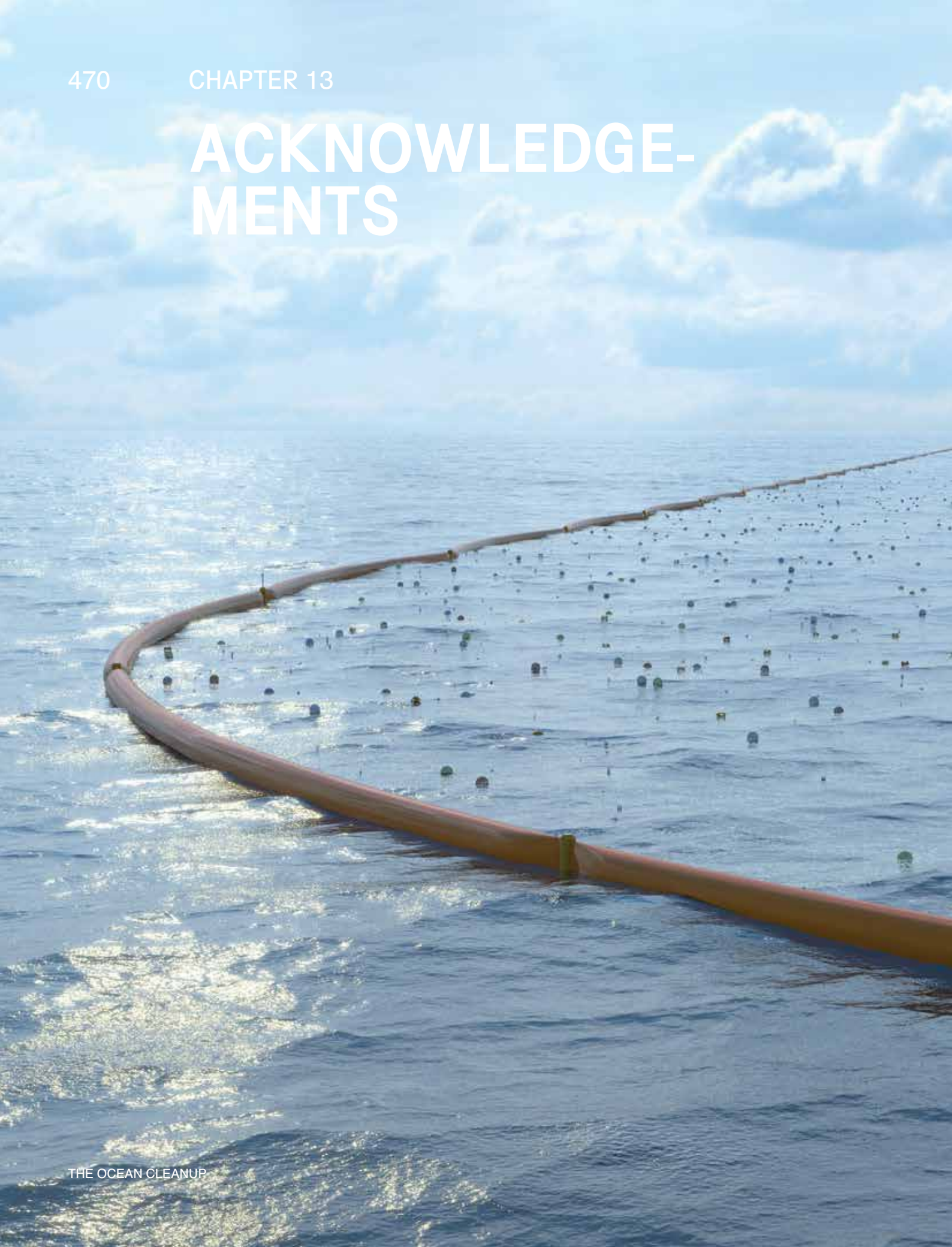
13.1 AUTHORS AND VOLUNTEERS

We would like to thank all the researchers, authors, editors and coordinators of this study for their time, dedication and hard work that they, mostly voluntarily, put into this feasibility study.

Furthermore, we would like to thank all our other volunteers that helped make The Ocean Cleanup function as an organization capable of facilitating this research.

BOARD

Boyan Slat	Founder & President
Ir. Frans Ratelband, MSc	Secretary
Femke Hoes	Treasurer, bookkeeper

MANAGEMENT

Boyan Slat	Founder & President
Florian Dirkse	General Manager
Jan de Sonneville, PhD	Lead Engineer, Project Manager Feasibility Study

FEASIBILITY STUDY COORDINATORS

Norbert Fraunholcz, PhD	Processing and Recycling Coordinator / Senior materials processing technologist
Ir. Leonid Pavlov, MSc	CFD/CM Coordinator
Julia Reisser, MSc	Lead Physical Oceanographer
Nicholas P. Katsepontes BA, LLB, LLM	Maritime & Environmental Law Coordinator
Robbert Zuijderwijk, BSc	Ecology Coordinator
Bernd van Dijk, MSc	Coordinator Financials

RESEARCHERS, AUTHORS AND EDITORS

Wouter Jansen	Intern Computational modelling
Bruno Sainte-Rose	2D CFD modelling expert
David Kauzlaric	Expert 3D CFD modelling
Nandini Sivasubramanian	Intern CFD modelling
Niklas Wehkamp	3D CFD modelling expert
Dr. Tim Landgraf	Computational modeller
Stephan Koch	Computational modeller
Alexander Rau	Computational modeller
Maximilian Michels	Computational modeller
Jaime López	Physical Oceanographer
Hyke Brugman	Intern Physical Testing
Raphael Klein, BSc	Coordinator boom engineering
Sebastiaan van Rossum	Intern Hydraulic Engineering
Ezra Hildering van Lith, BSc	Engineer
Joost de Haan, BSc	Offshore Engineer
Sebastiaan van Schie	Engineer

Richard Martini	Offshore Engineering advisor	**COMMUNICATIONS AND OFFICE**	
Marijn Dekker	Marine Engineer	Joost Niepoth	Lead Communications officer
Sjoerd Drenkelford	Intern Transport & Logistics	Joram Falkenburg	Communications
Dr. Gabrielle S. Prendergast	Biofouling Expert	Ianthe Dickhoff	Communications officer
Mark van Dijk, MSc	Plankton Ecologist	Sandra Quirijns	Communications officer
Pauline Horng	Ecologist	Marloes Loos	Communications officer
Moritz Schmid	Ecologist	Rene Coppens	Communications officer
Tadzio Holtrop	Ecologist		Webmaster
Marleen Roelofs	Plankton Biologist	Pieter Stalenhoef	Internal communications
Katherine Schmidt	Ecologist	Rob Gargett	Proofreader
Stella Diamant	Ecologist	Gerard Neil	Proofreader
Nathan Walworth	Ecologist	Marchien Bel	Videography/Photo
Evelien Bolle	Carbon Footprint Analyst		Coordinator
John Clinton Geil	Legal researcher	Helena Meresman	Social media coordinator
Paula Walker	Legal researcher	Manissa Ruffles	PA Boyan Slat
Richard Hildreth	Legal researcher	Stefanos Malandrakis	Merchandise Coordinator
Holly Campbell. J.D., LLM., Ph.D	Legal researcher	Alison O'Keeffe	Social media coordinator
Adam Walters	Legal researcher		
Rebecca Rushton	Legal researcher	**FINANCE AND FUNDING**	
Jill Randolph	Legal researcher	Dario Grassini, CPA	Accountant
Nick Howard	Legal researcher	Arthur van de Graaf	Crowdfunding Coordinator
Jochem A. Jonkman	Plastic sample analyser	Emmanuel Osiga	Communications officer
Dr. Kauê Pelegrini	Polymers Expert	Fadia Alabbar	Communications officer
Pierre-Louis Christiane	Financial Impact Analyst		
Jort Hammer	Ecological Impact Analist	**LEGAL**	
Bonnie Monteleone	Feasibility study co-author	Pauline Phoa	Legal coordinator
Goli Habibi-Kenari	Feasibility Study Editor	Martin Krüger	Legal coordinator
Kelly Marie Osborn	Feasibility Study Editor		
Elizabeth Ooi	Feasibility Study Editor	**IT**	
Mukul Kumar	Feasibility Study Editor	Steven Bink	IT Coordinator
Edd Hornsby	Feasibility Study Editor		
Agnes Ardiyanti	Feasibility Study Editor	**HR**	
Johanna Buurman	Feasibility Study Editor	Layla Groeneweg	HR Coordinator
Hester Jansen	Feasibility Study Editor		
Michiel van der Spek	Feasibility Study Editor		
Sergio Castellanos	Prototyping Engineer		
Wart Luscuere	Testing and Manufacturing		
Freddy Vlot	Workshop assistant		
Jan Schoemaker	Workshop assistant		
Erik van Vliet	Workshop assistant		
Bink van Drongelen	Workshop assistant		

13.2 SPONSORS AND COLLABORATORS

Thanks to the extensive support of these companies and institutes The Ocean Cleanup has been able to perform a large amount of research, with only a very limited amount of time and resources. We would like to sincerely thank them for their courage in supporting us in this early phase of the project.

Company/ Organisation	Website	Type of assistance	Special thanks to
Institutions			
Royal Netherlands Institute for Sea Research (NIOZ)	www.nioz.nl	Enabling The Ocean Cleanup to test in their racetrack-flume, and invited The Ocean Cleanup to join a research expedition through the NAG.	Henk Brinkhuis, Corina Brussaard, Kristina Mojica, Tjeerd Bouma, Klaas Timmermans, Henk de Haas
Delft University of Technology	www.tudelft.nl	Advising in the mechanical engineering field, and supplying office and workshop space.	Wim Thijs, Professor Kaminski, Professor Garcia Espallargas, Professor Lodewijks, Professor Baller, Michel van Baal, Kees Baardolf
Freiburg Institute of Advanced Studies	www.frias.uni-freiburg.de	Performing the 3D CFD analyses.	Dr. David Kauzlaric
Companies			
Recycling Avenue	www.recycling-avenue.nl	Processing and Recycling Research.	Dr. Norbert Fraunholcz, who has been of great help to the project, right from the early days. and Jochem Jonkman
Solidworks	www.solidworks.com	Supplying access to their network of engineers through design contests.	Bertrand Sicot, Jeroen Buring and Matthew West for the unique opportunities they've supplied us with
USG Engineering	www.usgengineering.nl	Sponsoring The Ocean Cleanup's lead engineer.	Bart Monster, Cees Hartman, Remco Boshuis for the great support throughout the feasibility study

Company/ Organisation	Website	Type of assistance	Special thanks to
Companies			
&Associates	www.usgengineering.nl	Website and design.	Ward Nicolaas Suzanne Volder
Websols	www.websols.nl	Web development.	Ralph Klerk
Iemants Steel Constructions	www.iemants.com	Platform engineering.	Rob Godden Patrick Maes
Vuyk Engineering Rotterdam	www.vuykrotterdam.com	Force simulation engineering.	Marc Oele Annemarie Damen
El-Tec	www.el-tec.nl	Electrical engineering.	Ruud Wanders, Remko Leinenga, Herbert Peek
Vryhof Anchors	www.vryhof.com	Mooring engineering.	Senol Ozmutlu Christophe Limouzin
Huisman Equipment	www.huismanequipment.com	Boom engineering.	Joop Roodenburg, Eric Romeijn, Stefan van Ruyven, Sam van der Horst, Emile Arens, Sophie Weusthof
Citigate First Financial	www.citigateff.nl	PR assistance.	Lord Chadlington, Uneke Dekkers, Geert Pielage, Vivian ten Have, Claire Verhagen
Hekkelman Advocaten	www.hekkelman.nl	Legal assistance.	Bavo Konig
Nubis	www.nub.is	Social Media.	Jelle Oskam & team

13.3 DONATIONS

This study has been funded in its entirety though donations and crowd funding.
We would like to thank all 3000 funders in supplying us with the funding needed to perform this feasibility study.

Fiona Campbell, A.	Amy Polzin	Bas Paumen	Catherine Sweere
Joanna Siegla, A.	Anais Leroux	Bas te Grotenhuis	Celestin Bache
A.A.S. Kruit	Anastassia Nefedova	Bas van Rossum	CH Allen
A.H. Rozendaal	Anders Astberg Neuman	Bas Verheul	Charles Hagema
A.J. Meerburg	Andre Piacentini	Ben Hinssen	Charles King
A.J. Rijsoort	Andrea Kollmann	Benjamin Gregory	Charlotte Schell
Aadne Kolbjoernshus	Andrea Ponza	Benjamin Quinto	Chauvin Charles
Aaron Job	Andrea Scholz	Bernadett Parrag	Cheryl Richard
Aaron Wheeler	Andrea Teaggi	Beth Rollison	Chris McWilliam
Acadia Bunn	Andreas Aanonson Normann	Bettina Brunner	Chris Page
Achim Zien	Andreas Kimpfler	BGPC van Baar	Christian Ehnis
Adam Eeuwens	Andrew John Mc Leod	Bimla Chall	Christian Engweiler
Adam Kaye	Andrew Young	Bjorn Bartel	Christian Gayed
Adam Verheyen	Angela Davies	Blake Dishman	Christian Human
Adedayo	Anita Prinsen	Bonnie Campbell	Christian Nerdrum
Adelheid Hansen	Anja Thiele	Boris Morel	Christian Wiegang
Adriana May	Anne Myllyaho	Boudewijn Pasman	Christina Morrell
Adrien Salvo	Anne Philippe	Boudewijn Tjeertes	Christina Sarich
Agnes Zuidam	Anneliese Pratt	Bradley Mc Millan	Christine Fiedler
Aida Gutkauskaite	Annemarie Labree	Bram Engelhard	Christine Gable
Aimar Molero	Annette Stucken Flinterman	Brent Reitze	Christine Lamsvelt
Albert Santing	Anouk Carlier	Brian Heise	Christine Vogeley Luetter
Alberto Coretti	Anton Koschier	Brian Reed	Christoff Snyders
Alejandro Decastro	Anton Mishel	Brigitte Blanken	Christoph Templer
Alessandro Brembati	Antonin Grazia	Brittany Johnstone	Christopher Jones
Alessandro Leoni	April Johnson	Bronwyn Belling	Christopher Rubio
Alex Leydenfrost	Arjan Blok	Bruce Schinkel	Christopher Winterhoff
Alex Meulenbroeks	Arjan Brienen	C. Zwezerijnen	Claire Lochet
Alexander Mascini	Arjen Hoven	C.J.M. van Greunsven	Claire Wallerstein
Alexander Smouha	Arnaud Touchard	C.M. Nelis	Clare Probert
Alexander Whitton	Aroena Nijman	Calvin Mayer	Claudia Bufalari
Alexandra Taylor	Arrigo Tosi	Camille Ballon	Clemens Wais
Alexandre Bugnon	Asdis Valdimarsdottir	Camille Vassart	Cloe Byruck
Alexis Vincent	Ashley Benson	Carlos Toriello	Colby Johnson
Alfred Joly	ATR Bogerd	Caro van der Schueren	Colton Weeks
Alisa Pena	Attila Antal	Carol Masterson	Connor Patrick
Alison Currie	Aude Berliner	Carolina Dahlberg	Cora Cox Matze
Allegra F. Snyder	August Aime van Kammen	Carolyn Corbin	Cristina Calasanz
Allen Johnson	Bapke Mayoh	Carolyn M Blake	D.V. Dwinger
Amanda White	Barbara Kortbeek	Cathelijne Engelvaart	Daniel Goriounov
Amandine Graff	Barbara Marcelis	Catherine Gauthier	Daniel Raffa
Amy Caruso	Bart van Putten	Catherine Julian	Daniel St-Yves

Danielle Frucci	Edward Slaght	Floris Hulsmann	Gwen Steel
Danielle Rock	Eelko Lommers	Frances Beek	H.J.C. Siteur
Daria de Pede	Efrem Terraneo	Frances Stark	H.W. van Oordt
David Bruce	Ehsan Farshid	Francesca Hampton	Hanna Visser
David Corner	Eileen Adams	Francis Stouffs	Hannah Boone
David Gross	Elisabeth Kastin	Francisco Iglesias Leon	Hans Doggen
David Kirshbaum	Elizabeth Spitz	Franck Langevin	Hans Wouters
David Landskov	Elliot Bouchard	Franck Massa	Haro Hollertt
David Pham	Elly Smit	Francois Ihuillery	Harry Eggens
David Pronk	Elsje Nagels	Francois Klein	Harry van Durme
David Rodrigues	Emily Anderson	Frank de la Bey	Heather Howard
David Rylander	Emily Vincent	Frank Gubbi	Heidi Wood
David Wilner	Emma Lord	Franklin Ard	Heloise Thomson
Davide Camisa	Emmanuelle Begon	Frederic Heeren	Hendrik Ahlen
Dawna Venzon	Emmery Cheung	Frederic Peters	Henk van Abeelen
Debbie Spalding	ER de Groot	Frederik Peters	Henning Focks
Delphine	Eric aan de Stegge	Frederik van Zande	Hermien Heveraet
Denise Pendexter	Eric Bauchau	G.C. Thurkow	Holly Johnson
Derek Salvi	Eric Case	Gaby Michels	Hubert Hol
Diana	Eric Darchis	Gareth Browne	Hynek Opolecky
Diana Alvarez Marin	Eric Lambot	Gary DeCarrico	Ian Coggan
Dick van Wielink	Erica Blyther	Gary Jahns	Ianthe Dickhoff
Diederik Van Remoortere	Erik Trudelle	Geert Popelier	Ines Laranjinha
Dieter Camps	Erik van Beek	Georges Braud	Ingolf Christian Ernst
Dieuwertje Ewalts	Erik Versaevel	Gerdahendrike Schokkin	Ingrid Matthys
Dieuwke Ingenegeren	Erik Versaevel	Gert Jan Peeters	Irene Gonzalez
Dominic de Bruijn	Erwan Rabenevanana Man Wai	Giorgio Buonocore	Ivona Cetinic
Dominica Corless	Esther Monks	Gisela Bongardt	J. Renouf
Dominique Verleye	Esther Schoemakers	Glenn Ellis	J.C. Bouwmeester
Doran Gaston	Evangelia Tseki	Greg Tanner	J.C. Vingerling
Dorian Severin-Eudes	Evert Langebeeke	Gregor Golob	J.C.J. Bouwmeester
Douglas Taylor	F.L.J. Waarsenburg	Gregory Sarno	J.J. Schakel
Douwe de Vries	F.P.M. Verhoeven	Gretchen Spletzer	J.M. Dekter
Drs. J.A.L.H. Bloks	Fabio Francisco	Guglielmo Gemignani	J.M. Ricker
E.A. Hoogstrate	Feillais Frederic	Guido Heezen	J.R. Plantinga
E.G. de Lange	Felix Becerra	Guido Schlegel	Jacobien Schreurs
E.J. van Pelt	Fleur Helluin Corblin	Guilhem Bec	Jacqueline Wentink
E.J. Vles	Floor Smit Vos	Guillaume Dache	James Fike
EC Meijer	Florian Cornu	Guy Andre	James Goodwin
Ed Weinberg	Florian Fenkl	Guy Andrea Yerro	James Hutchison
Edward de Vries	Floriane Herrero	Guy Michaud	Jan Christopher Bernhammer
Edward Lewis	Floris Honee	Gwen de Visser	Jan Cirkola

Jan Hanus	John Martens	Kerim Idris	M.C. Spaan
Jan Naveau	John Prigogine	Kim Kingsbury	M.C.L. Kempers
Jan Schoemaker	John Taylor	Kim Langer	M.C.M. Sommeling-Pronk
Jan van de Kamp	Jonas Ringer	Kira Sanders	M.K. Vaartjes
Jan van der Velden	Jonathan Pang	Kirk Chen	M.L. Salmond
Janice Ryan	Jonathan Pujo	Koen Muurling	Maaike Cotterink
Janneke Kimstra	Jonathon Pollard	Kristy Wheeldon	Maaike Joerink
Jantine Bresser	Joop de Kok	Kurt Seematter	Maarten Brons
Jao Pedro Torres	Jorgen Ilstad	L.S. Jongeneel	Maarten Endlich
Jaquelin Pearson	Josepf Pedro Pinto	Lars Lok	Maddison Whitford
Jared Bendifallah	Joseph Fordham	Lars Widmark	Magdalene McCann
Jared Chipkin	Joseph Sharp	Laura Blevins	Mallory Lyman
Jascha Drel	Josje Erkelens	Laurel Maloney	Mandy de Visser
Jason Marsh	Jouni Koso	Lauren Leisk	Mani White
Jasper Brugman	Judit Zila-Oroszlan	Leah Shields	Marc Meyer
Jasper Versteege	Judith Bardoel	Leo Smits	Marc van Thillo
Jean Contamin	Judith Keanzle	Lewis Gersh	Marchien Spier
Jean Francois Morin	Judith Lautner	Liesbeth de Bruyn	Marco Boero
Jean Marie Lepage	Judith Linders	Lincoln Justice	Marco Volker
Jeanne Davidson	Judy E. Rhodes	Linda Slaets	Marcus Briody
Jeffrey Barbee	Judy Galbraith	Linda Zegwaard	Marcus Rebok
Jeffrey Fish	Judy Hollingsworth	Lindy Elliot	Mareike Breitschuh
Jelmer Ter Haar	Julee Johnson	Lionel Moretti	Margaret Finnerty
Jennifer-Jessica Trumino	Julia Rhode	Lisa Boureau	Maria Dobler
Jenny Robb	Julie Dedieu	Lisa Kline	Maria E Wahrenberger
Jeremy Agnew	Julie Gaudin	Lisa Wagener	Maria Madrigal
Jeremy Chan	Julie Kestermans	Live Lomo	Maria Purzner
Jeremy Green	Julien Rabier	Liz StLawrence	Maria Regina Barona Leon
Jeroen Havenaar	Juliet Roth	Liz Wald	Mariana Barbosa
Jerome Glorie	Kara Lacey	Loretta Ramos	Marie Therese Cortina
Jesse Gaucher	Karen Doyle	Luciana Plocki	Marie Villeneuve
Jessi Nabuurs	Karen Yee	Lucie Cosson	Marie-Clair Renneson
Jessica Morales	Karima Charania	Lucie Patrowicz	Marielle Eilers
Jisca Huisman	Karin Hunt	Lucie Vetele	Marije Huis in t Veld
Joachim Wespel	Karin Vatter	Lucien Harteveld	Marijke Hoen
Jodi Ruschin	Kasper Thor	Ludovic Denis	Marijke Pardoel
Joel Assaizky	Katherine Loucks	Ludovic Painchaud Tremblay	Marin van Sprang
Joelle Laplante	Katja van Boxel	Lulamay Craufurd Gormly	Marina de Paula Souza
Jofrey Bellanger	Katrin Maria Kaluza	M Alexander Jurkat	Marion Undusk
Johanna Bloomberg	Katrina Hopkins	M. van der Lee	Marius Acke
Johannes van Dijk	Keith Gordon	M. Vives Batista	Marjan Willemsen
John Mann	Ken Green	M. Weltje Poldervaart	Mark Anderson

Mark Braafhart	Michael Lipinski	Nicholas Schneble	Peter Benedikt von Niebelschatz
Mark McElhaw	Michael Mangelschots	Nicholas Stone	Peter Bielatowicz
Mark Todd	Michael Novello	Nicola Di Gaetano	Peter Green
Mark Todd	Michael Palmer	Nicolas Blanchy	Peter Sitsen
Marko Lukaa	Michael Royston	Nicolas Gonot	Peter Speak
Markus Schulte	Michael Salemink	Niels Nijs	Peter ten Wolde
Marlon Spaans	Michael Tenenbaum	Nienke Beintema	Peter van Bogget
Martijn Arendsen	Michel Bergijk	Niklas Carling	Peter Vouk
Martijn Arendsen	Michele Martin	Niko Wojtynia	Peter Vrambout
Martijn Arendsen	Michelle Sites	Nils Gabriel	Petra Borrmann
Martin Weber	Michiel Erkelens	Nina Aarstrand	Philippe
Martina van Hooreweghe	Miguel Silvestre	Nitesh Hemlani	Phillip Ayres
Martine Reimerink	Mikael Schober	Norina Hammerling	Pierre Alain Geiser
Martinus Doekes	Mikael Teern	Odilia Borchert	Pierre Marie Noterdeame
Mary Ellen Degnan	Miles Cheverton	Oliver Henke	Piet Valkier
Mary Mathias	Minni Mc Master	Oliver Madgett	Pieter van der Marel
Mary Meyer	Miriam Vesma	Olivia Whatley	Pim Clous
Mary Richter	MLEF Bruins Slot	Olivier Dehaybe	Piotr Bielatowicz
Mathias Clement	Molly Watt Stokes	Olivier Grandhenry	PJB Steggerda
Mathias Tholey	Mona van Zuilekom	Olivier Steiner	Pleuntjr Schimmelpennink
Matina Morber	Monica Damele	Onno van Manen	Quentin Janssens
Matthew Parker	Monique Bergmans	Oscar Garcia Bofill	Quinta Mustamu
Matthew Vest	Monique Dontje	Owen Abrey	R. Griek
Matthieu Oldfield	Monique Slot	P.C. Kamp	R. vd den Biggerlaar
Matthijs Al	Muneyuki Kato	P.M.H. van Vloten	R.F. Dronkers
Matthijs de Kievit	Myfanwy Alderson	P.Prins	R.J. Avans en P. Bon
Matti Ahonen	Myfanwy Rowlands	Pablo Muruzabal Lamberti	R.M. Hermans
Maurits Dolmans	Myra Pearse	Pascal Moser	Rachael Hawkey
Maxime Baque	N. Beijer	Patrick Balleur	Rachel Soper
Maxine Ruffles	N.A. Slijkhuis	Patrick de Kok	Rafael Monteiro
MCM Dontje	Nada Gejic	Patrick Fecheyr Lippens	Ralf Hekkenberg
Meadow Meadow	Nadege Hopman	Patrick Healy	Ramona Muntean
Melanie Madon	Nadine Coumou	Patrizia Costa	Ramsey Metcalf
Melanie Roy	Nadine Djeha	Paul Belserene	Rebecca Mutton
Melissa Demmers	Nadine Henry	Paul Bergen	Rebecca Peterson
Melissa Keays	Nadine Michelin	Paul Camus	Remko Stobel
Meredith Rose	Nancy Linneman	Paul Charles	Rene Verbeek
Merry Henderson	Nancy Wiser	Paul Cotton	Rhonda Peterson
Michael Bennett	Naomi Kawase	Paul Giraud	Ricardo Martins
Michael Dorazio	Nathan Baily	Paul Rispens	Richard Kelly
Michael Escobar	Nicholas Hair	Peggy Malmaison	Richard Korebrit
Michael Flowers	Nicholas Neild	Per Fagrell	Richard Moore

Richard Urwin	Sally Hipwood	Stef Smits	Titia Sjenitzer
Richard Voget	Samuel Buyst	Stefaan Galle	Tobias Boonstoppel
Rick Ikkersheim	Sander den Ouden	Steffanie Igel	Tobias Sutor
Rick Westelaken	Sander Dercksen	Stephanie Coulter	Tom Boot
Riikka Oderychev	Sandra de Bruijn	Stephen Harwin Harwin	Tom Jourdan
Riwan Raejon	Sanne Plomp	Stephen Jervey	Tom Kerremans
RJ Schipper	Sara Bishop	Steven Bink	Tom Provo
Rob Dirksen	Sara Hajbane	Steven Heijtel	Tom Scott
Rob Morris	Sarah Beek	Susan Houston	Ton Geurts
Rob Wannyn	Sarah Grenon	Susanna Schultze	Tony Marlow
Robbe Vancayseele	Sarah Lines	Suzanne Eijsbouts	Tricia Graham
Robbert van der Sloot	Sarah Whiteford	SV Perfilyeva	Tyler Jessenberger
Robby Thater	Sayaka Chatani	Sven Willemse	Tyson Schleppe
Robert Byrne	Scheherezade O'Neill	Tahnee Woolf	Ursula Zimmermann
Robin Groenewold	Sebastian Engstrom	Tamara Kelly	Valentina Scollo
Rodrigo Marcon	Sebastian Heuft	Tammy Beaulieu	Valerie Rijckmans
Roel van Eerd	Sebastian Knoerr	Tara Fleming	Veerle Lenaerts
Roeland Maas	Sebastien Audy	Tars van Hoof	Veronica Nessim
Roger Coleman	Sebastien Barbieri	Teja Hudson	Veronique Rotkopf
Rogier Herrebout	Sebastien Cayzac	Teresa Ledesma	Vicki Kable
Roland Everaert	Seppe Cockx	Teresa Rodriguez	Victor Schermer Voest
Roland Preisach	Sergio Martinez Lahidalga	Tero Lehtonen	Vika Jagucanskyte
Roland Wolters	Seth Pullen	Terri Hager	Vincent Massaut
Romaric Tousseyn	Shayna Stott	Tessel Hengeveld	Vincent Thilly
Ronald Ruffles	Shery Cotton	Therese Howell	Visala Hohlbein
Ronald Thorne	Shiri Takacs	Thibaut Guignard	Vitor
Rosa Klitgaard	Shubham Garg	Thierry Kortekaas	Vittorio Prada
Rosemary Gehrig Mills	Signe Westi Henriksen	Thijs Biersteker	Walter Borgstein
Ruben van den Brink	Simon Warwick	Thomas Borghus	Walter Downarowicz
Runar Holen	Simone Willems	Thomas Haack	Warren Mc Allister
Russel Girard	Siu Ling Koo	Thomas Kineshanko	Wart Luscuere
Russel Todd	Sjoerd Bermans	Thomas Moreau	Wendy Marvin
Russell Braun	Skerolf Dickinger	Thomas Mueller	Werner Winkler
Russell Brown	Skylar Bayer	Thomas Pacoureau	Wiebke Siemann
Rutger van Zuidam	Slobodan Milnovic	Thomas Pakenham	Wilco Rietberg
Ruud Lagemann	Sofya Manukyan	Thomas Wahlgren	Wilfried Rymenans
Ruurd Klein Langenhorst	Sol Ines Zunin	Thorge Hiebner	Willem Glasbergen
S. van Leusden	Sonja Fasel	Tibor von Merey	Willem Max
S.L. Wiersma	Sophie Korenhof	Tim Spelmans	William Cisney
S.M. Lensink	Soren B. Daugaard	Tim Tuerlinckx	William MacDonald
S.W.F. Maathuis	Spathis Nikolaos	Tim Verhees	William van Tongeren
Sabrina Greensea	Steef van Oosterhout	Tim Winton Brown	Wim Willems

Winifred Chang

Winnifred Tovey

Wouter Luberti

Yann Bayo

Yannis Doulgeroglou

Yasin Jensen

Yegor Jbanov

Yili Sun

Yona Hummels

Yves Durinck

Yvonne Lefave

Zane Wylie

Zelis Niegaard

Zinaida V Skachinsky

thing we've ever towed with this boat".

- Wiebbe and Wiebbe Anne Bonsink (HEBO Maritiemservice) for the help testing the multi-level trawl

- Richard Bot and Michel Pattiasina (BDO Auditors and Advisors) for preliminary financial advice about Non Profit Organizations in The Netherlands

- Sven Gerhardt, Steven van der Kaaij and Bram Buijs from graphic design agency HOAX for helping us design the feasibility study report and book

- John Bos (Fontijne Grotnes) for helping us with pressing the Ocean Plastic covers of the report.

- Ellese Jobin, Adam Bazadona and Thomas Akey (Cut and Run) for helping us with editing a video of the first phase of the project.

- Ewa Miller and Dave Hodge (Fingermusic) for helping us out with the release event and audiovisual needs

- Japheth Yin (Chongqing Lange Machinery Group Co., Ltd.) for supplying us with quotes.

....and all other individuals, companies and institutes that helped (or offered their help) making this feasibility study possible.

APPENDICES

SLAT, B. • LUSCUERE, W., • HILDERING VAN LITH, E.
DE SONNEVILLE, J.

VERTICAL DISTRIBUTION DATA

JULIA REISSER • ROBBERT ZUIJDERWIJK • BOYAN SLAT
HYKE BRUGMAN

During the two expeditions in the North Atlantic Gyre, a total of 12 trawls were conducted. The available environmental conditions and sample results are listed in Table A1.1. An 'x' indicates a discarded or non-recorded sample.

	EXPEDITION 1			
	Trawl 1	**Trawl 2**	**Trawl 3**	**Trawl 4**
Date	11/18/13	11/19/13	11/19/13	11/20/13
Starting coordinate latitude (deg.min.milli)	N 21°45.89	N 19°56.22	N 19°57.85	N 18°16.59
Starting coordinate longitude(deg.min.milli)	W 64°28.92	W 64°35.93	W 64°35.16	W 64°50.97
Ending coordinate Latitude(deg.min.milli)	N 21°46.89	N 19°58.88	N 19°59.56	N 18°16.49
Ending coordinate Longitude(deg.min.milli)	W 64°28.19	W 64°35.06	W 64°34.96	W 64°49.41
Starting time (UTC)	15:52	11:17	13:37	9:04
Ending time (UTC)	16:52	13:20	15:41	10:07
Trawl duration	1:00 h	1:57 h	1:04 h	1:03 h
Vessel speed (Kts)	06-1.8 Kts	1.3 Kts	1.5Kts	1.5Kts
Vessel speed (ms-1)	0.3-0.9 ms^{-1}	0.7 ms^{-1}	0.8 ms^{-1}	0.8 ms^{-1}
Vessel course	050°T	040°T	035°T	102°T
Wind speed (Kts)	20Kts	6Kts	5Kts	10Kts
Wind speed (ms-1)	10 ms^{-1}	3 ms^{-1}	2,6 ms^{-1}	5 ms^{-1}
Wind direction	040°T	050°T	030°T	97°T
Wave height (ft)	6-9ft.	1-4ft	1-2ft	1ft
Wave height (m)	1.8-2.7 m	0.3-1.2 m	0.3-0.6 m	0.3 m
Flow value difference	6586	8239	2763	1178
Sampled water volume per net	316,13m³	395,47m³	132,62m³	56,54m³
Net 1 total plastic mass [g]	0.0026	0.0013	0.0061	0.001
Net 1 number of plastic particles	8	4	15	1
Net 2 total plastic mass [g]	0.0103	0.0081	0.0298	0
Net 2 number of plastic particles	4	17	25	0
Net 3 total plastic mass [g]	0.0017	0.0003	x	x
Net 3 number of plastic particles	5	2	x	x
Net 4 total plastic mass [g]	0.006	0.0001	0.0005	<0,00005
Net 4 number of plastic particles	4	6	2	1
Net 5 total plastic mass [g]	* 0,0012 (0,0021)	0	x	x
Net 5 number of plastic particles	1 (3)	0	x	x
Net 6 total plastic mass [g]	** 0,0032	0.0016	0	0
Net 6 number of plastic particles	5	4	0	0
Net 7 total plastic mass [g]	0	<0,00005	0.0003	0.0006
Net 7 number of plastic particles	0	1	5	1
Net 8 total plastic mass [g]	<0,00005	0.0007	0.0002	0
Net 8 number of plastic particles	3	1	3	0
Net 9 total plastic mass [g]	x	0.0001	0.0013	x
Net 9 number of plastic particles	x	5	1	x
Net 10 total plastic mass [g]	x	0.0001	0.0006	<0,00005
Net 10 number of plastic particles	x	6	3	1
Net 11 total plastic mass [g]	0.0044	<0,00005	0.0055	0
Net 11 number of plastic particles	7	3	7	0

	EXPEDITION 2			
	Trawl 5	Trawl 6	Trawl 7	Trawl 8
Date	12/21/13	12/22/13	12/23/13	12/24/13
Starting coordinate latitude (deg.min.milli)	N 29°589,592	N 29°753,591	N 29°782,073	N 32°344,079
Starting coordinate longitude(deg.min.milli)	W 61°108,742	W 58°843,688	W 57°109,372	W 57°169,484
Ending coordinate Latitude(deg.min.milli)	N 29°593,498	N 29°732,629	N 29°780,574	N 32°339,993
Ending coordinate Longitude(deg.min.milli)	W 61°079,299	W 58°838,799	W 57°100,461	W 57°153,289
Starting time (UTC)	20:22:34	16:33:54	11:36:50	13:14:54
Ending time (UTC)	21:34:31	17:57:52	12:43:07	14:19:18
Trawl duration	1:14 h	1:25 h	1:07 h	1:05 h
Vessel speed (Kts)	1Kts	1Kts	1Kts	1Kts
Vessel speed (ms-1)	0.5 ms-1	0.5 ms-1	0.5 ms-1	0.5 ms-1
Vessel course	71°T	20°T	338°T	111°T
Wind speed (Kts)	17,5Kts	19Kts	19Kts	8Kts
Wind speed (ms-1)	9 ms-1	10 ms-1	10 ms-1	4 ms-1
Wind direction	354°T	24°T	15°T	42°T
Wave height (ft)	4-5ft	4-5ft	4-5ft	5-6ft
Wave height (m)	1.4 m	1.3 m	1.5 m	1.6
Flow value difference	6224	6040	5222	3241
Sampled water volume per net	298,75m³	289,92m³	250,66m³	155,57m³
Net 1 total plastic mass [g]	x	x	x	0.0002
Net 1 number of plastic particles	x	x	x	1
Net 2 total plastic mass [g]	0.0563	0.152	0	< 0,00005
Net 2 number of plastic particles	1	15	0	1
Net 3 total plastic mass [g]	<0,00005	0.0987	0	0
Net 3 number of plastic particles	1	13	0	0
Net 4 total plastic mass [g]	0.0016	0.0445	x	0.0008
Net 4 number of plastic particles	3	11	x	5
Net 5 total plastic mass [g]	0.0108	0.0585	0.005	0.0012
Net 5 number of plastic particles	6	8	15	4
Net 6 total plastic mass [g]	<0,00005	0.0013	0.0055	0.0012
Net 6 number of plastic particles	1	3	11	3
Net 7 total plastic mass [g]	0.0033	0.0431	0.0009	0
Net 7 number of plastic particles	3	7	3	0
Net 8 total plastic mass [g]	0.0003	0.0731	0.0023	< 0,00005
Net 8 number of plastic particles	4	6	13	3
Net 9 total plastic mass [g]	0.0014	0.0168	0.0033	0.0023
Net 9 number of plastic particles	3	5	15	2
Net 10 total plastic mass [g]	1.3788	0.0113	0.0225	0
Net 10 number of plastic particles	10	25	25	0
Net 11 total plastic mass [g]	0.0006	0.0084	0.0074	0.005
Net 11 number of plastic particles	2	8	19	25

* T1A5 (T1A5(2))

** T1Afliepel

	EXPEDITION 2			
	Trawl 9	**Trawl 10**	**Trawl 11**	**Trawl 12**
Date	12/25/13	27-12-2013	12/28/13	12/29/13
Starting coordinate latitude (deg.min.milli)	N 33°157,226	N 34°005,371	N 34°153,733	N 34°400,515
Starting coordinate longitude(deg.min.milli)	W 54°439,435	W 47°718,114	W 44°325,164	W 39°726,328
Ending coordinate Latitude(deg.min.milli)	N 33°147,064	N 34°014,145	N 34°137,086	N 34°412,154
Ending coordinate Longitude(deg.min.milli)	W 54°448,475	W 47°704,645	W 44°320,812	W 39°731,319
Starting time (UTC)	12:15:37	16:26:32	12:23:55	15:21:05
Ending time (UTC)	13:14:31	17:42:47	13:32:05	16:30:10
Trawl duration	1:01 h	1:16 h	1:09 h	1:09 h
Vessel speed (Kts)	1Kts	1Kts	1Kts	1Kts
Vessel speed (ms-1)	0.5 ms-1	0.5 ms-1	0.5 ms-1	0.5 ms-1
Vessel course	163°T	154°T	130°T	19°T
Wind speed (Kts)	23Kts	18Kts	19Kts	21Kts
Wind speed (ms-1)	12 ms-1	9 ms-1	10 ms-1	11 ms-1
Wind direction	359°T	12°T	38°T	349°T
Wave height (ft)	10-11ft	4-5ft	7-8ft	5-6ft
Wave height (m)	3.3 m	1.5 m	2.4	1.6 m
Flow value difference	6281	5716	6106	4460
Sampled water volume per net	301,49m³	274,37m³	293.09	214.08
Net 1 total plastic mass [g]	x	x	x	x
Net 1 number of plastic particles	x	x	x	x
Net 2 total plastic mass [g]	0.0024	0.0248	0.0001	0.0182
Net 2 number of plastic particles	1	14	8	2
Net 3 total plastic mass [g]	0.0122	0.0083	0.0308	0.0717
Net 3 number of plastic particles	3	6	8	2
Net 4 total plastic mass [g]	0.0132	<0,00005	x	0.0111
Net 4 number of plastic particles	3	4	x	5
Net 5 total plastic mass [g]	0.0045	0	0.0209	0.0184
Net 5 number of plastic particles	4	0	6	6
Net 6 total plastic mass [g]	0	0.0199	0.002	0.0196
Net 6 number of plastic particles	0	7	3	2
Net 7 total plastic mass [g]	0.0024	0.0044	0.0416	0.0144
Net 7 number of plastic particles	1	2	5	6
Net 8 total plastic mass [g]	0.0077	0.0037	<0,00005	0.0034
Net 8 number of plastic particles	5	3	1	1
Net 9 total plastic mass [g]	0.0024	0.0553	x	0.004
Net 9 number of plastic particles	5	9	x	1
Net 10 total plastic mass [g]	0.0112	0.0223	0.0102	<0,00005
Net 10 number of plastic particles	19	5	3	1
Net 11 total plastic mass [g]	0.001	0.0037	x	0.002
Net 11 number of plastic particles	8	2	x	3

MULTILEVEL TRAWL MANUAL

HYKE BRUGMAN • JAN DE SONNEVILLE • BOYAN SLAT

This document outlines the steps performed to assemble a multi-level trawl.

Others are encouraged to use the designs to perform vertical distribution measurements around the world.
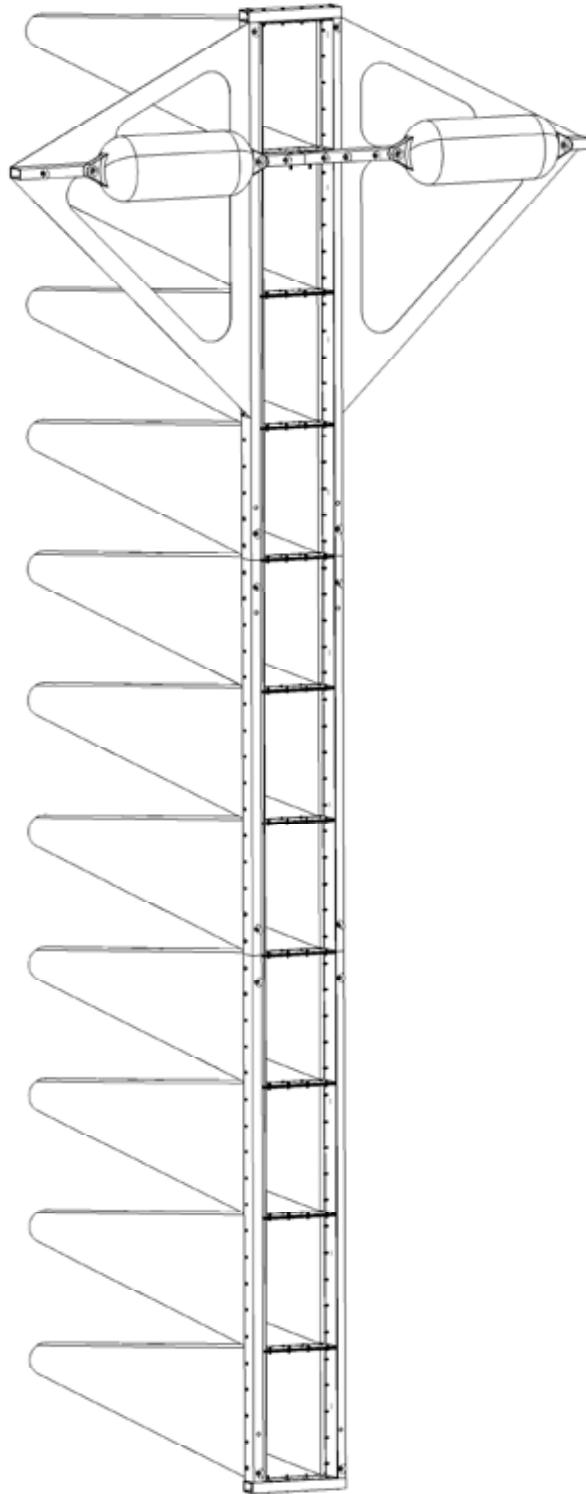
1. PART LIST
1.1. PARTS

TYPE		TYPE	
Half Rectangle 22x		Rubber 11x	
Spacer 9x		Nets 11x	
Bottom Vertical Tube 2x		Middle Vertical Tube 2x	
Top Vertical Tube 2x		Horizontal Tube 2x	
Left Wing 1x		Right Wing 1x	
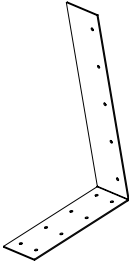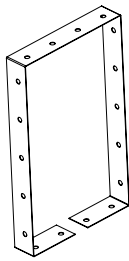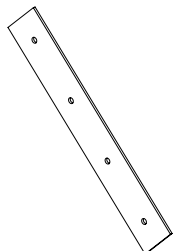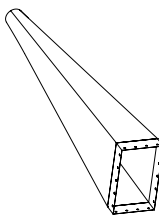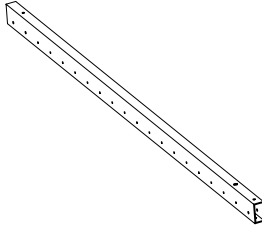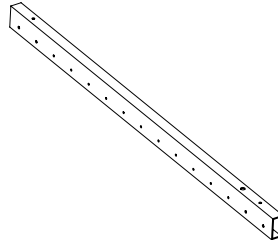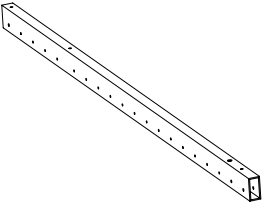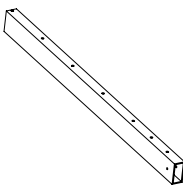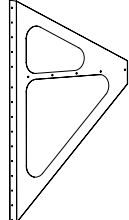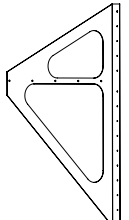
TYPE		TYPE	
Frame Tube 2x		Frame Block 4x	
Between Tube 1x		Horizontal Coupling 1x	
Vertical Coupling 4x		Buoy 2x	
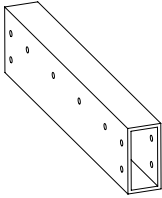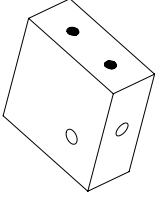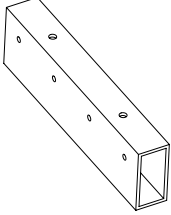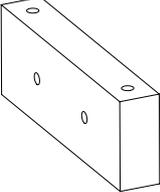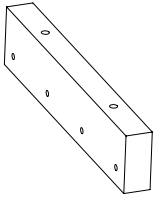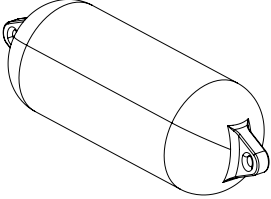
1. PART LIST

2. ASSEMBLY OF COMPONENTS

1.2. CONNECTING PARTS

2.1. OVERVIEW OF COMPONENTS

TYPE		TYPE	
Bolt M6x30 92x		The box 11x	
Bolt M8x60 20x		The frame bottom and top 2x	
Ringbolt M8x200 4x		The horizontal frame 1x	
Bolt M6x60 110x			
Ringbolt M8x120 22x			
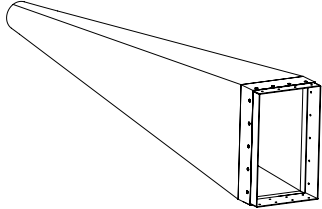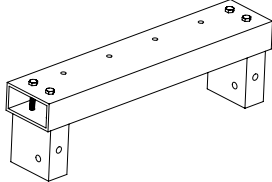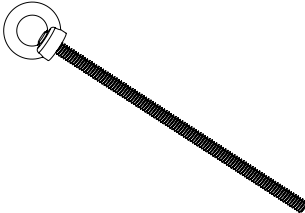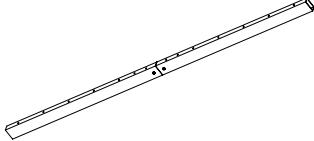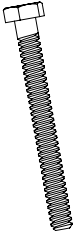
2. ASSEMBLY OF COMPONENTS

2.2. THE BOX

Step 1 Place one half rectangle in position.	
Step 2 1: Place a second half rectangle in position. Move it so it forms a rectangle. 2: Place the rubber in position. Slide it over the rectangle. 3: Place the net in position. Slide it over the rubber.	
Step 3 Repeat step 1 and 2 ten more times. Now eleven boxes are fully assembled.	
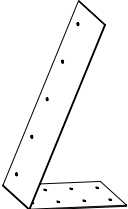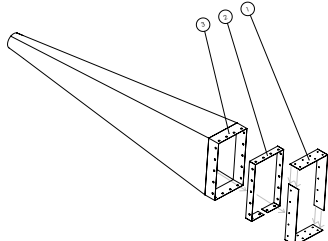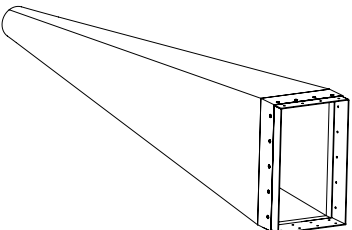
2. ASSEMBLY OF COMPONENTS

2.3. THE BOTTOM AND TOP

Step 1

1: top tube 2: Fasten the two blocks 3: Fasten four M6x60 bolts to the side holes of the bottom tube.
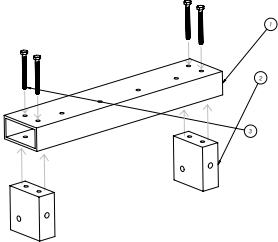
Step 2

Repeat step 1 for the bottom frame. Now the bottom and top frame are fully assembled.
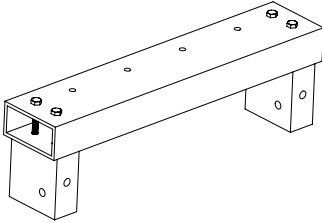
2.4. COMPONENT THE HORIZONTAL FRAME

Step 1

1: The horizontal connector 2: Place the left and right horizontal tube in position as in picture. Slide it over the horizontal connector. 3: Fasten two M8x60 bolts as in the picture .Tighten the nuts.
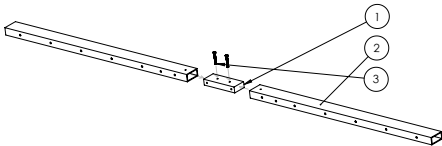
Step 2

The horizontal frame is now fully assembled.

3. FRAME ASSEMBLY

3.1. OVERVIEW OF FRAME ASSEMBLIES

TYPE	
Bottom frame assembly 1x	
Middle frame assembly 1x	
Top frame assembly 1x	
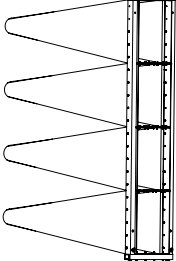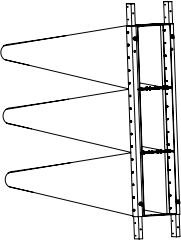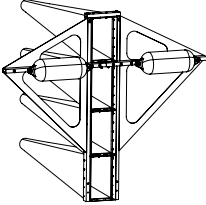
3. FRAME ASSEMBLY

3.2. BOTTOM FRAME ASSEMBLY

Step 1

1: The vertical tube 2: Fasten box 11.

3: Fasten four M6x60 bolts with the bottom vertical tube. Tighten the nuts.
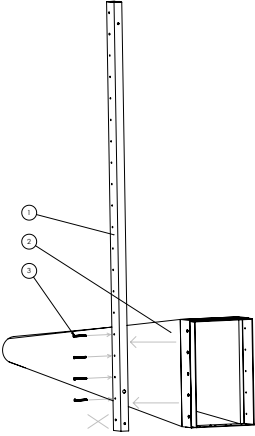
Step 2

1: Place a spacer between the boxes. Fasten it. 2 Fasten box 10. 3: Fasten eight M6x30 bolts to the lower rim of the box. Tighten the nuts.
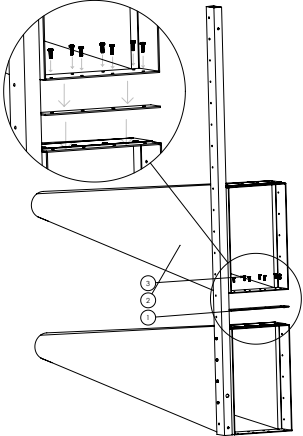
Step 3

1: Fasten five M6x60 bolts to the bottom vertical tube as shown in picture. Tighten the nuts.

3. FRAME ASSEMBLY

3.2. BOTTOM FRAME ASSEMBLY

Step 4

Attach box 9 and 8 as described in step 2 and 3. For box 8: fasten three M6x60 bolts with the bottom vertical tube as shown in picture. Skip the last two holes. Tighten the nuts.
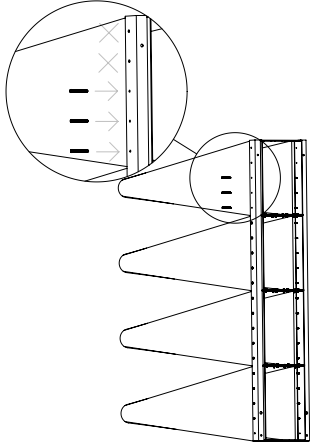
Step 5

1: Fasten a second bottom vertical tube as shown in picture. 2: Fasten seventeen M6x60 bolts to the bottom vertical tube. Skip one hole at the bottom and two at the top. Tighten the nuts.
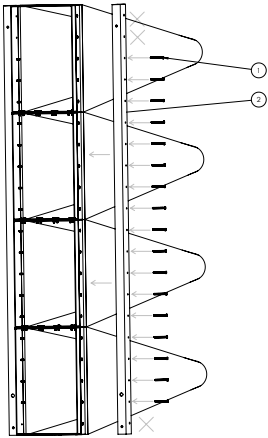
Step 6

1: Place the bottom component in position. Slide the blocks in the bottom vertical tube. 2: Fasten four M6x60 bolts in position as in picture. Tighten the nuts. 3: Fasten two M8x60 bolts as shown in picture. Tighten the nuts.
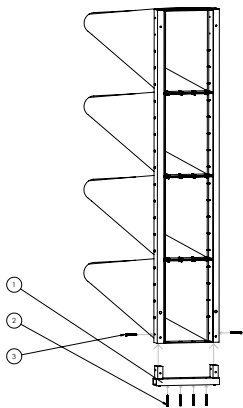
3. FRAME ASSEMBLY

3.2. BOTTOM FRAME ASSEMBLY

| **Step 7**
Fasten two M8x120 ringbolts as shown in picture. Tighten the nuts. | |
| **Step 8**
The bottom frame assembly is now fully assembled. | |
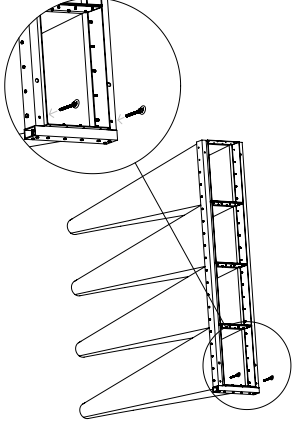
3. FRAME ASSEMBLY

3.3. MIDDLE FRAME ASSEMBLY

Step 9

1: The middle vertical tube 2: Fasten box 7. 3: Fasten three M6x60 bolts to the middle vertical tube as shown in picture. Skip the first two holes. Tighten the nuts.
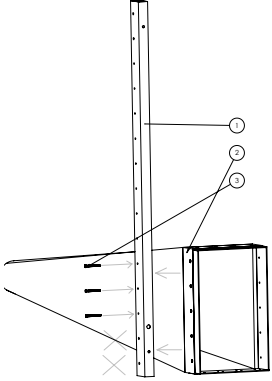
Step 10

Attach box 6 and 5 as described in step 2, 3 and 4. 1: Fasten the second middle vertical tube as shown in picture. 2: Fasten eleven M6x60 bolts to the middle vertical tube. Skip two holes on the bottom and top. Tighten the nuts.
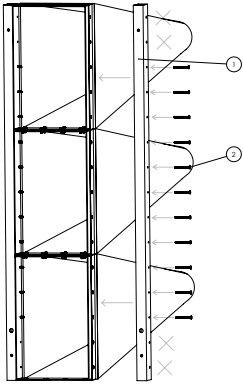
Step 11

1: Place four vertical connectors in position as shown in picture. Slide the connector in the middle vertical tube. 2: Fasten eight M8x60 bolts as shown in picture. Tighten the nuts.
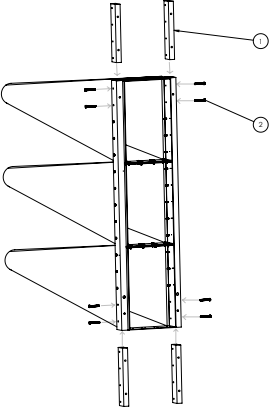
3. FRAME ASSEMBLY

3.3. MIDDLE FRAME ASSEMBLY

Step 12

Fasten four M8x120 ringbolts as shown in picture. Tighten the nuts.
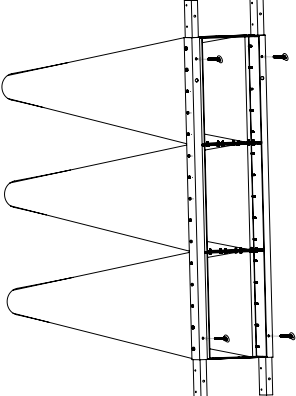
Step 13

The middle frame assembly is now fully assembled.
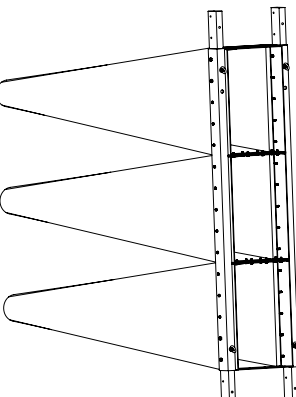
3. FRAME ASSEMBLY

3.4. THE TOP FRAME ASSEMBLY

Step 14

1: The top vertical tube 2: Fasten box 4. 3: Fasten three M6x60 bolts with the middle vertical tube. Skip the first two holes. Tighten the nuts.
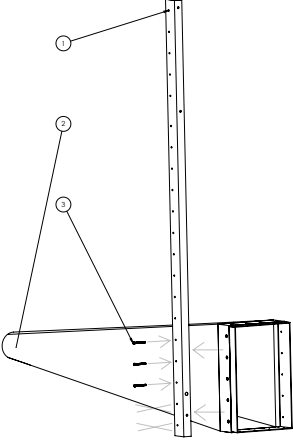
Step 15

Attach box 3 as describes in step 2. 1: Fasten the left wing as shown in picture. Fasten five M6x60 bolts to the left wing. Tighten the nuts.
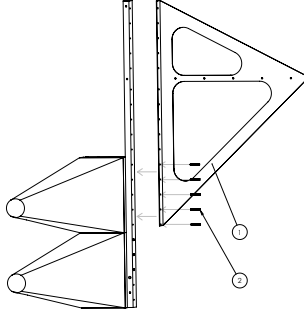
Step 16

Attach box 2 as described in step 2 and 3. 1 between tube 2: Fasten box 1. 3: Fasten four M6x60 bolts as shown in picture. Tighten the nuts.

**3. FRAME ASSEMBLY**

3.4. THE TOP FRAME ASSEMBLY

Step 17

Fasten four M6x60 bolts with the left wing. Skip the last hole. Tighten the nuts.
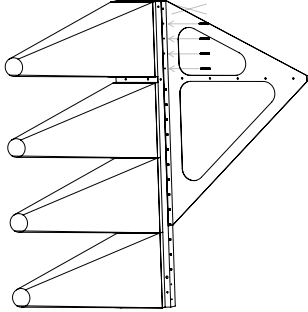
Step 18

1: Fasten Second vertical top tube. 2: Fasten right wing. 3: Fasten seventeen M6x60 bolts as shown in picture. Tighten the nuts.
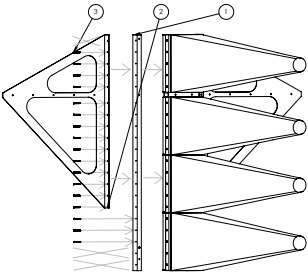
Step 19

Attach the top component as described in step 6. 1: Fasten the horizontal frame as shown in picture. 2: Fasten ten M8x120 ringbolts on outside of the horizontal frame. Tighten the nuts. 3: Fasten four M8x200 ringbolts on the center of the horizontal frame Tighten the nuts.
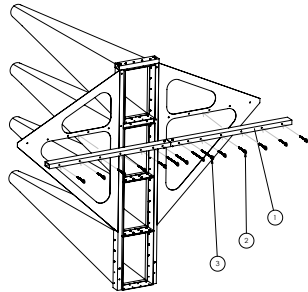
**3. FRAME ASSEMBLY**

3.4. THE TOP FRAME ASSEMBLY

Step 20

1: Fasten two M8x120 ringbolts in position as in picture. Tighten the nuts.
2: Place two buoy in position as in picture. Conect them with the ringbolts.
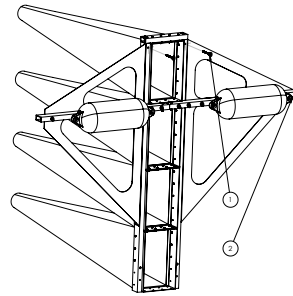
Step 21

The top frame assembly is now fully assembled.

4. THE MULTI-LEVEL TRAWL ASSEMBLY

Step 1 The bottom frame assembly.	
Step 2 1: Place the spacer as shown in picture. Fasten it. 2: Place the middle frame assembly as shown in picture. Slide the two vertical connectors in the bottom vertical tube's. 3: Fasten eight M6x30 bolts as shown in picture. Tighten the nuts. 4: Fasten four M8x60 bolts as in picture. Tighten the nuts.	
Step 3 1: Place the spacer as shown in picture. Fasten it. 2: Place the middle frame assembly as shown in picture. Slide the two vertical connectors in the bottom vertical tubes. 3: Fasten eight M6x30 bolts as shown in picture. Tighten the nuts. 4: Fasten four M8x60 bolts as in picture. Tighten the nuts	
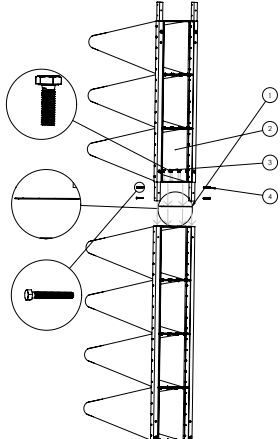
4. THE MULTI-LEVEL TRAWL ASSEMBLY

Step 4 Place four M8x120 ringbolts in position as in picture. Tighten the bolts.	
Step 5 The multi-level trawl in now fully assembled.	
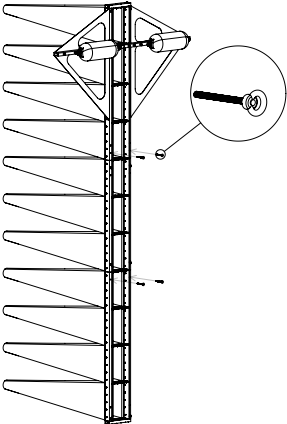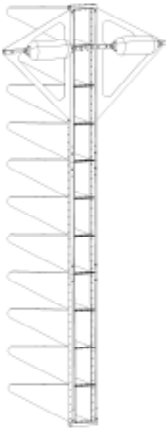
WAVE SCATTER DIAGRAM

SEBASTIAAN VAN ROSSUM

In Chapter 3.5, in order to determine the loads on a floating barrier at 95% conditions (at 30°N, 138°W) a Wave Scatter Diagram sourced from Octopus software was produced. The data itself is based on data from BMT Argoss.

In Table 1, the red area indicates conditions equal to 95.76% of the time. The yellow area equals 99.12%.

Table 1: Percentages of wave occurance

HS/TZ	3	3.5	4	4.5	5	5.5	6	6.5	7	7.5	8	8.5	9	9.5	10	10.5
13.5	0.00%	0.00%	0.00%	0.00%	0.00%	0.00%	0.00%	0.00%	0.00%	0.00%	0.00%	0.00%	0.00%	0.00%	0.00%	0.00%
13	0.00%	0.00%	0.00%	0.00%	0.00%	0.00%	0.00%	0.00%	0.00%	0.00%	0.00%	0.00%	0.00%	0.00%	0.00%	0.00%
12.5	0.00%	0.00%	0.00%	0.00%	0.00%	0.00%	0.00%	0.00%	0.00%	0.00%	0.00%	0.00%	0.00%	0.00%	0.00%	0.00%
12	0.00%	0.00%	0.00%	0.00%	0.00%	0.00%	0.00%	0.00%	0.00%	0.00%	0.00%	0.00%	0.00%	0.00%	0.00%	0.00%
11.5	0.00%	0.00%	0.00%	0.00%	0.00%	0.00%	0.00%	0.00%	0.00%	0.00%	0.00%	0.00%	0.00%	0.00%	0.00%	0.00%
11	0.00%	0.00%	0.00%	0.00%	0.00%	0.00%	0.00%	0.00%	0.00%	0.00%	0.00%	0.00%	0.00%	0.00%	0.00%	0.00%
10.5	0.00%	0.00%	0.00%	0.00%	0.00%	0.00%	0.00%	0.00%	0.00%	0.00%	0.00%	0.00%	0.00%	0.00%	0.00%	0.00%
10	0.00%	0.00%	0.00%	0.00%	0.00%	0.00%	0.00%	0.00%	0.00%	0.00%	0.00%	0.00%	0.00%	0.00%	0.00%	0.00%
9.5	0.00%	0.00%	0.00%	0.00%	0.00%	0.00%	0.00%	0.00%	0.00%	0.00%	0.00%	0.01%	0.01%	0.01%	0.01%	0.01%
9	0.00%	0.00%	0.00%	0.00%	0.00%	0.00%	0.00%	0.00%	0.00%	0.00%	0.01%	0.01%	0.01%	0.02%	0.02%	0.01%
8.5	0.00%	0.00%	0.00%	0.00%	0.00%	0.00%	0.00%	0.00%	0.00%	0.01%	0.01%	0.02%	0.02%	0.03%	0.03%	0.02%
8	0.00%	0.00%	0.00%	0.00%	0.00%	0.00%	0.00%	0.00%	0.00%	0.01%	0.02%	0.03%	0.04%	0.05%	0.04%	0.04%
7.5	0.00%	0.00%	0.00%	0.00%	0.00%	0.00%	0.00%	0.00%	0.01%	0.02%	0.04%	0.06%	0.08%	0.08%	0.07%	0.06%
7	0.00%	0.00%	0.00%	0.00%	0.00%	0.00%	0.00%	0.01%	0.02%	0.04%	0.08%	0.11%	0.12%	0.13%	0.11%	0.09%
6.5	0.00%	0.00%	0.00%	0.00%	0.00%	0.00%	0.00%	0.01%	0.04%	0.08%	0.13%	0.18%	0.20%	0.19%	0.17%	0.13%
6	0.00%	0.00%	0.00%	0.00%	0.00%	0.00%	0.01%	0.03%	0.07%	0.14%	0.22%	0.28%	0.30%	0.29%	0.24%	0.18%
5.5	0.00%	0.00%	0.00%	0.00%	0.00%	0.00%	0.02%	0.05%	0.13%	0.24%	0.35%	0.43%	0.45%	0.41%	0.34%	0.25%
5	0.00%	0.00%	0.00%	0.00%	0.00%	0.01%	0.03%	0.10%	0.22%	0.39%	0.54%	0.63%	0.63%	0.56%	0.44%	0.32%
4.5	0.00%	0.00%	0.00%	0.00%	0.00%	0.01%	0.06%	0.18%	0.37%	0.61%	0.80%	0.89%	0.86%	0.73%	0.56%	0.39%
4	0.00%	0.00%	0.00%	0.00%	0.00%	0.03%	0.11%	0.30%	0.59%	0.90%	1.13%	1.19%	1.10%	0.90%	0.66%	0.45%
3.5	0.00%	0.00%	0.00%	0.00%	0.01%	0.06%	0.21%	0.50%	0.90%	1.28%	1.51%	1.51%	1.32%	1.04%	0.74%	0.49%
3	0.00%	0.00%	0.00%	0.00%	0.02%	0.12%	0.36%	0.79%	1.30%	1.72%	1.89%	1.78%	1.48%	1.11%	0.76%	0.48%
2.5	0.00%	0.00%	0.00%	0.01%	0.05%	0.22%	0.60%	1.17%	1.77%	2.15%	2.20%	1.94%	1.53%	1.09%	0.71%	0.43%
2	0.00%	0.00%	0.00%	0.02%	0.11%	0.39%	0.94%	1.63%	2.21%	2.45%	2.31%	1.90%	1.40%	0.94%	0.58%	0.34%
1.5	0.00%	0.00%	0.00%	0.05%	0.22%	0.67%	1.36%	2.06%	2.48%	2.47%	2.11%	1.59%	1.08%	0.67%	0.39%	0.21%
1	0.00%	0.00%	0.01%	0.04%	0.15%	0.35%	0.59%	0.75%	0.77%	0.67%	0.50%	0.34%	0.21%	0.12%	0.06%	0.03%

11	11.5	12	12.5	13	13.5	14	14.5	15	15.5	16	16.5	17	17.5
0.00%	0.00%	0.00%	0.00%	0.00%	0.00%	0.00%	0.00%	0.00%	0.00%	0.00%	0.00%	0.00%	0.00%
0.00%	0.00%	0.00%	0.00%	0.00%	0.00%	0.00%	0.00%	0.00%	0.00%	0.00%	0.00%	0.00%	0.00%
0.00%	0.00%	0.00%	0.00%	0.00%	0.00%	0.00%	0.00%	0.00%	0.00%	0.00%	0.00%	0.00%	0.00%
0.00%	0.00%	0.00%	0.00%	0.00%	0.00%	0.00%	0.00%	0.00%	0.00%	0.00%	0.00%	0.00%	0.00%
0.00%	0.00%	0.00%	0.00%	0.00%	0.00%	0.00%	0.00%	0.00%	0.00%	0.00%	0.00%	0.00%	0.00%
0.00%	0.00%	0.00%	0.00%	0.00%	0.00%	0.00%	0.00%	0.00%	0.00%	0.00%	0.00%	0.00%	0.00%
0.00%	0.00%	0.00%	0.00%	0.00%	0.00%	0.00%	0.00%	0.00%	0.00%	0.00%	0.00%	0.00%	0.00%
0.00%	0.00%	0.00%	0.00%	0.00%	0.00%	0.00%	0.00%	0.00%	0.00%	0.00%	0.00%	0.00%	0.00%
0.01%	0.00%	0.00%	0.00%	0.00%	0.00%	0.00%	0.00%	0.00%	0.00%	0.00%	0.00%	0.00%	0.00%
0.01%	0.01%	0.01%	0.00%	0.00%	0.00%	0.00%	0.00%	0.00%	0.00%	0.00%	0.00%	0.00%	0.00%
0.02%	0.01%	0.01%	0.01%	0.00%	0.00%	0.00%	0.00%	0.00%	0.00%	0.00%	0.00%	0.00%	0.00%
0.03%	0.02%	0.01%	0.01%	0.00%	0.00%	0.00%	0.00%	0.00%	0.00%	0.00%	0.00%	0.00%	0.00%
0.04%	0.03%	0.02%	0.01%	0.01%	0.00%	0.00%	0.00%	0.00%	0.00%	0.00%	0.00%	0.00%	0.00%
0.07%	0.04%	0.03%	0.02%	0.01%	0.00%	0.00%	0.00%	0.00%	0.00%	0.00%	0.00%	0.00%	0.00%
0.09%	0.06%	0.04%	0.02%	0.01%	0.01%	0.00%	0.00%	0.00%	0.00%	0.00%	0.00%	0.00%	0.00%
0.13%	0.08%	0.05%	0.03%	0.02%	0.01%	0.00%	0.00%	0.00%	0.00%	0.00%	0.00%	0.00%	0.00%
0.17%	0.11%	0.06%	0.04%	0.02%	0.01%	0.01%	0.00%	0.00%	0.00%	0.00%	0.00%	0.00%	0.00%
0.21%	0.13%	0.08%	0.04%	0.02%	0.01%	0.01%	0.00%	0.00%	0.00%	0.00%	0.00%	0.00%	0.00%
0.25%	0.16%	0.09%	0.05%	0.03%	0.01%	0.01%	0.00%	0.00%	0.00%	0.00%	0.00%	0.00%	0.00%
0.29%	0.17%	0.10%	0.05%	0.03%	0.01%	0.01%	0.00%	0.00%	0.00%	0.00%	0.00%	0.00%	0.00%
0.30%	0.17%	0.10%	0.05%	0.03%	0.01%	0.01%	0.00%	0.00%	0.00%	0.00%	0.00%	0.00%	0.00%
0.29%	0.16%	0.09%	0.05%	0.02%	0.01%	0.01%	0.00%	0.00%	0.00%	0.00%	0.00%	0.00%	0.00%
0.25%	0.13%	0.07%	0.04%	0.02%	0.01%	0.00%	0.00%	0.00%	0.00%	0.00%	0.00%	0.00%	0.00%
0.18%	0.10%	0.05%	0.02%	0.01%	0.01%	0.00%	0.00%	0.00%	0.00%	0.00%	0.00%	0.00%	0.00%
0.11%	0.05%	0.03%	0.01%	0.01%	0.00%	0.00%	0.00%	0.00%	0.00%	0.00%	0.00%	0.00%	0.00%
0.01%	0.01%	0.00%	0.00%	0.00%	0.00%	0.00%	0.00%	0.00%	0.00%	0.00%	0.00%	0.00%	0.00%

ORCAFLEX MODEL PARAMETERS

JOOST DE HAAN • SEBASTIAAN VAN ROSSUM

This section acts as reference, indicating the used parameter values during Orcaflex simulations used in section 3.5.

4.1 GENERAL MODEL PROPERTIES

The axes:
- Z – direction is pointing vertical upwards
- Y – direction is pointing horizontal in the boom plane
- X – direction is pointing horizontal and normal to the boom

The general data of the model is as follows.

For the static analyses:
- Tolerance: 10^{-6}
- Min damping: 2.0
- Max damping: 80

For the dynamic analyses:
- Simulation build up from -250 – 0 s.
- Simulation time of 5,000 s.
- Time step of 0.01 s.

The rest of the data are left at their default values.

4.2 ENVIRONMENTAL MODEL PROPERTIES

- Sea surface: 0 m
- Kinematic Viscosity: $1.35*10^{-6}$ kPa·s
- Temperature: 10 °C
- Sea density: 1.025 t/m³
- Seabed: flat and at -100 m
- Current: 0.15 m/s normal to the boom

The waves have the following properties (used in section 3.5.2):

- Angle with respect to normal direction: 15 degrees
- Significant wave height: 5.5 m
- Mean wave period: 7.5 s
- Wave type: JONSWAP
- Number of wave directions: 5
- Spreading of wave directions: $\cos^{24}$*
- Spectral parameters: automatic
- Wave components: 40 per direction and a relative frequency range from 0.5 to 10.0

*The spreading function and the resulting wave direction are indicated by respectively the line and the dots in the Figure A4.1 below. This is the default spreading function in Orcaflex and it resulted in a more realistic sea state where waves come from several directions. In this figure, the normal direction is 90°.
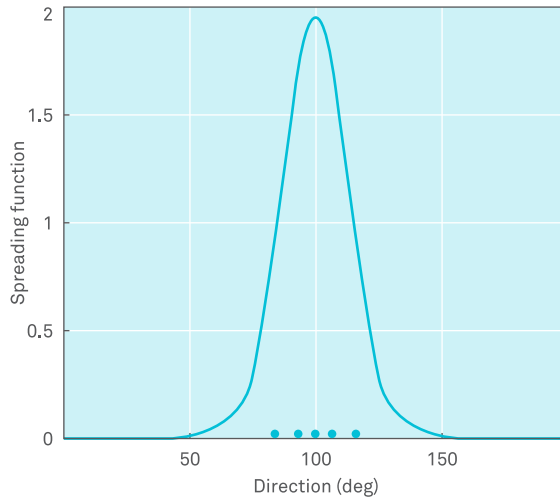
Figure A4.1 Wave spreading

Figure A4.2 Steel boom setup

STEEL SECTIONS

The boom consists of a total of 81 steel sections. The steel sections are 7.50 m long and with infinite connection stiffness connected to the links. Because the links have a relatively low stiffness compared to the connection, strains inside the connection are negligible compared to strains in the links. The connection stiffness can therefore be infinite in the model.

The steel sections have the following properties, based on the properties Orcaflex provides for a homogeneous steel pipe:

• Outer diameter: 1.55 m
• Inner diameter: 1.50 m
• Mass per unit length: 0.940 t/m
• Bending stiffness: $7.38*10^6$ kNm²
• Axial stiffness: $25.4*10^6$ kN
• Poisson ratio: 0.293
• Torsional stiffness: $5.71*10^6$ kNm²
• Drag Coefficient: 1.2 (Axial: 0.008)
• Number of segments: 1

LINKS BETWEEN STEEL SECTIONS

There are a total of 82 links. The links are 0.5 m long. The links have the following properties, based on the properties Orcaflex gives to a homogeneous pipe that consists of a material with a density of 1.1 t/m³ and a Young's modulus of 700 kPa.

• Outer diameter: 1.55 m
• Inner diameter: 1.35 m
• Mass per unit length: 0.501 t/m
• Bending stiffness: 84.2 kNm²
• Axial stiffness: 319 kN
• Poisson ratio: 0.50
• Torsional stiffness: 56 kNm²
• Drag Coefficient: 1.2 (Axial 0.008)
• Number of segments: 1

Density and Young's modulus for the links were based on neoprene properties (Materials Data Book, 2003).
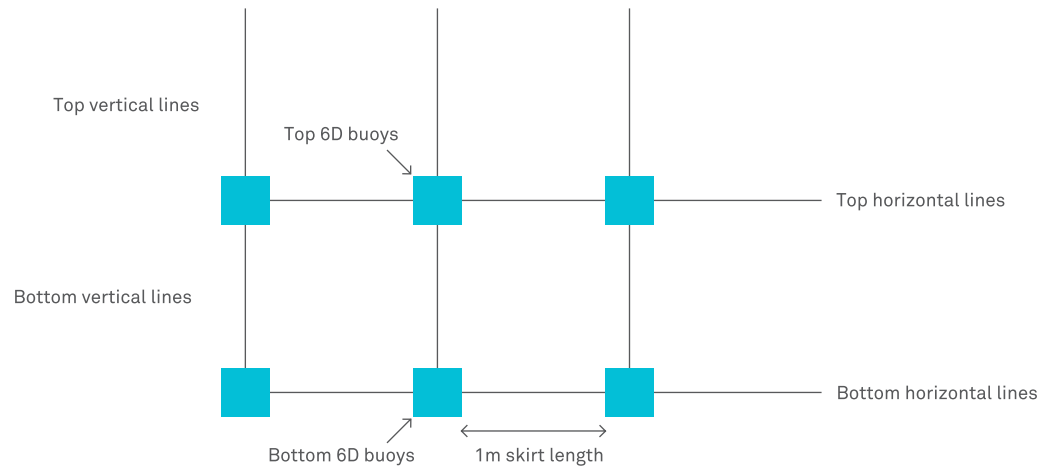
Figure A4.3 Setup of 1 m skirt length

CONNECTIONS BETWEEN LINKS AND STEEL SECTIONS

The steel sections and links are connected to each other through 6D Buoys. There are a total of 162 connections; in addition, both boom ends have an end buoy. The used connection buoys have the following properties:

- Mass: 0.694 t
- Mass moment of inertia: 0.01 t*m²
- Volume: $1.0 * 10^{-3}$ m³
- Height: 1 m
- Center of gravity: -0.1 m

The mass is based on a 0.05 m thick steel plate that would close off each section. The volume and mass moment of inertia are negligible because the steel sections have much larger dimensions.

Height is left as default as this only has an effect on the buoyancy forces in the model, which are negligible with the negligible volume. The center of gravity is placed underneath the center because the buoys tended to turn around their axis during static iterations for no apparent reason.

The end buoys are needed to prevent the end of the boom to sink due to the submerged weight of the mooring lines. The used end buoys have the following properties:

- Mass: 1.0 t
- Mass moment of inertia: 0.610 t*m²
- Volume: 7 m³
- Height: 1.91 m
- Center of gravity: -0.1 m
- Drag area: 3.66 m²
- Drag coefficient: 1.5

The mass is left at default; the buoy has been given a mass moment of inertia and drag area based on its mass and dimensions. The drag coefficient is set to 1.5.

MODELING OF THE SKIRT IN THE STEEL BOOM MODEL

Orcaflex does not support calculations for flat shapes, so the skirt needs to be modelled by means of lines. This is successfully done by creating an array of lines that are connected to each other through 6D Buoys, as is also done with the links and steel sections.

ARRAY OF LINES

The skirt is hanging from the boom. Each meter of skirt is build up by four lines as shown in Figure A4.3.
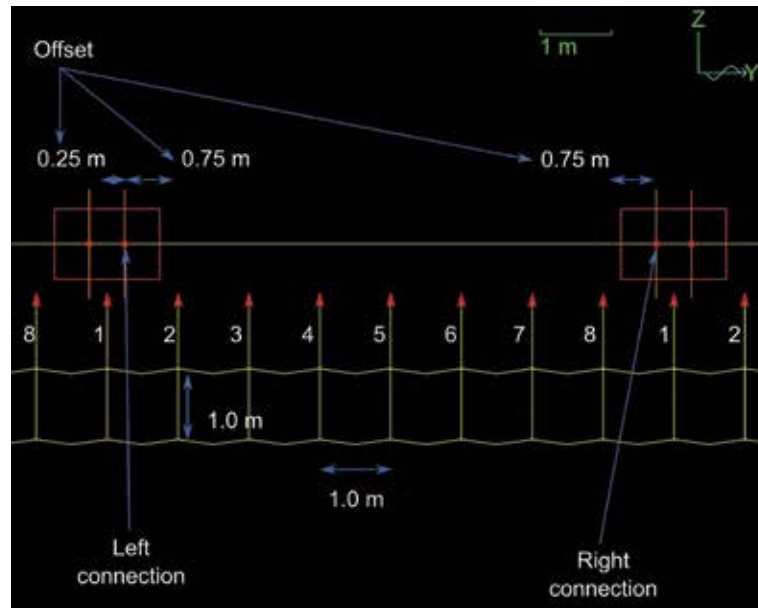
Figure A4.4 Skirt line-up

All lines have a vertical offset of 0.75 m below their connection point (-0.75 m in z direction). The lines are numbered from 1 to 8 in Figure A4.4. Lines 1 to 4 are connected to the left connection and lines 5 to 8 are connected to the right connection.

Lines 1 to 4 are connected with a horizontal offset (in y-direction) of respectively -0.25 m, 0.75 m, 1.75 m and 2.75 m with respect to the left connection point. Lines 5 to 8 are connected with a horizontal offset (in y-direction) of respectively -3.75 m, -2.75 m, -1.75 m and -0.75 m with respect to the right connection point.

By applying the lines in this way beneath each section of the boom, it is possible to get a continuous array of lines for the skirt. The possibility of connecting the lines to 6D Buoys with an offset reduces the calculation time significantly in comparison to placing a 6D Buoy for every line that needs to be connected to the boom.

It is possible to do this because the steel sections themselves are so rigid that no important relative displacements will take place between the top of the vertical lines and the point on the steel section where they should actually be connected to.

The lines have the following properties (as determined from tests done to optimize ballast and skirt thickness for further simulations). See also subchapter 3.5

- Length: 1.0 m
- Diameter: $5.0 * 10^{-3}$ m
- Mass per unit length: $2.9 * 10^{-3}$ t/m
- Bending stiffness: 0.292 kNm²
- Axial stiffness: 3.5 kN
- Poisson ratio: 0.50
- Torsional stiffness: 10 kNm²
- X drag coefficient: 0.1 (the x direction of the lines is 00 defined in the skirt plane, perpendicular to the line)
- Y drag coefficient: 1.2 (the y direction of the lines is defined normal to the skirt plane, perpendicular to the line)
- Z drag coefficient: 0.1 (the z direction is the axial direction of a line)
- Drag diameter: 0.6 m
- Added mass coefficients: 0.01 in x and z direction; 1.0 in y direction
- Number of segments: 2

Due to the facts that each meter of skirt is modelled by 4 lines, and each of those lines has a drag diameter of 0.6 m, the resulting surface area of the skirt for drag purposes will be 2.4 m²/m length.

CONNECTION BUOYS
Underneath each steel section, there are 8 top 6D Buoys and 8 bottom 6D Buoys at the intersections of the top respectively bottom lines. They connect the skirt lines to each other and are not visible in Figure A4.4. A detailed view is shown however, in Figure A4.3.

The top buoys have the following properties:
- Mass: $1.0*10^{-3}$ t
- Height: 1 m

The bottom buoys have the following properties (as determined from tests done to optimize ballast and skirt thickness for further simulations). This is done in subchapter 3.5:
- Mass: 0.05 t
- Mass moment of inertia: $0.29*10^{-3}$ t*m²
- Volume: $6.4*10^{-3}$ m³
- Height: 0.185 m

4.4 MODELING OF THE NEOPRENE BOOM
This model is build up out of 2 parts: neoprene sections and the connections between those sections.

NEOPRENE SECTIONS
The neoprene boom consists of a total of 96 neoprene sections of 1 m long. Each section is connected to the next with infinite bending stiffness. In this way a continuous neoprene tube is modelled. Based on the links in the steel boom model the properties of the neoprene sections are given by:

- Outer diameter: 1.55 m
- Inner diameter: 1.35 m
- Mass per unit length: 0.750 t/m
- Bending stiffness: 170 kNm²
- Axial stiffness: 825 kN
- Poisson ratio: 0.50
- Torsional stiffness: 114 kNm²
- Drag Coefficient: 1.2 (Axial: 0.008)

To create more stability in the model, the stiffness is based upon neoprene sections with 0.3 m wall thickness (instead of 0.1 m).

The mass is here defined so that the waterline is at nearly the same height as the centreline of the neoprene sections in a static situation. This is because OrcaFlex gives the best estimate for the draft of floating tubular sections when their centreline is near the waterline.

CONNECTION BETWEEN NEOPRENE SECTIONS
The neoprene sections are connected to each other through 6D Buoys. There are a total of 95 connections; in addition, both boom ends have an end buoy. The used connection buoys have the following properties:

- Mass: $1.0*10^{-3}$ t
- Mass moment of inertia: 0.01 t*m²
- Volume: $1.0*10^{-3}$ m³
- Height: 1 m
- Center of gravity: -0.1 m

The mass of the connection buoys is reduced to a negligible value in this model because the connections do not have any physical meaning in the flexible boom. They are present however, to be able to connect the skirt to the neoprene sections.

MODELING OF THE SKIRT IN THE NEOPRENE BOOM MODEL

ARRAY OF LINES
In the flexible boom model the skirt is defined in the same way and has the same properties as for the steel boom, with one exception.

Each vertical top line now has its own buoy between the boom sections to connect to, as can be seen in the Figure A4.5 below. This is instead of the offsets to a buoy as described in chapter 4.2, section "Array of Lines" (see above).
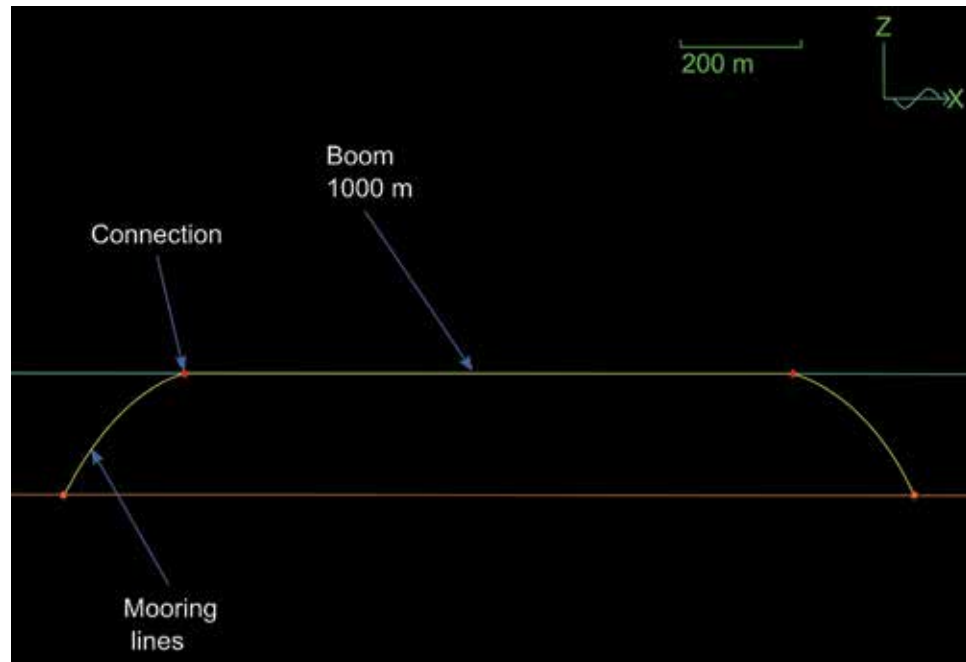
Figure A4.6 Mooring in wave climate model

The reason is that the flexible boom does not have the rigidity of the steel boom and connecting the vertical lines with offsets to a point several meters away will create relative displacements between the boom and the top of the vertical line at that point which cannot be neglected. Disadvantage is that this also results in longer calculation times per stretching meter of boom, because the segmentation is greater and more buoys are present.

CONNECTION BUOYS

The connection buoys for the flexible boom are as described in the previous section A4.3, paragraph Connection buoys.

A4.5 SEA STATE MODEL

Because the boom needs to be simulated in a lot of different wave climates, a very simple model has been created from 3 lines. One line models the boom and the other 2 attach the boom to the sea floor.

GENERAL MODEL PROPERTIES

The general data of the model is as follows

For the dynamic analyses:
- Simulation build up from -50 – 0 s.
- Simulation time of 500 s.
- Time step of 0.1 s.

MODELING OF THE MOORING

For this model the mooring is modelled by 1 line on each side of the boom, instead of 3. Only the mooring lines parallel to the boom are kept. This can be seen in Figure A4.6.

The mooring lines are fixed at the bottom at a horizontal distance of 200 m (instead of 100 m in the main model) from the boom end. The depth of the sea in this model is 200 m (instead of 100 m in the main model), therefore the vertical distance between anchor point and boom end is 200 m. The mooring lines are 290 m long.

The mooring lines have the following properties, based on the properties Orcaflex gives to a Polypropylene (8-strand Multiplair) rope with a nominal diameter of 0.050 m:

- Diameter: 0.040 m
- Mass per unit length: $1.1*10^{-3}$ t/m
- Axial Stiffness: 2,650 kN
- Poisson Ratio: 0.50
- Torsional Stiffness: 80.0 kNm²
- Drag Coefficients: 1.2 (Axial: 0.008)

Due to this change of mooring line, it is not necessary to have a buoyant buoy to compensate for the submerged weight of it because this line has a lower density than water.

MODELING OF THE BOOM

For these calculations it is chosen to have a boom defined by a 1,000 m long line between the end buoys as can be seen in Figure A4.6. It has the following properties, based on the properties Orcaflex gives to a homogeneous pipe that consists of a material with a density of 1.23 t/m³ and a Young's modulus of 700 kPa:

- Outer diameter: 1.5 m
- Inner diameter: 1.4 m
- Mass per unit length: 0.280 t/m
- Bending stiffness: 42.0 kNm²
- Axial stiffness: 159 kN
- Poisson ratio: 0.50
- Torsional stiffness: 28.0 kNm²
- Drag Coefficient: 1.2 (Axial: 0.008)
- Drag diameter: 3 m
- Number of segments: 1,000
- Contents: uniformly filled with a density of 0.407 t/m³

End buoys are present only to connect the boom to the mooring lines, they have negligible properties. The boom and the mooring are connected to each other through these buoys without any connection stiffness.

The drag diameter is set at 3 m as an estimate to compensate for the fact that the skirt is not present in this model. Later, it was found that this sort of simplification requires an even higher drag diameter/drag coefficient (Chapter A4.6). This is not as crucial for the results in this chapter as it will just give an indication of the difference between wave climates.

The contents are set to 0.407 t/m³ in order to let the boom center line to be at the same height as the water line.

MODELING OF THE SKIRT

No skirt was modelled for this purpose.

A4.6 ADJUSTMENTS FOR SKIRT AND BALLAST WEIGHT OPTIMIZATION

In order to be able to model several variables, the model was simplified. Only the adjusted model properties will be shown, the rest is as described in chapter A4.3.

GENERAL

The general data of the model is changed to the following:
- Simulation build up from -250 – 0 s.
- Simulation time of 10,800 s.
- Time step of 0.1 s.

The shortest simulation became unstable at 454.7 s while the longest simulation lasted for the full simulation period.

ENVIRONMENT

The environmental data of the model is changed to the following:

- Significant wave height: 4 m
- Mean wave period 6.5 s

A less severe wave climate is chosen to come to a longer stable simulation time for the in the model less stable combinations of skirt and ballast.

SKIRT

The skirt is here only applied to the middle 6 sections of the boom to save calculation time and to be able to simulate more varieties of properties. The variable properties are those of the lines and the bottom buoys. All combinations of the following properties have been modelled.

The lines forming the skirt can have the following properties:
- Diameter: $5.0*10^{-3}$ m
- Mass: 0.0029 t/m
- Bending stiffness: 0.292 kNm²
- Axial stiffness: 3.5 kN

Or:
- Diameter: $50*10^{-3}$ m
- Mass: 0.019 t/m
- Bending stiffness: 2.920 kNm²
- Axial stiffness: 35 kN

While the bottom buoys can have the following properties:
- Mass: 0.01 t
- Mass moment of inertia: $0.020*10^{-3}$ tm²
- Volume: $1.3*10^{-3}$ m³
- Height: 0.108 m

Or:
- Mass: 0.05 t
- Mass moment of inertia: $0.29*10^{-3}$ tm²
- Volume: $6.4*10^{-3}$ m³
- Height: 0.185 m

Or:
- Mass: 0.1 t
- Mass moment of inertia: $0.91*10^{-3}$ tm²
- Volume: $13*10^{-3}$ m³
- Height: 0.234 m

The line diameter is based on the skirt thickness. One skirt, which will be called the heavy skirt from here on, has a thickness of $50*10^{-3}$ m. The other skirt, which will be called the light skirt, has a thickness of $5.0*10^{-3}$ m which is 10 times thinner in order to see clear differences between the results.

The mass is based on the skirt thickness too. With a thickness of $5.0*10^{-3}$ m the skirt should weigh about .

As may be noticed, a density of 1.16 t/m³ is used here instead of the before used density of 1.1 t/m³ for the neoprene connections between the steel sections.

It should probably be emphasized that the used materials are not fully defined and will not be defined by this model; therefore a lot of material properties may change in the final design of the boom and these slight differences that got into the model during creation should not be important.

However, it is important to know which properties are used within the model exactly in order to determine whether using another material will have significant effects on the results of the model.

Each meter of skirt is defined by 4 lines as explained in chapter A4.3, section "Array of Lines". So the mass of the lines in the light skirt should be 0.0116/4 = $2.9*10^{-3}$ t/m while the mass of the lines in the heavy skirt should be $10 * 2.9 *10^{-3} = 29*10^{-3}$ t/m. To enhance the visibility of the effects of adding ballast to the model, this mass for the lines in the heavy skirt is reduced to $19*10^{-3}$ t/m.

The bending stiffness is chosen in such a way that the lines do not bend too much in the plane of the skirt, which would create instabilities in the model.

Top 6D buoys

Height vertical lines

Height horizontal lines
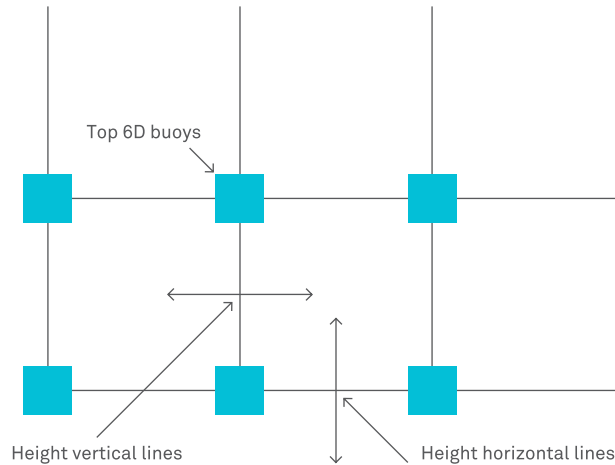
Figure A4.7 Skirt line height

It is defined by the EI each line should represent in that plane: $E * t * h^3/12 = 700 * 0.005 * 1^3/12 = 0.292$ kNm².

A line represents a height for the bending stiffness of 1 m because they are separated in a grid of 1 m and thus each line is a beam with a height of 1 m (as defined in Figure A4.7) and a width (thickness of skirt) of 0.005 m. The heavy skirt has 10 times this width and thus has an EI of 2.92 kNm².

Normal to the skirt plane the light skirt should have an EI of $E * 1 * t^3/12 = 700 * 0.005^3/12 = 7.29 * 10^{-6}$ kNm².

The EI of the heavy skirt should then be $700 * 0.05^3/12 = 7.29 * 10^{-3}$ kNm² .

The lower stiffness in normal direction is not integrated into the model as it would still need to be applied to the lines. When a line has a weak and a strong direction, it will just turn around its axis until the force acts on its weak direction. This creates unstable models and thus is not applied.

Because of the hinged connections between skirt and boom, it is possible for the skirt to have lateral movements relative to the boom. These movements have been found realistic from observations in the model. The difference in skirt movements between reality and the model due to the high estimate of the stiffness in normal direction is therefore assumed to remain small.

The axial stiffness of the skirt is also concentrated in the lines in the same way. So each line has an axial stiffness of $E * A = 700 * 1 * 0.005 = 3.5$ kN in the light skirt and $3.5 * 10 = 35$ kN in the heavy skirt.

Based on small model tests beforehand, 3 ballast masses have been chosen for comparison. A mass of 10 kg/m, another of 50 kg/m and one of 100 kg/m, the mass is applied to the bottom 6D Buoys in the skirt as they are introduced in chapter A4.3.

In this way they are concentrated masses at the points where the skirt axial stiffness is also concentrated. Their volume is linked to the density of steel of 7,850 kg/m³ through the formula:

$V = m/p = 50/1,850 = 6.37 * 10^{-3}$ m³.

For the height they are assumed as cubic and thus the height (and length of the sides) would be:

$h = \sqrt[3]{V} = \sqrt[3]{(6.37 * 10^{-3})} = 0.185$ m.

With these values, a mass moment of inertia of $(2*h^2*m)/12 = (2*0.185^2*0.05)/12 = 0.29 * 10^{-3}$ t * m² is calculated and used. As an example the numbers were filled in for the ballast mass of 50 kg/m, the values for the other masses are different.

A4.7 ADJUSTMENTS TO THE MODEL FOR FORCE CALCULATION

GENERAL
Only the time step has been increased to 0.1 s

ENVIRONMENT
The option to include the current speed in the static analyses is now used. In this way, the forces caused by the current only can also be shown.

MODELING OF THE STEEL BOOM
The skirt is removed. To compensate for the drag properties of the skirt, the steel sections have been given the following adaptations:
- Mass: 1.0 t/m
- Drag diameter: 5.0 m
- Drag coefficient: 1.8

The links between the steel sections now have the following properties changed to the values:
- Drag diameter: 5.0 m
- Drag coefficient: 1.8

It has been found through running the model with increasing values for drag diameter and drag coefficients that these parameters of the boom would result in a conservative estimate of the forces in the model.

All 6D Buoys between the links and steel sections were removed. They were not required anymore for connecting the boom to the skirt and the links. The skirt is removed and the line that models the boom is now one long line that is divided into 7.5 m long steel sections and 0.5 m long neoprene sections with properties as given in chapter A4.3 and above in this paragraph.

A top view of the boom and the waves acting upon it is shown in the Figure A4.8 below. This view shows the shortest modelled steel boom of 648 m length. The boom was also modelled with lengths of 1296 m and 1944 m.

Booms with longer lengths were also used, but only the resulting forces from the current could be obtained because this could be included in the static calculations. The longer booms did not reach their final shape under the influence of waves within the simulation period.

These longer lengths are modelled with boom lengths of 3,992 m, 7,984 m and 19,960 m. The 2 last models could not be created without additional 6D Buoys because the model of 3,992 m reached the maximum number of sections in one line.

Additional lines of the same length were attached to each other with 6D Buoys with negligible properties until the boom lengths of 7,984 m and 19,960 m were reached. It was still necessary however, to place the center of mass of these 6D Buoys at -0.1 m to obtain a stable iteration sequence during the static analyses.
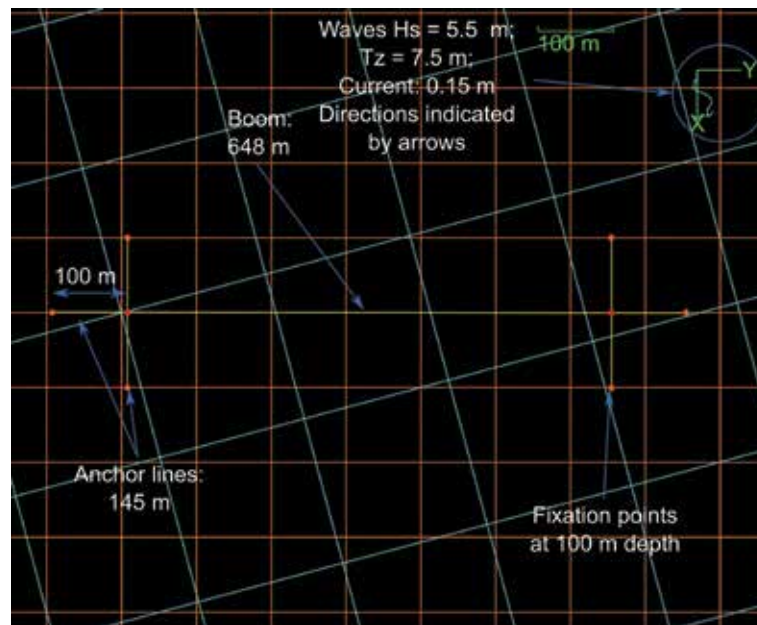
Figure A4.8 Top view of acting waves and current on the modelled boom

MODELING OF THE NEOPRENE BOOM

For the flexible boom, other boom properties have been found to compensate for the removal of the skirt to get to a conservative estimate:

- Mass: 0.75 t/m
- Drag diameter: 5.0 m
- Drag coefficient: 2.2

A secondary flexible boom with increased axial stiffness has been introduced with the axial stiffness increased to: $96.1*10^3$ kN. This is an increase of $95.3*10^3$ kN based on a 200 tonne Dyneema cable: FM-D200 ("Fibremax Dyneema Cable," n.d.) In kN, this cable has a tensile strength of . Using a load carrying cable came forward from a new design of the flexible boom, as described in Chapter 3.2. The boom without Dyneema cable is for the remainder of this chapter called 'neoprene', the boom with Dyneema cable will be called 'Dyneema'

Dynamic results of Dyneema were obtained for boom lengths of 288 m, 648 m and 1,296 m. For neoprene, they were obtained for boom lengths of 648 m, 1,296 m and 2,000 m.

Static results (in which the current was included, but no waves are present) are also obtained for boom lengths of 4,000 m and 10,000 m.

CAD MODEL FOR CFD

RAPHAEL KLEIN

This CAD Drawing illustrates the basic dimensions that have been used in the Computational Fluid Dynamics simulations in chapter 3.4. The generic boom design features a tube for floatation, a skirt to capture sub-surface debris, and ballast to maintain a vertical profile.

Isometric view
Scale: 1:200

20000

2950.45

1499.85

374.7

Front view
Scale: 1:200

25

30

25

Left view
Scale: 1:200

This drawing is our property. It can't be reproduced or communicated without our written agreement.

DRAWN BY	DATE				
Raphael	10/16/2013				
CHECKED BY	DATE	SIZE	DRAWING NUMBER		REV
XXX	xxx	A4	Part1		X
DESIGNED BY	DATE	SCALE 1:1	WEIGHT(kg) 0.00	SHEET	1/1
XXX	xxx				

The Ocean Cleanup

DRAWING TITLE

Simple Boom Design

ABOUT THE OCEAN CLEANUP

Boyan Slat (1994) combines environmentalism, entrepreneurism and technology to tackle global issues of sustainability.

While diving in Greece at the age of 16, he became frustrated by coming across more plastic bags than fish, and wondered: "why can't we clean this up?" While still in secondary school, he then decided to dedicate half a year of research to understand plastic pollution and the problems associated with cleaning it up. This ultimately led to the passive cleanup concept, which he presented at a TEDx conference in 2012.

Unfazed by the critics who claimed it was impossible to rid the oceans from plastic, Boyan put his aerospace engineering studies on hold, assembled a global team of more than 100 people, and crowdfunded $100,000 to investigate the feasibility of his concept. The Ocean Cleanup report marks the end to the first phase of the project, and shares with the world for the first time the results of this remarkable, yearlong tour-de-force.